Springer Handbook of Auditory Research

Alain Dabdoub
Bernd Fritzsch
Arthur N. Popper
Richard R. Fay *Editors*

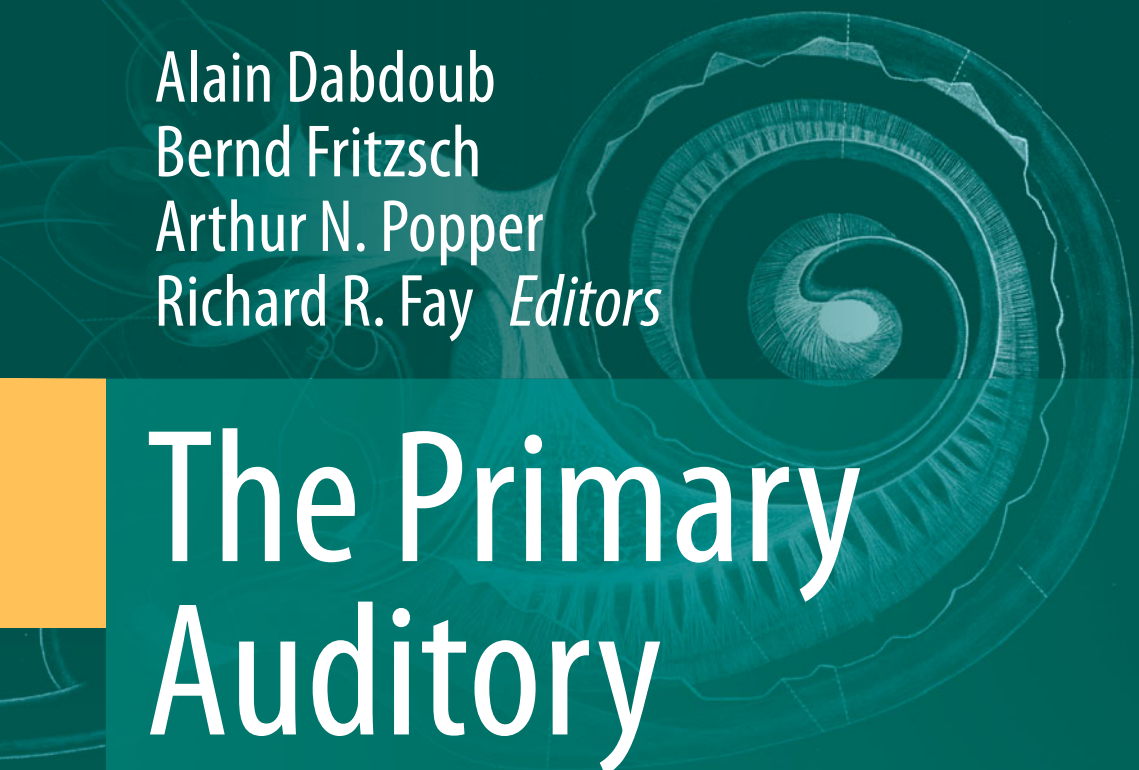

The Primary Auditory Neurons of the Mammalian Cochlea

Springer

Springer Handbook of Auditory Research

Volume 52

More information about this series at http://www.springer.com/series/2506

Alain Dabdoub · Bernd Fritzsch
Arthur N. Popper · Richard R. Fay
Editors

The Primary Auditory Neurons of the Mammalian Cochlea

With 58 Illustrations

Springer

Editors
Alain Dabdoub
Department of Otolaryngology—Head and Neck Surgery, Sunnybrook Research Institute
University of Toronto
Toronto, ON
Canada

Bernd Fritzsch
Department of Biology
University of Iowa
Iowa City, IA
USA

Arthur N. Popper
Department of Biology
University of Maryland
College Park, MD
USA

Richard R. Fay
Marine Biological Laboratory
Woods Hole, MA
USA

ISSN 0947-2657 ISSN 2197-1897 (electronic)
Springer Handbook of Auditory Research
ISBN 978-1-4939-3030-2 ISBN 978-1-4939-3031-9 (eBook)
DOI 10.1007/978-1-4939-3031-9

Library of Congress Control Number: 2015944172

Springer New York Heidelberg Dordrecht London

Printed on acid-free paper

Springer Science+Business Media LLC New York is part of Springer Science+Business Media (www.springer.com)

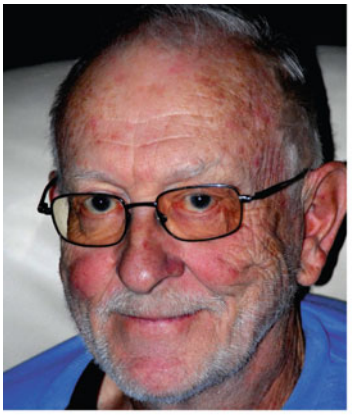

J. Morup Jørgensen

Elizabeth M. Keithley

Bruce J. Gantz (*right*) along with actress Marlee Matlin and Senator Tom Harkin (*left*)

The editors dedicate this volume to three individuals who touched their scientific communities at multiple levels as close friends, advisors, mentors, and important figures at the national and international level. J. Morup Jørgensen has been a collaborator, admired mentor, and longtime friend to the editors. His research and thinking about hair cell evolution stimulated the evolutionary thinking of two senior editors. Bruce J. Gantz served as a clinical role model to stimulate translational research for all editors. Beyond that, through his interaction with Senator Tom Harkin and

with the help of many, including actress Marlee Matlin, Bruce was involved in founding the National Institute of Deafness and Other Communication Disorders (NIDCD) at the NIH. Bruce has directly and indirectly influenced all ear-related research in the USA and, particularly fitting for the current volume, all spiral ganglion-related research. We also recognize Elizabeth M. Keithley in appreciation of her contributions to auditory neuroscience, especially documenting more than three decades ago that loss of spiral ganglion neurons is not simply retrograde degeneration following hair cell loss, but occurs as a result of some process that is intrinsic to these neurons. We also recognize her selfless mentorship, her efforts in education, and her support for hearing loss research.

Series Preface

The following preface is the one that we published in Volume 1 of the Springer Handbook of Auditory Research back in 1992. As anyone reading the original preface, or the many users of the series, will note, we have far exceeded our original expectation of eight volumes. Indeed, with books published to date, and those in the pipeline, we are now set for more than 50 volumes in SHAR, and we are still open to new and exciting ideas for additional books.

We are very proud that there seems to be consensus, at least among our friends and colleagues, that SHAR has become an important and influential part of the auditory literature. While we have worked hard to develop and maintain the quality and value of SHAR, the real value of the books is very much because of the numerous authors who have given their time to write outstanding chapters and to our many coeditors who have provided the intellectual leadership to the individual volumes. We have worked with a remarkable and wonderful group of people, many of whom have become great personal friends of both of us. We also continue to work with a spectacular group of editors at Springer, currently Ann Avouris. Indeed, several of our past editors have moved on in the publishing world to become senior executives. To our delight, this includes the current president of Springer US, Dr. William Curtis.

But the truth is that the series would and could not be possible without the support of our families, and we want to take this opportunity to dedicate all of the SHAR books, past and future, to them. Our wives, Catherine Fay and Helen Popper, and our children, Michelle Popper Levit, Melissa Popper Levinsohn, Christian Fay, and Amanda Fay, have been immensely patient as we developed and worked on this series. We thank them, and state, without doubt, that this series could not have happened without them. We also dedicate the future of SHAR to our next generation of (potential) auditory researchers—our grandchildren—Ethan and Sophie Levinsohn; Emma Levit; and Nathaniel, Evan, and Stella Fay.

Preface 1992

The Springer Handbook of Auditory Research presents a series of comprehensive and synthetic reviews of the fundamental topics in modern auditory research. The volumes are aimed at all individuals with interests in hearing research including advanced graduate students, postdoctoral researchers, and clinical investigators. The volumes are intended to introduce new investigators to important aspects of hearing science and to help established investigators to better understand the fundamental theories and data in the fields of hearing that they may not normally follow closely.

Each volume presents a particular topic comprehensively, and each serves as a synthetic overview and guide to the literature. As such, the chapters present neither exhaustive data reviews nor original research that has not yet appeared in peer-reviewed journals. The volumes focus on the topics that have developed a solid data and conceptual foundation rather than on those for which a literature is only beginning to develop. New research areas will be covered on a timely basis in the series as they begin to mature.

Each volume in the series consists of a few substantial chapters on a particular topic. In some cases, the topics will be ones of traditional interest for which there is a substantial body of data and theory, such as auditory neuroanatomy (Vol. 1) and neurophysiology (Vol. 2). Other volumes in the series deal with topics that have begun to mature more recently, such as development, plasticity, and computational models of neural processing. In many cases, the series editors are joined by a coeditor having special expertise in the topic of the volume.

Richard R. Fay, Falmouth, MA, USA
Arthur N. Popper, College Park, MD, USA

Volume Preface

The primary auditory neurons of the inner ear, or spiral ganglion neurons, are critical for hearing as they transmit auditory information in the form of electrical signals from mechanosensory hair cells in the inner ear to the cochlear nuclei in the brain stem. Loss of these auditory neurons and/or hair cells is the leading cause of congenital and acquired neurosensory hearing loss affecting hundreds of millions of people worldwide. The most common therapeutic strategies for hearing loss utilize either hearing aids to increase hair cell stimulation or cochlear implants as an electronic substitute for hair cells. These devices, as well as normal hearing, all require the presence of healthy functional spiral ganglion neurons.

This volume provides an up-to-date source of information on spiral ganglion neurons. From neurogenesis to biophysics and stem cell replacement therapy, the comprehensive and wide-ranging subjects encompassed will ensure that this volume will enlighten and function as a catalyst for future research and discovery. Although loss of auditory neurons has been considered secondary to hair cell loss, an increasing body of evidence clearly indicates that auditory neurons can degenerate as a result of noise exposure and aging, while hair cells remain intact. Therefore, auditory neurons are a primary target for regeneration, and a better understanding of these neurons will ultimately result in long-term maintenance and accelerate regenerative therapies. A comprehensive review of spiral ganglion neurons is important for researchers not only in the inner ear field but also for those working in development, neuroscience, biophysics, as well as neural networks.

The first chapter by Dabdoub and Fritzsch provides an overview of this volume and the current research on auditory neurons, including a perspective on future directions of research. Chapter 2 by Goodrich describes the molecular and genetic factors responsible for the neurogenesis of the spiral ganglion neurons. Chapter 3 by Fritzsch Kersigo, Yan, Jahan, and Pan explains the role of neurotrophic factors in spiral ganglion neuron maintenance. The electrophysiological properties as well as the tonotopic organization of spiral ganglion neurons are detailed in Chap. 4 by Davis and Crozier. Chapter 5 by Moser and Rutherford and Chap. 6 by Muniak, Connelly, Suthakar, Milinkeviciute, Ayeni, and Ryugo reveal the connectivity

details of the auditory neurons with hair cells in the inner ear and the cochlear nucleus in the brain stem, respectively. Chapter 7 by Green, Bailey, Kopelovich, and Hansen details gains in our cellular and molecular understanding of spiral ganglion neurons derived from various in vitro techniques invented during the last 100 years to achieve a mechanistic understanding of enhanced translation. In Chap. 8, Lang reviews processes of spiral ganglion neuron loss and degeneration and their relationship to hearing loss. The final Chap. 9 by Nayagam and Edge introduces stem cell research to replace lost auditory neurons.

As is often the case, chapters in earlier SHAR volumes complement the work presented in the current volume. This is particularly the case for the many chapters in earlier volumes that focus on the sensory hair cell and eighth nerve. For example, several chapters in *Synaptic Mechanisms in the Auditory System* (Vol. 41, edited by Trussell, Popper, and Fay, 2012) consider synapses associated with spiral ganglion neurons, while chapters in *Deafness* (Vol. 47, edited by Kral, Popper, and Fay, 2013) provide a consideration of the relationship of spiral ganglion neurons to hearing loss, as do chapters in *Auditory Prostheses: New Horizons* (Vol. 39, edited by Zeng, Fay, and Popper, 2011).

Alain Dabdoub, Toronto, Canada
Bernd Fritzsch, Iowa City, IA, USA
Arthur N. Popper, College Park, MD, USA
Richard R. Fay, Falmouth, MA, USA

Contents

1 Connecting the Inner Ear to the Central Auditory System: Molecular Development and Characteristics of the Primary Auditory Neurons and Their Network 1
Alain Dabdoub and Bernd Fritzsch

2 Early Development of the Spiral Ganglion 11
Lisa V. Goodrich

3 Neurotrophic Factor Function During Ear Development: Expression Changes Define Critical Phases for Neuronal Viability 49
Bernd Fritzsch, Jennifer Kersigo, Tian Yang, Israt Jahan and Ning Pan

4 The Electrophysiological Signature of Spiral Ganglion Neurons 85
Robin L. Davis and Robert A. Crozier

5 The Ribbon Synapse Between Type I Spiral Ganglion Neurons and Inner Hair Cells 117
Mark A. Rutherford and Tobias Moser

6 Central Projections of Spiral Ganglion Neurons 157
Michael A. Muniak, Catherine J. Connelly, Kirupa Suthakar, Giedre Milinkeviciute, Femi E. Ayeni and David K. Ryugo

7 The Spiral Ganglion in an Out-of-Body Experience: A Brief History of in Vitro Studies of the Spiral Ganglion 191
Steven H. Green, Erin M. Bailey, Jonathan C. Kopelovich and Marlan R. Hansen

8 Loss, Degeneration, and Preservation of the Spiral Ganglion Neurons and Their Processes 229
Hainan Lang

9 Stem Cells for the Replacement of Auditory Neurons 263
Bryony A. Nayagam and Albert S.B. Edge

Contributors

Femi E. Ayeni Garvan Institute of Medical Research, Sydney, NSW, Australia; School of Medical Sciences, University of New South Wales, Sydney, NSW, Australia

Erin M. Bailey Department of Biology, University of Iowa, Iowa City, IA, USA

Catherine J. Connelly Garvan Institute of Medical Research, Sydney, NSW, Australia; School of Medical Sciences, University of New South Wales, Sydney, NSW, Australia

Robert A. Crozier Department of Cell Biology and Neuroscience, Rutgers University, Piscataway, NJ, USA

Alain Dabdoub Department of Otolaryngology—Head and Neck Surgery, Sunnybrook Research Institute, University of Toronto, Toronto, Canada

Robin L. Davis Department of Cell Biology and Neuroscience, Rutgers University, Piscataway, NJ, USA

Albert S.B. Edge Eaton-Peabody Laboratory, Massachusetts Eye and Ear Infirmary, Harvard Medical School, Boston, MA, USA

Bernd Fritzsch Department of Biology, University of Iowa, Iowa City, IA, USA

Lisa V. Goodrich Department of Neurobiology, Harvard Medical School, Boston, MA, USA

Steven H. Green Department of Biology, University of Iowa, Iowa City, IA, USA

Marlan R. Hansen Department of Otolaryngology—HNS, University of Iowa, Iowa City, IA, USA

Israt Jahan Department of Biology, University of Iowa, Iowa City, IA, USA

Jennifer Kersigo Department of Biology, University of Iowa, Iowa City, IA, USA

Jonathan C. Kopelovich Department of Otolaryngology, Children's Hospital Colorado and University of Colorado School of Medicine, Aurora, CO, USA

Hainan Lang Department of Pathology and Laboratory Medicine, Medical University of South Carolina, Charleston, SC, USA

Giedre Milinkeviciute Garvan Institute of Medical Research, Sydney, NSW, Australia; School of Medical Sciences, University of New South Wales, Sydney, NSW, Australia

Tobias Moser Institute for Auditory Neuroscience and Inner Ear Lab, Collaborative Research Center 889, University Medical Center Göttingen, Göttingen, Germany

Michael A. Muniak Garvan Institute of Medical Research, Sydney, NSW, Australia

Bryony A. Nayagam Department of Audiology and Speech Pathology, University of Melbourne, Parkville, VIC, Australia

Ning Pan Department of Biology, University of Iowa, Iowa City, IA, USA

Mark A. Rutherford Department of Otolaryngology, Central Institute for the Deaf, Washington University School of Medicine, St. Louis, MO, USA

David K. Ryugo Garvan Institute of Medical Research, Sydney, NSW, Australia; School of Medical Sciences, University of New South Wales, Sydney, NSW, Australia

Kirupa Suthakar Garvan Institute of Medical Research, Sydney, NSW, Australia; School of Medical Sciences, University of New South Wales, Sydney, NSW, Australia

Tian Yang Department of Biology, University of Iowa, Iowa City, IA, USA

Chapter 1
Connecting the Inner Ear to the Central Auditory System: Molecular Development and Characteristics of the Primary Auditory Neurons and Their Network

Alain Dabdoub and Bernd Fritzsch

Keywords Auditory neuron · Deafness · Hearing loss · Inner ear · Network · Neurogenesis · Neurotrophic factor · Regenerative therapy · Reinnervation · Spiral ganglion · Stem cells · Transcription factor

1.1 Introduction

Humans are dependent on their auditory system for communication; therefore, hearing loss is an insidious problem that has a potentially devastating impact on the quality of life. It might lead not only to communication problems but also to social isolation and depression. Moreover, the economic impact of hearing loss is experienced both at an individual and a social level. As many of the conditions that lead to hearing loss are age related, the prevalence of hearing impairment is on the rise as the world's population ages. According to the World Health Organization (WHO), hearing impairment is the most common sensory defect, affecting at least three in 1000 newborns, 5 % of people younger than age 45, and 50 % of people by age 70 worldwide. The WHO estimates that around 900 million people might be hard of hearing (defined as a 25 dB SPL loss in sound sensitivity) by 2050 (Yamasoba et al., 2013). Given the future demographics of an increasingly aging population throughout the world, this staggering number will likely remain unchanged over the foreseeable future.

In the mammalian cochlea, the spiral ganglion neurons are the primary afferent auditory neurons. They have a critical function in hearing, as these neurons are responsible for transmitting auditory information from the mechanosensory hair cells

A. Dabdoub (✉)
Department of Otolaryngology—Head and Neck Surgery, Sunnybrook Research Institute, University of Toronto, 2075 Bayview Avenue, ON M4N 3M5 Toronto, Canada
e-mail: alain.dabdoub@sri.utoronto.ca

B. Fritzsch
Department of Biology, University of Iowa, Iowa City 52242, IA, USA
e-mail: bernd-fritzsch@uiowa.edu

A. Dabdoub et al. (eds.), *The Primary Auditory Neurons of the Mammalian Cochlea*, Springer Handbook of Auditory Research 52,
DOI 10.1007/978-1-4939-3031-9_1

in the organ of Corti to the auditory cochlear nuclei in the brain stem (Fig. 1.1). Based on the position of the cell body relative to the central process (usually referred to as the axon) and the peripheral process (usually referred to as the dendrite), two types of spiral ganglion neurons have been characterized: bipolar type I spiral ganglion neurons connecting the inner hair cells to the cochlear nuclei of the hindbrain and pseudounipolar type II spiral ganglion neurons connecting outer hair cells of the organ of Corti to the cochlear nuclei. The traditional nomenclature follows the information flow, with dendrites being the receiving end and axons the emitting end of a neuron. However, as the peripheral process or dendrite matures it acquires the properties of an axon in terms of action potential conduction. Peripheral to the soma, mature type I spiral ganglion neurons have a highly modified process that has functional and morphological characteristics of an axon, including myelination. Based on these characteristics one can refer to the myelinated peripheral process as an axon sending information toward the soma and to the unmyelinated part that receives synaptic input as a dendrite.

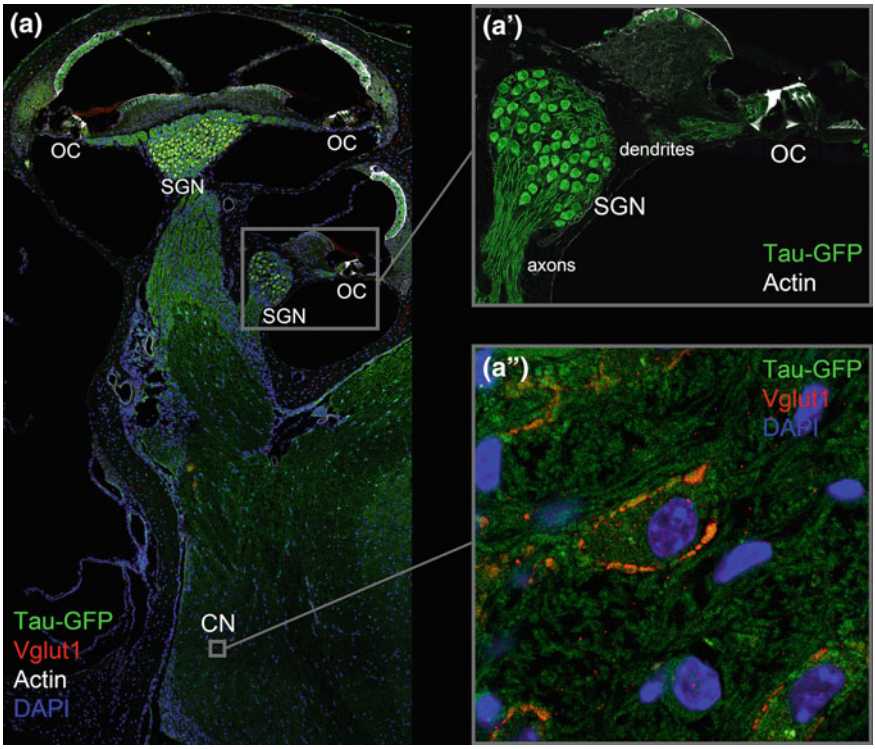

Fig. 1.1 Auditory neurons connect mechanosensory hair cells in the organ of Corti to cochlear nuclei neurons in the brain stem. **a** Cross section through the cochlea and brain stem of an adult tau-GFP neuron reporter mouse (2 months old). *SGN* spiral ganglion neurons; *OC* organ of Corti; *CN* cochlear nucleus. **a′** High-magnification view of the spiral ganglion neurons showing the dendrites extending in the periphery to the organ of Corti (OC) and the axons traveling to the central nervous system. **a″** High-magnification view demonstrating the spiral ganglion neuron endings (*red* Vglut1, vesicular glutamate transporter 1) on the neurons of the cochlear nucleus (*green* tau-GFP, with blue nuclei). Work performed by Dr. Koji Nishimura

1.2 Historical Perspective

The development of the auditory neurons and their connectivity was studied by early anatomists such as Gustaf Retzius, Fredrich-Christian Rosenthal, Alfonso Corti, Rudolph Albert von Kölliker, and Rafael Lorente de Nó. Indeed, the synapse between the hair cell and the sensory neurons was defined already by Retzius (1884) and made him one of the first adopters of the newly formulated neuron theory proposed by S. Ramon y Cajal. Retzius' silver impregnations showed a sharp stop at hair cells and thus led him to believe that the proposed discontinuity of sensory neurons and hair cells was in line with the neuron theory, which contrasted with the prevailing reticular theory of a syncytial nerve net (Retzius, 1884; Grant, 2011). Retzius' studies also presented the first detailed account of the development and cellular organization of the organ of Corti, the hearing organ of mammals. In addition, they clarified much of the evolution of the human organ of Corti from the basilar papilla found in other tetrapods (Retzius, 1884; Fritzsch et al., 2013). At the end of the 19th century, Retzius' ear studies provided the most detailed and comprehensive analysis of any vertebrate organ system development and evolution. Based on his standing in science at the time, Retzius was nominated for the Nobel Prize 11 times, without ever receiving it.

It took about 50 years before another great neuroanatomist, R. Lorente de Nó, could surpass the achievements of Retzius. As summarized in his 1981 volume (Lorente de Nó, 1981), Lorente de Nó in the 1930s showed, in great detail, how spiral ganglion neurons project to the organ of Corti (Fig. 1.2) and how the central projections into the cochlear nuclei are cochleotopically organized (Fig. 1.3). This beautiful work, unfortunately, followed the perception of Lorente de Nó's teacher, Ramon y Cajal, in assuming that there is no efferent system to the ear. Because of this bias, Lorente de Nó showed both afferent and efferent fibers in the organ of Corti in a bewildering complexity of a rich variety of spiral ganglion neurons (Fig. 1.2). In contrast to the baffling differences in peripheral projections, the central projections drawn by Lorente de Nó (Fig. 1.3) showed a much greater uniformity. The discovery that efferents to the ear exist (Rasmussen, 1953; Simmons et al., 2011; Sienknecht et al., 2014) and that spiral ganglion neurons comprise only two distinct types (Spoendlin & Schrott, 1989) overturned much of the early interpretations of Lorente de Nó. However, these different interpretations do not invalidate the information presented in the exquisite drawings that followed in great detail those of his teacher, S. Ramon y Cajal. Indeed, it took 100 years before modern techniques were developed that matched or exceeded the resolution of the Golgi technique to study spiral ganglion neurons (Figs. 1.1, 1.2, 1.3) and their peripheral and central projections. The present SHAR volume provides insights that go well beyond those early stages of the neurobiology of the spiral ganglion by adding molecular and physiological dimensions that will inform future clinical applications how to combat hearing impairment.

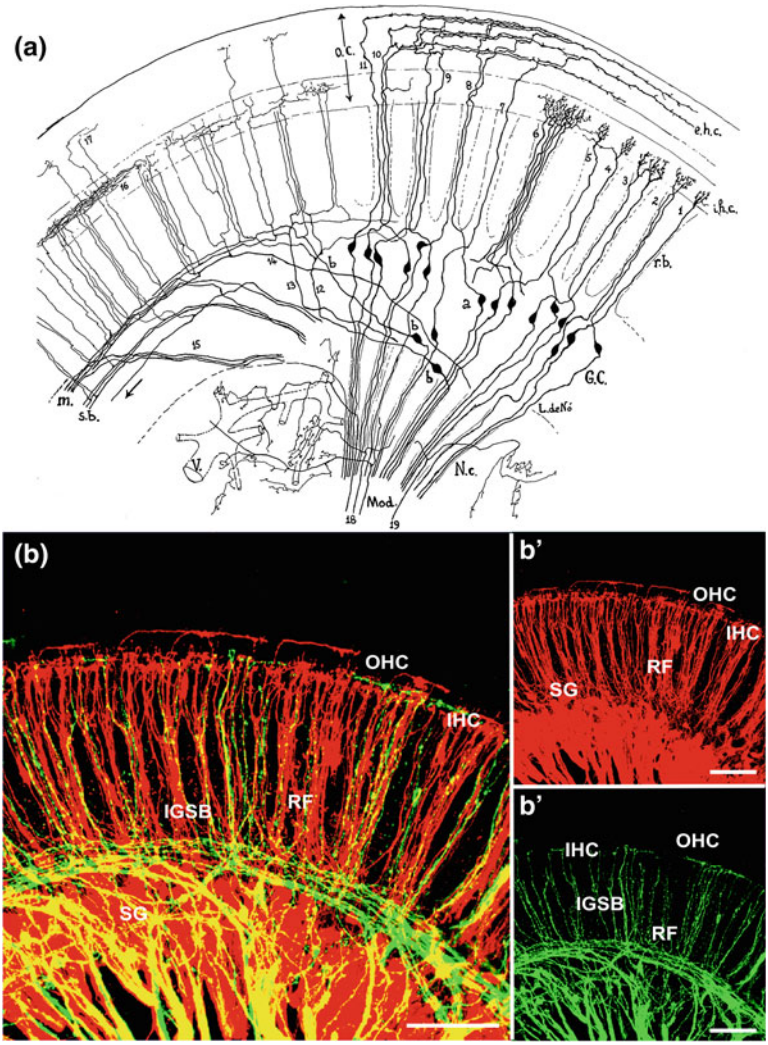

Fig. 1.2 Lorente de Nó (1981) showed in exquisite detail the organization of spiral ganglion neurons and their projections to the organ of Corti in postnatal mice (**a**). Note that only the right half of the image shows indeed the two types of spiral ganglion cells; on the far right the type I bipolar ganglion cells reaching to inner hair cells; and in the center the type II, partially pseudounipolar ganglion cells reaching to outer hair cells. The left side of this drawing shows what is now known as efferents but was interpreted by Lorente de Nó as a different set of spiral ganglion neurons. Only modern tracing techniques using injections of different colored tracers into the efferents (*green* in **b**) and cochlear nucleus (*red* in **b**) of mice around birth showed that efferents and afferents take partially overlapping but distinct trajectories. Although they overlap in radial fiber bundles (RF), only efferents contribute to the intraganglionic spiral bundle (IGSB). Both afferents and efferents form distinct terminals on outer (OHC) and inner hair cells (IHC) of the organ of Corti. Images are from Lorente de Nó (1981) and Simmons et al. (2011)

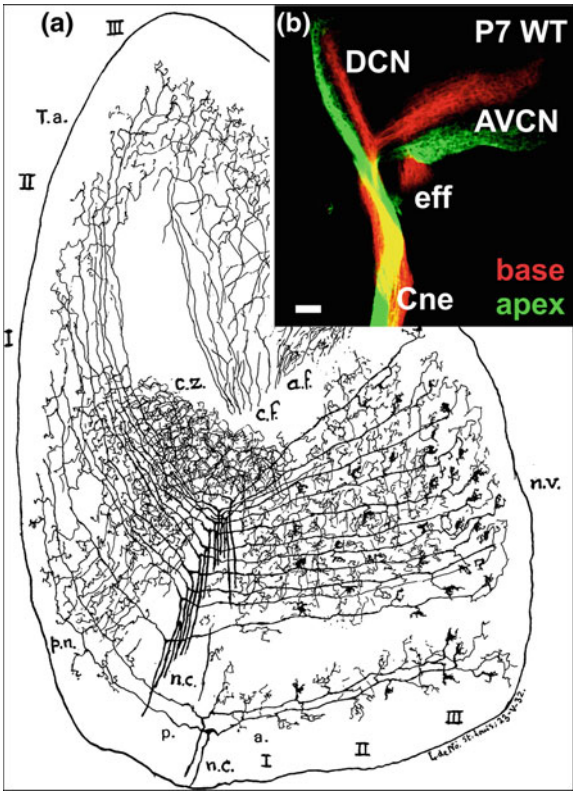

Fig. 1.3 Lorente de Nó used his Golgi impregnations (**a**) to demonstrate the topological organization of spiral ganglion afferents in the cochlear nuclei of postnatal rodents and the vastly different terminals in the different parts of the cochlear nucleus complex. Note that each fiber provides multiple contacts with different second-order neurons that have radically different morphologies. Modern techniques using differently colored tracers show that indeed the cochlear nuclei receive fibers from distinct nonoverlapping areas of the organ of Corti in this mouse embryo (**b**). Injections into the base (*red*) label fibers terminating dorsally, whereas injections into the apex (*green*) label fibers terminating ventrally in the cochlear nucleus complex. In addition, efferent fibers (eff) segregate from the cochlear nerve (Cne) to enter the brain via the vestibular root. AVCN, anteroventral cochlear nucleus; DCN, dorsal cochlear nucleus. Images taken from Lorente de Nó (1981) and Fritzsch et al. (2015)

1.3 Objectives of the Book

Beyond these early neuroanatomical insights, research over the last 30 years has shown that loss or damage of hair cells and/or spiral ganglion neurons is the leading cause of congenital and acquired hearing loss affecting millions of humans (Yamasoba et al., 2013). The most common therapeutic strategies for hearing loss are based on either using hearing aids to increase hair cell stimulation in moderate

hearing loss or utilizing cochlear implants (CIs) as an electronic substitute for hair cells in cases of severe hearing loss resulting from severe hair cell loss (Zeng et al., 2011). However, both scenarios depend on the presence of functional spiral ganglion neurons to achieve a positive outcome. Indeed clinical data suggest that the function of CIs depends critically on the remaining number of spiral ganglion neurons (Nadol et al., 1989; Reiss et al., 2012). Thus, the development of methodologies that could be used in the maintenance, repair, and regeneration of spiral ganglion neurons in a damaged ear have significant implications for future advances in cochlear implant technology and the treatment of neurosensory hearing loss.

The aim of this volume is to present the main concepts in spiral ganglion neuron research to guide translation into clinical settings. This book elucidates the molecular basis of development, degeneration, and loss of the auditory neurons and their environment, connectivity, and neurophysiological function with the goal of teaching and enlightening interested scientists new to this important field. In this volume the necessary groundwork toward maintenance, repair, and regeneration of these essential auditory neurons is succinctly presented. In addition to providing a broad overview of the current state of the art in this research field, each chapter looks back to define the underlying questions and concepts and also looks forward by offering insights into the building blocks for new and innovative investigations to be carried out by current and future scientists. The hope is that this snapshot of auditory neuron research will fuel original discovery-driven investigations that ultimately lead to translational research benefitting the millions who suffer some degree of hearing loss and the millions more who will suffer from this ailment in the near future. In terms of regenerative therapy, the loss of auditory neurons has been considered secondary to hair cell loss; here, we provide an increasing body of evidence that clearly indicates that auditory neurons can degenerate as a result of noise exposure and aging while hair cells remain intact. The potential clinical value in the amelioration of hearing impairment is tremendous, as the development of methodologies that could be used to induce the regeneration of the auditory neurons in a damaged ear have significant implications for future advances in cochlear implant technology and the treatment of hearing loss.

1.4 Overview of the Book

In Chap. 2, Goodrich lays out the molecular landscape responsible for the generation and development of the spiral ganglion neurons. This chapter details the developmental path of these neurons that arise from the proneurosensory domain present in the early otocyst. Further, the mechanisms responsible for spiral ganglion neuron development as well as the transcriptional networks that reinforce the neurosensory fate differentiation are eloquently reviewed and presented. Although not fully elucidated yet, the data presented provide a compelling molecular groundwork to promote and direct attempts to regenerate these essential neurons.

In Chap. 3, Fritzsch, Kersigo, Yang, Jahan, and Pan provide a comprehensive overview of the neurotrophic theory and how the spiral ganglion neurons present an exemplary model of this theory that was originally explored in the groundbreaking work of the late Nobel laureate R. Levi-Montalcini (Levi-Montalcini, 1949). The chapter illustrates how the two neurotrophins present in the inner ear, brain-derived neurotrophic factor (BDNF) and neurotrophin 3 (NT-3), and their receptors tyrosine kinase B (TrkB) and TrkC respectively, are both necessary and sufficient for the maturation and maintenance of all auditory neurons.

In Chap. 4, Davis and Crozier present and elaborate on the full richness of the electrophysiological characteristics of auditory neurons including the distribution of ion channels and synaptic proteins. As these are the first neurons in the auditory pathway, the authors describe these electrophysiological specializations within the framework of the coding requirements and the need for accuracy and reliability in conveying sounds from the environment with great topological precision. Such precision is necessary to refine and detail the tonotopic or cochleotopic presentation of the cochlear frequency distribution in the auditory nuclei of the brain stem.

In Chap. 5, Moser and Rutherford introduce the first auditory synapse in the cochlea, which is responsible for encoding sound. The chapter provides an overview of synaptogenesis, with special attention to how synaptic morphology matures over postnatal development as its function changes around the onset of hearing. The excitatory ribbon synapse that exists between the inner hair cells presynaptically and the type I spiral ganglion neurons postsynaptically triggers action potentials of the auditory nerve. Synaptic heterogeneities that may contribute to the diversity of sound-response properties among spiral ganglion neurons are concisely described.

The precise central connection of spiral ganglion neurons is essential for the frequency representation of the organ of Corti to form a tonotopic or cochleotopic map of afferent projections such that the base (high-frequency end) is presented in the dorsal part and the apex (low-frequency end) in the ventral part of the cochlear nuclei. Chapter 6 by Muniak and Ryugo expertly details the connectivity established by the spiral ganglion afferents onto the various second-order neurons of the cochlear nuclei, a crucial first connection for the auditory information processing in the brain.

Much of what we understand about the molecular details of pathfinding, neurotrophic signaling, and molecular basis of synapse formation was originally derived from studies of various tissue cultures of spiral ganglion neurons. To appreciate the profound insights that technology has contributed over the years to the current level of our understanding, Chap. 7 by Green, Bailey, Kopelovich, and Hansen provides an historical review of these contributions and brings us to the current state of the art. In a practical approach to studying these neurons encased in the strongest bone in the body, we are informed, for example, about approaches to elucidate in vitro guidance molecules to enhance efficiency of contact formation between spiral ganglion neuron processes and cochlear implants for a higher fidelity of information transmission through a larger set of electrode stimulations to more spiral ganglion neurons.

In Chap. 8, Lang explores data on spiral ganglion neuron degeneration, with an emphasis on recent studies describing primary and age-related spiral ganglion neuron degeneration. As hearing is dependent on the integrity of the spiral ganglion neurons, Lang adeptly reviews a wide range of studies that connect cellular and molecular degeneration of the auditory neurons to hearing loss. Results from animal models of spiral ganglion neuron degeneration and a discussion of possible methods that could lead to the preservation of these neurons in vivo are presented in this chapter.

The volume ends with an insightful review in Chap. 9 in which Nayagam and Edge present data on the use of stem cells to replace damaged or lost auditory neurons. Drawing from development and molecular biology studies presented in other chapters of this volume, as well as stem cell discoveries, the review revolves around the necessary characteristics of the replacement neurons. For the auditory network to function accurately, the stem cell–derived auditory neurons need to connect to their peripheral and central nervous system targets and reestablish an auditory circuit that behaves similarly to the original.

1.5 Looking Ahead

The volume could not be complete without a perspective of what needs to be accomplished in spiral ganglion neuron research; accordingly, each chapter ends with a section on future directions and major questions in the field. The goal of research is to maintain these auditory neurons long term under conditions of organ of Corti loss and possibly restore hearing with various means using these remaining neurons (see Chaps. 7 by Green et al., 8 by Lang, and 9 by Nayagam and Edge). A priority for basic research should therefore be to understand how to maintain auditory neurons in the absence of a peripheral target and how to enhance their abilities to regrow peripheral processes to either hair cells (should they remain or be regenerated) or cochlear implants (in cases of complete loss of the organ of Corti with little hope to restore such a complicated cellular system in the immediate future). Another priority is regenerating auditory neurons as loss of spiral ganglion neurons can be induced by various means (see Chap. 8 by Lang) and various trophic factors can play a role in both maintenance and fiber guidance (see Chaps. 3 by Fritzsch et al., 4 by Davis and Crozier, as well as 7 by Green et al.) but much remains to be investigated to use the basic knowledge to guide clinical work. Growing peripheral processes back to hair cells after long-term and/or loud sound exposure will lead to functional gain only if the synaptic architecture is restored (see Chap. 5 by Rutherford and Moser). As outlined in Chap. 9 Nayagam and Edge, replacement of spiral ganglion neurons is possible under certain circumstances. However, using such approaches to reliably and cost-effectively restore spiral ganglion neurons in a growing number of patients remains a prospect to be realized sometime in the future. Using the basic understanding of the molecular biology of neuronal development (see Chaps. 2 by Goodrich, 3 by Fritzsch et al. and 9 by

Nayagam and Edge) could provide molecular means to induce spiral ganglion neuron differentiation in vivo to expand and replenish remaining populations of spiral ganglion neurons. Should such approaches be feasible, it would be important to connect such cells not only to the hair cells of the organ of Corti, but also to the cochlear nuclei to establish the proper cochleotopic presentation of afferents (see Chaps. 4 by Davis and Crozier and 6 by Muniak et al., as well as Chap. 9 by Nayagam and Edge). Future success in ameliorating hearing deficits will depend on changes in the aims of restoration of hearing beyond the current focus on hair cells, emphasizing a stronger focus on spiral ganglion neurons.

In addition to the clinical value in hearing loss repair, regeneration of neurons in a degenerated spiral ganglion is a potential model system for neural network regeneration. Spiral ganglion neurons have only two targets: the peripheral cochlear hair cells and the neurons of the cochlear nuclei, offering a less complex network that can serve as an exceptionally suitable platform to dissect the molecular basis of topologically well-organized connections that are almost two dimensional in their distribution, reflecting the tonotopic organization of the organ of Corti and the cochlear nuclei. Once fully developed, the spiral ganglion could serve as a unique model to unravel otherwise difficult to dissect molecular interactions and could thus bring the ear back into the forefront of developmental research as in the first half of the 20th century, when neuronal viability were identified by Levi-Montalcini (1949). It is hoped that the concepts and data presented here will help propel the primary auditory neurons into the forefront of research in the 21st century, needed now more than ever to prevent and ameliorate hearing loss in hundreds of millions of people in aging societies worldwide.

Acknowledgments This work was supported by grants from NIH (P30 DC 010362), NASA Base Program, and the University of Iowa (B. F.); the Hearing Regeneration Initiative at Sunnybrook Research Institute (A. D.); and the Department of Otolaryngology—Head and Neck Surgery, University of Toronto (A. D.).

References

Fritzsch, B., Pan, N., Jahan, I., Duncan, J. S., Kopecky, B. J., Elliott, K. L., Kersigo, J., & Yang, T. (2013). Evolution and development of the tetrapod auditory system: An organ of Corti-centric perspective. *Evolution & Development*, 15(1), 63–79.

Fritzsch, B., Pan, N., Jahan, I., & Elliott, K. L. (2015). Inner ear development: Building a spiral ganglion and an organ of Corti out of unspecified ectoderm. *Cell & Tissue Research*, 363, 1–18.

Grant, G. (2011). Gustaf Retzius (1842–1919). *Journal of Neurology*, 258(4), 706–707.

Levi-Montalcini, R. (1949). The development of the acoustico-vestibular centres in the chick embryo in the absence of the afferent root fibers and of descending fiber tracts. *Journal of Comparative Neurology*, 91(2), 209–241.

Lorente de Nó, R. (1981). *The primary acoustic nuclei*. New York: Raven Press.

Nadol, J. B., Young, Y. S., & Glynn, R. J. (1989). Survival of spiral ganglion cells in profound sensorineural hearing loss: Implications for cochlear implantation. *Annals of Otology, Rhinology & Laryngology*, 98(6), 411–416.

Rasmussen, G. L. (1953). Further observations of the efferent cochlear bundle. *Journal of Comparative Neurology*, 99(1), 61–74.

Reiss, L. A., Turner, C. W., Karsten, S. A., Erenberg, S. R., Taylor, J., & Gantz, B. J. (2012). Consonant recognition as a function of the number of stimulation channels in the Hybrid short-electrode cochlear implant. *The Journal of the Acoustical Society of America,* 132(5), 3406–3417.

Retzius, G. (1884). *Das Gehörorgan der Wirbeltiere*, Band 2: *Das Gehörorgan der Reptilien, der Vögel und der Säugetiere*. Stockholm: Samson & Wallin.

Sienknecht, U. J., Koppl, C., & Fritzsch, B. (2014). Evolution and development of hair cell polarity and efferent function in the inner ear. *Brain, Behaviour and Evolution*, 83(2), 150–161.

Simmons, D., Duncan, J., de Caprona, D. C., & Fritzsch, B. (2011). Development of the inner ear efferent system Auditory and vestibular efferents. In D. K. Ryugo, R. F. Fay, and A. N. Popper (Eds.), *Auditory and vestibular efferents* (pp. 187–216). New York: Springer Science+Business Media.

Spoendlin, H., & Schrott, A. (1989). Analysis of the human auditory nerve. *Hearing Research,* 43 (1), 25–38.

Yamasoba, T., Lin, F. R., Someya, S., Kashio, A., Sakamoto, T., & Kondo, K. (2013). Current concepts in age-related hearing loss: Epidemiology and mechanistic pathways. *Hearing Research,* 303, 30–38.

Zeng, F.-G., Popper, A. N., & Fay, R. R. (2011). *Cochlear implants: Auditory prostheses and electric hearing*. New York: Springer Science+Business Media.

Chapter 2
Early Development of the Spiral Ganglion

Lisa V. Goodrich

Keywords Auditory neuroblast · Neural progenitor · Neurosensory progenitor · Otic vesicle · Otic neurogenesis · Sensory progenitor

2.1 Introduction: Morphogenesis of the Spiral Ganglion

The spiral ganglion develops in parallel with the patterning and morphogenesis of the inner ear (Fig. 2.1). The inner ear arises from the otic placode, an ectodermal thickening that forms adjacent to the 5th and 6th rhombomeres of the hindbrain in vertebrates other than the lamprey (Kuratani et al., 1998). This occurs at the 8–10 somite stage of development, which corresponds to E8.5 in mouse (*Mus musculus*) (Anniko & Wikstrom, 1984) and stage 10 in chicken (*Gallus gallus*) (Hemond & Morest, 1991a). In birds and rodents, the placode subsequently invaginates and deepens to become an otic cup (Knowlton, 1967; Marovitz et al., 1977; Anniko & Schacht, 1984). The otic cup then detaches from the ectoderm and seals to form an ovoid otic vesicle that is closely apposed to the hindbrain and surrounded by mesenchyme.

Inner ear neurons develop from precursors in the anteroventral quadrant of the otic vesicle, which leave the epithelium and proliferate to form the cochlear-vestibular ganglion (CVG) just rostral to the developing inner ear. At this stage, the cochlear and vestibular ganglia are distinct yet closely associated with each other, as well as with the geniculate ganglion (Fig. 2.1), forming a three-ganglion complex. Morphologically, neuroblasts can be recognized during otic cup stages as otic epithelial cells that lose their columnar morphology and delaminate from the epithelium (Carney & Silver, 1983; Hemond & Morest, 1991b), forming a distinct CVG by the 22–24 somite stage in mice (Wikstrom &

L.V. Goodrich (✉)
Department of Neurobiology, Harvard Medical School, 200 Longwood Avenue,
MA, Boston 02115, USA
e-mail: lisa_goodrich@hms.harvard.edu

A. Dabdoub et al. (eds.), *The Primary Auditory Neurons of the Mammalian Cochlea*, Springer Handbook of Auditory Research 52,
DOI 10.1007/978-1-4939-3031-9_2

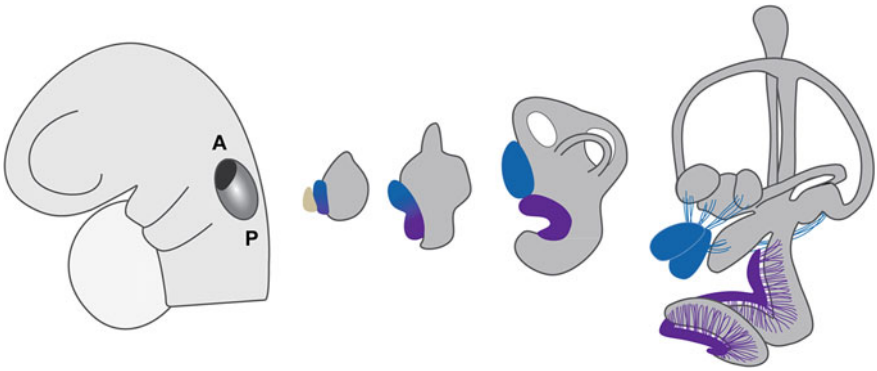

Fig. 2.1 Morphogenesis of the spiral ganglion. The spiral ganglion develops from a proneurosensory region (*dark gray*) in the anteroventral quadrant of the otic cup, beginning around E9 in mouse. Over the next week, the otic cup invaginates and acquires its mature three-dimensional structure. In parallel, the neurons delaminate to form a cochlear-vestibular ganglion (CVG). The vestibular (*blue*) and spiral (*purple*) ganglia gradually separate and eventually innervate the vestibular and auditory sensory epithelia respectively. The geniculate ganglion (tan) is initially attached to the CVG laterally (shown only for E10.5). This ganglion is separated from the CVG by the facial nerve and originates from a distinct placode

Anniko, 1987), with the auditory division positioned medial and ventral to the vestibular division and the entire neural anlage still attached to the geniculate ganglion (Sher, 1972). The spiral ganglion grows and extends together with the cochlear duct over the next several days (Carney & Silver, 1983), gradually separating from the vestibular and geniculate ganglia.

The basic sequence of events during spiral ganglion development is conserved across species, with a few notable exceptions. In every species examined, neurons seem to be the first differentiated cell type to appear in the inner ear. In both mice and birds, neurogenesis begins during otic cup stages and continues after the otic vesicle has closed and become free from the overlying ectoderm (Carney & Silver, 1983; Hemond & Morest, 1991a). However, the structures for hearing exhibit distinct forms. In mammals, the auditory sensory epithelium (the organ of Corti) spirals within a coiled cochlear duct. Birds (and reptiles) instead detect sound via the basilar papilla, which is located in the tube-like lagenar recess. To underscore its similar function, the avian hearing organ is often referred to as the cochlear duct, but it is important to note that these structures are not strictly analogous, as the lagenar recess also houses an additional sensory epithelium, the lagena macula, that is not present in the cochlea.

The lagena macula is a sensory organ found in birds, fish, reptiles, and amphibians but not in mammals (Harada et al., 2001). Most often considered vestibular in nature, its function remains unclear and may vary among species (Fritzsch & Straka, 2014). In pigeons, there is intriguing evidence for a role in magnetoreception, which is the ability to orient in response to the Earth's magnetic field (Wu & Dickman, 2011). From an evolutionary point of view, the lagena macula seems to

have been lost from mammals, possibly having been incorporated into the apex of the organ of Corti, which itself evolved from the basilar papilla (reviewed in Fritzsch et al., 2013). Because of these differences, auditory and vestibular neurons form distinct ganglia in mammals but remain as a CVG in birds. Whether this difference in organization affects the development of the auditory neurons is not clear, but the presence of the lagena macula should be borne in mind when making comparisons between species, especially because this sensory epithelium is innervated by a subset of neurons that project to distinct targets centrally (Mahmoud et al., 2013).

The fish inner ear also exhibits a number of salient differences from both the avian and mammalian ears. Most strikingly, fish such as the common model organism zebrafish (*Danio rerio*) do not develop a cochlea-like structure and have no basilar papilla, as fish rely instead on hair cells in the saccule and lagena for auditory function (Bigelow, 1904). This raises the question of whether the neurons that innervate the saccule and lagena in fish are more analogous to vestibular or auditory neurons in mammals. Circuit tracing studies have confirmed that the primary sensory neurons that innervate each of these structures convey information to different regions of the brain, suggesting that fish use the information from sound-induced vibrations in the saccule and lagena differently from the movement-induced vibrations of the utricle and semicircular canals (McCormick & Wallace, 2012). However, in many brainstem nuclei, there is also considerable overlap with projections that are vestibular in nature. In addition to the murky understanding of auditory versus vestibular identity, the timing of neurogenesis is also slightly different in fish. Whereas in birds and mammals, hair cells typically develop after neurons, both populations are produced at the same time in fish (Haddon & Lewis, 1996) and continue to be added long after hatching (Popper & Hoxter, 1984). Fish also differ in the size of the ganglion, which contains only a few hundred neurons (Popper & Hoxter, 1984) compared to approximately 8000 in mice (Johnson et al., 2011) and approximately 9000 in chickens (Ard & Morest, 1984).

The human spiral ganglion is even larger, with approximately 30,000 neurons (Rasmussen, 1940; Nadol, 1988; Spoendlin & Schrott, 1989), although it appears to pass through developmental stages similar to what has been described in mice and chickens (Streeter, 1906; Bibas et al., 2006; Locher et al., 2013). In addition, there is accumulating evidence that the same basic pathways operate in fish, mice, and chickens, though different specific players may be involved in each species (see Groves & Fekete, 2012 for review). Much less is known about the molecular basis of human spiral ganglion neuron development, but to date, no obvious differences have been described. Nevertheless, it is important to keep in mind that differences between species may exist, both among model organisms and between model organisms and humans. Because of the closer parallels to the human system, findings from chicken and rodents will be emphasized here. The chick has served as an excellent system for working out the earliest stages of neurogenesis because of its accessibility for acute embryological manipulations. Mice offer the advantage of genetics plus closer parallels to the human.

Morphogenesis of the spiral ganglion depends on a coordinated series of extrinsic and intrinsic patterning events that begin in the early otic vesicle with the

production of multipotent neurosensory progenitors. Neurosensory progenitors are progressively directed toward the spiral ganglion neuron (SGN) fate through a series of fate decisions. In parallel, the number and location of SGNs is controlled by selective expansion and culling of progenitor populations as well as directed migration away from the otic vesicle into the surrounding mesenchyme. As a result of these developmental events, the mature cochlea houses a population of SGNs that have both the intrinsic properties and the precise connections necessary for accurate transmission of sound information from hair cells to the central nervous system. Building on decades of careful anatomical and embryological studies, we now have a broad understanding of how these events unfold at the cellular level, and have begun to identify many of the signaling pathways and transcriptional networks that initiate and regulate early SGN development.

2.2 Origin of Inner Ear Neurons

2.2.1 The Otic Vesicle

In all species, neurogenesis is confined to spatially restricted regions of the otic cup, partially overlapping with zones that produce the sensory cells but excluded from those fated for non-neurosensory tissues in the mature inner ear. In rodents and birds, the neurons of the inner ear arise in the anteroventral quadrant of the otic vesicle (Figs. 2.1 and 2.2). Although intuited from histological studies, which revealed an obvious region of delamination (Knowlton, 1967; Carney & Silver, 1983), in vitro fate mapping studies ultimately confirmed that this portion of the otocyst produces neurons when dissected and cultured in isolation (Li et al., 1978; Adam et al., 1998), but that more dorsal and more posterior regions do not (Li et al., 1978). Similarly, dye labeling of the chick otic cup (Hamburger Hamilton [HH] stage 12) showed that CVG neurons are produced from the anterior compartment (Abello et al., 2007). Moreover, cells in this region rarely mixed with cells in the neighboring "non-neuronal" compartment and respected gene expression boundaries, indicating that the region of neurogenesis is patterned at an early stage.

The neurogenic zone itself appears to be further patterned, as vestibular neurons are generated before auditory neurons and from spatially distinct populations, as evidenced by dye labeling experiments in chicks (Bell et al., 2008) and genetic tracing experiments in mice (Koundakjian et al., 2007). Indeed, auditory and vestibular neurons appear to delaminate from different regions of the otic vesicle, with vestibular neurons developing close to the vestibular sensory epithelia and most auditory neurons instead delaminating from the boundary between the cochlea and saccule and then from the middle and apical turns of the cochlea itself (reviewed in Yang et al., 2011). Such spatial segregation is particularly extreme in fish, in which there are two separate neurogenic zones, with the anterior region producing neurons

that innervate the utricle and the posterior region producing neurons that innervate the saccule, with anterior neurogenesis occurring slightly earlier (Haddon & Lewis, 1996; Haddon et al., 1998; Sapede & Pujades, 2010).

Importantly, in each species, the neurogenic zone is closely associated with regions of the epithelium that produce sensory cells, namely the hair cells and supporting cells of the utricle, saccule, cristae, and cochlea. Hence, the neurogenic zone is actually contained within a larger "proneurosensory domain" (PNSD) that contains both neural and sensory progenitors, with the neurogenic region overlapping with the nascent sensory epithelia for the utricle and saccule (Cole et al., 2000; Raft et al., 2007). Other sensory areas, such as those for the cristae, can arise either from apparently non-neurogenic regions in the PNSD or outside of the PNSD altogether, as suggested by expression of sensory markers and fate mapping (reviewed in Fekete & Wu, 2002).

2.2.2 Other Potential Sources for SGNs

Although the otic vesicle is the primary source for inner ear neurons, there is a long history of studies considering the possibility of a contribution from the neural crest and/or neuroepithelium. In fact, Bartelmez argued strongly that auditory neurons derive from the neural tube based on his histological analysis of early human embryos (Bartelmez, 1922). In contrast, early embryological experiments using the larval salamander indicated that most if not all neurons derive from the otic placode, whereas the neural crest produces the Schwann cells that myelinate the inner ear neurons (Yntema, 1937). Similarly, when neural crest cells were transplanted from quails to chicks, many quail-derived glia populated the mature ganglia and eighth nerve, confirming that auditory Schwann cells share the same neural crest origin as those in the rest of the peripheral nervous system (D'Amico-Martel & Noden, 1983). More surprisingly, some quail-derived cells also appeared to develop as neurons, but these seemed more likely to be vestibular based on their location. However, it was not possible to rule out a contaminating non-neural crest cell population, nor were markers used to verify the neuronal identity of the quail-derived cells.

More recently, an argument for a neural crest contribution was made based on genetic fate mapping studies in mice (Freyer et al., 2011). In these experiments, neural crest cells were permanently marked by Cre-mediated recombination of fluorescent reporters. In mice that produce Cre under the control of the *Pax3* promoter, which is active throughout the dorsal neural tube, fluorescent cells could be seen moving from the neural tube into the otic vesicle, eventually contributing to the ganglion, maculae, and cochlea. However, these types of experiments can be difficult to interpret, as even undetectably low and likely physiologically irrelevant levels of Cre protein might be sufficient to induce recombination. In addition, *Pax3*

expression is not restricted to the neural crest, so many of these cells may be occasional neuroepithelial precursors that accidentally found themselves in the otic cup, which is pressed up against the hindbrain, but were nonetheless able to proliferate and differentiate within this new environment. In fact, dye labeling of cells in the early embryonic chick hindbrain revealed a similar contribution to various tissues of the inner ear, including the CVG (Ali et al., 2003). Hemond & Morest, (1991b) further noted a possible contribution from migratory cells formed at the boundary of the otic cup in chicks. These so-called "otic crest" cells seemed to stream toward multiple ganglia, but a specific contribution to the CVG was not defined.

In fact, many experiments argue that any non-otic contribution to the neurons of the inner ear is minimal or even nonexistent. For instance, complementary fate mapping studies using multiple independent *Cre* lines with expression in the otic vesicle, namely *Foxg1–Cre* (Hebert & McConnell, 2000), *Pax2–Cre* (Ohyama & Groves, 2004), and *Pax8–Cre* (Bouchard et al. 2004), suggest that the vast majority if not all inner ear neurons do in fact derive from the otic epithelium. In addition, fate mapping with *Wnt1–Cre* as well as a more restricted *Pax3–Cre* driver did not reveal any substantial contribution to the inner ear besides Schwann cells (Sandell et al., 2014). The conflicting results for *Wnt1–Cre* could reflect variation in the level of Cre activity in combination with different reporters and on different genetic backgrounds. Because the currently available "otic" *Cre* lines also mediate recombination in the neuroepithelium, albeit within highly restricted regions (Hebert & McConnell, 2000; Bouchard et al., 2004; Ohyama & Groves, 2004), generation of a truly otic-specific *Cre* line may be necessary for final resolution of this issue. Nonetheless, most studies indicate that the otic vesicle does indeed serve as the primary source for inner ear neurons.

2.3 Overview of SGN Development

SGNs pass through a number of developmental stages, from their origin in the proneurosensory domain to their final differentiation and maturation within the cochlea. Following on the careful descriptive studies performed by embryologists and anatomists at the beginning of the 20th century, our understanding of how SGN development progresses has been greatly aided by the more recent identification of genes that are expressed in a subset of cells and that have been shown to affect specific features of inner ear neuronal development. The first step is the production of proneurosensory progenitors, which are recognized by expression of Lunatic fringe (Lfng) (Morsli et al., 1998; Cole et al., 2000), Sox2 (Kiernan et al., 2005; Neves et al., 2007), and fibroblast growth factor 10 (FGF10; Pirvola et al., 2000; Alsina et al., 2004). Subsequently, a subset of proneurosensory cells upregulate expression of Delta-like 1 (Dll1) and Neurogenin1 (Neurog1) (Adam et al., 1998; Ma et al., 1998; Alsina et al., 2004; Brooker et al., 2006). Neurog1-positive precursors begin to express *Neurod1* as they delaminate from the otic vesicle (Liu et al.,

2000; Kim et al., 2001; Bell et al., 2008) and quickly down-regulate *Neurog1* (Evsen et al., 2013).

Delaminated neuroblasts continue to divide within the nascent ganglion, exiting the cell cycle along the basal-apical axis, starting in the mid-base region around E9.5 in mouse, with only a few neurons still dividing in the apical turn at E13.5 and none at E14.5 (Ruben, 1967; Matei et al., 2005). This general progression fits with *Neurog1*-based birthdating studies (Koundakjian et al., 2007), though it is important to bear in mind that onset of *Neurog1* precedes cell-cycle exit, so different aspects of timing are measured by these two methods. Early neuroblasts express Islet-1 (Adam et al., 1998; Li et al., 2004), which is sustained beyond the transient expression of Neurod1 (Radde-Gallwitz et al., 2004; Deng et al., 2014). The delaminated neurons begin expressing first Pou4f1 and then, after becoming postmitotic, Pou4f2 (Deng et al., 2014). Maturation is also marked by production of βIII-tubulin (i.e., TuJ1) (Radde-Gallwitz et al., 2004; Bell et al., 2008), which is maintained as the neurons differentiate and coalesce in distinct vestibular and spiral ganglia.

As they mature, neurons extend processes back toward the otic epithelium (Carney & Silver, 1983). In mice, neurons mature first in the base, with neurites present along the path by E11.5 (Carney & Silver, 1983) and peripheral processes extending into the cochlea by E12.5 (Farinas et al., 2001; Koundakjian et al., 2007; Appler et al., 2013). In parallel, SGNs extend central axons out of the ear and toward the auditory brainstem to form the auditory division of the eighth cranial nerve. The axons reach the hindbrain by E11.5 and quickly bifurcate, extending an ascending process rostrally toward the developing anterior ventral cochlear nucleus and a descending process caudally toward the posterior ventral cochlear nucleus and dorsal cochlear nucleus (Lu et al., 2011). By E15.5, SGN peripheral processes have penetrated the cochlear duct along its entire extent, and the central processes are topographically organized within each division of the developing cochlear nuclei (Koundakjian et al., 2007). The arrival of peripheral and central axons at their targets coincides with a peak in cell death first in the vestibular system and then in the cochlea (Nishizaki et al., 1998; Farinas et al., 2001). A similar sequence of events occurs in chicks (Ard & Morest, 1984; Whitehead & Morest, 1985; Molea & Rubel, 2003).

In mammals, there are two clear subtypes of SGNs that can be distinguished based on morphology by late embryogenesis (Bruce et al., 1997; Koundakjian et al., 2007). Type I SGNs extend radial projections directly toward the inner hair cells, whereas a minority population of Type II SGNs instead grow toward the outer hair cells and spiral toward the base. Initially, all SGNs produce Peripherin, but this expression is eventually restricted to Type II SGNs at postnatal stages (Hafidi, 1998). SGNs are further classified based on their spontaneous firing rates (Liberman, 1980) and variation in firing properties and gene expression (reviewed in Davis & Liu, 2011), but to date there are no molecular markers for early Type II SGNs or any other well-defined SGN subtype.

Efforts to understand the molecular pathways that govern early SGN development have uncovered important roles for several extrinsic pathways that pattern the otic

vesicle; promote neurogenesis; and control the specification, proliferation, and survival of committed SGN precursors. Many familiar signaling pathways are involved, often exerting distinct effects at different stages. Of particular importance are Notch signaling, as well as pathways activated by fibroblast growth factors (FGFs), bone morphogenetic proteins (BMPs), Sonic hedgehog (Shh), insulin growth factor (IGF), and the neurotrophins. In Sect. 2.4, the cellular and molecular events that govern SGN development are described, including the specific impact of relevant signaling pathways at each stage. Excellent reviews outlining the details of these pathways and their broader contributions to inner ear development are available for additional information (Wright & Mansour, 2003a; Varela-Nieto et al., 2004; Yang et al., 2011; Groves & Fekete, 2012; Kiernan, 2013; Neves et al., 2013).

2.4 Patterning the Proneurosensory Domain

Inner ear neurogenesis begins with the formation of the PNSD in the anterior otic cup during the earliest stages of development. As such, development of the PNSD is essentially a matter of establishing the anterior–posterior axis of the otic cup. The appearance of *L-fng* and other PNSD markers in the anterior otocyst is accompanied by a gradual restriction in the expression of nonsensory markers, such as Lmx1a/1b (Abello et al., 2007; Nichols et al., 2008; Vazquez-Echeverria et al., 2008) and Tbx1 (Raft et al., 2004), to the posterolateral domain as early as the 10–12 somite stage in mice (Fig. 2.2). Genetic fate mapping studies have confirmed that *Tbx1*-positive cells are excluded from the neurogenic zone (Xu et al., 2007). However, similar genetic fate mapping data for *L-fng* and *FGF10* are not available, leaving open the question of the degree of fate restriction within the PNSD at this early stage.

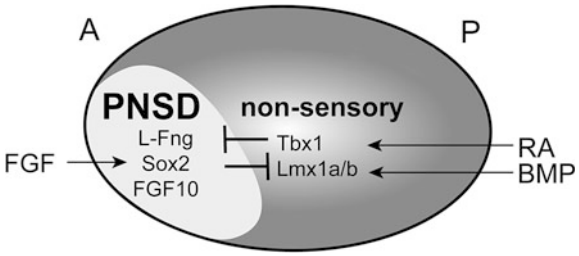

Fig. 2.2 Patterning the proneurosensory domain (PNSD). Extrinsic signals pattern the anterior–posterior (A-P) axis of the otic cup, with FGF inducing neurosensory development in the anterior and retinoic acid (RA) and BMPs inducing development of nonsensory structures in the posterior. As a result, PNSD markers such as L-fng, Sox2, and FGF10 are restricted to the anteroventral quadrant. These fate decisions are reinforced intrinsically by mutually antagonistic transcriptional networks, with Sox2 promoting the neurosensory fate and Tbx1 promoting the nonsensory fate

2.4.1 Patterning Signals from Outside of the Inner Ear

Initial efforts to understand how the PNSD is patterned showed that the anterior–posterior axis is fixed remarkably early. For instance, anterior pieces of the chick otic epithelium are able to generate neurons in vitro, even in the absence of any surrounding tissues (Adam et al., 1998). Similarly, when otic cups were transplanted with a reversed orientation in HH stage 16 chick embryos, the PNSD remained in its original position (Wu et al., 1998). However, a similar manipulation between HH stages 10–12 caused the *L-fng* domain to form in what was originally the posterior half of the otic cup (Bok et al., 2005). Thus, signals from the surrounding tissue initially influence where the PNSD will form, but the axis is fixed just after the 16 somite stage (HH stage 12). In contrast, the dorsal–ventral axis remains sensitive to changes in orientation for longer, with important cues provided by the notochord, floorplate, and dorsal neural tube (Wu et al., 1998; Bok et al., 2005). Changes to the dorsal–ventral axis can also affect the position of the neurogenic domain (Bok et al., 2005; Riccomagno et al., 2005), highlighting the complexity of the interactions that ultimately shape the PNSD. However, the timing of events suggests that signals along the anterior–posterior axis provide the primary cues for PNSD formation.

Embryological experiments have helped narrow down the possible source of the cues that pattern the otic cup. The hindbrain does not appear to provide essential anterior-posterior information, as rotations prior to the 16 somite stage did not affect the location of the PNSD (Bok et al., 2005). Instead, signals seem to come from the nearby periotic ectoderm and somatic mesoderm (Bok et al., 2011). A major component of this signal is retinoic acid (RA), which prevents neurogenesis when ectopically expressed in chicks or mice. Conversely, blockade of RA signaling causes expanded neurogenesis. Further, RA and other components of the pathway are present and actively maintained in tissues surrounding the early otic cup in chicks. A similar role for RA has been described in zebrafish (Radosevic et al., 2011), suggesting this is an evolutionarily conserved mechanism, though differences among species likely exist in terms of the source of RA, how the gradient is established, and how the signal is interpreted. Indeed, the complex expression patterns and wide range of teratogenic effects across species indicate that RA can affect multiple aspects of inner ear development (reviewed in Romand et al., 2006).

Additional critical patterning information appears to be provided by FGFs. In chicks, FGF8 is expressed close to the otic territory prior to the onset of neurogenesis and can promote neurogenesis when expressed ectopically (Abello et al., 2010). Conversely, broad pharmacological inhibition of FGF signaling caused a loss of PNSD markers, accompanied by an expansion of the nonsensory marker *Lmx1b*. Similar alterations in BMP signaling had no effect on neurogenesis, but did influence *Lmx1b* expression, confirming a role in anterior–posterior patterning. The expansion of a nonsensory marker in the absence of an effect on neurogenesis

indicates that FGF and BMPs may act independently to pattern the axis, with additional signals such as RA influencing the final outcome. For instance, as in chicks, an FGF ligand is required for anterior-posterior patterning in fish (Hammond & Whitfield, 2011), but some of these effects may be due to changes in expression of genes required for RA metabolism (Radosevic et al., 2011).

Whether FGFs regulate PNSD formation in mice remains unclear, due in part to differences in how and when neuronal development has been assessed. The PNSD appears to be present in *FGF3* mutants, though the CVG is noticeably smaller once it forms (Hatch et al., 2007; Vazquez-Echeverria et al., 2008). However, loss of both *FGF3* and *FGF10* can cause expanded neurogenesis (Vazquez-Echeverria et al., 2008). Similarly, *Neurod1*-positive cells form in ectopic locations in *Kreisler* mutant mice, which suffer from hindbrain patterning defects including reduced expression of *FGF3* and *FGF10*, and this phenotype can be partially rescued by restoration of either FGF. On the other hand, loss of the FGF2R (IIIb) receptor, which binds both FGF3 and FGF10, does not impair early CVG development (Pirvola et al., 2000; Pauley et al., 2003). However, because early PNSD development was not assessed, it is possible that a similar phenotype was missed in these animals (Pirvola et al., 2000). Altogether, the exact contribution of FGF3/FGF10 signaling is difficult to pinpoint due to the variability of reported double mutant phenotypes (Wright & Mansour, 2003b; Vazquez-Echeverria et al., 2008) and the fact that the phenotypes do not recapitulate what is seen in *FGF2R* mutants (Pirvola et al., 2000; Pauley et al., 2003). Why FGFs may antagonize neurogenesis in some contexts yet induce neurogenesis in others, as well as the specific contributions of various family members, will be important to work out in the future.

Although anterior–posterior signaling pathways function first, the final shape and size of the PNSD is also influenced by cues that pattern the dorsal–ventral axis. Shh from the notochord and floor plate provides a potent ventralizing signal that is necessary for normal expression of sensory and nonsensory markers (Brown & Epstein, 2011). However, loss of the PNSD from *Shh* mutant mice does not appear to be a direct effect on otic vesicle patterning, as otic-specific ablation of the Shh receptor Smoothened did not reproduce this effect. Instead, the change in PNSD gene expression appears to be secondary to expanded Wnt signaling from the neural tube, which is dorsalized in *Shh* mutants (Chiang et al., 1996; Riccomagno et al., 2005). In support of this idea, activation of Wnt signaling also inhibits neurogenesis (Ohyama et al., 2006; Brown & Epstein, 2011). However, importantly, Wnt signaling is not necessary for neurogenesis per se (Ohyama et al., 2006). Hedgehog proteins may play a more direct role during anterior–posterior patterning of the zebrafish otic vesicle, where they appear to work in parallel with—yet independently of—FGFs (Hammond et al., 2003, 2010; Hammond & Whitfield, 2011). The basis of these apparent differences among species is unclear but could reflect unique features of different types of vertebrate ears.

2.4.2 Intrinsic Patterning Mechanisms

Although signals extrinsic to the ear likely initiate the events that place the PNSD in the anterior otic cup, transcriptional networks and local cell–cell interactions play an important role in reinforcing these decisions and ensuring the neurosensory competence of cells within this domain. The transcriptional networks serve two complementary functions: to ensure expression of genes necessary for that cell's needs at that point in time and to control the activity of the network itself. The Cell–cell interactions coordinate these intrinsic events with the surrounding tissue.

One important player in the PNSD is the transcription factor Tbx1, whose expression is restricted to the posterolateral (i.e. nonsensory) region of the otocyst as early as the 10 somite stage in mice (Raft et al., 2004). *Neurog1* and *Neurod1*, which mark neural progenitors in the PNSD, are expressed in a complementary pattern to *Tbx1* in the otocyst (Fig. 2.2). In mice with excess *Tbx1*, neurogenesis is reduced, particularly in the posterior of the PNSD (Raft et al., 2004; Freyer et al., 2013). Conversely, in *Tbx1* mutant mice, *Neurog1* and *Neurod1* expression is increased (Raft et al., 2004; Xu et al., 2007), likely due to an expansion of the PNSD (Raft et al., 2004). Moreover, in *Tbx1* mutants, cells from the *Tbx1* domain populate the ganglion, something that never occurs in wild-type animals (Xu et al., 2007). Thus, Tbx1 actively represses the PNSD fate in nonsensory cells, thereby confining neurogenesis to a restricted domain. Extra *Neurog1*- and *Neurod1*-positive cells also develop in *Tbx1* mutant fish (Radosevic et al., 2011), and spiral ganglion defects have been reported in human patients with velocardiofacial/DiGeorge syndrome (Schmidt, 1985), which is linked to *TBX1* mutations (Yagi et al., 2003; Zweier et al., 2007). Hence, Tbx1 appears to play a basic, evolutionarily conserved role in determining where neurogenesis will occur.

If Tbx1 acts to prevent the neurosensory fate within the nonsensory region of the otocyst, then what factors promote this fate in the PNSD? The positively acting pathways are more complex, involving multiple transcriptional networks that interact with each other to drive production not only of neurons, but also of hair cells and supporting cells that will form the organ of Corti. One factor that appears to participate in many of these fate decisions is the SoxB1 family member Sox2. In mice, Sox2 is expressed in the ventral rim of the otic cup by E8.5 (Wood & Episkopou, 1999; Zou et al., 2008) and then in the ventrolateral otocyst at E9.5 (Mak et al., 2009). Subsequently, Sox2 can be detected both in delaminating neuroblasts and in the developing sensory epithelia (Kiernan et al., 2005; Mak et al., 2009). *Sox* genes show a similar expression in the PNSD in chicks, with expression complementing *Tbx1* and *Lmx1b* by the 10 somite stage (Abello et al., 2007, 2010).

Just as Tbx1 promotes the nonsensory fate, so does Sox2 drive cells down the neurosensory path. In mice harboring mutations in *Sox2*, neurosensory development is severely disrupted, with an early loss of both the prosensory domain (Kiernan et al., 2005) and of neurons (Puligilla et al., 2010). The loss of both cell types

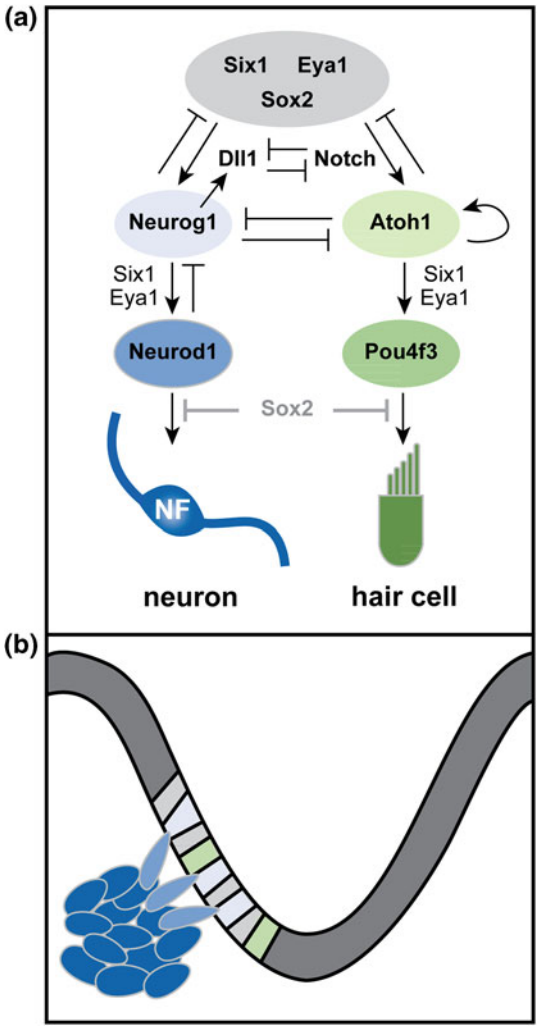

suggests that Sox2 may be required for the initial specification of precursors in the PNSD. Moreover, in chicks, ectopic expression of Sox3 inhibits *Lmx1b*, hinting that mutually antagonistic interactions may solidify the nonsensory versus PNSD fate decision (Abello et al., 2010): wherever Tbx1 is on, Sox2 will be off and vice versa. Interestingly, *Tbx1* expression was not affected. Similarly, *Lmx1a* but not *Tbx1* shows reduced expression in *Kreisler* mutant mice, indicating there may be multiple parallel pathways that influence the nonsensory fate (Vazquez-Echeverria et al., 2008). Indeed, in *Lmx1a* mutant mice, *Sox2* expression expands, followed by the formation of fused sensory epithelia and a larger CVG (Nichols et al., 2008; Koo et al., 2009).

◀ **Fig. 2.3** Transcriptional control of neurogenesis. **a** Six1, Eya1, and Sox2 cooperate in PNSD progenitors (*gray*) to promote the neurosensory fate. Lateral inhibition mediated by Delta-like 1 (Dll1) and Notch steers neurosensory precursors toward either the neuronal (*blue*) or sensory (*green*) fate. In neural precursors, Neurog1 works with Six1 and Eya1 to promote differentiation, resulting in expression of Neurod1 and production of mature, neurofilament (NF)-positive neurons. Similarly, in prosensory progenitors (*green*), Atoh1 promotes its own expression and cooperates with Six1 and Eya1 to induce hair-cell differentiation pathways (i.e. Pou4f3) and production of hair cells. In some contexts, Neurog1 and Atoh1 show mutually antagonistic interactions. Downregulation of Sox2 occurs in differentiating neurons and hair cells; maintained expression of Sox2 interferes with maturation, suggesting that a decrease in Sox2 levels may be necessary for normal differentiation. **b** Diagram of neurogenesis in the context of the developing otocyst. Neuronal precursors are specified in the otic epithelium and then delaminate into the mesenchyme, where they continue to proliferate and then differentiate. Sensory precursors remain in the otic epithelium, where they ultimately produce both the hair cells and supporting cells of the organ of Corti (not shown)

As early acting factors such as Sox2 direct cells toward the neurosensory fate, additional transcriptional networks cooperate to determine whether individual progenitors will produce neurons, sensory cells, or both (Fig. 2.3). Unraveling the logic of this progressive fate restriction has been complicated by the fact that there seem to be multiple types of neurosensory progenitors within the PNSD. In favor of this idea, fate mapping in zebrafish has revealed three different types of precursors: neurosensory, neural, and sensory (Sapede et al., 2012). Similarly, in chicks, there is solid evidence that a common neurosensory progenitor produces both hair cells and neurons in the utricular maculae, but not in the other sensory organs, consistent with the presence of a heterogeneous precursor population (Satoh & Fekete, 2005).

The basis of the observed precursor heterogeneity remains unclear. One possibility is that hair cells and neurons derive from a similar early neurosensory progenitor that gradually shifts its potential over time, with the latest remnants of this population showing an extended ability to produce both hair cells and neurons in the maculae. Such a progenitor would be difficult to detect using standard fate mapping techniques. Alternatively, there may be a spatial segregation within the PNSD, with common progenitors limited to one subregion. Indeed, across species, proven bipotent progenitors exist in regions where the sensory domain, presaged, for example, by expression of *BMP4*, is found within the PNSD itself (Cole et al., 2000; Raft et al., 2007; Sapede et al., 2012).

Within the otocyst, local cell–cell interactions reinforce the intrinsic pathways that ultimately determine which cells will contribute to the neuronal lineage, influencing both the initial formation of the PNSD and the subsequent segregation of neuronal and sensory precursors. Both of these binary fate decisions appear to be under the control of the Notch pathway. As initially established in *Drosophila*, the Notch receptor interacts with a transmembrane ligand called Delta to mediate lateral inhibition and thereby promote the acquisition of distinct cell fates within a field of multipotent progenitors (reviewed in Schwanbeck et al., 2011). A second related ligand, Jagged, plays a similar role. In mammals, the basic pathway is conserved, with four Notch receptors, three Delta-like ligands, and two Jagged ligands. Ligand

binding induces cleavage of the intracellular domain (ICD) of the Notch receptor protein in the neighboring cell. The Notch-ICD then enters the nucleus to directly regulate expression of target genes. Among the target genes are additional transcription factors that feedback to increase expression of Notch itself while simultaneously decreasing Delta production in that cell. The overall consequence is that neighboring cells ultimately express either Delta or Notch and therefore adopt one of two possible fates, for instance, whether to become a neuron. Because of the lateral inhibition mechanism, early uniform expression of the ligand and receptor is often followed by a more salt-and-pepper–like appearance within that field of cells, reflecting the gradual emergence of two distinct cell fates. Thus, activation of the Notch receptor by a Delta-family ligand offers a direct way to convert an extrinsic signal into an intrinsic change in gene expression.

Understanding the precise effects of Notch signaling in otic neurogenesis has been challenging because of the presence of multiple ligands and receptors, as well as differences in the effects of these molecules throughout development (reviewed in Kiernan, 2013). However, several lines of evidence suggest that Notch signaling promotes neurogenesis during inner ear development. For instance, like Lfng (Morsli et al., 1998), which is a known regulator of the Notch pathway, the *Delta* homolog *Delta-like 1* (*Dll1*) is expressed in the PNSD at early stages (Abello et al., 2007; Daudet et al., 2007). In addition, pharmacological inhibition of Notch signaling in chicks can increase the number of Dll1+ cells (Daudet et al., 2007). Conversely, when *Dll1* is absent in mice, too many neurons develop, consistent with a loss of lateral inhibition between Dll1+ neurons and the surrounding cells (Brooker et al., 2006). Interestingly, the production of extra neurons in *Dll1* mutant mice apparently comes at the expense of the saccular and utricular maculae, whereas there is an increase in hair cell number in the cochlea, providing further evidence that there is a defined common neurosensory progenitor for only a subset of hair cells and neurons. Jagged ligands, on the other hand, may not be involved in inner ear neurogenesis (Zhang et al., 2000; Brooker et al., 2006; Neves et al., 2011).

One of the key consequences of Notch signaling is to induce expression of potent basic helix loop helix (bHLH) transcription factors, which act both to regulate Notch–Delta production and to induce cell-type–specific programs of gene expression. Similarly, whereas many genes are uniformly expressed in the PNSD, *Dll1* shows a more irregular pattern, apparently reflecting upregulation in early neuronal precursors (Adam et al., 1998; Abello et al., 2007; Daudet et al., 2007) which express the proneural bHLH transcription factors Neurog1 and Neurod1. In *Neurog1* mutant mice, no inner ear neurons form and *Dll1* expression is lost, consistent with the classic model of lateral inhibition, with Neurog1 acting both to enhance production of Dll1 and promote the neuronal fate (Ma et al., 1998; Raft et al., 2007). The Dll1- cells, on the other hand, likely adopt a prosensory fate, which is promoted by a different bHLH transcription factor, Atoh1 (formerly Math1), which is required for hair cell development in mice (Bermingham et al., 1999). When signaling downstream of Notch is prevented, *Neurog1* expression increases, as would be expected if Dll1 is no longer able to inhibit expression of *Neurog1* in neighboring cells (Raft et al., 2007). In addition, pharmacological inhibition of

Notch in chicks enhances the local upregulation of Dll1, indicating that lateral inhibition normally segregates Notch+ and Dll1+ populations within the PNSD (Daudet et al., 2007). Indeed, ectopic expression of the Notch-ICD is sufficient to create ectopic sensory regions and can divert neuroblasts to the hair cell fate in vivo (Daudet & Lewis, 2005; Hartman et al. 2010; Pan et al., 2010; Liu et al., 2012).

Because Neurog1 and Atoh1 are essential for neuronal and sensory development respectively, one attractive idea is that these two transcription factors participate in mutually antagonistic interactions within PNSD precursors that ultimately produce dedicated neuronal (i.e., Neurog1+) or sensory (i.e., Atoh1+) progenitors. If this model is true, then Neurog1 and Atoh1 must be coexpressed, at least at low levels, in any common neurosensory progenitor. This clearly appears to be the case in the utricle and saccule, where stripes of *Atoh1* expression appear within the neurogenic domain (Raft et al., 2007). Moreover, descendants of Neurog1+ cells, as marked by genetic fate mapping, do indeed populate the maculae, exactly as predicted both by gene expression studies and viral fate mapping (Morsli et al., 1998; Cole et al., 2000; Satoh & Fekete, 2005). Additional evidence has come from analysis of *Neurog1* and *Atoh1* mutant mice: loss of *Neurog1* is accompanied by an increased number of *Atoh1*-positive hair cell precursors in the developing utricular macula, whereas there are more neural precursors in the maculae of *Atoh1* mutant mice (Raft et al., 2007). Ultimately, however, fewer hair cells develop in *Neurog1* mutants, particularly in the saccule, indicating that the extra *Atoh1*-positive progenitors may not differentiate properly (Ma et al., 2000; Raft et al., 2007).

Together, these findings provide strong support for a common neurosensory progenitor in the maculae. Notably, the three major drivers of neuronal and hair cell fates in vertebrates—Neurog1, Neurod1, and Atoh1—are all bHLH factors that are closely related to each other and to bHLH factors with similar functions in sensory development in invertebrates. Indeed, it has been proposed that transient coexpression and cross-regulation of Neurog1, Neurod1, and Atoh1 may reflect an evolutionarily ancient series of interactions, with an expansion within the family eventually leading to a situation where individual bHLH factors segregate to neural versus sensory precursors (Pan et al., 2012).

The situation in the cochlea is less clear. First, *Atoh1* expression does not appear to overlap with the neurogenic region of the cochlea (Raft et al., 2007). Accordingly, genetic fate mapping revealed no contribution of *Atoh1*-positive progenitors to the CVG (Yang et al., 2010). Conversely, the *Neurog1* population does not produce any cochlear hair cells (Raft et al., 2007), despite massive labeling of the spiral ganglion neurons (Koundakjian et al., 2007; Raft et al., 2007). Nevertheless, there are some tantalizing phenotypes in the cochlea that suggest that Atoh1–Neurog1 interactions may occur, though perhaps only transiently. During normal development, neurons exit the cell cycle before hair cells (Matei et al., 2005). In contrast, in *Neurog1* mutants, hair cell precursors exit the cell cycle prematurely (Matei et al., 2005), and extra rows of hair cells develop in some regions (Ma et al., 2000). This phenotype can be explained in part by the absence of SGNs, which normally produce a Shh cue that prevents hair cells from exiting the cell cycle (Bok et al., 2013). However, intrinsic effects might also contribute: when Neurog1 is lost, a progenitor that

would normally become a neuron may instead select the alternate fate and differentiate as a hair cell (Matei et al., 2005).

According to this model, such a progenitor may in fact express extremely low levels of Atoh1, just not at high enough levels to drive Cre-mediated recombination for genetic fate mapping. In fact, Atoh1 positively regulates its own expression (Raft et al., 2007), so it is possible that the loss of Neurog1 relieves a block on this autoregulation, thereby allowing Atoh1 expression to accumulate and therefore divert a neural precursor to the sensory fate. This would explain the failure to observe any major contribution of Atoh1-derived cells to the ganglion in wild type mice: Neurog1 may be so efficient at promoting the neural fate that common progenitors per se do not exist in the wild-type cochlea, and any binary potential is revealed only once the Neurog1–Atoh1 feedback loop is disrupted.

Additional evidence that the Atoh1–Neurog1 feedback loop is evident only in restricted contexts has come from zebrafish. As in mice, neural (*neurod1*) and hair cell (*atoh1a*) markers are largely segregated, overlapping only in the posterior macula and not in the anterior (Sapede et al., 2012). Moreover, *Neurog1* mutant fish exhibit not only a loss of ganglion neurons, but also an increase in the number of hair cells, which differentiate prematurely and appear to derive from a *Neurog1*-positive progenitor. However, the phenotype is restricted to the site of overlapping expression, namely the posterior macula. Hence, as in mice, atoh1+/neurog1+ progenitors are restricted, in this case to the posterior maculae, with cells in the anterior maculae already committed to either the neural or sensory fate. Indeed, additional fate mapping studies in zebrafish suggest that precursors can become committed to the neuronal fate as early as the otic placode stage (Hans et al., 2013). Whether orthologous factors define restricted neural and sensory precursors in the early mouse otic vesicle remains to be determined.

2.5 Otic Neurogenesis

Within the PNSD population, neuronal precursors are ultimately specified through complex networks of transcription factors that involve both the pro-neurosensory factor Sox2 and the pro-neural factor Neurog1. Unravelling these interactions has been difficult, as many of the earliest acting factors have broad effects on inner ear morphogenesis in addition to their specific effects on auditory neurogenesis. For instance, loss of the transcription factor Six1 causes increased cell death and decreased cell proliferation throughout the otic vesicle by E9.5, which remains cystic with no CVG at E12.5 (Zheng et al., 2003). Hence, the failure in neurogenesis could in principle be secondary to gross patterning or growth defects. However, a series of studies indicate instead that Six1 and its partner Eya1 cooperate with Sox2 to control early neurogenesis directly.

2.5.1 *Six1 and Eya1*

Six1 and Eya1 cooperate in a network that reinforces the initial neurosensory versus nonsensory patterning of the otic vesicle and then plays an ongoing role in the maintenance of Neurog1. Six1 is a homeodomain protein that interacts with the Eya1 transactivator to control gene expression (Wong et al., 2013). Both Six1 and Eya1 are expressed in the ventral otic cup and are then maintained in the developing ganglion (Kalatzis et al., 1998; Zheng et al., 2003; Ahmed et al., 2012a). Six1 and Eya1 appear to act synergistically, with a range of phenotypes emerging in mice with differing degrees of Six1/Eya1 activity. When the network is completely blocked, PNSD development arrests early (Ahmed et al., 2012a). On the other hand, in single mutant mice, the PNSD appears to form (Zou et al., 2004). However, neurogenesis is clearly impaired from the earliest stages (Zou et al., 2004; Friedman et al., 2005). These results are consistent with the idea that Six1 and Eya1 act first during PNSD formation and subsequently during neurogenesis.

Analysis of an allelic series for *Eya1* revealed dose dependent effects that further confirm multiple roles for these genes (Zou et al., 2008). In *Eya1* null mutants, PNSD development is severely disrupted, with a loss of *L-fng* and expansion of *Tbx1* (Friedman et al., 2005; Zou et al., 2008). By contrast, in *Eya1* hypomorphs, *L-fng* expression is only reduced and *Tbx1* expression remains largely normal (Friedman et al., 2005). Nevertheless, *Neurog1* expression is still diminished, consistent with a role in neurogenesis that is independent of PNSD patterning. Although Six1 and Eya1 bind to each other and likely function within a common transcriptional complex (reviewed in Wong et al., 2013), it is important to remember that Eya1 is also a phosphatase and could therefore mediate some of its effects through signaling independent of Six1-mediated gene transcription.

2.5.2 *Sox2*

The effects of Six1 and Eya1 are influenced in part by the presence of Sox2. Indeed, in addition to its role in the early PNSD, Sox2 plays an ongoing role in neurosensory development, as reflected by its dynamic expression pattern and changing functions over time. At each stage, Sox2 is present in cells that exhibit some developmental plasticity. For instance, Sox2 is expressed initially throughout the PNSD, which has the potential to produce hair cells, supporting cells, or neurons (Wood & Episkopou, 1999; Mak et al., 2009). Subsequently, Sox2 continues to be produced in the prosensory domain (Dabdoub et al., 2008) and in developing neuroblasts (Puligilla et al., 2010). As the prosensory domain differentiates to form the organ of Corti, Sox2 is downregulated in hair cells, but maintained in supporting cells, which can behave like inner ear progenitors at neonatal stages (White et al., 2006). Sox2 is also expressed in Kölliker's organ (also called the greater epithelial ridge), a transient structure adjacent to the organ of Corti that eventually

becomes the inner sulcus. With the introduction of transcription factors such as Atoh1 (Woods et al., 2004) or Neurog1 (Puligilla et al., 2010), cells here can express markers for hair cells or neurons respectively, indicating that cells in Kölliker's organ are not yet locked into one defined fate.

Consistent with its expression in cells that have not yet committed to a final fate, Sox2 seems to inhibit differentiation. For instance, introduction of Sox2 can actually prevent cells from developing as hair cells, even if Atoh1 is present (Dabdoub et al., 2008). Atoh1, in turn, can inhibit *Sox2* expression. This leads to a model where Sox2 + precursors begin to produce Atoh1, which in turn increases its own expression and inhibits expression of both *Neurog1* and *Sox2*, thereby ushering the precursor from proliferation to differentiation. In support of this idea, hair cells differentiate prematurely in *Sox2* hypomorphs (Dabdoub et al., 2008). However, although Sox2 can antagonize hair cell differentiation when overexpressed, the presence of Sox2 is not fundamentally incompatible with hair cell differentiation, as Sox2 protein is in fact present in differentiating hair cells (Mak et al., 2009).

Sox2 may have similar effects on the behavior of neural precursors in the inner ear. Although the introduction of Sox2 was sufficient to cause cells in Kölliker's organ to express the neuronal marker βIII-tubulin (Puligilla et al., 2010), neither *Neurog1* nor *Neurod1* was induced, and the neurons failed to mature. In addition, only 39 % of electroporated cells took on a neuronal-like phenotype and this number decreased with developmental time. Sox2's potency is likely influenced by both Neurog1 and Neurod1 (Evsen et al., 2013). In fact, expression of *Sox2* is lower in delaminated neuroblasts, which instead express high levels of *Neurod1*. When Sox2 levels were forced to stay high by electroporation into the chick otic cup, *Neurog1* was induced, but the cells failed to progress to the next stage and neurogenesis failed. In contrast, electroporation of either *Neurog1* or *Neurod1* inhibited expression of *Sox2* and therefore increased the number of neurons. Together, these studies suggest that downregulation of Sox2 is necessary for neuronal differentiation, paralleling the situation for hair cell differentiation.

2.5.3 *Regulation of Transcriptional Activity in Neurosensory Progenitors*

Given the broad expression and function of transcription factors such as Six1, Eya1, and Sox2, how might such a network be poised to have specific effects on auditory neurogenesis? Like other transcriptional networks, the answer lies both in the presence of other transcription factors as well as the overall epigenetic status of the cell. For instance, the presence of the Notch-ICD appears to have important consequences for the outcome of Sox2 activity: when both are present, there is an expansion of sensory regions at the expense of neuroblasts (Hartman et al., 2010; Pan et al., 2010), and ectopic expression of Notch-ICD is sufficient to redirect neuroblasts to the hair cell fate in vivo (Pan et al., 2013). Similarly, Six1 and Eya1 can have dual effects on neuronal versus hair cell fate depending on the context

(Bricaud & Collazo, 2011; Ahmed et al., 2012b). Moreover, coexpression of Neurog1 and Neurod1 is only able to initiate neurogenesis, as the neurons that form fail to advance to a more mature state, as signaled by expression of neurofilament (NF). Hence, additional factors must influence how each of these regulators affects neuronal differentiation.

One important variable appears to be chromatin structure, which can affect which specific binding sites are available for active transcription (reviewed in Ronan et al., 2013). Although neither Eya1 nor Six1 is able to induce formation of ßIII-tubulin-positive neurons in the embryonic cochlea, co-electroporation of both induces production of Neurog1 and Neurod1, albeit with low efficiency, as most transfected cells instead adopt a hair cell fate (Ahmed et al., 2012a). However, when Six1 and Eya1 are introduced together with components of the SWI/SNF chromatin remodeling complex, approximately 85 % of the transfected neurons now express both Neurod1 and NF, with many fewer cells expressing hair cell markers. This effect requires Sox2, which apparently antagonizes the differentiation of Six1/Eya1+ cells into hair cells (Dabdoub et al., 2008; Ahmed et al., 2012a). Indeed, addition of Sox2 further augments the effectiveness of this treatment, such that 99 % of the transfected cells in Kölliker's organ now express NF. This might be influenced in part by the fact that cells in Kölliker's organ are derived from cells that once expressed *Neurog1* and may therefore already be biased toward the neuronal fate (Raft et al., 2007). The same transcriptional network (i.e., Six1, Eya1, SWI/SNF, and Sox2) can convert 3T3 fibroblasts into NF+ neurons with high efficiency, likely acting in part through synergistic effects on the activity of Neurog1 and Neurod1, which are induced in parallel (Ahmed et al., 2012a).

To add further complexity, the nature of the transcriptional complexes governing neurogenesis also evolves over time. For instance, in the developing chick inner ear, *Sox2* and *Neurog1* levels decrease in neuroblasts that have begun to express enhanced levels of *Neurod1* (Evsen et al., 2013). Moreover, Neurog1 and Neurod1 are able to promote neurogenesis when introduced into the chick otic cup, and these effects are accompanied by a loss of *Sox2*, likely through direct binding of these transcription factors to an enhancer in the *Sox2* locus. Presumably, the failure of Neurog1 and Neurod1 to induce mature neurons in cultured cochlear explants (Puligilla et al., 2010) reflects a difference in the availability of Sox2 in these two systems: Sox2 is naturally downregulated in the chick otic cup, but not in Kölliker's organ.

Taken together, a model emerges in which an Eya1/Six1/Sox2/SWI/SNF complex activates Neurog1 and Neurod1, which subsequently cooperate with a Sox2-negative complex that drives neuronal differentiation (Ahmed et al., 2012a; Wong et al., 2013). The importance of epigenetic regulation for SGN development is further underscored by analysis of CHD7, another chromatin remodeling enzyme that is responsible for CHARGE syndrome in humans, a disorder marked by hearing loss and many other developmental anomalies (Layman et al., 2010; Zentner et al., 2010). In mice, loss of *CHD7* impairs *Neurog1* expression and inner ear neurogenesis (Hurd et al., 2010). Hence, there are likely multiple pathways coordinating which regions of the genome are accessible to pro-neurogenic transcriptional complexes.

2.6 Delamination and Differentiation

Although the onset of *Neurog1* marks an important milestone in SGN development, this initial specification must be paired with tightly controlled delamination and differentiation to create a spiral ganglion with the correct number of cells in the proper location. Once specified, Neurog1+ neuroblasts pass through additional stages as they mature, with intrinsic factors endowing neuroblasts both with the ability to leave the otic epithelium and to respond appropriately to mitogenic and trophic cues in the environment.

2.6.1 Delamination

One of the earliest signs of maturation in Neurog1+ neuroblasts is expression of the closely related bHLH factor Neurod1 (Fig. 2.3). Neurod1 seems to take over from Neurog1 after the neuroblasts are specified, as hinted at by the upregulation of *Neurod1* and downregulation of *Neurog1* in post-delaminated neuroblasts (Evsen et al., 2013). Neurod1 is present at modest levels in the PNSD of the otic epithelium, but is more strongly expressed in the nascent ganglion (Liu et al., 2000; Kim et al., 2001). Consistent with this observation, Neurod1 is lost from *Neurog1* mutant mice (Ma et al., 1998), whereas Neurog1 expression is sustained and even increased in the absence of *Neurod1*, placing Neurod1 downstream in this hierarchy (Jahan et al., 2010a).

Neurod1 is clearly required for normal CVG development, likely affecting multiple stages of neuronal differentiation. In *Neurod1* mutant mice, the CVG is strongly reduced (Liu et al., 2000; Kim et al., 2001). This phenotype may have two origins. First, the neurons do not seem to delaminate normally. Many cells meant to produce Neurod1, as indicated by a β-galactosidase reporter, remain in the otic epithelium (Liu et al., 2000; Kim et al., 2001). Second, there is an increase in cell death, accompanied by reduced expression of two neurotrophin receptors: TrkB (Liu et al., 2000) and TrkC (Kim et al., 2001).

Although loss of cells is an early and drastic consequence, Neurod1 also appears to influence SGN differentiation beyond survival. For instance, activation of Neurod1 can have potent and long term effects for neuronal production in chicks (Evsen et al., 2013). In addition, analysis of *Neurod1* conditional knockouts has revealed changes in cochlear innervation (Jahan et al., 2010a). Whether these effects reflect intrinsic changes in SGN differentiation or instead are secondary to defects in the organ of Corti remains unclear as Neurod1 also affects the onset of hair cell differentiation (Jahan et al., 2010b).

Little is known about what controls the initial delamination of neurons out of the PNSD or the subsequent separation of the CVG into a distinct SG and VG. On delaminating, SGN neuroblasts come into contact with a new environment consisting of mesenchyme and neural crest cells, which will produce the glia of the

inner ear (D'Amico-Martel & Noden, 1983; Freyer et al., 2011; Sandell et al., 2014). The cells in this region are histologically distinct because they form a funnel-shaped structure, through which the differentiating SGNs appear to extend their earliest processes (Carney & Silver, 1983). Indeed, the earliest CVG neuroblasts appear to be enveloped by a "sleeve" of neural crest cells emanating from the fourth rhombomere of the hindbrain (Sandell et al., 2014). Similarly, neural crest cells form passages for migration of other placodally derived neurons (Freter et al., 2013). Ablation of neural crest in this region impairs extension of axons from differentiating CVG neurons (Sandell et al., 2014). In addition, when the cochlea is depleted of Schwann cells genetically, SGNs coalesce too close to the modiolus and can even migrate outside of the otic capsule (Morris et al., 2006; Mao et al., 2014).

The nature of the molecules that mediate the cell-cell interactions that guide SGN movements is not well understood. As in mice lacking Schwann cells, SGNs are displaced toward the modiolus in neurons lacking the transcription factor Gata3. This may mean that Gata3 determines how SGNs respond to glial-derived signals, though other interpretations are also possible (Appler et al., 2013). FGF2 has been put forward as one possible migratory signal, due to its ability to affect the migration of neuroblasts in vitro (Hossain et al., 2002). However, clear delamination defects have not been reported in any FGF mutant mice, though the CVG is often affected in poorly understood ways (Wright & Mansour, 2003a). One intriguing possibility is that canonical axon guidance molecules play a role. For instance, SGN cell bodies are somewhat mispositioned in the absence of Slit/Robo signaling (Wang et al., 2013). However, this phenotype arises after E13, suggesting that other signals direct the initial positioning of the SGN with Slit/Robo acting instead to keep SGNs in the proper location.

2.6.2 *Control of Proliferation and Differentiation*

After delaminating from the PNSD, Neurod1+ neuroblasts continue to proliferate before exiting the cell cycle and differentiating. FGF signals may influence how much proliferation occurs, though exactly how this works remains unclear because of the pleiotropic and redundant effects of various family members in vivo (Wright & Mansour, 2003a). This issue has been partly overcome by manipulating the FGF pathway acutely in cultured chick inner ear neurons. These studies revealed that in addition to its earlier role in neuronal specification, FGF also inhibits cell proliferation and drives neuroblasts to differentiate (Alsina et al., 2004). Conversely, pharmacological inhibition of FGF signaling has the opposite effect. A slightly different role has been proposed in zebrafish, in which exposure to high levels of FGF5 prevents slowly dividing neuroblasts in the nascent ganglion from differentiating (Vemaraju et al., 2012). These studies also uncovered a dose dependence that may influence the ultimate outcome of each FGF signal.

How FGFs affect the delamination and expansion of neuroblasts in mouse is not known. In mice lacking the shared FGF3/FGF10 receptor FGFR2, CVG neurons

seem to delaminate as they should, but the ganglion is obviously abnormal by E11 and exhibits excess cell death by E13 (Pirvola et al., 2000), with few neurons remaining by E18.5 (Pauley et al., 2003). Similarly, the CVG is smaller in *FGF3* mutants (Hatch et al., 2007), though the fact that FGF3 is restricted to the vestibular neurogenic zone (Koo et al., 2009) suggests this could reflect a selective loss of vestibular neurons. No obvious change in the CVG was noted in *FGF10* mutants (Pauley et al., 2003), and the phenotypes in *FGF3/10* double mutants are complicated to interpret because of the possible actions of each ligand at multiple stages of CVG development, as well as phenotypic variability (Wright & Mansour, 2003b; Vazquez-Echeverria et al., 2008).

As in other regions of the nervous system, the final number of neurons in the SG reflects a balance of proliferation and apoptosis. In chicks, IGF activation of the PI3 K/Akt pathway may contribute to the expansion of neuroblasts before they start to differentiate, influencing both proliferation and survival (Camarero et al., 2003; Varela-Nieto et al., 2004; Aburto et al., 2012). In contrast, IGF1 does not appear to be required for early SGN development in mice (Camarero et al., 2001). However, otic neuroblasts do show evidence of Akt pathway activation in mice, and there is a severe loss of Neurod1+ cells by E10.5 and increased cell death by E11.5 in mice with abnormal Akt signaling (Kim et al., 2013). Thus, early neuroblasts require signaling through the Akt pathway for their survival.

Apoptosis also affects subsequent stages of SGN development, after the neurons have exited the cell cycle and differentiated. Classic in vitro assays originally showed that SGN survival depends on target-derived cues present both in the sensory epithelia and in the hindbrain (Zhou & Van De Water, 1987). In vivo, apoptosis peaks in the SGN between E15.5 and E16.5 in mouse (Nishizaki et al., 1998), which coincides with the arrival of peripheral neurites in the organ of Corti (Farinas et al., 2001). Consistent with this observation, the total number of neurons in the spiral ganglion decreases from E15.5 to E17.5 (Farinas et al., 2001). A similar wave of cell death occurs after connections have been made in the chick basilar papilla (Ard & Morest, 1984). This naturally occurring period of cell death likely reflects a culling of SGNs that were unable to establish proper connections in the sensory epithelia.

There is abundant evidence that the brain-derived neurotrophic factor (BDNF) and neurotrophin (NT-3) neurotrophins are crucial for the survival of SGNs that have reached their target (reviewed in Yang et al., 2011). Both BDNF and NT-3 are produced in the developing sensory epithelia of the inner ear, whereas their respective receptors TrkB and TrkC are present in the developing neurons (Farinas et al., 2001). In the cochlea, NT-3 and BDNF are produced at slightly different times and in opposing apical-basal gradients. In addition, whereas NT-3 is broadly present in supporting cells, including those in Kölliker's organ, BDNF seems to be more restricted to hair cells. Consistent with these differing expression patterns, SGNs are strongly dependent on NT-3, particularly in the base where there is no BDNF during the initial stages of neurite outgrowth (Fritzsch et al., 1998; Farinas et al., 2001). This is exactly what would be predicted if NT-3 normally keeps SGNs alive as they extend processes into the cochlear duct. Although NT-3 appears to be the dominant player, BDNF is also involved, as inner ear neurons are completely

lost in *BDNF/NT-3* double mutants (Ernfors et al., 1995) and deletion of *TrkB* enhances the *TrkC* phenotype (Fritzsch et al., 1998). Importantly, in addition to these classic roles, BDNF and NT-3 also influence many other features of SGN differentiation, including axon guidance, synaptogenesis, and maturation of firing properties (reviewed in Yang et al., 2011 and Green et al., 2012. See also Chaps. 3 by Fritzsch et al., 4 by Davis and Crozier, and 7 by Green et al.).

2.7 SGN Specification

The astonishing diversity of neurons in the central nervous system has long captured the attention of developmental neurobiologists. Efforts to understand how different neuronal subtypes are generated have established a model where early acting transcription factors induce more generic fates that are progressively restricted over time, as shown both for spinal cord motor neurons and in the cortex (Leone et al., 2008; Philippidou & Dasen, 2013). Although the SG might at first glance appear to be comparatively homogeneous, similar subtype specification must still occur. First and foremost is the specification of the auditory and vestibular fates. In addition, within the auditory population in mammals, SGNs are further divided into Type I and Type II neurons. Type I SGNs, which comprise approximately 95 % of the population, innervate inner hair cells, whereas the minority Type II SGNs instead innervate outer hair cells (Spoendlin, 1972; Perkins & Morest, 1975). Type I SGNs can be further classified based on their firing properties, varying both along the tonotopic axis (Davis & Liu, 2011) and with regard to threshold sensitivity (Taberner & Liberman, 2005). Unfortunately, our knowledge of how these different types of SGNs arise during development remains rudimentary (Fig. 2.4).

2.7.1 Auditory Versus Vestibular

The decision whether to populate the auditory or vestibular division of the inner ear appears to be made quite early in development, with neuroblasts assigned to an auditory or vestibular fate prior to delamination. Histologically, the auditory neurons have more densely packed nuclei than the vestibular neurons, which develop more laterally (Sher, 1972) and are noticeably larger (Ard & Morest, 1984). As early as E12.5 in mouse, the two ganglia are already clearly distinct, though still attached (Carney & Silver, 1983). More recent studies further suggested that auditory and vestibular ganglion neurons can be distinguished even earlier, with vestibular ganglion neurons extending peripheral neurites along the future paths of

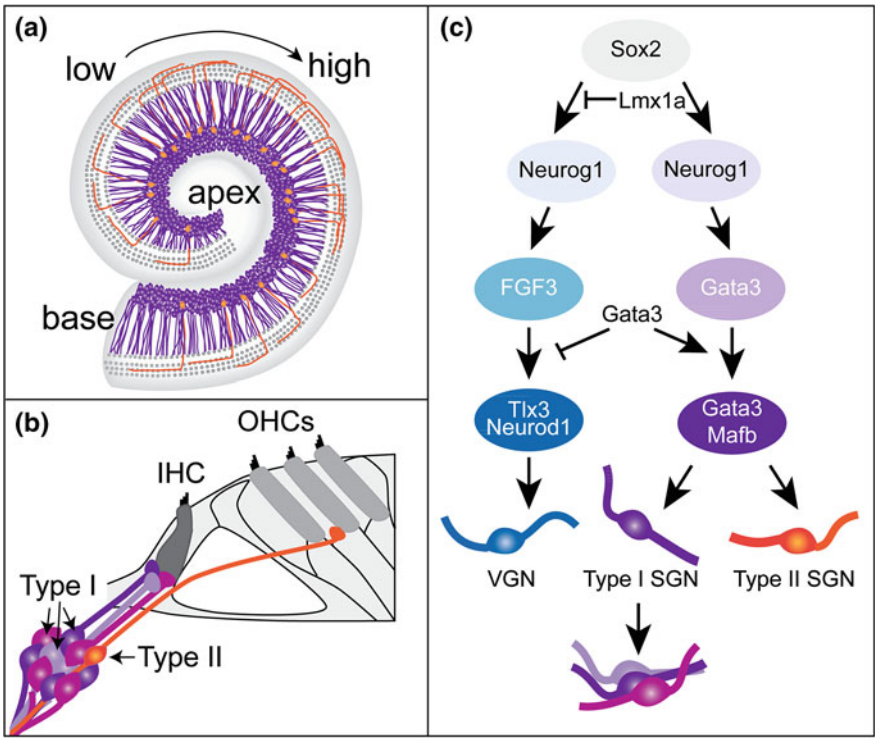

Fig. 2.4 Specification of SGNs. **a**, **b** SGNs are organized tonotopically from the apex to the base of the cochlea and show different firing properties depending on their location. Two basic types of SGNs can be recognized morphologically, with Type I SGNs (*purple*) projecting to inner hair cells (IHC) and Type II SGNs (*orange*) projecting to outer hair cells (OHCs). At any one point along the tonotopic axis, SGNs show additional heterogeneity, as evidenced by differences in spontaneous firing rates and gene expression. **c** Precursors for spiral (*purple*) and vestibular (*blue*) ganglion neurons are specified early in development. Lmx1a sets a medial–lateral boundary in the PNSD. Subsequently, early SGN progenitors maintain expression of Gata3, which both promotes auditory-specific programs of development and inhibits the vestibular fate. Mafb acts downstream of Gata3 to promote terminal differentiation of SGNs. The mechanisms that further diversify the SGN population remain unknown

the inferior and superior vestibular nerves at E10.5, followed 1 day later by the emergence of a fan of cochlear processes into the growing cochlear duct (Sandell et al., 2014).

Neurons in the murine vestibular ganglion also exit the cell cycle (Ruben, 1967) and express *Neurog1* (Koundakjian et al., 2007) earlier than those in the spiral ganglion. Similarly, in chicks, vestibular ganglion neurons are produced earlier (Bell et al., 2008). This temporal patterning is mirrored by a spatial patterning of the PNSD, with expression of the transcription factor Gata3 restricted to the medial PNSD (Lawoko-Kerali et al., 2004) and FGF3 marking the lateral division (Koo et al., 2009). Similarly, the earliest delaminated neuroblasts adjacent to these

domains express either auditory (i.e. Gata3) (Karis et al., 2001) or vestibular (i.e., Tlx3) markers (Lu et al., 2011).

Additional evidence for a spatial segregation of precursors within the PNSD has come from fate mapping studies in chicks, where neurons destined to innervate auditory or vestibular epithelia arise from physically distinct populations of precursors (Bell et al., 2008). Intriguingly, the same pattern was observed for the corresponding sensory epithelia, leading to a model where the PNSD is patterned along the dorsal-ventral axis, with neurogenesis preceding sensory cell production within defined regions for each sensory organ. In support of this idea, virus-based fate mapping in chicks has revealed that auditory and vestibular neurons rarely develop from a common neural precursor (Satoh & Fekete, 2005).

Which extrinsic cues may establish this pattern in the PNSD is not known. SGNs can still develop in the absence of Shh activity (Brown & Epstein, 2011). However, ectopic Wnt signaling can impose a "dorsal" identity and lead to the development of vestibular-like hair cells within the chicken cochlea (Stevens et al., 2003). As the lagena macula is a vestibular sensory epithelium that develops close to the basilar papilla, it is also possible that Wnt signaling acts more locally to affect the auditory-vestibular fate decision.

Although nothing is known about the extrinsic cues that might control the auditory versus vestibular neurogenic fate, the intrinsic factor Lmx1a may be involved in setting and reinforcing the boundaries that have been revealed by fate mapping. In the early otic vesicle, *Lmx1a* is present everywhere except for a small wedge where the neurosensory precursors are located (Nichols et al., 2008). However, *Lmx1a* is not fully excluded from the PNSD, but is in fact expressed within the auditory division (Koo et al., 2009). Here, *Lmx1a* appears to set the boundary between auditory and vestibular regions of the PNSD, as evidenced by ectopic production of vestibular neurons within the auditory domain in *Lmx1a* mutant mice. Interestingly, vestibular-like hair cells also appear in the cochlea of *Lmx1a* mutant mice, as predicted by the boundaries established by the fate mapping studies in chick (Bell et al., 2008). However, it remains unclear whether this phenotype reflects a change in the identity of a common "auditory" neurosensory progenitor or whether "vestibular" neurosensory progenitors are aberrantly migrating into the auditory zone.

The eventual differentiation of neurons with either auditory or vestibular-appropriate properties is controlled by intrinsic factors acting downstream of Neurod1. In fact, there are hints that Neurod1 may participate in this early segregation. After its initial role in generic neurogenesis, Neurod1 is selectively maintained in vestibular but not in more mature auditory neurons (Lawoko-Kerali et al., 2004; Jones & Warchol, 2009). Projections from auditory and vestibular ganglion neurons intermingle inappropriately in ear-specific *Neurod1* knockout mice, underscoring a possible role in subtype-specific properties of differentiation (Jahan et al., 2010a).

Another key player is Gata3, which is enriched in the medial PNSD where SGNs develop (Karis et al., 2001; Lawoko-Kerali et al., 2002, 2004). Moreover, Gata3 is maintained at high levels in SGNs throughout embryonic development and after

birth (Karis et al., 2001; Lawoko-Kerali et al., 2002, 2004; Appler et al., 2013). Although clearly auditory-enriched, *Gata3* is also transcribed transiently in the vestibular ganglion (VG), with a smattering of Gata3-positive vestibular ganglion neurons (VGNs) present by E11 (Lu et al., 2011). This observation suggests that Gata3 may not be the sole mediator of SGN identity. In support of this idea, in chicks, Gata3 is not expressed in dividing or migrating neuroblasts and is only upregulated in auditory neurons as they differentiate (Jones & Warchol, 2009). Together, these results indicate that Gata3 may play an important role beyond SGN specification.

As predicted by its auditory-enriched expression even within the PNSD, SGNs are lost from *Gata3* null embryos by E15, leaving only an apparent VG (Karis et al., 2001; Duncan et al., 2011). Similarly, conditional deletion of *Gata3* from the early otic vesicle prevents SGN development, while VGNs develop with no gross abnormalities (Duncan & Fritzsch, 2013). Thus, Gata3 clearly plays a primary role in SGNs, though more minor defects in a subpopulation of VGNs cannot be ruled out. Notably, the neurons that remain in *Gata3* null mutants still try to produce Gata3, as indicated by a lacZ reporter (Karis et al., 2001). This further suggests that Gata3's main function may be to drive execution of the auditory fate, but that other intrinsic factors are involved in the initial specification.

Analysis of other mouse mutants revealed an ongoing need for Gata3 after specification. When Gata3 is removed slightly later in development (Duncan & Fritzsch, 2013), the initial production of neurons appears normal, but the SGNs subsequently undergo cell death beginning at E12.5, apparently independent of any change in neurotrophin availability or responsiveness (Luo et al., 2013). In addition, the few remaining SGNs make highly abnormal connections both peripherally and centrally (Duncan & Fritzsch, 2013; Luo et al., 2013), indicating that Gata3 affects not only SGN specification and survival, but also differentiation.

Consistent with this interpretation, when *Gata3* is deleted after the neuroblasts have delaminated, SGNs differentiate prematurely (Appler et al., 2013). In these mice, Gata3 protein is preserved in the developing cochlea, and the organ of Corti shows no major defects, confirming that the changes in cochlear wiring reflect a direct role for Gata3 in SGNs. Although many features of the auditory identity are maintained, the mutant SGNs aberrantly express several vestibular markers and fail to transcribe some key auditory markers, including the transcription factor Mafb, which begins to be expressed in the base of the SG at E14.5 and is then maintained in postmitotic neurons (Yu et al., 2013). Mafb, in turn, acts downstream of Gata3 to direct later features of SGN differentiation. Taken together with the fact that many Gata3 target genes are not SGN-specific but are in fact expressed in both spiral and vestibular neurons in the wild-type scenario (Appler et al., 2013), these studies suggest that Gata3 guides SGNs through a prolonged period of differentiation by coordinating activation of generic and auditory-specific neuronal differentiation programs.

2.7.2 SGN Diversification

Even less is known about the further diversification of SGNs once they have been directed down the auditory path. SGNs are typically divided into two basic classes based on their morphology and pattern of innervation (Spoendlin, 1972). The vast majority are Type I SGNs, which are myelinated and extend unbranched radial processes to contact the inner hair cells. The remaining Type II SGNs, which comprise 5 % of the population, are unmyelinated, have smaller cell bodies, and extend thin processes that spiral along the cochlea to innervate multiple outer hair cells. A much stronger acoustic signal is required to evoke responses from Type II SGNs than from Type I SGNs, although both receive glutamatergic input (Weisz et al., 2009). These two populations are best recognized by their innervation patterns and by enriched expression of Peripherin in postnatal Type II SGNs (Hafidi, 1998). Although there is also heterogeneity among the auditory neurons in chickens (Whitehead & Morest, 1981; Rebillard & Pujol, 1983), Type I and Type II neurons analogous to those in humans have not been described, so only mammals are discussed here.

In the absence of early markers, it has been difficult to pinpoint exactly when Type II SGNs first appear in development. Electron microscopic studies confirmed the presence of Type II SGNs at birth in cats and mice, but not earlier (Romand & Romand, 1990). Similarly, the final pattern of Type I versus Type II innervation is not set until postnatal stages, with apparent rearrangement of neurites (Echteler, 1992; Huang et al., 2007), synaptic pruning (Huang et al., 2012), and differential cell death (Echteler et al., 2005; Barclay et al., 2011). With no reliable independent markers, however, it remains unclear which SGN populations are affected by each of these events. Nevertheless, Type II SGNs can be recognized during embryonic stages, as evidenced by the presence of a large growth cone that turns toward the base and grows among the region where the outer hair cells will eventually differentiate (Bruce et al., 1997; Koundakjian et al., 2007). In addition, Type I SGNs appear to be intrinsically programmed to avoid the outer hair cell region during synaptogenesis, as only Type I SGNs express EphA4 and signaling through this receptor is necessary to confine Type I neurites to the inner hair cell region (Defourny et al., 2013). Identifying the intrinsic programs that activate and maintain these differences is an important challenge for the future.

The Type I SGN population is itself further diversified at a functional level, though the extent and nature of this heterogeneity remain poorly defined. For instance, Type I SGNs exhibit different firing properties depending on their location along the tonotopic axis of the cochlea (see Chap. 4 by Davis and Crozier). These differences correlate with changes in protein expression, indicating that at least some of this variation may be genetically programmed (Flores-Otero et al., 2007). SGNs also express varying levels of calretinin and calbindin, but these differences have not yet been correlated with any clear electrophysiological differences (Liu & Davis, 2014).

Aside from these molecular differences, Type I SGNs also vary in their baseline firing profiles and respond to sound stimulation at different thresholds (Taberner & Liberman, 2005). SGNs with low spontaneous firing rates (low-SR) have higher dynamic range and thus contribute to hearing at higher sound intensities compared to those with high spontaneous firing rates (high-SR). These physiological differences come with morphological differences, as well (Liberman, 1980, 1982; Kawase & Liberman, 1992; Taberner & Liberman, 2005). Low-SR fibers preferentially innervate the modiolar side of the inner hair cell and develop smaller postsynaptic densities than the high-SR fibers, which instead cluster on the pillar side of the hair cell (Liberman et al., 2011). However, to date, there are no markers for either population, leaving open the question of when or how these differences are established.

2.8 Summary

The past decade has witnessed a remarkable flurry of discoveries into mechanisms of SGN development, made possible largely by the availability of improved molecular tools that overcome the technical hurdles for studying the cochlea. These studies have uncovered multiple extrinsic signaling pathways that determine when, where, and how many SGNs will develop. In parallel, complex transcriptional networks endow developing neurons with their unique properties, while simultaneously inhibiting alternative fates. This involves activation of cell-type–specific programs, as well as feedback loops within the pathway that turn off "early" genes and drive progenitors toward a progressively more differentiated state. Many transcription factors act at multiple stages and in multiple progenitor populations, with specificity achieved through the action of a few potent regulators.

Looking forward, this body of knowledge provides an important foundation for the next generation of scientific inquiry. Now that we have begun to gain traction on the question of how auditory fate is imposed on SGNs, it will be important to identify the pathways that further diversify this population, starting with the identification of reliable cell-type–specific markers. In addition, we still have very little grasp on the extrinsic pathways that divide the auditory and vestibular populations, let alone the cues that may promote any additional heterogeneity within the SGN population.

A deeper understanding both of the intrinsic and extrinsic pathways that act at each step of SGN development is crucial for current efforts to design effective stem cell-based therapies for deafness. For instance, with improved knowledge of the relevant signaling pathways that act at each step, scientists will be able to design protocols to steer naïve stem cells toward a specific fate, similar to approaches that have proven so successful for motor neurons (reviewed in Davis-Dusenbery et al., 2014). It may also be possible to reawaken developmental potential within cells in the mature cochlea by introducing cocktails of transcription factors such as Eya1/Six1 and Gata3, together with drugs that influence the chromatin state in these cells (see Chap. 9 by Nayagam and Edge).

Acknowledgments Thank you to Dr. Doris Wu, Dr. Donna Fekete, Dr. Amy Kiernan, Dr. Matthew Kelley, and Dr. Bernd Fritzsch for their insightful comments and many engaging discussions about spiral ganglion neuron development over the years, as well as to Dr. Cindy Lu, Dr. Noah Druckenbrod, Dr. Brikha Shrestha, and Ms. Andrea Yung for assistance with final preparation of the manuscript and figures.

References

Abello, G., Khatri, S., Giraldez, F., & Alsina, B. (2007). Early regionalization of the otic placode and its regulation by the Notch signaling pathway. *Mechanisms of Development*, 124(7–8), 631–645.

Abello, G., Khatri, S., Radosevic, M., Scotting, P. J., Giraldez, F., & Alsina, B. (2010). Independent regulation of Sox3 and Lmx1b by FGF and BMP signaling influences the neurogenic and non-neurogenic domains in the chick otic placode. *Developmental Biology*, 339(1), 166–178.

Aburto, M. R., Magarinos, M., Leon, Y., Varela-Nieto, I., & Sanchez-Calderon, H. (2012). AKT signaling mediates IGF-I survival actions on otic neural progenitors. *PLoS One*, 7(1), e30790.

Adam, J., Myat, A., Le Roux, I., Eddison, M., Henrique, D., Ish-Horowicz, D., & Lewis, J. (1998). Cell fate choices and the expression of Notch, Delta and Serrate homologues in the chick inner ear: Parallels with *Drosophila* sense-organ development. *Development*, 125(23), 4645–4654.

Ahmed, M., Xu, J., & Xu, P. X. (2012a). EYA1 and SIX1 drive the neuronal developmental program in cooperation with the SWI/SNF chromatin-remodeling complex and SOX2 in the mammalian inner ear. *Development*, 139(11), 1965–1977.

Ahmed, M., Wong, E. Y., Sun, J., Xu, J., Wang, F., & Xu, P. X. (2012b). Eya1–Six1 interaction is sufficient to induce hair cell fate in the cochlea by activating Atoh1 expression in cooperation with Sox2. *Developmental Cell*, 22(2), 377–390.

Ali, M. M., Jayabalan, S., Machnicki, M., & Sohal, G. S. (2003). Ventrally emigrating neural tube cells migrate into the developing vestibulocochlear nerve and otic vesicle. *International Journal of Developmental Neuroscience*, 21(4), 199–208.

Alsina, B., Abello, G., Ulloa, E., Henrique, D., Pujades, C., & Giraldez, F. (2004). FGF signaling is required for determination of otic neuroblasts in the chick embryo. *Developmental Biology*, 267(1), 119–134.

Anniko, M., & Wikstrom, S. O. (1984). Pattern formation of the otic placode and morphogenesis of the otocyst. *American Journal of Otolaryngology*, 5(6), 373–381.

Anniko, M., & Schacht, J. (1984). Inductive tissue interactions during inner ear development. *Archives of Oto-Rhino-Laryngology*, 240(1), 17–33.

Appler, J. M., Lu, C. C., Druckenbrod, N. R., Yu, W. M., Koundakjian, E. J., & Goodrich, L. V. (2013). Gata3 is a critical regulator of cochlear wiring. *Journal of Neuroscience*, 33(8), 3679–3691.

Ard, M. D., & Morest, D. K. (1984). Cell death during development of the cochlear and vestibular ganglia of the chick. *International Journal of Developmental Neuroscience*, 2(6), 535–547.

Barclay, M., Ryan, A. F., & Housley, G. D. (2011). Type I vs type II spiral ganglion neurons exhibit differential survival and neuritogenesis during cochlear development. *Neural Development*, 6, 33.

Bartelmez, G. W. (1922). The origin of the otic and optic primordia in man. *Journal of Comparative Neurology*, 34(2), 201–232.

Bell, D., Streit, A., Gorospe, I., Varela-Nieto, I., Alsina, B., & Giraldez, F. (2008). Spatial and temporal segregation of auditory and vestibular neurons in the otic placode. *Developmental Biology*, 322(1), 109–120.

Bermingham, N. A., Hassan, B. A., Price, S. D., Vollrath, M. A., Ben-Arie, N., Eatock, R. A., Bellen, H. J., Lysakowski, A., & Zoghbi, H. Y. (1999). Math1: An essential gene for the generation of inner ear hair cells. *Science*, 284(5421), 1837–1841.

Bibas, A., Hornigold, R., Liang, J., Michaels, L., Anagnostopoulou, S., & Wright, A. (2006). The development of the spiral ganglion in the human foetus. *Folia Morphologica*, 65(2), 140–144.

Bigelow, H. B. (1904). The sense of hearing in the goldfish *Carassius Auratus L. The American Naturalist*, 38(448), 275–284.

Bok, J., Bronner-Fraser, M., & Wu, D. K. (2005). Role of the hindbrain in dorsoventral but not anteroposterior axial specification of the inner ear. *Development*, 132(9), 2115–2124.

Bok, J., Raft, S., Kong, K. A., Koo, S. K., Drager, U. C., & Wu, D. K. (2011). Transient retinoic acid signaling confers anterior-posterior polarity to the inner ear. *Proceedings of the National Academy of Sciences of the USA*, 108(1), 161–166.

Bok, J., Zenczak, C., Hwang, C. H., & Wu, D. K. (2013). Auditory ganglion source of Sonic hedgehog regulates timing of cell cycle exit and differentiation of mammalian cochlear hair cells. *Proceedings of the National Academy of Sciences of the USA*, 110(34), 13869–13874.

Bouchard, M., Souabni, A., & Busslinger, M. (2004). Tissue-specific expression of cre recombinase from the Pax8 locus. *Genesis*, 38(3), 105–109.

Bricaud, O., & Collazo, A. (2011). Balancing cell numbers during organogenesis: Six1a differentially affects neurons and sensory hair cells in the inner ear. *Developmental Biology*, 357(1), 191–201.

Brooker, R., Hozumi, K., & Lewis, J. (2006). Notch ligands with contrasting functions: Jagged1 and Delta1 in the mouse inner ear. *Development*, 133(7), 1277–1286.

Brown, A. S., & Epstein, D. J. (2011). Otic ablation of smoothened reveals direct and indirect requirements for Hedgehog signaling in inner ear development. *Development*, 138(18), 3967–3976.

Bruce, L. L., Kingsley, J., Nichols, D. H., & Fritzsch, B. (1997). The development of vestibulocochlear efferents and cochlear afferents in mice. *International Journal of Developmental Neuroscience*, 15(4–5), 671–692.

Camarero, G., Avendano, C., Fernandez-Moreno, C., Villar, A., Contreras, J., de Pablo, F., Pichel, J. G., & Varela-Nieto, I. (2001). Delayed inner ear maturation and neuronal loss in postnatal Igf-1–deficient mice. *Journal of Neuroscience*, 21(19), 7630–7641.

Camarero, G., Leon, Y., Gorospe, I., De Pablo, F., Alsina, B., Giraldez, F., & Varela-Nieto, I. (2003). Insulin-like growth factor 1 is required for survival of transit-amplifying neuroblasts and differentiation of otic neurons. *Developmental Biology*, 262(2), 242–253.

Carney, P. R., & Silver, J. (1983). Studies on cell migration and axon guidance in the developing distal auditory system of the mouse. *Journal of Comparative Neurology*, 215(4), 359–369.

Chiang, C., Litingtung, Y., Lee, E., Young, K. E., Corden, J. L., Westphal, H., & Beachy, P. A. (1996). Cyclopia and defective axial patterning in mice lacking Sonic hedgehog gene function. *Nature*, 383(6599), 407–413.

Cole, L. K., Le Roux, I., Nunes, F., Laufer, E., Lewis, J., & Wu, D. K. (2000). Sensory organ generation in the chicken inner ear: Contributions of bone morphogenetic protein 4, serrate1, and lunatic fringe. *Journal of Comparative Neurology*, 424(3), 509–520.

Dabdoub, A., Puligilla, C., Jones, J. M., Fritzsch, B., Cheah, K. S., Pevny, L. H., & Kelley, M. W. (2008). Sox2 signaling in prosensory domain specification and subsequent hair cell differentiation in the developing cochlea. *Proceedings of the National Academy of Sciences of the USA*, 105(47), 18396–18401.

D'Amico-Martel, A., & Noden, D. M. (1983). Contributions of placodal and neural crest cells to avian cranial peripheral ganglia. *American Journal of Anatomy*, 166(4), 445–468.

Daudet, N., & Lewis, J. (2005). Two contrasting roles for Notch activity in chick inner ear development: Specification of prosensory patches and lateral inhibition of hair-cell differentiation. *Development*, 132(3), 541–551.

Daudet, N., Ariza-McNaughton, L., & Lewis, J. (2007). Notch signalling is needed to maintain, but not to initiate, the formation of prosensory patches in the chick inner ear. *Development*, 134 (12), 2369–2378.

Davis, R. L., & Liu, Q. (2011). Complex primary afferents: What the distribution of electrophysiologically-relevant phenotypes within the spiral ganglion tells us about peripheral neural coding. *Hearing Research*, 276(1–2), 34–43.

Davis-Dusenbery, B. N., Williams, L. A., Klim, J. R., & Eggan, K. (2014). How to make spinal motor neurons. *Development*, 141(3), 491–501.

Defourny, J., Poirrier, A. L., Lallemend, F., Mateo Sanchez, S., Neef, J., Vanderhaeghen, P., Soriano, E., Peuckert, C., Kullander, K., Fritzsch, B., Nguyen, L., Moonen, G., Moser, T., & Malgrange, B. (2013). Ephrin-A5/EphA4 signalling controls specific afferent targeting to cochlear hair cells. *Nature Communications*, 4, 1438.

Deng, M., Yang, H., Xie, X., Liang, G., & Gan, L. (2014). Comparative expression analysis of POU4F1, POU4F2 and ISL1 in developing mouse cochleovestibular ganglion neurons. *Gene Expression Patterns*, 15(1), 31–37.

Duncan, J. S., & Fritzsch, B. (2013). Continued expression of GATA3 is necessary for cochlear neurosensory development. *PLoS One*, 8(4), e62046.

Duncan, J. S., Lim, K. C., Engel, J. D., & Fritzsch, B. (2011). Limited inner ear morphogenesis and neurosensory development are possible in the absence of GATA3. *International Journal of Developmental Biology*, 55(3), 297–303.

Echteler, S. M. (1992). Developmental segregation in the afferent projections to mammalian auditory hair cells. *Proceedings of the National Academy of Sciences of the USA*, 89(14), 6324–6327.

Echteler, S. M., Magardino, T., & Rontal, M. (2005). Spatiotemporal patterns of neuronal programmed cell death during postnatal development of the gerbil cochlea. *Brain Research. Developmental Brain Research*, 157(2), 192–200.

Ernfors, P., Van De Water, T., Loring, J., & Jaenisch, R. (1995). Complementary roles of BDNF and NT-3 in vestibular and auditory development. *Neuron*, 14(6), 1153–1164.

Evsen, L., Sugahara, S., Uchikawa, M., Kondoh, H., & Wu, D. K. (2013). Progression of neurogenesis in the inner ear requires inhibition of Sox2 transcription by neurogenin1 and neurod1. *Journal of Neuroscience*, 33(9), 3879–3890.

Farinas, I., Jones, K. R., Tessarollo, L., Vigers, A. J., Huang, E., Kirstein, M., de Caprona, D. C., Coppola, V., Backus, C., Reichardt, L. F., & Fritzsch, B. (2001). Spatial shaping of cochlear innervation by temporally regulated neurotrophin expression. *Journal of Neuroscience*, 21(16), 6170–6180.

Fekete, D. M., & Wu, D. K. (2002). Revisiting cell fate specification in the inner ear. *Current Opinion in Neurobiology*, 12(1), 35–42.

Flores-Otero, J., Xue, H. Z., & Davis, R. L. (2007). Reciprocal regulation of presynaptic and postsynaptic proteins in bipolar spiral ganglion neurons by neurotrophins. *Journal of Neuroscience*, 27(51), 14023–14034.

Freter, S., Fleenor, S. J., Freter, R., Liu, K. J., & Begbie, J. (2013). Cranial neural crest cells form corridors prefiguring sensory neuroblast migration. *Development*, 140(17), 3595–3600.

Freyer, L., Aggarwal, V., & Morrow, B. E. (2011). Dual embryonic origin of the mammalian otic vesicle forming the inner ear. *Development*, 138(24), 5403–5414.

Freyer, L., Nowotschin, S., Pirity, M. K., Baldini, A., & Morrow, B. E. (2013). Conditional and constitutive expression of a Tbx1–GFP fusion protein in mice. *BMC Developmental Biology*, 13(1), 33.

Friedman, R. A., Makmura, L., Biesiada, E., Wang, X., & Keithley, E. M. (2005). Eya1 acts upstream of Tbx1, Neurogenin 1, NeuroD and the neurotrophins BDNF and NT-3 during inner ear development. *Mechanisms of Development*, 122(5), 625–634.

Fritzsch, B., & Straka, H. (2014). Evolution of vertebrate mechanosensory hair cells and inner ears: Toward identifying stimuli that select mutation driven altered morphologies. *Journal of Comparative Physiology A: Neuroethology, Sensory, Neural, and Behavioral Physiology*, 200 (1), 5–18.

Fritzsch, B., Barbacid, M., & Silos-Santiago, I. (1998). The combined effects of trkB and trkC mutations on the innervation of the inner ear. *International Journal of Developmental Neuroscience*, 16(6), 493–505.

Fritzsch, B., Pan, N., Jahan, I., Duncan, J. S., Kopecky, B. J., Elliott, K. L., Kersigo, J., & Yang, T. (2013). Evolution and development of the tetrapod auditory system: An organ of Corti-centric perspective. *Evolution & Development*, 15(1), 63–79.

Green, S. H., Bailey, E., Wang, Q., & Davis, R. L. (2012). The Trk A, B, C's of neurotrophins in the cochlea. *Anatomical Record*, 295(11), 1877–1895.

Groves, A. K., & Fekete, D. M. (2012). Shaping sound in space: The regulation of inner ear patterning. *Development*, 139(2), 245–257.

Haddon, C., & Lewis, J. (1996). Early ear development in the embryo of the zebrafish, *Danio rerio*. *Journal of Comparative Neurology*, 365(1), 113–128.

Haddon, C., Jiang, Y. J., Smithers, L., & Lewis, J. (1998). Delta-Notch signalling and the patterning of sensory cell differentiation in the zebrafish ear: Evidence from the mind bomb mutant. *Development*, 125(23), 4637–4644.

Hafidi, A. (1998). Peripherin-like immunoreactivity in type II spiral ganglion cell body and projections. *Brain Research*, 805(1–2), 181–190.

Hammond, K. L., & Whitfield, T. T. (2011). Fgf and Hh signalling act on a symmetrical pre-pattern to specify anterior and posterior identity in the zebrafish otic placode and vesicle. *Development*, 138(18), 3977–3987.

Hammond, K. L., Loynes, H. E., Folarin, A. A., Smith, J., & Whitfield, T. T. (2003). Hedgehog signalling is required for correct anteroposterior patterning of the zebrafish otic vesicle. *Development*, 130(7), 1403–1417.

Hammond, K. L., van Eeden, F. J., & Whitfield, T. T. (2010). Repression of Hedgehog signalling is required for the acquisition of dorsolateral cell fates in the zebrafish otic vesicle. *Development*, 137(8), 1361–1371.

Hans, S., Irmscher, A., & Brand, M. (2013). Zebrafish Foxi1 provides a neuronal ground state during inner ear induction preceding the Dlx3b/4b-regulated sensory lineage. *Development*, 140(9), 1936–1945.

Harada, Y., Kasuga, S., & Tamura, S. (2001). Comparison and evolution of the lagena in various animal species. *Acta Oto-Laryngologica*, 121(3), 355–363.

Hartman, B. H., Reh, T. A., & Bermingham-McDonogh, O. (2010). Notch signaling specifies prosensory domains via lateral induction in the developing mammalian inner ear. *Proceedings of the National Academy of Sciences of the USA*, 107(36), 15792–15797.

Hatch, E. P., Noyes, C. A., Wang, X., Wright, T. J., & Mansour, S. L. (2007). Fgf3 is required for dorsal patterning and morphogenesis of the inner ear epithelium. *Development*, 134(20), 3615–3625.

Hebert, J. M., & McConnell, S. K. (2000). Targeting of cre to the Foxg1 (BF-1) locus mediates loxP recombination in the telencephalon and other developing head structures. *Developmental Biology*, 222(2), 296–306.

Hemond, S. G., & Morest, D. K. (1991a). Ganglion formation from the otic placode and the otic crest in the chick embryo: Mitosis, migration, and the basal lamina. *Anatomy and Embryology*, 184(1), 1–13.

Hemond, S. G., & Morest, D. K. (1991b). Formation of the cochlea in the chicken embryo: Sequence of innervation and localization of basal lamina-associated molecules. *Brain Research. Developmental Brain Research*, 61(1), 87–96.

Hossain, W. A., Brumwell, C. L., & Morest, D. K. (2002). Sequential interactions of fibroblast growth factor-2, brain-derived neurotrophic factor, neurotrophin-3, and their receptors define critical periods in the development of cochlear ganglion cells. *Experimental Neurology*, 175(1), 138–151.

Huang, L. C., Thorne, P. R., Housley, G. D., & Montgomery, J. M. (2007). Spatiotemporal definition of neurite outgrowth, refinement and retraction in the developing mouse cochlea. *Development*, 134(16), 2925–2933.

Huang, L. C., Barclay, M., Lee, K., Peter, S., Housley, G. D., Thorne, P. R., & Montgomery, J. M. (2012). Synaptic profiles during neurite extension, refinement and retraction in the developing cochlea. *Neural Development*, 7, 38.

Hurd, E. A., Poucher, H. K., Cheng, K., Raphael, Y., & Martin, D. M. (2010). The ATP-dependent chromatin remodeling enzyme CHD7 regulates pro-neural gene expression and neurogenesis in the inner ear. *Development*, 137(18), 3139–3150.

Jahan, I., Kersigo, J., Pan, N., & Fritzsch, B. (2010a). Neurod1 regulates survival and formation of connections in mouse ear and brain. *Cell and Tissue Research*, 341(1), 95–110.

Jahan, I., Pan, N., Kersigo, J., & Fritzsch, B. (2010b). Neurod1 suppresses hair cell differentiation in ear ganglia and regulates hair cell subtype development in the cochlea. *PLoS One*, 5(7), e11661.

Johnson, S. B., Schmitz, H. M., & Santi, P. A. (2011). TSLIM imaging and a morphometric analysis of the mouse spiral ganglion. *Hearing Research*, 278(1–2), 34–42.

Jones, J. M., & Warchol, M. E. (2009). Expression of the Gata3 transcription factor in the acoustic ganglion of the developing avian inner ear. *Journal of Comparative Neurology*, 516(6), 507–518.

Kalatzis, V., Sahly, I., El-Amraoui, A., & Petit, C. (1998). Eya1 expression in the developing ear and kidney: Towards the understanding of the pathogenesis of branchio-oto-renal (BOR) syndrome. *Developmental Dynamics*, 213(4), 486–499.

Karis, A., Pata, I., van Doorninck, J. H., Grosveld, F., de Zeeuw, C. I., de Caprona, D., & Fritzsch, B. (2001). Transcription factor GATA-3 alters pathway selection of olivocochlear neurons and affects morphogenesis of the ear. *Journal of Comparative Neurology*, 429(4), 615–630.

Kawase, T., & Liberman, M. C. (1992). Spatial organization of the auditory nerve according to spontaneous discharge rate. *Journal of Comparative Neurology*, 319(2), 312–318.

Kiernan, A. E. (2013). Notch signaling during cell fate determination in the inner ear. *Seminars in Cell and Developmental Biology*, 24(5), 470–479.

Kiernan, A. E., Pelling, A. L., Leung, K. K., Tang, A. S., Bell, D. M., Tease, C., Lovell-Badge, R., Steel, K. P., & Cheah, K. S. (2005). Sox2 is required for sensory organ development in the mammalian inner ear. *Nature*, 434(7036), 1031–1035.

Kim, H. J., Woo, H. M., Ryu, J., Bok, J., Kim, J. W., Choi, S. B., Park, M. H., Park, H. Y., & Koo, S. K. (2013). Conditional deletion of pten leads to defects in nerve innervation and neuronal survival in inner ear development. *PLoS One*, 8(2), e55609.

Kim, W. Y., Fritzsch, B., Serls, A., Bakel, L. A., Huang, E. J., Reichardt, L. F., Barth, D. S., & Lee, J. E. (2001). NeuroD-null mice are deaf due to a severe loss of the inner ear sensory neurons during development. *Development*, 128(3), 417–426.

Knowlton, V. Y. (1967). Correlation of the development of membranous and bony labyrinths, acoustic ganglia, nerves, and brain centers of the chick embryo. *Journal of Morphology*, 121 (3), 179–207.

Koo, S. K., Hill, J. K., Hwang, C. H., Lin, Z. S., Millen, K. J., & Wu, D. K. (2009). Lmx1a maintains proper neurogenic, sensory, and non-sensory domains in the mammalian inner ear. *Developmental Biology*, 333(1), 14–25.

Koundakjian, E. J., Appler, J. L., & Goodrich, L. V. (2007). Auditory neurons make stereotyped wiring decisions before maturation of their targets. *Journal of Neuroscience*, 27(51), 14078–14088.

Kuratani, S., Horigome, N., Ueki, T., Aizawa, S., & Hirano, S. (1998). Stereotyped axonal bundle formation and neuromeric patterns in embryos of a cyclostome, *Lampetra japonica*. *Journal of Comparative Neurology*, 391(1), 99–114.

Lawoko-Kerali, G., Rivolta, M. N., & Holley, M. (2002). Expression of the transcription factors GATA3 and Pax2 during development of the mammalian inner ear. *Journal of Comparative Neurology*, 442(4), 378–391.

Lawoko-Kerali, G., Rivolta, M. N., Lawlor, P., Cacciabue-Rivolta, D. I., Langton-Hewer, C., van Doorninck, J. H., & Holley, M. C. (2004). GATA3 and NeuroD distinguish auditory and vestibular neurons during development of the mammalian inner ear. *Mechanisms of Development*, 121(3), 287–299.

Layman, W. S., Hurd, E. A., & Martin, D. M. (2010). Chromodomain proteins in development: Lessons from CHARGE syndrome. *Clinical Genetics*, 78(1), 11–20.

Leone, D. P., Srinivasan, K., Chen, B., Alcamo, E., & McConnell, S. K. (2008). The determination of projection neuron identity in the developing cerebral cortex. *Current Opinion in Neurobiology*, 18(1), 28–35.

Li, C., Van De Water, T., & Ruben, R. (1978). The fate mapping of the eleventh and twelfth day mouse otocyst: An in vitro study of the sites of origin of the embryonic inner ear sensory structures. *Journal of Morphology*, 157(3), 249–267.

Li, H., Liu, H., Sage, C., Huang, M., Chen, Z. Y., & Heller, S. (2004). Islet-1 expression in the developing chicken inner ear. *Journal of Comparative Neurology*, 477(1), 1–10.

Liberman, L. D., Wang, H., & Liberman, M. C. (2011). Opposing gradients of ribbon size and AMPA receptor expression underlie sensitivity differences among cochlear-nerve/hair-cell synapses. *Journal of Neuroscience*, 31(3), 801–808.

Liberman, M. C. (1980). Morphological differences among radial afferent fibers in the cat cochlea: An electron-microscopic study of serial sections. *Hearing Research*, 3(1), 45–63.

Liberman, M. C. (1982). Single-neuron labeling in the cat auditory nerve. *Science*, 216(4551), 1239–1241.

Liu, M., Pereira, F. A., Price, S. D., Chu, M. J., Shope, C., Himes, D., Eatock, R. A., Brownell, W. E., Lysakowski, A., & Tsai, M. J. (2000). Essential role of BETA2/NeuroD1 in development of the vestibular and auditory systems. *Genes and Development*, 14(22), 2839–2854.

Liu, W., & Davis, R. L. (2014). Calretinin and calbindin distribution patterns specify subpopulations of type I and type II spiral ganglion neurons in postnatal murine cochlea. *Journal of Comparative Neurology*, 522(10), 2299–2318.

Liu, Z., Owen, T., Fang, J., & Zuo, J. (2012). Overactivation of Notch1 signaling induces ectopic hair cells in the mouse inner ear in an age-dependent manner. *PLoS One*, 7(3), e34123.

Locher, H., Frijns, J. H., van Iperen, L., de Groot, J. C., Huisman, M. A., & Chuva de Sousa Lopes, S. M. (2013). Neurosensory development and cell fate determination in the human cochlea. *Neural Development*, 8, 20.

Lu, C. C., Appler, J. M., Houseman, E. A., & Goodrich, L. V. (2011). Developmental profiling of spiral ganglion neurons reveals insights into auditory circuit assembly. *Journal of Neuroscience*, 31(30), 10903–10918.

Luo, X. J., Deng, M., Xie, X., Huang, L., Wang, H., Jiang, L., Liang, G., Hu, F., Tieu, R., Chen, R., & Gan, L. (2013). GATA3 controls the specification of prosensory domain and neuronal survival in the mouse cochlea. *Human Molecular Genetics*, 22(18), 3609–3623.

Ma, Q., Chen, Z., del Barco Barrantes, I., de la Pompa, J. L., & Anderson, D. J. (1998). neurogenin1 is essential for the determination of neuronal precursors for proximal cranial sensory ganglia. *Neuron*, 20(3), 469–482.

Ma, Q., Anderson, D. J., & Fritzsch, B. (2000). Neurogenin 1 null mutant ears develop fewer, morphologically normal hair cells in smaller sensory epithelia devoid of innervation. *Journal of the Association for Research in Otolaryngology*, 1(2), 129–143.

Mahmoud, A., Reed, C., & Maklad, A. (2013). Central projections of lagenar primary neurons in the chick. *Journal of Comparative Neurology*, 521(15), 3524–3540.

Mak, A. C., Szeto, I. Y., Fritzsch, B., & Cheah, K. S. (2009). Differential and overlapping expression pattern of SOX2 and SOX9 in inner ear development. *Gene Expression Patterns*, 9 (6), 444–453.

Mao, Y., Reiprich, S., Wegner, M., & Fritzsch, B. (2014). Targeted deletion of Sox10 by Wnt1–cre defects neuronal migration and projection in the mouse inner ear. *PLoS One*, 9(4), e94580.

Marovitz, W. F., Khan, K. M., & Schulte, T. (1977). Ultrastructural development of the early rat otocyst. *Annals of Otology, Rhinology, and Laryngology*, 86(1 Pt 2 Supplement 35), 9–28.

Matei, V., Pauley, S., Kaing, S., Rowitch, D., Beisel, K. W., Morris, K., Feng, F., Jones, K., Lee, J., & Fritzsch, B. (2005). Smaller inner ear sensory epithelia in Neurog 1 null mice are related to earlier hair cell cycle exit. *Developmental Dynamics*, 234(3), 633–650.

McCormick, C. A., & Wallace, A. C. (2012). Otolith end organ projections to auditory neurons in the descending octaval nucleus of the goldfish, *Carassius auratus*: A confocal analysis. *Brain, Behavior and Evolution*, 80(1), 41–63.

Molea, D., & Rubel, E. W. (2003). Timing and topography of nucleus magnocellularis innervation by the cochlear ganglion. *Journal of Comparative Neurology*, 466(4), 577–591.

Morris, J. K., Maklad, A., Hansen, L. A., Feng, F., Sorensen, C., Lee, K. F., Macklin, W. B., & Fritzsch, B. (2006). A disorganized innervation of the inner ear persists in the absence of ErbB2. *Brain Research*, 1091(1), 186–199.

Morsli, H., Choo, D., Ryan, A., Johnson, R., & Wu, D. K. (1998). Development of the mouse inner ear and origin of its sensory organs. *Journal of Neuroscience*, 18(9), 3327–3335.

Nadol, J. B., Jr. (1988). Quantification of human spiral ganglion cells by serial section reconstruction and segmental density estimates. *American Journal of Otolaryngology*, 9(2), 47–51.

Neves, J., Kamaid, A., Alsina, B., & Giraldez, F. (2007). Differential expression of Sox2 and Sox3 in neuronal and sensory progenitors of the developing inner ear of the chick. *Journal of Comparative Neurology*, 503(4), 487–500.

Neves, J., Parada, C., Chamizo, M., & Giraldez, F. (2011). Jagged 1 regulates the restriction of Sox2 expression in the developing chicken inner ear: A mechanism for sensory organ specification. *Development*, 138(4), 735–744.

Neves, J., Abello, G., Petrovic, J., & Giraldez, F. (2013). Patterning and cell fate in the inner ear: A case for Notch in the chicken embryo. *Development Growth and Differentiation*, 55(1), 96–112.

Nichols, D. H., Pauley, S., Jahan, I., Beisel, K. W., Millen, K. J., & Fritzsch, B. (2008). Lmx1a is required for segregation of sensory epithelia and normal ear histogenesis and morphogenesis. *Cell and Tissue Research*, 334(3), 339–358.

Nishizaki, K., Anniko, M., Orita, Y., Karita, K., Masuda, Y., & Yoshino, T. (1998). Programmed cell death in the developing epithelium of the mouse inner ear. *Acta Oto-Laryngologica*, 118 (1), 96–100.

Ohyama, T., & Groves, A. K. (2004). Generation of Pax2–Cre mice by modification of a Pax2 bacterial artificial chromosome. *Genesis*, 38(4), 195–199.

Ohyama, T., Mohamed, O. A., Taketo, M. M., Dufort, D., & Groves, A. K. (2006). Wnt signals mediate a fate decision between otic placode and epidermis. *Development*, 133(5), 865–875.

Pan, N., Kopecky, B., Jahan, I., & Fritzsch, B. (2012). Understanding the evolution and development of neurosensory transcription factors of the ear to enhance therapeutic translation. *Cell and Tissue Research*, 349(2), 415–432.

Pan, W., Jin, Y., Stanger, B., & Kiernan, A. E. (2010). Notch signaling is required for the generation of hair cells and supporting cells in the mammalian inner ear. *Proceedings of the National Academy of Sciences of the USA*, 107(36), 15798–15803.

Pan, W., Jin, Y., Chen, J., Rottier, R. J., Steel, K. P., & Kiernan, A. E. (2013). Ectopic expression of activated notch or SOX2 reveals similar and unique roles in the development of the sensory cell progenitors in the mammalian inner ear. *Journal of Neuroscience*, 33(41), 16146–16157.

Pauley, S., Wright, T. J., Pirvola, U., Ornitz, D., Beisel, K., & Fritzsch, B. (2003). Expression and function of FGF10 in mammalian inner ear development. *Developmental Dynamics*, 227(2), 203–215.

Perkins, R. E., & Morest, D. K. (1975). A study of cochlear innervation patterns in cats and rats with the Golgi method and Nomarkski Optics. *Journal of Comparative Neurology*, 163(2), 129–158.

Philippidou, P., & Dasen, J. S. (2013). Hox genes: Choreographers in neural development, architects of circuit organization. *Neuron*, 80(1), 12–34.

Pirvola, U., Spencer-Dene, B., Xing-Qun, L., Kettunen, P., Thesleff, I., Fritzsch, B., Dickson, C., & Ylikoski, J. (2000). FGF/FGFR-2(IIIb) signaling is essential for inner ear morphogenesis. *Journal of Neuroscience*, 20(16), 6125–6134.

Popper, A. N., & Hoxter, B. (1984). Growth of a fish ear: 1. Quantitative analysis of hair cell and ganglion cell proliferation. *Hearing Research*, 15(2), 133–142.

Puligilla, C., Dabdoub, A., Brenowitz, S. D., & Kelley, M. W. (2010). Sox2 induces neuronal formation in the developing mammalian cochlea. *Journal of Neuroscience*, 30(2), 714–722.

Radde-Gallwitz, K., Pan, L., Gan, L., Lin, X., Segil, N., & Chen, P. (2004). Expression of Islet1 marks the sensory and neuronal lineages in the mammalian inner ear. *Journal of Comparative Neurology*, 477(4), 412–421.

Radosevic, M., Robert-Moreno, A., Coolen, M., Bally-Cuif, L., & Alsina, B. (2011). Her9 represses neurogenic fate downstream of Tbx1 and retinoic acid signaling in the inner ear. *Development*, 138(3), 397–408.

Raft, S., Nowotschin, S., Liao, J., & Morrow, B. E. (2004). Suppression of neural fate and control of inner ear morphogenesis by Tbx1. *Development*, 131(8), 1801–1812.

Raft, S., Koundakjian, E. J., Quinones, H., Jayasena, C. S., Goodrich, L. V., Johnson, J. E., Segil, N., & Groves, A. K. (2007). Cross-regulation of Ngn1 and Math1 coordinates the production of neurons and sensory hair cells during inner ear development. *Development*, 134(24), 4405–4415.

Rasmussen, A. T. (1940). Studies of the VIIIth cranial nerve of man. *The Laryngoscope*, 50(1), 67–83.

Rebillard, M., & Pujol, R. (1983). Innervation of the chicken basilar papilla during its development. *Acta Oto-Laryngologica*, 96(5–6), 379–388.

Riccomagno, M. M., Takada, S., & Epstein, D. J. (2005). Wnt-dependent regulation of inner ear morphogenesis is balanced by the opposing and supporting roles of Shh. *Genes and Development*, 19(13), 1612–1623.

Romand, M. R., & Romand, R. (1990). Development of spiral ganglion cells in mammalian cochlea. *Journal of Electron Microscopy Technique*, 15(2), 144–154.

Romand, R., Dolle, P., & Hashino, E. (2006). Retinoid signaling in inner ear development. *Journal of Neurobiology*, 66(7), 687–704.

Ronan, J. L., Wu, W., & Crabtree, G. R. (2013). From neural development to cognition: Unexpected roles for chromatin. *Nature Revies Genetics*, 14(5), 347–359.

Ruben, R. J. (1967). Development of the inner ear of the mouse: A radioautographic study of terminal mitoses. *Acta Oto-Laryngologica Supplementum*, 220, 221–244.

Sandell, L. L., Butler Tjaden, N. E., Barlow, A. J., & Trainor, P. A. (2014). Cochleovestibular nerve development is integrated with migratory neural crest cells. *Developmental Biology*, 385 (2), 200–210.

Sapede, D., & Pujades, C. (2010). Hedgehog signaling governs the development of otic sensory epithelium and its associated innervation in zebrafish. *Journal of Neuroscience*, 30(10), 3612–3623.

Sapede, D., Dyballa, S., & Pujades, C. (2012). Cell lineage analysis reveals three different progenitor pools for neurosensory elements in the otic vesicle. *Journal of Neuroscience*, 32 (46), 16424–16434.

Satoh, T., & Fekete, D. M. (2005). Clonal analysis of the relationships between mechanosensory cells and the neurons that innervate them in the chicken ear. *Development*, 132(7), 1687–1697.

Schmidt, J. M. (1985). Cochlear neuronal populations in developmental defects of the inner ear. Implications for cochlear implantation. *Acta Oto-Laryngologica*, 99(1–2), 14–20.

Schwanbeck, R., Martini, S., Bernoth, K., & Just, U. (2011). The Notch signaling pathway: Molecular basis of cell context dependency. *European Journal of Cell Biology*, 90(6–7), 572–581.

Sher, A. (1972). The embryonic and postnatal development of the inner ear of the mouse. *Acta Oto-Laryngologica Supplementum*, 285, 1–77.

Spoendlin, H. (1972). Innervation densities of the cochlea. *Acta Oto-Laryngologica*, 73(2), 235–248.

Spoendlin, H., & Schrott, A. (1989). Analysis of the human auditory nerve. *Hearing Research*, 43 (1), 25–38.

Stevens, C. B., Davies, A. L., Battista, S., Lewis, J. H., & Fekete, D. M. (2003). Forced activation of Wnt signaling alters morphogenesis and sensory organ identity in the chicken inner ear. *Developmental Biology*, 261(1), 149–164.

Streeter, G. L. (1906). On the development of the membranous labyrinth and the acoustic and facial nerves in the human embryo. *American Journal of Anatomy*, 6(1), 139–165.

Taberner, A. M., & Liberman, M. C. (2005). Response properties of single auditory nerve fibers in the mouse. *Journal of Neurophysiology*, 93(1), 557–569.

Varela-Nieto, I., Morales-Garcia, J. A., Vigil, P., Diaz-Casares, A., Gorospe, I., Sanchez-Galiano, S., Canon, S., Camarero, G., Contreras, J., Cediel, R., & Leon, Y. (2004). Trophic effects of insulin-like growth factor-I (IGF-I) in the inner ear. *Hearing Research*, 196(1–2), 19–25.

Vazquez-Echeverria, C., Dominguez-Frutos, E., Charnay, P., Schimmang, T., & Pujades, C. (2008). Analysis of mouse kreisler mutants reveals new roles of hindbrain-derived signals in the establishment of the otic neurogenic domain. *Developmental Biology*, 322(1), 167–178.

Vemaraju, S., Kantarci, H., Padanad, M. S., & Riley, B. B. (2012). A spatial and temporal gradient of Fgf differentially regulates distinct stages of neural development in the zebrafish inner ear. *PLoS Genetics*, 8(11), e1003068.

Wang, S. Z., Ibrahim, L. A., Kim, Y. J., Gibson, D. A., Leung, H. C., Yuan, W., Zhang, K. K., Tao, H. W., Ma, L., & Zhang, L. I. (2013). Slit/Robo signaling mediates spatial positioning of spiral ganglion neurons during development of cochlear innervation. *Journal of Neuroscience*, 33(30), 12242–12254.

Weisz, C., Glowatzki, E., & Fuchs, P. (2009). The postsynaptic function of type II cochlear afferents. *Nature*, 461(7267), 1126–1129.

White, P. M., Doetzlhofer, A., Lee, Y. S., Groves, A. K., & Segil, N. (2006). Mammalian cochlear supporting cells can divide and trans-differentiate into hair cells. *Nature*, 441(7096), 984–987.

Whitehead, M. C., & Morest, D. K. (1981). Dual populations of efferent and afferent cochlear axons in the chicken. *Neuroscience*, 6(11), 2351–2365.

Whitehead, M. C., & Morest, D. K. (1985). The development of innervation patterns in the avian cochlea. *Neuroscience*, 14(1), 255–276.

Wikstrom, S. O., & Anniko, M. (1987). Early development of the stato-acoustic and facial ganglia. *Acta Oto-Laryngologica*, 104(1–2), 166–174.

Wong, E. Y., Ahmed, M., & Xu, P. X. (2013). EYA1–SIX1 complex in neurosensory cell fate induction in the mammalian inner ear. *Hearing Research*, 297, 13–19.

Wood, H. B., & Episkopou, V. (1999). Comparative expression of the mouse Sox1, Sox2 and Sox3 genes from pre-gastrulation to early somite stages. *Mechanisms of Development*, 86(1–2), 197–201.

Woods, C., Montcouquiol, M., & Kelley, M. W. (2004). Math1 regulates development of the sensory epithelium in the mammalian cochlea. *Nature Neuroscience*, 7(12), 1310–1318.

Wright, T. J., & Mansour, S. L. (2003a). FGF signaling in ear development and innervation. *Current Topics in Developmental Biology*, 57, 225–259.

Wright, T. J., & Mansour, S. L. (2003b). Fgf3 and Fgf10 are required for mouse otic placode induction. *Development*, 130(15), 3379–3390.

Wu, D. K., Nunes, F. D., & Choo, D. (1998). Axial specification for sensory organs versus non-sensory structures of the chicken inner ear. *Development*, 125(1), 11–20.

Wu, L. Q., & Dickman, J. D. (2011). Magnetoreception in an avian brain in part mediated by inner ear lagena. *Current Biology*, 21(5), 418–423.

Xu, H., Viola, A., Zhang, Z., Gerken, C. P., Lindsay-Illingworth, E. A., & Baldini, A. (2007). Tbx1 regulates population, proliferation and cell fate determination of otic epithelial cells. *Developmental Biology*, 302(2), 670–682.

Yagi, H., Furutani, Y., Hamada, H., Sasaki, T., Asakawa, S., Minoshima, S., Ichida, F., Joo, K., Kimura, M., Imamura, S., Kamatani, N., Momma, K., Takao, A., Nakazawa, M., Shimizu, N., & Matsuoka, R. (2003). Role of TBX1 in human del22q11.2 syndrome. *Lancet*, 362(9393), 1366–1373.

Yang, H., Xie, X., Deng, M., Chen, X., & Gan, L. (2010). Generation and characterization of Atoh1–Cre knock-in mouse line. *Genesis*, 48(6), 407–413.

Yang, T., Kersigo, J., Jahan, I., Pan, N., & Fritzsch, B. (2011). The molecular basis of making spiral ganglion neurons and connecting them to hair cells of the organ of Corti. *Hearing Research*, 278(1–2), 21–33.

Yntema, C. L. (1937). An experimental study of the origin of the cells which constitute the VIIth and VIIIth cranial ganglia and nerves in the embryo of *Amblystoma punctatum*. *Journal of Experimental Zoology*, 75(1), 75–101.

Yu, W. M., Appler, J. M., Kim, Y. H., Nishitani, A. M., Holt, J. R., & Goodrich, L. V. (2013). A Gata3–Mafb transcriptional network directs post-synaptic differentiation in synapses specialized for hearing. *Elife*, 2, e01341.

Zentner, G. E., Hurd, E. A., Schnetz, M. P., Handoko, L., Wang, C., Wang, Z., Wei, C., Tesar, P. J., Hatzoglou, M., Martin, D. M., & Scacheri, P. C. (2010). CHD7 functions in the nucleolus as a positive regulator of ribosomal RNA biogenesis. *Human Molecular Genetics*, 19(18), 3491–3501.

Zhang, N., Martin, G. V., Kelley, M. W., & Gridley, T. (2000). A mutation in the Lunatic fringe gene suppresses the effects of a Jagged2 mutation on inner hair cell development in the cochlea. *Current Biology*, 10(11), 659–662.

Zheng, W., Huang, L., Wei, Z. B., Silvius, D., Tang, B., & Xu, P. X. (2003). The role of Six1 in mammalian auditory system development. *Development*, 130(17), 3989–4000.

Zhou, X., & Van De Water, T. R. (1987). The effect of target tissues on survival and differentiation of mammalian statoacoustic ganglion neurons in organ culture. *Acta Oto-Laryngologica*, 104 (1–2), 90–98.

Zou, D., Silvius, D., Fritzsch, B., & Xu, P. X. (2004). Eya1 and Six1 are essential for early steps of sensory neurogenesis in mammalian cranial placodes. *Development*, 131(22), 5561–5572.

Zou, D., Erickson, C., Kim, E. H., Jin, D., Fritzsch, B., & Xu, P. X. (2008). Eya1 gene dosage critically affects the development of sensory epithelia in the mammalian inner ear. *Human Molecular Genetics*, 17(21), 3340–3356.

Zweier, C., Sticht, H., Aydin-Yaylagul, I., Campbell, C. E., & Rauch, A. (2007). Human TBX1 missense mutations cause gain of function resulting in the same phenotype as 22q11.2 deletions. *American Journal of Human Genetics*, 80(3), 510–517.

Chapter 3
Neurotrophic Factor Function During Ear Development: Expression Changes Define Critical Phases for Neuronal Viability

Bernd Fritzsch, Jennifer Kersigo, Tian Yang, Israt Jahan and Ning Pan

Keywords Brain-derived neurotrophic factor · Cell death · Cochlea · Ear development · Expression changes · Neuronal loss · Neurotrophins · Neurotrophin 3 · Neurotrophin tyrosine kinase 2 (Ntrk2 or TrkB) · TrkC · Ntrk3 or Trkc

3.1 Introduction

Neurosensory development leads to quantitative matching of two populations of neurons and their connections for optimized information processing. Data from multiple developing systems indicate that numerical matching requires a two-step process. The first step generates the initial number of neurons or sensory cells of both populations through independently regulated proliferation. The second step matches the cell numbers by eliminating about 50 % of supernumerary neurons through programmed cell death and fine tunes connections by pruning of aberrant projections (Oppenheim, 1991). These generative and degenerative developmental steps constitute the basis of the neurotrophic theory (Oppenheim, 1989). This theory assumes that numerical matching and pruning of aberrant projections is mediated by competition for the limited access to trophic factors. Many of these

B. Fritzsch (✉) · J. Kersigo · T. Yang · I. Jahan · N. Pan
Department of Biology, University of Iowa, Iowa City, IA 52242, USA
e-mail: bernd-fritzsch@uiowa.edu

J. Kersigo
e-mail: jennifer-kersigo@uiowa.edu

T. Yang
e-mail: tian-yang@uiowa.edu

I. Jahan
e-mail: israt-jahan@uiowa.edu

N. Pan
e-mail: ning-pan@uiowa.edu

A. Dabdoub et al. (eds.), *The Primary Auditory Neurons of the Mammalian Cochlea*, Springer Handbook of Auditory Research 52,
DOI 10.1007/978-1-4939-3031-9_3

ideas were originally developed to explain the effects of embryonic ear manipulations on the developing brain (Levi-Montalcini, 1949) and have now been expanded to include the molecular basis of these interactions in the ear and elsewhere (Rubel & Fritzsch, 2002; Dekkers et al., 2013).

This chapter provides a historical overview of the trophic interactions in the embryonic sculpting of ear connections followed by an analysis of the predictions of the neurotrophic theory of numerical matching through cell death and pruning for the fine tuning of inner ear connection development. In particular, the role played by the molecularly well-characterized neurotrophic factors released from sensory epithelia to prevent cell death of spiral and vestibular ganglion neurons and guide their developing projections will be discussed. Spiral and vestibular ganglion neurons develop in the ear, migrate to their final positions, and establish specific connections to both their peripheral targets [the organ of Corti and the five vestibular sensory epithelia (Lewis et al., 1985; Fritzsch et al., 2013)] and central targets [the cochlear and vestibular nuclei of the brain stem] to process sound and vestibular inputs (Nayagam et al., 2011; Straka et al., 2014). The establishment of these projections for information processing is likely to involve multiple levels of molecular guidance cues (see Chap. 2 by Goodrich), comparable to those required for the "fine tuning" in the visual system (Triplett, 2014), but also the neurotrophins for neuronal survival, process guidance and pruning (Yang et al., 2011). In addition, this chapter explores yet to be fully defined mechanisms through which sensory neurons affect both central and peripheral target cell viability. Overall, trophic support via known and unknown factors play distinct roles at different stages of development and in aging, with the trophically supported viability of sensory neurons being center stage throughout a vertebrate's life.

3.1.1 Embryonic Development: Historical Overview Leading to the Neurotrophic Theory

The first evidence for a dependency of inner ear related neurons on unknown factors was provided by the late Nobel laureate Rita Levi-Montalcini (Levi-Montalcini, 1949). In her seminal paper, Levi-Montalcini showed that auditory nucleus neurons in the brain stem of chickens depend on inner ear innervation for normal development, whereas only one vestibular nucleus showed similar dependency on innervation. She later went on to discover the neurotrophin nerve growth factor (NGF), which became the basis for her Nobel Prize in 1986. Her earlier work on inner ear development was continued by others (Benes et al., 1977; Peusner & Morest 1977; Fritzsch, 1981).

Forty years after Levi-Montalcini's (1949) paper, the neurotrophic theory was formulated, claiming that neuronal cell death is a way to regulate survival of neurons to numerically match interacting populations. The neurotrophic theory assumes that neurons compete for access to neurotrophic supply provided by their target (Oppenheim, 1991). Naturally occurring "programmed" cell death was

conjectured to adjust the number of neurons to the available target support by preventing cell death of those neurons that are appropriately connected, killing misconnected neurons. Exaggerated cell death induced by peripheral manipulations, such as removal of the entire inner ear or the cochlea alone, was considered to expand the naturally occurring cell death, possibly following the same principles. Meanwhile, one family of neurotrophins and their receptors (Fig. 3.1) have been characterized through targeted deletion in ear development (Ernfors et al., 1995; Fritzsch et al., 2004). Other neurotrophic factors that play a role in neuronal survival through the prevention of naturally occurring or induced cell death have been identified (Lindholm & Saarma, 2010; Dekkers et al., 2013), but these factors seem to play little role in embryonic ear development.

More recently it has become clear that the original formulation of the neurotrophic theory, meant to explain how neurotrophins regulate the viability of properly connected neurons for normal function of the adult system, was too simple. Some receptors play dual roles as "dependence receptors": They are death promoting,

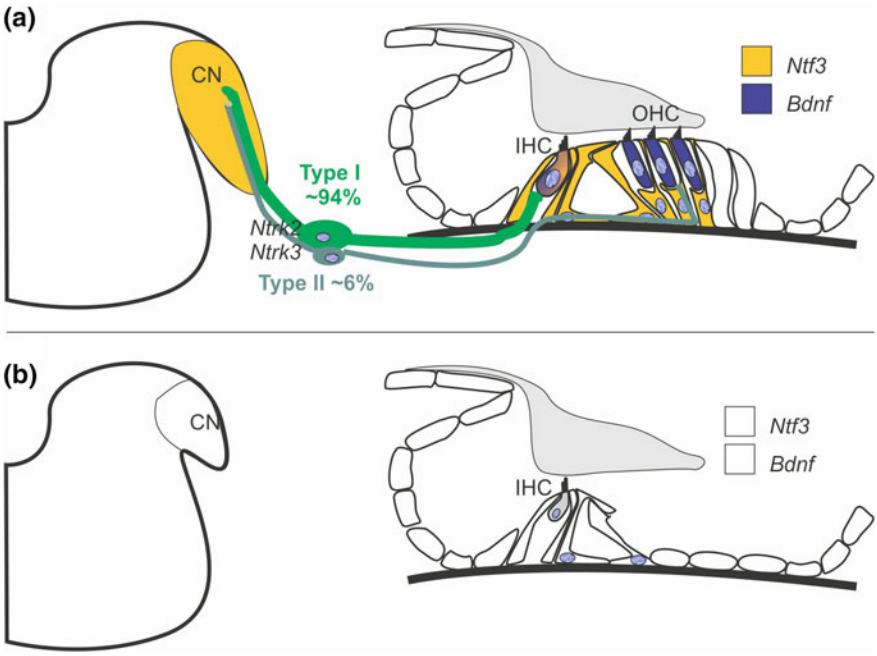

Fig. 3.1 Overview of neurotrophin expression and effects of neurotrophin loss. Two neurotrophins, *Bdnf* and *Ntf3*, are expressed in the developing organ of Corti. *Bdnf* is nearly exclusively found in hair cells and *Ntf3* mostly in supporting cells but also IHCs (**a**). *Ntf3* is also expressed in the developing cochlear nuclei (CN). Two types of spiral ganglion neurons (type I, type II) project to IHCs and OHCs, respectively, and coexpress the two neurotrophin receptors, *Ntrk2* and *Ntrk3*. **b** Loss of either both neurotrophins or both neurotrophin receptors results in complete loss of all spiral ganglion neurons at birth, reduction in cochlear nucleus size, and, after several months, loss of OHCs followed by loss of IHCs

pro-apoptotic without neurotrophins, but prevent death with neurotrophins (Taylor et al., 2012; Dekkers et al., 2013). Moreover, even deletion of two neurotrophins has only a very limited effect on the central nervous system (CNS) (Fritzsch et al., 1997c), indicating that perhaps CNS cell death is not regulated the same way as in the peripheral nervous system (PNS) (Dekkers & Barde, 2013). These new insights suggest not only that the neurotrophic theory may have limited value for the CNS but also that even in the developing PNS many examples do not fit well to the theory. As will be apparent in the narrative that follows, ear development superficially fits the neurotrophic theory. Closer examination reveals, however, that neither correction of misguided afferents through elimination of parental neurons or pruning, nor an easy numerical correlation of afferents to target hair cells, occurs in the ear.

The molecular basis supporting the viability of sensory neurons by the developing sensory epithelia of the inner ear has been clarified through targeted mutational analysis in mice. Genetic ablation of two neurotrophic factor genes or their two receptors (Fig. 3.1) rapidly kills all sensory neurons during embryonic development (Ernfors et al., 1995; Fritzsch et al., 1997c). In contrast to molecular understanding of neuronal dependency on factors released by sensory epithelia, progress in understanding the molecular basis of cochlear nuclei dependency on afferents has been limited. It has been suggested that cochlear nucleus neurons depend on either transmitter release and/or co-release of yet to be determined substance(s) from spiral ganglion neurons for survival (Rubel & Fritzsch, 2002). In addition, neurons of one vestibular nucleus of birds (Shao et al., 2009), but not of several other vestibular nuclei in birds and mammals, critically depend on inner ear afferents for survival. Even those vestibular and cochlear nuclei that show induced cell death on denervation lose fewer than 50 % of all neurons, comparable to other developing systems (Oppenheim, 1991). This limited effect of denervation on central nuclei contrasts sharply with loss of neurotrophins on ganglion neurons: all vestibular and spiral ganglion neurons degenerate after genetically engineered removal of both neurotrophin factors or receptors (Yang et al., 2011).

To complicate matters further, mice genetically engineered to be unable to release synaptic or dense core vesicles (Fig. 3.2) through the mutation of proteins needed for vesicle docking show normal assembly and synapse formation in the absence of any vesicular release (Verhage et al., 2000; Varoqueaux et al., 2002). Importantly, dense core vesicles are believed to store and release neurotrophins (Kuczewski et al., 2009; van de Bospoort et al., 2012), in particular pro-forms (Dieni et al., 2012). In vesicular docking defected mutants, there is a phase of enhanced neurodegeneration (Verhage et al., 2000), and neurotrophins can offset the neuronal loss for some time (Heeroma et al., 2004), arguing that the cell death in these mutant mice may be caused by other intracellular functions such as intracellular vesicular fusion to Golgi cisternae (Ma et al., 2013). This conclusion is further supported through data in related mutant mice that have no synaptic transmitter release, show no enhanced cell death, but do show normal development of the brain until birth as well as normal synaptogenesis in postnatal brain tissue culture (Varoqueaux et al., 2002). Combined, the data on vesicular docking mutants

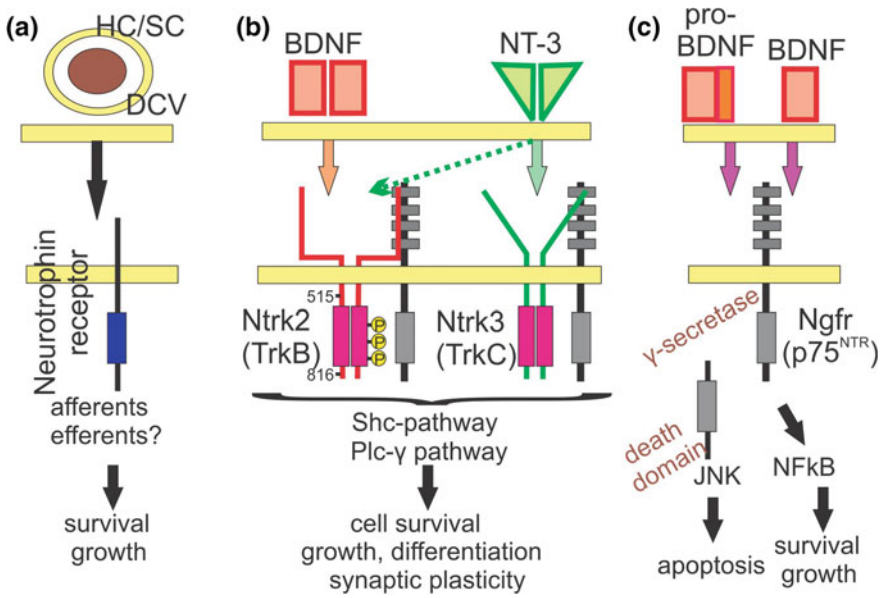

Fig. 3.2 Neurotrophin receptors, ligands, and functions. Neurotrophins are stored in dense core vesicles (DCV) in hair cells (HC) or supporting cells (SC) at or near a synapse and stimulate both survival and growth in innervating neurons (**a**). The ear expresses only two neurotrophins (BDNF, NT-3) that signal through their specific receptors (Ntrk2, Ntrk3, Ngfr) in a complex fashion (**b**). Some in vitro data suggest NT-3 signaling through Ntrk3 (*dotted arrows*). On dimerized ligand binding, Ntrk receptors activate a complex intracellular cascade via two pathways (Shc pathway, Plcγ pathway) to support cells by antagonizing the pro-apoptotic function of pro-BDNF, induce growth of cells and processes including some guidance, and play a role in synaptic plasticity. Pro-BDNF can bind to Ngfr to induce apoptosis via γ-secretase mediated cleaving of the intracellular death domain (**c**). Ngfr can also interact with tyrosine kinase receptors (Nrtk's) to support cell survival through interaction with mature BDNF (**c**). (Adopted from Panja & Bramham, 2014)

strongly support the notion that during embryonic development there is little evidence for activity mediated fine-tuning of connections facilitated by vesicular release. Deletion of vesicular docking proteins only in sensory neurons is needed to verify that connection development can progress without vesicle release. Such mutant mice should demonstrate postnatal neuronal loss comparable to cochlear ablation (Harris & Rubel, 2006). Depending on the outcome of such an experiment, it might be necessary to reconcile possibly conflicting data with the prevailing view and interpretation in the current literature on the role of activity dependency mediated by vesicle release (Marrs & Spirou, 2012). In summary, neuronal activity of cochlear afferents leading to glutamate release, possibly paired with co-release of dense core vesicles containing an unknown factor(s), may be the basis of afferent support of cochlear nuclei (Rubel & Fritzsch, 2002).

Much like removal of the cochlea has demonstrated the dependency of cochlear nuclei neurons on afferents (Levi-Montalcini, 1949; Harris & Rubel, 2006), transplantation experiments (Ard et al., 1985; Zhou & Van de Water, 1987) and

Table 3.1 Nomenclature and abbreviations used throughout this text combined with a summary of effects of genetic deletion

Gene (mouse)	Aliases	Description	Function revealed by embryonic elimination of the gene
Atoh1	*Math1*	Atonal homolog 1	Loss of development of all hair cells
Bdnf	*BDNF*	Brain-derived neurotrophic factor	Loss of canal crista innervation, reduction of innervation to apex
Ngf	*NGF*	Nerve growth factor	No loss in the ear, loss of autonomic ganglia
Ngfr	*p75NTR*	Nerve growth factor receptor	No loss in the ear, reduced motoneuron death
Ntf3	*NT-3*	Neurotrophin 3	No loss in the vestibular system, loss of basal turn spiral ganglion neurons
Ntf4	*NT-4*	Neurotrophin 4	No loss in the ear, some loss of epibranchial placode derived ganglia
Ntrk1	*TrkA*	Neurotrophic tyrosine kinase, receptor type 1	No loss in the ear, loss of autonomic ganglia
Ntrk2	*TrkB*	Neurotrophic tyrosine kinase, receptor type 2	Loss of canal crista innervation, reduction of innervation to apex
Ntrk3	*TrkC*	Neurotrophic tyrosine kinase, receptor type 3	No loss in the vestibular system, loss of basal turn spiral ganglion neurons
Plcg1	*PLC-γ*	Phospholipase C, gamma 1	Reduced and misguided innervation of the vestibular system
Pou4f3	*Brn3c*	POU domain, class 4, Transcription factor 3	Delayed loss of all differentiated hair cells
Shc1	*SHC*	Src homology 2 domain transforming protein 1	Reduced and misguided innervation of the vestibular system
Sox2	*Lcc*	SRY (sex determining region Y)-box 2	Loss of all sensory epithelia development of the ear

selective deletion of cochlear nucleus neurons (Maricich et al., 2009) indicate that cochlear nuclei support sensory neurons in addition to their support from their peripheral targets. These data suggest that inner ear ganglion neurons are not exclusively dependent on the periphery (i.e., sensory epithelia support sensory neurons which support central neurons) but participate in a more complex interaction involving possible feedback loops whereby both central neurons and sensory epithelia provide support, in turn supported by neurons. Although it is clear that many cochlear nucleus neurons depend on innervation for their viability during a critical phase (Harris & Rubel, 2006), recent data suggest that some cochlear hair cells may also depend on innervation for their long-term maintenance (Kersigo & Fritzsch, 2015). Unfortunately, although retrograde signaling from the target cells across synapses to presynaptic neurons is the most studied signal in the CNS in the context of synaptic plasticity (Panja & Bramham, 2014), such retrograde signals have rarely been considered in the ear (Maricich et al., 2009; Singer et al., 2014).

Nomenclature and abbreviations used throughout this text combined with a summary of effects of genetic deletion are given in Table 3.1.

3.2 Evolution of Neurotrophins and Their Receptors

As indicated in the introduction, neurotrophins and their receptors are essential for the maintenance of inner ear innervation. Neurotrophins belong to a family of excreted proteins (Hallbook, 1999) that bind as ligands to a set of tyrosine kinase receptors (Hallbook et al., 2006) and the Ngfr ($p75^{NTR}$) receptor (Bothwell, 2006). The tyrosine kinase receptors mediate their intracellular effects through a phosphorylation cascade (Fig. 3.2) that is integral to promote cell survival and synaptic plasticity (Sciarretta et al., 2010; Bramham & Panja, 2014). Although mammalian nerve growth factor (*Ngf*) was the first ligand to be isolated and characterized, the later discovered brain-derived nerve growth factor (*Bdnf*) was subsequently found to be closer to the ancestral neurotrophic ligand out of which the others apparently evolved through gene duplication and mutational diversification (Hallbook, 1999). *Bdnf* doubled again and these duplications evolved into neurotrophin 3 (*Ntf3*) and *Ngf* respectively. A later, additional duplication of *Bdnf* generated neurotrophin 4 (*Ntf4*). Bony fishes, with their additional duplication of the whole genome, have several additional neurotrophins. Most interestingly, the expression of *bdnf* in lampreys is in hair cells of the inner ear (Hallbook et al., 1998), much like in other vertebrates (Pirvola et al., 1992; Farinas et al., 2001), suggesting a historic involvement of this neurotrophin with vertebrate inner ear innervation.

The receptor for BDNF, neurotrophin tyrosine kinase 2 (*Ntrk2* or *TrkB*), appears to be close to the ancestral receptor. The neurotrophin tyrosine kinase 1 receptor (Ntrk1 or TrkA) that binds Ngf and the neurotrophin tyrosine kinase 3 receptor (Ntrk3 or TrkC) that binds NT-3 formed through duplications (Hallbook et al., 2006). In contrast to the ligands, the receptors duplicated only twice and BDNF and NT-4 both signal through the Ntrk2 receptor. In addition, both *Ntrk2* and *Ntrk3* receptors can produce, by alternative splicing of unique exons, a number of different receptor genes isoforms, including some without an intracellular tyrosine kinase domain used for the canonical signaling. While experimental work has verified that Ntrk2 has indeed only two docking sites on amino acid 515 and 816 (Fig. 3.2) that provide for the intracellular cascade leading to neuronal survival and fiber growth (Sciarretta et al., 2010), docking on amino acid 478 plays additional roles in Ntrk2 signaling (Miyamoto et al., 2006). Likewise, in addition to its pro-survival function, Ntrk3 has additional effects on nerve fiber growth via activation by one of its truncated receptor isoforms (Esteban et al., 2006).

The Ngfr ($p75^{NTR}$) receptor has a different structure and function compared to the Ntrk receptors (Bothwell, 2006). Although all neurotrophins can signal through this receptor, it is the unprocessed, pro-form of BDNF that appears to be the preferred ligand of Ngfr, collaborating with the co-receptor sortilin for binding (Dekkers et al., 2013). In many systems, the Ngfr receptor, activated by pro-BDNF, acts in a pro-apoptotic way to stimulate cell death and appears to be responsible for some motoneuron death (Taylor et al., 2012). In contrast, mature BDNF binds with higher affinity to Ntrk2 and is clearly anti-apoptotic to rescue neurons as further explained in Sect. 3.3 (Fig. 3.2).

In summary, *Bdnf* and its *Ntrk2* receptor are found in all vertebrates associated with hair cell/sensory neurons and may be close to the ligand–receptor pairing that evolved in early vertebrates, when the single neurosensory cell diversified into a sensory neuron/hair cell pair (Lindholm & Saarma, 2010; Pan et al., 2012b). In contrast, *Ntf3* is associated with supporting cells and some hair cells only in the developing mammalian ear whereas its receptor *Ntrk3* is already found in the ear-of nonmammals (Pirvola et al., 1997). Neither *Ntf4*, *Ngf*, nor the *Ngf* receptor, *Ntrk1*, is found in measurable levels in the embryonic ear (Pirvola et al., 1992) and seem to have no role compared to the effects of *Bdnf*/*Ntf3* or *Ntrk2*/*Ntrk3* With this conceptual framework of the role of trophic factors in the support of ear innervation in mind (Figs. 3.1 and 3.2), Sect. 3.3 explores how neurons are supported by and support their central and peripheral targets.

3.3 Embryonic Dependency of Spiral Ganglion Cells on the Cochlea

The vestibular/auditory system of chicken has a natural cell death phase with a loss of about 25 % of inner ear neurons between embryonic days 8 and 14 (E8–14) (Ard & Morest, 1984), about 6 days after the first afferent fibers enter the brain (Fritzsch et al., 1993). This loss partially overlaps with the phase during which central auditory and vestibular nuclei are particularly sensitive to loss of innervation in the chicken (Peusner & Morest, 1977; Rubel & Fritzsch, 2002). This sensitivity on innervation of auditory nuclei seems to continue after hatching (Born & Rubel, 1985). In the rat, degenerating spiral ganglion neurons are most frequent between E18 and E19 (Nikolic et al., 2000), resulting in a loss of approximately 20 % of neurons (Stenqvist et al., 2005). A possible additional loss of 22 % of spiral ganglion neurons (Rueda et al., 1987) occurs in early postnatal mammals when central auditory neurons are particularly vulnerable to loss of innervation (Harris & Rubel, 2006). Experimental data in mice and chicken show that inner ear neurons depend on support from both the hindbrain and the ear, with a combination of both tissues providing the best support (Ard et al., 1985; Zhou & Van de Water, 1987). These developmental data suggest a natural delay of several days between terminal mitosis of sensory neurons and hair cells (Ruben, 1967) and naturally occurring cell death in sensory neurons. Hair cells seem to develop without cell death (Nikolic et al., 2000) even in the absence of all afferents (Ma et al., 2000). Overall, these data fit the neurotrophic theory well, indicating that one population remains constant (hair cells) whereas the projecting ganglion neurons numerically adjusted by about 50 % cell death, much like in many other developing systems (Oppenheim, 1991).

In contrast to these descriptive developmental data, induced neuronal cell death caused by loss of neurotrophins is happening much earlier (Farinas et al., 2001), indicating a limited temporal overlap of natural and experimentally induced cell death. Despite this temporal discrepancy, targeted deletion of neurotrophins or their

receptors show that neurotrophic factors, thought to be released primarily from the developing sensory epithelia, are essential for spiral and vestibular ganglion cell survival (Ernfors et al., 1995; Yang et al., 2011; Kersigo & Fritzsch, 2015). Additional support for such a prominent dependency role of sensory neurons on the peripheral target comes from data showing a severe reduction of spiral ganglion neurons in the absence of organ of Corti development (Fritzsch et al., 2005c; Pan et al., 2011). Interestingly enough, the effects caused by the removal of hair cells of the organ of Corti are less profound in terms of embryonic loss of sensory neurons compared to loss of neurotrophins. This suggests that during embryonic development the neurotrophins are all that is needed for neuronal maintenance of cochlear innervation and beyond that, there is no additional support provided by the hair cells or supporting cells. Because all of these effects happen at a time when afferents are growing to the undifferentiated hair cells, there is no possible involvement of synaptic transmission via glutamatergic receptors. In summary, cell death caused by loss of neurotrophins occurs much earlier compared to the peak of natural cell death. In the ear, it is therefore questionable whether such induced cell death is comparable to naturally occurring cell death, which in mammals occurs up to a week later (Rueda et al., 1987; Farinas et al., 2001).

3.4 Embryonic Dependency of Cochlear Nucleus Neurons on Innervation

Whereas neurotrophic dependency of sensory neurons in the developing ear is 100 %, the dependency of cochlear and vestibular nucleus neurons shows dramatic variation in magnitude, onset, and progression after peripheral lesion (Peusner & Morest, 1977; Born & Rubel, 1985; Harris & Rubel, 2006). Even within a given species such as chicken, the magnitude of effects caused by lesions can vary between nearly 50 % in one nucleus to almost nothing in another. In mammals, the magnitude of cochlear nucleus loss depends on the species and the time of afferent lesion (Harris & Rubel, 2006). In addition, the onset of these effects coincides with the beginning of synaptogenesis and may be influenced by synapse formation. However, in some nuclei cell death starts before synaptogenesis (Peusner & Morest, 1977; Petralia et al., 1991; Rubel & Fritzsch, 2002), suggesting different dependence of certain neurons at different times. In fact, cell death shows a critical phase even in individual neurons after ear ablation (Elliott et al., 2015b).

Obviously, 60 years after the effects of loss of innervation on vestibular and cochlear nuclei were first described in the developing chicken (Levi-Montalcini, 1949), our detailed description has improved but our understanding of the variability within and between different nuclei of different species at different time points is still limited. Even within a given nucleus there is profound variation in the responses of individual neurons to the loss of afferents, ruling out simple explanations for dependency effects. New models are needed to clarify these effects at a

cellular and a molecular level. Beyond statistical effects across a large cohort of possibly molecularly different neurons reflecting different stages of development, such models should provide correlations of cell death and dendritic growth matching inner ear afferents with cellular gene expression profiles. Such correlative studies could be conducted in aquatic vertebrates as they have a pair of large, bilaterally symmetrical Mauthner cells (neurons that mediate the escape response or c-start) that respond with cell death and dendritic changes to loss of afferents at various times in development (Fritzsch, 1990; Elliott et al., 2015a, b).

3.5 Embryonic Dependency of Hair Cells on Innervation

Obviously, if neurons critically depend on neurotrophins released from hair cells and surrounding supporting cells (Fig. 3.1), one would expect that the initial development of hair cells should not depend on innervation and that hair cells drive, through neurotrophins, the matching of afferents as predicted by the neurotrophic theory (Oppenheim, 1991). Indeed, consistent with this prediction, numerous in vitro and in vivo studies have shown that during embryonic and some postnatal development, hair cells are independent of any innervation (Fritzsch et al., 1997c; Rusch et al., 1998; Ma et al., 2000). However, in other sensory systems such as the taste buds in mammals (Fritzsch et al., 1997b), the electroreceptive organs in fishes (Fritzsch et al., 1990), and the lateral line hair cells in salamanders (Jones & Singer, 1969), there is a variable dependency of the sensory cells on innervation with a fickle time constant. It cannot be ruled out that hair cells of the inner ear might depend on afferent and possibly efferent innervation in the long term as suggested in the very similar lateral line neuromast studies (Jones & Singer, 1969). Unfortunately, such long-term viability tests have not yet been conducted (Rusch et al., 1998), with the possible exception of primary neuropathy in which the etiology is mostly unknown and the loss of neurons may differ between ears (Buchman et al., 2006, 2011). As systemic deletion of neurotrophins or their *Ntrk* receptors is lethal, cell-type specific conditional deletion of either both *Bdnf* and *Ntf3* or both their receptors, *Ntrk2* and *Ntrk3*, is needed to generate viable mice without any sensory neurons to test the possible dependence of hair cells on innervation. Consistent with these suggestions are recent data on limited long-term hair cell viability after conditional deletion of both neurotrophins (Kersigo & Fritzsch, 2015).

3.6 Late Embryonic and Early Postnatal Development

The postnatal decline of the expression level of neurotrophins (Pirvola et al., 1992), with the exception of *Ntf3* in the inner hair cells (IHCs) (Pirvola et al., 1994), suggests that the major function of these ligands is during embryonic development.

Overall, the downregulation of neurotrophins relates closely to what has been referred to as the "critical phase" of postnatal development of cochlear nuclei (Harris & Rubel, 2006). Like cochlear nucleus neurons, it is possible that sensory neurons are becoming progressively less dependent on neurotrophin support as they age. Beyond the diminishing role of neurotrophins, there are other effects related to specific differentiation aspects of neurotrophins that are mostly covered in other chapters (see Chaps. 7 by Green et al. and 4 by Davis and Crozier). In Sect. 4.4.1 we outline only two major points of late embryonic and early neonatal function, allegedly associated with neurotrophins: fiber sorting and fiber branching as revealed by complete or targeted ligand deletion or misexpression.

3.6.1 *Sorting Two Types of Afferents to Two Types of Hair Cells*

All sensory epithelia of amniotes consist of two distinct hair cell types (Lewis et al., 1985). In the vestibular system these are type I and type II hair cells, distinguished by the presence or absence of calyx innervation (Rusch et al., 1998). These two types of hair cells can differentiate without any innervation (Ma et al., 2000). In contrast, the hair cell innervation by a calyx may depend on the level and distribution of neurotrophins, in particular BDNF, the main factor for ganglion neuron survival in the vestibular system (Ernfors et al., 1995). Indeed, calyx formation is disrupted in mutants missing one of the two intracellular pathways downstream of the Ntrk2 receptor for BDNF (Sciarretta et al., 2010). Likewise, the few remaining fibers in *Bdnf* null mice ($Bdnf^{-/-}$) show only occasional and partial formation of calyces indicating that the presence of BDNF, and to a lesser degree of NT-3, drives calyx formation. The process by which this is achieved is unclear, but it may relate to the well-known function of BDNF in long-term potentiation (LTP) plasticity in the developing and adult nervous system (Bramham & Panja, 2014).

The mammalian organ of Corti also has two distinct types of hair cells. In contrast to the random distribution of vestibular hair cell types, cochlear hair cell types are very orderly and differentially distributed into one row of inner hair cells (IHCs) and three rows of outer hair cells (OHCs). Each cochlear hair cell type is innervated by a different set of spiral ganglion neurons. Numerous theories have been proposed as to how the type I spiral ganglion afferents organize the innervation of 10–30 fibers on a single IHC and the growth of type II afferents to OHCs, innervating 20 or more OHCs by a single fiber (Simmons et al., 2011; Bulankina & Moser, 2012), including a possible function of neurotrophins and their receptors. Early work suggested a simple correlation: NT-3 and Ntrk2 regulate innervation to IHCs whereas BDNF and Ntrk2 regulate the innervation to OHCs (Ernfors et al., 1995; Schimmang et al., 1995). It remained unclear how such simple correlations can be reconciled with the overlapping expression of *Ntrk2* and *Ntrk3* in spiral ganglion neurons and of *Bdnf* in all hair cells (Pirvola et al., 1992; Ylikoski et al., 1993; Farinas et al., 2001). In contrast to these simple correlations of one

neurotrophin/neurotrophin receptor with a given pairing of spiral ganglion cell/hair cell type, other work showed a sophisticated change in expression (Fig. 3.3) during the growth of afferents (Fritzsch et al., 1995, 1997a). Follow-up work using mouse models with replacement of either *Ntf3* with *Bdnf* [$Ntf3^{tgBdnf}$ (Coppola et al., 2001; Tessarollo et al., 2004)] or *Bdnf* with *Ntf3* [$Bdnf^{tgNtf3}$ (Agerman et al., 2003)] revealed functional equivalence of BDNF and NT-3 during most inner ear innervation development. However, more recent work suggested that the differential density of IHC and OHC innervation may be related to quantitative expression differences of neurotrophins (Yang et al., 2011). It is possible that single IHC innervation by 10–30 type I spiral ganglion neurons may depend on the late embryonic coexpression of *Ntf3 and Bdnf* in IHCs. In contrast, type II fibers contact many OHCs, possibly to accumulate enough BDNF for viability. Clearly, either *Bdnf* (Farinas et al., 2001; Tessarollo et al., 2004) or *Ntf3* expression (Agerman et al., 2003) in OHCs can provide enough support to maintain type II fibers. However, neurotrophins are unlikely candidates to explain why these fibers grow to the outer compartment of the organ of Corti in the first place. Obviously, the high level of expression of both neurotrophins in and around IHCs (Fig. 3.3) would argue that they should remain in the inner compartment of the cochlea.

Nevertheless, the sorting of afferent fibers to various hair cell types has superficial resemblance to the basic assumption of the neurotrophic theory to achieve numerical matching of source and target (Oppenheim, 1991). However, closer examination reveals that simple numerical matching of fibers to target(s) is difficult to apply in the ear. In contrast to other developing systems, such as skeletal muscle fibers (Oppenheim, 1989), the ear shows variable ratios of afferents to hair cells, all seemingly related to the variable distribution of just two neurotrophins expressed during the time of fiber sorting in late embryos and early neonates:

1. In the vestibular system, there can be a 1:1 ratio of afferents to type I hair cells. Whereas calyces are found throughout the vestibular epithelia, calyces without afferent branches are associated with the striola region in the utricle and saccule (Desai et al., 2005b), which expresses *Ntf3* and *Bdnf* early in development (Farinas et al., 2001). It is conceivable that the coexpression of *Ntf3* and *Bdnf* allows this unusual 1:1 ratio to develop whereas afferents outside the coexpression zone of *Bdnf* and *Ntf3* form additional branches to many more hair cells [mixed afferents (Desai et al., 2005b)]. The formation of some calyces in *Bdnf* null mutants ($Bdnf^{-/-}$) as well as in *Ntrk2* point mutants [$Ntrk2^{PLC/PLC}$ (Sciarretta et al., 2010)] is consistent with this hypothesis.
2. In the vestibular type II hair cells and the OHCs of the organ of Corti, a single fiber can converge on multiple hair cells (Fritzsch, 2003; Desai et al., 2005a; Nayagam et al., 2011). This aspect is particularly difficult to reconcile with the neurotrophic theory as it indicates a highly variable numerical match or no obvious match at all.
3. In the IHCs of the organ of Corti, 10–30 or more type I afferent fibers converge onto a single IHC (Nayagam et al., 2011).

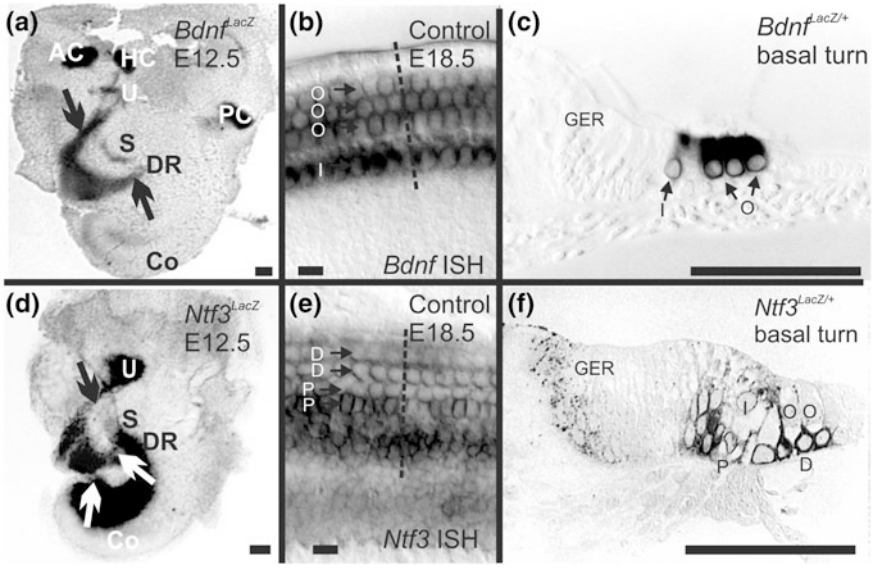

Fig. 3.3 Neurotrophin and neurotrophin receptor expression revealed by ß-galactosidase staining in *LacZ*-knockin mice and in situ hybridization. *Bdnf* is expressed early on in the three canal cristae (anterior crista, AC; horizontal crista, HC; posterior crista, PC); the early differentiating hair cells of the utricle (U) and saccule (S), and the apex of the cochlea (Co); and in delaminating neurons (*arrows* in **a**). Later *Bdnf* is primarily expressed in hair cells, with limited expression in supporting cells (**b**, **c**). In contrast, *Ntf3* is not expressed in early embryonic canal cristae but shows strong expression in the utricle, saccule and the basal turn of the cochlea as well as in delaminating neurons (*arrows* in **d**). In older mouse embryos, *Ntf3* is primarily expressed in supporting cells of the cochlea (**e**, **f**) and the IHCs (I) but not in the OHCs (O). D, Deiters' cells; DR, ductus reuniens; GER, greater epithelial ridge; P, pillar cell (Compiled after Farinas et al., 2001). *Bar* indicates 100 µm (**a**, **c**, **d**, **f**) and 20 µm (**b**, **e**)

Clearly, the highly variable innervation density of different inner ear hair cells conflicts with a simple quantitative afferent-to-target ratio sorting in the ear, as specified in the original formulation of the neurotrophic theory. Obviously, if multiple afferents can be supported by a single hair cell, there is no easy explanation why only a single afferent is supported by other hair cells and multiple hair cells are needed to support yet another set of afferents. However, the complex qualitative and quantitative expression of the two neurotrophic factors and their receptors could accommodate for such variable numerical ratios between fibers and hair cells. Further assessments combining conditional deletion with misexpression of neurotrophins (Agerman et al., 2003; Tessarollo et al., 2004) are needed to resolve these interactions beyond the limited available data supporting such a notion (Yang et al., 2011). Most recent data demonstrate that induced overshooting of afferents beyond areas of hair cells is not corrected through elimination of these fibers (Mao et al., 2014), indicating limits to redirecting misguided fibers in the ear, clearly not in agreement with the neurotrophic theory (Oppenheim, 1991). In summary, while

overall the ear appears to be an ideal system to establish the basic assumptions of the neurotrophic theory, the details uncovered thus far do not support that "programmed" cell death or pruning of fibers to eliminate aberrant projections is at all easily applicable in the ear.

3.6.2 *Promoting Branching and Targeting in the Cochlear Nuclei*

Both spiral ganglion fiber types terminate adjacent in the cochlear nucleus despite their very different peripheral distribution (Nayagam et al., 2011). Afferent growth into the cochlear nuclei occurs early and follows a simple temporal order: the basal spiral ganglion neurons become postmitotic first and reach the cochlear nucleus first, branching to reach all subdivisions (Fritzsch, 2003; Matei et al., 2005; Fritzsch et al., 2014). Consistent with other developing hindbrain sensory systems (Fritzsch et al., 1997b, 2005a), initial projection to cochlear nuclei develop prior to hair cell differentiation and can progress in their absence (Xiang et al., 2003). Although some immunocytochemical data suggest the presence of both neurotrophins at different times in the cochlear and vestibular nuclei, in situ hybridization shows that only *Ntf3* is expressed in the embryonic cochlear nuclei. Obviously, this neurotrophin could provide additional support to spiral ganglion afferents consistent with data indicating that the cochlear nuclei provide some neurotrophic support (Maricich et al., 2009). It is possible that the presence of neurotrophins in the target nuclei can affect the branching proportional to the overall vitality of neurons [better supported neurons branch more profusely (Elliott et al., 2015b)] as compared to more specific branching effects. In contrast, embryonic vestibular nucleus neurons seem to express very little if any neurotrophins, suggesting that expression of neurotrophins in the cochlear nucleus is unique to that nucleus and is possibly related to the unique molecular development of these nuclei, distinct from vestibular nuclei (Fritzsch et al., 2006; Duncan & Fritzsch, 2013). Deletion of neurotrophins only in the ear or only in the cochlear nucleus is needed to dissect the molecular basis of the sorting processes and to expand the role of neurotrophins in conjunction with spontaneous activity (Marrs & Spirou, 2012).

3.7 Embryonic Expression of Neurotrophins and Their Receptors

While embryonic viability of all inner ear neurons hinges on only two neurotrophins and their receptors (Ernfors et al., 1995; Fritzsch et al., 1997c), losing only one or the other neurotrophin or its receptor leads to complicated patterns of incomplete loss of inner ear neurons and complicated patterns of residual innervation (Fig. 3.4). Understanding the differential effects of spiral ganglion and vestibular neuronal loss is seemingly directly

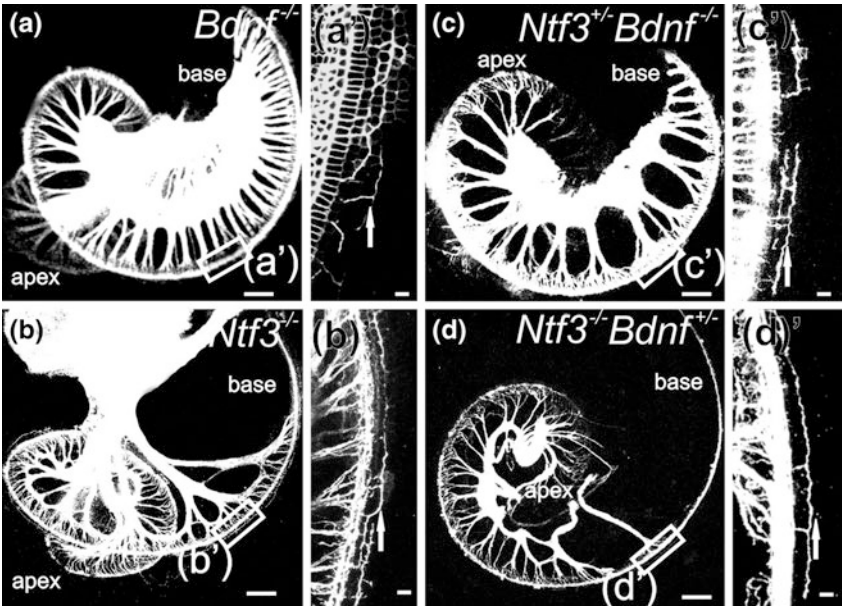

Fig. 3.4 Effects of single neurotrophin deletions and additive effects of haploinsufficiency of the second neurotrophin. Loss of *Bdnf* results in wider spacing of radial bundles in the apex but not base (**a**). Loss of *Ntf3* alone (**b**) or with a partial loss of *Bdnf* (**d**) results in complete loss of spiral ganglion neurons in the base with middle turn afferents spiraling along IHCs to the basal tip. Loss of *Bdnf* compounded with haploinsufficiency of *Ntf3* results in an exaggerated phenotype of $Bdnf^{-/-}$ with a variable, wider spacing radial fibers (RF) throughout the cochlea (**c**). Note that the innervation of OHCs is reduced in all mutants with the most profound reduction in *Ntf3* mutants (*arrows* in **a′**–**d′**). Bar = 100 μm (**a**–**d**) and 10 μm (**a′**–**d′**). (Modified after Yang et al., 2011)

related to the differential expression of the two neurotrophins (Fig. 3.3) that support all inner ear sensory neurons during embryonic development. Thus, whereas loss of *Bdnf* and *Ntf3* shows distinct effects in the vestibular system, their loss in the cochlea may be largely quantitative, reflecting their differential expression levels during development (Yang et al., 2011) rather than a unique function. Understanding the data around the common and unique function of neurotrophins requires some background information on the structure and function of these ligands.

3.7.1 The Two Survival Promoting Neurotrophins of the Ear Have a Dynamic Embryonic Pattern of Expression

In mice, neurotrophins are expressed as early as the first postmitotic neurons begin to differentiate [E10 (Farinas et al., 2001; Durruthy-Durruthy et al., 2014)]. Expression starts in the ear prior to hair cell formation and is also transiently

expressed in delaminating sensory neurons (Farinas et al., 2001; Fritzsch et al., 2002; Yang et al., 2011). The coexpression of *Bdnf* and *Ntf3* in delaminating neurons is one of the strongest arguments that all neurons derive from the ear (Rubel & Fritzsch, 2002) as such expressions are unknown for neural crest derived neurons. The early expression is initially over large areas of the otocyst but focuses rapidly to the future sensory epithelia (Pirvola et al., 1992). Expression of neurotrophins is prior to the differentiation of the hair cells (Fig. 3.3), suggesting that some neurotrophin expression is independent of hair cell differentiation. Consistent with this early expression in the undifferentiated sensory epithelia precursors is the expression of *Bdnf* in sensory epithelia that fail to differentiate hair cells. Specifically, in *Atoh1* null mice ($Atoh1^{Hprt-/-}$; $Bdnf^{lacz+/-}$), there is expression of *Bdnf-ß-galactosidase* in all three canal cristae and in the apex of the cochlea (Fritzsch et al., 2005b; Jahan et al., 2012). In contrast, the gravity sensing epithelia (utricle, saccule) and the base of the cochlea show virtually no expression of *Bdnf*, suggesting that in certain epithelia expression will appear only after hair cells differentiate whereas in other epithelia, expression of *Bdnf* is independent of hair cell differentiation. The restricted and faint expression of *Bdnf* in these hair cell–deficient mutants limits innervation to areas of residual expression of *Bdnf* (Fritzsch et al., 2005b; Pan et al., 2011).

In contrast to *Bdnf*, which is expressed primarily in hair cells during early embryonic development of the mouse (Fig. 3.3), the expression of *Ntf3* is mainly in supporting cells. In newborn mice, *Ntf3* expression moves into the IHCs of the cochlea (Pirvola et al., 1992; Farinas et al., 2001). As with *Bdnf*, *Ntf3* is expressed before hair cell differentiation and remains expressed in undifferentiated sensory patches in the absence of hair cell differentiation in mice lacking hair cells. Mice with embryonic (Fritzsch et al., 2005b) or postnatal hair cell loss (Xiang et al., 2003) retain more innervation compared to neurotrophin null mice (Yang et al., 2011) but these fibers fail to reach into the undifferentiated organ of Corti (Fritzsch et al., 2005b; Pan et al., 2011). The expression of *Ntf3* mimics that of *Sox2*, a gene needed to initiate sensory epithelia differentiation (Dabdoub et al., 2008).

Beyond the differential and changing expression in cells of sensory epithelia, both neurotrophins show variable expression topology in different epithelia over time. For *Bdnf*, this continued expression change is possibly related to the multiple promoter sites of *Bdnf* that can all lead to the same transcript (Koppel et al., 2010; Koppel & Timmusk, 2013). This may allow for their activity-mediated expression (Pruunsild et al., 2011), which in turn may mediate some of the synaptic plasticity associated effects of *Bdnf* (Panja & Bramham, 2014). *Bdnf* is the first and most profoundly expressed neurotrophin in the canal cristae, as *Ntf3* expression is limited and late (Farinas et al., 2001). In contrast, the utricle and saccule express both neurotrophins nearly simultaneously, starting in mice around E11.5. However, *Ntf3* is more widely expressed whereas *Bdnf* is restricted to the first differentiating hair cells near the line of polarity reversal (striola).

Most complicated is the progressive change in neurotrophin expression in the organ of Corti. *Bdnf* seemingly follows the cell cycle exit of hair cells (Matei et al.,

2005; Kopecky et al., 2013) and progresses from the apex (E12.5) toward the base. In contrast, *Ntf3* follows the differentiation of the organ of Corti and progresses from the base toward the apex (Farinas et al., 2001; Jahan et al., 2013). This countercurrent of embryonic expression change indicates that each area of the organ of Corti is unique with respect to the time of coexpression of these two neurotrophins, relative to cell cycle exit and onset of hair cell differentiation. In addition, there is a radial cellular expression change: *Bdnf* starts expression around undifferentiated postmitotic IHCs of the apex to progress toward the basal turn OHCs whereas *Ntf3* starts around the basal turn OHCs and progresses over embryonic time toward the IHCs of the apex. As will be apparent from the neurotrophin targeted deletion data provided (see Sect. 3.6), these progressive and differential expression changes are meaningful for the viability of sensory neurons projecting to different regions. Moreover, they suggest that the complex *Bdnf* promoter architecture may be an important part of this expression regulation (Koppel et al., 2010).

Obviously, the continued expression of neurotrophins in undifferentiated sensory epithelia after deletion of hair cells (Fritzsch et al., 2005b; Pan et al., 2012a) could be meaningful for long-term neurosensory maintenance in the absence of hair cells. However, continued cellular dedifferentiation of sensory epithelia in the absence of hair cells lead to progressive loss of neurotrophin expression. Differences in embryonic, compared to postnatal hair cell loss, suggests a longer retention of afferents after postnatal loss of hair cells (Fritzsch et al., 2005b; Pauley et al., 2008). Importantly, because neurotrophins are expressed in both hair cells and supporting cells, even if sensory epithelia never differentiate, manipulating this expression could lead to therapeutic neurotrophin expression in cases of progressive hair cell loss to retain long-term innervation for better use of cochlear implants.

It should be noted that several reports describe postnatal expression of neurotrophins that is radically different from what is reported by in situ hybridization (Pirvola et al., 1992; Pan et al., 2011) or knockin-*LacZ* expression (Farinas et al., 2001; Fritzsch et al., 2005b). This discrepancy could be caused by the detection of neurotrophin protein that has not been synthesized by the cell itself (von Bartheld & Fritzsch, 2006). For example, BDNF immunopositivity in supporting cells (Singer et al., 2014) may not reflect synthesis in these cells but rather uptake of BDNF synthesized in hair cells (Fritzsch et al., 1999). In addition, many anti-neurotrophin and anti-neurotrophin receptor antibodies have been shown to be unspecific (Dieni et al., 2012) and give false positive labeling, even in null mutant mice. In summary, reports on neurotrophin or neurotrophin receptor expression based exclusively on immunocytochemistry need to be treated with caution and require confirmation by demonstrating direct gene expression by other means. Worst of all, some antibodies are known to ‘recognize’ neurotrophins or their receptors in null mutants for these genes.

3.7.2 The Three Neurotrophin Receptors Show Limited Developmental Expression Dynamics in the Ear

In contrast to the puzzling expression changes of the two neurotrophins, there is little expression change in the three neurotrophin receptors in the ear. In situ hybridization and immunocytochemistry shows early expression for *Ntrk2*, *Ntrk3* and Ngfr in all sensory neurons (von Bartheld et al., 1991; Ylikoski et al., 1993), which is apparently unchanged over the embryonic period. However, after birth the Ngfr receptor is downregulated in the rodent spiral ganglion neurons but is maintained in the vestibular ganglion neurons. In addition, the Ngfr receptor is transiently expressed in the inner pillar cells of the organ of Corti. No changes in expression have been reported for *Ntrk2* and *Ntrk3*, which apparently are co-expressed in differentiating sensory neurons as soon as neurites begin to grow toward the brain and the sensory epithelia (Farinas et al., 2001; Fritzsch et al., 2002).

3.7.3 Neurotrophin Expression in the Central Target Nuclei

All vestibular afferents project to the vestibular nuclei (Maklad & Fritzsch, 2003) and cerebellum (Maklad et al., 2010) whereas all cochlear afferents project only to the cochlear nuclei, as visualized by labeling with the spiral ganglion specific marker *Gata3* (Fritzsch et al., 2006; Duncan & Fritzsch, 2013). Various reports claim the presence of neurotrophin ligands in these targets, but some claims of *Bdnf* expression in cochlear nuclei seemingly mistake the *tgPax2–cre* mediated expression of β-galactosidase as presenting expression of the floxed *Bdnf* gene (Zuccotti et al., 2012). Based on these considerations, embryonic expression of *Bdnf* is restricted to the ear whereas *Ntf3* has additional expression in the cochlear nuclei (Maricich et al., 2009). As will be obvious from data on conditional deletion of neurotrophins described in Sect. 3.6, the expression of *Ntf3* in developing cochlear nuclei is in line with gene deletion effects.

3.7.4 Predictions of Expression Changes on Loss of Innervation in Null Mutants

Whereas neurotrophins show sophisticated patterns of expression changes in the ear (Fig. 3.3), their receptors show limited changes. The postnatal downregulation of neurotrophin expression correlates with the less severe reduction of sensory neurons in mutants that lose hair cells in neonates (Xiang et al., 2003) instead of late embryos (Fritzsch et al., 2005b). Given the rather stable co-expression of *Ntrk2* and *Ntrk3* one would expect that loss of neither results in patterned loss of neurons, given that both BDNF and NT-3 seem to be mostly functionally equivalent

(Agerman et al., 2003; Tessarollo et al., 2004). In contrast to this stability in embryonic expression of receptors, the alterations in expression overlap of *Bdnf* and *Ntf3* could result in sophisticated patterns of loss, depending on the degree through which one neurotrophin can compensate for the other based on co-localization. This picture is more complicated for *Ntf3* compared to *Bdnf* because of the obvious additional expression of *Ntf3* in the cochlear nuclei. One would thus expect that conditional deletion of *Ntf3* in the ear alone should have a less profound effect compared to the systemic loss of *Ntf3* in the ear and the cochlear nuclei whereas either conditional deletion of *Bdnf* in the ear alone or complete systemic loss of *Bdnf* should have the same effect.

3.8 Deletion (Knockouts) of Neurotrophin Ligands and Receptors

As outlined in Sect. 3.5, interpretation of innervation defects in the ear of mice missing single neurotrophins or neurotrophin receptors varies in the three distinct sensory systems of the ear, each with a different co-expression pattern of *Bdnf* and *Ntf3*: *Bdnf* is almost exclusively in the canal cristae, it partially overlaps with *Ntf3* in the utricle and saccule, and has complicated and changing expression gradients in the organ of Corti.

3.8.1 Early Hypotheses and Their Technical Limitations

The earliest papers on neurotrophin and neurotrophin receptor mutations reported differential effects in the loss of vestibular and cochlear neurons and the innervation of sensory epithelia. Unfortunately, because of an incomplete assessment of the vestibular epithelia, these papers emphasized differential innervation effects in vestibular versus cochlear sensory epithelia (Ernfors et al., 1995; Schimmang et al., 1995). Subsequent work clarified that different vestibular organs respond differently to neurotrophin and neurotrophin receptor loss (Fritzsch et al., 1995; Farinas et al., 2001). Indeed, loss of either *Bdnf* or *Ntrk2* results in near complete loss of all innervation to the canal cristae but only in a reduced innervation of the utricle and saccule (Fritzsch et al., 2005c), consistent with the nearly exclusive expression of *Bdnf* in the canal cristae (Pirvola et al., 1992). In the cochlea, the initial approximation in spiral ganglion losses of the mutant mice led to the suggestions that *Bdnf*/*Ntrk2* supports innervation to OHCs whereas *Ntf3*/*Ntrk3* supports innervation to IHCs (Ernfors et al., 1995; Schimmang et al., 1995). However, a parallel analysis showed that without *Ntf3* or *Ntrk3* there is remaining innervation in some IHCs but not in the OHCs in a regionally variable pattern (Fritzsch et al., 1995; Fritzsch et al., 1997a). Furthermore, recent data suggest that loss of innervation to the OHCs in the organ of Corti is largely dependent on the concentration of neurotrophins (Yang et al., 2011).

3.8.2 Loss of Neurons in Neurotrophin Deficient Mice Correlates with Their Pattern of Expression

A number of studies have shown that the loss of innervation in neurotrophin deficient mice (Fig. 3.4) correlates well with their pattern of expression during inner ear development (Fritzsch et al., 2004). This is particularly obvious in the vestibular sensory epithelia (Fig. 3.5). In fact, because only *Bdnf* is expressed in the canal cristae at the time its absence exerts its maximal effect (Farinas et al., 2001), nearly all innervation to this area is lost in either *Bdnf* or *Ntrk2* null mutants. In contrast, there is overlapping expression of *Ntf3* and *Bdnf* in the utricle and saccule (Fig. 3.3) and as a result, the simple loss of *Bdnf* leaves some fairly dense innervation in these epithelia (Fig. 3.5). Overall, there is a loss of approximately 85 % of vestibular ganglion neurons in *Bdnf*/*Ntrk2* null mice whereas only approximately 20 % of the vestibular ganglion neurons are lost in *Ntf3*/*Ntrk3* null mice. Why the much earlier and more profound expression of *Ntf3* in the saccule and utricle (Fig. 3.3) has so little overall effect on vestibular ganglion viability remains unexplained.

The quantitative effects of neurotrophin or receptor loss in the cochlea fit closely with the pattern of expression changes of neurotrophins. *Ntf3* is earlier and more highly expressed in particular in the undifferentiated basal turn of the cochlea (Fig. 3.3). Thus, loss of 85 % of spiral ganglion neurons in *Ntf3* null mice and only 7 % after *Bdnf* loss seems to correlate well with their differential longitudinal pattern of expression (Ernfors et al., 1995; Farinas et al., 2001). Surprisingly, these data do not agree with the loss caused by *Ntrk3* (51–66 %) or *Ntrk2* (15–20 %) deletion raising the possibility that NT-3 may cross-talk to Ntrk2. Alternatively, Ntrk3 acts as a "dependence" receptor killing neurons in the absence of a ligand (Dekkers et al., 2013). However, the first Ntrk3 mutation was incomplete with disruption of only the kinase isoform of *Ntrk3* (Klein et al., 1994). A complete *Ntrk3* mutant mouse, with disruption of all isoforms including the truncated one (Tessarollo et al., 1997; Esteban et al., 2006), has a phenotype closely resembling the *Ntf3* null phenotype (Fig. 3.6). These more recent data reduce the apparent discrepancy between *Ntf3* and *Ntrk3* null mutants, and thus questions the need to invoke additional functions of neurotrophin–receptor interactions. It should also be noted that most of the quantification was not conducted using proper dissector techniques, the standard for quantification in the cochlea (Richter et al., 2011) and few comparisons were actually conducted using the same counting procedures in the same laboratory. Additional data from new mouse models discussed in Sect. 3.7 support the notion that, at least in the ear, neurotrophins signal in vivo specifically through their preferred receptor with little to no cross talk.

The loss of innervation in *Ntf3*/*Ntrk3* null mice primarily in the base and of *Bdnf*/*Ntrk2* null mice in the apex of the cochlea (Figs. 3.4 and 3.6) is consistent with the progressing longitudinal expression profile of *Bdnf* and *Ntf3* (Fig. 3.3). Most revealing is the cumulative effect of *Bdnf* heterozygosity on the *Ntf3* null phenotype ($Bdnf^{+/-}$; $Ntf3^{-/-}$) showing an even more profound loss of basal turn afferents and innervation with only few neurons surviving in the apex (Figs. 3.4 and 3.6).

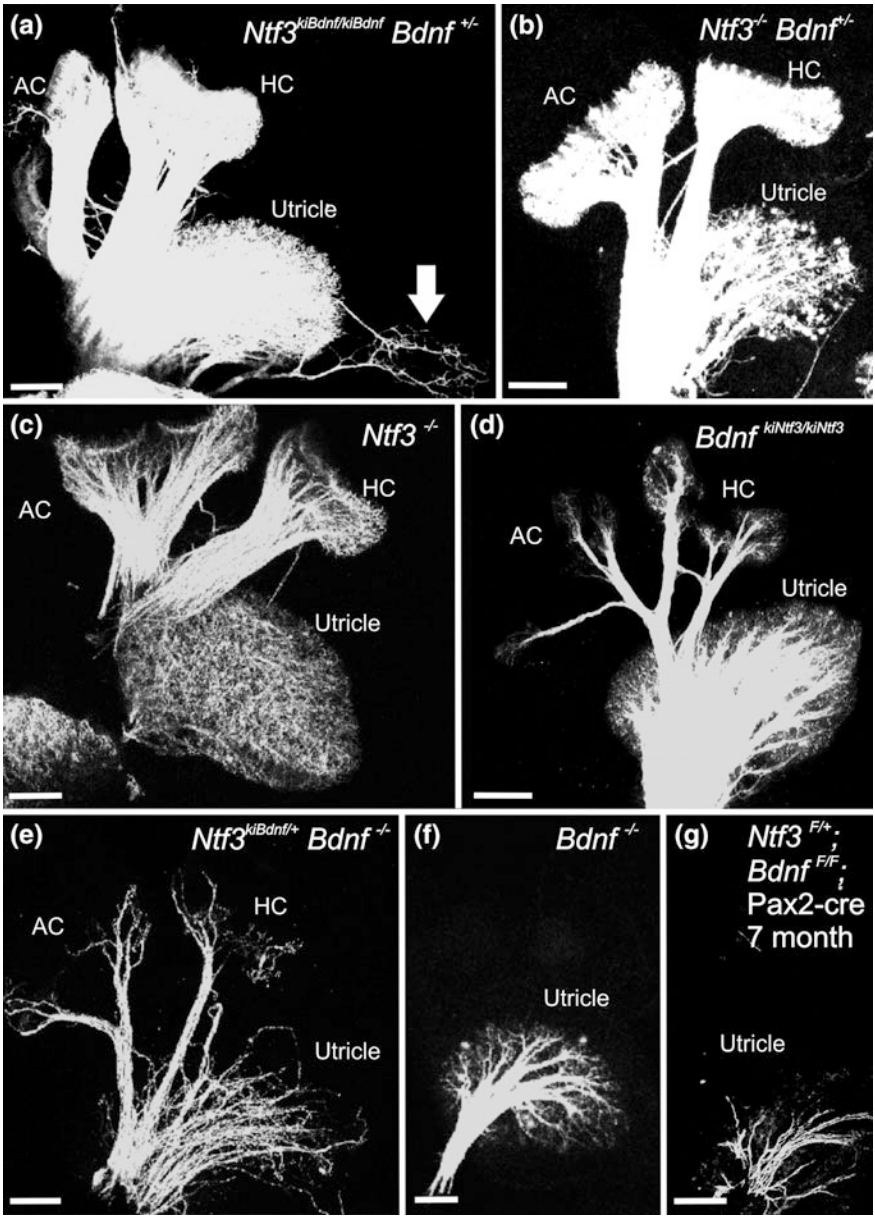

Likewise, *Bdnf* null mutants combined with *Ntf3* heterozygosity ($Bdnf^{-/-}$; $Ntf3^{+/-}$) show a more profound loss of apical turn neurons, in complete agreement with the prediction that both neurotrophins have equivalent function for the survival of embryonic spiral ganglion neurons. Interestingly, whereas apical radial fiber density is reduced proportional to the loss of spiral ganglion neurons in *Bdnf* null mutants,

◀ **Fig. 3.5** Vestibular innervation defects reveal distinct *Bdnf* and *Ntf3* signaling effects. Vestibular epithelia show a constant pattern of neurotrophin expression with little change allowing for an easier understanding of complex mutants replacing one neurotrophin by another on the innervation. The highest density of innervation, including fibers overshooting to nonsensory areas of limited *Ntf3* expression (*arrow* in **a**) are misexpressors of *Bdnf* in the *Ntf3* locus with one or two alleles of native *Bdnf* (**a**). Even reducing all neurotrophins to a single allele of *Bdnf* can nearly maintain the overall innervation (**b**), consistent with the fact that loss of *Ntf3* has virtually no effect on the density of innervation (**c**). Replacing *Bdnf* by *Ntf3* reduces the density of innervation to the canal cristae, but not to the utricle (**d**). A similar limited density of innervation can be obtained if one *Ntf3* allele is replaced by *Bdnf* and there is no *Bdnf* expression under its own promoter control (**e**). This contrast with the complete loss of *Bdnf*, where no fibers reach the canal cristae (**f**). Likewise, conditional deletion of *Bdnf* in the ear eliminates all canal cristae innervation but retains a limited innervation of the utricle for at least 7 months (**g**). *Bars* indicate 100 μm (Data are from Hellard et al., 2004; Tessarollo et al., 2004)

there is an exaggerated growth of fibers to the OHCs and beyond (Yang et al., 2011), contrasting sharply with earlier claims about the function of BDNF to be essential for OHC innervation growth. Likewise, in contrast to earlier data suggesting that in *Ntrk3* or *Ntf3* null mice the IHCs should be denervated, new results show that the only basal turn hair cells that may be innervated are the IHCs (Fig. 3.4) whereas the OHCs receive no innervation at all (Yang et al., 2011; Kersigo & Fritzsch 2015). Interestingly, such radial fiber deficits have also been reported in null mutants lacking *Slitrk6*, a receptor affecting Ntrk receptor signaling (Katayama et al., 2009).

Despite absence of dynamic alterations in expression, various combinations of *Ntrk2* and *Ntrk3* mutant alleles (Fig. 3.6) show a patchy and variable loss of spiral ganglion neurons (Fritzsch et al., 1998). These differential effects may in part be due to incomplete *Ntrk3* deletion, reflecting the presence of the residual truncated *Ntrk3* isoform signaling in the ear (Esteban et al., 2006).

3.8.3 *Conditional Deletion of Neurotrophins in the Ear*

Both neurotrophins exist as floxed alleles in mouse (Bates et al., 1999; Ma et al., 1999; Gorski et al., 2003) and have already been used in combination with various *Cre* lines to generate viable mice with a topologically restricted deletion to test postnatal function of neurotrophins in the ear (Zilberstein et al., 2012). Here, we focus on the simple aspect of specific embryonic deletion of either neurotrophin in the ear to evaluate the possible developmental support from central nuclear targets. As outlined in Sect. 3.5, *Bdnf* is expressed in the embryonic mouse ear mostly in hair cells (Figs. 3.1 and 3.3). Consequently, crossing the conditional allele with a *tgPax2–cre* line that eliminates the floxed *Bdnf* only in the ear ($Bdnf^{fl/f}$; *Pax2–cre*), while sparing mostly the brain stem, should have an identical phenotype, provided there is no expression of *Bdnf* in the embryonic brain. Indeed, vestibular and cochlear innervation defects are virtually identical in the conditional ($Bdnf^{fl/f}$; *Pax2–cre*) and systemic

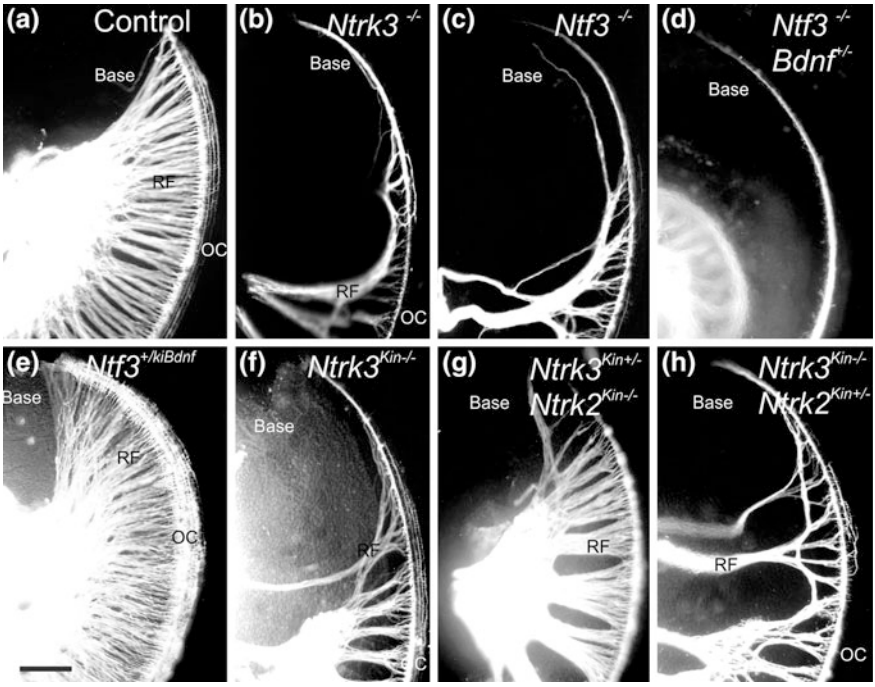

Fig. 3.6 Effects of various neurotrophin and neurotrophin receptor deletions on the basal turn innervation at birth. The basal turn innervation shows dense radial fibers (RF) emanating from spiral ganglion neurons to reach the organ of Corti (OC) in newborn wild type mice (**a**). In contrast, the basal turn has no spiral ganglion neurons and radial fibers in *Ntrk3* (**b**) and *Ntf3* (**c**) null mice. Afferents expand along the IHCs from middle turn neurons in *Ntf3* null mice (**c**), particularly if combined with *Bdnf* heterozygosity (**d**). This is not a specific function of *Ntf3* but rather reflects the early expression only of *Ntf3* in the basal turn as demonstrated by the complete retention of spiral ganglion neurons and very dense radial fibers in mice in which *Ntf3* has been replaced by *Bdnf* (**e**). Unfortunately, early mutations of the *Ntrk3* gene focused on the kinase domain, leaving some additional signaling capacity. In these *Ntrk3* kinase mutants some basal turn spiral ganglion cells remain, generating an apparent difference (**f**) relative to the complete null of *Ntrk3* (**b**) and the *Ntf3* null mice (**c**). Combining in various ways the kinase domain of *Ntrk2* and *Ntrk3* null mice shows sophisticated patterns of partial loss of spiral ganglion neurons with increased spacing between radial fibers (**g**) or a more profound loss of basal turn innervation approaching the *Ntf3* null mutant phenotype (**h**). *Bar* indicates 100 μm (Images compiled after Fritzsch et al., 1998, 2004)

($Bdnf^{-/-}$) *Bdnf* null mice (Kersigo & Fritzsch, 2015). In addition, if *Bdnf* expression is eliminated only in hair cells, a more profound innervation to the sensory epithelia should remain, consistent with the fact that some epithelia have neurotrophin expression in supporting cells as well.

In contrast, the pattern of innervation loss after specific deletion of *Ntf3* in the ear ($Ntf3^{f/f}$; *Pax2–cre*) is very different from the *Bdnf* scenario because it shows a less severe innervation defect compared to the null mutant mouse ($Ntf3^{-/-}$). However, if one single allele of *Bdnf* is removed in combination with loss of *Ntf3* ($Ntf3^{f/f}$; $Bdnf^{f/+}$;

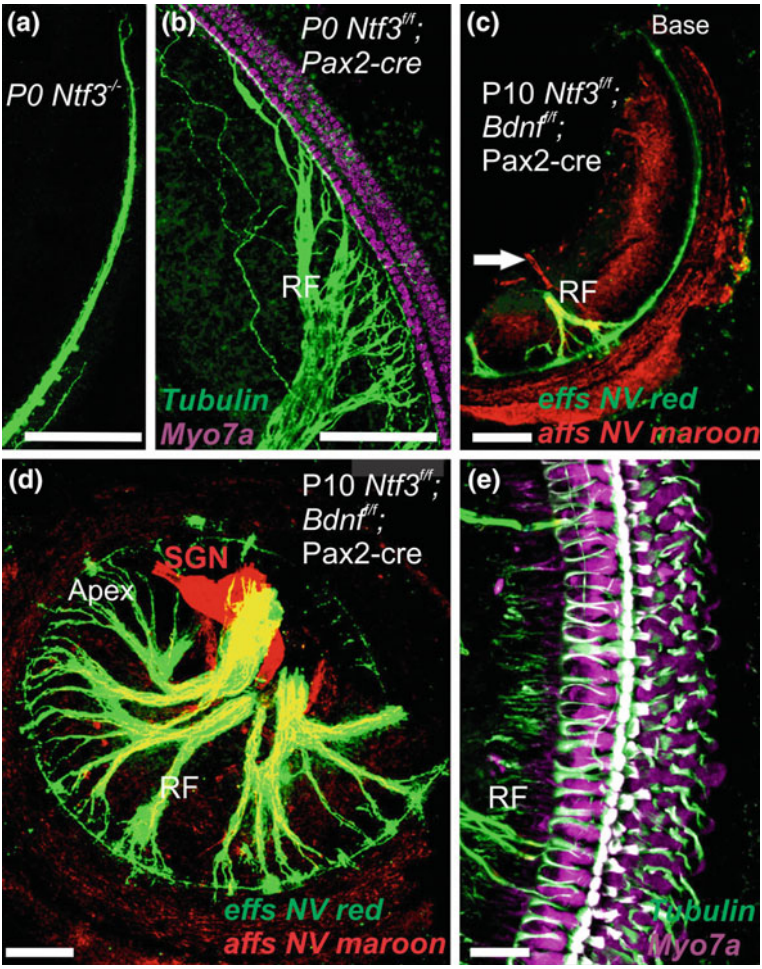

Fig. 3.7 Conditional deletion of one or more neurotrophins in the ear reveals support from cochlear nuclei. Whereas simple *Ntf3* null mutants lose almost all innervation of the base with fibers spiraling up from the middle turn (**a**), there is more retention of fibers after conditional deletion of *Ntf3* only in the ear, suggesting some support from the spared expression of *Ntf3* in the cochlear nuclei. However, if combined with conditional *Bdnf* loss, afferent loss is more profound and comparable to a simple *Ntf3* loss (**c** compared to **a**). In fact, in contrast to the complete loss of all innervation in double neurotrophin nulls, double conditional neurotrophin null mutants have some radial fibers (RF) left until about postnatal day 10 (**c**–**e**). This suggests that the expression of *Ntf3* in the cochlear nuclei provides at least some transient support. SGN, spiral ganglion neuron. *Bar* indicates 100 μm (Modified after Kersigo & Fritzsch, 2015)

Pax2–cre), the innervation loss approaches that of a complete *Ntf3* null mutant mouse (Fig. 3.7). Importantly, the conditional deletion of both neurotrophins in the ear (*Ntf3*$^{f/f}$; *Bdnf*$^{f/f}$; *Pax2–cre*) shows substantial residual innervation compared to the full, systemic null mutant (Fig. 3.7), clearly supporting the notion that additional

neurotrophic support is provided by neurotrophins expressed in the cochlear/vestibular nuclei, with *Ntf3* expressed in the cochlear nuclei being the most likely candidate (Maricich et al., 2009). Together these data demonstrate mice with ear specific deletions of neurotrophins are an excellent model to study postnatal function of neurotrophins. They also provide an excellent tool to investigate the development of ears without any innervation, thus allowing researchers to study the long-term effects of absence of afferents on cochlear and vestibular nuclei during development, an aspect that has thus far been limited to postnatal developmental stages (Harris & Rubel, 2006; Peusner et al., 2009). Indeed, these mutant mice show a severe reduction of the cochlear nuclei already at birth, earlier than any other previously reported study in mice. Moreover, these mice also allow the study of the long-term effects of loss of afferents on hair cells (Kersigo & Fritzsch, 2015), suggesting a surprisingly long-term dependency of organ of Corti hair cells on innervation.

3.9 Misexpressions (Knockin) of Neurotrophins by Gene Replacement Strategy

If neurotrophin distribution and expression levels are the two parameters that define the pattern of inner ear neuronal survival and innervation, one would expect that partial or complete misexpression of one or another neurotrophin should have a profound effect on inner ear innervation. Indeed, such experiments replacing *Bdnf* with *Ntf3* [$Bdnf^{kiNtf3}$ (Agerman et al., 2003)] or *Ntf3* with *Bdnf* [$Ntf3^{kiBdnf}$ (Coppola et al., 2001; Tessarollo et al., 2004)] have been performed and the data so far support largely the predictions for the function of these neurotrophins in the cochlea, but not entirely in the vestibular system.

3.9.1 Effects of Bdnf Knocked into the Ntf3 Locus ($Ntf3^{kiBdnf}$)

As indicated previously, deletion of *Ntf3* results in profound topological loss of basal turn innervation (Figs. 3.4, 3.6, and 3.7). If there is equivalence of signal between the two neurotrophins, *Bdnf* replacement of *Ntf3* should rescue the fiber growth to the basal turn, which is precisely what was found (Coppola et al., 2001). Thus, BDNF and NT-3 apparently can equally support spiral ganglion neurons at least to the extent that the typical loss of basal turn spiral ganglion neurons associated with lack of *Ntf3* expression does not occur. Somewhat consistent with the expectation that BDNF may promote growth of type II afferents to the OHCs is an abundance of growth of afferents to the outer compartment of the basal turn (Fig. 3.6). These data suggest two possibilities: Either (1) BDNF is more effective

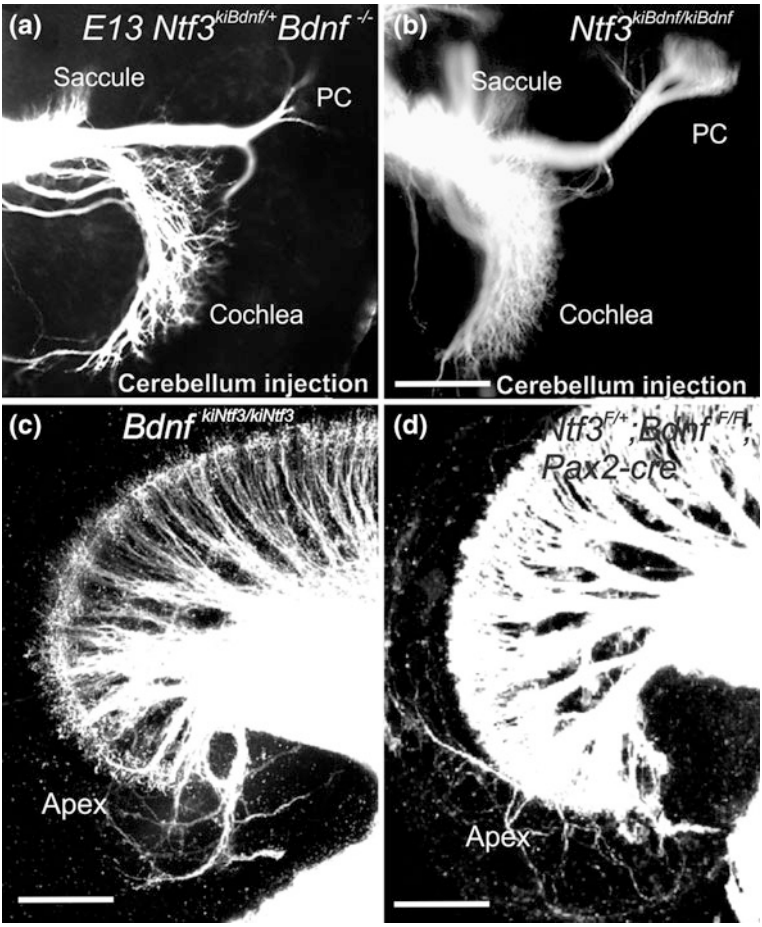

Fig. 3.8 *Bdnf* expression affects targeting of vestibular afferents. Misexpression of *Bdnf* under *Ntf3* promoter control reroutes vestibular afferents from the saccule and the posterior canal crista (PC) to the basal turn of the cochlea (**a**, **b**). This rerouting is more profound from the posterior canal crista if *Bdnf* is eliminated in addition (**a**). Elimination of *Bdnf* either by replacing it with *Ntf3* (**c**) or in a conditional deletion of *Bdnf* (**d**) shows that radial fiber bundle (RF) spacing is affected and fibers overshoot at the apex (**c**, **d**). *Bar* indicates 100 μm. (Data modified after Tessarollo et al., 2004)

in rescuing spiral ganglion neurons and promoting their growth to OHC, or (2) fibers are rerouted from the vestibular organs. Additional work demonstrated that many of these extra fibers are indeed rerouted vestibular afferents (Tessarollo et al., 2004), primarily from the posterior canal crista and the saccule (Fig. 3.8). A complicating problem with this approach is that in these mutant mice there is an overabundance of BDNF because *Bdnf* is expressed both under its own promoter as well as under the control of the *Ntf3* promoter.

A logical way of minimizing this additional problem is to combine the *Ntf3*^{kiBdnf} mutation with a mutant null for *Bdnf* (*Nt-3*$^{kiBdnf/kiBdnf}$; *Bdnf*$^{-/-}$), thus allowing for only one set of the neurotrophin promoters to express *Bdnf* i.e., under the control of the *Ntf3* promoter). If in such a model, that expresses only *Bdnf* under the control of the *Ntf3* promoter control, there is rescue of the basal turn innervation even if the endogenous *Bdnf* is missing, it would demonstrate that the neurotrophin expression pattern rather than intrinsic characteristic of each neurotrophin is responsible for supporting inner ear innervation. Indeed, depending on the level of *Bdnf* misexpression and loss, more vestibular afferents reroute to the basal turn of the cochlea and more afferents are growing to the outer compartment of the organ of Corti, apparently in a simple concentration-dependent manner (Yang et al., 2011). These mutants show overshooting of afferents in the apex of the cochlea (Fig. 3.8) consistent with a guidance function of BDNF now more widely expressed under the *Ntf3* promoter. Most interestingly, the great majority of misrouted vestibular afferents do not grow through the habenula perforata into the organ of Corti, but rather stay in the scala tympani side of the basilar membrane (Tessarollo et al., 2004). Similar inability of fibers entering into the organ of Corti has been found after conditional ablation of Schwann cells (Mao et al., 2014). These data suggest that only spiral ganglion cells have the ability to respond to an additional cue provided by hair cells/supporting cells to grow into the organ of Corti and require proper guidance by Schwann cells to enter the organ of Corti.

Data from mice with misexpression of *Bdnf* in the *Ntf3* locus with or without loss of endogenous *Bdnf* expression provide insight into the possible function of Ngfr as a death receptor (Fig. 3.2) and of Ntrk3 as a "dependence" receptor. Obviously, if Ngfr interacts in the ear with pro-BDNF generated from both the *Ntf3* and the *Bdnf* locus, one would expect a more profound loss of sensory neurons (Taylor et al., 2012) expressing Ngfr given the overabundance of pro-BDNF. Likewise, if Ntrk3 would act in the ear as a "dependence" receptor that initiates cell death without a ligand (Dekkers & Barde, 2013; Dekkers et al., 2013), one would expect that expression of *Bdnf* instead of *Ntf3* should increase spiral ganglion loss due to such actions. However, such possibilities are not supported by the apparent overgrowth of afferent fibers to the cochlea in such mutants (Yang et al., 2011). In fact, both the cochlea (Figs. 3.6 and 3.8) and the vestibular system (Fig. 3.5) show overgrowth of fibers in these mutant mice instead of the predicted additional cell death mediated by the availability of pro-BDNF to the Ngfr receptor and the Ntf3-deprived Ntrk3 receptors (Figs. 3.5 and 3.6). Nevertheless, it is possible that an exaggerated cell death exists in very early stages of developing spiral ganglion neurons that is thus far undetected. Clearly, although unlikely, this assumption requires additional work to investigate the presence of degenerating neurons by terminal deoxynucleotidyl for example transferase dUTP nick end labeling (TUNEL; (Yang et al., 2013), anti-Cleaved Caspase-3 immunochemistry, or PSVue® Probe staining techniques, for example (Kersigo et al., 2011). Comparing the spiral ganglion loss in *Ntf3*^{kiBdnf} mutant mice with or without conditional deletion of *Bdnf* would also verify if and to what extent these recent ideas on trophic dependency may affect ear neuronal development in terms of a more or less profound increase in the early phase of

spiral ganglion neuronal cell death. Given that the efferents to the ear are derived from facial branchial motoneurons (Simmons et al., 2011), and express Ngfr much like other motoneurons, it is possible that they are specifically reduced by additional pro-BDNF comparable to spinal motor neurons (Taylor et al., 2012).

3.9.2 *Effects of Ntf3 Knocked into the Bdnf Locus (Bdnf^{kiNtf3})*

The effects of replacement of *Bdnf* by *Ntf3* (*Bdnf^{kNtf3}*) are largely consistent with the data presented in Sect. 3.7.1 in the cochlea with a minor reduction of fiber growth to the OHCs (Agerman et al., 2003). Of course, this effect could also relate to the more profound attraction of fibers by BDNF to the high concentration around IHCs (Fig. 3.3), thus blocking them from growing to the OHCs in the presence of excessive BDNF in and around the IHCs. The effects of this knockin line on the innervation of the vestibular epithelia are more interesting. Based on the ubiquitous and overlapping expression of *Ntrk2* and *Ntrk3* in vestibular ganglion neurons (Ylikoski et al., 1993; Pirvola et al., 1994; Farinas et al., 2001), one would expect a lack of specific effect caused by this replacement, which is not what has been reported (Agerman et al., 2003). Instead of the approximately 80 % loss of vestibular neurons caused by *Bdnf* deletion, these knockin mice lose about 60 % of these neurons by P0 and about 75 % by P17. This indicates that the additional *Ntf3* expressed under the *Bdnf* promoter can sustain additional neurons only as long as there is a substantial level of neurotrophin expression before the postnatal decline in expression level. These data agree with those from a mouse model with a targeted deletion of *Ntrk2* receptor signaling docking sites which also show profound vestibular but not cochlear innervation defects (Postigo et al., 2002; Sciarretta et al., 2010), suggesting that Ntrk2 activation plays a unique role in vestibular innervation, in particular of the unusually large calyx around type I vestibular hair cells. The substantial innervation of all vestibular organs suggests that NT-3's ability to attract and maintain innervation is only quantitatively different from that of BDNF (Fig. 3.5). These data are also consistent with the ability of BDNF to direct fiber growth more profoundly than NT-3, an effect that is particularly obvious in the derailed growth of afferents in the apex of the organ of Corti in various *Bdnf* mutants (Figs. 3.4 and 3.8).

To further test claims that Ntrk2 can interact with the ligand NT-3, *Bdnf^{kiNtf3}* mice were crossed with either *Ntrk3* or *Ntrk2* null mice (Stenqvist et al., 2005). If indeed NT-3 can cross-talk to Ntrk2 mice with a deletion of *Ntrk2* in combination with expression of only *Bdnf* under both the *Ntf3* and its own promoter control (hence lack NT-3 protein) should not show any innervation defects. Conversely, if NT-3 is the sole ligand for Ntrk3 and cannot interact in vivo with Ntrk2 a combination of endogenous *Ntf3* expression combined with expression of *Ntf3* under the *Bdnf* promoter and a *Ntrk3* null mutation should result in the complete loss of all

innervation, similar to double ligand and receptor null mutants (Yang et al., 2011). Indeed, the results are consistent with this latter prediction, providing evidence that in the ear BDNF and NT-3 each signal through its own receptor (Stenqvist et al., 2005). This result is also consistent with data generated with the complete *Ntrk3* mutants when compared to partial *Ntrk3* knockouts (Fritzsch et al., 2004). What remains to be shown now is that the $Ntf3^{kiBdnf}$ mice, combined with *Ntrk3* or *Ntrk2* null mutations, show no loss ($Ntf3^{kiBdnf}$; $Ntrk3^{-/-}$) or complete loss ($Ntf3^{kiBdnf}$; $Ntrk2^{-/-}$) of all ear innervation, including the well-known vestibular fiber rerouting to the cochlea.

In summary, misexpression and conditional deletion experiments have helped to clarify that in the developing ear there is a simple correlation of one ligand to one receptor (*Bdnf*/*Ntkr2*; *Ntf3*/*Ntrk3*), and that there is neither evidence for a specific function of Ngfr in early development as a pro-apoptotic receptor, nor of a Ntrk3 function as a pro-apoptotic "dependence" receptor. Moreover, elimination of all neurotrophins in the ear through conditional deletion results in transient retention of some innervation to the cochlea, presumably via the remaining *Ntf3* expression in the cochlear nuclei. Fine-tuning the obvious involvement of neurotrophins in fiber growth and formation of innervation requires going beyond the neonatal viability options of these mutants to generate viable combinations of conditionally deleted neurotrophins with misexpressed ones, ultimately expressing *Ntf3* only from the *Bdnf* promoter and *Bdnf* only from the *Ntf3* promoter. Such data will clarify the postnatal effects of these growth factors on the developing pattern of innervation of the cochlea (see Chaps. 4 by Davis and Crozier and 7 by Green et al.).

3.10 Summary and Conclusion

The data presented in this review demonstrate that only two neurotrophins, BDNF and NT-3, and their respective receptors, Ntrk2 and Ntrk3, are necessary and sufficient for the entire trophic support of developing inner ear neurons. Losses of these neurotrophins have a more profound effect on innervation than even the loss of all hair cells (Fig. 3.9). Overall, the effects follow the simple model of the neurotrophic theory that loss of trophic support leads to neuronal death, with more profound effects being achieved with progressive loss of more neurotrophin alleles. In the ear, there is no evidence for an embryonic role of the Ngfr receptor as a "death" receptor or for the Ntrk3 receptor acting as a pro-apoptotic "dependence" receptor to induce neuronal death without a ligand. Most revealing for these conclusions are the available knockin mouse models that swap the ligands. Conditional deletions of neurotrophins provide evidence for neurotrophic support from the cochlear nuclei and also show that hair cells are supported by neurons for the long term. The molecular basis of the neuronal support of cochlear nuclei remains unclear, in particular, in light of results from recently generated mutants that eliminate all vesicle release of either neurotransmitters or neurotrophins. Although much of this data are consistent with the original formulation of the neurotrophic

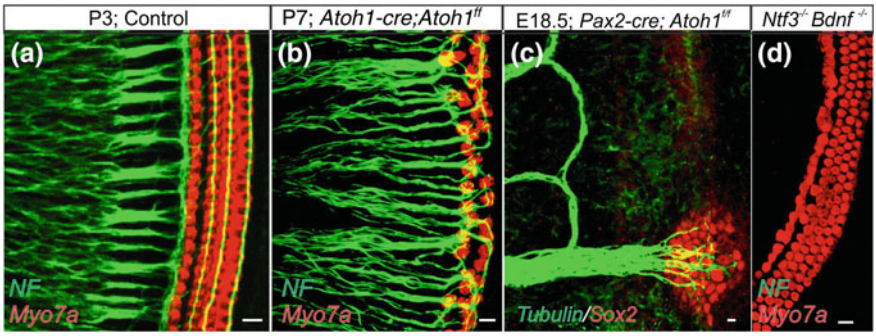

Fig. 3.9 Innervation defects without HC development are less profound compared to loss of all neurotrophins. These images compare the innervation of hair cells (**a**, **b**, **d**) or their precursors (c) using neurofilament (NF) or tubulin immunocytochemistry. Normally, there is a dense projection of radial fibers to IHCs with three rows of type II spiral ganglion afferents to OHCs (**a**). A "self-terminating" conditional deletion of *Atoh1* results in loss of many hair cells with little reduction of afferents but a change in innervation pattern due to IHC loss (**b**). Deletion of *Atoh1* using *Pax2–cre* eliminates all hair cell differentiation but leaves patches of organ of Corti precursors that express Sox2 (**c**). Note that only the patches of Sox2-immunopositive cells (*red*) receive innervation (*green*). Eliminating both neurotrophins results in complete loss of all afferents and reorganization of hair cells due to stunted cochlear extension (**d**). This demonstrates that the two neurotrophins carry all relevant information for afferent retention in the developing organ of Corti. *Bar* indicates 10 μm (Modified after Yang et al., 2011; Jahan et al., 2013)

theory as a process that induces death of neurons on limited access of neurotrophins, the quantitative ratio of afferents to hair cells with their highly different convergence and divergence ratio and lack of correction of overshooting processes in certain mutants are not easily reconcilable with this theory.

Acknowledgments This work was supported by NASA Base Grant (BF), a P30 core grant (DC 010362), an RO3 grant (DC013655 to IJ) and an R01 grant (DC 005590) to BF. The support of the Office of the Vice President for Research (OVPR) of the University of Iowa is gratefully acknowledged. We thank Dr. Lino Tessarollo for his expert review, comments, and suggestions of an earlier version and the SHAR editors for their helpful suggestions.

References

Agerman, K., Hjerling-Leffler, J., Blanchard, M. P., Scarfone, E., Canlon, B., Nosrat, C., & Ernfors, P. (2003). BDNF gene replacement reveals multiple mechanisms for establishing neurotrophin specificity during sensory nervous system development. *Development*, 130(8), 1479–1491.

Ard, M. D., & Morest, D. K. (1984). Cell death during development of the cochlear and vestibular ganglia of the chick. *International Journal of Developmental Neuroscience*, 2(6), 535–547.

Ard, M. D., Morest, D. K., & Hauger, S. H. (1985). Trophic interactions between the cochleovestibular ganglion of the chick embryo and its synaptic targets in culture. *Neuroscience*, 16(1), 151–170.

Bates, B., Rios, M., Trumpp, A., Chen, C., Fan, G., Bishop, J. M., & Jaenisch, R. (1999). Neurotrophin-3 is required for proper cerebellar development. *Nature Neuroscience*, 2(2), 115–117.

Benes, F. M., Parks, T. N., & Rubel, E. W. (1977). Rapid dendritic atrophy following deafferentation: An EM morphometric analysis. *Brain Research*, 122(1), 1–13.

Born, D. E., & Rubel, E. W. (1985). Afferent influences on brain stem auditory nuclei of the chicken: Neuron number and size following cochlea removal. *Journal of Comparative Neurology*, 231(4), 435–445.

Bothwell, M. (2006). Evolution of the neurotrophin signaling system in invertebrates. *Brain, Behavior and Evolution*, 68(3), 124–132.

Bramham, C. R., & Panja, D. (2014). BDNF regulation of synaptic structure, function, and plasticity. *Neuropharmacology*, 76 *Pt C*, 601–602.

Buchman, C. A., Roush, P. A., Teagle, H. F., Brown, C. J., Zdanski, C. J., & Grose, J. H. (2006). Auditory neuropathy characteristics in children with cochlear nerve deficiency. *Ear and Hearing*, 27(4), 399–408.

Buchman, C. A., Teagle, H. F., Roush, P. A., Park, L. R., Hatch, D., Woodard, J., Zdanski, C., & Adunka, O. F. (2011). Cochlear implantation in children with labyrinthine anomalies and cochlear nerve deficiency: Implications for auditory brainstem implantation. *Laryngoscope*, 121(9), 1979–1988.

Bulankina, A. V., & Moser, T. (2012). Neural circuit development in the mammalian cochlea. *Physiology (Bethesda)*, 27(2), 100–112.

Coppola, V., Kucera, J., Palko, M. E., Martinez-De Velasco, J., Lyons, W. E., Fritzsch, B., & Tessarollo, L. (2001). Dissection of NT-3 functions in vivo by gene replacement strategy. *Development*, 128(21), 4315–4327.

Dabdoub, A., Puligilla, C., Jones, J. M., Fritzsch, B., Cheah, K. S., Pevny, L. H., & Kelley, M. W. (2008). Sox2 signaling in prosensory domain specification and subsequent hair cell differentiation in the developing cochlea. *Proceedings of the National Academy of Sciences of the USA*, 105(47), 18396–18401.

Dekkers, M. P., & Barde, Y. A. (2013). Developmental biology: Programmed cell death in neuronal development. *Science*, 340(6128), 39–41.

Dekkers, M. P., Nikoletopoulou, V., & Barde, Y. A. (2013). Cell biology in neuroscience: Death of developing neurons: New insights and implications for connectivity. *Journal of Cell Biology*, 203(3), 385–393.

Desai, S. S., Ali, H., & Lysakowski, A. (2005a). Comparative morphology of rodent vestibular periphery. II. Cristae ampullares. *Journal of Neurophysiology*, 93(1), 267–280.

Desai, S. S., Zeh, C., & Lysakowski, A. (2005b). Comparative morphology of rodent vestibular periphery. I. Saccular and utricular maculae. *Journal of Neurophysiology*, 93(1), 251–266.

Dieni, S., Matsumoto, T., Dekkers, M., Rauskolb, S., Ionescu, M. S., Deogracias, R., Gundelfinger, E. D., Kojima, M., Nestel, S., & Frotscher, M. (2012). BDNF and its pro-peptide are stored in presynaptic dense core vesicles in brain neurons. *The Journal of Cell Biology*, 196(6), 775–788.

Duncan, J. S., & Fritzsch, B. (2013). Continued expression of GATA3 is necessary for cochlear neurosensory development. *PLoS One*, 8(4), e62046.

Durruthy-Durruthy, R., Gottlieb, A., Hartman, B. H., Waldhaus, J., Laske, R. D., Altman, R., & Heller, S. (2014). Reconstruction of the mouse otocyst and early neuroblast lineage at single-cell resolution. *Cell*, 157(4), 964–978.

Elliott, K. L., Houston, D. W., & Fritzsch, B. (2015a). Sensory afferent segregation in three-eared frogs resemble the dominance columns observed in three-eyed frogs. *Scientific Reports*, 5, 8338.

Elliott, K. L., Houston, D. W., DeCook, R., & Fritzsch, B. (2015b). Ear manipulations reveal a critical period for survival and dendritic development at the single-cell level in Mauthner neurons. *Developmental Neurobiology*, doi: 10.1002/dneu.22287.

Ernfors, P., Van De Water, T., Loring, J., & Jaenisch, R. (1995). Complementary roles of BDNF and NT-3 in vestibular and auditory development. *Neuron*, 14(6), 1153–1164.

Esteban, P. F., Yoon, H. Y., Becker, J., Dorsey, S. G., Caprari, P., Palko, M. E., Coppola, V., Saragovi, H. U., Randazzo, P. A., & Tessarollo, L. (2006). A kinase-deficient TrkC receptor

isoform activates Arf6–Rac1 signaling through the scaffold protein tamalin. *Journal of Cell Biology*, 173(2), 291–299.

Farinas, I., Jones, K. R., Tessarollo, L., Vigers, A. J., Huang, E., Kirstein, M., de Caprona, D. C., Coppola, V., Backus, C., Reichardt, L. F., & Fritzsch, B. (2001). Spatial shaping of cochlear innervation by temporally regulated neurotrophin expression. *The Journal of Neuroscience*, 21 (16), 6170–6180.

Fritzsch, B. (1981). Transneuronal vestibular afferent influence on the nodular molecular layer synaptogenesis. *Anatomy and Embryology (Berlin)*, 162(2), 199–208.

Fritzsch, B. (1990). Experimental reorganization in the alar plate of the clawed toad, *Xenopus laevis*. I. Quantitative and qualitative effects of embryonic otocyst extirpation. *Brain Research, Developmental Brain Research*, 51(1), 113–122.

Fritzsch, B. (2003). Development of inner ear afferent connections: Forming primary neurons and connecting them to the developing sensory epithelia. *Brain Research Bulletin*, 60(5–6), 423–433.

Fritzsch, B., Zakon, H. H., & Sanchez, D. Y. (1990). Time course of structural changes in regenerating electroreceptors of a weakly electric fish. *Journal of Comparative Neurology*, 300 (3), 386–404.

Fritzsch, B., Christensen, M. A., & Nichols, D. H. (1993). Fiber pathways and positional changes in efferent perikarya of 2.5- to 7-day chick embryos as revealed with DiI and dextran amines. *Journal of Neurobiology*, 24(11), 1481–1499.

Fritzsch, B., Silos-Santiago, I., Smeyne, R., Fagan, A., & Barbacid, M. (1995). Reduction and loss of inner ear innervation in trkB and trkC receptor knockout mice: A whole mount DiI and scanning electron microscopic analysis. *Auditory Neuroscience*, 1(2), 401–417.

Fritzsch, B., Farinas, I., & Reichardt, L. F. (1997a). Lack of neurotrophin 3 causes losses of both classes of spiral ganglion neurons in the cochlea in a region-specific fashion. *Journal of Neuroscience*, 17(16), 6213–6225.

Fritzsch, B., Sarai, P. A., Barbacid, M., & Silos-Santiago, I. (1997b). Mice with a targeted disruption of the neurotrophin receptor trkB lose their gustatory ganglion cells early but do develop taste buds. *International Journal of Developmental Neuroscience*, 15(4–5), 563–576.

Fritzsch, B., Silos-Santiago, I. I., Bianchi, L. M., & Farinas, I. I. (1997c). Effects of neurotrophin and neurotrophin receptor disruption on the afferent inner ear innervation. *Seminars in Cell and Developmental Biology*, 8(3), 277–284.

Fritzsch, B., Barbacid, M., & Silos-Santiago, I. (1998). The combined effects of trkB and trkC mutations on the innervation of the inner ear. *International Journal of Developmental Neuroscience*, 16(6), 493–505.

Fritzsch, B., Pirvola, U., & Ylikoski, J. (1999). Making and breaking the innervation of the ear: Neurotrophic support during ear development and its clinical implications. *Cell and Tissue Research*, 295(3), 369–382.

Fritzsch, B., Beisel, K. W., Jones, K., Farinas, I., Maklad, A., Lee, J., & Reichardt, L. F. (2002). Development and evolution of inner ear sensory epithelia and their innervation. *Journal of Neurobiology*, 53(2), 143–156.

Fritzsch, B., Tessarollo, L., Coppola, V., & Reichardt, L. F. (2004). Neurotrophins in the ear: Their roles in sensory neuron survival and fiber guidance. *Progress in Brain Research*, 146, 265–278.

Fritzsch, B., Gregory, D., & Rosa-Molinar, E. (2005a). The development of the hindbrain afferent projections in the axolotl: Evidence for timing as a specific mechanism of afferent fiber sorting. *Zoology (Jena)*, 108(4), 297–306.

Fritzsch, B., Matei, V. A., Nichols, D. H., Bermingham, N., Jones, K., Beisel, K. W., & Wang, V. Y. (2005b). Atoh1 null mice show directed afferent fiber growth to undifferentiated ear sensory epithelia followed by incomplete fiber retention. *Developmental Dynamics*, 233(2), 570–583.

Fritzsch, B., Pauley, S., Matei, V., Katz, D. M., Xiang, M., & Tessarollo, L. (2005c). Mutant mice reveal the molecular and cellular basis for specific sensory connections to inner ear epithelia and primary nuclei of the brain. *Hearing Research*, 206(1–2), 52–63.

Fritzsch, B., Pauley, S., Feng, F., Matei, V., & Nichols, D. (2006). The molecular and developmental basis of the evolution of the vertebrate auditory system. *International Journal of Comparative Psychology*, 19(1), 1–24.

Fritzsch, B., Pan, N., Jahan, I., Duncan, J. S., Kopecky, B. J., Elliott, K. L., Kersigo, J., & Yang, T. (2013). Evolution and development of the tetrapod auditory system: An organ of Corti-centric perspective. *Evolution & Development*, 15(1), 63–79.

Fritzsch, B., Pan, N., Jahan, I., & Elliott, K. L. (2014). Inner ear development: Building a spiral ganglion and an organ of Corti out of unspecified ectoderm. *Cell and Tissue Research*, 361, 7–24.

Gorski, J. A., Zeiler, S. R., Tamowski, S., & Jones, K. R. (2003). Brain-derived neurotrophic factor is required for the maintenance of cortical dendrites. *The Journal of Neuroscience*, 23 (17), 6856–6865.

Hallbook, F. (1999). Evolution of the vertebrate neurotrophin and Trk receptor gene families. *Current Opinion in Neurobiology*, 9(5), 616–621.

Hallbook, F., Lundin, L. G., & Kullander, K. (1998). Lampetra fluviatilis neurotrophin homolog, descendant of a neurotrophin ancestor, discloses the early molecular evolution of neurotrophins in the vertebrate subphylum. *The Journal of Neuroscience*, 18(21), 8700–8711.

Hallbook, F., Wilson, K., Thorndyke, M., & Olinski, R. P. (2006). Formation and evolution of the chordate neurotrophin and Trk receptor genes. *Brain Behavior & Evolution*, 68(3), 133–144.

Harris, J. A., & Rubel, E. W. (2006). Afferent regulation of neuron number in the cochlear nucleus: Cellular and molecular analyses of a critical period. *Hearing Research*, 2166–217, 127–137.

Heeroma, J. H., Roelandse, M., Wierda, K., van Aerde, K. I., Toonen, R. F., Hensbroek, R. A., Brussaard, A., Matus, A., & Verhage, M. (2004). Trophic support delays but does not prevent cell-intrinsic degeneration of neurons deficient for munc18-1. *The European Journal of Neuroscience*, 20(3), 623–634.

Hellard, D., Brosenitsch, T., Fritzsch, B., & Katz, D. M. (2004). Cranial sensory neuron development in the absence of brain-derived neurotrophic factor in BDNF/Bax double null mice. *Developmental Biology*, 275(1), 34–43.

Jahan, I., Pan, N., Kersigo, J., & Fritzsch, B. (2013). Beyond generalized hair cells: Molecular cues for hair cell types. *Hearing Research*, 297, 30–41.

Jahan, I., Pan, N., Kersigo, J., Calisto, L.E., Morris, K.A., Kopecky, B., Duncan, J.S., Beisel, K. W., Fritzsch, B. (2012). Expression of Neurog1 instead of Atoh1 can partially rescue organ of Corti cell survival. PLoS One, 7: e30853.

Jones, D. P., & Singer, M. (1969). Neurotrophic dependence of the lateral-line sensory organs of the newt, Triturus viridescens. *The Journal of Experimental Zoology*, 171(4), 433–442.

Katayama, K., Zine, A., Ota, M., Matsumoto, Y., Inoue, T., Fritzsch, B., & Aruga, J. (2009). Disorganized innervation and neuronal loss in the inner ear of Slitrk6-deficient mice. *PLoS One*, 4(11), e7786.

Kersigo, J., & Fritzsch, B. (2015). Inner ear hair cells deteriorate in mice engineered to have no or diminished innervation. *Frontiers in Aging Neuroscience*, 7, 33.

Kersigo, J., D'Angelo, A., Gray, B. D., Soukup, G. A., & Fritzsch, B. (2011). The role of sensory organs and the forebrain for the development of the craniofacial shape as revealed by Foxg1-cre-mediated microRNA loss. *Genesis*, 49(4), 326–341.

Klein, R., Silos-Santiago, I., Smeyne, R. J., Lira, S. A., Brambilla, R., Bryant, S., Zhang, L., Snider, W. D., & Barbacid, M. (1994). Disruption of the neurotrophin-3 receptor gene trkC eliminates la muscle afferents and results in abnormal movements. *Nature*, 368(6468), 249–251.

Kopecky, B. J., Jahan, I., & Fritzsch, B. (2013). Correct timing of proliferation and differentiation is necessary for normal inner ear development and auditory hair cell viability. *Developmental Dynamics*, 242(2), 132–147.

Koppel, I., & Timmusk, T. (2013). Differential regulation of Bdnf expression in cortical neurons by class-selective histone deacetylase inhibitors. *Neuropharmacology*, 75, 106–115.

Koppel, I., Aid-Pavlidis, T., Jaanson, K., Sepp, M., Palm, K., & Timmusk, T. (2010). BAC transgenic mice reveal distal cis-regulatory elements governing BDNF gene expression. *Genesis*, 48(4), 214–219.

Kuczewski, N., Porcher, C., Lessmann, V., Medina, I., & Gaiarsa, J. L. (2009). Activity-dependent dendritic release of BDNF and biological consequences. *Molecular Neurobiology*, 39(1), 37–49.

Levi-Montalcini, R. (1949). The development to the acoustico-vestibular centers in the chick embryo in the absence of the afferent root fibers and of descending fiber tracts. *Journal of Comparative Neurology*, 91(2), 209–241.

Lewis, E. R., Leverenz, E. L., & Bialek, W. S. (1985). *The vertebrate inner ear.* Boca Raton, FL: CRC Press.

Lindholm, P., & Saarma, M. (2010). Novel CDNF/MANF family of neurotrophic factors. *Developmental Neurobiology*, 70(5), 360–371.

Ma, C., Su, L., Seven, A. B., Xu, Y., & Rizo, J. (2013). Reconstitution of the vital functions of Munc18 and Munc13 in neurotransmitter release. *Science*, 339(6118), 421–425.

Ma, L., Reis, G., Parada, L. F., & Schuman, E. M. (1999). Neuronal NT-3 is not required for synaptic transmission or long-term potentiation in area CA1 of the adult rat hippocampus. *Learning & Memory*, 6(3), 267–275.

Ma, Q., Anderson, D. J., & Fritzsch, B. (2000). Neurogenin 1 null mutant ears develop fewer, morphologically normal hair cells in smaller sensory epithelia devoid of innervation. *Journal of the Association of Research in Otolaryngology*, 1(2), 129–143.

Maklad, A., & Fritzsch, B. (2003). Development of vestibular afferent projections into the hindbrain and their central targets. *Brain Research Bulletin*, 60(5–6), 497–510.

Maklad, A., Kamel, S., Wong, E., & Fritzsch, B. (2010). Development and organization of polarity-specific segregation of primary vestibular afferent fibers in mice. *Cell and Tissue Research*, 340(2), 303–321.

Mao, Y., Reiprich, S., Wegner, M., & Fritzsch, B. (2014). Targeted deletion of Sox10 by Wnt1-cre defects neuronal migration and projection in the mouse inner ear. *PLoS One*, 9(4), e94580.

Maricich, S. M., Xia, A., Mathes, E. L., Wang, V. Y., Oghalai, J. S., Fritzsch, B., & Zoghbi, H. Y. (2009). Atoh1-lineal neurons are required for hearing and for the survival of neurons in the spiral ganglion and brainstem accessory auditory nuclei. *The Journal of Neuroscience*, 29(36), 11123–11133.

Marrs, G. S., & Spirou, G. A. (2012). Embryonic assembly of auditory circuits: spiral ganglion and brainstem. *Journal of Physiology*, 590(Part 10), 2391–2408.

Matei, V., Pauley, S., Kaing, S., Rowitch, D., Beisel, K. W., Morris, K., Feng, F., Jones, K., Lee, J., & Fritzsch, B. (2005). Smaller inner ear sensory epithelia in Neurog1 null mice are related to earlier hair cell cycle exit. *Developmental Dynamics*, 234(3), 633–650.

Miyamoto, Y., Yamauchi, J., Tanoue, A., Wu, C., & Mobley, W. C. (2006). TrkB binds and tyrosine-phosphorylates Tiam1, leading to activation of Rac1 and induction of changes in cellular morphology. *Proceedings of the National Academy of Sciences of the USA*, 103(27), 10444–10449.

Nayagam, B. A., Muniak, M. A., & Ryugo, D. K. (2011). The spiral ganglion: Connecting the peripheral and central auditory systems. *Hearing Research*, 278(1–2), 2–20.

Nikolic, P., Jarlebark, L. E., Billett, T. E., & Thorne, P. R. (2000). Apoptosis in the developing rat cochlea and its related structures. *Brain Research, Developmental Brain Research*, 119(1), 75–83.

Oppenheim, R. (1991). Cell death during development of the nervous system. *Annual Review of Neuroscience*, 14(1), 453–501.

Oppenheim, R. W. (1989). The neurotrophic theory and naturally occurring motoneuron death. *Trends in Neurosciences*, 12(7), 252–255.

Pan, N., Jahan, I., Kersigo, J., Duncan, J., Kopecky, B., & Fritzsch, B. (2012a). A novel Atoh1 'self-terminating' mouse model reveals the necessity of proper Atoh1 expression level and duration for inner ear hair cell differentiation and viability. *PLoS One*, 7(1), e30358.

Pan, N., Kopecky, B., Jahan, I., & Fritzsch, B. (2012b). Understanding the evolution and development of neurosensory transcription factors of the ear to enhance therapeutic translation. *Cell and Tissue Research*, 349, 415–432.

Pan, N., Jahan, I., Kersigo, J., Kopecky, B., Santi, P., Johnson, S., Schmitz, H., & Fritzsch, B. (2011). Conditional deletion of Atoh1 using Pax2–Cre results in viable mice without differentiated cochlear hair cells that have lost most of the organ of Corti. *Hearing Research*, 275(1–2), 66–80.

Panja, D., & Bramham, C. R. (2014). BDNF mechanisms in late LTP formation: A synthesis and breakdown. *Neuropharmacology*, 76(Part C), 664–676.

Pauley, S., Kopecky, B., Beisel, K., Soukup, G., & Fritzsch, B. (2008). Stem cells and molecular strategies to restore hearing. *Panminerva Medica*, 50(1), 41–53.

Petralia, R. S., Gill, S. S., & Peusner, K. D. (1991). Ultrastructural evidence that early synapse formation on central vestibular sensory neurons is independent of peripheral vestibular influences. *Journal of Comparative Neurology*, 310(1), 68–81.

Peusner, K., Vidal, P. P., Minor, L., Cullen, K., Yates, B., Shao, M., & Dutia, M. (2009). Vestibular compensation: New clinical and basic science perspectives. *Journal of Vestibular Research*, 19(5–6), 143–146.

Peusner, K. D., & Morest, D. K. (1977). Neurogenesis in the nucleus vestibularis tangentialis of the chick embryo in the absence of the primary afferent fibers. *Neuroscience*, 2(2), 253–270.

Pirvola, U., Ylikoski, J., Palgi, J., Lehtonen, E., Arumae, U., & Saarma, M. (1992). Brain-derived neurotrophic factor and neurotrophin 3 mRNAs in the peripheral target fields of developing inner ear ganglia. *Proceedings of the National Academy of Science USA*, 89(20), 9915–9919.

Pirvola, U., Arumae, U., Moshnyakov, M., Palgi, J., Saarma, M., & Ylikoski, J. (1994). Coordinated expression and function of neurotrophins and their receptors in the rat inner ear during target innervation. *Hearing Research*, 75(1–2), 131–144.

Pirvola, U., Hallbook, F., Xing-Qun, L., Virkkala, J., Saarma, M., & Ylikoski, J. (1997). Expression of neurotrophins and Trk receptors in the developing, adult, and regenerating avian cochlea. *Journal of Neurobiology*, 33(7), 1019–1033.

Postigo, A., Calella, A. M., Fritzsch, B., Knipper, M., Katz, D., Eilers, A., Schimmang, T., Lewin, G. R., Klein, R., & Minichiello, L. (2002). Distinct requirements for TrkB and TrkC signaling in target innervation by sensory neurons. *Genes & Development*, 16(5), 633–645.

Pruunsild, P., Sepp, M., Orav, E., Koppel, I., & Timmusk, T. (2011). Identification of cis-elements and transcription factors regulating neuronal activity-dependent transcription of human BDNF gene. *The Journal of Neuroscience*, 31(9), 3295–3308.

Richter, C. P., Kumar, G., Webster, E., Banas, S. K., & Whitlon, D. S. (2011). Unbiased counting of neurons in the cochlea of developing gerbils. *Hearing Research*, 278(1–2), 43–51.

Rubel, E. W., & Fritzsch, B. (2002). Auditory system development: Primary auditory neurons and their targets. *Annual Review of Neuroscience*, 25, 51–101.

Ruben, R. J. (1967). Development of the inner ear of the mouse: A radioautographic study of terminal mitoses. *Acta Oto-Laryngolocia Supplementum*, 220, 221–244.

Rueda, J., de la Sen, C., Juiz, J. M., & Merchan, J. A. (1987). Neuronal loss in the spiral ganglion of young rats. *Acta Oto-Laryngologica*, 104(5–6), 417–421.

Rusch, A., Lysakowski, A., & Eatock, R. A. (1998). Postnatal development of type I and type II hair cells in the mouse utricle: Acquisition of voltage-gated conductances and differentiated morphology. *The Journal of Neuroscience*, 18(18), 7487–7501.

Shao, M., Popratiloff, A., Hirsch, J. C., & Peusner, K. D. (2009). Presynaptic and postsynaptic ion channel expression in vestibular nuclei neurons after unilateral vestibular deafferentation. *Journal of Vestibular Research*, 19(5–6), 191–200.

Schimmang, T., Minichiello, L., Vazquez, E., San Jose, I., Giraldez, F., Klein, R., & Represa, J. (1995). Developing inner ear sensory neurons require TrkB and TrkC receptors for innervation of their peripheral targets. *Development*, 121(10), 3381–3391.

Sciarretta, C., Fritzsch, B., Beisel, K., Rocha-Sanchez, S. M., Buniello, A., Horn, J. M., & Minichiello, L. (2010). PLCgamma-activated signalling is essential for TrkB mediated sensory neuron structural plasticity. *BMC Developmental Biology*, 10, 103.

Simmons, D., Duncan, J., Crapon de Caprona, D., & Fritzsch, B. (2011). Development of the inner ear efferent system. In D. K. Ryugo, R. R. Fay, & A. N. Popper (Eds.), *Auditory and vestibular efferents.* (pp. 187–216.). New York: Springer Science+Business Media.

Singer, W., Panford-Walsh, R., & Knipper, M. (2014). The function of BDNF in the adult auditory system. *Neuropharmacology*, 76(Part C), 719–728.

Stenqvist, A., Agerman, K., Marmigere, F., Minichiello, L., & Ernfors, P. (2005). Genetic evidence for selective neurotrophin 3 signalling through TrkC but not TrkB in vivo. *EMBO Reports*, 6(10), 973–978.

Straka, H., Fritzsch, B., & Glover, J. C. (2014). Connecting ears to eye muscles: Evolution of a 'simple'reflex arc. *Brain, Behavior and Evolution*, 83(2), 162–175.

Taylor, A. R., Gifondorwa, D. J., Robinson, M. B., Strupe, J. L., Prevette, D., Johnson, J. E., Hempstead, B., Oppenheim, R. W., & Milligan, C. E. (2012). Motoneuron programmed cell death in response to proBDNF. *Developmental Neurobiology*, 72(5), 699–712.

Tessarollo, L., Tsoulfas, P., Donovan, M. J., Palko, M. E., Blair-Flynn, J., Hempstead, B. L., & Parada, L. F. (1997). Targeted deletion of all isoforms of the trkC gene suggests the use of alternate receptors by its ligand neurotrophin-3 in neuronal development and implicates trkC in normal cardiogenesis. *Proceedings of the National Academy of Sciences of the USA*, 94(26), 14776–14781.

Tessarollo, L., Coppola, V., & Fritzsch, B. (2004). NT-3 replacement with brain-derived neurotrophic factor redirects vestibular nerve fibers to the cochlea. *The Journal of Neuroscience*, 24(10), 2575–2584.

Triplett, J. W. (2014). Molecular guidance of retinotopic map development in the midbrain. *Current Opinion in Neurobiology*, 24, 7–12.

van de Bospoort, R., Farina, M., Schmitz, S. K., de Jong, A., de Wit, H., Verhage, M., & Toonen, R. F. (2012). Munc13 controls the location and efficiency of dense-core vesicle release in neurons. *The Journal of Cell Biology*, 199(6), 883–891.

Varoqueaux, F., Sigler, A., Rhee, J. S., Brose, N., Enk, C., Reim, K., & Rosenmund, C. (2002). Total arrest of spontaneous and evoked synaptic transmission but normal synaptogenesis in the absence of Munc13-mediated vesicle priming. *Proceedings of the National Academy of Sciences of the USA*, 99(13), 9037–9042.

Verhage, M., Maia, A. S., Plomp, J. J., Brussaard, A. B., Heeroma, J. H., Vermeer, H., Toonen, R. F., Hammer, R. E., van den Berg, T. K., Missler, M., Geuze, H. J., & Sudhof, T. C. (2000). Synaptic assembly of the brain in the absence of neurotransmitter secretion. *Science*, 287 (5454), 864–869.

von Bartheld, C. S., & Fritzsch, B. (2006). Comparative analysis of neurotrophin receptors and ligands in vertebrate neurons: Tools for evolutionary stability or changes in neural circuits? *Brain, Behavior and Evolution*, 68(3), 157–172.

von Bartheld, C. S., Patterson, S. L., Heuer, J. G., Wheeler, E. F., Bothwell, M., & Rubel, E. W. (1991). Expression of nerve growth factor (NGF) receptors in the developing inner ear of chick and rat. *Development*, 113(2), 455–470.

Xiang, M., Maklad, A., Pirvola, U., & Fritzsch, B. (2003). Brn3c null mutant mice show long-term, incomplete retention of some afferent inner ear innervation. *BMC Neuroscience*, 4(1), 2.

Yang, T., Bassuk, A. G., & Fritzsch, B. (2013). Prickle1 stunts limb growth through alteration of cell polarity and gene expression. [Research Support, N.I.H., Extramural]. *Developmental Dynamics*, 242(11), 1293–1306.

Yang, T., Kersigo, J., Jahan, I., Pan, N., & Fritzsch, B. (2011). The molecular basis of making spiral ganglion neurons and connecting them to hair cells of the organ of Corti. *Hearing Research*, 278(1–2), 21–33.

Ylikoski, J., Pirvola, U., Moshnyakov, M., Palgi, J., Arumae, U., & Saarma, M. (1993). Expression patterns of neurotrophin and their receptor mRNAs in the rat inner ear. *Hearing Research*, 65(1–2), 69–78.

Zhou, X. N., & Van de Water, T. R. (1987). The effect of target tissues on survival and differentiation of mammalian statoacoustic ganglion neurons in organ culture. *Acta Oto-Laryngologica*, 104(1–2), 90–98.

Zilberstein, Y., Liberman, M. C., & Corfas, G. (2012). Inner hair cells are not required for survival of spiral ganglion neurons in the adult cochlea. *Journal of Neuroscience*, 32(2), 405–410.

Zuccotti, A., Kuhn, S., Johnson, S. L., Franz, C., Singer, W., Hecker, D., Geisler, H. S., Kopschall, I., Rohbock, K., Gutsche, K., Dlugaiczyk, J., Schick, B., Marcotti, W., Ruttiger, L., Schimmang, T., & Knipper, M. (2012). Lack of brain-derived neurotrophic factor hampers inner hair cell synapse physiology, but protects against noise-induced hearing loss. *The Journal of Neuroscience*, 32(25), 8545–8553.

Chapter 4
The Electrophysiological Signature of Spiral Ganglion Neurons

Robin L. Davis and Robert A. Crozier

Keywords Accommodation · Brain-derived neurotrophic factor · Membrane potential · Neurotrophin 3 · Primary auditory afferents · Threshold · Voltage-gated ion channels

4.1 Introduction

Every neuronal type in the peripheral and central nervous system (PNS and CNS, respectively) displays characteristic electrophysiological properties that shape the transmitted electrical signal for effective and efficient coding. From the regular firing of cortical pyramidal cells to the complex bursting observed in cerebellar Purkinje cells, firing patterns vary widely (Bean, 2007). For primary sensory afferent neurons, accommodation is a hallmark feature that defines different response types (Loewenstein & Mendelson, 1965; Cleland et al., 1971; Crozier & Davis, 2014). Further, it is also clear that the shape of a single action potential can vary. Some are prolonged, as evidenced by midbrain dopaminergic neurons (Puopolo et al., 2007), compared to the more abbreviated action potentials observed in other areas of the brain such as fast-spiking cells of the neocortex (McCormick et al., 1985). Another example is the calcium spike that typifies neuromodulatory neurons such as those that secrete serotonin, acetylcholine, and dopamine, in which the increased calcium entry likely enhances neurotransmitter release at the presynaptic terminals (Klein & Kandel, 1980). Thus, the shape of action potentials and patterns of firing are critical features for determining the specific contributions any particular neuron supplies to coding paradigms.

R.L. Davis (✉) · R.A. Crozier
Department of Cell Biology and Neuroscience, Rutgers University, 604 Allison Road, Piscataway NJ 08854, USA
e-mail: rldavis@dls.rutgers.edu

R.A. Crozier
e-mail: crozier@dls.rutgers.edu

A. Dabdoub et al. (eds.), *The Primary Auditory Neurons of the Mammalian Cochlea*, Springer Handbook of Auditory Research 52,
DOI 10.1007/978-1-4939-3031-9_4

Interestingly, the phenotype of spiral ganglion neurons is exquisitely diverse and uniquely specialized. These electrophysiologically relevant specializations are likely tailored to promote accuracy and reliability within the neurons themselves to meet the challenge of conveying rapidly acquired stimuli with precision. This should be considered within the context of the coding requirements of the first neuronal element in the auditory system. Spiral ganglion neurons must first receive input from the peripherally located sensory receptors, project through the PNS, traverse the Schwann–glial border into the CNS, and then synapse onto multiple targets located within the cochlear nucleus (CN). All told, spiral ganglion neurons must transmit signals from the PNS to the CNS over relatively long distances, on the order of hundreds of microns (Fekete et al., 1984). Moreover, they must also meet the added demand of conveying their signals with precision. In addition to allowing discrimination of frequency, intensity, patterns, and timbre of sound stimuli (Bizley & Walker, 2010), accurate transmission of interaural time and intensity differences are necessary to enable the system to build meaningful sound localization maps in the brain stem (Grothe et al., 2010). Once these maps are constructed, the acoustic information is fully transformed into an area in the brain that represents location in space. Yet, for these transformations to take place with accuracy, the demands on the afferents to deliver signals with precision in timing and intensity are unquestionably stringent (Carr et al., 2001).

4.2 Electrophysiologically Relevant Morphological Specializations

4.2.1 An Electrophysiological Perspective on Innervation Patterns

The innervation patterns that define the type I and type II spiral ganglion neurons, described in Chaps. 1 by Dabdoub and Fritzsch and 2 by Goodrich, illustrate a distinctive anatomical organization that can lend insights into the functional coding requirements of each class of primary afferent. For example, the type I neurons, which compose up to 95 % of the ganglion, make one-to-one synaptic connections with inner hair cell (IHC) receptors; thus they have the ability to code the smallest receptive field that can be directly delivered by the cochlear machinery (Fig. 4.1a, b; Held, 1926; Brödel & Malone, 1946). Similar to other sensory afferents, most notably those innervating the retinal fovea and touch receptors on a fingertip, this type of organization delivers sensory information with high resolution (Mountcastle et al., 1966; Ahmad et al., 2003). Because the major modality in the cochlea is frequency, this type of organization subserves precision in coding information in the temporal domain. Further, the 10–30 afferents/IHC also form a classic divergent

pathway (see Rutherford and Moser, Chap. 5) in which the information received and conveyed synaptically by the receptor cell is delivered to the brain via multiple pathways. Thus, in addition to conveying high-resolution information about the acoustic environment, the type I neurons also exhibit the first stages of parallel processing in which submodalities are split into separate pathways and transmitted concurrently.

A consideration of the role played by type I spiral ganglion neurons in afferent signal transmission would be incomplete without some discussion of the extensive descending efferent control that is exerted at the neuronal postsynaptic membrane. Neurotransmitters released from the lateral efferent system include acetylcholine (ACh), γ-aminobutryic acid (GABA), calcitonin gene–related peptide (CGRP), dopamine, serotonin, adenosine triphosphate (ATP), and opioids such as dynorphin and enkephalin (Dulon et al., 2006; Ciuman, 2010). This list includes both excitatory (ACh, CGRP, dynorphin) and inhibitory (GABA and dopamine) transmitter types (Simmons et al., 2011). Further, combinations of transmitters can reside within the same presynaptic terminals (e.g., ACh and dynorphin), thus complicating an already intricate microchemical environment (Altschuler et al., 1985; Safieddine & Eybalin, 1992). This indicates that the receptor-generated synaptic signal is exquisitely controlled within the first moments of synaptic transmission, even before the action potential is generated at the spike initiation zone. This complex organization at the source of electrical signal generation, together with its innervation pattern, suggests that the type I primary afferent is specialized to precisely shape a high-resolution neural signal that is a subcomponent of the total output of a single IHC.

The type II spiral ganglion neurons are a second, enigmatic class of primary afferents that compose the remaining 5 % of the ganglion. Although little is known about their in vivo responses to sound stimuli, their peripheral synaptic connections, like the type I afferents, also illuminate aspects of their potential role in coding. As described in Chaps. 1 by Dabdoub and Fritzsch and 2 by Goodrich, type II afferents innervate multiple outer hair cells (OHCs; Fig. 4.1b; Spoendlin, 1973; Perkins & Morest, 1975). This classically convergent pathway is designed for signal integration rather than resolution, and has a proposed role in the sensory determinations of threshold detection and pain perception (Spoendlin, 1973; Brown, 1994), two functions that, although divergent in their sensory input, similarly require the specialization of signal integration. What ultimately distinguishes one function from the other is the detection characteristics of the sensory receptors themselves. In this regard, one might expect that the network of OHCs is highly sensitive to sound stimuli due to cellular specializations such as the transduction channels at the tips of the stereocilia, indicating a role in threshold detection. Conversely, because synaptic input from satellite cells may contribute to the synaptic potential generated onto apical type II spiral ganglion neurons (Burgess et al., 1997), it is possible that input is also gathered from high-intensity events, perhaps indicating a role in pain

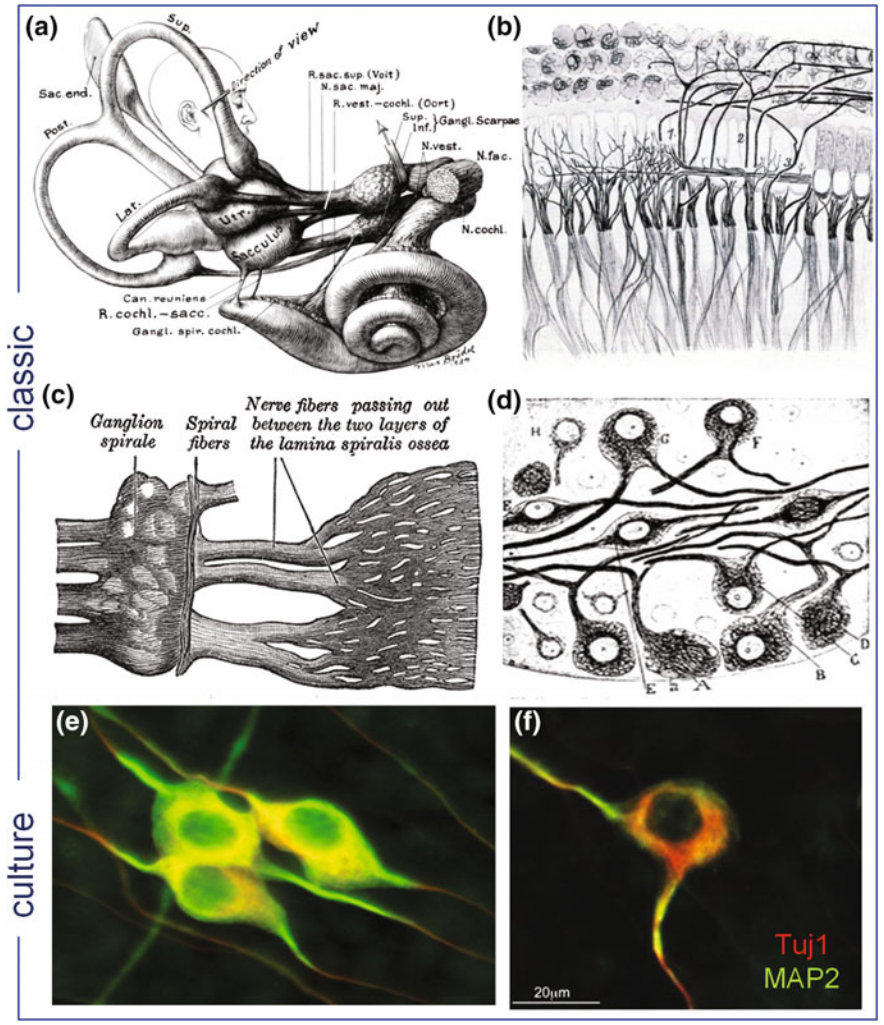

perception. It is possible that both views may be correct with regard to type II neurons, acting either individually or as an overall population and being capable of integrating an array of input with widely divergent intensities, potentially contributing to a broad detection range with low resolution. Thus, investigators have found that whether type II neurons receive, process, and transmit low threshold input, high-intensity stimuli, or both, their endogenous membrane properties reflect the underlying requirement to mediate signal integration across a wide range of sensory input, including prolonged time constants (Reid et al., 2004; Weisz et al., 2014).

A description of the role of type II afferents in sensory processing is also incomplete without a consideration of efferent innervation. In this case, the efferent

◀ **Fig. 4.1** The peripheral innervation patterns and classical morphologies of spiral ganglion neurons are illustrative of their respective functional specializations. **a** Image of the vestibular and auditory bony structures within the inner ear. (Adapted from Brödel & Malone, 1946.) **b** Illustration of the anatomical arrangements within the organ of Corti with many type I spiral ganglion fibers innervating a single inner hair cell and individual type II fibers innervating multiple outer hair cells. (Adapted from Held, 1926. Die Cochlea der Säuger und der Vögel, ihre Entwicklung und ihr Bau. In *Handbuch der Physiologie*.) **c–f** The classically bipolar and pseudomonopolar spiral ganglion neuronal cell bodies described in vivo are also observed in tissue culture. **c** Bipolar primary afferent neurons compose the spiral ganglion. (From Gray & Lewis, 1918.) **d** Pseudomonopolar profiles are highlighted in a longitudinal section through a spiral ganglion of a chick embryo on the 12th day of incubation using the reduced silver nitrate method. The figure illustrates the full range of morphologies, although the relative percentages are not representative. (From Santiago Ramón y Cajal 1995. *Histology of the nervous system*, Vol 1., Figure 33. Oxford University Press.) **e**, **f** Examples of bipolar **e** and pseudomonopolar **f** neurons in vitro isolated from their peripheral and central synaptic targets and co-labeled with anti-MAP2 antibody (*green*) and anti-neuron-specific β-III tubulin antibody (red). (Adapted from Chen et al., 2011, cover illustration) and F. L. Smith and R. L. Davis (in preparation), respectively

innervation originates from the medial superior olivary (MSO) complex and is delivered directly to the OHCs (Guinan, 2011). However, what is unique about efferent cochlear controls at the level of the OHCs is that type II neurons themselves exert a postulated feedback control on OHCs through reciprocal synapses (Thiers et al., 2008). Thus, type II afferents may serve as a local efferent regulator, in addition to their role as integrators of multiple sensory receptor inputs.

Beyond the spiral ganglion neuronal classes and their innervation patterns, a concerted effort has been made in recent years to characterize the intrinsic electrophysiological features of these cells. This goal was made possible by in vitro systems that allow access to whole-cell and single-channel patch-clamp recordings and provide a stable environment for manipulating experimental conditions. Although it is necessary to separate the neurons from their peripheral and central targets to determine unequivocally their endogenous characteristics, it is critical that many of their overall features remain unchanged. Evaluations have shown that at the most basic level, spiral ganglion neurons retain their distinctive features. As shown (Fig. 4.1c–f), their bipolar and pseudomonopolar soma shapes are evident, and they elaborate long processes that, in many culture conditions, reiterate their simple in vivo branching patterns (Whitlon et al., 2006). Further, intermediate filaments that distinguish type I from type II spiral ganglion neurons in vivo (Hafidi, 1998; see also Muniak et al., Chap. 6) are retained in vitro (Mou et al., 1998), which makes it possible to separate the firing features of type I from type II neurons even when isolated from their peripheral targets. Moreover, immunocytochemical studies have shown that many voltage-gated ion channels characterized for these neurons in vitro are also detected in postnatal and adult spiral ganglion tissue sections. Thus, although there inevitably will be differences found between the electrophysiologically relevant phenotype of isolated spiral ganglion neurons in vitro and those still connected to their synaptic partners in vivo, these studies allow a more

comprehensive view of the capabilities of the neurons on their own so that the role of the spiral ganglion can be assessed as a component part of the auditory neural pathway.

4.2.2 An Unusual Neuron

The functional challenges carried out by the convergent and divergent pathways formed by the primary auditory afferents are met by a class of neurons with an unusual morphological configuration. Compared to the entirety of the nervous system, the type I spiral ganglion neurons that compose the VIIIth cranial nerve are unique because of their bipolar and pseudomonopolar configurations, in which the somata are part of the conduction pathway (Fig. 4.1). In many species, the type I spiral ganglion somata, interposed in the conduction pathway, possesses a unique form of myelin, termed loose myelin (Rosenbluth, 1962), whereas in humans the interposing somata are unmyelinated (Nadol, 1988). Thus, the configuration of this class of primary afferents is unlike that of a typical central neuron in which electrical input is received in the dendrites and integrated at the soma *before* generating an action potential at the spike initiation zone. Instead, in the spiral ganglion, the action potential is initiated in the type I cells proximal to the sensory receptors and transmitted along the axonal segment, which is interrupted by a large expanse of soma membrane (Hossain et al., 2005). Without specific compensatory electrophysiological specializations, one might expect that this configuration would create an impedance mismatch that leads to action potential failure (Despres et al., 1994), much like that observed at asymmetric axonal branch points (Luscher and Shiner 1990; Debanne et al., 2011). However, the bipolar spiral ganglion somata have multiple morphological specializations, such as the close proximity of surrounding nodes and differential diameter of their central versus peripheral initial processes (Liberman & Oliver, 1984; Spoendlin & Schrott, 1989), which presumably counteract "branch failures" that, if unchecked, would ultimately impede action potential conduction into the CNS.

Why would a high-precision system evolve to interpose the soma in the conduction pathway only to necessarily overcome its presence? One might speculate that these elaborate morphological specializations are designed to filter or modify, rather than block, signal transmission. The electrophysiological significance of the soma is compounded by the fact that spiral ganglion somata sizes are graded along the cochlear contour. Although heterogeneous, neurons in the apex are significantly smaller than those in the base (Nadol et al., 1990). Yet, rather than the soma area differences being rigidly graded, one observes small but systematic size increases from the apex through the mid-basal region, and then the soma area abruptly increases in the most extreme end of the base (Echteler & Nofsinger, 2000). One study that addressed the electrophysiological consequences of this size disparity concluded that soma area is related to action potential filtering (Robertson, 1976). An additional possibility is that the soma size regulates conduction time through the

soma (Lawson & Waddell, 1991), which is also dependent on input resistance, the length constant, and membrane area (Johnston et al., 1995). Whether these somatic specializations contribute to filtering, transmission delays, or other aspects of shaping the endogenous electrical profile, the system design appears to support specialized processes separately for low–mid- versus high-frequency regions.

The unique soma placement and presence of loose myelin initially suggest that the soma, itself, is an internodal axonal structure that serves exclusively to transmit signals. However, there is evidence that the soma is electrogenic and therefore potentially capable of integrating signals as well as conducting them (Robertson, 1976). In support of this latter view, microtubule-associated protein 2 (MAP2), a marker of dendrites and somatic integrating regions, was shown to be present in spiral ganglion neuron somata (Chen et al., 2011) in both bipolar (Fig. 4.1e, green/yellow) and pseudomonopolar (Fig. 4.1f, green/yellow) cell types. This staining extends into the processes that emanate from the soma, yet was not observed along their axons (Fig. 4.1e, f red). Thus, despite their axonal location, spiral ganglion neuronal somata possess a dendritic marker, suggesting a distinct functionality that is separated from the postsynaptic dendritic region by a length of myelinated axon. Further, a related protein, CASPR, known to flank the nodes of Ranvier and found within the spike initiation zone (Peles et al., 1997), has also been localized to the somatic region (Hossain et al., 2005), along with multiple types of voltage-gated ion currents (Rusznak & Szucs, 2009). Thus, it appears that spiral ganglion neurons are unusual, not because they lack a soma that can potentially integrate and shape electrical signals, but because this region is morphologically discontinuous from the postsynaptic membrane and primary spike initiation zone.

Further evidence that spiral ganglion somata may contribute to shaping the signals that they ultimately transmit comes from the now well-established presence of somatic voltage-gated ion channels located beneath the loose myelin. A first step toward determining whether resident voltage-gated ion channels affect electrogenicity was performed on neurons from the goldfish (*Carassius auratus*) saccular nerve, which are bipolar myelinated neurons (Fig. 4.2a, b) that convey sound (Furshpan & Furukawa, 1962). Mechanical microdissection of the myelin (Fig. 4.2c, d) permitted single-channel patch-clamp recordings from the underlying somatic membrane (Davis, 1996). Recordings indeed showed multiple classes of voltage-gated ion channels (Fig. 4.2e–h). Four separate K^+ channel types were identified based on their distinctive kinetics, conductances, and inactivation profiles (Fig. 4.2e–g), one of which was the large-conductance, voltage- and calcium-activated potassium (BK) channel (Fig. 4.2g, h). These experiments revealed that voltage-gated channels were functional in the cell bodies of primary auditory afferents, despite their location beneath myelin, and thus highlighted the electrogenic capacity of these neurons. Further, these studies show that the complexity of the electrophysiological profile of the soma membrane goes well beyond the simple combination of nodal Na^+ channels and paranodal delayed rectifier K^+ channels (Rasband & Trimmer, 2001).

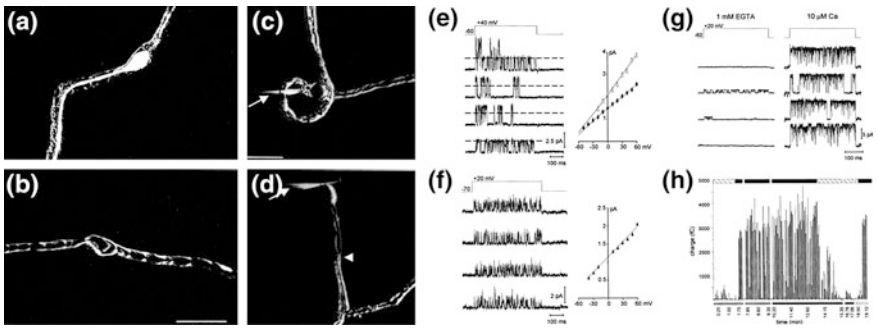

Fig. 4.2 Identification of K^+ channels in acutely demyelinated primary auditory neurons. **a** Bipolar goldfish saccular neuron encased in myelin labeled intracellularly with Lucifer Yellow. **b** The myelin covering was labeled independently by breaking through the Schwann cell membrane surrounding a bipolar goldfish saccular neuron. **c** The initial stage of mechanical demyelination. A glass micropipette was used to penetrate the myelin sheath without affecting the neuronal membrane. The *arrow* indicates the pipette position after the myelin above the soma membrane had been partially removed. **d** The pipette (*arrow*) was subsequently threaded between the remaining myelin and neuronal membrane and then lifted to remove the soma from the myelin covering. *Arrowhead* indicates the edge of the myelin. **e**–**h** Evidence for multiple types of somatic voltage-gated K^+ channels obtained from patch-clamp recordings of the internodal membrane. **e** Overlapping openings of different amplitudes indicate the presence of two distinct K^+ channel types. Right, current-to-voltage relationships for the small (*filled diamond*) and large (*open triangle*) channel openings. The conductances were 18 and 30 pS, respectively, for the small and large conductance channels. **f** Similar to **e** but this channel type had much briefer openings. *I*–*V* graph to the right indicates a conductance of 14 pS and a reversal potential of −81 mV for this channel. **g** An inside-out single-channel recording revealed the presence of a large-conductance K^+ channel that was activated following elevation of external Ca^{2+} (compare left side sweeps with the right when 10 μM Ca^{2+} was added). **h** Plot of charge (fC) calculated for each sweep over the course of a recording of a BK channel. Below the *x*-axis (time, min) are the voltage protocols used (hatched bars, −60 mV holding potential, stepped to 0 mV; black bars, −40 mV holding potential, 0 mV step potential; white bars, −60 mV holding potential, +10 mV step potential). Represented above the graph are durations of EGTA application (*hatched bar*) and 10 μM Ca^{2+} (*black bars*). Note the increase in charge with the addition of Ca^{2+}. (Adapted from Figs. 1–3 of Davis, 1996)

4.3 The Basic Firing Patterns

The unusual morphological configuration of the spiral ganglion neuron, in which an electrogenic cell soma lies directly in the signal conduction pathway, makes it imperative to characterize the firing properties of isolated neurons to understand better their contribution to coding. The first intracellular recordings of this type were made from adult spiral ganglion neurons (Santos-Sacchi, 1993). Voltage-clamp traces revealed a transient inward Na^+ current, which could be blocked by tetrodotoxin (TTX), followed by an outward current with properties that typified a classic delayed rectifier (Fig. 4.3a_1; Santos-Sacchi, 1993). Although current-clamp traces showed an atypical gradation in amplitude, a fully formed action potential was evident at the highest depolarization (Fig. 4.3a_2). This basic

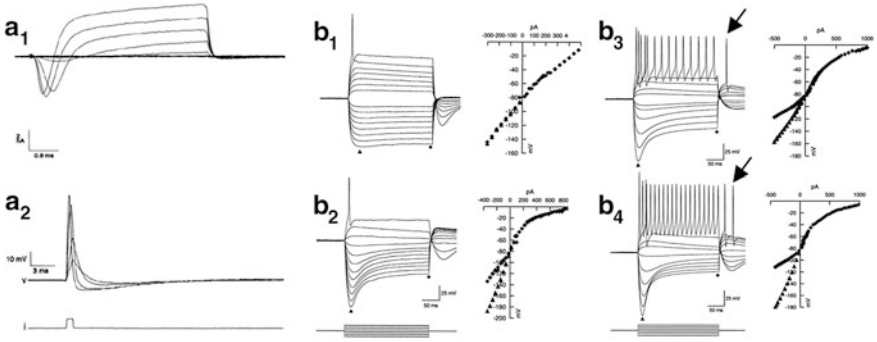

Fig. 4.3 Somatic electrophysiological recordings of spiral ganglion neurons in culture confirm electrogenicity and display a wide range of firing features. a_1 Whole-cell voltage-clamp traces demonstrate the presence of an inward Na^+ current and an outward K^+ current from an isolated, adult rat spiral ganglion neuron in culture. a_2 Current-clamp recording from the cell shown in the top panel. Increasing amounts of current injection elicit a fast depolarization followed by a rapid repolarization and an after-hyperpolarization that are consistent with an action potential. (From Fig. 2 of Santos-Sacchi, 1993.) **b** Whole-cell patch-clamp recordings and voltage-current (V–I) relationships for rapidly accommodating (RA) and slowly accommodating (SA) neurons. b_1 Voltage responses of an RA neuron. Depolarizing current injection resulted in a single action potential. Hyperpolarizing current injection (downward-going traces) produced a nearly ohmic response. Together, they result in a nearly linear V–I relationship (*right*). Current injection is shown below b_2. b_2 Another RA neuron but the voltage sag produced by hyperpolarizing current injection resulted in a nonlinear V–I relationship. The voltage sag is observed as the difference in magnitude between the peak (*filled triangle*) and plateau (*filled diamond*). Note the difference in voltage sag magnitude between b_1 and b_2. b_3 and b_4 were similarly analyzed SA neurons. Note the difference in the maximum number of action potentials fired between b_3 and b_4. In response to hyperpolarizing current injection, both neurons fired rebound action potentials (shown by *arrows*). (From Figs. 7 and 8 of Mo & Davis, 1997b)

electrophysiological profile is consistent with standard single-unit recordings in vivo, in which post-stimulus time histograms revealed rapid and dynamic firing patterns in response to pure tone stimuli (Kiang, 1965). These findings prompted the examination of responses to prolonged stimuli to determine whether primary auditory afferents are capable of displaying the more varied properties expected of a sophisticated sensory system that could also potentially account for the nonstandard behavior of some reported single-unit recordings (Kiang, 1990).

Experiments that evaluated murine postnatal spiral ganglion neurons using longer pulse durations expanded the view of the electrophysiological complexity of these cells (Fig. 4.3b_1–b_4). Some neurons showed a rapid accommodation (RA) profile in which action potentials ceased to fire during a prolonged depolarizing current injection (Fig. 4.3b_1, b_2; Mo & Davis, 1997b). The majority of the neurons within this class of cells fired only a single action potential even at the highest levels of current injection. The other neurons within this class, while accommodating during the depolarizing stimulus, typically fired fewer than eight action potentials just following the onset of the stimulus (Mo and Davis, 1997b).

Slowly accommodating (SA) neurons, which fired action potentials throughout a prolonged depolarizing current injection, were also detected (Fig. 4.3b_3, b_4; Mo & Davis, 1997b). Examination of responses to a series of current injections revealed that the maximal number of action potentials a cell was capable of firing varied from neuron to neuron. This variation was largely the result of differences in the maximum firing rate (minimum interspike interval). For example, the two cells illustrated in Fig. 4.3b_3, b_4, although firing the maximum number of action potentials do so at different rates. Coincident with these depolarization-evoked responses, a distinctive voltage response was also noted in these neurons to hyperpolarizing constant current injections. Some neurons displayed essentially linear responses (Fig. 4.3b_1), whereas most others showed a hyperpolarizing sag indicative of the hyperpolarization-activated (I_h) cationic current (Fig. 4.3b_2–b_4; Chen, 1997; Liu & Davis, 2007; Kim & Holt, 2013). As seen from the examples, the magnitude of the hyperpolarizing sag does not appear to correlate with the degree of accommodation, revealing an additional point of electrophysiological diversity (Fig. 4.3b_1–b_4).

4.4 Voltage-Gated Ion Channels: The Fundamental Building Blocks

The levels of accommodation from mammalian cells, whether categorized as rapidly accommodating (RA) or slowly accommodating (SA), require a greater ensemble of voltage-gated ion channel types than the classic transient Na^+ and delayed rectifier K^+ channels described by Hodgkin and Huxley (Hodgkin & Huxley, 1952; Hodgkin et al., 1952). Using pharmacological, molecular, genetic, and immunocytochemical approaches, evidence for an abundance of voltage-gated channel types has indeed been found in spiral ganglion neurons.

4.4.1 Ionic Currents Present in Spiral Ganglion Neurons

Initial studies pairing electrophysiology with pharmacological blockers paved the way for identifying the basic underlying voltage-dependent ion channels that shape the membrane properties in spiral ganglion neurons. Multiple voltage-gated K^+ channels, through their varied time course and voltage dependence, have a profound regulatory effect on neuronal firing patterns (Hille, 2001). Recordings from spiral ganglion neuron somata using tetraethylammonium (TEA) revealed a delayed rectifier current while experiments with 4-aminopyridine (4-AP) provided evidence for a transient inactivating current (Fig. 4.4a–d; Garcia-Diaz, 1999; Szabo et al., 2002). Further, α-dendrotoxin and dendrotoxin-K, specific blockers of delayed rectifier subtypes $K_V1.1$, $K_V1.2$ and $K_V1.6$, were effective in revealing both low-voltage- and high-voltage-activated K^+ currents that contributed to the overall whole-cell outward current (Mo et al., 2002). In addition, application of linopirdine,

a blocker of the K_V7 family (KCNQ) of channels, identified these currents in dissociated cultures of mouse spiral ganglion (Lv et al., 2010). These observations were further refined to specifically include $K_V7.4$, which was genetically deleted in mice (Beisel et al., 2005).

Although the investigations summarized in the preceding text provide evidence for the diversity of the membrane K^+ currents, other studies have identified additional current types. For example, of the 10 voltage-gated calcium channel (VGCC) α-subunits identified to date (Catterall et al., 2005), 8 are expressed in the ganglion and 7 were found to be localized to the neurons in differing intra- and intercellular distributions in postnatal and adult animals (Lopez et al., 2003; Chen et al., 2011). Electrophysiological analysis indicates that L-type calcium channels predominate; however, evidence exists for T-, P/Q-, N-, and R-type calcium channels actively contributing to the endogenous membrane properties (Fig. 4.4e; Yamaguchi and Ohmori 1990; Szabo et al., 2002; Lv et al., 2012). Another current type, underlying

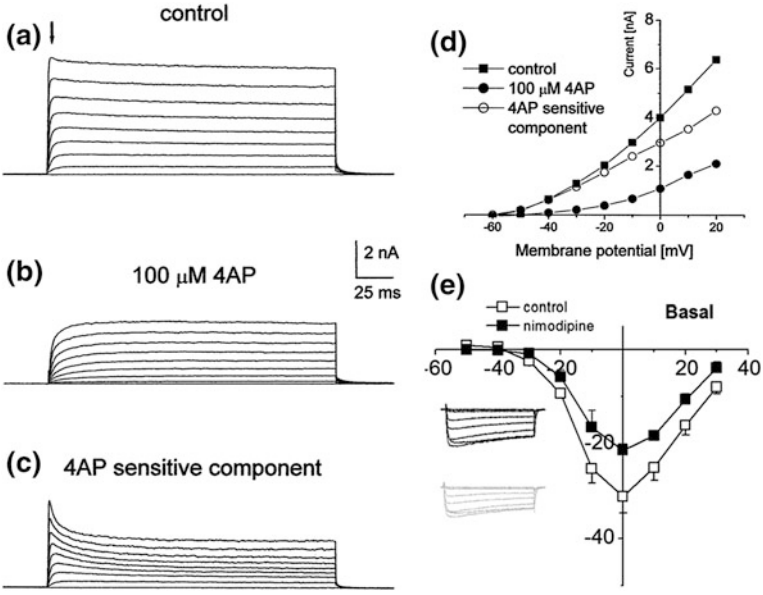

Fig. 4.4 The sensitivity of spiral ganglion neurons to pharmacological blockers. **a**–**d** Cultured guinea pig neurons were voltage clamped at −60 mV and stepped to 20 mV in 10-mV increments. **a** Outward currents prior to 4-AP application and **b** after 100 μM 4-AP application. **c** Subtracted traces (**b** from **a**) reveals the 4-AP-sensitive currents. **d** I–V plots of control (*filled square*), 4-AP (*filled circle*), and subtracted component (*open circle*). The scale bar for sweeps is shown between **a** and **b**. The measurements for the I–V plots were taken from the peak current (*downward arrow* in **a**). (From Fig. 4 of Szabo et al., 2002.) **e** Sensitivity of basal neurons to nimodipine. I–V plot of whole-cell voltage-clamp recordings from 3-month-old mouse spiral ganglion neurons in culture demonstrates the presence of L-type Ca^{2+} channels. The amplitude of the control (*open squares*) was clearly reduced by nimodipine (*filled squares*). *Inset* shows the effect of nimodipine before (*dark traces*) and after (*gray traces*). (Adapted from Fig. 3 of Lv et al., 2012)

the aforementioned hyperpolarizing sag, is the cationic I_h current, identified in spiral ganglion neurons using the blockers Cs^+ and ZD-7288, polymerase chain reaction of of HCN1-4, and genetic deletions of HCN1 and -2 (Kim & Holt, 2013; Liu et al., 2014a). Interestingly, the voltage dependence of activation showed unusually broad heterogeneity under the control of cAMP (Banks et al., 1993; Mo and Davis, 1997a), supporting the variations in hyperpolarizing sag first noted in current-clamp recordings (Fig. 4.3b).

Together, several somatic whole-cell patch-clamp studies have identified a range of voltage-gated currents from the classic rapidly inactivating Na^+ current to multiple types of K^+ and Ca^{2+} currents to I_h currents. These findings are important because they reveal a functional complexity beyond that expected for the axonally localized neuronal cell body. The abundance and diversity of ion channel types found in neurons will likely increase with additional studies.

4.4.2 *Currents that Contribute to the Complex Firing Patterns*

To understand better the functional impact of the aforementioned currents on the firing patterns of spiral ganglion neurons, pharmacological blockers were applied during whole-cell current-clamp recordings to evaluate changes in the voltage responses. In this way, the altered firing patterns caused by a pharmacological blocker can be compared to control conditions to determine how a specific current type contributes to the overall neuronal firing.

A pharmacological blocker of BK currents, charybdotoxin, altered the firing patterns of spiral ganglion neurons (Fig. 4.5a), thus confirming the presence of this large conductance voltage- and calcium-activated K^+ channel in mammalian, as well as goldfish, primary afferents (Davis, 1996; Adamson et al., 2002b). These experiments support the idea that BK currents exert multiple effects. At voltages close to action potential threshold, BK currents reduced the onset time course, whereas at suprathreshold levels, BK currents increased accommodation.

The K_V1 blocker α-dendrotoxin also had a profound effect on the endogenous firing patterns of spiral ganglion neurons. Neurons exposed to the toxin showed predominantly SA responses, depolarized resting membrane potentials (RMPs), and lower thresholds, resulting in greater overall excitability (Fig. 4.5b; Mo et al., 2002; Liu et al., 2014b). Conversely, cells exposed to the broad-spectrum blocker TEA showed very little alteration of threshold or RMP, but instead slowed action potential repolarization (Fig. 4.5c). This effect on repolarization has implications not only for individual action potentials but also for prolonging the interspike intervals of neurons that fire more than once. These examples demonstrate that K^+ channel types, which are responsible for hyperpolarizing the membrane, do so at distinct voltages, and therefore can affect firing patterns in very different ways.

In addition to effects of K^+ currents, depolarization contributed by VGCCs can also alter firing patterns, and, similar to K^+ channels, the voltage dependence of a

particular Ca^{2+} channel can affect the mechanism of action. Thus, blocking Ca^{2+} currents with the broad-spectrum blocker cadmium produced effects at both threshold and suprathreshold voltages (Chen et al., 2011). Cadmium application eliminated a depolarization near threshold to increase response latency (Fig. 4.5d) and abolished a subtle plateau-like potential on the falling phase of the action potential that resulted in a spike with faster repolarization (Fig. 4.5e, arrows). The Ca^{2+} effect on action potential duration was clearly revealed with the application of TEA. Following an initial rapid repolarization was a pronounced plateau that substantially prolonged the action potential duration (Fig. 4.5f, arrows), which is a hallmark of a Ca^{2+} spike (Mason & Leng, 1984; Sundgren-Andersson & Johansson, 1998). Thus, despite the rapidity with which these neurons are capable of firing action potentials, buried beneath the powerful repolarizing currents carried by delayed rectifiers and BK channels is a capacity for prolonged depolarization that could have significant effects on signal transmission and, ultimately, neurotransmitter release (Borst & Sakmann, 1999; Yang & Wang, 2006).

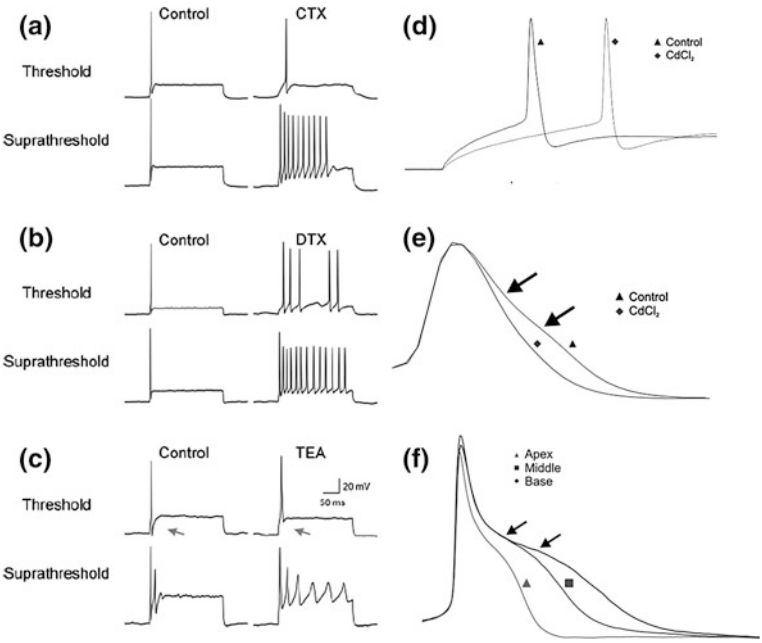

Fig. 4.5 Effects of K^+ and Ca^{2+} channel blockers illustrate the diversity of spiral ganglion neuron firing properties. **a** Charybdotoxin (CTX), a BK channel blocker, was most effective at suprathreshold stimulation levels as shown by the increase in the number of action potentials. **b** Dendrotoxin (DTX), a K_V1 channel blocker, was effective at both threshold and suprathreshold levels. **c** TEA application blocked the after-hyperpolarization at threshold (denoted with *arrows*) and also changed the firing at suprathreshold levels by increasing the number and duration of the action potentials. **d**, **e** Effect of Cd^{2+} on action potential latency at threshold **d** and action potential duration **e**. **f** TEA application revealed tonotopic differences in action potential duration. (**a**–**c** from Fig. 6 of Adamson et al., (2002b) and **d**–**f** adapted from Figs. 2 and 4 of Chen et al., 2011)

4.5 Multidimensional Distribution Patterns

The highly ordered innervation patterns of spiral ganglion neurons described in Sect. 4.2.1, and in greater detail in Chap. 1 by Dabdoub and Fritzsch, form a stable framework in which to explore the distribution patterns of electrophysiological features and relevant proteins. The base-to-apex tonotopic contour representing a high-to-low frequency map is punctuated in the middle by the most sensitive region of hearing (Rosowski, 1991; Ruggero & Temchin, 2002; see also Goodrich, Chap. 2) and is transected by an orthogonal, scala vestibuli/scala tympani (SV/ST) organization of spontaneous rate and threshold (Leake & Snyder, 1989). In early postnatal animals, the base-to-apex developmental progression is still in motion, and therefore may be responsible for some of the variations in ion channel distribution and firing features. Recent studies mapping out the distribution patterns of particular attributes have revealed novel patterns potentially representing heretofore undiscovered organizational principles that will lead to a new appreciation of spiral ganglion coding capabilities.

4.5.1 Tonotopic Distributions Related to Membrane Kinetics and Timing

A unifying feature within the auditory system is its tonotopic specializations. From the stiffness gradient along the basilar membrane and specialized cellular features within the cochlea to the receptive fields in the primary auditory cortex (A1), frequency coding is clearly an imperative of sound processing (Rubel & Fritzsch, 2002). Similarly, the spiral ganglion, with its role to reliably receive and transmit frequency-specific information into the brain, also displays frequency-dependent features. Most obvious is its tonotopically related morphology, such as axon diameter and soma size (Ryugo, 1992). However, it was discovered that postnatal spiral ganglion neuron firing properties could also be tonotopically mapped. The first indication of these frequency-specific electrophysiological specializations was the observation that the membrane kinetics and action potential profiles were distinctly different when recordings were made from high-frequency basal neurons and compared with low-frequency apical neurons (Fig. 4.6a). Action potential latency and onset time course at threshold were significantly more rapid for basal than apical neurons, and the action potential duration was prolonged in the apex compared to the base (Fig. 4.6a, insert). Further, multiple accommodation patterns (Fig. 4.6b) were distinctively distributed. Neurons from the base were predominantly RA, mostly firing only a single action potential in response to prolonged

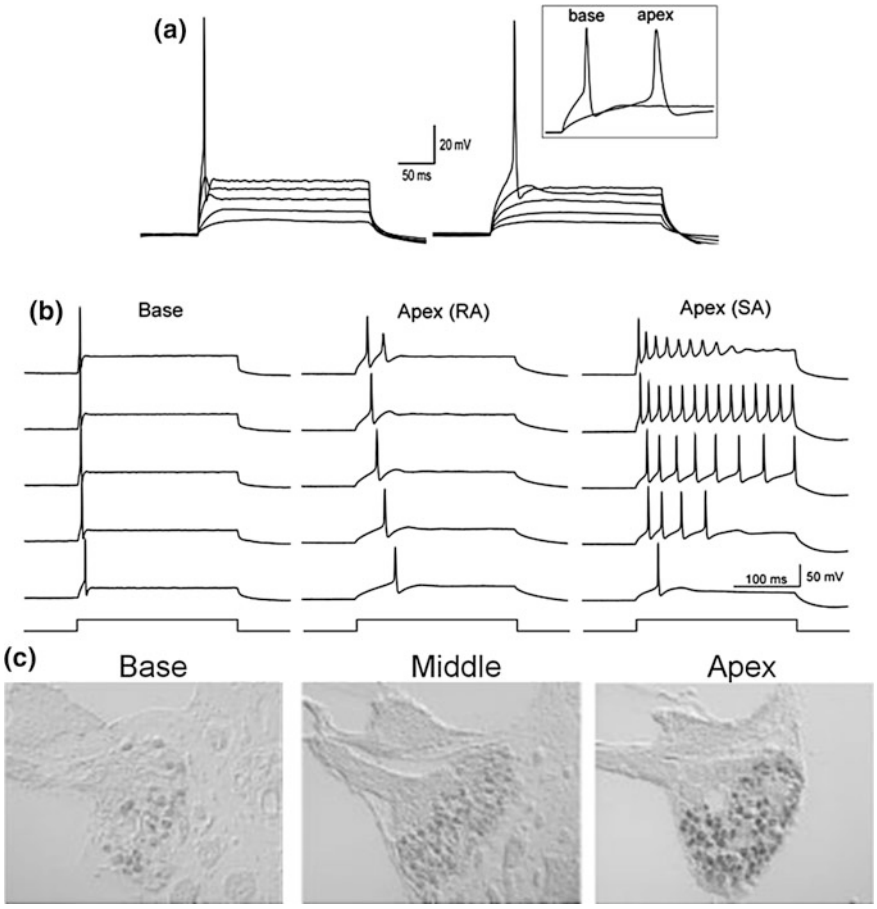

Fig. 4.6 Tonotopic differences in spiral ganglion electrophysiologically relevant features. **a** Depolarizing constant current injections elicit action potentials with different kinetics from basal neurons (*left*) and apical neurons (*right*). *Inset* shows the difference in threshold response latencies between the two regions with apical neurons being generally slower than basal neurons. **b** Stacked sweeps show example responses of basal and apical neurons. At suprathreshold stimulation, the neuron from the base (*left*) fires only a single action potential whereas the two different apical neurons have more complicated firing patterns with the apical (RA) neuron in the middle column firing two action potentials and the neuron on the right (SA) firing multiple action potentials that eventually ceased as the stimulation level increased. (**a** adapted from Fig. 5 and **b** from Fig. 3 of Adamson et al., 2002b.) **c** In situ hybridization of KCNMB4 (the β4 regulatory subunit of BK channels) of P16 rat cochlea. Note the tonotopic progression in the detection of the β4 subunit with highest levels in the apex (*left panel*) and lowest levels in the base (*right panel*). (Adapted from Fig. 11 of Langer et al., 2003)

depolarizing stimulation. Those from the apex, conversely, showed a wider range of accommodation profiles ranging from RA to SA, separated by a naturally occurring gap in the data between the RA and SA categories (Mo & Davis, 1997b).

Overall, the different kinetic features and degree of accommodation displayed by basal and apical neuron recordings suggest that their respective complements of voltage-gated ion channels may also vary from the base to the apex. In agreement with this hypothesis, isolated postnatal basal neurons in tissue culture had substantial immunolabeling for $K_V1.1$, $K_V3.1$, and BK, all channels that would give rise to faster kinetics (Adamson et al., 2002a, b). Apical postnatal neurons, however, showed labeling for the aforementioned ion channels but at lower levels than basal neurons and also had higher immunolabeling with anti-$K_V4.2$ antibodies, a channel type that could contribute to the comparatively longer action potential latencies observed in these neurons at threshold (Kanold & Manis, 1999; Shibata et al., 2000).

Although these results are clearly consistent with an electrophysiological complexity within the ganglion, they alone cannot distinguish between tonotopic-specific or developmental processes because the recordings were made in maturing postnatal neurons. However, knowing the channel types specifically associated with regulated electrophysiological features permits comparative investigations of the channel composition in adult neurons using immunocytochemistry and in situ hybridization techniques. Studies of this kind have shown that the basal-apical postnatal differences were also seen in adult animals (Adamson et al., 2002b). Labeling of adult cochlear sections with anti-$K_V1.1$, anti-$K_V3.1$, and anti-BK antibodies showed that the higher immunostaining in basal neurons was preserved, while higher anti-$K_V4.2$ antibody labeling was maintained in the apical ganglion. Further, the BK channel regulatory subunit, BKβ4, also shows a tonotopic pattern that might be predicted by its properties, but this was not evident until postnatal day 16 (Fig. 4.6c; Langer et al., 2003).

4.5.2 Mid-Cochlear Distributions Related to Neuron Excitability and Intensity Coding

When considering the sound waveforms that must be transduced into electrical signals (i.e., action potentials) and transmitted into the brain, it is clearly more than just frequency information that defines the richness of hearing. Signal intensity is another parameter of the acoustic stimulus. Behavioral threshold, defined by the lowest intensity sound that an animal can detect, is a frequency-dependent parameter that varies from species to species (Heffner & Heffner, 1980; Kojima 1990). A comparison of tuning curves constructed from primary afferent single-unit recordings to the behavioral threshold reveals two important features of spiral ganglion neuron organization. First, the tips of the tuning curves, which represent the frequency at which a neuron is most sensitive, show a variation with some neurons responding at behavioral threshold, while others require much higher stimulus intensities to produce a response. Second, the tips of the tuning curves

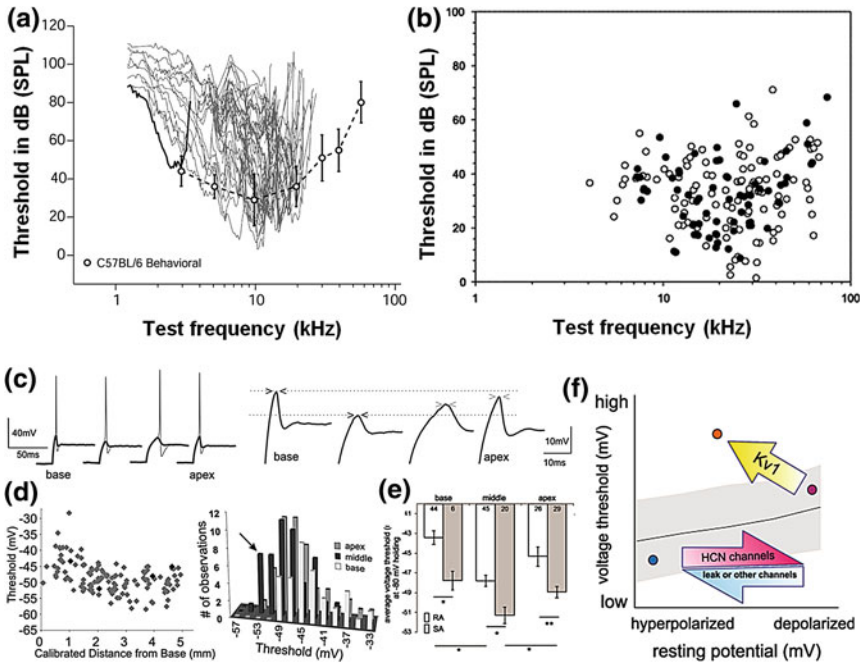

Fig. 4.7 Heterogeneity and enhanced sensitivity of individual nerve fiber responses and cultured neuron recordings in the mid-ganglion region. **a** Tuning curves (*gray lines*) from several C57Bl/6 auditory nerves with one recording highlighted (*black line*). Comparative behavioral data from C57Bl/6 mice were overlaid (*dotted line* with open symbols). **b** Auditory nerve recordings from another mouse strain, CBA/J, show the characteristic frequency at threshold as a function of frequency. Horseradish peroxidase–filled neurons confirmed their location (*black circles*) and the remainder were unsuccessfully filled neurons (*open circles*). (**a** from Fig. 10 of Taberner & Liberman, 2005) and **b** from Fig. 3 of Muller et al., 2005.) Data from gangliotopic cultures **c**, **d** and explant cultures **e**, **f** are shown. **c** Threshold recordings from four different neurons that are arranged from base to apex. The thick *black trace* is the just-subthreshold response and the *gray trace* is the threshold action potential. The gangliotopic preparation preserves positional information such that the original in vivo location can be determined with accuracy. To the *right* are the same subthreshold recordings as the *left* panel highlight the location-related thresholds. Note the neuron from the base had the highest threshold while neurons from the middle region had the lowest thresholds. **d** *Left*, plot of thresholds (*gray symbols*) obtained from all recordings as a function of position (calibrated distance from base). The *black* symbols are recordings in **c**. **d** *Right*, histogram relates threshold and gangliotopic position. The *arrow* highlights the most sensitive neurons were found in the middle. **e** Relationship of threshold to accommodation category. RA, rapid accommodation; SA, slow accommodation. Thresholds from both SA neurons and RA neurons were consistently more hyperpolarized in the middle. **f** Visual illustration of three identified mechanisms that contribute to the diversity of RMP and thresholds. The first mechanism, as shown by the *blue* and *magenta arrows*, regulates RMP—more HCN channels and/or fewer leak or chloride channels would depolarize the RMP along the *x*-axis. The *line* and *shadow* plot indicate a second mechanism that involves an indirect regulation of threshold through RMP. Combining mechanisms 1 and 2 slides the position from the *blue circle* to the *magenta circle*. The third mechanism involves K_v1 dual-regulation of RMP and threshold and is illustrated by the *yellow arrow*. As levels of K_v1 current increase both RMPs would hyperpolarize and the threshold would elevate as shown by the *yellow arrow* moving from the *magenta circle* to the *orange circle*. **c**, **d** adapted from Fig. 3 of Liu & Davis, 2007 and **e**, **f** from Figs. 4 and 8 of Liu et al., 2014b)

define a broad set of responses that have the greatest heterogeneity and excitability within the most sensitive mid-cochlear region (Fig. 4.7a, b).

To accomplish the above organization mechanistically, intensity information from an individual hair cell must be parsed into 10–30 innervating spiral ganglion neurons (Keithley & Schreiber, 1987; Liberman, 1982; Liberman et al., 1990). One postulated mechanism involves the synapses themselves. The presynaptic machinery and the apposed postsynaptic membrane areas vary systematically along the contour of individual hair cells that are innervated by low- to high-threshold neurons, which could potentially account for the variation in sensitivity (Meyer et al., 2009; Liberman et al., 2011). Based on the evidence that spiral ganglion neurons possess both regional heterogeneity, as well as general tonotopic differences, a second plausible hypothesis is that the endogenous membrane properties of the neurons also contribute.

Two endogenous neuronal membrane properties that, if contributing factors, would likely play a role are threshold and RMP. Together, these parameters can set the excitably of a neuron. For example, the closer the RMP is to threshold, the less current is required to fire an action potential. Accordingly, more hyperpolarized thresholds would also require less current to move the voltage from RMP to threshold. Thus, the most excitable neurons possess a depolarized RMP combined with a hyperpolarized threshold, whereas those with a hyperpolarized RMP and depolarized threshold are the least excitable. To tailor the properties of neurons between these two extremes one might expect that the lowest RMPs are not always aligned with the highest thresholds and vice versa. Thus, interspersing these two parameters would result in intermediate excitatory levels and the most heterogeneity.

What emerges from recordings of spiral ganglion neurons in vitro is the broad diversity in their thresholds regardless of the regularity of other properties (Fig. 4.7c, d; Mo & Davis, 1997b; Liu et al., 2014b). Thus, even without hair cell presynaptic input, spiral ganglion neurons in isolation already vary in the membrane potentials at which they are initially capable of firing an action potential (Liu et al., 2014b). Further examination of this feature revealed that although heterogeneity did not diminish when comparing the neurons isolated from different cochlear regions, the neurons with the lowest (most sensitive) thresholds were localized to the mid to apical region, whereas the neurons with the highest thresholds (least sensitive) were localized to the basal region (Fig. 4.7c, d). This distribution was robust in that it did not specifically depend on firing pattern; both RA and SA neurons had the same enhancement in threshold sensitivity in the middle region (Fig. 4.7e).

The second parameter that contributes to neuronal excitability, RMP, is more difficult to measure with standard electrophysiological methods because these approaches are generally invasive and disrupt the intracellular milieu. Thus, the very act of breaking through the cell membrane to assess RMP very likely changes the parameter being measured. The most accurate method for determining the RMP is noninvasive and utilizes cell-attached single channel recording methodology to determine the reversal potential of a K^+ channel and then calculate RMP based on

the Nernst equation (Verheugen et al., 1999; Liu et al., 2014b). RMPs assessed noninvasively in spiral ganglion neurons averaged −68.7 mV (base), −65.3 mV (middle), and −65.5 mV (apex) (Liu et al., 2014b). Each of these levels were shifted by approximately −6 mV as compared to measurements made using standard whole-cell current clamp (Liu et al., 2014b) and are consistent with measurements of RMP in a variety of species and ages (Rusznak & Szucs, 2009). Importantly, both approaches consistently showed that neurons from mid-apical regions were significantly more depolarized than those from the base. The tonotopic RMP distribution corresponded to observations of threshold: the mid-apical neurons consistently had the lowest average thresholds and the highest average RMP.

Yet, taken together these two parameters did not appear to align specifically to yield neurons with discrete levels of excitably. This issue was assessed with recordings from neurons that were maintained at their calculated endogenous RMP and then tested for their threshold responsiveness. Rather than observing discrete populations of neurons displaying the extremes of excitability, neurons with many combinations were found (Liu et al., 2014b). Neurons had depolarized RMPs that were paired with high thresholds, hyperpolarized RMPs that were paired with low thresholds, and combinations in between. This organization served to emphasize the heterogeneity of excitability across the population, while maintaining the mid-apical tonotopic sensitivity displayed by each parameter on its own (Liu et al., 2014b). This distributed combination of the two basic properties that regulate excitability, threshold and RMP, is reminiscent of the patterns observed in vivo (Fig. 4.7a, b). Although these observations do not prove the connection between intrinsic neuronal membrane properties and intensity coding, they open the door to future investigations.

As neuronal excitably is dependent on ion channels that are active at relatively hyperpolarized voltages, it is likely that many of the low-voltage-activated ion channels found in spiral ganglion neurons exert a regulatory role. Studies exploring this issue have shown that two such ion channels, HCN and K_V1, were involved in control of neuronal excitability (Liu et al., 2014b). In this regard, the effect of the I_h current carried by HCN channels, assessed before and after cesium block, was limited to altering the RMP. In agreement with the range of RMPs observed in spiral ganglion neurons, the voltage dependence from cell to cell was also remarkably diverse (Mo and Davis 1997a), suggesting that it may contribute to the observed heterogeneity (Fig. 4.7f). In parallel with HCN, $K_V1.1$ affected RMP, but studies with α-dendrotoxin showed that it had an impact on threshold as well. Consistent with electrophysiological assessments, basal turn neurons that displayed the highest levels of anti-$K_V1.1$ antibody labeling were the least excitable, whereas middle turn neurons that displayed the lowest levels of $K_V1.1$ were the most excitable (Liu et al., 2014b). Thus, in accord with their role in regulating neuronal excitability, $K_V1.1$ channels appear to have the lowest immunostaining levels in the mid-turn ganglionic region (Liu et al., 2014b).

4.5.3 *Heterogeneous Distributions Across the Tonotopic Contour*

As described in Sects. 4.2, 4.3, 4.5.1, and 4.5.2, heterogeneity is routinely observed in many aspects of the spiral ganglion neuron phenotype, including anatomical connections, morphological attributes, and physiological features. Even when a particular parameter shows a clear region-specific distribution, a marked heterogeneity is still often present within each region. For example, ion channels such as BK and $K_V1.1$ that are associated with kinetics and threshold, respectively, and distributed accordingly (tonotopic, mid-cochlear, respectively), still display prominent local variations in ion channel density as evaluated by immunocytochemistry (Rosenblatt et al., 1997; Adamson et al., 2002b; Liu et al., 2014b). Heterogeneity has also been found in calcium-binding proteins, which in some neurons were reported to affect neuronal firing patterns (Schwaller et al., 2002; Orduz et al., 2013). Neurons labeled with anti-calbindin or anti-calbindin antibody, showed high, intermediate, or low levels that were interspersed within each tonotopic region, despite the uniform immunolabeling of the neuron-specific β-III tubulin antibody (Liu & Davis, 2014). Another example of local heterogeneity was observed in adult chinchillas when the authors explored the distribution of α1A–E Ca^{2+} channels (Fig. 4.8a–d; Lopez et al., 2003). Although not explicitly mentioned, heterogeneity was apparent between cells for a given subunit, as well as in the

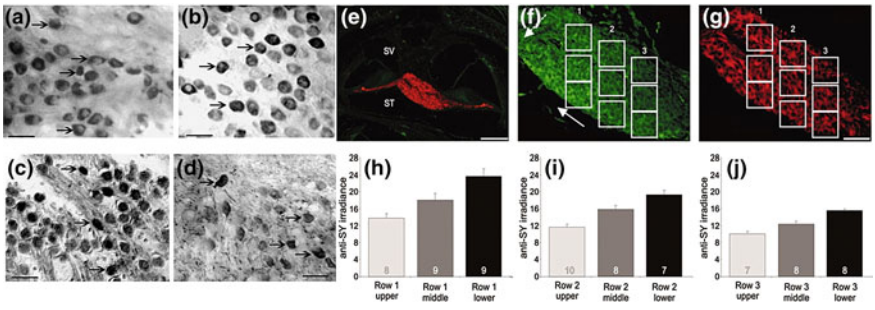

Fig. 4.8 Expression and local heterogeneity of Ca^{2+} channel subunits and synaptophysin immunolabeling. **a** α1B (*arrows* in this and subsequent panels denote neuron somata). **b** α1C. **c** α1D. **d** α1E. (Adapted from Fig. 6 of Lopez et al., 2003.) **e–j** Synaptophysin tonotopic immunolabeling is also locally graded in a scala vestibuli (SV) to scala tympani (ST) orthogonal orientation. **e** Low-magnification view of a postnatal mouse cochlear section stained with anti-synaptophysin (α-SY, *green*) and anti-β-III tubulin (α-, β-Tubulin, red). **f** α-SY staining showed dual gradients. The first was a base-to-apex gradient (*arrow*) and the second extended from SV to ST (*dashed arrow*). Based on this pattern, SY staining was highest in apical neurons proximal to ST (where the two arrowheads would meet). **g** β-Tubulin staining was relatively uniform throughout the cochlear section. **h–j** Analysis of α-SY irradiance from SV to ST (*white boxes* in **b** and **c**) as a function of tonotopic location (rows 1, 2, and 3). **h** Row 1 analysis from upper box (*light gray bar*) to lower box (*black bar*). **i** Same analysis as **d** but for row 2. **j** Same analysis as **d** but for row 3. (Adapted from Fig. 9 of Flores-Otero & Davis, 2011)

relative expression levels between the subunits. When evaluating immunocytochemical results in this context, however, it is critical to use a marker that uniformly labels all neurons to distinguish between true heterogeneous labeling and an artifact, such as differential antibody penetration. Indeed, with that caveat in mind, there are many observed heterogeneous distribution patterns in the ganglion. Other examples of protein labeling throughout the ganglion that show local heterogeneity are Ca^{2+} channel α-subunits (Chen et al., 2011), osteopontin (Lopez et al., 1995), synaptophysin and SNAP-25 (Flores-Otero & Davis, 2011), and neurofilament proteins (Despres et al., 1994).

4.5.4 Dual Gradients

Whereas most molecules that have been investigated show a distinctive gradation in a single dimension, one electrophysiologically relevant protein, synaptophysin, a presynaptic vesicle-associated protein (Sudhof et al., 1987), shows a two-dimensional distribution pattern (Flores-Otero & Davis, 2011). Superimposed on its tonotopic gradient, which is highest in apical compared to basal neurons, is an orthogonal one (Fig. 4.8e–j). Thus, the local heterogeneity observed within each tonotopic region is graded; the highest immunolabeling density was found in neurons closest to the scala tympani (ST) while the lowest density was found within neurons closest to the scala vestibule (SV). This distribution pattern is notable because it not only correlated with the frequency distribution along the tonotopic contour, but it also simultaneously correlated with spontaneous rate and threshold distributions that are aligned along the SV/ST axis.

4.5.5 Multiple Phenotypic Distributions Within a Single Ganglion

Mapping the distributions of electrophysiologically related proteins reveals a complex overall phenotype represented within spiral ganglion neurons. Not only do discrete patterns relate to their potential functional significance, but the differential localization of specific proteins also shows that their effects on neuronal firing patterns and the regulatory mechanisms that control them are potentially separable.

Features under the global heading of timing, representing parameters such as action potential latency, duration at threshold, and the onset time course (τ) of subthreshold responses, are controlled separately by fast (blue base to apex gradient) and slow (rose apex to base gradient) components (Fig. 4.9), such as the $K_V3.1$ and $K_V4.2$ voltage-gated ion channels, respectively. Distinguishable from frequency and timing, are the parameters that potentially contribute to sensitivity, which peaks within the central region (Fig. 4.9, green rectangle). The lowest thresholds (Fig. 4.9, green rectangle, white dotted line) and highest RMPs (Fig. 4.9,

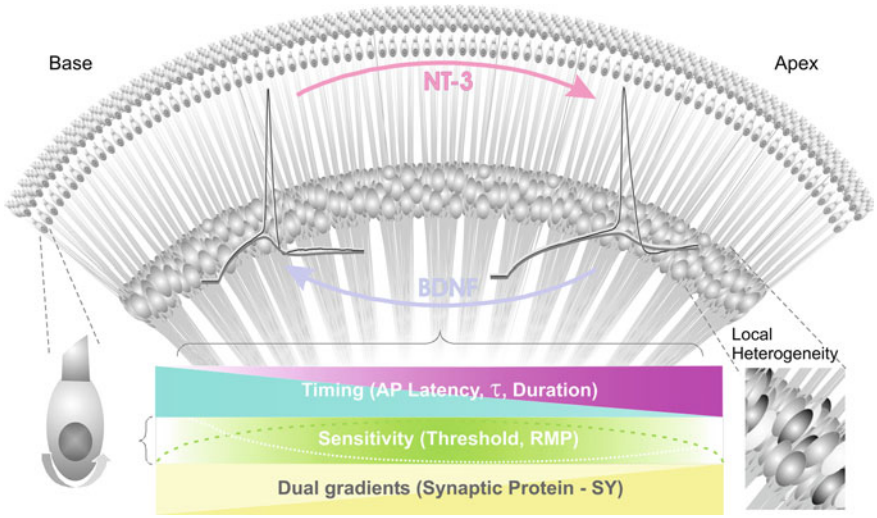

Fig. 4.9 Depiction of the multidimensional tonotopic electrophysiological phenotype across the spiral ganglion. Specific aspects of these features are regulated by both intrinsic and extrinsic factors. Intrinsic factors, described in Figs. 4.5, 4.6, 4.7, and 4.8, are responsible for an individual neuron's particular response profile and are related to tonotopic position. For example, $K_V1.1$, which has its lowest levels within the mid-ganglion, likely contributes to the middle being the most sensitive location with the most depolarized RMP (*green rectangle*, *green dashed line*) and hyperpolarized voltage thresholds (*green rectangle*, *white dotted line*). Neurons with more K_V1, K_V3, and BK (toward the base) would possess shorter onset time constants (τ) and action potential latencies relative to apical neurons and narrower action potentials (*blue gradient*). On the other hand, neurons toward the apex possess greater levels of $K_V4.2$, which could delay response properties (*magenta gradient*). The synaptic protein synaptophysin (SY; *yellow rectangle*) manifests two orthogonal tonotopic gradients corresponding to tonotopy and the SV/ST contour. Local heterogeneity is also prevalent within cochlear locations for many ion channel types and electrophysiological features (shown by *highlighted box*, *lower right*). Finally, extrinsic factors including brain-derived neurotrophic factor (BDNF, *purple curved arrow*) and neurotrophin 3 (NT-3, *pink curved arrow*) affect timing, sensitivity, and synaptic protein gradients, and, ultimately, firing features (example sweeps from a basal (*left*) and apical (*right*) neuron at the same time and voltage calibrations). NT-3 converts basal neurons to the apical phenotype and, conversely, BDNF converts apical neurons to the basal phenotype

green rectangle, green dashed line) were found in the mid-cochlear region, thus rendering the mid-ganglion neurons with endogenous properties that were potentially the most sensitive with the greatest heterogeneity. The ion channel having the largest contribution to reducing the sensitivity of spiral ganglion neurons, $K_V1.1$, was distributed such that its lowest levels were within the mid-frequency region (Liu et al., 2014b).

Although frequency and intensity are the major components of the signal processing that takes place at the level of the cochlea and spiral ganglion, the degree of heterogeneity observed in the population of spiral ganglion neurons suggests that additional types of analysis may be present. For example, the variation found for many of the VGCCs, voltage-gated K^+ channels, BK, calcium binding proteins, and

synaptic proteins indicates that multiple parameters are likely coded by parallel processing mechanisms (Fig. 4.9, lower right, "Local Heterogeneity"). The orthogonal gradients of synaptophysin (Fig. 4.9, yellow rectangle) are a good example, in this case, of enabling an interaction between the modalities of both frequency and spontaneous rate/threshold.

4.6 Altering the Electrophysiological Phenotype with Neurotrophins

The neurotrophins brain derived neurotrophic factor (BDNF) and neurotrophin 3 (NT-3) have been extensively characterized in the spiral ganglion because of their prominent role in auditory development and maintenance (see Goodrich, Chap. 2 and Rubel & Fritzsch, 2002). Among their extensive functions that range from regulating survival (Barde et al., 1982; Huang & Reichardt, 2001) to modifying synaptic strength (Levine et al., 1995), BDNF and NT-3 play a significant role in tailoring the electrophysiological phenotype of spiral ganglion neurons. This is, in part, carried out through mechanisms that up- or downregulate the very voltage-gated ion channels that contribute to spiral ganglion intrinsic firing properties. Although some of the BDNF and NT-3 effects can undoubtedly be mediated through selective survival, experiments that evaluated electrophysiological changes under conditions in which survival remained constant showed that the neuronal phenotype could be directly altered by neurotrophins (Zhou et al., 2005).

What is noteworthy about BDNF and NT-3 regulation of spiral ganglion intrinsic membrane properties is that these two neurotrophins generally work in opposition to one another. Exposure to BDNF, on the one hand, enhances the properties that ultimately increase the response kinetics of spiral ganglion neurons. These effects were most clearly observed in neurons with slower features, such as those isolated from the apical region. Their latency, onset time course at threshold, action potential duration, and accommodation became more rapid, while the same features for basal neurons remained unchanged (Fig. 4.10a). Consistent with these findings were the increased anti-$K_V1.1$, anti-$K_V3.1$, and anti-BK antibody labeling in apical neurons exposed to BDNF, which were similar to levels measured from basal neurons maintained in control conditions (Adamson et al., 2002a). Thus, addition of physiologically relevant amounts of BDNF to neurons from the apical spiral ganglion produces overall electrophysiological phenotypes that are essentially indistinguishable from the neurons in the basal region.

In contrast, NT-3 serves to enhance the properties that ultimately slow the response kinetics of spiral ganglion neurons. These effects were most clearly observed in basal neurons which possess faster features. Their latency, onset time course at threshold, action potential duration, and accommodation became

significantly prolonged, while the same features for apical neurons remain either unchanged or became even slower (Fig. 4.10b). Consistent with these findings, basal neurons exposed to NT-3 showed increased $K_V4.2$ antibody labeling and reduced anti-$K_V3.1$ and anti-BK antibody labeling, results that were similar to the levels measured from apical neurons maintained in control conditions (Adamson et al., 2002a).

It is not only the ion channels that contribute to the intrinsic firing properties of the neurons that are affected, but also the synaptic proteins synaptophysin, SNAP-25, and α-amino-3-hydroxy-5-methyl-4-isoxazolepropionic acid (AMPA) receptors, $GluA_2$ and $GluA_3$ (Collingridge et al., 2009), which are oppositely regulated by BDNF and NT-3 (Flores-Otero et al., 2007). For example, the upregulation of synaptophysin protein by NT-3 and downregulation by BDNF predicts the tonotopic gradient shown in Fig. 4.9. Open questions include how the orthogonal gradient is achieved and whether it is through additional modulators or the influence of regulated release mechanisms (Greenberg et al., 2009) that could underlie the differences observed in the IHC synaptic profiles (Merchan-Perez & Liberman, 1996).

There are a number of important conclusions that can be drawn from these observations. First, the ion channels that control the intrinsic firing properties of spiral ganglion neurons can be directly regulated to alter the overall firing patterns. Second, the ion channel distributions clearly reflect the changes in electrophysiology, allowing functional predictions to be made from measurements of ion channel density. Third, the opposite regulation by BDNF and NT-3 sets up many of the differences that distinguish basal from apical neurons. A straightforward prediction is that these neurotrophins, or their high-affinity receptors, tropomyosin receptor kinase B (TrkB) and TrkC, are expressed in oppositely oriented tonotopic gradients. Consistent with this, NT-3 has higher expression levels in the apical cochlea and ganglion, whereas BDNF has a higher concentration in basal hair cells and ganglion neurons in neonates and adults (Farinas et al., 2001; Sugawara et al., 2007). Lastly, if every spiral ganglion neuron could potentially respond similarly to BDNF and NT-3 as a result of near equal distribution of TrkB and TrkC (Farinas et al., 2001), then a uniform application of a particular neurotrophin may result in the full population of neurons throughout the ganglion having either uniform basal-like or apical-like response properties. This final conclusion is noteworthy when undertaking neurotrophin infusions in the cochlea to enhance neuronal survival for cochlear implants. Although enhanced neuronal survival may be beneficial, the uniformity in the firing properties may not. From these studies, therefore, it is clear that understanding how BDNF and NT-3 orchestrate aspects of the complex spiral ganglion phenotype should be considered carefully when developing novel therapeutic approaches.

A summary of the tonotopically distributed voltage-gated ion channels and electrophysiologically relevant proteins assessed to date shows the elegance of the underlying regulatory mechanisms. A protein that is found at higher levels in the base is upregulated by BDNF, and in most cases downregulated by NT-3. Conversely, a protein that is found at higher levels in the apex is upregulated by

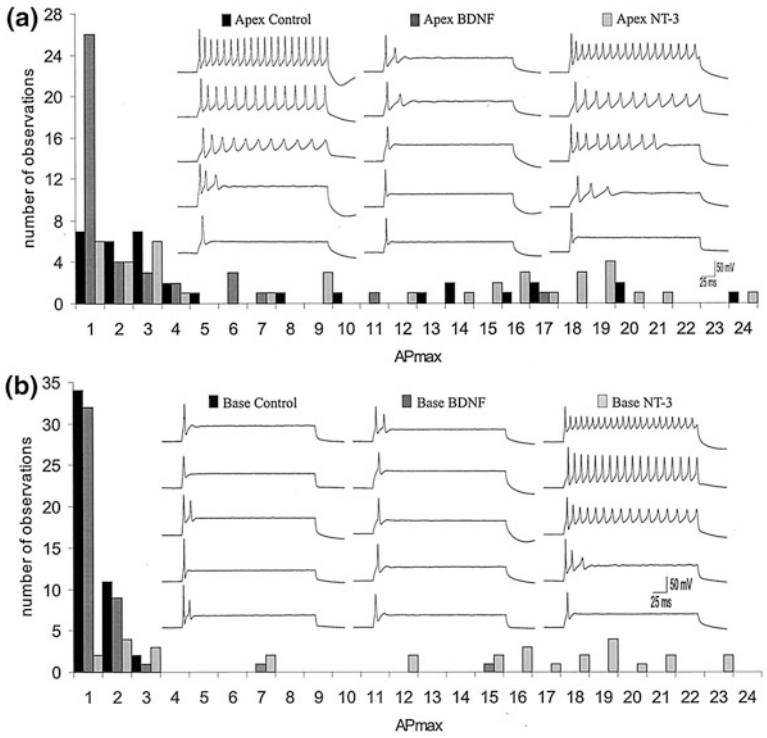

Fig. 4.10 Opposing actions of BDNF and NT-3 on postnatal spiral ganglion neurons in culture. **a** BDNF exposure (5 ng/mL, 6 DIV) converted apical neurons to a rapidly accommodating, basal neuron phenotype. NT-3 (5 ng/mL, 6 DIV) had essentially no effect on accommodation. Apex control (*black square*), apex BDNF (*dark gray*), and apex NT-3 (*light gray*). Beneath the stacked traces is a histogram that documents the effects of the neurotrophins on the maximum number of action potentials that a cell was capable of firing (APmax). Note the leftward shift in APmax for the BDNF-treated neurons. **b** Similar experiment as in **a** but on basal neurons. In this case, NT-3 produced an increase in accommodation in basal neurons while BDNF was without effect. The histogram, beneath the stacked sweeps, shows the effect in the population of neurons in this experiment. Note the rightward shift in APmax in the NT-3-treated neurons. (**a** from Fig. 1 and **b** from Fig. 2 of Adamson et al., 2002a)

NT-3 and in most cases downregulated by BDNF (Flores-Otero et al., 2007). As more electrophysiological elements are tested for their regulation by neurotrophins in the spiral ganglion, it will be informative to determine whether this same simple pattern remains or whether more complex interactions that underlie the different ganglionic distribution patterns exist. The complexity of the multiple sources of neurotrophins (including their pro-neurotrophin precursors), their interactions with both high- and low-affinity receptors, and their intricate release mechanisms are some of the features that suggest that much of the phenotypic complexity can result solely from just two neurotrophins. Nevertheless, it is important to identify other regulators of the spiral ganglion phenotype. As powerful as BDNF and NT-3 are in

modifying the density of voltage-gated ion channels and electrophysiologically relevant proteins, they are likely not the sole regulators as evidenced by the heterogeneity that persists.

4.7 Summary

The neurons that convey sound information from the periphery to the brain display prodigious differences throughout the spiral ganglion. In fact, one might speculate that every neuron, whether a type I or type II, is modified subtly to be slightly different from every other neuron. Thus, for a rodent spiral ganglion, which consists of approximately 30,000 neurons, one could observe 30,000 different electrophysiologically relevant signatures. Further, should the ion channel types that contribute to each of these distinct phenotypes change over time to alter response properties dynamically, then the range of possibilities would likely expand well beyond the number of neurons.

The exquisitely organized distributions of the ion channels and synaptic proteins make a compelling case for taking the next steps—to identify their impact on electrical signaling and development. Whether one considers the embryonic, postnatal, or adult spiral ganglion, it is impossible to ignore the sophistication of the features intrinsic to the neurons. The superimposed distributions of voltage-gated ion channels, modulating subunits, synaptic proteins, neurotransmitter receptors, and Ca^{2+} binding proteins are only examples of the wide variety of elements that are regulated. Determining their distribution patterns in the precisely ordered ganglion will undoubtedly lend a new level of understanding to the initial stages of auditory coding.

Acknowledgments We thank Dr. Mark R. Plummer for discussions and a critical reading of the manuscript. This work is supported by NIH NIDCD RO1 DC01856.

References

Adamson, C. L., Reid, M. A., & Davis, R. L. (2002a). Opposite actions of brain-derived neurotrophic factor and neurotrophin-3 on firing features and ion channel composition of murine spiral ganglion neurons. *The Journal of Neuroscience*, 22(4), 1385–1396.

Adamson, C. L., Reid, M. A., Mo, Z. L., Bowne-English, J., & Davis, R. L. (2002b). Firing features and potassium channel content of murine spiral ganglion neurons vary with cochlear location. *The Journal of Comparative Neurology*, 447(4), 331–350.

Ahmad, K. M., Klug, K., Herr, S., Sterling, P., & Schein, S. (2003). Cell density ratios in a foveal patch in macaque retina. *Visual Neuroscience*, 20(2), 189–209.

Altschuler, R. A., Hoffman, D. W., Reeks, K. A., & Fex, J. (1985). Localization of dynorphin B-like and alpha-neoendorphin-like immunoreactivities in the guinea pig organ of Corti. *Hearing Research*, 17(3), 249–258.

Banks, M. I., Pearce, R. A., & Smith, P. H. (1993). Hyperpolarization-activated cation current (Ih) in neurons of the medial nucleus of the trapezoid body: Voltage-clamp analysis and enhancement by norepinephrine and cAMP suggest a modulatory mechanism in the auditory brain stem. *Journal of Neurophysiology*, 70(4), 1420–1432.

Barde, Y. A., Edgar, D., & Thoenen, H. (1982). Purification of a new neurotrophic factor from mammalian brain. *EMBO Journal*, 1(5), 549–553.

Bean, B. P. (2007). The action potential in mammalian central neurons. *Nature Reviews Neuroscience*, 8(6), 451–465.

Beisel, K. W., Rocha-Sanchez, S. M., Morris, K. A., Nie, L., Feng, F., Kachar, B., Yamoah, E. N., & Fritzsch, B. (2005). Differential expression of KCNQ4 in inner hair cells and sensory neurons is the basis of progressive high-frequency hearing loss. *The Journal of Neuroscience*, 25(40), 9285–9293.

Bizley, J. K., & Walker, K. M. (2010). Sensitivity and selectivity of neurons in auditory cortex to the pitch, timbre, and location of sounds. *Neuroscientist*, 16(4), 453–469.

Borst, J. G., & Sakmann, B. (1999). Effect of changes in action potential shape on calcium currents and transmitter release in a calyx-type synapse of the rat auditory brainstem. *Philosophical Transactions of the Royal Society of London B: Biological Sciences*, 354(1381), 347–355.

Brödel, M., & Malone, P. D. (1946). *Three unpublished drawings of the anatomy of the human ear*. Philadelphia and London: W. B. Saunders Company.

Brown, M. C. (1994). Antidromic responses of single units from the spiral ganglion. *Journal of Neurophysiology*, 71(5), 1835–1847.

Burgess, B. J., Adams, J. C., & Nadol, J. B., Jr. (1997). Morphologic evidence for innervation of Deiters' and Hensen's cells in the guinea pig. *Hearing Research*, 108(1–2), 74–82.

Carr, C. E., Soares, D., Parameshwaran, S., & Perney, T. (2001). Evolution and development of time coding systems. *Current Opinion in Neurobiology*, 11(6), 727–733.

Catterall, W. A., Perez-Reyes, E., Snutch, T. P., & Striessnig, J. (2005). International Union of Pharmacology. XLVIII. Nomenclature and structure-function relationships of voltage-gated calcium channels. *Pharmacological Reviews*, 57(4), 411–425.

Chen, C. (1997). Hyperpolarization-activated current (Ih) in primary auditory neurons. *Hearing Research*, 110(1–2), 179–190.

Chen, W. C., Xue, H. Z., Hsu, Y. L., Liu, Q., Patel, S., & Davis, R. L. (2011). Complex distribution patterns of voltage-gated calcium channel alpha-subunits in the spiral ganglion. *Hearing Research*, 278(1–2), 52–68.

Ciuman, R. R. (2010). The efferent system or olivocochlear function bundle—fine regulator and protector of hearing perception. *International Journal of Biomedical Science*, 6(4), 276–288.

Cleland, B. G., Dubin, M. W., & Levick, W. R. (1971). Sustained and transient neurones in the cat's retina and lateral geniculate nucleus. *The Journal of Physiology*, 217(2), 473–496.

Collingridge, G. L., Olsen, R. W., Peters, J., & Spedding, M. (2009). A nomenclature for ligand-gated ion channels. *Neuropharmacology*, 56(1), 2–5.

Crozier, R. A., & Davis, R. L. (2014). Unmasking of spiral ganglion neuron firing dynamics by membrane potential and neurotrophin-3. *The Journal of Neuroscience*, 34(29), 9688–9702.

Davis, R. L. (1996). Differential distribution of potassium channels in acutely demyelinated, primary-auditory neurons in vitro. *Journal of Neurophysiology*, 76(1), 438–447.

Debanne, D., Campanac, E., Bialowas, A., Carlier, E., & Alcaraz, G. (2011). Axon physiology. *Physiological Reviews*, 91(2), 555–602.

Despres, G., Leger, G. P., Dahl, D., & Romand, R. (1994). Distribution of cytoskeletal proteins (neurofilaments, peripherin and MAP-tau) in the cochlea of the human fetus. *Acta Oto-Laryngologica*, 114(4), 377–381.

Dulon, D., Jagger, D. J., Lin, X., & Davis, R. L. (2006). Neuromodulation in the spiral ganglion: shaping signals from the organ of corti to the CNS. *The Journal of Membrane Biology*, 209(2–3), 167–175.

Echteler, S. M., & Nofsinger, Y. C. (2000). Development of ganglion cell topography in the postnatal cochlea. *The Journal of Comparative Neurology*, 425(3), 436–446.

Farinas, I., Jones, K. R., Tessarollo, L., Vigers, A. J., Huang, E., Kirstein, M., de Caprona, D. C., Coppola, V., Backus, C., Reichardt, L. F., & Fritzsch, B. (2001). Spatial shaping of cochlear innervation by temporally regulated neurotrophin expression. *The Journal of Neuroscience*, 21 (16), 6170–6180.

Fekete, D. M., Rouiller, E. M., Liberman, M. C., & Ryugo, D. K. (1984). The central projections of intracellularly labeled auditory nerve fibers in cats. *The Journal of Comparative Neurology*, 229(3), 432–450.

Flores-Otero, J., & Davis, R. L. (2011). Synaptic proteins are tonotopically graded in postnatal and adult type I and type II spiral ganglion neurons. *The Journal of Comparative Neurology*, 519 (8), 1455–1475.

Flores-Otero, J., Xue, H. Z., & Davis, R. L. (2007). Reciprocal regulation of presynaptic and postsynaptic proteins in bipolar spiral ganglion neurons by neurotrophins. *The Journal of Neuroscience*, 27(51), 14023–14034.

Furshpan, E. J., & Furukawa, T. (1962). Intracellular and extracellular responses of the several regions of the Mauthner cell of the goldfish. *Journal of Neurophysiology*, 25, 732–771.

Garcia-Diaz, J. F. (1999). Development of a fast transient potassium current in chick cochlear ganglion neurons. *Hearing Research*, 135(1–2), 124–134.

Gray, H., & Lewis, W. H. (1918). *Anatomy of the human body* (20th ed.). Philadelphia and New York: Lea & Febiger.

Greenberg, M. E., Xu, B., Lu, B., & Hempstead, B. L. (2009). New insights in the biology of BDNF synthesis and release: Implications in CNS function. *The Journal of Neuroscience*, 29 (41), 12764–12767.

Grothe, B., Pecka, M., & McAlpine, D. (2010). Mechanisms of sound localization in mammals. *Physiological Reviews*, 90(3), 983–1012.

Guinan, J. (2011). Physiology of the medial and lateral olivocochlear systems. In D. K. Ryugo & R. R. Fay (Eds.), *Auditory and vestibular efferents* (pp. 39–81). New York: Springer Science +Business Media.

Hafidi, A. (1998). Peripherin-like immunoreactivity in type II spiral ganglion cell body and projections. *Brain Research*, 805(1–2), 181–190.

Heffner, R., & Heffner, H. (1980). Hearing in the elephant (*Elephas maximus*). *Science*, 208(4443), 518–520.

Held, H. (1926). Die Cochlea der Säuger und der Vögel, ihre Entwicklung und ihr Bau. In W. Buddenbrock, M. H. Fischer, M. Frey, K. Frisch, M. Gildemeister, A. Goldscheider, K. Grahe, H. Held, H. Henning, H. Herter, F. B. Hofmann, E. M. Hornbostel, L. Jost, A. Kleyn, W. Koehler, W. Kolmer, A. Kreidl, W. Kümmel, R. Magnus, E. Mangold, T. Masuda, H. Rhese, F. Rohrer, H. Runge, A. Seybold, H. Sierp, E. Skramlik, P. Stark, J. Teufer, E. Waetzmann, V. Weizsaecker & C. Zarniko (Eds.), *Receptionsorgane I* (pp. 467–534). Munich: J. F. Bergmann-Verlag.

Hille, B. (2001). *Ion channels of excitable membranes*, 3rd ed. Sunderland, MA: Sinauer.

Hodgkin, A. L., & Huxley, A. F. (1952). Currents carried by sodium and potassium ions through the membrane of the giant axon of *Loligo*. *The Journal of Physiology*, 116(4), 449–472.

Hodgkin, A. L., Huxley, A. F., & Katz, B. (1952). Measurement of current-voltage relations in the membrane of the giant axon of *Loligo*. *The Journal of Physiology*, 116(4), 424–448.

Hossain, W. A., Antic, S. D., Yang, Y., Rasband, M. N., & Morest, D. K. (2005). Where is the spike generator of the cochlear nerve? Voltage-gated sodium channels in the mouse cochlea. *The Journal of Neuroscience*, 25(29), 6857–6868.

Huang, E. J., & Reichardt, L. F. (2001). Neurotrophins: Roles in neuronal development and function. *Annual Review of Neuroscience*, 24, 677–736.

Johnston, D., Wu, S. M.-S., & Gray, R. (1995). *Foundations of cellular neurophysiology*. Cambridge, MA: MIT Press.

Kanold, P. O., & Manis, P. B. (1999). Transient potassium currents regulate the discharge patterns of dorsal cochlear nucleus pyramidal cells. *The Journal of Neuroscience*, 19(6), 2195–2208.

Keithley, E. M., & Schreiber, R. C. (1987). Frequency map of the spiral ganglion in the cat. *Journal of the Acoustic Society of America*, 81(4), 1036–1042.

Kiang, N. Y.-s. (1965). *Discharge patterns of single fibers in the cat's auditory nerve.* Cambridge, MA: MIT Press.

Kiang, N. Y. (1990). Curious oddments of auditory-nerve studies. *Hearing Research*, 49(1–3), 1–16.

Kim, Y. H., & Holt, J. R. (2013). Functional contributions of HCN channels in the primary auditory neurons of the mouse inner ear. *Journal of General Physiology*, 142(3), 207–223.

Klein, M., & Kandel, E. R. (1980). Mechanism of calcium current modulation underlying presynaptic facilitation and behavioral sensitization in *Aplysia*. *Proceedings of the National Academy of Sciences of the USA*, 77(11), 6912–6916.

Kojima, S. (1990). Comparison of auditory functions in the chimpanzee and human. *Folia Primatologica (Basel)*, 55(2), 62–72.

Langer, P., Grunder, S., & Rusch, A. (2003). Expression of Ca^{2+}-activated BK channel mRNA and its splice variants in the rat cochlea. *The Journal of Comparative Neurology*, 455(2), 198–209.

Lawson, S. N., & Waddell, P. J. (1991). Soma neurofilament immunoreactivity is related to cell size and fibre conduction velocity in rat primary sensory neurons. *The Journal of Physiology*, 435, 41–63.

Leake, P. A., & Snyder, R. L. (1989). Topographic organization of the central projections of the spiral ganglion in cats. *The Journal of Comparative Neurology*, 281(4), 612–629.

Levine, E. S., Dreyfus, C. F., Black, I. B., & Plummer, M. R. (1995). Brain-derived neurotrophic factor rapidly enhances synaptic transmission in hippocampal neurons via postsynaptic tyrosine kinase receptors. *Proceedings of the National Academy of Sciences of the USA*, 92 (17), 8074–8077.

Liberman, L. D., Wang, H., & Liberman, M. C. (2011). Opposing gradients of ribbon size and AMPA receptor expression underlie sensitivity differences among cochlear-nerve/hair-cell synapses. *The Journal of Neuroscience*, 31(3), 801–808.

Liberman, M. C. (1982). Single-neuron labeling in the cat auditory nerve. *Science*, 216(4551), 1239–1241.

Liberman, M. C., & Oliver, M. E. (1984). Morphometry of intracellularly labeled neurons of the auditory nerve: Correlations with functional properties. *Journal of Comparative Neurology*, 223(2), 163–176.

Liberman, M. C., Dodds, L. W., & Pierce, S. (1990). Afferent and efferent innervation of the cat cochlea: Quantitative analysis with light and electron microscopy. *The Journal of Comparative Neurology*, 301(3), 443–460.

Liu, Q., & Davis, R. L. (2007). Regional specification of threshold sensitivity and response time in CBA/CaJ mouse spiral ganglion neurons. *Journal of Neurophysiology*, 98(4), 2215–2222.

Liu, Q., Manis, P. B., & Davis, R. L. (2014a). I and HCN channels in murine spiral ganglion neurons: Tonotopic variation, local heterogeneity, and kinetic model. *Journal of the Association for Research in Otolaryngology*, 15(4), 585–599.

Liu, Q., Lee, E., & Davis, R. L. (2014b). Heterogeneous intrinsic excitability of murine spiral ganglion neurons is determined by Kv1 and HCN channels. *Neuroscience*, 257, 96–110.

Liu, W., & Davis, R. L. (2014). Calretinin and calbindin distribution patterns specify subpopulations of type I and type II spiral ganglion neurons in postnatal murine cochlea. *The Journal of Comparative Neurology*, 522, 2299–2318.

Loewenstein, W. R., & Mendelson, M. (1965). Components of receptor adaptation in a Pacinian corpuscle. *The Journal of Physiology*, 177, 377–397.

Lopez, C. A., Olson, E. S., Adams, J. C., Mou, K., Denhardt, D. T., & Davis, R. L. (1995). Osteopontin expression detected in adult cochleae and inner ear fluids. *Hearing Research*, 85 (1–2), 210–222.

Lopez, I., Ishiyama, G., Acuna, D., Ishiyama, A., & Baloh, R. W. (2003). Immunolocalization of voltage-gated calcium channel alpha1 subunits in the chinchilla cochlea. *Cell and Tissue Research*, 313(2), 177–186.

Luscher, H. R., & Shiner, J. S. (1990). Simulation of action potential propagation in complex terminal arborizations. *Biophysical Journal*, 58(6), 1389–1399.

Lv, P., Wei, D., & Yamoah, E. N. (2010). Kv7–type channel currents in spiral ganglion neurons: Involvement in sensorineural hearing loss. *Journal of Biological Chemistry*, 285(45), 34699–34707.

Lv, P., Sihn, C. R., Wang, W., Shen, H., Kim, H. J., Rocha-Sanchez, S. M., & Yamoah, E. N. (2012). Posthearing $Ca(^{2+})$ currents and their roles in shaping the different modes of firing of spiral ganglion neurons. *The Journal of Neuroscience*, 32(46), 16314–16330.

Mason, W. T., & Leng, G. (1984). Complex action potential waveform recorded from supraoptic and paraventricular neurones of the rat: Evidence for sodium and calcium spike components at different membrane sites. *Experimental Brain Research*, 56(1), 135–143.

McCormick, D. A., Connors, B. W., Lighthall, J. W., & Prince, D. A. (1985). Comparative electrophysiology of pyramidal and sparsely spiny stellate neurons of the neocortex. *Journal of Neurophysiology*, 54(4), 782–806.

Merchan-Perez, A., & Liberman, M. C. (1996). Ultrastructural differences among afferent synapses on cochlear hair cells: Correlations with spontaneous discharge rate. *The Journal of Comparative Neurology*, 371(2), 208–221.

Meyer, A. C., Frank, T., Khimich, D., Hoch, G., Riedel, D., Chapochnikov, N. M., Yarin, Y. M., Harke, B., Hell, S. W., Egner, A., & Moser, T. (2009). Tuning of synapse number, structure and function in the cochlea. *Nature Neuroscience*, 12(4), 444–453.

Mo, Z. L., & Davis, R. L. (1997a). Heterogeneous voltage dependence of inward rectifier currents in spiral ganglion neurons. *Journal of Neurophysiology*, 78(6), 3019–3027.

Mo, Z. L., & Davis, R. L. (1997b). Endogenous firing patterns of murine spiral ganglion neurons. *Journal of Neurophysiology*, 77(3), 1294–1305.

Mo, Z. L., Adamson, C. L., & Davis, R. L. (2002). Dendrotoxin-sensitive $K(^{+})$ currents contribute to accommodation in murine spiral ganglion neurons. *The Journal of Physiology*, 542(Pt 3), 763–778.

Mou, K., Adamson, C. L., & Davis, R. L. (1998). Time-dependence and cell-type specificity of synergistic neurotrophin actions on spiral ganglion neurons. *The Journal of Comparative Neurology*, 402(1), 129–139.

Mountcastle, V. B., Talbot, W. H., & Kornhuber, H. H. (1966). The neural transformation of mechanical stimuli delivered to the monkey's hand. In *Ciba Foundation Symposium: Hormonal Factors in Carbohydrate Metabolism (Colloquia on Endocrinology)* (pp. 325–351). Chichester, UK: John Wiley & Sons.

Muller, M., von Hunerbein, K., Hoidis, S., & Smolders, J. W. (2005). A physiological place-frequency map of the cochlea in the CBA/J mouse. *Hearing Research*, 202(1–2), 63–73.

Nadol, J. B., Jr. (1988). Comparative anatomy of the cochlea and auditory nerve in mammals. *Hearing Research*, 34(3), 253–266.

Nadol, J. B., Jr., Burgess, B. J., & Reisser, C. (1990). Morphometric analysis of normal human spiral ganglion cells. *Annals of Otology, Rhinology, and Laryngology*, 99(5 Pt 1), 340–348.

Orduz, D., Bischop, D. P., Schwaller, B., Schiffmann, S. N., & Gall, D. (2013). Parvalbumin tunes spike-timing and efferent short-term plasticity in striatal fast spiking interneurons. *The Journal of Physiology*, 591(Pt 13), 3215–3232.

Peles, E., Nativ, M., Lustig, M., Grumet, M., Schilling, J., Martinez, R., Plowman, G. D., & Schlessinger, J. (1997). Identification of a novel contactin-associated transmembrane receptor with multiple domains implicated in protein-protein interactions. *EMBO Journal*, 16(5), 978–988.

Perkins, R. E., & Morest, D. K. (1975). A study of cochlear innervation patterns in cats and rats with the Golgi method and Nomarkski optics. *The Journal of Comparative Neurology*, 163(2), 129–158.

Puopolo, M., Raviola, E., & Bean, B. P. (2007). Roles of subthreshold calcium current and sodium current in spontaneous firing of mouse midbrain dopamine neurons. *The Journal of Neuroscience*, 27(3), 645–656.

Rasband, M. N., & Trimmer, J. S. (2001). Developmental clustering of ion channels at and near the node of Ranvier. *Developmental Biology*, 236(1), 5–16.

Reid, M. A., Flores-Otero, J., & Davis, R. L. (2004). Firing patterns of type II spiral ganglion neurons in vitro. *The Journal of Neuroscience*, 24(3), 733–742.

Robertson, D. (1976). Possible relation between structure and spike shapes of neurones in guinea pig cochlear ganglion. *Brain Research*, 109(3), 487–496.

Rosenblatt, K. P., Sun, Z. P., Heller, S., & Hudspeth, A. J. (1997). Distribution of Ca^{2+}-activated K^+ channel isoforms along the tonotopic gradient of the chicken's cochlea. *Neuron*, 19(5), 1061–1075.

Rosenbluth, J. (1962). The fine structure of acoustic ganglia in the rat. *Journal of Cell Biology*, 12, 329–359.

Rosowski, J. J. (1991). The effects of external- and middle-ear filtering on auditory threshold and noise-induced hearing loss. *Journal of the Acoustic Society of America*, 90(1), 124–135.

Rubel, E. W., & Fritzsch, B. (2002). Auditory system development: primary auditory neurons and their targets. *Annual Review of Neuroscience*, 25, 51–101

Ruggero, M. A., & Temchin, A. N. (2002). The roles of the external, middle, and inner ears in determining the bandwidth of hearing. *Proceedings of the National Academy of Sciences of the USA*, 99(20), 13206–13210.

Rusznak, Z., & Szucs, G. (2009). Spiral ganglion neurones: An overview of morphology, firing behaviour, ionic channels and function. *Pflugers Archiv—European Journal of Physiology*, 457(6), 1303–1325.

Ryugo, D. (1992). The auditory nerve: Peripheral innervation, cell body morphology, and central projections. In D. Webster, A. Popper, & R. Fay (Eds.), *The mammalian auditory pathway: Neuroanatomy* (pp. 23–65). New York: Springer-Verlag.

Safieddine, S., & Eybalin, M. (1992). Triple immunofluorescence evidence for the coexistence of acetylcholine, enkephalins and calcitonin gene-related peptide within efferent (olivocochlear) neurons of rats and guinea-pigs. *European Journal of Neuroscience*, 4(10), 981–992.

Santos-Sacchi, J. (1993). Voltage-dependent ionic conductances of type I spiral ganglion cells from the guinea pig inner ear. *The Journal of Neuroscience*, 13(8), 3599–3611.

Schwaller, B., Meyer, M., & Schiffmann, S. (2002). 'New' functions for 'old' proteins: The role of the calcium-binding proteins calbindin D-28k, calretinin and parvalbumin, in cerebellar physiology. Studies with knockout mice. *Cerebellum*, 1(4), 241–258.

Shibata, R., Nakahira, K., Shibasaki, K., Wakazono, Y., Imoto, K., & Ikenaka, K. (2000). A-type K^+ current mediated by the Kv4 channel regulates the generation of action potential in developing cerebellar granule cells. *The Journal of Neuroscience*, 20(11), 4145–4155.

Simmons, D., Duncan, J., de Caprona, D. C., & Fritzsch, B. (2011). Development of the inner ear efferent system. In D. K. Ryugo, R. R. Fay, & A. N. Popper (Eds.), *Auditory and vestibular efferents* (pp. 187–216). New York: Springer Science+Business Media.

Spoendlin, H. (1973). The innervation of the cochlear receptor. In A.R. Møller (Ed.), *Basic mechanisms in hearing* (pp. 185–234). New York: Academic Press.

Spoendlin, H., & Schrott, A. (1989). Analysis of the human auditory nerve. *Hearing Research*, 43 (1), 25–38.

Sudhof, T. C., Lottspeich, F., Greengard, P., Mehl, E., & Jahn, R. (1987). A synaptic vesicle protein with a novel cytoplasmic domain and four transmembrane regions. *Science*, 238(4830), 1142–1144.

Sugawara, M., Murtie, J. C., Stankovic, K. M., Liberman, M. C., & Corfas, G. (2007). Dynamic patterns of neurotrophin 3 expression in the postnatal mouse inner ear. *The Journal of Comparative Neurology*, 501(1), 30–37.

Sundgren-Andersson, A. K., & Johansson, S. (1998). Calcium spikes and calcium currents in neurons from the medial preoptic nucleus of rat. *Brain Research*, 783(2), 194–209.

Szabo, Z. S., Harasztosi, C. S., Sziklai, I., Szucs, G., & Rusznak, Z. (2002). Ionic currents determining the membrane characteristics of type I spiral ganglion neurons of the guinea pig. *European Journal of Neuroscience*, 16(10), 1887–1895.

Taberner, A. M., & Liberman, M. C. (2005). Response properties of single auditory nerve fibers in the mouse. *Journal of Neurophysiology*, 93(1), 557–569.

Thiers, F. A., Nadol, J. B., Jr., & Liberman, M. C. (2008). Reciprocal synapses between outer hair cells and their afferent terminals: Evidence for a local neural network in the mammalian cochlea. *Journal of the Association for Research in Otolaryngology*, 9(4), 477–489.

Verheugen, J. A., Fricker, D., & Miles, R. (1999). Noninvasive measurements of the membrane potential and GABAergic action in hippocampal interneurons. *The Journal of Neuroscience*, 19(7), 2546–2555.

Weisz, C. J., Glowatzki, E., & Fuchs, P. A. (2014). Excitability of type II cochlear afferents. *The Journal of Neuroscience*, 34(6), 2365–2373.

Whitlon, D. S., Ketels, K. V., Coulson, M. T., Williams, T., Grover, M., Edpao, W., & Richter, C. P. (2006). Survival and morphology of auditory neurons in dissociated cultures of newborn mouse spiral ganglion. *Neuroscience*, 138(2), 653–662.

Yamaguchi, K., & Ohmori, H. (1990). Voltage-gated and chemically gated ionic channels in the cultured cochlear ganglion neurone of the chick. *The Journal of Physiology*, 420, 185–206.

Yang, Y. M., & Wang, L. Y. (2006). Amplitude and kinetics of action potential-evoked Ca^{2+} current and its efficacy in triggering transmitter release at the developing calyx of held synapse. *The Journal of Neuroscience*, 26(21), 5698–5708.

Zhou, Z., Liu, Q., & Davis, R. L. (2005). Complex regulation of spiral ganglion neuron firing patterns by neurotrophin-3. *The Journal of Neuroscience*, 25(33), 7558–7566.

Chapter 5
The Ribbon Synapse Between Type I Spiral Ganglion Neurons and Inner Hair Cells

Mark A. Rutherford and Tobias Moser

Keywords Action potential generation · Active zone · Cochlea · Exocytosis · Glutamate receptor · Nanodomain · Synaptic heterogeneity · Synaptic ribbon · Synaptic vesicle · Voltage-gated calcium channel $Ca_v1.3$

5.1 Introduction

5.1.1 Overview

Sound pressure waves induce vibrations in the cochlea that produce graded receptor potentials in presynaptic sensory inner hair cells (IHCs). Ultimately, sounds are represented in the output of the cochlea by patterns of action potentials (APs) in spiral ganglion neurons (SGNs). These APs travel to the brain along the afferent fibers of the auditory nerve, which are myelinated axons of SGNs. This transformation of vibrations to electrical impulses is an analog-to-digital conversion taking place in the organ of Corti. Information about acoustic stimuli is encoded through IHC–SGN synaptic transmission and subsequent AP generation in the postsynaptic SGN.

M.A. Rutherford (✉)
Department of Otolaryngology, Central Institute for the Deaf, Washington University School of Medicine, 660 South Euclid Ave, St. Louis, MO 63110, USA
e-mail: rutherfordm@ent.wustl.edu

T. Moser (✉)
Institute for Auditory Neuroscience and Inner Ear Lab, Collaborative Research Center 889, University Medical Center Göttingen, Robert-Kochstr. 40, 37075 Göttingen, Germany
e-mail: tmoser@gwdg.de

A. Dabdoub et al. (eds.), *The Primary Auditory Neurons of the Mammalian Cochlea*, Springer Handbook of Auditory Research 52,
DOI 10.1007/978-1-4939-3031-9_5

5.1.2 The Type I Spiral Ganglion Neuron

The peripheral connectivity of type I SGNs, from the spiral ganglion to the organ of Corti, is shown for one tonotopic position in Fig. 5.1. Tonotopy determines the frequency of maximum sensitivity. Moreover, the APs in each type I SGN contain information about temporal dynamics and sound level in their precise timing and mean rate. The synapses between cochlear outer hair cells and type II SGNs are not covered in this chapter; therefore we will refer to type I SGNs simply as SGNs.

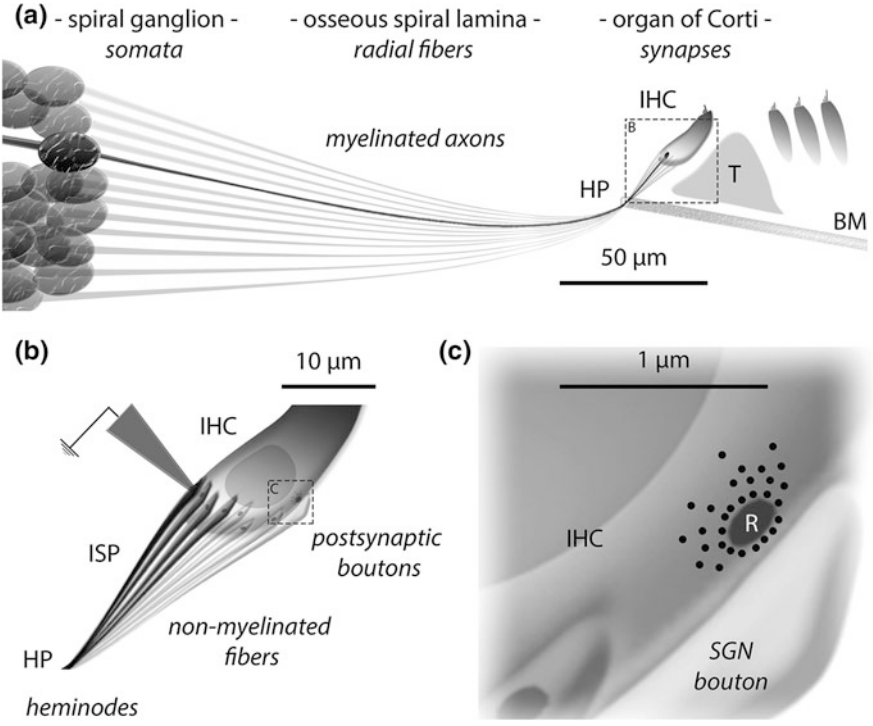

Fig. 5.1 Radial section schematic of spiral ganglion neurons in the cochlea. **a** The spiral ganglion is on *left*, showing several somas of type I spiral ganglion neurons (*SGNs*) all connected to one inner hair cell (*IHC*) in the organ of Corti on *right*, each via a single myelinated axon called a radial fiber. The radial fibers go through habenulas perforata (*HP*) to reach the neuropil of the inner spiral plexus (*ISP*) underneath IHCs in the organ of Corti. See *boxed* region enlarged in **b**. T, tunnel of Corti; BM, basilar membrane. One SGN is highlighted in *black*. *SGN anatomical parts* are labeled in *italic font*. **b** Synaptic transmission initiates a postsynaptic depolarization in the bouton and nonmyelinated fiber that triggers an action potential (*AP*) at the heminode near the HP (Sect. 5.4.4). An AP then propagates along the peripheral myelinated axon **a** via nodes of Ranvier to the soma in the spiral ganglion, then along the centrally projecting axon (not shown). **c** Each SGN receives excitatory synaptic input via one IHC presynaptic active zone, marked by a presynaptic ribbon (*R*), and surrounded by synaptic vesicles. (Modified from Rutherford et al., 2012). Spike encoding of neurotransmitter release timing by spiral ganglion neurons of the cochlea. *The Journal of Neuroscience*, 32(14), 4773–4789)

Starting from the periphery, in the organ of Corti, each SGN contacts a single synapse on one IHC via a single postsynaptic bouton (Fig. 5.1). The bouton is connected to the soma via the SGN's short nonmyelinated segment and longer peripheral myelinated axon. Beyond the SGN soma in the spiral ganglion, the myelinated central axon projects to the brain stem (see Muniak et al., Chap. 6).

As the SGN fiber exits the organ of Corti into the osseous spiral lamina, the cable thickens and the myelin begins just beyond the habenula perforata (HP; Fig. 5.1a, b). APs are likely initiated there, relatively near the IHC–SGN synapses in the neuropil of the inner spiral plexus (ISP; Fig. 5.1b). In the neuropil environment of the ISP between bouton and HP, the SGN fiber is surrounded by other afferent fibers, presynaptic terminals of efferent fibers, and nonneuronal glia-like supporting cells. It is unclear whether this part of the SGN should be called a nonmyelinated axon or a dendrite. The great majority of SGN fibers do not branch (Liberman, 1980). Therefore, in general AP generation in each SGN depends on excitatory input to its postsynaptic bouton from a single presynaptic ribbon-type active zone (AZ) of one IHC (Fig. 5.1c).

5.1.3 The Inner Hair Cell

IHCs are the primary sensory receptors in the organ of Corti. They mediate mechanotransduction through the hair bundle comprised of stereocilia. Ionic current through the bundle drives the receptor potential continuously, depolarizing the IHC to modulate the opening of voltage-gated Ca^{2+} channels at synapses. IHCs release glutamate at rest and in response to sound, initiating the postsynaptic depolarization that generates spontaneous and evoked APs in SGNs. Each IHC excites multiple SGNs. For example, cochleae of mammals such as mice and rats have around 1000 IHCs and approximately 20,000 SGNs.

In murine species and other mammals as well, the number of SGNs per IHC varies tonotopically (Spoendlin, 1972; Bohne et al., 1982). As illustrated in Fig. 5.1, in the developed ears of cats and mice, for example, each SGN is excited by a single ribbon-type AZ (i.e., a single ribbon synapse on one IHC). Therefore, like the number of SGNs, the number of ribbon synapses per IHC varies tonotopically (Meyer et al., 2009). In general, there are fewer than 10 afferent synapses per IHC in the extreme cochlear base and apex, and 15–30 synapses per IHC in the mid-cochlea. Greater synaptic density correlates with greater hearing acuity for mid-cochlear frequencies. For example, the tonotopic location of peak innervation density corresponds to frequencies of peak behavioral sensitivity (Ehret, 1976).

The 1:1 connection between ribbon synapse and SGN means that each IHC AZ provides the sole excitatory input to its SGN. In this way, each IHC AZ has one private line of communication from ear to brain. The specific sound-response properties of these communication lines differ from each other, depending greatly on mechanisms inherent to the given IHC AZ and its paired SGN. Through these

heterogeneous synaptic connections, information diverges from one IHC receptor potential to multiple SGNs with different response properties (Sect. 5.5).

5.1.4 The IHC Ribbon-Type Active Zone

The presynaptic AZ of each afferent synapse is occupied by a synaptic ribbon, a vesicle-tethering presynaptic electron-dense structural hallmark of the IHC–SGN synapse (Smith & Sjöstrand, 1961). Synaptic ribbons, found in cell types that release transmitter in response to graded stimulus-evoked receptor potentials, are composed predominantly of Ribeye (Schmitz et al., 2000; Khimich et al., 2005), a protein with both an enzymatic function (Schwarz et al., 2011) and an aggregating property thought to bind the ribbon together (Magupalli et al., 2008). Each synaptic ribbon has tens of vesicles tethered to it, a fraction of which are also tethered to the plasma membrane of the AZ (Frank et al., 2010). Structurally and molecularly, synaptic ribbons seem to be exocytosis nanomachines (Lenzi & von Gersdorff, 2001; Rutherford & Pangršič, 2012). One hypothesis is that ribbons inexhaustibly support high rates of transmitter release at continuously active sensory synapses by promoting the association of Ca^{2+} channels with fusion-competent vesicles. However, the complete functions of synaptic ribbons in IHC–SGN sensory encoding remain incompletely understood.

Ribbon-type AZs are large relative to AZs in the brain. Relative to each other, the ribbon-type AZs of hair cells exhibit marked heterogeneity in size. Putatively, differences in AZ size and protein content significantly influence AZ function (Sect. 5.5). In the absence of sound, different SGNs fire APs at mean rates that range from fewer than 1 to greater than 100 APs per second (s^{-1}). These so-called "spontaneous" APs are not generated cell-endogenously. Rather, both spontaneous and sound-evoked APs require the endocochlear potential, IHC depolarization, voltage-gated Ca^{2+} influx, and glutamate release from the IHC AZ onto its paired SGN bouton (Sewell, 1984; Glowatzki & Fuchs, 2002; Robertson & Paki, 2002).

5.1.5 Voltage-Gated Ca^{2+} Channels Controlling Exocytosis

Continuous, graded receptor potentials arise from mechanoelectrical and voltage-gated conductances (Corey & Hudspeth, 1979; Roberts et al., 1990). These changes in hair cell transmembrane potential modulate the temporal pattern of synaptic voltage-gated Ca^{2+} channel activity. Gating of Ca^{2+} channels modulates synaptic transmission by triggering exocytosis of glutamate from synaptic vesicles. In the cochlea, the receptor potential of each IHC is sampled over time by several SGNs, separately, based on the details of Ca^{2+} channel activity at each presynaptic AZ. Therefore the synaptic transfer function can differ among synapses stimulated by the same IHC receptor potential.

Hair cells are said to release neurotransmitter continuously because their synapses are never truly at rest. From IHC AZs, glutamate is released in an ongoing temporal sequence of discrete quanta. These packets of glutamate arrive onto the SGN bouton at rates that increase with the level of depolarization of the IHC receptor potential, which changes in response to sound. In IHCs, the voltage-gated Ca^{2+} channels controlling exocytosis are not prone to use-dependent inactivation. Thus, IHC depolarization produces an increase in Ca^{2+} channel activity at each ribbon synapse that is sustained for the duration of the depolarization. The opening of just one voltage-gated Ca^{2+} channel may be sufficient to trigger exocytosis of glutamate onto the SGN postsynaptic bouton (Sect. 5.3).

5.1.6 Abbreviations Used in This Chapter

AMPAR	α-Amino-3-hydroxy-5-methyl-4-isoxazolepropionic acid receptor
AP	Action potential
AZ	Active zone
BAPTA	1,2-*bis*(o-aminophenoxy)ethane-*N*,*N*,*N*′,*N*′-tetraacetic acid, "fast" Ca^{2+} chelator
$[Ca^{2+}]$	Ca^{2+} concentration
C_2	Ca^{2+}-binding protein domain
CaBP	Ca^{2+} binding protein
$Ca_V1.3$	Voltage-gated Ca^{2+} channel, L-type, pore-forming α-1D subunit
$Ca_Vß$	Auxiliary ß-subunit of voltage-gated Ca^{2+} channel
$Ca_Vα2δ$	Auxiliary α2δ-subunit of voltage-gated Ca^{2+} channel
CDI	Ca^{2+}-dependent inactivation
CtBP2	C-terminal binding protein 2
EGTA	Ethylene glycol-*bis*(2-aminoethylether)-*N*,*N*,*N*′,*N*′-tetraacetic acid, "slow" Ca^{2+} chelator
EPSC/P	Excitatory postsynaptic current/potential
ex vivo	Experiments in acutely explanted organs
GluA	Glutamate receptor subunit type, comprising AMPARs
HCN	Hyperpolarization-activated, cyclic nucleotide-gated nonspecificationic current (I_h)
IHC	Inner hair cell
K_V	Voltage-gated K^+ channel
m	Apparent Ca^{2+} cooperativity of exocytosis; from a power function fit to the relationship between exocytosis and Ca^{2+} influx
Na_V	Voltage-gated Na^+ channel
PSD	Postsynaptic density
px	Postnatal day *x*
RRP	Readily releasable pool of vesicles
SGN	Type I spiral ganglion neuron, also called auditory nerve fiber, cochlear nerve fiber, or auditory nerve single-unit

SNARE Soluble NSF attachment protein receptors, including SNAP, syntaxin, and synaptobrevin proteins
SR Spontaneous AP rate of a SGN (in the absence of sound)

5.2 Synaptogenesis of IHC and Type I Spiral Ganglion Neuron

5.2.1 Development from Pattern Generator to Sound Receiver

Before the onset of sensory function, IHCs drive patterned APs in the auditory nerve that seem to be required for normal wiring of the auditory brain (Walsh & McGee, 1987; Clause et al., 2014). These presensory APs in SGNs are driven by synaptic transmission, evoked by Ca^{2+} spikes in immature IHCs (Fig. 5.2a–c). Calcium spikes are regenerative potentials, similar to Na^{+} APs in neurons. Spike-driven exocytosis in immature IHCs (Kros et al., 1998; Beutner & Moser, 2001) is mediated predominantly by $Ca_V1.3$ Ca^{2+} channels (Brandt et al., 2003; Marcotti et al., 2003). Although mature IHCs do not spike, they use the same type of voltage-gated Ca^{2+} channels to mediate hearing.

By the onset of hearing, at approximately postnatal day 14 (p14) in mice and rats, reduction in number of $Ca_V1.3$ channels (Brandt et al., 2003) and upregulation of K^{+} channels disable regenerative Ca^{2+} spikes in IHCs. For example, the large-conductance Ca^{2+}- and voltage-activated K^{+} channels (BK channels) carry a hyperpolarizing conductance that ensures a nonspiking, graded response of the mature IHC transmembrane potential (Kros et al., 1998; Oliver et al., 2006). Another developmentally upregulated K^{+} channel, $K_V7.4$ ($KCNQ_4$,), defective in human deafness DFNA2 (Kubisch et al., 1999), is partially active when IHCs are at rest, and contributes to setting the IHC resting membrane potential (Oliver et al., 2003). Many aspects of IHC development depend on thyroid hormone signaling (Rüsch et al., 2001; Sendin et al., 2007).

Presensory spiking in IHCs generates bursts of APs in SGNs at p10 in vivo (Fig. 5.2c). These bursts are replaced by mature-looking AP trains in SGNs around p14 (Wong et al., 2013). Experiments in organ of Corti explants have investigated what underlies the temporal pattern of Ca^{2+} spikes in IHCs, but the mechanism is still under debate. Release of ATP onto IHCs from cells in the developmentally transient Kölliker's organ may be important for hair cell excitation (Tritsch et al., 2007; Tritsch & Bergles, 2010), although patterned activity proceeded in the presence of inhibitors of ionotropic purinoceptors (Sendin et al., 2014). Alternatively, patterned electrical activity may be intrinsic to the IHC but modulated by ATP release (Johnson et al., 2011).

There is general agreement that presensory activity is likely regulated by inhibition of IHCs via the efferent synapses of olivocochlear neurons. Inhibitory

cholinergic transmission could periodically interrupt the IHC depolarization resulting from resting mechanotransduction (Walsh & Romand, 1992; Glowatzki & Fuchs, 2000; Sendin et al., 2014), similar to efferent inhibition of mature outer hair cells (Géléoc & Holt, 2003). However, olivocochlear neurons have somas in the brain, and it is unclear how intrinsic activity in their axons is altered in the excised organ of Corti. Whatever the mechanism, dramatic changes in SGN AP trains between p10 and p14 (Fig. 5.2c–f) are concurrent with IHC synaptic maturation.

5.2.2 Anatomical and Physiological Synaptic Maturation

In mice, SGN fibers reach cells in the differentiating organ of Corti already at birth. The numbers of fibers and synapses in the organ of Corti appear to increase in number during the first postnatal week (Lenoir et al., 1980; Shnerson et al., 1981). Then, presynaptic ribbons and postsynaptic densities (PSDs) decrease in number (Huang et al., 2007, 2012). By p21, IHC–SGN synapses are predominantly mature (Sobkowicz et al., 1982; Grant et al., 2010). This section highlights some structural and functional aspects of synaptic maturation and discusses underlying molecular-anatomical mechanisms.

In the first postnatal week, the IHC Ca^{2+} current and exocytosis increase as they approach their peak sizes. Then, during the second postnatal week, they decline differently as the efficiency with which Ca^{2+} influx triggers exocytosis increases. The number of $Ca_V1.3$ channels decreases but the smaller Ca^{2+} current of mature IHCs causes comparably large amounts of exocytosis (Beutner & Moser, 2001; Brandt et al., 2005; Zampini et al., 2010). Immunofluorescence microscopy in fixed tissue (Fig. 5.3a–c) as well as Ca^{2+} imaging in live tissue revealed that overall $Ca_V1.3$ immunoreactivity declined while it accumulated synaptically and the Ca^{2+} influx increased specifically at the ribbon synapses (Wong et al., 2013, 2014). Thus, maturation involved reduction of extrasynaptic Ca^{2+} channels not directly coupled to synaptic vesicle exocytosis. Unlike immature IHCs, Ca^{2+} influx in mature IHCs is largely confined to AZs.

Individual IHC–SGN synapses at p6 displayed several small appositions of AZs and PSDs, only some of them occupied by a presynaptic ribbon. These groups of appositions encircled the perimeter of the bouton contact (Wong et al., 2014). Only after the onset of hearing was a single juxtaposed AZ–PSD complex found per SGN bouton (Fig. 5.3).

As AZs and PSDs decreased in number they increased in size, as shown via electron microscopy (Fig. 5.3e, f) and corroborated with confocal immunohistochemistry using antibodies against $Ca_V1.3$ Ca^{2+} channels, GluA2/3 glutamate receptors, and the ribbon protein CtBP2 (Fig. 5.3a–c; Wong et al., 2014). The ratio of ribbons to glutamate receptor puncta increased to nearly 1 by p20, indicating that ribbonless AZs disappeared and the 1:1 connection between ribbons and PSDs prevailed for each SGN.

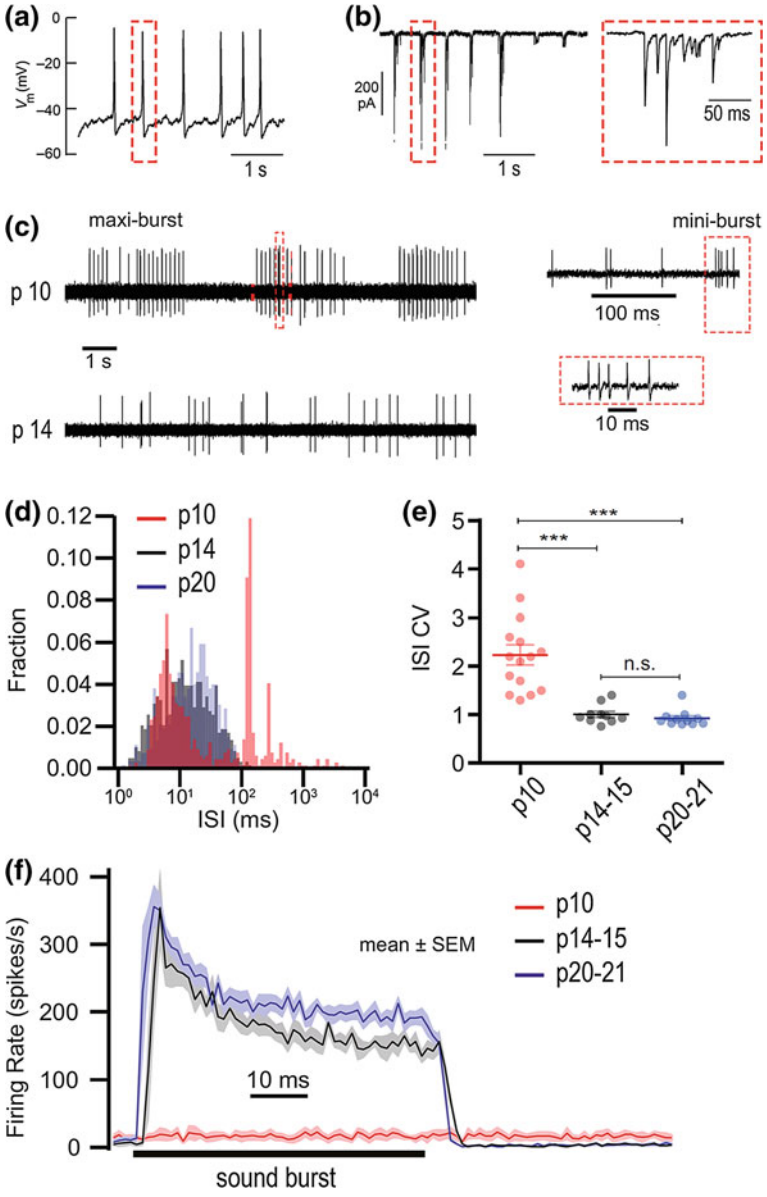
(a)
0
−20
−40
−60
V_m (mV)
1 s
(b)
200 pA
1 s
50 ms
(c)
maxi-burst
mini-burst
p 10
1 s
100 ms
10 ms
p 14
(d)
0.12
0.10
0.08
0.06
0.04
0.02
0.00
Fraction
p10
p14
p20
10^0
10^1
10^2
10^3
10^4
ISI (ms)
(e)
5
4
3
2
1
0
ISI CV
***
***
n.s.
p10
p14-15
p20-21
(f)
400
300
200
100
0
Firing Rate (spikes/s)
mean ± SEM
p10
p14-15
p20-21
10 ms
sound burst

◀ **Fig. 5.2** Functional maturation from pattern generator to stimulus transducer. **a** Patch-clamp recording of a semiperiodic sequence of Ca^{2+} spikes in a developing IHC. **b** *Left*, bursts of EPSCs in a patch-clamp recording of a developing SGN, due to presynaptic Ca^{2+} spikes in the IHC. *Right*, one burst is enlarged. Each Ca^{2+} spike and EPSC burst lasts for approximately 100 ms and consists of several events of exocytosis. **c** *Upper*, in vivo SGN spontaneous AP train at p10 showing semiperiodic discharge. Each SGN AP mini-burst (*red dashed boxes* in **c**) is evoked by a burst of EPSCs (*red dashed box* in **b**) triggered by a Ca^{2+} spike in the presynaptic IHC (*red dashed box* in **a**). The timing between each mini-burst in a maxi-burst (the interburst interval) corresponds to the interspike interval in the immature IHC **a**. The periods between maxi-bursts represent durations over which the IHC is not spiking. *Lower*, SGN spontaneous AP train at p14 is relatively irregularly timed. **d** Interspike interval histograms for SGN spontaneous AP trains at p10, p14, and p20. The distribution of intervals changes from bimodal to unimodal between p10 and p14, and then remains relatively unchanged by p20. **e** Interspike interval coefficients of variation (CV: variance/mean) for individual SGN recordings (*filled circles*) and their means (*horizontal bars*) are significantly less by p14 because of the absence of long intervals that made the bimodal distribution at p10 **d**. **f** Mean instantaneous AP rates for repetitions of 50 ms sound bursts (*horizontal bar*) at the three developmental stages. After the onset of hearing (after p14) the SGNs exhibit an onset response that adapts and approaches a steady-state spike rate of $\sim$200 s^{-1}. (Modified from Wong et al., 2013. Concurrent maturation of inner hair cell synaptic Ca^{2+} influx and auditory nerve spontaneous activity around hearing onset in mice. *Journal of Neuroscience*, 33 (26), 10661–10666)

Ribbons are synaptically anchored via the presynaptic protein bassoon (Khimich et al., 2005). In keeping with the notion that Ca^{2+} channels cluster underneath ribbons in the presynaptic density (schematized in Fig. 5.3d, g), bassoon and $Ca_V1.3$ immunofluorescence closely aligned in elongated stripes at p19 when measured with two-color stimulated emission depletion (STED) microscopy (Wong et al., 2014; Rutherford, 2015). In contrast, before the onset of hearing synaptic $Ca_V1.3$ channels formed only smaller spot-like clusters.

Two candidate mechanisms for this anatomical refinement are (1) merging—small AZs or PSDs of a synaptic contact coalesce via interactions of scaffold molecules possibly involving transsynaptic regulation and (2) pruning—small AZs and PSDs are selectively eliminated via protein degradation. Bassoon and the similar protein piccolo each inhibit ubiquitin ligase activity (Waites et al., 2013). Their greater abundance might protect the largest of the initially formed AZs.

These structural refinements are accompanied by developmental changes in synaptic function and changes in molecular composition. At p0, rodent IHCs show relatively little Ca^{2+} current or exocytosis. As mentioned previously in this section, this is followed by an increase during week 1, then a decrease in Ca^{2+} current but relatively little decrease in exocytosis during week 2. This increase in efficiency of exocytosis is at least partially due to the positioning of more $Ca_V1.3$ channels at AZs and fewer $Ca_V1.3$ channels away from AZs (Fig. 5.3a). Moreover, during the first postnatal week exocytosis seems to employ a different molecular program than later in development. For example, otoferlin, essential for exocytosis in mature IHCs, seems dispensable for presynaptic function at this early stage while the neuronal Ca^{2+} sensor of exocytosis synaptotagmin 2 is temporarily expressed (Beurg et al., 2010; Reisinger et al., 2011). In addition to the increase in efficiency

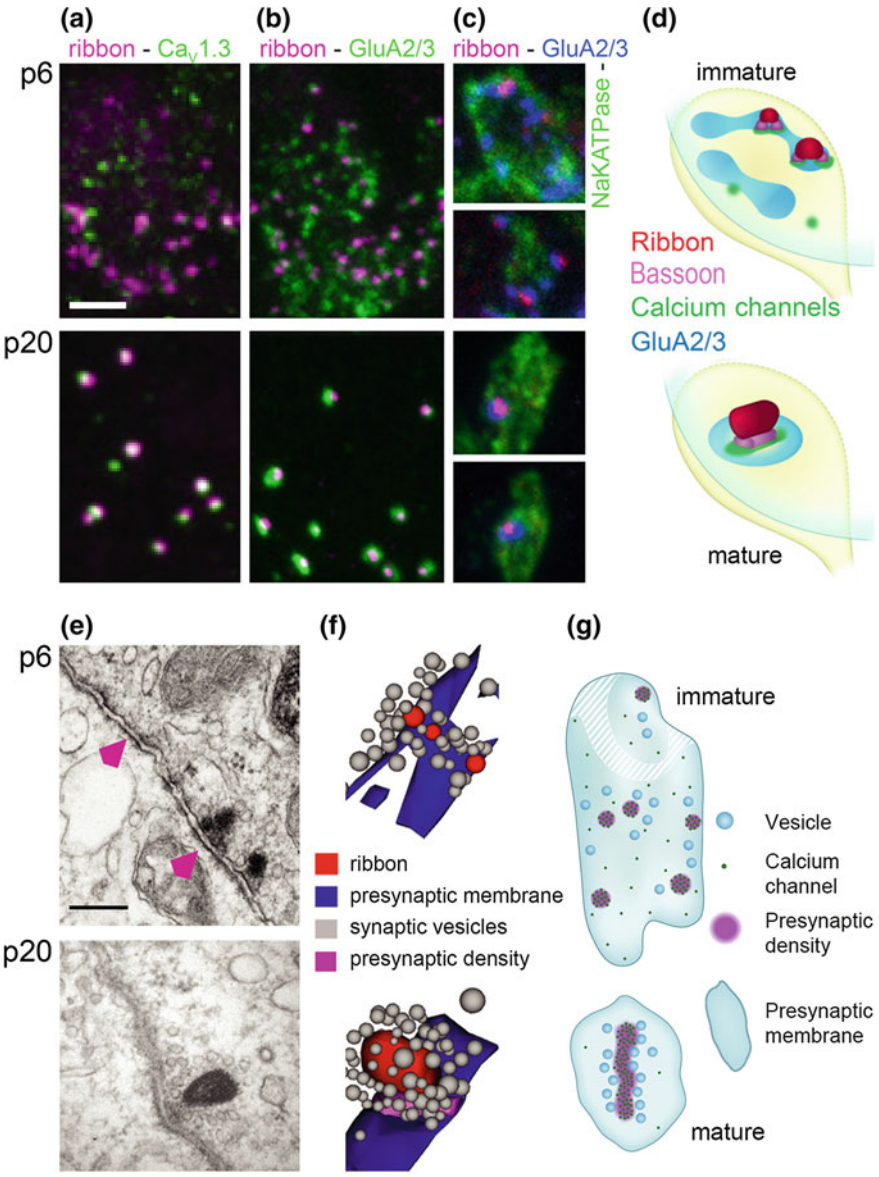
(a)
ribbon - $Ca_V1.3$
(b)
ribbon - GluA2/3
(c)
ribbon - GluA2/3
NaKATPase -
p6
p20
(d)
immature
Ribbon
Bassoon
Calcium channels
GluA2/3
mature
(e)
p6
p20
(f)
ribbon
presynaptic membrane
synaptic vesicles
presynaptic density
(g)
immature
Vesicle
Calcium channel
Presynaptic density
Presynaptic membrane
mature

◀ **Fig. 5.3** Structural maturation of IHC-SGN ribbon synapses. **a** Ribbons (anti-CtBP2, *magenta*) and voltage-gated Ca^{2+} channels (anti-$Ca_V1.3$, *green*) in one IHC at p6 (immature, *upper*) and one IHC at p20 (mature, *lower*). **b** Similar to **a** but with AMPA-type glutamate receptors on the green channel (anti-GluA2/3). Between p6 and p20, presynaptic voltage-gated Ca^{2+} channels and postsynaptic glutamate receptors become restricted to ribbons at IHC–SGN connections. **c** Ribbons (*magenta*), GluA2/3 (*blue*), and NaKATPase (*green*, labeling SGN boutons) demonstrate refinement of molecular anatomy within the synaptic regions defined by each bouton contact. **d** Schematic of changes in **a–c** illustrates the development of 1:1 connectivity between ribbons and SGNs between p6 and p20. **e** Electron micrographs of IHC–SGN synaptic contacts. At p6, some postsynaptic densities are juxtaposed to presynaptic ribbons while others are not (*magenta arrowheads*). By p20, almost all synapses have a single, larger ribbon. **f** Three-dimensional AZ reconstructions of a few small immature ribbons (p6, *upper*) and one large mature ribbon (p20, *lower*) anchored to the presynaptic membrane and surrounded by vesicles. **g** Schematic of IHC–SGN synapses shows a more ordered arrangement of voltage-gated Ca^{2+} channels and synaptic vesicles upon maturity. (Modified from Wong et al., 2014. Developmental refinement of hair cell synapses tightens the coupling of Ca^{2+} influx to exocytosis. *The EMBO Journal*, 33(3), 247–264; Copyright Wiley-VCH Verlag GmbH & Co. KGaA. Reproduced with permission)

of exocytosis, a change is also observed in the apparent Ca^{2+} dependence of exocytosis when manipulating the Ca^{2+} current by changing the number of open channels (Johnson et al., 2005; Wong et al., 2014).

Two mechanisms have been proposed to contribute to changes in the Ca^{2+} efficiency and apparent Ca^{2+} dependence of exocytosis in IHCs around the onset of hearing: (1) the intrinsic Ca^{2+} dependence of exocytosis changes due to a switch in synaptic protein type and/or (2) tightening of the spatial coupling between Ca^{2+} channels and vesicles at the AZ. A developmental upregulation of synaptotagmin IV has been proposed to underlie the increase in Ca^{2+} efficiency and the linearization of the apparent Ca^{2+} dependence of IHC exocytosis around the onset of hearing (Johnson et al., 2010), which might support hypothesis 1.

The intrinsic Ca^{2+} dependence of exocytosis in mouse IHCs was compared before and after the onset of hearing by measuring the Ca^{2+}-dependent rate constant of the fast component of exocytosis, elicited by step changes of $[Ca^{2+}]$ in response to intracellular Ca^{2+} uncaging (Wong et al., 2014). The intrinsic Ca^{2+} dependence was found to be similar, which does not support hypothesis 1. In contrast, when changing the Ca^{2+} current by manipulating the number of open channels, a developmental difference was found in the apparent Ca^{2+} dependence (or cooperativity) of exocytosis. The apparent Ca^{2+} cooperativity of exocytosis was supralinear before hearing onset but near linear in mature IHCs, suggesting a transition from Ca^{2+} *micro*-domain control of exocytosis before the onset of hearing to Ca^{2+} *nano*-domain control of exocytosis after the onset of hearing. Development of Ca^{2+} nanodomain control of exocytosis upon maturation implies tightening of the spatial coupling between Ca^{2+} influx and exocytosis, which supports hypothesis 2. Indeed, the topography of membrane-proximal vesicles, assumed to form the readily releasable pool, is more ordered around presynaptic densities after the onset of hearing (Fig. 5.3g). For more on the subjects of intrinsic and apparent Ca^{2+}

cooperativity as well as Ca^{2+} microdomain and nanodomain control of exocytosis, see Sect. 5.3.3.

5.3 Presynaptic Mechanisms Encoding Sound

5.3.1 Presynaptic Ca^{2+} Influx

Unlike typical L-type Ca^{2+} currents known in other systems to be activated by high-voltage (e.g., in cardiomyocytes of the heart), the L-type Ca^{2+} currents in hair cells of the inner ear activate at relatively hyperpolarized potentials, exhibit fast activation, and undergo slow and mild inactivation (Fuchs et al., 1990; Roberts et al., 1990; Spassova et al., 2001). In mouse cochlea, the pore-forming alpha subunit is $Ca_V1.3$ (Platzer et al., 2000; Brandt et al., 2003; Dou et al., 2004). Without Ca^{2+} influx through this channel, IHC synaptic exocytosis is abolished (Moser & Beutner, 2000; Brandt et al., 2003) and there is profound deafness in rodents and humans (Zhang et al., 1999; Platzer et al., 2000; Baig et al., 2011).

Hair cells are thusly similar to retinal photoreceptors and bipolar neurons, which also employ L-type Ca^{2+} channels, have synaptic ribbons, and transduce graded receptor potentials for controlling transmitter release (Barnes & Hille, 1989; Heidelberger & Matthews, 1992; Tachibana et al., 1993). They are different from conventional central nervous system (CNS) synapses that use N- and P/Q-type Ca^{2+} channels for transmitter release. The number of channels depends on species, developmental stage, and AZ number which varies by tonotopic location but, on average, the number of Ca^{2+} channels per mature mouse IHC is approximately 1700, with the majority being synaptic (Brandt et al., 2005; Frank et al., 2010; Wong et al., 2014). Evidence from various technical approaches agrees that each AZ of a mature auditory hair cell has on average approximately 100 Ca^{2+} channels in the frog (Roberts et al., 1990; Issa & Hudspeth, 1996; Rodriguez-Contreras & Yamoah, 2001), turtle (Tucker & Fettiplace, 1995), and mouse (Brandt et al., 2005; Zampini et al., 2013).

IHC $Ca_V1.3$ currents have little Ca^{2+}-dependent inactivation (CDI) and activate at relatively negative potentials (Koschak et al., 2001), likely due to the IHC-specific molecular composition of the $Ca_V1.3$ Ca^{2+} channel complex and specific intracellular modulators of its activity. $Ca_V\beta_2$ was identified to be the predominant ß-subunit of IHCs that co-regulates channel inactivation and enables sufficient numbers of Ca^{2+} channels to accumulate at the AZ (Neef et al., 2009). The $Ca_V\alpha2\delta$ subunit(s) involved in the IHC Ca^{2+} channel remain to be identified. Calmodulin, an obligate mediator of CDI (Lee et al., 2000), is expressed in IHCs, where it regulates CDI of $Ca_V1.3$ channels (Grant & Fuchs, 2008). However, calmodulin-mediated CDI of $Ca_V1.3$ channels is antagonized by Ca^{2+} binding proteins (CaBPs), several of which are expressed in IHCs (Yang et al., 2006; Cui

et al., 2007). In humans, mutation in the gene coding for CaBP2 results in hearing impairment DFNB93 (Schrauwen et al., 2012).

The list of putative regulators of the IHC $Ca_V1.3$ Ca^{2+} channel complex is steadily growing and includes bassoon, Rab3-interacting molecule (RIM), RIM-binding protein (Hibino et al., 2002), harmonin, and otoferlin. Of the two described mechanisms of interaction between RIM and Ca^{2+} channels, via RIM–PDZ binding to the proline-rich PDZ interacting motif in the C-terminus of $Ca_V\alpha$ or via RIM C-terminal C_2 domain binding to Ca_Vß, the $Ca_V1.3$ Ca^{2+} channel complex seems to employ only the C_2 domain-Ca_Vß binding (Gebhart et al., 2010; Kaeser et al., 2011). Harmonin, a scaffold protein mutated in Usher 1C syndrome (Verpy et al., 2000), is an important organizer of the mechanotransduction machinery in the hair bundle. Harmonin also interacts with $Ca_V1.3$ via binding of its second PDZ domain to the proline-rich PDZ interacting motif in the $Ca_V1.3$ C-terminus (Gregory et al., 2011). In this interaction harmonin imposes an inhibition on $Ca_V1.3$ gating that is relieved by depolarization, thereby contributing to voltage-dependent facilitation of $Ca_V1.3$. In addition, harmonin appears to facilitate ubiquitination and proteasomal degradation of $Ca_V1.3$, potentially co-regulating the abundance of Ca^{2+} channels at the presynaptic AZ (Gregory et al., 2011). Finally, proper number and morphology of $Ca_V1.3$ Ca^{2+} channel clustering have been attributed to the presynaptic scaffold protein bassoon and/or its associated supramolecular ribbon nanomachine (Frank et al., 2010; Jing et al., 2013). IHCs from mice lacking function of bassoon protein had fewer ribbons and less Ca^{2+} channel immunofluorescence at AZs (Fig. 5.4a). Reduction of Ca^{2+} channel immunoreactivity was greatest at the ribbonless AZs. Because the remaining ribbons were more loosely anchored to the AZ than wild-type ribbons (Fig. 5.4b, c), the extent to which functional deficits were due to lack of bassoon alone versus disruption of the entire ribbon complex is unclear.

Presynaptic Ca^{2+} influx has been imaged in living hair cells with confocal microscopy in excised inner ear endorgans. On strong depolarization, spatially confined Ca^{2+} signals rapidly rise and decay with two time constants (Issa & Hudspeth, 1996; Frank et al., 2009), dependent on cytosolic diffusion of free and buffered Ca^{2+} (Roberts, 1993). Among IHC AZs, a marked heterogeneity of Ca^{2+} signal amplitude and voltage of half-maximal activation was observed (Frank et al., 2009). This presynaptic heterogeneity may enable the IHC to decompose sound amongst SGNs having different sensitivities, to encode the entire audible range of sound pressures at any characteristic frequency. For more about synaptic heterogeneity, see Sect. 5.5.

5.3.2 *Presynaptic Transmitter Release*

The ensuing Ca^{2+} signal drives rapid exocytosis of the readily releasable pool (RRP) of synaptic vesicles at the AZ, which releases glutamate onto the postsynaptic SGN bouton (Sect. 5.4). The IHC AZ has a molecular composition and

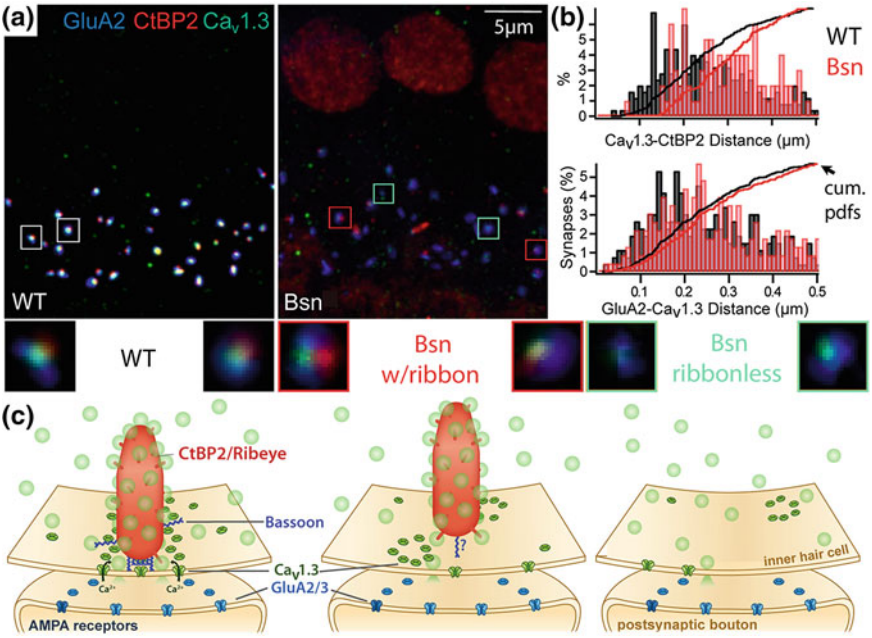

Fig. 5.4 Bassoon anchors the ribbon to the active zone, organizing Ca^{2+} channels and vesicles. **a** AMPA receptors (anti-GluA2, *blue*), ribbons (anti-CtBP2, *red*), and Ca^{2+} channels (anti- $Ca_V1.3$, *green*) in mature IHCs of wild-type mice (*left*, WT) or bassoon-deficient mice (*right*, Bsn). In Bsn IHCs, a minority of ribbons remained and all AZs appeared to have fewer Ca^{2+} channels. Small boxes are centered on individual AZs enlarged below for WT synapses (*white boxes, left*), ribbon-occupied Bsn synapses (*red boxes, center*), and ribbonless Bsn synapses (*aqua boxes, right*). **b** Analysis per AZ: without bassoon (*red*, Bsn) the distances between CtBP2 and $Ca_V1.3$ puncta (*upper*) are greater than in wild-type (*black*, WT). The distance between GluA2 and $Ca_V1.3$ puncta (*lower*) was relatively unaffected. *Vertical bars* are frequency histograms and lines are cumulative probability density functions (cum. pdfs). **c** Schematic of protein localizations at AZs of WT (*left*), ribbon-occupied Bsn (*middle*), and Bsn ribbonless IHCs (*right*). (Modified from Jing et al., 2013. Disruption of the presynaptic cytomatrix protein bassoon degrades ribbon anchorage, multiquantal release, and sound encoding at the hair cell afferent synapse. *Journal of Neuroscience*, 33(10), 4456–4467)

structure that enables temporally precise release at high rates over long periods of time, as required for normal hearing (Moser et al., 2006; Matthews & Fuchs, 2010; Rutherford & Pangršič, 2012). The synaptic ribbon tethers synaptic vesicles to its ellipsoid-like surface. Moreover, two rows of vesicles align with the presynaptic membrane density at the base of the ribbon (Frank et al., 2010), some tethered to the plasma membrane. Because of their number and their preferential loss during stimulation, these vesicles are often considered to be the ultrastructural substrate of a finite RRP measured physiologically (Moser & Beutner, 2000; Lenzi et al., 2002). The vesicles immediately surrounding and near ribbons are thought to refill the RRP. Vesicle density can differ between high- and low-frequency hair cells, which

may be an important tonotopic specialization (Schnee et al., 2005). After fusion with the plasma membrane, vesicles are regenerated via endocytosis in the perisynaptic space (Neef et al., 2014).

Sound-response properties of single auditory nerve units have been measured with extracellular electrophysiological recording of APs from the central axon of single SGNs in vivo (Kiang, 1965; Taberner & Liberman, 2005). The 1:1 connectivity between IHC AZ and SGN makes these recordings extremely valuable for understanding sound encoding at the IHC afferent synapse but also, more generally for neuroscience, because there is probably no other synaptic connection for which an in vivo readout of a single AZ exists. Computational models have used the acoustic signal as input and the APs of individual SGNs as measured output to describe cochlear filter properties mathematically (Weiss, 1966; Meddis, 2006).

To measure exocytosis of synaptic vesicles, the patch-clamp technique was applied to hair cells in inner ear explants (Parsons et al., 1994). Patch-clamp measurements of presynaptic plasma membrane capacitance allow one to monitor exocytosis and endocytosis because fusion and fission of synaptic vesicle membrane with plasma membrane cause increases and decreases, respectively, in surface area that are proportional to capacitance. Applied to the whole cell, measurements of capacitance changes report the summed activity of all synapses. On average, each AZ in a mouse IHC has RRP of about one dozen vesicles that undergoes exocytosis with a time constant of about 10 ms and is replenished with fast and slow time constants of about 140 ms and 3 s (Moser & Beutner, 2000). For single AZ measurements of exocytosis and synaptic transmission with the patch-clamp technique applied to SGN boutons, see Sect. 5.4.2.

Insights into the molecular composition of transmitter release have been provided along three main avenues of investigation: (1) candidate gene approaches driven by knowledge of conventional synapses (e.g., Safieddine & Wenthold, 1999; Nouvian et al., 2011), (2) genetics of human deafness (e.g., Yasunaga et al., 1999; Ruel et al., 2008), and (3) proteomics (Uthaiah & Hudspeth, 2010; Kantardzhieva et al., 2012; Duncker et al., 2013). The synaptic ribbon is composed primarily of the protein Ribeye (Schmitz et al., 2000), a splice variant of the transcriptional co-repressor CtBP2 that has lysophosphatidylacyl-transferase activity (Schwarz et al., 2011). The presence of ribeye at AZs seem to promote endocytic vesicle regeneration, vesicle tethering/docking/priming, and Ca^{2+}-channel clustering in hair cells (Frank et al., 2010; Sheets et al., 2011; Jing et al., 2013; Khimich et al., 2005).

Some components of the presynaptic AZ machinery seem not to be conserved between conventional neuronal synapses and ribbon-type synapses of IHCs, specifically the proteins that mediate Ca^{2+} sensing and lipid membrane fusion. Otoferlin, a multi-C_2-domain ferlin protein specifically expressed in inner ear hair cells is defective in human deafness DFNB9 (Yasunaga et al., 1999) and is currently the best candidate for a vesicular Ca^{2+} sensor. Exocytosis was nearly abolished in otoferlin-deficient IHCs despite the presence of synaptic vesicles at the AZ (Roux et al., 2006). A definitive conclusion on otoferlin as a Ca^{2+} sensor of fusion will require mutagenesis of Ca^{2+} binding sites, biochemical characterization of altered Ca^{2+} binding, and physiological assessment of the Ca^{2+} dependence of IHC

exocytosis with the mutant otoferlin. In addition to its putative role as Ca^{2+} sensor, otoferlin seems to facilitate vesicle replenishment (Pangršič et al., 2010).

The core membrane fusion machinery is thought to be conserved at all synapses. In neurons it consists of the soluble NSF attachment protein receptors (SNAREs) synaptobrevin 1 or 2, SNAP25, and syntaxin 1. However, experiments that used neurotoxins and genetic mutations to disable SNARE proteins indicated that IHC exocytosis may operate without neuronal SNARE proteins (Nouvian et al., 2011). Interestingly, otoferlin has been shown to interact with neuronal SNAREs (Roux et al., 2006; Ramakrishnan et al., 2009) but hair cells seem to lack SNARE regulators such as synaptotagmins (Beurg et al., 2010; Reisinger et al., 2011) and complexins (Strenzke et al., 2009; Uthaiah & Hudspeth, 2010). Investigations into the fusion machinery of IHCs are ongoing.

5.3.3 *Stimulus–Secretion Coupling*

There is an intimate functional relationship and perhaps even direct molecular binding between release-ready vesicles and Ca^{2+} channels in a proximity of 10–30 nm. From the perspective of the Ca^{2+}-sensing protein on a given release-ready synaptic vesicle, it seems that only one or very few $Ca_V1.3$ channels dominate the local $[Ca^{2+}]$ (Brandt et al., 2005; Goutman & Glowatzki, 2007; Graydon et al., 2011). In other words, Ca^{2+} control of exocytosis appears to operate in nanodomains. Alternatively, vesicle fusion at a given AZ may be controlled by a Ca^{2+} microdomain (Johnson et al., 2008, 2010; Heil & Neubauer, 2010), in which many Ca^{2+} channels contribute to the local $[Ca^{2+}]$ signal acting on individual vesicles.

To test the nanodomain versus microdomain hypotheses, the relative number of $Ca_V1.3$ channels contributing to exocytosis can be experimentally tested by studying the incremental dependence of RRP exocytosis on Ca^{2+} influx. The apparent Ca^{2+} cooperativity m is obtained by fitting a power function to the relationship between exocytosis and transmembrane Ca^{2+} charge (Q_{Ca}): exocytosis = $A(Q_{Ca})^m$, where A is the amplitude of the exocytic response and the exponent m is the apparent cooperativity. Different data points are obtained by manipulating the Ca^{2+} influx, either by changing the number of open channels or by changing the charge through each channel, while depolarizing the IHC for a brief duration to probe the RRP. If m is smaller when manipulating Ca^{2+} influx by changing the number of open Ca^{2+} channels than it is when changing the current through a given channel, then Ca^{2+} nanodomain control of exocytosis is suggested. If m is close to unity then the dependence of RRP exocytosis on Ca^{2+} influx is near linear. This implies little or no cooperativity of Ca^{2+} in its coupling to vesicle fusion and suggests nanodomain stimulus-secretion coupling. In the extreme interpretation of nanodomain, one vesicle undergoes exocytosis for each opening of a Ca^{2+} channel because a sufficient $[Ca^{2+}]$ is reached to saturate the sensor. Ca^{2+} from further channels would be insufficient. On the other hand, if comparable estimates of m are obtained for these two types of manipulation of Ca^{2+} influx (changing the number of open Ca^{2+}

channels versus changing the current through a given channel), then m should be similar to the intrinsic biochemical Ca^{2+} cooperativity of IHC exocytosis ($m = 4$; Beutner et al., 2001). This would suggest Ca^{2+} microdomain control (Augustine et al., 1991). In a Ca^{2+} microdomain control of exocytosis, many channels must open with overlapping effects before [Ca^{2+}] is high enough to evoke fusion.

Evidence for a nanodomain-like control as described in the preceding text was obtained using membrane capacitance measurements to assay the Ca^{2+} dependence of exocytosis in mature IHCs (Brandt et al., 2005; Wong et al., 2014). When changing the number of open Ca^{2+} channels, m was approximately 1.4. When changing the charge through each channel, m was above 3. Considering the number and open probability of Ca^{2+} channels, the distance to vesicles, the concentration and binding kinetics of Ca^{2+} buffers, and the Ca^{2+} binding properties of the Ca^{2+} sensor on the vesicle (Matveev et al., 2011), biophysical modeling was performed to evaluate the Ca^{2+} nanodomain hypothesis. The model predicted a vesicle-to-sensor coupling of less than 20 nm (Wong et al., 2014), in agreement with experiments that tested the differential effects on exocytosis of synthetic Ca^{2+} chelators having different binding rates (EGTA and BAPTA, Moser & Beutner, 2000; Goutman & Glowatzki, 2007). Therefore, the IHC–SGN synapse seems to operate in a nanodomain regime. In vestibular hair cells the Ca^{2+} influx per ribbon is significantly less; however, the nanodomain stimulus–secretion coupling may be even tighter than in mature IHCs (Vincent et al., 2014).

5.4 Synaptic Transmission and Action Potential Generation

5.4.1 Latency and Rate

After presynaptic Ca^{2+} influx evokes vesicular exocytosis of glutamate into the cleft, the transmitter binds to transmembrane proteins of the PSD: ionotropic α-amino-3-hydroxy-5-methyl-4-isoxazolepropionic acid (AMPA)-type glutamate receptors (AMPARs) on the SGN bouton (Glowatzki & Fuchs, 2002). This binding induces a conformational change in the receptor that initiates the final step in the process of synaptic transmission, influx of cations, which can be measured as an event of synaptic transmission called an excitatory postsynaptic current (EPSC). When the EPSC creates an excitatory postsynaptic potential (EPSP) in the SGN bouton that is large enough to depolarize the nearby AP generator to AP threshold, then an AP is initiated in the SGN. Note the electrophysiological concept of AP threshold (e.g., mV required to generate an AP) is distinct from the concept of SGN sound response threshold (decibels of sound pressure level (dB SPL) required to evoke a criterion AP rate; see Sect. 5.5).

SGN boutons have maximum dimensions of 1 or 2 µm where they contact IHCs (Merchan-Perez & Liberman, 1996). On this contact membrane is a ring-like postsynaptic array of AMPA receptors approximately 0.8 µm in outer diameter and

0.4 μm in inner diameter, on average (Meyer et al., 2009). If this array has an AMPA receptor density of 3000 μm^{-2} (freeze-fracture electron microscopy; Saito, 1990), then one bouton has approximately 1500 AMPA receptors, on average. By comparison, pyramidal spines in the hippocampus are estimated to have, at most, 10 times fewer AMPA receptors (Nusser et al., 1998). In the SGN, the large number of AMPA receptors allows for potent glutamatergic excitation of the electrically compact bouton and its connected cable, which has a diameter of only 0.1–0.8 μm (Liberman, 1980).

The IHC–SGN synaptic delay is approximately 0.8 ms of the 1.3 ms between sound onset and spike recorded in the auditory nerve (Palmer & Russell, 1986). Presynaptic voltage-gated Ca^{2+} channels are tightly coupled to synaptic vesicles at the AZ and activate with microsecond kinetics (Sects. 5.2 and 5.3). Still, synaptic transmission—including Ca^{2+} influx and binding to the exocytosis machinery, formation of the fusion pore, diffusion and binding of glutamate, and opening of the AMPA receptors—is the slowest of the processes between sound onset (i.e., stimulation at the eardrum) and SGN spike.

In mature cochlear IHCs, in the absence of an applied sound each AZ already releases neurotransmitter onto its postsynaptic bouton in a Ca^{2+}-dependent mechanism that depends on depolarization of the hair cell resting potential by the resting mechanoelectrical transduction current through the hair bundle (Sewell, 1984; Robertson & Paki, 2002; Farris et al., 2006). This background level of transmission is evident as a sequence of EPSPs that excite the SGN to fire a spontaneous pattern of APs at irregular intervals (Walsh et al., 1972; Siegel, 1992; Glowatzki & Fuchs, 2002). These APs in the absence of sound occur at a mean rate termed the spontaneous rate (SR); their relatively irregular timing is likely due to the stochastic nature of presynaptic release (reviewed by Kim et al., 2013).

To encode sound, mechanoelectrical transduction of an auditory stimulus depolarizes the IHC from its resting potential (Russell & Sellick, 1978). The depolarization-evoked activation of synaptic Ca^{2+} channels increases the rate of release events from the presynaptic IHC, thus raising the rates of EPSCs and APs in the SGN. At SGN sound response threshold (i.e., the SPL required to produce a just detectable increase in SGN AP rate; Galambos & Davis, 1944), the IHC is depolarized by less than 1 mV from its resting potential (Dallos, 1985). SGN sound response threshold is thought to be the underlying basis of perceptual hearing threshold.

One measure of response speed is the latency of the first AP after sound onset in electrophysiological recordings of SGNs in vivo. In response to sounds of moderate intensity and rapid onset (80 dB, submillisecond rise time), the first-spike latency in many SGNs is less than 2 ms (Buran et al., 2010). Response speed depends on stimulus strength: more intense stimuli evoke faster responses. For hearing, perceptual threshold is a function of temporal integration of sound pressure over time (Heil & Irvine, 1997; Heil & Neubauer, 2003). Evidence suggests that the integration happens in the ear at the IHC–SGN synapse and that loud sounds are heard before soft sounds because with increasing sound level the EPSC rate becomes greater, making first-spike latencies briefer (Heil & Neubauer, 2001). Biophysical

modeling showed how the initial EPSC rate depends on stimulus size and number of RRP vesicles to determine the latency and jitter of the first AP (Wittig & Parsons, 2008; Buran et al., 2010). IHCs from bassoon mutant mice had a smaller RRP and fewer Ca^{2+} channels at AZs (Frank et al., 2010). Their hearing phenotype was impaired coding of sound onset with delayed and jittered first-APs (Buran et al., 2010), leading to a drastic reduction of the spiral ganglion compound action potential (Khimich et al., 2005).

Paired IHC–SGN patch-clamp recordings showed most directly how initial EPSC latency and amplitude depend on stimulus properties. Increasing the level of the IHC depolarization reduced the latency and increased the amplitude of the onset EPSC in the SGN bouton (Goutman, 2012). The amplitude increase was likely due to EPSC superposition at stimulus onset rather than a change in the individual EPSC size (Sect. 5.4.3). In addition to this speeding of transmitter release latency by stronger IHC depolarization, the increased EPSC amplitude in the SGN will further reduce first-spike latency by accelerating AP generation (Rutherford et al., 2012). Thus, at the onset of a strong stimulus, expedited IHC exocytosis and faster SGN AP generation produce shorter first-spike latencies in the auditory nerve, explaining the faster perception of sound onset with increasing sound pressure level.

Gradations of the IHC receptor potential represent changes in sound pressure level but are limited in speed by the low-pass filter property of the IHC membrane resistance (R_m) and capacitance (C_m), which define the membrane time constant $\tau = R_m C_m$. For frequencies admitted by the RC time constant of the IHC membrane (generally, below a few kilohertz) periodic stimuli evoke periodic APs in SGNs. These APs occur at preferred times within the cycle of the periodic stimulus, in a phenomenon known as phase-locking (Galambos & Davis, 1944) that underlies localization of sounds in the horizontal plane (Knudsen & Konishi, 1979). The brain calculates the angle of the horizontal vector to the source of low-frequency sound by comparing the arrival times of APs between the two ears. The accuracy and reproducibility of encoding this interaural time difference in the ear and its transmission to the brain depends on the precision of IHC–SGN transmission and AP generation.

When the level of a pure tone is increased, the preferred phase of phase-locked spikes remains relatively unchanged (Rose et al., 1967; reviewed by Fuchs, 2005). A plausible biophysical explanation is offered by the hypothesis of a Ca^{2+} nanodomain control of exocytosis (Sect. 5.3). If exocytosis is evoked by a nanometer-spaced Ca^{2+} channel, then a high-micromolar $[Ca^{2+}]$ directly around the vesicle could make Ca^{2+} binding to the sensor occur at saturated rate. In this case, the speed of exocytosis would be limited by vesicle fusion with the plasma membrane once the nearby channel has opened, no matter how many other channels opened. Stimulus intensity would then primarily affect the number of activated channels, while having relatively little effect on kinetics of exocytosis and SGN response, given an adequate RRP (Moser et al., 2006). By making interaural time difference relatively insensitive to stimulus level, the brain could be provided with binaural cues that enable calculation of sound source location regardless of intensity.

Paired recordings from IHC–SGN synapses showed how multiple presynaptic mechanisms may combine to produce consistent release latencies across stimulus

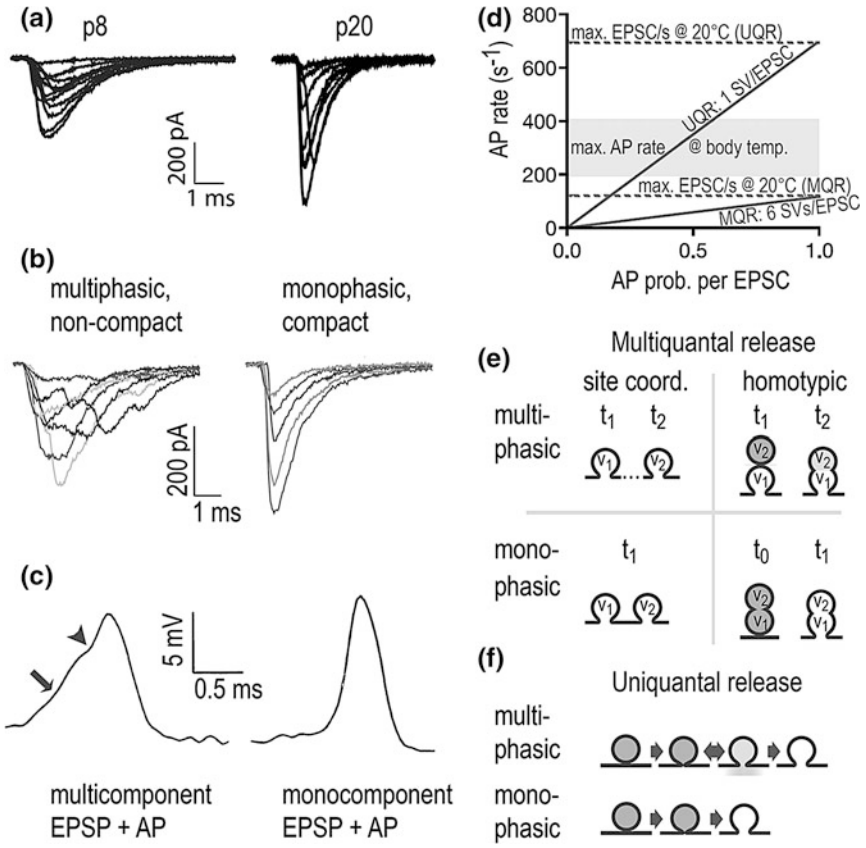

levels in response to the ongoing part of a periodic stimulus. The latency of synaptic transmission depended on the level of IHC depolarization. At the same time, it depended on stimulus history effects on presynaptic [Ca^{2+}] and the availability of release-ready vesicles (Goutman & Glowatzki, 2011 see also in the frog papilla: Cho et al., 2011; Li et al., 2014). A balance between Ca^{2+}-dependent presynaptic facilitation and vesicle supply-dependent presynaptic depression may underlie the near phase constancy of release as an ongoing periodic stimulus to the IHC is changed in intensity (Goutman, 2012).

5.4.2 Quantal Characteristics of Synaptic Transmission

It is believed that when transmission from an AZ is uniquantal, independent exocytosis of individual neurotransmitter-filled vesicles prevails. In contrast, in vivo intracellular recordings of SGN subthreshold potentials suggested that release of

◀ **Fig. 5.5** Synaptic vesicle exocytosis and postsynaptic response. **a** Between p8 and p20, monophasic EPSCs become larger and faster, as shown with patch-clamp intracellular recordings from SGN boutons. **b** Some EPSCs are temporally noncompact or multiphasic (*left*), but most are temporally compact or monophasic (*right*). **c** In vivo recordings of EPSPs demonstrate multiphasic (*left*) and monophasic (*right*) events of synaptic transmission preceding spontaneous APs. At *left*, the arrow points between two phases of the EPSP; *arrowhead* points to the onset of AP discharge. **d** *Diagonal lines* AP rate versus probability per EPSC under conditions of uniquantal release (UQR: one synaptic vesicle per EPSC) or multiquantal release (MQR: six synaptic vesicles per EPSC), assuming a maximum vesicle replenishment rate of 700 s^{-1}, as measured ex vivo at room temperature. The maximum EPSC rates for UQR (700 s^{-1}) and MQR (117 s^{-1}) are indicated by *dashed horizontal lines*. The *gray shaded area* indicates maximum sustained AP rates for SGNs in vivo at body temperature. **e** Schematic representation of two prominent hypotheses of synchronized multiquantal release: release site temporal coordination by a common Ca^{2+} nanodomain (*left*) and homotypic vesicle-to-vesicle fusion preceding compound exocytosis (*right*). Each mechanism could produce multiphasic (*upper*) or monophasic waveforms (*lower*). **f** The hypothesis of UQR with a dynamic fusion pore proposes that multiphasic (*upper*) and monophasic EPSCs (*lower*) result from flickering fusion and full fusion pore events, respectively. (**a** adapted from Grant et al. 2010. Two modes of release shape the postsynaptic response at the inner hair cell ribbon synapse. *The Journal of Neuroscience*, 30(12), 4210–4220. **b**, **d**, and **f** modified from Chapochnikov et al. 2014. Uniquantal release through a dynamic fusion pore is a candidate mechanism of hair cell exocytosis. *Neuron*, 83(6), 1389–1403. **c** adapted from Siegel 1992. Spontaneous synaptic potentials from afferent terminals in the guinea pig cochlea. *Hearing Research*, 59(1), 85–92)

multiple vesicles is synchronized even for generation of spontaneous APs (Siegel, 1992). Some EPSPs were brief while others were temporally dispersed, suggesting somewhat less synchronized release of several vesicles (Fig. 5.5c).

Pioneering intracellular patch-clamp recordings from SGN postsynaptic boutons of pre-hearing rats revealed enormous variability in EPSC amplitudes and waveforms (Glowatzki & Fuchs, 2002). Most EPSCs were waveforms that resembled alpha functions, with a fast and singular peak (i.e., monophasic) followed by a slower exponential decay. Although their peak amplitudes ranged from less than 30 pA to greater than 800 pA, monophasic EPSCs had similar kinetics. Some EPSCs had multiple peaks (multiphasic EPSCs). Monophasic EPSCs are temporally compact and multiphasic EPSCs are temporally dispersed (Fig. 5.5b). Although no precise mechanism is understood, monophasic and multiphasic EPSCs have been interpreted, respectively, as the postsynaptic responses to highly synchronized and poorly synchronized presynaptic release of multiple vesicles from a single AZ. Thus, IHC–SGN synaptic transmission seems more complex than what is expected under assumptions of uniquantal release. EPSC peak-amplitude distributions deviated from Gaussian, having high variance and positive skew, and means far greater than modes (means of 130–190 pA vs. modes of ∼36 pA). If the modal release event of approximately 30 pA represents release of one synaptic vesicle, then an EPSC of mean amplitude has a quantal content of four to six synaptic vesicles and the largest EPSCs have a content of approximately 20 vesicles (Glowatzki & Fuchs, 2002, their Fig. 4).

During maturation from p8 to p20, multiphasic EPSCs became even less frequent whereas monophasic EPSCs became larger and faster (Fig. 5.5a). The distribution of peak amplitudes became near Gaussian and the modal peak moved to approximately 375 pA as larger EPSCs became more frequent. Monophasic rise and decay times decreased from 0.6 to 0.3 ms and from 1.5 to 0.5 ms, respectively (Grant et al., 2010). The observation that the largest monophasic EPSCs can be as fast as the smallest monophasic EPSCs suggested that the range of EPSC peak amplitudes resulted from an extremely synchronized multiquantal multivesicular mechanism (Glowatzki & Fuchs, 2002, their Fig. 2; Keen & Hudspeth, 2006, their Fig. 2; Li et al., 2009, their Fig. 1).

Potential mechanisms of multiquantal release are schematized in Fig. 5.5e. One mechanism is pre-fusion of a variable number of vesicles followed by a single exocytic event (compound exocytosis; Fig. 5.5e, lower right: monophasic waveform at t_1 arising from homotypic multivesicular pre-fusion at t_0). Another possible mechanism is synchronous exocytosis of a variable number of single quanta (release-site coordination, Fig. 5.5e, lower left: monophasic event arising from simultaneous multivesicular release from multiple release sites at t_1), coordinated by, for example, a common Ca^{2+} signal (Graydon et al., 2011). Multiphasic EPSCs could represent the temporal overlap of nearly synchronous but staggered events of exocytosis, either through release site coordination or homotypic "piggy-back" fusion (Fig. 5.5e, upper left and right). These multivesicular mechanisms assume that exocytosis releases the full neurotransmitter content of each vesicle, such that transmission scales with the number of vesicles.

Assuming the mean EPSC quantal content to be 1 (i.e., uniquantal) or 6 (i.e., multiquantal) predicts quite different estimates of the numbers of vesicles required to support experimentally observed maximum sustained AP rates in SGNs in vivo, generally 200–400 s^{-1}. Given the rate of sustained IHC exocytosis from membrane capacitance measurements at room temperature, the maximal vesicle supply rate per AZ is estimated to be about 700 s^{-1} (Pangrsic et al., 2010). If each EPSC generates one AP and contains six vesicles on average, then an ongoing AP rate of 300 s^{-1} would require at least 1800 vesicles s^{-1} per AZ at body temperature. If each EPSC is univesicular, then higher AP rates are achievable with fewer vesicles (Fig. 5.5d), making release from a uniquantal vesicle seem more realistic. However, at body temperature, exocytosis from mature intact IHCs in response to sound is expected to exceed the maximal vesicle turnover rate per AZ of 700 s^{-1} estimated from patch-clamp electrophysiology at room temperature. This would increase the predicted AP rates in both the uniquantal and multiquantal scenarios.

As an alternative to multivesicular release, a uniquantal hypothesis is considered (Fig. 5.5f). Computational modeling of data on AMPA receptor number and ring-like morphology on SGN boutons suggested that EPSCs of maximum size can be evoked by the glutamate content of a single vesicle regardless of the precise location of the fusion event (Chapochnikov et al., 2014). This study suggested that short openings and flickering of the exocytic fusion pore could create multiphasic EPSCs and variably sized monophasic EPSCs from single vesicles. Additional variability between EPSCs arising from exocytosis of single vesicles could arise

from differences in vesicle volume (doubling the sphere diameter multiplies the volume by eight) or differences in neurotransmitter concentration (Wu et al., 2007). Experiments that combine electrophysiology and imaging may be required to elucidate the precise exocytosis mechanisms and, if they coexist, their relative contributions at hair cell ribbon synapses in different endorgans, species, and developmental stages.

How is AP generation in SGNs affected by EPSC variability? For the SR, the great majority of EPSPs successfully triggered an AP in vivo (~12 % failure rate, Siegel, 1992). Similarly, in the explanted organ of Corti, bouton recordings from relatively mature rats (p19) showed that the rates and interval distributions for EPSCs and APs were nearly identical (Rutherford et al., 2012). The nearly 1-to-1 conversion of EPSPs into APs for spontaneous AP rates, which are relatively low, indicated that in the absence of neural refractoriness only the smallest release events failed to trigger an AP in the SGNs tested. The situation may be different at higher rates, or in auditory endorgans of the turtle and frog, in which multiple hair cell AZs provide convergent input to each afferent neuron (Schnee et al., 2013; Li et al., 2014).

For the SR, it may seem wasteful that typical EPSCs (~300 pA) should so exceed the EPSC size required to reach AP voltage threshold. Indeed, when currents were injected into boutons through patch-pipettes, EPSC-like waveforms with amplitudes of less than 50–100 pA were already sufficient to depolarize the SGNs tested to spike threshold. However, the large EPSCs are likely required to achieve high AP rates in the presence of postsynaptic refractoriness. Further, large EPSCs improve the speed and precision of AP generation. Although small EPSCs triggered APs, increasing their size to the mean EPSC amplitude dramatically reduced latency and jitter. Spike-onset latencies improved from 1.5 to 0.5 ms when increasing the EPSC from 100 to 300 pA at room temperature (Rutherford et al., 2012).

5.4.3 *Short-Term Synaptic Depression Contributes to Spike Rate Adaptation*

The temporal pattern of sound-evoked APs depends on adaptation to stimulus history. Early experiments in the auditory nerve of cats demonstrated a progressive diminution in size of the population response during continued stimulation, which was not accompanied by any reduction in the gross cochlear potential (Derbyshire & Davis, 1935). This suggested that the IHC receptor potential was relatively nonadapting, and that sensorineural adaptation took place at the IHC–SGN synapse.

For example, fast AP rate adaption in the auditory nerve is an exponential decrement in AP rate following the initial peak at the onset of a sustained sound (Kiang, 1965). For tone bursts, this fast adaptation has two time constants of about 0.5 and 10 ms (Westerman & Smith, 1984). A similar reduction was not seen in the hair cell receptor potential or Ca^{2+} current (Russell & Sellick, 1978; Hudspeth & Lewis, 1988). Thus, fast adaptation is thought to arise from mechanisms

downstream from the Ca^{2+} current, like exhaustion of the RRP of synaptic vesicles (Furukawa & Matsura, 1978; Furukawa et al., 1982). Depletion of the RRP was indeed demonstrated by membrane capacitance measurements in hair cells and was shown to have similar kinetics as fast spike-rate adaptation in the same species (Moser & Beutner, 2000; Spassova et al., 2004; Buran et al., 2010). Figure 5.6b demonstrates the sustained IHC Ca^{2+} current for the duration of the stimulus. Exhaustion of the RRP at single AZs was observed directly with SGN recordings of EPSC trains during sustained IHC Ca^{2+} current (Fig. 5.6c, d; Goutman & Glowatzki, 2007).

Indeed, AP-rate decrement during a brief stimulus as well as AP-rate recovery between stimuli occur with time courses that mirror depletion and recovery, respectively, of the RRP. In recordings from IHC–SGN pairs in the organ of Corti explant (Fig. 5.6a), the recovery time constant of 37 ms for postsynaptic current amplitude in paired-pulse experiments ex vivo (Goutman, 2012) was similar to the time for half-recovery of the SGN AP rate in forward masking experiments in vivo (23 ms; Frank et al., 2010). Comparably fast paired-pulse recovery was measured in frog auditory hair cells at native temperature (Cho et al., 2011). Taken together, presynaptic mechanisms in the IHC seem to directly influence spike rate adaptation in SGNs.

The contributions of postsynaptic (i.e., SGN-intrinsic) mechanisms to SGN AP rate adaptation are less clear. However, fast adaptation is thought to be a mixture of both presynaptic depression and SGN refractoriness (Buran et al., 2010; Frank et al., 2010). Another form of response adaptation observed at the level of single SGNs in the auditory nerve is an adjustment of dynamic range—the range of sound pressure levels over which the SGN AP rate changes form minimum to maximum. Dynamic range adaptation depends on the mean level of sound in a continuously varying, dynamic stimulus (Wen et al., 2009). Future studies should address its underlying mechanisms.

5.4.4 Action Potential Generation

The distal-most segment of the SGN peripheral process, within the organ of Corti (i.e., within the inner spiral plexus, Fig. 5.1b), is sometimes called a dendrite. It has a compact morphology that supports potent synaptic transmission and robust AP generation. Patch-clamp recordings from SGN boutons of the rat showed high input resistance ($R_m \sim 0.5$–$3\ G\Omega$) and small input capacitance ($C_m \leq \sim 1$ pF; Glowatzki & Fuchs, 2002; Rutherford et al., 2012). A short distance away from the bouton ($\sim$20–40 µm) the SGN exits the organ of Corti, enters the spiral lamina, and gains myelin. There lies a heminode shown to contain voltage-gated Na^+ and K^+ channels ($Na_V1.6$ and $K_V1.2$; Lacas-Gervais et al., 2004; Hossain et al., 2005). The compact morphology and the voltage-gated conductances at the nearby heminode make the SGN very responsive to injected current.

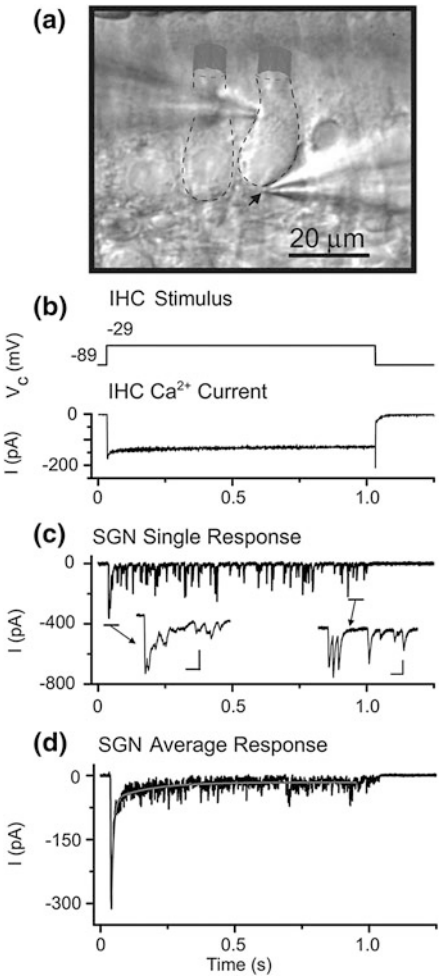

Fig. 5.6 Paired pre- and post-synaptic recordings demonstrate sustained presynaptic Ca^{2+} influx and depletion of the synaptic vesicle pool during prolonged IHC depolarization. **a** Photograph of a paired IHC–SGN electrophysiological recording in rat organ of Corti excised just before hearing onset. Two IHCs are outlined. The pipette on *left* records from an IHC while the pipette on *right* records from a SGN postsynaptic bouton (*arrow*). **b** The IHC is depolarized (*upper*) and the presynaptic voltage-gated Ca^{2+} current is activated and sustained (*lower*). **c** Example of the response recorded in the postsynaptic bouton. Each downward deflection is an individual EPSC; they superimpose somewhat at stimulus onset before the EPSC rate adapts. **d** Average of several responses from the same SGN illustrates depression of transmission due primarily to exhaustion of the presynaptic supply of releasable vesicles. (Adapted from Goutman and Glowatzki. Time course and calcium dependence of transmitter release at a single ribbon synapse. *Proceedings of the National Academy of Sciences of the USA*, 104(41), 16341–16346; Copyright (2007) National Academy of Sciences, USA)

In organ of Corti explants from mature rats (p19) SGN AP discharge was typically rapidly adapting, or phasic. When SGN boutons were depolarized with sustained current injection they fired only a single AP, at stimulus onset (Rutherford et al., 2012). Thus, high AP rates seem to require rapid repolarization of the SGN in between events of exocytosis, which may be aided by dendritic HCN channels (Yi et al., 2010). The molecular anatomy of primary afferent neurons in the inner ear is only beginning to be understood (Lysakowski et al., 2011). The phasic property is possibly due to SGN Na^+ channel inactivation (Santos-Sacchi, 1993). Curiously, the principal Na^+ channel isoform located at axon initial segments and nodes of Ranvier at neuronal synapses in the brain, $Na_V1.6$, is relatively resistant to inactivation and seems to promote repetitive firing (Raman et al., 1997). Other factors such as K^+ currents likely influence this phasic onset-response property in SGNs. This phasic property of SGN AP generation might prevent multiple APs during longer EPSCs, and thereby enhance the locking of AP times to the onsets of neurotransmitter release events (Rutherford et al., 2012).

5.5 Synaptic Heterogeneity and the Diversity of SGN Response Properties

5.5.1 Range Fractionation Through Synaptic Heterogeneity

Active amplification of cochlear vibrations at low sound levels and compression at high sound levels allows the entire 120 dB perceptual range of hearing to be encoded in the receptor potential of IHCs (Russell & Sellick, 1978). In contrast, individual SGNs have a smaller dynamic range: They change their AP rates from minimum to maximum over a more limited range of 10–40 dB of sound pressure level in cat, guinea pig, and gerbil (Sachs et al., 1989; Winter et al., 1990; Ohlemiller et al., 1991). In the mouse, most SGNs have dynamic ranges of less than 15 dB (Taberner & Liberman, 2005). Thus, the range of stimulus levels over which AP- rate changes in an individual SGN is much smaller than either the range over which loudness judgments can be made psychophysically or the range over which microphonic potentials measured at the round window increase in amplitude (Stevens & Davis, 1938/1983; Wever & Lawrence, 1954). One key hypothesis of wide dynamic range encoding is that information from one IHC receptor potential is somehow decomposed into the AP trains of multiple SGNs, each having different dynamic ranges: the hypothesis of range fractionation. A single mouse IHC has 7–20 presynaptic AZs and is innervated by 7–20 unbranched SGNs (Meyer et al., 2009), each of which encodes a fraction of the audible sound pressure range (Zagaeski et al., 1994).

To describe the diversity of response properties among single auditory nerve fibers recorded in vivo, SGNs can be categorized in terms of their SR and sensitivities to sound. These properties are interrelated and thought to arise from

underlying mechanisms that establish and maintain the firing behavior of a given SGN. In silence IHC AZs release glutamate at relatively low rates, evoking SRs that differ among SGNs from less than 1 to greater than 100 APs s^{-1}. Neurons with high SR are more sensitive to sound (i.e., lower threshold) than those with medium or low SR (Kiang, 1965; Liberman, 1978). SGNs of all characteristic frequencies exhibit this diversity. Therefore, SGNs with the same frequency tuning but different SRs and sound sensitivities are thought to emanate from neighboring if not the same IHC in the organ of Corti (Merchan-Perez & Liberman, 1996; Winter et al., 1990). The determinants of this afferent diversity are, however, unknown.

Downstream from cochlear mechanics and mechanoelectrical transduction, the specific sound-response properties of a given SGN depend on the details of the presynaptic AZ and the input–output function of the SGN itself. Thus, IHCs and SGNs may form diverse synaptic connections for SGNs to collectively encode the entire audible range. Differential sound encoding among SGNs may be regulated by afferent connections having different pre- and postsynaptic properties (Frank et al., 2009; Grant et al., 2010; Liberman et al., 2011) and by adjacent efferent synapses having different properties (Ruel et al., 2001). However, the ways in which SGNs and IHCs regulate synaptic heterogeneity are not clear.

5.5.2 *Presynaptic Heterogeneity*

The ribbon-type AZs of hair cells are large relative to AZs of conventional CNS synapses. Each IHC–SGN synapse is comprised of an AZ having several release-ready vesicles (i.e., the RRP) that can fuse with the plasma membrane in a few milliseconds after stimulation (Moser & Beutner, 2000). Neurotransmitter is released in response to graded depolarization, activating graded fractions of the population of voltage-gated Ca^{2+} channels at each AZ. The presence of numerous tethered synaptic vesicles and voltage-gated Ca^{2+} channels per IHC AZ plus evidence that relatively few of those Ca^{2+} channels regulate the exocytosis of individual vesicles (Sects. 5.3 and 5.4) contributed to the emerging view that individual IHC AZs are composed of multiple vesicular release sites (Nouvian et al., 2006).

Numerous release sites per IHC AZ is a property that seems essential for normal encoding of sound (Wittig & Parsons, 2008; Buran et al., 2010). The number of release sites likely scales with AZ size, which seems to differ among the AZs of a given IHC (Merchan-Perez & Liberman, 1996; Meyer et al., 2009). Understanding the differences in size among AZs in the IHC is a topic of current investigation. Synaptic ribbon size is a proxy for AZ size in hair cells. In the basilar papilla of the chick, the amplitude of the depolarization-evoked whole-cell Ca^{2+} current correlated positively with the whole-cell sum of ribbon cross sections (Martinez-Dunst et al., 1997). A systematic, tonotopic gradient was observed in which high-frequency basal hair cells had larger Ca^{2+} currents and larger AZ areas than hair cells in the low-frequency apex, suggesting that Ca^{2+} channel number and release site area are causally related.

In live Ca^{2+} imaging experiments, depolarization-evoked presynaptic Ca^{2+} signals around ribbons are termed Ca^{2+} microdomains (Fig. 5.7a). Ca^{2+} microdomain amplitudes are highly heterogeneous and positively correlated with the fluorescence intensity of ribbon-binding peptide (Fig. 5.7b), suggesting that larger Ca^{2+} microdomains arise from bigger AZs that contained more Ca^{2+} channels (Frank et al., 2009, 2010). The variance of Ca^{2+}-microdomain peak amplitudes in live tissue was larger than the variance of $Ca_V1.3$-immunofluorescence peak amplitudes in fixed tissue, suggesting that differences in channel regulation as well as channel number might contribute to synaptic heterogeneity among AZs. Indeed, the Ca^{2+} microdomain voltage dependence varies among the AZs within a given IHC. Ca^{2+}-microdomain variance exceeds that of the voltage dependence of whole-cell current activation between cells (Fig. 5.7c). This finding may reflect variation in composition among the supramolecular $Ca_V1.3$ channel complexes at each AZ. Each IHC decomposes auditory information into functionally diverse SGNs by divergence of its receptor potential through AZs that vary in synaptic strength.

Presynaptic Ca^{2+} influx is well known as a positive indicator of synaptic strength. In postnatal development of the mouse cochlea, IHC AZs with large-amplitude Ca^{2+} microdomains emerge around the onset of hearing, as do SGNs of high SR (Wong et al., 2013). In mature mice lacking function of bassoon protein, synaptic $Ca_V1.3$ channels are fewer in number. Ca^{2+} microdomains are smaller because there is less Ca^{2+} influx at AZs compared with wild-type (Fig. 5.7d, e; Bsn vs. WT). As a result there is less exocytosis from the IHC and abnormal encoding of sound in the auditory nerve (Khimich et al., 2005). SGNs in mice lacking bassoon have lower SRs and smaller dynamic ranges (Fig. 5.7f).

Like Ca^{2+} microdomains, presynaptic ribbons are heterogeneous in size. Larger ribbons and higher amplitude Ca^{2+} microdomains were observed more frequently on the modiolar-facing sides of IHCs (Meyer et al., 2009). If $Ca_V1.3$ expression, AZ size, and number of release sites are causally related, then modiolar-facing IHC AZs are expected to have stronger presynaptic function. However, cat SGNs with high SR and low threshold (i.e., high sensitivity to sound) were found more frequently on the pillar faces of IHCs, where ribbons are smaller (Merchan-Perez & Liberman, 1996). Thus, the relationships between AZ size, synaptic strength, and firing properties of the postsynaptic SGN are not clear. Moreover, this may constitute a conundrum. If $Ca_V1.3$ channel number scales with ribbon size and release site area, then how might larger ribbons with a larger RRP provide the synaptic input to SGNs that have lower SRs and lower sensitivities to sound?

Additional clues regarding the loci of heterogeneity contributing to SGN response diversity come from studies of facilitation, depression, and recovery in response to sounds in vivo and in response to direct IHC depolarization in organ of Corti explants. In response to pairs of clicks, the AP rates of low-SR SGNs facilitated while those of high-SR SGNs did not (Siegel & Relkin, 1987). Moreover, low-SR SGNs recovered from depression more slowly (Relkin & Doucet, 1991). Facilitation and depression are best understood as Ca^{2+}-dependent presynaptic mechanisms that depend on the probability of release and the availability of synaptic vesicles. At IHC synapses, facilitation and depression are at least partly

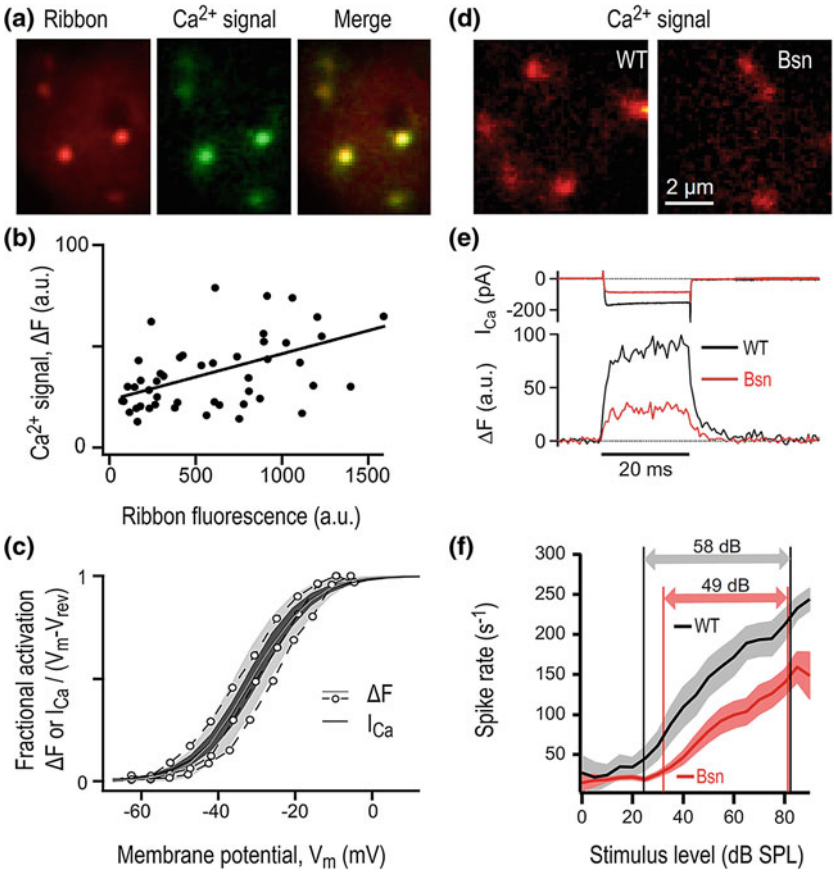

Fig. 5.7 Presynaptic Ca^{2+} influx and SGN response properties. **a** Live Ca^{2+} imaging with the indicator Fluo-5 N (*green*) and simultaneous detection of fluorescent ribbon binding peptide (*red*) demonstrates Ca^{2+} microdomains restricted to IHC AZs. **b** AZs with greater ribbon fluorescence (*x*-axis) tended to have more intense Ca^{2+} microdomain signals (*y*-axis). **c** Fractional activation of fluorescent Ca^{2+} signals by membrane potential illustrates heterogeneity in voltage dependence among AZs. *Open circles* connected by *dashed lines* show voltage activation of Ca^{2+} fluorescence for three individual AZs in one IHC. *Dark shaded area* is mean ± SD for the whole-cell Ca^{2+} current across cells; *light shaded area* is mean ± SD for synaptic Ca^{2+} microdomain fluorescence changes across AZs. **d** In bassoon-deficient IHCs (Bsn, *right*) Ca^{2+} microdomains were less intense than in wild-type (WT, *left*). **e** *Upper*, individual traces of whole-cell Ca^{2+} current in WT (*black*) and Bsn mouse IHCs (*red*). *Lower*, single AZ fluorescence changes indicate greater Ca^{2+} influx in WT. **f** AP rate versus sound pressure level for SGN recordings in vivo in WT (*black*) or Bsn (*red*). Solid lines are means across cells and shaded areas are ± SD. WT SGNs have greater SRs, steeper slopes, and larger dynamic ranges (10–90 % of maximum AP rate indicates dynamic range by *vertical lines*. (**a**–**c** adapted from Frank et al. 2009. Mechanisms contributing to synaptic Ca^{2+} signals and their heterogeneity in hair cells. *Proceedings of the National Academy of Sciences of the USA*, 106(11), 4483–4488. **d**, **e** adapted from Frank et al. 2010. Bassoon and the synaptic ribbon organize Ca^{2+} channels and vesicles to add release sites and promote refilling. *Neuron*, 68 (4), 724–738. **f** adapted from Wong et al. 2013. Concurrent maturation of inner hair cell synaptic Ca^{2+} influx and auditory nerve spontaneous activity around hearing onset in mice. *The Journal of Neuroscience*, 33(26), 10661–10666)

presynaptic and Ca^{2+} dependent (Goutman & Glowatzki, 2011; Goutman, 2012), suggesting that differences between IHC AZs contribute directly to the diversity observed in SGN firing properties.

Even without significant differences in postsynaptic efficacy of the SGNs innervating one IHC, diversity of SGN SRs might arise from heterogeneity in the presynaptic rate of release events (the EPSC rate). Curiously, when high- and low-SR synapses of the cat were compared quantitatively, the presynaptic ribbon sizes and vesicle numbers were similar (Kantardzhieva et al., 2013), suggesting that unseen presynaptic differences or postsynaptic neuron-intrinsic differences might influence SGN response diversity.

5.5.3 Postsynaptic Heterogeneity

Comparatively little is known about how rates of glutamate-evoked APs may be modulated by SGN-intrinsic mechanisms, either over time or among a population of SGNs. This section reviews observations in whole animals and in organ of Corti explants. Other SGN endogenous properties are covered in Chap. 4 by Davis and Crozier.

In some mammals, synapses of SGNs with different SRs can be distinguished by their size, morphology, and location on the IHC (Liberman, 1982). High-SR SGNs tended to innervate the pillar faces of IHCs, where synaptic ribbons were smaller (Liberman, 1980). The fibers of high-SR SGNs were also thicker, with greater mitochondrial content than fibers of low-SR SGNs. Like the larger mammals mainly used in studies of auditory nerve fiber physiology in vivo—cats, guinea pigs, gerbils, and chinchillas—mice also have SGNs with diverse firing properties (Taberner & Liberman, 2005) and AZs with heterogeneous morphologies (Meyer et al., 2009; Liberman et al., 2011). It remains to be determined if SGNs segregate around the IHC circumference according to SR and sensitivity in mice and humans, as they do in cats.

Species differences have been reported. For example in the gerbil, in contrast to the guinea pig and cat, differences between SGN terminal thicknesses were not seen around the IHC perimeter (Slepecky et al., 2000).

Among SGNs, potential mechanisms for diversity of excitability are postsynaptic heterogeneities of synaptic strength and AP generation. In this scenario, SGNs might be expected to vary markedly in the level of input required to evoke an EPSC of equivalent size or an AP of equivalent latency. The same concentration of glutamate in the cleft might produce EPSCs of different sizes in different SGNs. A variable-amplitude train of EPSCs might evoke high AP rates in one SGN but low rates in another.

On postsynaptic boutons in the mouse, immunohistochemistry with an antibody to AMPAR subunits GluA2/3 demonstrated that SGN boutons innervating the pillar faces of IHCs had larger immunoreactivity than those innervating the modiolar sides (Liberman et al., 2011), congruent with pillar SGNs corresponding to high-SR

fibers. Immunolabeled glutamate receptor clusters appear to vary significantly in overall intensity between SGN postsynaptic boutons (Meyer et al., 2009; Jing et al., 2013). However, the relationships among postsynaptic AMPAR expression, presynaptic $Ca_V1.3$ expression, and Ca^{2+}-microdomain amplitude as a function of synapse position within IHCs are not yet clear.

5.6 Summary and Conclusion

Deciphering the pre- and postsynaptic mechanisms of synaptic transmission at the hair cell ribbon synapse, the first afferent synapse in the auditory system, is essential for understanding how sound is encoded. We are only beginning to comprehend the molecular anatomy and physiology of the hair cell ribbon synapse, but it has become evident that it differs from that of a conventional CNS synapse. Synaptic specializations between a single IHC AZ and a single SGN PSD enable them to achieve unparalleled performance in terms of sustained high rates of temporally precise synaptic communication. Synaptic ribbons and associated scaffolds promote a large complement of presynaptic Ca^{2+} channels and fusion-competent vesicles that are likely to be molecularly coupled in a nanodomain signaling regime. Heterogeneity of Ca^{2+} channel number and properties among AZs seems essential for the synaptic diversity that enables decomposition of auditory information into functionally distinct SGNs. The fusion machinery still largely awaits discovery but involves unconventional and IHC-specific proteins such as the C_2 domain protein otoferlin, which is required for vesicle fusion and replenishment. The SGN efficiently turns presynaptic glutamate release into APs via sensitive glutamate detection tightly coupled with AP generation. Before attaining its mature structure and function as sound receiver in hearing animals, the hair cell synapse is active during development to provide presensory activity important for formation of the central auditory pathway.

Acknowledgments This work was supported by the Department of Otolaryngology at Washington University in St. Louis (M. A. R.) and a grant of the Deutsche Forschungsgemeinschaft to T. M. through the Collaborative Research Center 889.

References

Augustine, G. J., Adler, E. M., & Charltonc, M. P. (1991). The calcium signal for transmitter secretion from presynaptic nerve terminals. *Annals of the New York Academy of Sciences*, 635 (1), 365–381.

Baig, S. M., Koschak, A., Lieb, A., Gebhart, M., Dafinger, C., Nürnberg, G., Ali, A., Ahmad, I., Sinnegger-Brauns, M. J., & Brandt, N. (2011). Loss of CaV1. 3 (CACNA1D) function in a human channelopathy with bradycardia and congenital deafness. *Nature Neuroscience*, 14(1), 77–84.

Barnes, S., & Hille, B. (1989). Ionic channels of the inner segment of tiger salamander cone photoreceptors. *The Journal of General Physiology (JGP)*, 94(4), 719–743.

Beurg, M., Michalski, N., Safieddine, S., Bouleau, Y., Schneggenburger, R., Chapman, E. R., Petit, C., & Dulon, D. (2010). Control of exocytosis by synaptotagmins and otoferlin in auditory hair cells. *The Journal of Neuroscience*, 30(40), 13281–13290.

Beutner, D., & Moser, T. (2001). The presynaptic function of mouse cochlear inner hair cells during development of hearing. *The Journal of Neuroscience*, 21(13), 4593–4599.

Beutner, D., Voets, T., Neher, E., & Moser, T. (2001). Calcium dependence of exocytosis and endocytosis at the cochlear inner hair cell afferent synapse. *Neuron*, 29(3), 681–690.

Bohne, B. A., Kenworthy, A., & Carr, C. D. (1982). Density of myelinated nerve fibers in the chinchilla cochlea. *The Journal of the Acoustical Society of America*, 72(1), 102–107.

Brandt, A., Khimich, D., & Moser, T. (2005). Few CaV1.3 channels regulate the exocytosis of a synaptic vesicle at the hair cell ribbon synapse. *The Journal of Neuroscience*, 25(50), 11577–11585.

Brandt, A., Striessnig, J., & Moser, T. (2003). CaV1.3 channels are essential for development and presynaptic activity of cochlear inner hair cells. *The Journal of Neuroscience*, 23(34), 10832–10840.

Buran, B. N., Strenzke, N., Neef, A., Gundelfinger, E. D., Moser, T., & Liberman, M. C. (2010). Onset coding is degraded in auditory nerve fibers from mutant mice lacking synaptic ribbons. *The Journal of Neuroscience*, 30(22), 7587–7597.

Chapochnikov, N. M., Takago, H., Huang, C. H., Pangršič, T., Khimich, D., Neef, J., Auge, E., Göttfert, F., Hell, S. W., Wichmann, C., Wolf, F., & Moser, T. (2014). Uniquantal release through a dynamic fusion pore is a candidate mechanism of hair cell exocytosis. *Neuron*, 83(6), 1389–1403.

Cho, S., Li, G. L., & von Gersdorff, H. (2011). Recovery from short-term depression and facilitation is ultrafast and Ca^{2+}-dependent at auditory hair cell synapses. *The Journal of Neuroscience*, 31(15), 5682–5692.

Clause, A., Kim, G., Sonntag, M., Weisz, C. J. C., Vetter, D. E., Rűbsamen, R., & Kandler, K. (2014). The precise temporal pattern of prehearing spontaneous activity is necessary for tonotopic map refinement. *Neuron*, 82(4), 822–835.

Corey, D. P., & Hudspeth, A. J. (1979). Ionic basis of the receptor potential in a vertebrate hair cell. *Nature*, 281(5733), 675–677.

Cui, G., Meyer, A. C., Calin-Jageman, I., Neef, J., Haeseleer, F., Moser, T., & Lee, A. (2007). Ca^{2+}-binding proteins tune Ca^{2+}-feedback to CaV1.3 channels in mouse auditory hair cells. *The Journal of Physiology*, 585(3), 791–803.

Dallos, P. (1985). Response characteristics of mammalian cochlear hair cells. *The Journal of Neuroscience*, 5(6), 1591–1608.

Derbyshire, A. J., & Davis, H. (1935). The action potentials of the auditory nerve. Boston, MA: Department of Physiology, Harvard Medical School.

Dou, H., Vazquez, A. E., Namkung, Y., Chu, H., Cardell, E. L., Nie, L., Parson, S., Shin, H. S., & Yamoah, E. N. (2004). Null mutation of α1D Ca^{2+} channel gene results in deafness but no vestibular defect in mice. *Journal of the Association for Research in Otolaryngology (JARO)*, 5 (2), 215–226.

Duncker, S. V., Franz, C., Kuhn, S., Schulte, U., Campanelli, D., Brandt, N., Hirt, B., Fakler, B., Blin, N., & Ruth, P. (2013). Otoferlin couples to clathrin-mediated endocytosis in mature cochlear inner hair cells. *The Journal of Neuroscience*, 33(22), 9508–9519.

Ehret, G. (1976). Development of absolute auditory thresholds in the house mouse (*mus musculus*). *Ear and Hearing*, 1(5), 179–184.

Farris, H. E., Wells, G. B., & Ricci, A. J. (2006). Steady-state adaptation of mechanotransduction modulates the resting potential of auditory hair cells, providing an assay for endolymph [Ca^{2+}]. *The Journal of Neuroscience*, 26(48), 12526–12536.

Frank, T., Khimich, D., Neef, A., & Moser, T. (2009). Mechanisms contributing to synaptic Ca^{2+} signals and their heterogeneity in hair cells. *Proceedings of the National Academy of Sciences of the USA*, 106(11), 4483–4488.

Frank, T., Rutherford, M. A., Strenzke, N., Neef, A., Pangršič, T., Khimich, D., Fejtova, A., Gundelfinger, E. D., Liberman, M. C., Harke, B., Bryan, K. E., Lee, A., Egner, A., Riedel, D., & Moser, T. (2010). Bassoon and the synaptic ribbon organize Ca^{2+} channels and vesicles to add release sites and promote refilling. *Neuron*, 68(4), 724–738.

Fuchs, P. A. (2005). Time and intensity coding at the hair cell's ribbon synapse. *The Journal of Physiology*, 566(1), 7–12.

Fuchs, P. A., Evans, M. G., & Murrow, B. W. (1990). Calcium currents in hair cells isolated from the cochlea of the chick. *The Journal of Physiology*, 429(1), 553–568.

Furukawa, T., & Matsuura, S. (1978). Adaptive rundown of excitatory post-synaptic potentials at synapses between hair cells and eight nerve fibres in the goldfish. *The Journal of Physiology*, 276(1), 193–209.

Furukawa, T., Kuno, M., & Matsuura, S. (1982). Quantal analysis of a decremental response at hair cell-afferent fibre synapses in the goldfish sacculus. *The Journal of Physiology*, 322(1), 181–195.

Galambos, R., & Davis, H. (1944). *The response of single auditory-nerve fibers to acoustic stimulation*. Boston, MA: Department of Physiology, Harvard Medical School.

Gebhart, M., Juhasz-Vedres, G., Zuccotti, A., Brandt, N., Engel, J., Trockenbacher, A., Kaur, G., Obermair, G. J., Knipper, M., Koschak, A., & Striessnig, J. (2010). Modulation of cav1.3 ca2+ channel gating by rab3 interacting molecule. *Molecular and Cellular Neuroscience*, 44(3), 246–259.

Géléoc, G. S., & Holt, J. R. (2003). Auditory amplification: Outer hair cells *pres* the issue. *Trends in Neurosciences*, 26(3), 115–117.

Glowatzki, E., & Fuchs, P. A. (2000). Cholinergic synaptic inhibition of inner hair cells in the neonatal mammalian cochlea. *Science*, 288(5475), 2366–2368.

Glowatzki, E., & Fuchs, P. A. (2002). Transmitter release at the hair cell ribbon synapse. *Nature Neuroscience*, 5(2), 147–154.

Goutman, J. D. (2012). Transmitter release from cochlear hair cells is phase locked to cyclic stimuli of different intensities and frequencies. *The Journal of Neuroscience*, 32(47), 17025–17036.

Goutman, J. D., & Glowatzki, E. (2007). Time course and calcium dependence of transmitter release at a single ribbon synapse. *Proceedings of the National Academy of Sciences of the USA*, 104(41), 16341–16346.

Goutman, J. D., & Glowatzki, E. (2011). Short-term facilitation modulates size and timing of the synaptic response at the inner hair cell ribbon synapse. *The Journal of Neuroscience*, 31(22), 7974–7981.

Grant, L., & Fuchs, P. (2008). Calcium-and calmodulin-dependent inactivation of calcium channels in inner hair cells of the rat cochlea. *The Journal of Neurophysiology*, 99(5), 2183–2193.

Grant, L., Yi, E., & Glowatzki, E. (2010). Two modes of release shape the postsynaptic response at the inner hair cell ribbon synapse. *The Journal of Neuroscience*, 30(12), 4210–4220.

Graydon, C. W., Cho, S., Li, G. L., Kachar, B., & von Gersdorff, H. (2011). Sharp Ca^{2+} nanodomains beneath the ribbon promote highly synchronous multivesicular release at hair cell synapses. *The Journal of Neuroscience*, 31(46), 16637–16650.

Gregory, F. D., Bryan, K. E., Pangršič, T., Calin-Jageman, I. E., Moser, T., & Lee, A. (2011). Harmonin inhibits presynaptic CaV1.3 Ca^{2+} channels in mouse inner hair cells. *Nature Neuroscience*, 14(9), 1109–1111.

Heidelberger, R., & Matthews, G. (1992). Calcium influx and calcium current in single synaptic terminals of goldfish retinal bipolar neurons. *The Journal of Physiology*, 447(1), 235–256.

Heil, P., & Irvine, D. R. (1997). First-spike timing of auditory-nerve fibers and comparison with auditory cortex. *Journal of Neurophysiology*, 78(5), 2438–2454.

Heil, P., & Neubauer, H. (2001). Temporal integration of sound pressure determines thresholds of auditory-nerve fibers. *The Journal of Neuroscience*, 21(18), 7404–7415.

Heil, P., & Neubauer, H. (2003). A unifying basis of auditory thresholds based on temporal summation. *Proceedings of the National Academy of Sciences of the USA*, 100(10), 6151–6156.

Heil, P., & Neubauer, H. (2010). Summing across different active zones can explain the quasi-linear Ca^{2+}-dependencies of exocytosis by receptor cells. *Frontiers in Synaptic Neuroscience*, 2.

Hibino, H., Pironkova, R., Onwumere, O., Vologodskaia, M., Hudspeth, A. J., & Lesage, F. (2002). Rim binding proteins (RBPs) couple rab3-interacting molecules (RIMs) to voltage-gated Ca^{2+} channels. *Neuron*, 34(3), 411–423.

Hossain, W. A., Antic, S. D., Yang, Y., Rasband, M. N., & Morest, D. K. (2005). Where is the spike generator of the cochlear nerve? Voltage-gated sodium channels in the mouse cochlea. *The Journal of Neuroscience*, 25(29), 6857–6868.

Huang, L. C., Thorne, P. R., Housley, G. D., & Montgomery, J. M. (2007). Spatiotemporal definition of neurite outgrowth, refinement and retraction in the developing mouse cochlea. *Development*, 134(16), 2925–2933.

Huang, L. C., Barclay, M., Lee, K., Peter, S., Housley, G. D., Thorne, P. R., Montgomery, J. M., & others (2012). Synaptic profiles during neurite extension, refinement and retraction in the developing cochlea. *Neural Development*, 7 1–17.

Hudspeth, A. J., & Lewis, R. S. (1988). Kinetic analysis of voltage-and ion-dependent conductances in saccular hair cells of the bull-frog, *rana catesbeiana*. *The Journal of Physiology*, 400(1), 237–274.

Issa, N. P., & Hudspeth, A. J. (1996). The entry and clearance of Ca^{2+} at individual presynaptic active zones of hair cells from the bullfrog's sacculus. *Proceedings of the National Academy of Sciences of the USA*, 93(18), 9527–9532.

Jing, Z., Rutherford, M. A., Takago, H., Frank, T., Fejtova, A., Khimich, D., Moser, T., & Strenzke, N. (2013). Disruption of the presynaptic cytomatrix protein bassoon degrades ribbon anchorage, multiquantal release, and sound encoding at the hair cell afferent synapse. *The Journal of Neuroscience*, 33(10), 4456–4467.

Johnson, S. L., Marcotti, W., & Kros, C. J. (2005). Increase in efficiency and reduction in Ca^{2+} dependence of exocytosis during development of mouse inner hair cells. *The Journal of Physiology*, 563(1), 177–191.

Johnson, S. L., Forge, A., Knipper, M., Munkner, S., & Marcotti, W. (2008). Tonotopic variation in the calcium dependence of neurotransmitter release and vesicle pool replenishment at mammalian auditory ribbon synapses. *The Journal of Neuroscience*, 28(30), 7670–7678.

Johnson, S. L., Franz, C., Kuhn, S., Furness, D. N., Rüttiger, L., Münkner, S., Rivolta, M. N., Seward, E. P., Herschman, H. R., & Engel, J. (2010). Synaptotagmin IV determines the linear Ca^{2+} dependence of vesicle fusion at auditory ribbon synapses. *Nature Neuroscience*, 13(1), 45–52.

Johnson, S. L., Eckrich, T., Kuhn, S., Zampini, V., Franz, C., Ranatunga, K. M., Roberts, T. P., Masetto, S., Knipper, M., Kros, C. J., & Marcotti, W. (2011). Position-dependent patterning of spontaneous action potentials in immature cochlear inner hair cells. *Nature Neuroscience*, 14 (6), 711–717.

Kaeser, P. S., Deng, L., Wang, Y., Dulubova, I., Liu, X., Rizo, J., & Südhof, T. C. (2011). RIM proteins tether Ca^{2+} channels to presynaptic active zones via a direct PDZ-domain interaction. *Cell*, 144(2), 282–295.

Kantardzhieva, A., Peppi, M., Lane, W. S., & Sewell, W. F. (2012). Protein composition of immunoprecipitated synaptic ribbons. *Journal of Proteome Research*, 11(2), 1163–1174.

Kantardzhieva, A., Liberman, M. C., & Sewell, W. F. (2013). Quantitative analysis of ribbons, vesicles, and cisterns at the cat inner hair cell synapse: Correlations with spontaneous rate: hair cell synaptic ribbons. *Journal of Comparative Neurology*, 521(14), 3260–3271.

Keen, E. C., & Hudspeth, A. J. (2006). Transfer characteristics of the hair cell's afferent synapse. *Proceedings of the National Academy of Sciences of the USA*, 103(14), 5537–5542.

Khimich, D., Nouvian, R., Pujol, R., tom Dieck, S., Egner, A., Gundelfinger, E. D., and Moser, T. (2005). Hair cell synaptic ribbons are essential for synchronous auditory signalling. *Nature*, 434, 889–894.

Kiang, N. Y. S. (1965). *Discharge patterns of single fibers in the cat's auditory nerve*. Cambridge, MA: MIT Press.

Kim, M. H., Li, G. L., & von Gersdorff, H. (2013). Single Ca^{2+} channels and exocytosis at sensory synapses. *The Journal of Physiology*, 591(13), 3167–3178.

Knudsen, E. I., & Konishi, M. (1979). Mechanisms of sound localization in the barn owl (*tyto alba*). *Journal of Comparative Physiology*, 133(1), 13–21.

Koschak, A., Reimer, D., Huber, I., Grabner, M., Glossmann, H., Engel, J., & Striessnig, J. (2001). Alpha 1D (CaV1. 3) subunits can form L-type Ca^{2+} channels activating at negative voltages. *The Journal of Biological Chemistry (jbc)*, 276(25), 22100–22106.

Kros, C. J., Ruppersberg, J. P., & Rüsch, A. (1998). Expression of a potassium current in inner hair cells during development of hearing in mice. *Nature*, 394(6690), 281–284.

Kubisch, C., Schroeder, B. C., Friedrich, T., Lütjohann, B., El-Amraoui, A., Marlin, S., Petit, C., & Jentsch, T. J. (1999). KCNQ4, a novel potassium channel expressed in sensory outer hair cells, is mutated in dominant deafness. *Cell*, 96(3), 437–446.

Lacas-Gervais, S., Guo, J., Strenzke, N., Scarfone, E., Kolpe, M., Jahkel, M., De Camilli, P., Moser, T., Rasband, M. N., Solimena, M. (2004). βIVΣ1 spectrin stabilizes the nodes of Ranvier and axon initial segments. *The Journal of Cell Biology (JCB)*, 166(7), 983–990.

Lee, A., Scheuer, T., & Catterall, W. A. (2000). Ca^{2+}/calmodulin-dependent facilitation and inactivation of P/Q-type Ca^{2+} channels. *The Journal of Neuroscience*, 20(18), 6830–6838.

Lenoir, M., Shnerson, A., & Pujol, R. (1980). Cochlear receptor development in the rat with emphasis on synaptogenesis. *Anatomy and Embryology*, 160(3), 253–262.

Lenzi, D., & von Gersdorff, H. (2001). Structure suggests function: The case for synaptic ribbons as exocytotic nanomachines. *Bioessays*, 23(9), 831–840.

Lenzi, D., Crum, J., Ellisman, M. H., & Roberts, W. M. (2002). Depolarization redistributes synaptic membrane and creates a gradient of vesicles on the synaptic body at a ribbon synapse. *Neuron*, 36(4), 649–659.

Li, G. L., Keen, E., Andor-Ardo, D., Hudspeth, A. J., & von Gersdorff, H. (2009). The unitary event underlying multiquantal EPSCs at a hair cell's ribbon synapse. *The Journal of Neuroscience*, 29(23), 7558–7568.

Li, G. L., Cho, S., & von Gersdorff, H. (2014). Phase-locking precision is enhanced by multiquantal release at an auditory hair cell ribbon synapse. *Neuron*, 83(6), 1404–1417.

Liberman, M. C. (1978). Auditory-nerve response from cats raised in a low-noise chamber. *The Journal of the Acoustical Society of America*, 63(2), 442–455.

Liberman, M. C. (1980). Morphological differences among radial afferent fibers in the cat cochlea: An electron-microscopic study of serial sections. *Hearing Research*, 3(1), 45–63.

Liberman, M. C. (1982). Single-neuron labeling in the cat auditory nerve. *Science*, 216(4551), 1239–1241.

Liberman, L. D., Wang, H., & Liberman, M. C. (2011). Opposing gradients of ribbon size and AMPA receptor expression underlie sensitivity differences among cochlear-nerve/hair-cell synapses. *The Journal of Neuroscience*, 31(3), 801–808.

Lysakowski, A., Gaboyard-Niay, S., Calin-Jageman, I., Chatlani, S., Price, S. D., & Eatock, R. A. (2011). Molecular microdomains in a sensory terminal, the vestibular calyx ending. *The Journal of Neuroscience*, 31(27), 10101–10114.

Magupalli, V. G., Schwarz, K., Alpadi, K., Natarajan, S., Seigel, G. M., & Schmitz, F. (2008). Multiple ribeye-ribeye interactions create a dynamic scaffold for the formation of synaptic ribbons. *The Journal of Neuroscience*, 28(32), 7954–7967.

Marcotti, W., Johnson, S. L., Rusch, A., & Kros, C. J. (2003). Sodium and calcium currents shape action potentials in immature mouse inner hair cells. *The Journal of Physiology*, 552(3), 743–761.

Martinez-Dunst, C., Michaels, R. L., & Fuchs, P. A. (1997). Release sites and calcium channels in hair cells of the chick's cochlea. *The Journal of Neuroscience*, 17(23), 9133–9144.

Matthews, G., & Fuchs, P. (2010). The diverse roles of ribbon synapses in sensory neurotransmission. *Nature Reviews Neuroscience*, 11(12), 812–822.

Matveev, V., Bertram, R., & Sherman, A. (2011). Calcium cooperativity of exocytosis as a measure of Ca^{2+} channel domain overlap. *Brain Research*, 1398 126–138.

Meddis, R. (2006). Auditory-nerve first-spike latency and auditory absolute threshold: A computer model. *The Journal of the Acoustical Society of America*, 119(1), 406–417.

Merchan-Perez, A., & Liberman, M. C. (1996). Ultrastructural differences among afferent synapses on cochlear hair cells: Correlations with spontaneous discharge rate. *Journal of Comparative Neurology*, 371(2), 208–221.

Meyer, A. C., Frank, T., Khimich, D., Hoch, G., Riedel, D., Chapochnikov, N. M., Yarin, Y. M., Harke, B., Hell, S. W., Egner, A., & Moser, T. (2009). Tuning of synapse number, structure and function in the cochlea. *Nature Neuroscience*, 12(4), 444–453.

Moser, T., & Beutner, D. (2000). Kinetics of exocytosis and endocytosis at the cochlear inner hair cell afferent synapse of the mouse. *Proceedings of the National Academy of Sciences of the USA*, 97(2), 883–888.

Moser, T., Neef, A., & Khimich, D. (2006). Mechanisms underlying the temporal precision of sound coding at the inner hair cell ribbon synapse. *The Journal of Physiology*, 576(1), 55–62.

Neef, J., Gehrt, A., Bulankina, A. V., Meyer, A. C., Riedel, D., Gregg, R. G., Strenzke, N., & Moser, T. (2009). The Ca^{2+} channel subunit β2 regulates Ca^{2+} channel abundance and function in inner hair cells and is required for hearing. *The Journal of Neuroscience*, 29(34), 10730–10740.

Neef, J., Jung, S., Wong, A. B., Reuter, K., Pangrsic, T., Chakrabarti, R., Kugler, S., Lenz, C., Nouvian, R., Boumil, R. M., Frankel, W. N., Wichmann, C., & Moser, T. (2014). Modes and regulation of endocytic membrane retrieval in mouse auditory hair cells. *The Journal of Neuroscience*, 34(3), 705–716.

Nouvian, R., Beutner, D., Parsons, T. D., & Moser, T. (2006). Structure and function of the hair cell ribbon synapse. *Journal of Membrane Biology*, 209(2–3), 153–165.

Nouvian, R., Neef, J., Bulankina, A. V., Reisinger, E., Pangršič, T., Frank, T., Sikorra, S., Brose, N., Binz, T., & Moser, T. (2011). Exocytosis at the hair cell ribbon synapse apparently operates without neuronal snare proteins. *Nature Neuroscience*, 14(4), 411–413.

Nusser, Z., Lujan, R., Laube, G., Roberts, J. D. B., Molnar, E., & Somogyi, P. (1998). Cell type and pathway dependence of synaptic AMPA receptor number and variability in the hippocampus. *Neuron*, *21*(3), 545–559.

Ohlemiller, K. K., Echteler, S. M., & Siegel, J. H. (1991). Factors that influence rate-versus-intensity relations in single cochlear nerve fibers of the gerbil. *The Journal of the Acoustical Society of America*, 90(1), 274–287.

Oliver, D., Knipper, M., Derst, C., & Fakler, B. (2003). Resting potential and submembrane calcium concentration of inner hair cells in the isolated mouse cochlea are set by KCNQ-type potassium channels. *The Journal of Neuroscience*, 23(6), 2141–2149.

Oliver, D., Taberner, A. M., Thurm, H., Sausbier, M., Arntz, C., Ruth, P., Fakler, B., & Liberman, M. C. (2006). The role of BK_{Ca} channels in electrical signal encoding in the mammalian auditory periphery. *The Journal of Neuroscience*, 26(23), 6181–6189.

Palmer, A. R., & Russell, I. J. (1986). Phase-locking in the cochlear nerve of the guinea-pig and its relation to the receptor potential of inner hair cells. *Hearing Research*, 24(1), 1–15.

Pangršič, T., Lasarow, L., Reuter, K., Takago, H., Schwander, M., Riedel, D., Frank, T., Tarantino, L. M., Bailey, J. S., Strenzke, N., Brose, N., Müller, U., Reisinger, E., & Moser, T. (2010). Hearing requires otoferlin-dependent efficient replenishment of synaptic vesicles in hair cells. *Nature Neuroscience*, 13(7), 869–876.

Parsons, T. D., Lenzi, D., Almers, W., & Roberts, W. M. (1994). Calcium-triggered exocytosis and endocytosis in an isolated presynaptic cell: Capacitance measurements in saccular hair cells. *Neuron*, 13(4), 875–883.

Platzer, J., Engel, J., Schrott-Fischer, A., Stephan, K., Bova, S., Chen, H., Zheng, H., & Striessnig, J. (2000). Congenital deafness and sinoatrial node dysfunction in mice lacking class D L-type Ca^{2+} channels. *Cell*, 102(1), 89–97.

Ramakrishnan, N. A., Drescher, M. J., & Drescher, D. G. (2009). Direct interaction of otoferlin with syntaxin 1a, SNAP-25, and the L-type voltage-gated calcium channel CaV1.3. *The Journal of Biological Chemistry (jbc)*, 284(3), 1364–1372.

Raman, I. M., Sprunger, L. K., Meisler, M. H., & Bean, B. P. (1997). Altered subthreshold sodium currents and disrupted firing patterns in purkinje neurons of *SCN8A* mutant mice. *Neuron*, 19 (4), 881–891.

Reisinger, E., Bresee, C., Neef, J., Nair, R., Reuter, K., Bulankina, A., Nouvian, R., Koch, M., Buckers, J., Kastrup, L., Roux, I., Petit, C., Hell, S. W., Brose, N., Rhee, J. S., Kugler, S., Brigande, J. V., & Moser, T. (2011). Probing the functional equivalence of otoferlin and synaptotagmin 1 in exocytosis. *The Journal of Neuroscience*, 31(13), 4886–4895.

Relkin, E. M., & Doucet, J. R. (1991). Recovery from prior stimulation. I: Relationship to spontaneous firing rates of primary auditory neurons. *Hearing Research*, 55(2), 215–222.

Roberts, W. M. (1993). Spatial calcium buffering in saccular hair cells. *Nature*, 363, 74–76.

Roberts, W. M., Jacobs, R. A., & Hudspeth, A. J. (1990). Colocalization of ion channels involved in frequency selectivity and synaptic transmission at presynaptic active zones of hair cells. *The Journal of Neuroscience*, 10(11), 3664–3684.

Robertson, D., & Paki, B. (2002). Role of L-type Ca^{2+} channels in transmitter release from mammalian inner hair cells. II. Single-neuron activity. *Journal of Neurophysiology*, 87(6), 2734–2740.

Rodriguez-Contreras, A., & Yamoah, E. N. (2001). Direct measurement of single-channel Ca^{2+} currents in bullfrog hair cells reveals two distinct channel subtypes. *The Journal of Physiology*, 534(3), 669–689.

Rose, J. E., Brugge, J. F., Anderson, D. J., Hind, J. E., & others (1967). Phase-locked response to low-frequency tones in single auditory nerve fibers of the squirrel monkey. *Journal of Neurophysiology*, 30(4), 769–793.

Roux, I., Safieddine, S., Nouvian, R., Simmler, M. C., Bahloul, A., Perfettini, I., Le Gall, M., Rostaing, P., Hamard, G., & Triller, A. (2006). Otoferlin, defective in a human deafness form, is essential for exocytosis at the auditory ribbon synapse. *Cell*, 127(2), 277–289.

Ruel, J., Nouvian, R., d' Aldin, C. G., Pujol, R., Eybalin, M., & Puel, J. L. (2001). Dopamine inhibition of auditory nerve activity in the adult mammalian cochlea. *European Journal of Neuroscience*, 14(6), 977–986.

Ruel, J., Emery, S., Nouvian, R., Bersot, T., Amilhon, B., Van Rybroek, J. M., Rebillard, G., Lenoir, M., Eybalin, M., Delprat, B., Sivakumaran, T. A., Giros, B., El Mestikawy, S., Moser, T., Smith, R. J. H., Lesperance, M. M., & Puel, J. L. (2008). Impairment of SLC17A8 encoding vesicular glutamate transporter-3, VGLUT3, underlies nonsyndromic deafness DFNA25 and inner hair cell dysfunction in null mice. *The American Journal of Human Genetics*, 83(2), 278–292.

Rüsch, A., Ng, L., Goodyear, R., Oliver, D., Lisoukov, I., Vennström, B., Richardson, G., Kelley, M. W., & Forrest, D. (2001). Retardation of cochlear maturation and impaired hair cell function caused by deletion of all known thyroid hormone receptors. *The Journal of Neuroscience*, 21(24), 9792–9800.

Russell, I. J., & Sellick, P. M. (1978). Intracellular studies of hair cells in the mammalian cochlea. *The Journal of Physiology*, 284(1), 261–290.

Rutherford, M. A., & Pangršič, T. (2012). Molecular anatomy and physiology of exocytosis in sensory hair cells. *Cell Calcium*, 52(3), 327–337.

Rutherford, M. A., Chapochnikov, N. M., & Moser, T. (2012). Spike encoding of neurotransmitter release timing by spiral ganglion neurons of the cochlea. *The Journal of Neuroscience*, 32(14), 4773–4789.

Rutherford, M. A. (2015). Resolving the structure of inner ear ribbon synapses with STED microscopy. *Synapse*, 69(5), 242-255.

Sachs, M. B., Winslow, R. L., & Sokolowski, B. H. (1989). A computational model for rate-level functions from cat auditory-nerve fibers. *Hearing Research*, 41(1), 61–69.

Safieddine, S., & Wenthold, R. J. (1999). SNARE complex at the ribbon synapses of cochlear hair cells: Analysis of synaptic vesicle-and synaptic membrane-associated proteins. *European Journal of Neuroscience*, 11(3), 803–812.

Saito, K. (1990). Freeze-fracture organization of hair cell synapses in the sensory epithelium of guinea pig organ of corti. *Journal of Electron Microscopy Technique*, 15(2), 173–186.

Santos-Sacchi, J. (1993). Voltage-dependent ionic conductances of type I spiral ganglion cells from the guinea pig inner ear. *The Journal of Neuroscience*, 13(8), 3599–3611.

Schmitz, F., Königstorfer, A., & Südhof, T. C. (2000). RIBEYE, a component of synaptic ribbons: A protein's journey through evolution provides insight into synaptic ribbon function. *Neuron*, 28(3), 857–872.

Schnee, M. E., Lawton, D. M., Furness, D. N., Benke, T. A., & Ricci, A. J. (2005). Auditory hair cell-afferent fiber synapses are specialized to operate at their best frequencies. *Neuron*, 47(2), 243–254.

Schnee, M. E., Castellano-Muñoz, M., & Ricci, A. J. (2013). Response properties from turtle auditory hair cell afferent fibers suggest spike generation is driven by synchronized release both between and within synapses. *Journal of Neurophysiology*, 110(1), 204–220.

Schrauwen, I., Helfmann, S., Inagaki, A., Predoehl, F., Tabatabaiefar, M. A., Picher, M. M., Sommen, M., Seco, C. Z., Oostrik, J., Kremer, H., Dheedene, A., Claes, C., Fransen, E., Chaleshtori, M. H., Coucke, P., Lee, A., Moser, T., & Van Camp, G. (2012). A mutation in CaBP2, expressed in cochlear hair cells, causes autosomal-recessive hearing impairment. *The American Journal of Human Genetics*, 91(4), 636–645.

Schwarz, K., Natarajan, S., Kassas, N., Vitale, N., & Schmitz, F. (2011). The synaptic ribbon is a site of phosphatidic acid generation in ribbon synapses. *The Journal of Neuroscience*, 31(44), 15996–16011.

Sendin, G., Bulankina, A. V., Riedel, D., & Moser, T. (2007). Maturation of ribbon synapses in hair cells is driven by thyroid hormone. *The Journal of Neuroscience*, 27(12), 3163–3173.

Sendin, G., Bourien, J., Rassendren, F., Puel, J. L., & Nouvian, R. (2014). Spatiotemporal pattern of action potential firing in developing inner hair cells of the mouse cochlea. *Proceedings of the National Academy of Sciences of the USA*, 111(5), 1999–2004.

Sewell, W. F. (1984). The relation between the endocochlear potential and spontaneous activity in auditory nerve fibres of the cat. *The Journal of Physiology*, 347(1), 685–696.

Sheets, L., Trapani, J. G., Mo, W., Obholzer, N., & Nicolson, T. (2011). Ribeye is required for presynaptic CaV1.3 channel localization and afferent innervation of sensory hair cells. *Development*, 138(7), 1309–1319.

Shnerson, A., Devigne, C., & Pujol, R. (1981). Age-related changes in the C57Bl/6j mouse cochlea. II. ultrastructural findings. *Developmental Brain Research*, 2(1), 77–88.

Siegel, J. H. (1992). Spontaneous synaptic potentials from afferent terminals in the guinea pig cochlea. *Hearing Research*, 59(1), 85–92.

Siegel, J. H., & Relkin, E. M. (1987). Antagonistic effects of perilymphatic calcium and magnesium on the activity of single cochlear afferent neurons. *Hearing Research*, 28(2), 131–147.

Slepecky, N. B., Galsky, M. D., Swartzentruber-Martin, H., & Savage, J. (2000). Study of afferent nerve terminals and fibers in the gerbil cochlea: Distribution by size. *Hearing Research*, 144 (1), 124–134.

Smith, C. A., & Sjöstrand, F. S. (1961). Structure of the nerve endings on the external hair cells of the guinea pig cochlea as studied by serial sections. *Journal of Ultrastructure Research*, 5(6), 523–556.

Sobkowicz, H. M., Rose, J. E., Scott, G. E., & Slapnick, S. M. (1982). Ribbon synapses in the developing intact and cultured organ of corti in the mouse. *The Journal of Neuroscience*, 2(7), 942–957.

Spassova, M., Eisen, M. D., Saunders, J. C., & Parsons, T. D. (2001). Chick cochlear hair cell exocytosis mediated by dihydropyridine-sensitive calcium channels. *The Journal of Physiology*, 535(3), 689–696.

Spassova, M. A., Avissar, M., Furman, A. C., Crumling, M. A., Saunders, J. C., & Parsons, T. D. (2004). Evidence that rapid vesicle replenishment of the synaptic ribbon mediates recovery from short-term adaptation at the hair cell afferent synapse. *Journal of the Association for Research in Otolaryngology*, 5(4), 376–390.

Spoendlin, H. (1972). Innervation densities of the cochlea. *Acta Oto-Laryngologica*, 73(2),–(6), 235–248.

Stevens, S. S., & Davis, H. (1938/1983). *Hearing: Its psychology and physiology.* American Institute of Physics for the Acoustical Society of America.

Strenzke, N., Chanda, S., Kopp-Scheinpflug, C., Khimich, D., Reim, K., Bulankina, A. V., Neef, A., Wolf, F., Brose, N., Xu-Friedman, M. A., & Moser, T. (2009). Complexin-I is required for high-fidelity transmission at the endbulb of held auditory synapse. *The Journal of Neuroscience*, 29(25), 7991–8004.

Taberner, A. M. & Liberman, M. C. (2005). Response properties of single auditory nerve fibers in the mouse. *Journal of Neurophysiology*, 93(1), 557–569.

Tachibana, M., Okada, T., Arimura, T., Kobayashi, K., & Piccolino, M. (1993). Dihydropyridine-sensitive calcium current mediates neurotransmitter release from bipolar cells of the goldfish retina. *The Journal of Neuroscience*, 13(7), 2898–2909.

Tritsch, N. X., & Bergles, D. E. (2010). Developmental regulation of spontaneous activity in the mammalian cochlea. *The Journal of Neuroscience*, 30(4), 1539–1550.

Tritsch, N. X., Yi, E., Gale, J. E., Glowatzki, E., & Bergles, D. E. (2007). The origin of spontaneous activity in the developing auditory system. *Nature*, 450(7166), 50–55.

Tucker, T., & Fettiplace, R. (1995). Confocal imaging of calcium microdomains and calcium extrusion in turtle hair cells. *Neuron*, 15(6), 1323–1335.

Uthaiah, R. C., & Hudspeth, A. J. (2010). Molecular anatomy of the hair cell's ribbon synapse. *The Journal of Neuroscience*, 30(37), 12387–12399.

Verpy, E., Leibovici, M., Zwaenepoel, I., Liu, X. Z., Gal, A., Salem, N., Mansour, A., Blanchard, S., Kobayashi, I., & Keats, B. J. (2000). A defect in harmonin, a PDZ domain-containing protein expressed in the inner ear sensory hair cells, underlies Usher syndrome type 1C. *Nature Genetics*, 26(1), 51–55.

Vincent, P. F. Y., Bouleau, Y., Safieddine, S., Petit, C., & Dulon, D. (2014). Exocytotic machineries of vestibular type I and cochlear ribbon synapses display similar intrinsic otoferlin-dependent Ca^{2+} sensitivity but a different coupling to Ca^{2+} channels. *The Journal of Neuroscience*, 34(33), 10853–10869.

Waites, C. L., Leal-Ortiz, S. A., Okerlund, N., Dalke, H., Fejtova, A., Altrock, W. D., Gundelfinger, E. D., & Garner, C. C. (2013). Bassoon and piccolo maintain synapse integrity by regulating protein ubiquitination and degradation. *The EMBO Journal*, 32(7), 954–969.

Walsh, E. J., & McGee, J. (1987). Postnatal development of auditory nerve and cochlear nucleus neuronal responses in kittens. *Hearing Research*, 28(1), 97–116.

Walsh, E. J., & Romand, R. (1992). Functional development of the cochlea and the cochlear nerve. *Development of Auditory and Vestibular Systems*, 2 161–219.

Walsh, B. T., Miller, J. B., Gacek, R., & Kiang, N. Y. S. (1972). Spontaneous activity in the eighth cranial nerve of the cat. *International Journal of Neuroscience*, 3(5), 221–235.

Weiss, T. F. (1966). A model of the peripheral auditory system. *Kybernetik*, 3(4), 153–175.

Wen, B., Wang, G. I., Dean, I., & Delgutte, B. (2009). Dynamic range adaptation to sound level statistics in the auditory nerve. *The Journal of Neuroscience*, 29(44), 13797–13808.

Westerman, L. A., & Smith, R. L. (1984). Rapid and short-term adaptation in auditory nerve responses. *Hearing Research*, 15(3), 249–260.

Wever, E. G., & Lawrence, M. (1954). *Physiological acoustics*. Princeton, NJ: Princeton University Press.

Winter, I. M., Robertson, D., & Yates, G. K. (1990). Diversity of characteristic frequency rate-intensity functions in guinea pig auditory nerve fibres. *Hearing Research*, 45(3), 191–202.

Wittig, J. H., & Parsons, T. D. (2008). Synaptic ribbon enables temporal precision of hair cell afferent synapse by increasing the number of readily releasable vesicles: A modeling study. *The Journal of Neurophysiology*, 100(4), 1724–1739.

Wong, A. B., Jing, Z., Rutherford, M. A., Frank, T., Strenzke, N., & Moser, T. (2013). Concurrent maturation of inner hair cell synaptic Ca^{2+} influx and auditory nerve spontaneous activity around hearing onset in mice. *The Journal of Neuroscience*, 33(26), 10661–10666.

Wong, A. B., Rutherford, M. A., Gabrielaitis, M., Pangršič, T., Göttfert, F., Frank, T., Michanski, S., Hell, S., Wolf, F., Wichmann, C., & Moser, T. (2014). Developmental refinement of hair cell synapses tightens the coupling of Ca $^{2+}$ influx to exocytosis. *The EMBO Journal*, 33(3), 247–264.

Wu, X. S., Xue, L., Mohan, R., Paradiso, K., Gillis, K. D., & Wu, L. G. (2007). The origin of quantal size variation: Vesicular glutamate concentration plays a significant role. *Journal of Neuroscience*, 27(11), 3046–3056.

Yang, P. S., Alseikhan, B. A., Hiel, H., Grant, L., Mori, M. X., Yang, W., Fuchs, P. A., & Yue, D. T. (2006). Switching of Ca^{2+}-dependent inactivation of CaV1.3 channels by calcium binding proteins of auditory hair cells. *The Journal of Neuroscience*, 26(42), 10677–10689.

Yasunaga, S., Grati, M., Cohen-Salmon, M., El-Amraoui, A., Mustapha, M., Salem, N., El-Zir, E., Loiselet, J., & Petit, C. (1999). A mutation in OTOF, encoding otoferlin, a FER-1-like protein, causes DFNB9, a nonsyndromic form of deafness. *Nature Genetics*, 21(4), 363–369.

Yi, E., Roux, I., & Glowatzki, E. (2010). Dendritic HCN channels shape excitatory postsynaptic potentials at the inner hair cell afferent synapse in the mammalian cochlea. *Journal of Neurophysiology*, 103(5), 2532–2543.

Zagaeski, M., Cody, A. R., Russell, I. J., & Mountain, D. C. (1994). Transfer characteristic of the inner hair cell synapse: Steady-state analysis. *The Journal of the Acoustical Society of America*, 95(6), 3430–3434.

Zampini, V., Johnson, S. L., Franz, C., Lawrence, N. D., Munkner, S., Engel, J., Knipper, M., Magistretti, J., Masetto, S., & Marcotti, W. (2010). Elementary properties of CaV1.3 Ca^{2+} channels expressed in mouse cochlear inner hair cells. *The Journal of Physiology*, 588(1), 187–199.

Zampini, V., Johnson, S. L., Franz, C., Knipper, M., Holley, M. C., Magistretti, J., Masetto, S., & Marcotti, W. (2013). Burst activity and ultrafast activation kinetics of CaV1.3 Ca^{2+} channels support presynaptic activity in adult gerbil hair cell ribbon synapses. *The Journal of Physiology*, 591(16), 3811–3820.

Zhang, S. Y., Robertson, D., Yates, G., & Everett, A. (1999). Role of L-type Ca^{2+} channels in transmitter release from mammalian inner hair cells I. Gross sound-evoked potentials. *Journal of Neurophysiology*, 82(6), 3307–3315.

Chapter 6
Central Projections of Spiral Ganglion Neurons

Michael A. Muniak, Catherine J. Connelly, Kirupa Suthakar, Giedre Milinkeviciute, Femi E. Ayeni and David K. Ryugo

Keywords Auditory nerve · Characteristic frequency · Cochlear nucleus · Endbulb of Held · Ending morphology · Neuroanatomy · Spontaneous discharge rate · Synapses · Tonotopy · Type I fiber · Type II fiber · Ultrastructure

6.1 Introduction

Sensory systems function to detect and interpret the physical environment. Receptor organs convert external stimuli such as photons, mechanical energy, or chemicals into a series of electrical impulses. These impulses, or action potentials, are conveyed to the brain, where they are processed by neural circuits that identify the position and significance of the stimulus. This path between detection and interpretation involves many specializations particular to each sensory modality.

M.A. Muniak · C.J. Connelly · K. Suthakar · G. Milinkeviciute · F.E. Ayeni · D.K. Ryugo (✉)
Garvan Institute of Medical Research, Sydney, Nsw, 2010, Australia
e-mail: david.ryugo@gmail.com

M.A. Muniak
e-mail: m@muniak.com

C.J. Connelly
e-mail: c.connelly@garvan.org.au

K. Suthakar
e-mail: k.suthakar@garvan.org.au

G. Milinkeviciute
e-mail: g.milinkeviciute@garvan.org.au

F.E. Ayeni
e-mail: f.ayeni@garvan.org.au

C.J. Connelly · K. Suthakar · G. Milinkeviciute · F.E. Ayeni · D.K. Ryugo
School of Medical Sciences, University of New South Wales, Sydney, Nsw, 2052, Australia

A. Dabdoub et al. (eds.), *The Primary Auditory Neurons of the Mammalian Cochlea*, Springer Handbook of Auditory Research 52,
DOI 10.1007/978-1-4939-3031-9_6

The study of these specializations can provide valuable insight as to how the brain is able to process and act on sensory input.

In mammals, neurons of the spiral ganglion connect the brain to the physical world of sound. Spiral ganglion neurons send their peripheral processes out to the organ of Corti, where they form contacts with two types of acoustic receptor cells, the inner hair cells (IHCs) and the outer hair cells (OHCs). The central processes of these neurons coalesce to form the acoustic portion of the cochlear nerve. These primary auditory neurons terminate in the cochlear nucleus (CN), located on the dorsolateral side of the brain stem. Synapses are established with many different classes of cells throughout the CN, giving rise to multiple, parallel representations of the acoustic environment.

This chapter describes specializations in the central projections of spiral ganglion cells in mammals and discusses how these properties contribute to divergent pathways for information processing in the brain. First, the types of spiral ganglion neurons and features of their organization with respect to physiological parameters of sound are reviewed. Next, the projection patterns of auditory nerve fibers into the CN are discussed. Lastly, specializations in the morphology of primary afferent terminals are considered with respect to their effects on stimulus coding.

6.2 Spiral Ganglion Neurons

Spiral ganglion somata reside within Rosenthal's canal, medial to the osseous spiral lamina and flanked above and below by the scala vestibuli and scala tympani. Peripheral processes from the ganglion cells run radially along the osseous spiral lamina, enter the organ of Corti at the habenula perforata, and innervate the receptor hair cells. Many details regarding development (Goodrich, Chap. 1; Fritzsch et al. Chap. 2), endogenous properties (Davis and Crozier, Chap. 4), and peripheral innervation (Rutherford and Moser, Chap. 5) of these neurons are covered elsewhere in this volume. The characteristics of these primary auditory neurons that dictate the functional organization of their central projections are reviewed in this chapter.

6.2.1 Cell Types

Spiral ganglion neurons can be differentiated into two populations, classified according to somatic size, relative numbers, cytologic traits, and properties of their central and peripheral processes (Fig. 6.1; Spoendlin, 1971, 1973; Kiang et al., 1984). Type I ganglion cells represent the majority of auditory nerve fibers, comprising 90–95 % of the population in the cat (Spoendlin, 1971, 1973). These large, bipolar cells are rich in ribosomes and cytoplasmic organelles, and have myelinated central axons. The remaining 5–10 % of the population consists of type II ganglion

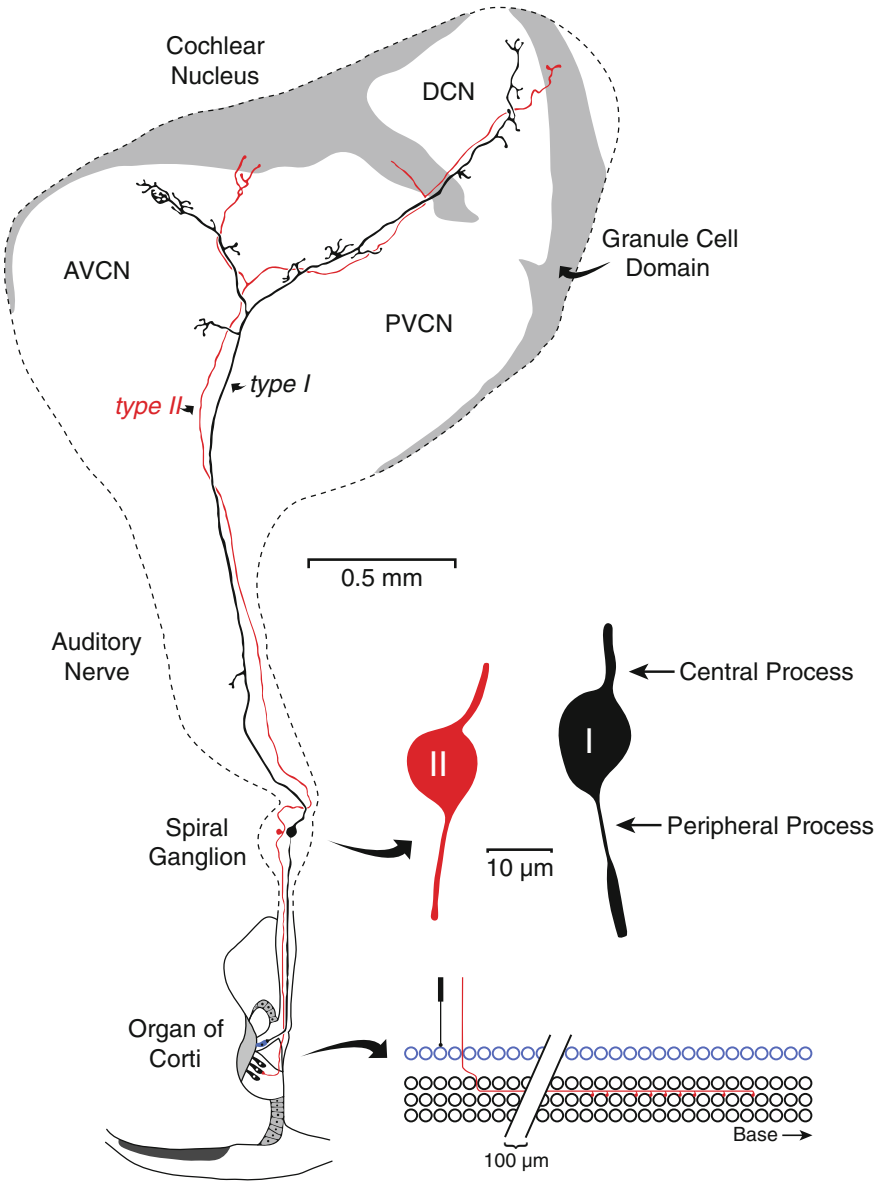

Fig. 6.1 Schematic drawing of spiral ganglion neurons and their central and peripheral terminations. The type I neuron (*black*) innervates a single IHC and projects in a topographic fashion into the CN. Fibers that innervate the basal hair cells project to dorsal regions of the CN, whereas fibers that innervate more apical hair cells project to progressively more ventral regions. This type I neuron is representative of its group. Note that a representative type II neuron (*red*) has a similar central projection pattern but with additional terminations in the GCD. The conundrum is that in spite of the differences in peripheral innervation, the central projections have a similar spatial pattern (Adapted from Brown et al., 1988)

cells, which tend to be smaller, pseudomonopolar (i.e., possessing a single axon that branches to produce central and peripheral processes), unmyelinated, and neurofilament rich (Kiang et al., 1982; Berglund & Ryugo, 1986). Type II cells also tend to reside in the periphery of Rosenthal's canal, closer to the osseous spiral lamina (Berglund & Ryugo, 1987). A key distinction between these two cell types is in their disparate peripheral innervation pattern: The radial fiber of a type I ganglion cell selectively innervates a single IHC, whereas an outer spiral fiber of a type II ganglion cell innervates multiple OHCs (reviewed by Fritzsch et al., Chap. 3 and Rutherford and Moser, Chap. 5). This distinction was first suggested by the differential survival patterns of ganglion neurons after auditory nerve transection (Spoendlin, 1971, 1973), and later confirmed by tracing individual labeled nerve fibers in the cat (Kiang et al., 1982). The numerical conundrum between proportions of spiral ganglion cell types and hair cell types is clarified by the number of contacts each fiber type makes with its respective hair cell target. Each type I radial fiber contacts a single IHC, but each IHC receives contact from numerous fibers. In contrast, type II outer spiral fibers are more promiscuous, reaching out to multiple OHCs, with each OHC receiving only a handful of contacts (for counts, refer to Tables 2 and 3 of Nayagam et al., 2011).

Morphological generalizations such as cell body size or shape (Berglund & Ryugo, 1987) may not always be sufficient in every species for distinguishing between spiral ganglion cell types. In such instances, the ratio of the diameter of the central and peripheral processes of spiral ganglion neurons, when measured in proximity to the soma, is informative (Kiang et al., 1982; Berglund & Ryugo, 1987). The calibers of both processes of type II cells are generally comparable, whereas the peripheral diameter of type I cell processes is characteristically much smaller than the central counterpart. This observation has been reported in a number of species including the cat, mouse, opossum (*Didelphimorphia*), guinea pig (*Cavia porcellus*), squirrel monkey (*Saimiri sciureus*), and human (Kiang et al., 1982, 1984; Berglund & Ryugo, 1987).

A number of staining techniques can also be employed to distinguish between spiral ganglion cell populations. Because of different cytoskeletal profiles, type II neurons can be selectively labeled using antibodies directed against the phosphorylated 200-kDa neurofilament protein (Berglund & Ryugo, 1986, 1991), or peripherin, a neuronal intermediate filament protein (Hafidi et al., 1993). It is also possible to label type I neurons rapidly and selectively using dextran-based neuronal tracers by applying dye crystals directly onto the freshly sectioned auditory nerve (Huang et al., 2007).

6.2.2 Physiology

Auditory nerve fibers exhibit a diverse range of intrinsic and evoked physiological response profiles (reviewed by Davis and Crozier, Chap. 4). Such variety in the afferent input to the central auditory system highlights the complexity of coding

strategies used by the brain to analyze the sound environment. The physiological properties of type I spiral ganglion neurons have been well characterized by recordings from their axons (Kiang et al., 1965; Evans, 1972). In contrast, virtually nothing is known about the in vivo response properties of type II cells because of their scarcity and fine axon caliber (Liberman, 1982a; Robertson, 1984). Recent progress has been made with recordings at type II afferent terminals under OHCs (Weisz et al., 2009, 2012), but how this information is functionally integrated at the type II soma and propagated to the central nervous system remains undetermined.

Type I fibers can be differentiated on the basis of three basic physiological properties: spontaneous discharge rate, response threshold, and characteristic frequency. Spontaneous discharge rate (SR) describes the firing activity of an individual nerve fiber in the absence of sound stimulation. The response threshold of auditory nerve fibers refers to the lowest sound pressure level that elicits a supra-threshold response (e.g., a firing rate 10 % above SR or an increase of one spike/stimulus above SR), typically measured in decibels (dB) relative to 20 μPa. Variations in threshold criteria, however, do not substantially change population groupings (Liberman, 1978; Geisler et al., 1985). Lastly, the characteristic frequency (CF) is defined as the sound frequency at which an individual auditory nerve fiber is most sensitive. The CF is determined by measuring a "tuning curve" (Kiang et al., 1965; Evans, 1972), which describes the collection of frequency and intensity combinations that evoke increases in the firing rate above SR of an auditory neuron. The tip of this excitatory tuning curve indicates both the response threshold and CF of the unit.

6.2.2.1 Characteristic Frequency

The mammalian cochlea acts as a biological frequency analyzer of sound, with a low-to-high frequency gradient established from the apex to the base of the cochlear spiral (von Békésy, 1960). Because each radial fiber contacts only a single IHC, the CF of each type I cell is determined by the position of its peripheral innervation along the basilar membrane (see also Rutherford and Moser, Chap. 5). This systematic relationship was demonstrated by physiologically characterizing and tracing labeled auditory nerve fibers back to their cochlear origin, establishing a place-frequency map of the cochlea. Such experiments have been performed in a variety of mammals including cat, rat, opossum, gerbil, guinea pig, chinchilla, mouse, and bat (Liberman, 1982b; Kössl & Vater, 1985; Vater et al., 1985; Müller, 1991, 1996; Müller et al., 1993, 2005, 2010; Tsuji & Liberman, 1997; Muniak et al., 2013).

The determination of cochlear place-frequency maps also shows that, in most species, frequency representation is approximately log-linear, giving equal weighting to frequency components across the physiological hearing range. Deviations from this log-linear trend are seen in some species, where frequency expansions—termed acoustic foveae—for high frequencies used in echolocation have been observed in horseshoe (*Rhinolophus rouxi*) and mustache (*Pteronotus parnellii*) bats (Bruns & Schmieszek, 1980; Kössl & Vater, 1985; Vater et al., 1985), and in the

low-frequency region of the African mole rat (*Cryptomys hottentotus*) cochlea (Müller et al., 1992). Whether specialized or generalized, the place-frequency map of the cochlea and its transfer to auditory nerve fibers establishes the range and sensitivity of hearing capabilities of the animal (Fay, 1988).

Type I spiral ganglion somata are distributed throughout Rosenthal's canal with respect to CF (Keithley & Schreiber, 1987). Cells with low CFs are located apically, whereas cells with progressively higher CFs can be found at progressively more basal regions. Hence, order is maintained in the connection between peripheral targets and cell bodies. An inverse relationship of unknown significance has also been observed between type I soma size and CF in the cat. Low-CF neurons exhibit the largest somatic silhouette area but soma size becomes progressively smaller with increasing CF until plateauing at approximately 4 kHz (Liberman & Oliver, 1984).

6.2.2.2 Spontaneous Discharge Rate and Threshold

Type I spiral ganglion neurons exhibit a broad range of SRs, which have been strongly correlated with response threshold (Kiang et al., 1965; Liberman, 1978). Cells with high SRs consistently display low thresholds for activation, whereas cells with low SRs tend to have higher thresholds. Across the audible frequency range, units with similar CFs can vary in SR from near 0 to greater than 100 spikes per second. A bimodal distribution of SRs is frequently observed in cats (Kiang et al., 1965; Liberman, 1978; Evans & Palmer, 1980) and guinea pigs (Tsuji & Liberman, 1997). In these species, 60–70 % of fibers have high SRs (>30 spikes/s), and the remaining 30–40 % have low SRs (<10 spikes/s). The low-SR population can be further subdivided into low-SR (<0.5 spikes/s) and medium-SR (>0.5 spikes/s) units. In gerbils, rats, and mice, a clear bimodal distribution of SRs is not observed (Schmiedt, 1989; Ohlemiller & Echteler, 1990; el Barbary, 1991; Taberner & Liberman, 2005). The inverse relationship between SR and response threshold, however, remains constant across CF, suggesting a general organizational feature of the auditory nerve.

The distinction of type I fibers on the basis of SR is also reflected in their peripheral anatomy. High-SR fibers are larger in caliber, and almost always contact the pillar side of IHCs (Liberman, 1982a; Liberman & Oliver, 1984; Merchan-Perez & Liberman, 1996). In contrast, low- and medium-SR fibers are smaller, and contact only the modiolar side of the IHC, indicating that differences in SR may partially stem from differences in their afferent innervation (Rutherford and Moser, Chap. 5). This segregation of fibers is maintained within the osseous spiral lamina, with high-SR fibers traveling closer to the scala tympani, and low- and medium-SR fibers residing closer to the scala vestibuli (Kawase & Liberman, 1992; Tsuji & Liberman, 1997). A similar pattern of divergence for type I somata within the spiral ganglion is also observed with respect to SR, although high-SR neurons tend to be found throughout the canal (Kawase & Liberman, 1992). Such a separation was not found in the guinea pig (Tsuji & Liberman, 1997). The dissociation of type I

auditory nerve fibers on the combined basis of SR, response threshold, and peripheral innervation strongly suggests that these disparate fiber classes may play separate roles in auditory perception.

6.3 Central Projections

The challenges of auditory coding confronted 20th-century physiologists such as Rafael Lorente de Nó (1933a, b, 1976, 1981), who marveled at the complicated nature of the task. He proposed that clues to understanding the physiology of hearing would be aided by anatomical research that described the distribution pattern of auditory nerve terminals and the cell types that received its inputs. He boldly declared that individual auditory nerve fibers were modular, with each fiber resembling the other and differing only in its origin in the cochlea. Moreover, he concluded that each fiber innervated every one of the 13 regions he described for the CN, contacting hundreds of the 40–50 neuron types (Lorente de Nó, 1933b). When Lorente de Nó (1937) described three patterns of ganglion cell innervation of the sensory receptors, he complicated the idea that divergent patterns of sensory receptor innervation would produce identical connections in the brain. As new data emerged, some of the major conclusions of Lorente de Nó have been abandoned but his observations have contributed significantly to our understanding of the auditory system and set the stage for modern hypothesis testing.

6.3.1 Auditory Nerve

The centrally projecting axons of spiral ganglion cells collect along the central axis of the cochlea within the modiolus. The total number of fibers contained within this bundle varies with species, ranging from 10,000 to 12,000 fibers in mice, 30,000 in humans, and 95,000 in dolphins (Guild et al., 1931; Rasmussen, 1940; Gacek & Rasmussen, 1961; Wever et al., 1971; Anniko & Arnesen, 1988; Nadol, 1988; Berglund & Ryugo, 1991; Chen et al., 2010; see Table 1 of Nayagam et al., 2011). Irrespective of absolute counts, the proportions of 90–95 % thick, myelinated type I fibers and 5–10 % unmyelinated type II fibers remain fairly constant (Alving & Cowan, 1971; Arnesen & Osen, 1978; Anniko & Arnesen, 1988).

Early electrophysiological experiments suggested that fibers with similar CFs were located near each other within the trunk of the auditory nerve (Kiang et al., 1965). Anatomical work confirmed this observation, showing an orderly arrangement of fibers within the modiolus from the spiral lamina through to the CN (Fig. 6.2; Sando, 1965; Arnesen & Osen, 1978; Anniko & Arnesen, 1988). Low-CF fibers originating from the apex of the cochlea are positioned within the central axis of the modiolar trunk. Fibers from more basal regions join the nerve bundle peripherally, progressively wrapping around its outer edge. This spatial pattern

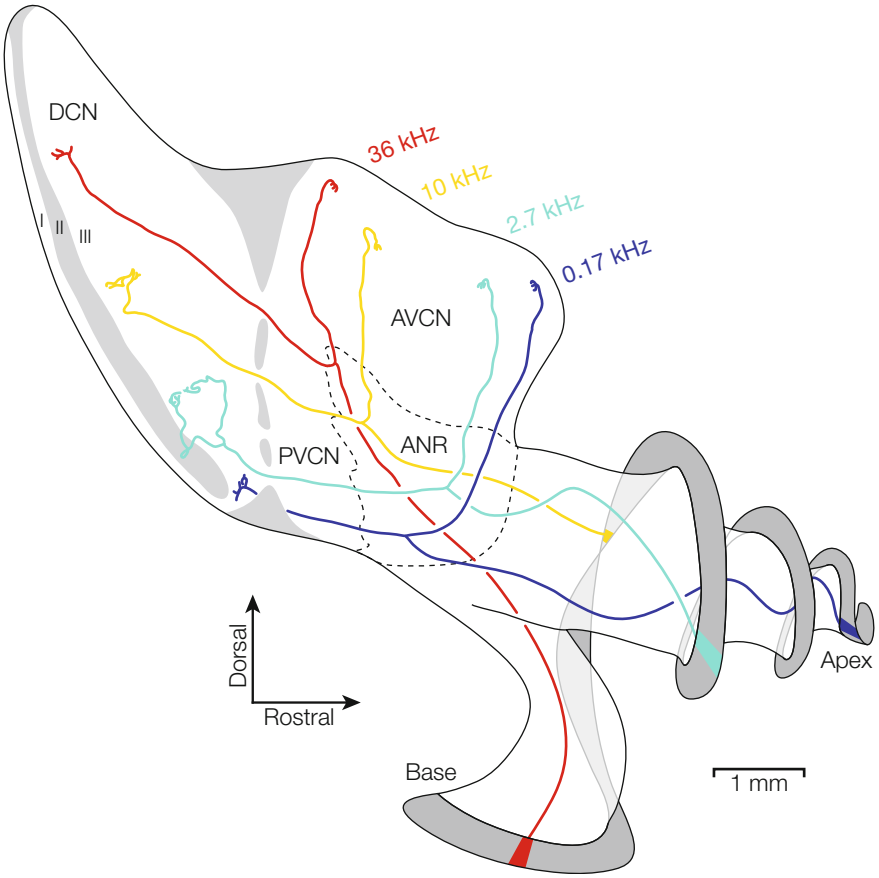

Fig. 6.2 Schematic diagram of the CN complex and cochlear nerve in cat, as shown from a dorsolateral aspect. The cochleotopic/tonotopic projections of four type I auditory nerve fibers are illustrated. Each fiber begins at the spiral lamina and twists through the cochlear nerve bundle to emerge in the auditory nerve root, where it bifurcates and gives rise to an ascending branch, which terminates within the AVCN, and a descending branch, which passes through the PVCN and terminates within layer III of the DCN. The position of each fiber along its entire path is frequency dependent. The auditory nerve root region is shown as a dotted outline, with the ventral boundary corresponding to the Schwann–glia border. The GCD and layer II of the DCN are indicated in gray. ANR, auditory nerve root; AVCN, anteroventral cochlear nucleus; DCN, dorsal cochlear nucleus; PVCN, posteroventral cochlear nucleus (Adapted from Arnesen & Osen, 1978; Ryugo & May, 1993)

within the nerve forms a helical twist, echoing that of the cochlea. The arrangement spirals through the internal auditory meatus and continues into the central nervous system by crossing the Schwann–glia border, where the bundle begins to unwrap as auditory nerve fibers make their topographic projections into the CN (Sando, 1965; Arnesen et al., 1978; Muniak et al., 2013).

6.3.2 Cochlear Nucleus

The CN is located on the dorsolateral aspect of the brain stem at the pontine–medullary junction. It is divided into a dorsal cochlear nucleus (DCN) and a ventral cochlear nucleus (VCN). These two divisions are visible externally, with a slight depression separating them along the lateral surface. The DCN is a laminated cortical structure reminiscent of a cerebellar folium (Ramón y Cajal, 1909; Lorente de Nó, 1933b). The internal organization of the VCN is less obvious. The two divisions are separated by a thin expanse of granule cells, which is visible in Nissl-stained sections (Mugnaini et al., 1980). The CN is the sole target of auditory nerve input (Fekete et al., 1984; Liberman, 1991). Individual auditory nerve fibers bifurcate on entering, and the zone of bifurcations roughly separates the VCN into an anterior and a posterior division (AVCN, PVCN; Ramón y Cajal, 1909). Cytoarchitectonic features such as size, shape, and packing density of cell bodies, dendritic branching, and fiber patterns can also be used to subdivide the nucleus (Harrison & Irving, 1965; Osen, 1969; Brawer et al., 1974). Different cell populations within these subdivisions may be further characterized by features of the cytology of the cell body, characteristics of the nucleus, afferent innervation, immunologic staining, axonal projections, and physiological response properties, but the borders between different populations are often fuzzy (for review, see Cant, 1992). Differential patterns of ascending projections from cells of the CN help to establish divergent representations of the sound environment along parallel central auditory pathways. The systematic and generally reliable relationship between anatomical and physiological properties suggests a role in stimulus coding and signal processing.

6.3.2.1 Type I Fibers

Auditory nerve fibers project into the CN following a stereotyped plan (Figs. 6.1 and 6.2; Ramón y Cajal, 1909; Lorente de Nó, 1933a). On crossing the Schwann–glia border, fibers ascend dorsally into the nucleus forming the root branch of the nerve. After traversing for some distance, the root branch bifurcates, giving rise to an ascending branch and a descending branch (collectively called “parent” branches). The ascending branch projects into the anterior region of the AVCN, where one of its most pronounced terminals is a large, axosomatic ending known as the endbulb of Held (Held, 1893). The descending branch is directed posteriorly through the PVCN and usually (85 % of cases in cats) continues onward and upward into the DCN (Fekete et al., 1984). Nodes of Ranvier can be observed at regular intervals along the parent branches, and the mean lengths of ascending and descending branches are similar irrespective of CF or SR (Fekete et al., 1984).

Each parent branch maintains a relatively straight trajectory and can give rise to short collaterals and multiple endings as they traverse through the nucleus. In the cat, the ascending branch produces an average of nine primary collaterals, and the

descending branch gives rise to an average of 11 primary collaterals (Fekete et al., 1984). These collaterals are thinner, divide several times, exhibit en passant and terminal swellings, and generally do not extend far from the parent branch. En passant swellings do not consistently display synapses, but terminal swellings always do (Fekete et al., 1984; Ryugo & Sento, 1991). Collaterals are scattered along the length of each parent branch, resulting in a patchy terminal field for any given auditory nerve fiber. In the cat, approximately 15 % of terminal swellings reside in the DCN, with the remainder scattered throughout the VCN (Ryugo & May, 1993). Fibers sharing similar CFs (see Sect. 6.3.2.2) occupy the same region, thus filling in the patches to form a solid terminal field along the length of the projection (Fekete et al., 1984; Ryugo & May, 1993). All terminals, however, remain within the magnocellular core of the VCN and the deep layer (III) of the DCN (Fekete et al., 1984; Liberman, 1991).

6.3.2.2 Organization with Respect to Frequency

Topographic maps are one of the fundamental principles of brain organization, defined by an orderly representation of sensory and motor systems (Kaas, 1997). In the auditory system, frequency maps are conserved throughout the ascending pathways, replicating the place-frequency map established at the cochlear sensory epithelium (Clopton et al., 1974). Tonotopy is thus imprinted upon the CN via the precise distribution of auditory nerve fibers relative to CF (Fekete et al., 1984; Ryugo & May, 1993). This organization can also be referred to as cochleotopy, which describes the organization of projections with respect to their position of origin on the cochlear spiral. Because of the orderly organization of the cochlear place-frequency map (Liberman, 1982b), the concepts of tonotopy and cochleotopy are often interchangeable. This correspondence is useful for interpreting anatomical studies from which physiological data may not be available.

An electrophysiological study first established that a complete representation of audible frequencies could be found within the CN (Rose et al., 1959). Electrode penetrations along a dorsal to ventral axis revealed frequency tunings that progressed from high to low CFs. The range of CFs encountered on a particular electrode track varied with location, but similar trends were observed in both dorsal and ventral divisions. Subsequent physiological experiments have expanded upon this view, establishing that frequency tuning is highly organized within the DCN, AVCN, and PVCN (Bourk et al., 1981; Spirou et al., 1993). Spatial reconstructions of electrode penetrations in these studies were sufficiently detailed to support the conclusion that frequency representations were conceptually organized into isofrequency laminae.

Exploration of the cochleotopic projection pattern of the auditory nerve into the CN began with the histologically stained material of early neuroanatomists (Ramón y Cajal, 1909; Poljak, 1927; Lorente de Nó, 1933a). Initial experimental studies verified a rough correspondence between a lesion point in the cochlea and the position of the silver grains attracted by degenerating axons to identify the

bifurcation of the root branch and the distribution of auditory nerve fiber projections (Sando, 1965; Osen, 1970; Webster, 1971). Apical parts of the cochlea, representing low CFs, projected to ventral regions of the CN, whereas basal, high-CF portions projected to dorsal areas. More direct results were obtained following small extracellular tracer deposits made in the cochlea that filled the axons and their terminations in the CN (Leake & Snyder, 1989; Brown & Ledwith, 1990). Another study involved small injections into defined frequency locations of the CN that backfilled auditory nerve fibers within the nucleus as well as peripheral terminations in the cochlea (Muniak et al., 2013). When analyzed in the coronal plane, these injections produced "slabs" of labeled fibers that coursed throughout the rostro-caudal extent of the nucleus. The dorsoventral position of these slabs was cochleotopic, giving an anatomical substrate to the isofrequency laminae observed electrophysiologically.

Further refinement of these findings was obtained through the reconstruction of physiologically characterized and intracellularly labeled auditory nerve fibers in the cat (Fekete et al., 1984; Liberman, 1991; Ryugo & May, 1993). Single-fiber studies not only provide excellent resolution for analyzing the fine details of primary projections but also yield unambiguous structure–function relationships. These results provided unequivocal evidence that the position of bifurcation of the root branch and the spatial distribution of the central axon is strongly correlated with the CF of the fiber (Fig. 6.2). Fibers with low CFs bifurcate almost immediately on entering the CN, with the ascending and descending branches distributed ventrally in the VCN and DCN. Fibers with progressively higher CFs bifurcate and distribute at progressively more dorsal locations.

One consequence of this organization is that the overall length of each auditory nerve fiber remains approximately constant across CFs (Arnesen & Osen, 1978; Fekete et al., 1984). Although apical fibers must traverse a greater distance from their entrance in the spiral lamina to the Schwann–glia border, this length is offset by a shorter distance to the point of bifurcation. In the cat, the total length of the ascending and descending branches after the point of bifurcation is 6–7 mm; the length of the intracochlear axon from the bifurcation to the habenula perforata is also about 6–7 mm. Within the DCN, auditory nerve terminal fields form an anisotropic spatial envelope, with the long axis oriented perpendicular to the ependymal surface and short axis confined to an isofrequency lamina (Ryugo & May, 1993). The orientation of the terminal field shifts systematically with CF, corresponding to the gradual curvature of the DCN.

Owing to technical constraints, most studies of fiber projections have historically analyzed and/or presented data using 2D plots, typically along a parasagittal plane to maximize the information yield across all subdivisions (Fekete et al., 1984; Ryugo & May, 1993). A limitation of such analyses is the difficulty in capturing the undulating variations of isofrequency laminae within all three dimensions. Recently, a quantitative 3D model of frequency representation in the CN was developed for the mouse (Fig. 6.3) that confirmed and extended the 2D projection pattern previously described (Fekete et al., 1984; Ryugo & May, 1993; Muniak et al., 2013). Visualizations of the helical twist of the nerve root and the angular

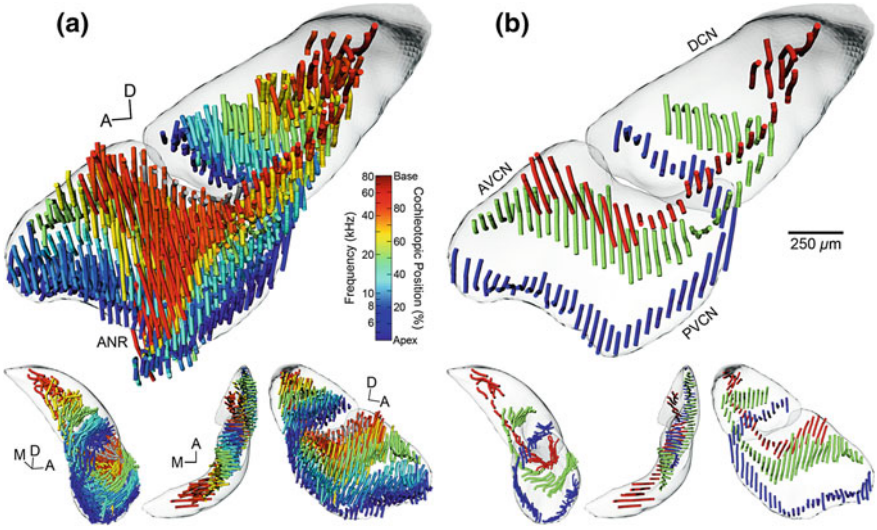

Fig. 6.3 3D tonotopic arrangement of auditory nerve fibers in the CN of the CBA/J mouse. **a** Reconstructed auditory nerve fiber trajectories from 24 experimental cases are shown after normalization to a template CN. Each tract is represented as a set of "noodles" and shaded according to its cochleotopic origin. An equivalent tonotopic value is calculated based on a place-frequency map of the cochlea. A clear tonotopic trend is evident in all three major subdivisions. DCN and VCN surfaces are also shown and rendered semi-opaque. The top figure is from a medial viewpoint. Lower figures are from alternate viewing angles; L-R: posterior, dorsal, and lateral. In the lower figures, the reconstructed root branch fibers have been removed. **b** Three cases from **a** are chosen to illustrate the trajectory of low-, middle-, and high-frequency fiber tracts more clearly. Examples shown correspond to values of 13.5 %/6.4 kHz, 53.0 %/20.5 kHz, and 87.0 %/55.8 kHz. Scale bar equals 250 μm for large figures only (Adapted from Muniak et al., 2013)

projection of fibers transitioning from PVCN to DCN were also possible (Sando, 1965; Arnesen & Osen, 1978). At the base of the nerve root, low-CF fibers spiral around the outer edge of the nerve bundle along a medial-to-rostral trajectory before bifurcating laterally. Higher-CF fibers enter the nerve root more centrally within the bundle, ultimately bifurcating both at more dorsal and more medial locations than those of lower CFs. Such reconstructions demonstrate that, although the dorsal-ventral axis may be the predominant orientation of fiber distribution with respect to CF, there is also a strong medial-lateral bias that must be considered (Fig. 6.4). The stereotyped primary projection to the CN may be described as forming "C"-shaped laminae that stack vertically upon one another with increasing CFs (Fig. 6.3).

The precise tonotopic projection pattern of auditory nerve fibers provides a solid grounding for observations of orderly frequency tuning in the CN (Bourk et al., 1981; Spirou et al., 1993). Some regions of the nucleus, however, exhibit tuning variations that are explainable on the basis of local perturbations in afferent input. In the first instance, fine-scale frequency organization was described as irregular in the

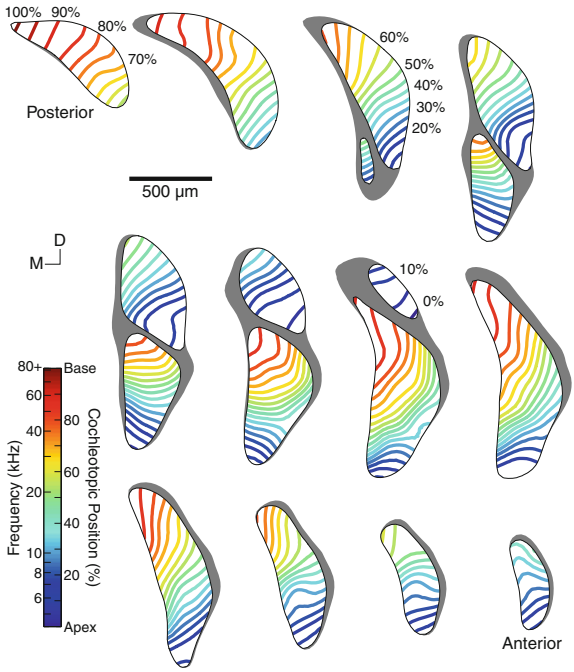

Fig. 6.4 Collection of "virtual slices" through a quantitative model of frequency representation in the CN of the CBA/J mouse. Evenly spaced (150 µm) parallel slices are presented in the coronal plane. Isofrequency lines are rendered within each slice at 5 % cochleotopic intervals, equivalent to 0.25-octave steps. Slices within each row or column are aligned with one another along the orthogonal axis. Frequency representation can be seen to change along both dorsal-ventral and medial-lateral gradients through each subdivision (Adapted from Muniak et al., 2013)

nerve root (Bourk et al., 1981), with high-CF units encountered in locations generally corresponding to low CFs. This circumstance is created by the presence of collaterals arising from the root branch prior to the bifurcation (Fekete et al., 1984). The numbers and lengths of these collaterals can vary widely, but are usually confined to the nerve root region. Fibers with high CFs tend to emit more numerous and extensive collaterals, which can intermingle with low-CF fibers and complicate frequency tuning. Octopus cells, a unique cell type of the PVCN, respond strongly to the onset of sounds or stimulus transients and represent another instance of unconventional tuning (Godfrey et al., 1975; Rhode & Smith, 1986). These cells show sharp tuning near threshold, but exhibit broader tuning 20 dB above threshold (Godfrey et al., 1975). The prominent dendrites of octopus cells intersect a broad swath of descending branch fibers (Osen, 1969), providing a likely substrate for broad tuning. On the other hand, it was noted that descending fibers with CFs greater than 4 kHz emit long collaterals oriented orthogonal to the parent branch, but parallel to octopus cell dendrites (Fekete et al., 1984). The combination of a dendrite intersecting a wide CF swath of auditory nerve terminals and collaterals

from a single fiber converging on the same dendritic branch could contribute to narrow tuning near threshold and broad tuning at higher levels.

There has been some question as to whether all frequencies are equally represented in each subdivision of the CN. In the mouse (Muniak et al., 2013) and gerbil (Müller, 1990), reconstructions of tissue volume with respect to CF suggest that proportional volumes of each subdivision are roughly dedicated to equivalent octave ranges (Fig. 6.4). In cats, however, electrode penetrations (Spirou et al., 1993) and fiber reconstructions (Fekete et al., 1984; Ryugo & May, 1993) suggest that greater amounts of tissue in the DCN may be dedicated to mid–high frequencies relative to that in the VCN. Complicating this interpretation, however, is that these data were analyzed with respect to linear distance, rather than tissue volume, which appears not to be uniform (i.e., narrowing cross sections) along the frequency axis. Interestingly, the bat appears to have an expanded representation of the echolocating frequency range (Feng & Vater, 1985). This expansion, however, reflects a similar "fovea" in its cochlear representation (Vater et al., 1985), suggesting that the presence (or absence) of cochlear specializations may be equivalently represented through the projection pattern of auditory nerve fibers.

6.3.2.3 Organization with Respect to Spontaneous Discharge Rate

Hearing involves more than simple analysis of the frequency spectrum. Accordingly, although the predominant organizational feature of auditory nerve projections into the CN is tonotopy, the central projections of type I fibers also exhibit variations with respect to SR, echoing observations in the periphery (Fig. 6.5). Fibers belonging to different SR classes have distinct physiological characteristics, particularly with respect to encoding dynamic range and representing vowel sounds (Sachs & Young, 1979; Evans & Palmer, 1980; May et al., 1996). High-SR fibers with low thresholds may operate best in quiet, whereas low-SR, high-threshold fibers may be optimized for loud and noisy environments. Different groupings of fibers likely contribute to separate roles in acoustic processing and so are expected to differ in their central terminations.

High-SR fibers give rise to short collaterals that produce on average 25–30 branches from both ascending and descending parents (Fekete et al., 1984). In contrast, low-SR fibers on average give rise to twice as many collateral branches, especially within the AVCN (Fekete et al., 1984; Liberman, 1991, 1993; Tsuji & Liberman, 1997). In cats, there are more and longer collateral branches arising from ascending low-SR fibers (Fekete et al., 1984). Low-SR fibers have an average of 5 mm of collaterals per ascending branch in cats, compared to 2.8 mm of collaterals per high-SR fiber (Fekete et al., 1984). This increase in branching results in approximately twice as many terminal endings in the AVCN. Similarly, terminal distributions are more widely spaced in the DCN for low-SR fibers (Ryugo & May, 1993). The arborizations of high-SR fibers also tend to decrease in width with increasing CF. These observations suggest that low-SR fibers may contact more neurons across a wider region of the CN compared to high-SR fibers. This divergent

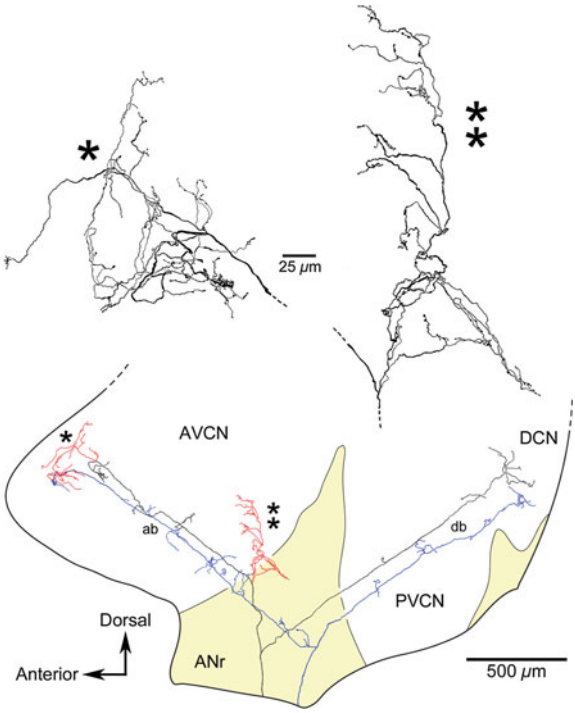

Fig. 6.5 Drawing tube reconstructions of a low-SR auditory nerve fiber (*black* and *red*; CF = 3.1 kHz; SR = 0.2 spikes/s; threshold = 26 dB SPL) and a high-SR auditory nerve fiber (*blue*; CF = 1.2 kHz; SR = 86 spikes/s; threshold = −3 dB SPL), as viewed laterally. The ascending branches take a relatively straight trajectory through the AVCN. Low-SR fibers are distinctive by the collaterals that arborize within the small cell cap (*red*). Otherwise, the main parts of the ascending and descending branches are similar for the different SR types. Higher magnification drawings are shown for each collateral. One collateral ramifies anterior to the endbulb (*), whereas the other ramifies laterally (**). The collaterals of high threshold, low-SR fibers ramify extensively within the small cell cap and are good candidates for serving as the afferent limb of the high threshold circuit that feeds back to the organ of Corti by way of the olivocochlear system (Ye et al., 2000). ab, ascending branch; ANr, auditory nerve root; AVCN, anteroventral cochlear nucleus; db, descending branch; PVCN, posteroventral cochlear nucleus (Adapted from Fekete et al., 1984; Ryugo, 2008)

innervation pattern may relate to the perception of loudness, which has been hypothesized to be proportional to the number of active neurons (Stevens & Davis, 1938). Low-SR, high-threshold fibers are activated by loud sounds, which would not only increase both the total number of active nerve fibers, but also produce a wider spread of activity within the CN, supplementing the responses of high-SR fibers that would already be saturated at such levels (Kiang et al., 1965).

The small cell cap of the CN preferentially receives auditory nerve input from low-SR fibers (Fig. 6.5; Liberman, 1991; Ryugo, 2008). This thin region is a collection of cells squeezed between the granule cell domain (GCD) and the

magnocellular VCN, particularly along the dorsal, lateral, and dorsomedial aspects of the AVCN (Osen, 1969; Cant, 1993). These small cells are characterized by a round, pale nucleus and dendrites filled with ribosomes. Low-SR collaterals form long, thin branches that arborize extensively within the small cell cap, often extending orthogonal to the isofrequency laminae of the adjacent magnocellular region (Ryugo, 2008). These collaterals can emerge from any position along the ascending branch, sometimes directly from the endbulb of Held or near the beginning of the ascending branch just beyond its exit from the nerve root zone. They produce numerous small terminals that selectively target the somata and dendrites of resident small cells within the small cell cap (Ryugo, 2008). The significance of this selective projection is that these small cells of the cap have been shown to send axons to the dendrites and somata of neurons of the medial olivocochlear efferent system (Ye et al., 2000). Cells of the cap also exhibit high thresholds for activation (Ghoshal & Kim, 1996, 1997), consistent with the low-SR inputs and the idea of encoding stimulus intensity. The picture that emerges is one of a high-threshold feedback circuit to the inner ear, in which low-SR auditory nerve fibers might initiate activation of medial olivocochlear efferent neurons via cells of the small cell cap.

6.3.2.4 Type II Fibers

The projections of unmyelinated type II auditory nerve fibers within the CN are less well characterized than their type I counterparts. As the physiological properties of these fibers continue to elude experimental inquiry, their organization can only be described with respect to cochleotopy and in comparison to myelinated fibers. Broadly speaking, type II axons adhere to the same stereotyped projection pattern described for type I fibers (Brown et al., 1988; Berglund & Brown, 1994). The enigma is that these cochleotopic central projections arise from separate fiber populations with distinctly different patterns of peripheral terminations (Fig. 6.1).

Extracellular tracer deposits are typically made in the spiral ganglion to label primary fibers. Type II fibers are readily distinguished from type I fibers by their small diameters (Fig. 6.6). The most comprehensive information about these fibers has been obtained from small mammals, such as mice (Brown et al., 1988). Complete fills of type II fibers are difficult to obtain in larger animals such as guinea pigs (Brown, 1987) and cats (Ryugo et al., 1991; Morgan et al., 1994), as the thin axon caliber and greater length of the auditory nerve impedes the transport of tracers.

Type II fibers bifurcate in a cochleotopic manner, forming ascending and descending branches that follow the same spatial organization of co-labeled type I fibers, but only 15 % of the descending branches will enter the DCN (Brown & Ledwith, 1990; Berglund & Brown, 1994). These parent branches produce fewer collaterals compared to type I fibers, with most swellings located in the neuropil in proximity to cell bodies, nodes of Ranvier of type I axons, and blood vessels. Only 18 % of type II terminal and en passant swellings appear to form synapses (Brown

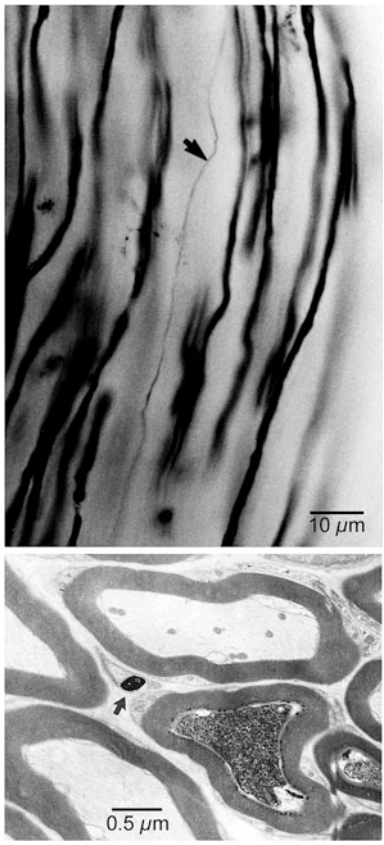

Fig. 6.6 Photomicrograph (*top*) and electron micrograph (*bottom*) of auditory nerve fibers in the cat labeled with horseradish peroxidase. Most of the fibers are 2–4 μm thick and represent the central axons of type I spiral ganglion cells. An occasional fiber is thin (*arrows*) and arises from the type II spiral ganglion cell. The thick fibers are myelinated, whereas the thin ones are not (Adapted from Ryugo et al., 1991)

et al., 1988; Ryugo et al., 1991; Berglund et al., 1996). Unlike type I fibers, type II fibers extend beyond the magnocellular core of the nucleus to ramify within the GCD (Brown et al., 1988). Type II fibers are not all equal: Ascending fibers from basal regions of the cochlea terminate most heavily in the GCD, whereas those from more apical regions do not always send collaterals to the GCD (Brown & Ledwith, 1990; Berglund & Brown, 1994). In contrast, descending fibers, irrespective of their cochlear origin, always project to the GCD, particularly in the region that separates the VCN and DCN. The projections to the GCD are not considered to be tonotopic (Berglund & Brown, 1994; Morgan et al., 1994). The lack of myelination means that signals that are conveyed by type II fibers will arrive in the CN with a delay of several milliseconds relative to that of type I fibers. These spatially topographic terminations with temporally separate arrivals are certainly cause for puzzlement. Moreover, the divergent pattern of peripheral innervation of the two fiber types seems incongruent with their topographic projections. Regardless, the differences in afferent innervation, myelination, central synapse morphology, and termination patterns suggest markedly different function in sensory processing.

6.4 Ending Morphology

The transfer of acoustic information from the auditory nerve to the CN depends not only on the broad axonal projection pattern with respect to physiological parameters, but also on the local cell types with which synapses are made and the fine details of nerve ending morphology. Auditory nerve fibers form a variety of ending types with their postsynaptic targets, including en passant, small bouton, medium complex, and large complex endings (Fig. 6.7). Type I fibers give rise to all four ending types, but type II fibers tend to give rise only to en passant and small bouton terminals. Although the morphology of each ending is relatively consistent within each ending group, there are variations with respect to the physiology and type of nerve fiber from which they arise.

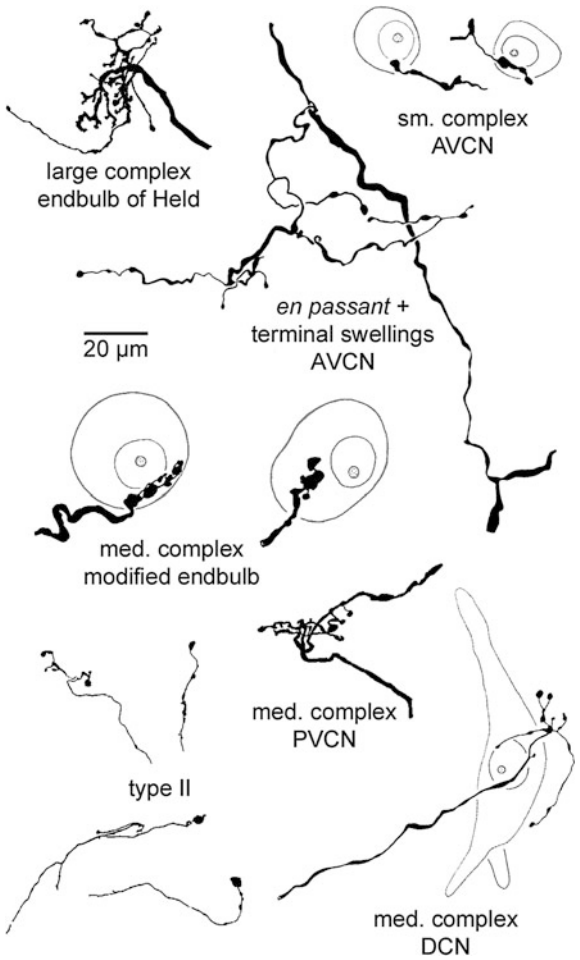

Fig. 6.7 Drawing-tube reconstructions of representative auditory nerve endings throughout the CN (Adapted from Fekete et al., 1984; Rouiller et al., 1986; Brown et al., 1988)

6.4.1 En Passant and Terminal Swellings

En passant swellings have been previously described as circumscribed enlargements located along the length of a fiber whose diameter is twice that of its parent axon branch or radiating collateral (Brown et al., 1988). Often they are rounded or oblong in shape, but in the cat some have also been described to have a more complex or "pedunculated" structure (Morgan et al., 1994). Type II fibers produce en passant swellings throughout the magnocellular neuropil of the CN and within the GCD lamina before terminating in the GCD. Swellings in the magnocellular core tend to have a smooth contour, whereas those along the lamina have been described as mostly angular and complex (Brown & Ledwith, 1990). Type II fibers give off few collaterals so the majority of these en passant boutons are located along its parent branch (Ryugo et al., 1991; Morgan et al., 1994). When studied with the electron microscope, many type II en passant swellings in the magnocellular core did not exhibit synaptic features (Ryugo et al., 1991). It is not clear to what extent en passant endings are nonsynaptic, or if this result is an artifact of tissue processing, degeneration, or evidence for mobile, transient swellings involved with organelle transport.

Small terminal boutons are defined similarly to en passant swellings, and are simple expansions ($\sim$5–7 μm^2) that reside at the terminus of an axon collateral. In combination with en passant swellings, they make up 94 % of swellings in the CN (Rouiller et al., 1986). Type I fibers make terminal endings more frequently throughout the CN when compared to type II fibers, which mostly terminate as small bouton endings in the GCD. Type I bouton terminals are predominately found within the neuropil, but are sometimes seen in close association with cell bodies, and are more frequently observed in the dorsal division. The size of these small endings can be correlated with SR. High-SR fibers give rise to slightly larger boutons (4.8 ± 0.14 μm^2) than low-SR fibers (3.1 ± 0.10 μm^2). High-SR fibers also produce more terminal boutons on their descending branch than their ascending branch, whereas low-SR fibers exhibit more small terminal boutons on their ascending branch (Rouiller et al., 1986). Morphological variations of type I terminals with respect to fiber CF have not been reported.

6.4.2 Medium Complex Endings

Medium-size complex endings are larger than terminal boutons, range in size from 12.9 to 125 μm^2 (Rouiller et al., 1986), and make up about 4 % of the auditory nerve ending population in the CN. They arise from collaterals of the main axon trunk, contacting a portion of the cell soma and terminating in a cluster of discrete swellings. Both ascending and descending branches give rise to these intermediate endings, but they are most often found stemming from the ascending branch. Type I high-SR fibers tend to have larger complex endings on average than low-SR fibers.

As with small bouton endings, high-SR fibers show a propensity to emit more medium-sized complex endings from the descending branch, whereas such endings from low-SR fibers are biased toward the ascending branch.

These medium complex endings contact the somata of spherical bushy cells and octopus cells, and terminate in the neuropil of layer II in the DCN. They are, however, most often found within the cochlear nerve root area where they form axosomatic contacts with globular bushy cells (Tolbert & Morest, 1982; Fekete et al., 1984). These endings have also been described as "modified endbulbs" (Harrison & Irving, 1966), owing to their resemblance to the larger endbulb of Held found in the anterior AVCN (see Sect. 6.4.3). One auditory nerve fiber may create two to four modified endbulbs along its length (Lorente de Nó, 1933b). Up to 50 modified endbulbs may contact a single globular bushy cell (Spirou et al., 1990; Rothman et al., 1993). Globular cells, in turn, send projections to the medial nucleus of the trapezoid body (Tolbert et al., 1982), delivering precisely timed signals required for sound localization computations in the superior olivary complex (Grothe et al., 2010). This relationship suggests that the structure of modified endbulbs and the nature of its association with globular bushy cells is crucial to its role in binaural localization.

6.4.3 Large Complex Endings: The Endbulb of Held

The largest ending created by primary auditory afferents is the endbulb of Held, which makes up approximately 2 % of the ending population in the CN (Rouiller et al., 1986). The endbulb was first described by Hans Held, (1893) in Golgi-stained tissue from kittens. It is one of the largest synaptic endings in the brain and every vertebrate species examined to date exhibits endbulbs at the tips of auditory nerve fibers (Fig. 6.8; Ryugo & Parks, 2003). This evolutionary conservation emphasizes the functional importance of this synaptic structure in early sound processing.

Endbulbs are found in the rostral portion of the AVCN, and typically emerge from the ascending parent branch of the auditory nerve, although a few endbulbs have been observed to spur from the root branch (Rouiller et al., 1986). The endbulb itself has a calyx-like appearance marked by the emergence of several thick, twisted branches that divide repeatedly to form an elaborate arborization of en passant and terminal swellings that clasp the postsynaptic spherical bushy cell. Up to three endbulbs may selectively contact a single bushy cell (Cant & Morest, 1979; Ryugo & Sento, 1991), although their arborizations do not interdigitate over the soma (Ryugo & Fekete, 1982); they maintain spatially separate domains and each endbulb contains up to 2000 release sites (Ryugo et al., 1996). Endbulb terminals have more than 1000 readily releasable vesicles and an average of more than 6000 voltage-gated Ca^{2+} channels on the presynaptic membrane, of which about half open during a single action potential, suggesting multiple voltage-gated Ca^{2+} channels influence the release of a single vesicle (Lin et al., 2011). These features allow the auditory nerve to transmit high rates of activity to the spherical

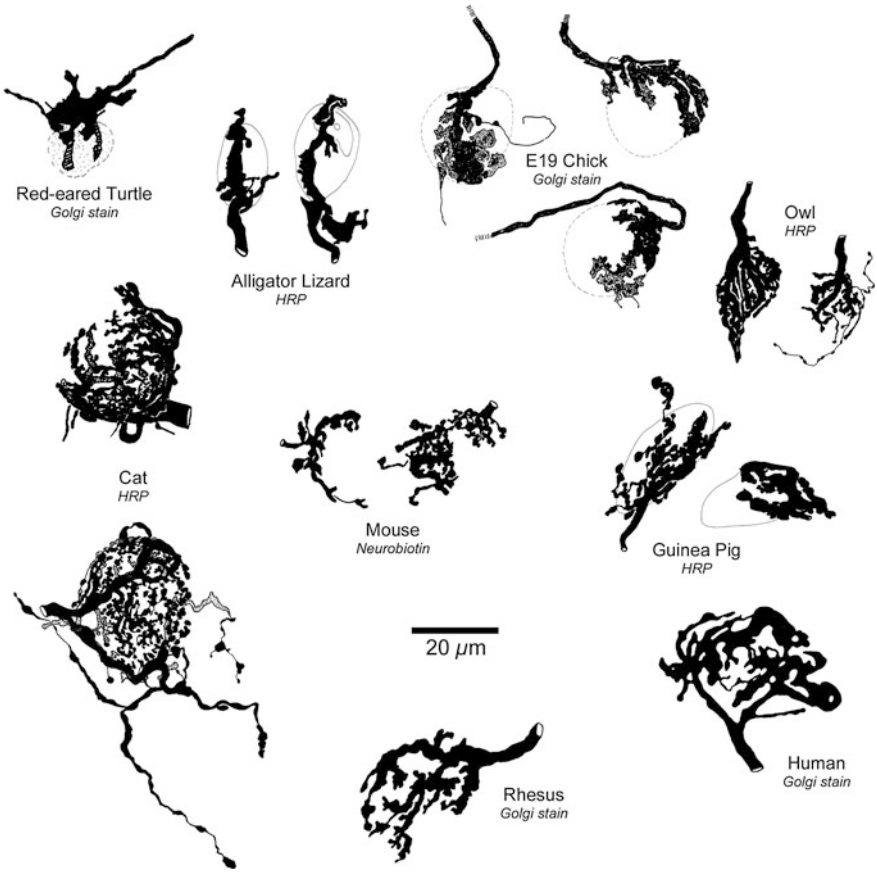

Fig. 6.8 Comparative view of endbulbs of Held from different terrestrial vertebrate species showing the evolutionary conservation of this large synapse (Adapted from Ryugo & Parks 2003)

bushy cell with great fidelity (Pfeiffer, 1966; Manis & Marx, 1991; Babalian et al., 2003). Spherical bushy cells project to the lateral and medial superior olivary nuclei (Cant & Casseday, 1986), where precision in signal timing is necessary for accurate sound localization (Grothe et al., 2010).

Endbulb morphology can be correlated with both the CF and SR of its parent axon. In the cat, type I fibers with CFs less than 4 kHz give rise to the largest endbulbs on average, whereas fibers with higher CFs produce slightly smaller endbulbs (Rouiller et al., 1986; Sento & Ryugo, 1989). High-SR endbulbs exhibit modest levels of branching with relatively large component swellings (Fig. 6.9). In contrast, low-SR endbulbs appear more elaborately branched with relatively small component swellings. When overall endbulb size is quantified by measuring its silhouette area, inconsistent results have been reported comparing high-SR and

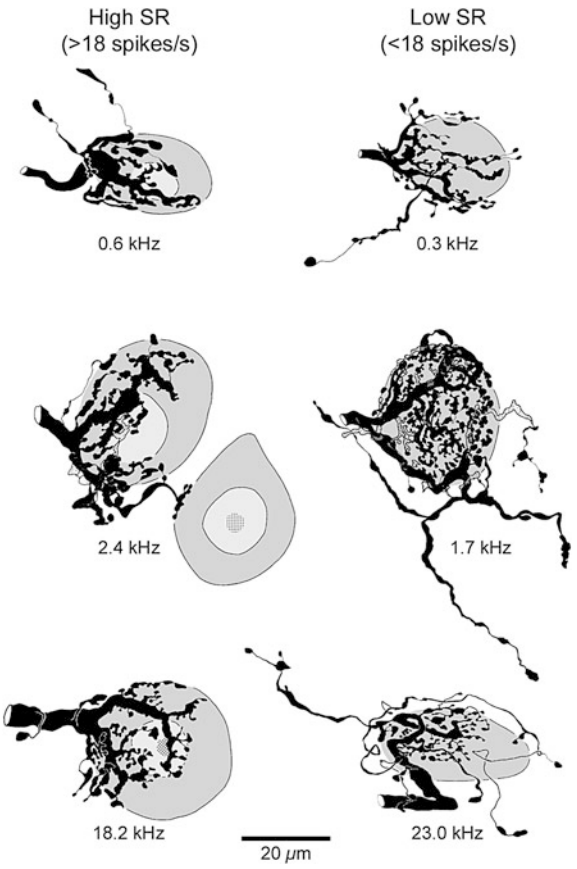

Fig. 6.9 Endbulbs of Held and activity-related morphology. The column on the left contains endbulbs from high-SR, low-threshold auditory nerve fibers; endbulbs on the right arise from low-SR, high-threshold fibers. *Left–right* pairs are approximately matched for CF. Endbulbs arising from low-SR fibers are more highly branched and elaborate compared to those of high-SR fibers. Such differences are observed even when pairs are matched in frequency sensitivity, implying the differences are due to activity differences (Adapted from Sento & Ryugo, 1989)

low-SR endbulbs. One study reported no differences in endbulb area (Sento & Ryugo, 1989), but a later study showed that high-SR endbulbs were significantly larger, even when matched for CF (Ryugo et al., 1996). However, differences in branching complexity were consistently confirmed by measuring fractal values: High-SR fibers have a form factor greater than 0.52 (no units), whereas low-SR endbulbs routinely fall below this value (Sento & Ryugo, 1989; Ryugo et al., 1996). A similar relationship between SR and endbulb morphology has also been observed in guinea pigs (Tsuji & Liberman, 1997), suggesting the differences in structural complexity reflect a reliable but as yet unknown specialization of function. Using metrics such as position, size, and form factor, it is therefore possible to estimate the CF and SR of an endbulb without physiological data.

Interestingly, endbulbs that converge onto the same bushy cell body share similar form factors, implying they are from the same SR group (Ryugo & Sento, 1991). Endbulbs may also form synapses with passing dendrites of neighboring cells, which often belong to other spherical bushy cells (Cant & Morest, 1979). These axodendritic contacts do not always originate from endbulbs sharing the

same SR as the primary axosomatic endings onto the cell (Ryugo & Sento, 1991). The function and influence of axodendritic endbulb synapses are unknown, but could be a way to disperse activity to other nearby cells.

6.4.4 *Ending Ultrastructure*

Synaptic terminals for both type I and type II fibers have similar general characteristics (Ryugo et al., 1991; Berglund et al., 1996). Although type II endings have fewer organelles compared to that of type I endings, all contain clear, round synaptic vesicles and mitochondria. Terminals also exhibit prominent asymmetrical postsynaptic densities (PSDs), which house receptors, transporters, ion channels, signal transduction proteins, and other molecular components necessary for transmission and cell adhesion. Type I fibers differ from type II fibers in that they tend to have large round vesicles (~50–60 nm diameter) associated with relatively small PSDs, whereas type II endings have small round vesicles (~40–50 nm diameter) associated with larger PSDs (Ryugo et al., 1991). Although the presence of round neurotransmitter vesicles following glutaraldehyde fixation is associated with excitatory neurotransmission (Uchizono, 1965), this difference in vesicle size might relate to other characteristics such as neurotransmitter type.

Some ultrastructural features of type I endings have been found to vary with SR, but others do not (Ryugo et al., 1993). In the cat, the synaptic vesicles of high-SR fibers are smaller (average diameter of 54.6 ± 8.9 nm), compared to those of low-SR fibers (55.9 ± 11.2 nm), but this difference is not statistically significant. The packing density of vesicles within the terminal was similar, as was the average length of the PSD. On the other hand, mitochondria were found to occupy approximately 25 % of the area of high-SR terminals, representing a 60 % increase compared to low-SR terminals. High-SR fibers also produce about 4.5 synapses per ending, compared to 1.3 per ending in low-SR fibers. The increase in mitochondrial content may be necessary to supply extra energy for the increased activity of high-SR fibers.

The ultrastructure of endbulbs of Held has been particularly well documented, owing to their large and readily identifiable appearance (Lenn & Reese, 1966; Ryugo & Sento, 1991; Ryugo et al., 1996). These terminals contain organelles typical of other type I fibers, and are distinguished by the presence of a convex, dome-shaped PSD (Fig. 6.10a). Although only 8–26 % of the membrane apposition of endbulbs is synaptic, endbulbs contain thousands of active zones (Ryugo & Sento, 1991), ensuring reliable synaptic transmission (Pfeiffer, 1966). PSDs of endbulbs vary with SR (Fig. 6.10b). Low-SR endbulbs produce PSDs that are larger but less curved than those from high-SR endbulbs (Ryugo et al., 1996). PSD size appears to be a feature of activity, which is consistent with observations in rats exposed to repetitive tones as a proxy for activity levels: Endbulbs from stimulated

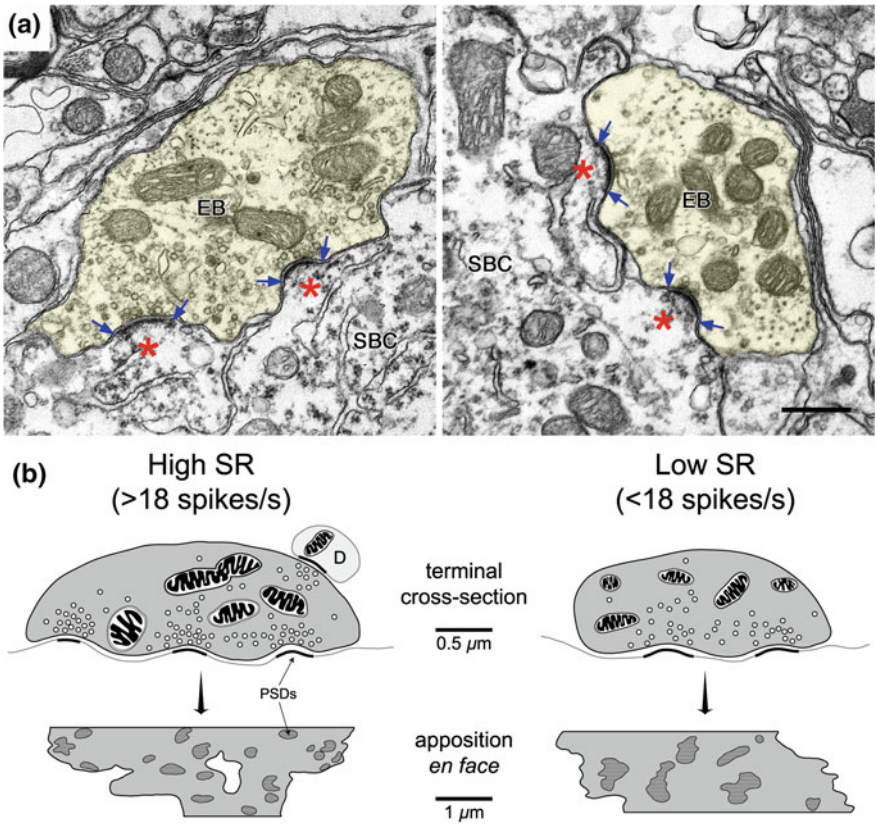

Fig. 6.10 Fine structure of endbulb synapses. **a** Electron micrographs through endbulbs of Held (*yellow shading*) from high-SR fibers in cat. PSDs (*asterisks*, delimited by *arrows*) are indicative of synaptic release sites and lie along the surface of the postsynaptic spherical bushy cells, evident by their dense, fuzzy appearance facing the synaptic cleft. Note especially the distinct dome-shaped PSDs at this synapse. Scale bar equals 0.5 μm (Adapted from O'Neil et al., 2010). **b** Schematic diagram highlighting structural features of endbulb of Held terminals with respect to fiber SR. Terminals on the left arise from high-SR, low-threshold auditory nerve fibers; terminals on the right arise from low-SR, high-threshold fibers. Cross sections through endbulb terminals (*top*) show intracellular features; lower figures are en face views of terminal appositions (*bold outline*) reconstructed from ultrathin sections (*horizontal lines*), showing synaptic area (*dark gray regions*). Low-SR fibers produce larger but fewer synapses and have smaller mitochondria. In contrast, endings of high-SR fibers express smaller but more numerous synapses, exhibit greater curvature of their postsynaptic densities, contain more synaptic vesicles, have larger mitochondria, and form more axodendritic (D) synapses (Adapted from Ryugo et al., 1996)

animals had smaller PSDs than those exposed to silence (Rees et al., 1985). It may be that small synapses increase synaptic efficiency for rapid and repetitive discharges by facilitating the diffusion of neurotransmitter away from the active zone.

6.5 Glutamate as the Neurotransmitter for Type I Spiral Ganglion Cells

The prime candidate for the excitatory neurotransmission of type I fibers is glutamate. It is known to facilitate rapid synaptic transmission (Raman & Trussell, 1992; Mosbacher et al., 1994), which would be ideal for mediating information transmission from the periphery to the central auditory system, particularly in pathways important for temporal sound coding. It has, however, been difficult to prove the presence of glutamate in nerve terminals because of its ubiquitous nature in the CN and difficulty in measuring its synaptic release. As such, studies have turned to immunohistochemistry to characterize its localization to type I terminals. Primary type I terminals containing large round vesicles have been stained positively with antibodies against glutamate, its precursor glutamine, and enzymes involved in glutamate metabolism (Hackney et al., 1996; Rubio & Juiz 1998). In addition, reduced immunolocalization of glutamate is seen in primary terminals that had been depleted of their vesicles by potassium-induced depolarization (Hackney et al., 1996). Virtually nothing is known about the neurotransmitter at central type II synapses.

The presence of glutamate at auditory nerve terminals is further supported by the localization of glutamatergic receptors in postsynaptic targets throughout the CN. Ionotropic α-amino-3-hydroxy-5-methyl-4-isoxazolepropionic acid (AMPA) receptors have rapid kinetics, with GluR3 and GluR4 subunits found to appose primary endings throughout the nucleus (Rubio & Wenthold, 1997; Wang et al., 1998). The GluR4 subunit is known for rapid gating (Mosbacher et al., 1994), facilitating high-fidelity synaptic transmission. The GluR2 subunit, typically associated with Ca^{2+} permeability, is found in dendritic spines postsynaptic to parallel fiber inputs in the DCN and in the basal dendrites of pyramidal cells postsynaptic to primary afferents (Gardner et al., 2001).

N-methyl-D-aspartate (NMDA) receptors have slower kinetics and are characterized by a voltage-dependent Ca^{2+} permeability, which is thought to mediate synaptic plasticity. The NR1 subunit is distributed throughout the CN, with other NMDA receptor subunits selectively distributed in different cell populations (Bilak et al., 1996; Petralia et al., 2000). NMDA receptor expression in the nucleus decreases with maturation (Isaacson & Walmsley, 1995; Futai et al., 2001), but still appears to play a role in the precise timing of synaptic transmission in bushy cells (Pliss et al., 2009). Metabotropic glutamate receptors have also been localized in the CN (Wright et al., 1996; Petralia et al., 2000), where second messenger activation might underlie long-term synaptic effects of acoustic responses.

Rapid glutamate signaling requires effective clearance of neurotransmitter from the synaptic cleft between bouts of release, which is achieved through a network of uptake and transporter molecules surrounding glutamatergic synapses (Bergles et al., 1999). It has been suggested such transporter molecules may reside within intracellular cisternae situated between primary endings and CN cells (Redd et al., 2000), which could be a mechanism for regulating synaptic strength (Turecek & Trussell, 2000). However, additional support for this idea is needed.

6.6 Plasticity

The development of the precise projection pattern of auditory nerve fibers into the CN largely emerges before hearing onset (reviewed by Appler & Goodrich, 2011), indicating the initial wiring plan occurs independent of sound-evoked activity. There is suggestive evidence, however, that changes in hearing status can modify this plan. In cats that have been ototoxically deafened prior to hearing onset, topographic projections of auditory nerve fibers into the CN are reported to be cochleotopically correct, but disproportionately broader than those seen in normal animals (Leake et al., 2008). This observation supports the idea that cochleotopy emerges independent of acoustic stimulation, but that such stimulation may be necessary for refinement of topographic precision.

The influence of SR on the morphology of endbulbs demonstrates that auditory nerve endings show activity-dependent influences on structure (Sento & Ryugo, 1989; Ryugo et al., 1996). Endbulbs of congenitally deaf cats exhibit significantly less branching and their PSDs become flattened and hypertrophied (Ryugo et al., 1997). Similar plastic changes to the PSD are also evident at synapses of modified endbulbs (Redd et al., 2000). That these alterations are influenced by primary afferent activity is further supported by observations in "hard-of-hearing" cats with elevated hearing thresholds, which show atrophic changes to the endbulb whose severity lies between those of normal and deaf subjects (Ryugo et al., 1998). Lastly, restoration of activity to the auditory nerve, in the form of electrical stimulation via a cochlear implant, has been observed to restore synapse morphology (Ryugo et al., 2005; O'Neil et al., 2010). These findings strongly support the idea that ending structure of auditory nerve fibers is under the influence of neural activity.

6.7 Summary

More than a century of scientific inquiry has revealed a complex organization in the delivery of acoustic information from the mammalian inner ear to the brain. Spiral ganglion neurons display a range of anatomical and physiological specializations for accurate encoding of sound features, and many of the characteristics observed in the periphery are reflected in the pattern of central projections of the auditory nerve into the CN. The dominant organizational principle of the auditory system is tonotopy, in which there is a topographic and systematic spatial ordering of frequency representation. Overlying this tonotopic organization is a second layer of complexity relating to the spontaneous discharge rate and sound intensity coding of spiral ganglion neurons. Different rates of activity result in different termination patterns, even within an isofrequency lamina, and can produce morphological differences in ending structure. Ending morphology and convergence also differ with respect to target cell types and physiological response properties in the CN, suggesting particular classes of connections are formed for representing different

aspects of the acoustic signal. Ultimately, neural activity initiated by the auditory nerve and sent along divergent, parallel pathways converges and recombines to form percepts of the sound environment.

Although researchers have made great strides in dissecting the intricacies of this pathway, many questions remain unanswered. Most of our understanding of central projections concerns type I auditory nerve fibers. The unmyelinated type II fibers remain an enigma of the auditory system. These latter neurons appear to adhere to the general topographic plan of type I afferents, yet we know next to nothing about their function. As neuroanatomical techniques continue to evolve, however, we may yet find ways to selectively target type II spiral ganglion neurons and unlock their secrets. Questions also linger about the segregation of high- and low-SR terminations: Endbulb analyses suggest that each bushy cell receives input from only one SR class. Does this segregated pattern of inputs extend to other cell types in the CN, and how does this facilitate sound processing? Along these lines, what is the function of the selective projection to the small cell cap? We also do not fully understand the ultrastructural diversity of primary afferent synapses: What is the functional significance of PSD size and shape with respect to spike activity? And why do PSDs of endbulbs exhibit a characteristic curvature? Knowledge of physiological attributes of neurons has advanced by the application of novel and sophisticated in vitro methods; likewise, neuroanatomy has experienced a renaissance through the application of molecular markers, transgenes, and imaging techniques. Researchers have the ability to genetically label or ablate specific cell types, seamlessly image large volumes of tissue with ultrastructural resolution, and automate the analysis of enormous datasets. We have come a long way from inferring connections on the basis of an affinity for silver on degenerating neurons. The strength of new techniques, however, lies in the strength of the question. Young researchers should find the field wide open with a vast array of questions where each answer prompts more questions.

Acknowledgments The authors gratefully acknowledge support from NHMRC grant 1009482, 1080652, and 1081478 Fairfax Foundation; Oticon Foundation; the Macquarie Development Group; and donations from Christian Vignes, Allen and Irene Moss, Hadyn and Sue Daw, Alan and Lynne Rydge, and Carol-Ann Kirkpatrick.

References

Alving, B. M., & Cowan, W. M. (1971). Some quantitative observations on the cochlear division of the eighth nerve in the squirrel monkey (*Saimiri sciureus*). *Brain Research*, 25(2), 229–239.

Anniko, M., & Arnesen, A. R. (1988). Cochlear nerve topography and fiber spectrum in the pigmented mouse. *Archives of Oto-Rhino-Laryngology*, 245(3), 155–159.

Appler, J. M., & Goodrich, L. V. (2011). Connecting the ear to the brain: Molecular mechanisms of auditory circuit assembly. *Progress in Neurobiology*, 93(4), 488–508.

Arnesen, A. R., & Osen, K. K. (1978). The cochlear nerve in the cat: Topography, cochleotopy, and fiber spectrum. *Journal of Comparative Neurology*, 178(4), 661–678.

Arnesen, A. R., Osen, K. K., & Mugnaini, E. (1978). Temporal and spatial sequence of anterograde degeneration in the cochlear nerve fibers of the cat. A light microscopic study. *Journal of Comparative Neurology*, 178(4), 679–696.

Babalian, A. L., Ryugo, D. K., & Rouiller, E. M. (2003). Discharge properties of identified cochlear nucleus neurons and auditory nerve fibers in response to repetitive electrical stimulation of the auditory nerve. *Experimental Brain Research*, 153(4), 452–460.

Bergles, D. E., Diamond, J. S., & Jahr, C. E. (1999). Clearance of glutamate inside the synapse and beyond. *Current Opinion in Neurobiology*, 9(3), 293–298.

Berglund, A. M., & Ryugo, D. K. (1986). A monoclonal antibody labels type II neurons of the spiral ganglion. *Brain Research*, 383(1–2), 327–332.

Berglund, A. M., & Ryugo, D. K. (1987). Hair cell innervation by spiral ganglion neurons in the mouse. *Journal of Comparative Neurology*, 255(4), 560–570.

Berglund, A. M., & Ryugo, D. K. (1991). Neurofilament antibodies and spiral ganglion neurons of the mammalian cochlea. *Journal of Comparative Neurology*, 306(3), 393–408.

Berglund, A. M., & Brown, M. C. (1994). Central trajectories of type II spiral ganglion cells from various cochlear regions in mice. *Hearing Research*, 75(1–2), 121–130.

Berglund, A. M., Benson, T. E., & Brown, M. C. (1996). Synapses from labeled type II axons in the mouse cochlear nucleus. *Hearing Research*, 94(1–2), 31–46.

Bilak, M. M., Bilak, S. R., & Morest, D. K. (1996). Differential expression of *N*-methyl-D-aspartate receptor in the cochlear nucleus of the mouse. *Neuroscience*, 75(4), 1075–1097.

Bourk, T. R., Mielcarz, J. P., & Norris, B. E. (1981). Tonotopic organization of the anteroventral cochlear nucleus of the cat. *Hearing Research*, 4(3–4), 215–241.

Brawer, J. R., Morest, D. K., & Kane, E. C. (1974). The neuronal architecture of the cochlear nucleus of the cat. *Journal of Comparative Neurology*, 155(3), 251–300.

Brown, M. C. (1987). Morphology of labeled afferent fibers in the guinea pig cochlea. *Journal of Comparative Neurology*, 260(4), 591–604.

Brown, M. C., & Ledwith, J. V. (1990). Projections of thin (type-II) and thick (type-I) auditory-nerve fibers into the cochlear nucleus of the mouse. *Hearing Research*, 49(1–3), 105–118.

Brown, M. C., Berglund, A. M., Kiang, N. Y., & Ryugo, D. K. (1988). Central trajectories of type II spiral ganglion neurons. *Journal of Comparative Neurology*, 278(4), 581–590.

Bruns, V., & Schmieszek, E. (1980). Cochlear innervation in the greater horseshoe bat: Demonstration of an acoustic fovea. *Hearing Research*, 3(1), 27–43.

Cant, N. B. (1992). The cochlear nucleus: Neuronal types and their synaptic organization. In D. B. Webster, A. N. Popper, & R. R. Fay (Eds.), *The mammalian auditory pathway: Neuroanatomy* (pp. 66–116). New York: Springer-Verlag.

Cant, N. B. (1993). The synaptic organization of the ventral cochlear nucleus of the cat: The peripheral cap of small cells. In M. A. Merchán, J. M. Juiz, D. A. Godfrey, & E. Mugnaini (Eds.), *The mammalian cochlear nuclei: Organization and function* (pp. 91–105). New York: Plenum Press.

Cant, N. B., & Morest, D. K. (1979). The bushy cells in the anteroventral cochlear nucleus of the cat. A study with the electron microscope. *Neuroscience*, 4(12), 1925–1945.

Cant, N. B., & Casseday, J. H. (1986). Projections from the anteroventral cochlear nucleus to the lateral and medial superior olivary nuclei. *Journal of Comparative Neurology*, 247(4), 457–476.

Chen, I., Limb, C. J., & Ryugo, D. K. (2010). The effect of cochlear-implant-mediated electrical stimulation on spiral ganglion cells in congenitally deaf white cats. *Journal of the Association for Research in Otolaryngology*, 11(4), 587–603.

Clopton, B. M., Winfield, J. A., & Flammino, F. J. (1974). Tonotopic organization: Review and analysis. *Brain Research*, 76(1), 1–20.

el Barbary, A. (1991). Auditory nerve of the normal and jaundiced rat. I. Spontaneous discharge rate and cochlear nerve histology. *Hearing Research*, 54(1), 75–90.

Evans, E. F. (1972). The frequency response and other properties of single fibres in the guinea-pig cochlear nerve. *Journal of Physiology*, 226(1), 263–287.

Evans, E. F., & Palmer, A. R. (1980). Relationship between the dynamic range of cochlear nerve fibers and their spontaneous activity. *Experimental Brain Research*, 40(1), 115–118.

Fay, R. R. (1988). *Hearing in vertebrates: A psychophysics databook*. Winnetka, IL: Hill-Fay Associates.

Fekete, D. M., Rouiller, E. M., Liberman, M. C., & Ryugo, D. K. (1984). The central projections of intracellularly labeled auditory nerve fibers in cats. *Journal of Comparative Neurology*, 229 (3), 432–450.

Feng, A. S., & Vater, M. (1985). Functional organization of the cochlear nucleus of rufous horseshoe bats (*Rhinolophus rouxi*): Frequencies and internal connections are arranged in slabs. *Journal of Comparative Neurology*, 235(4), 529–553.

Futai, K., Okada, M., Matsuyama, K., & Takahashi, T. (2001). High-fidelity transmission acquired via a developmental decrease in NMDA receptor expression at an auditory synapse. *Journal of Neuroscience*, 21(10), 3342–3349.

Gacek, R. R., & Rasmussen, G. L. (1961). Fiber analysis of the statoacoustic nerve of guinea pig, cat, and monkey. *Anatomical Record*, 139, 455–463.

Gardner, S. M., Trussell, L. O., & Oertel, D. (2001). Correlation of AMPA receptor subunit composition with synaptic input in the mammalian cochlear nuclei. *Journal of Neuroscience*, 21(18), 7428–7437.

Geisler, C. D., Deng, L., & Greenberg, S. R. (1985). Thresholds for primary auditory fibers using statistically defined criteria. *Journal of the Acoustical Society of America*, 77(3), 1102–1109.

Ghoshal, S., & Kim, D. O. (1996). Marginal shell of the anteroventral cochlear nucleus: Acoustically weakly-driven and not-driven units in the unanesthetized decerebrate cat. *Acta Oto-Laryngologica*, 116(2), 280–283.

Ghoshal, S., & Kim, D. O. (1997). Marginal shell of the anteroventral cochlear nucleus: Single-unit response properties in the unanesthetized decerebrate cat. *Journal of Neurophysiology*, 77(4), 2083–2097.

Godfrey, D. A., Kiang, N. Y., & Norris, B. E. (1975). Single unit activity in the posteroventral cochlear nucleus of the cat. *Journal of Comparative Neurology*, 162(2), 247–268.

Grothe, B., Pecka, M., & McAlpine, D. (2010). Mechanisms of sound localization in mammals. *Physiological Reviews*, 90(3), 983–1012.

Guild, S. R., Crowe, S. J., Bunch, C. C., & Polvogt, L. M. (1931). Correlations of differences in the density of innervation of the organ of Corti with differences in the acuity of hearing, including evidence as to the location in the human cochlea of the receptors for certain tones. *Acta Oto-Laryngologica*, 15(2–4), 269–308.

Hackney, C. M., Osen, K. K., Ottersen, O. P., StormMathisen, J., & Manjaly, G. (1996). Immunocytochemical evidence that glutamate is a neurotransmitter in the cochlear nerve: A quantitative study in the guinea-pig anteroventral cochlear nucleus. *European Journal of Neuroscience*, 8(1), 79–91.

Hafidi, A., Despres, G., & Romand, R. (1993). Ontogenesis of type II spiral ganglion neurons during development: Peripherin immunohistochemistry. *International Journal of Developmental Neuroscience*, 11(4), 507–512.

Harrison, J. M., & Irving, R. (1965). The anterior ventral cochlear nucleus. *Journal of Comparative Neurology*, 124, 15–41.

Harrison, J. M., & Irving, R. (1966). Ascending connections of the anterior ventral cochlear nucleus in the rat. *Journal of Comparative Neurology*, 126(1), 51–63.

Held, H. (1893). Die centrale Gehörleitung. *Archiv für Anatomie und Physiologie*, *Anatomische Abteilung*, 201–248.

Huang, L. C., Thorne, P. R., Housley, G. D., & Montgomery, J. M. (2007). Spatiotemporal definition of neurite outgrowth, refinement and retraction in the developing mouse cochlea. *Development*, 134(16), 2925–2933.

Isaacson, J. S., & Walmsley, B. (1995). Receptors underlying excitatory synaptic transmission in slices of the rat anteroventral cochlear nucleus. *Journal of Neurophysiology*, 73(3), 964–973.

Kaas, J. H. (1997). Topographic maps are fundamental to sensory processing. *Brain Research Bulletin*, 44(2), 107–112.

Kawase, T., & Liberman, M. C. (1992). Spatial organization of the auditory nerve according to spontaneous discharge rate. *Journal of Comparative Neurology*, 319(2), 312–318.

Keithley, E. M., & Schreiber, R. C. (1987). Frequency map of the spiral ganglion in the cat. *Journal of the Acoustical Society of America*, 81(4), 1036–1042.

Kiang, N. Y.-S., Watanabe, T., Thomas, E. C., & Clark, L. F. (1965). *Discharge patterns of single fibers in the cat's auditory nerve*. Cambridge, MA: MIT Press.

Kiang, N. Y.-S., Rho, J. M., Northrop, C. C., Liberman, M. C., & Ryugo, D. K. (1982). Hair-cell innervation by spiral ganglion cells in adult cats. *Science*, 217(4555), 175–177.

Kiang, N. Y.-S., Liberman, M. C., Gage, J. S., Northrup, C. C., Dodds, L. W., & Oliver, M. E. (1984). Afferent innervation of the mammalian cochlea. In L. Bolis, R. D. Keynes, & H. P. Maddrell (Eds.), *Comparative physiology of sensory systems* (pp. 143–161). Cambridge, UK: Cambridge University Press.

Kössl, M., & Vater, M. (1985). The cochlear frequency map of the mustache bat, *Pteronotus parnellii. Journal of Comparative Physiology A: Sensory*, *Neural*, *and Behavioral Physiology*, 157(5), 687–697.

Leake, P. A., & Snyder, R. L. (1989). Topographic organization of the central projections of the spiral ganglion in cats. *Journal of Comparative Neurology*, 281(4), 612–629.

Leake, P. A., Hradek, G. T., Bonham, B. H., & Snyder, R. L. (2008). Topography of auditory nerve projections to the cochlear nucleus in cats after neonatal deafness and electrical stimulation by a cochlear implant. *Journal of the Association for Research in Otolaryngology*, 9(3), 349–372.

Lenn, N. J., & Reese, T. S. (1966). The fine structure of nerve endings in the nucleus of the trapezoid body and the ventral cochlear nucleus. *American Journal of Anatomy*, 118(2), 375–389.

Liberman, M. C. (1978). Auditory-nerve response from cats raised in a low-noise chamber. *Journal of the Acoustical Society of America*, 63(2), 442–455.

Liberman, M. C. (1982a). Single-neuron labeling in the cat auditory nerve. *Science*, 216(4551), 1239–1241.

Liberman, M. C. (1982b). The cochlear frequency map for the cat: Labeling auditory-nerve fibers of known characteristic frequency. *Journal of the Acoustical Society of America*, 72(5), 1441–1449.

Liberman, M. C. (1991). Central projections of auditory-nerve fibers of differing spontaneous rate. I. Anteroventral cochlear nucleus. *Journal of Comparative Neurology*, 313(2), 240–258.

Liberman, M. C. (1993). Central projections of auditory nerve fibers of differing spontaneous rate, II: Posteroventral and dorsal cochlear nuclei. *Journal of Comparative Neurology*, 327(1), 17–36.

Liberman, M. C., & Oliver, M. E. (1984). Morphometry of intracellularly labeled neurons of the auditory nerve: Correlations with functional properties. *Journal of Comparative Neurology*, 223(2), 163–176.

Lin, K. H., Oleskevich, S., & Taschenberger, H. (2011). Presynaptic Ca^{2+} influx and vesicle exocytosis at the mouse endbulb of Held: A comparison of two auditory nerve terminals. *Journal of Physiology*, 589(Pt 17), 4301–4320.

Lorente de Nó, R. (1933a). Anatomy of the eighth nerve: The central projections of the nerve endings of the internal ear. *Laryngoscope*, 43(1), 1–38.

Lorente de Nó, R. (1933b). Anatomy of the eighth nerve. III. General plan of structure of the primary cochlear nuclei. *Laryngoscope*, 43(4), 327–350.

Lorente de Nó, R. (1937). Symposium: Neural mechanism of hearing: I. Anatomy and physiology. (b) The sensory endings in the cochlea. *Laryngoscope*, 47(6), 373–377.

Lorente de Nó, R. (1976). Some unresolved problems concerning the cochlear nerve. *Annals of Otology*, *Rhinology and Laryngology*, 85(Supplement 34), 1–28.

Lorente de Nó, R. (1981). *The primary acoustic nuclei*. New York: Raven Press.

Manis, P. B., & Marx, S. O. (1991). Outward currents in isolated ventral cochlear nucleus neurons. *Journal of Neuroscience*, 11(9), 2865–2880.

May, B. J., Huang, A., Le Prell, G., & Hienz, R. D. (1996). Vowel formant frequency discrimination in cats: Comparison of auditory nerve representations and psychophysical thresholds. *Auditory Neuroscience*, 3(2), 135–162.

Merchan-Perez, A., & Liberman, M. C. (1996). Ultrastructural differences among afferent synapses on cochlear hair cells: Correlations with spontaneous discharge rate. *Journal of Comparative Neurology*, 371(2), 208–221.

Morgan, Y. V., Ryugo, D. K., & Brown, M. C. (1994). Central trajectories of type II (thin) fibers of the auditory nerve in cats. *Hearing Research*, 79(1–2), 74–82.

Mosbacher, J., Schoepfer, R., Monyer, H., Burnashev, N., Seeburg, P. H., & Ruppersberg, J. P. (1994). A molecular determinant for submillisecond desensitization in glutamate receptors. *Science*, 266(5187), 1059–1062.

Mugnaini, E., Warr, W. B., & Osen, K. K. (1980). Distribution and light microscopic features of granule cells in the cochlear nuclei of cat, rat, and mouse. *Journal of Comparative Neurology*, 191(4), 581–606.

Müller, M. (1990). Quantitative comparison of frequency representation in the auditory brainstem nuclei of the gerbil, *Pachyuromys duprasi*. *Experimental Brain Research*, 81(1), 140–149.

Müller, M. (1991). Frequency representation in the rat cochlea. *Hearing Research*, 51(2), 247–254.

Müller, M. (1996). The cochlear place-frequency map of the adult and developing Mongolian gerbil. *Hearing Research*, 94(1–2), 148–156.

Müller, M., Laube, B., Burda, H., & Bruns, V. (1992). Structure and function of the cochlea in the African mole rat (*Cryptomys hottentotus*): Evidence for a low frequency acoustic fovea. *Journal of Comparative Physiology A: Sensory*, *Neural*, *and Behavioral Physiology*, 171(4), 469–476.

Müller, M., Wess, F. P., & Bruns, V. (1993). Cochlear place-frequency map in the marsupial *Monodelphis domestica*. *Hearing Research*, 67(1–2), 198–202.

Müller, M., von Hunerbein, K., Hoidis, S., & Smolders, J. W. (2005). A physiological place-frequency map of the cochlea in the CBA/J mouse. *Hearing Research*, 202(1–2), 63–73.

Müller, M., Hoidis, S., & Smolders, J. W. (2010). A physiological frequency-position map of the chinchilla cochlea. *Hearing Research*, 268(1–2), 184–193.

Muniak, M. A., Rivas, A., Montey, K. L., May, B. J., Francis, H. W., & Ryugo, D. K. (2013). 3D model of frequency representation in the cochlear nucleus of the CBA/J mouse. *Journal of Comparative Neurology*, 521(7), 1510–1532.

Nadol, J. B., Jr. (1988). Quantification of human spiral ganglion cells by serial section reconstruction and segmental density estimates. *American Journal of Otolaryngology*, 9(2), 47–51.

Nayagam, B. A., Muniak, M. A., & Ryugo, D. K. (2011). The spiral ganglion: Connecting the peripheral and central auditory systems. *Hearing Research*, 278(1–2), 2–20.

Ohlemiller, K. K., & Echteler, S. M. (1990). Functional correlates of characteristic frequency in single cochlear nerve fibers of the Mongolian gerbil. *Journal of Comparative Physiology A: Sensory*, *Neural*, *and Behavioral Physiology*, 167(3), 329–338.

O'Neil, J. N., Limb, C. J., Baker, C. A., & Ryugo, D. K. (2010). Bilateral effects of unilateral cochlear implantation in congenitally deaf cats. *Journal of Comparative Neurology*, 518(12), 2382–2404.

Osen, K. K. (1969). Cytoarchitecture of the cochlear nuclei in the cat. *Journal of Comparative Neurology*, 136(4), 453–484.

Osen, K. K. (1970). Course and termination of the primary afferents in the cochlear nuclei of the cat: An experimental anatomical study. *Archives Italiennes de Biologie*, 108(1), 21–51.

Petralia, R. S., Rubio, M. E., Wang, Y. X., & Wenthold, R. J. (2000). Differential distribution of glutamate receptors in the cochlear nuclei. *Hearing Research*, 147(1–2), 59–69.

Pfeiffer, R. R. (1966). Anteroventral cochlear nucleus: Wave forms of extracellularly recorded spike potentials. *Science*, 154(3749), 667–668.

Pliss, L., Yang, H., & Xu-Friedman, M. A. (2009). Context-dependent effects of NMDA receptors on precise timing information at the endbulb of Held in the cochlear nucleus. *Journal of Neurophysiology*, 102(5), 2627–2637.

Poljak, S. (1927). Über den allgemeinen Bauplan des Gehörsystems und über seine Bedeutung für die Physiologie, für die Klinik und für die Psychologie. *Zeitschrift für die Gesamte Neurologie und Psychiatrie*, 110(1), 1–49.

Raman, I. M., & Trussell, L. O. (1992). The kinetics of the response to glutamate and kainate in neurons of the avian cochlear nucleus. *Neuron*, 9(1), 173–186.

Ramón y Cajal, S. (1909). *Histologie du système nerveux de l'homme et des vertébrés*. Paris: Maloine.

Rasmussen, A. T. (1940). Studies of the VIIIth cranial nerve of man. *Laryngoscope*, 50, 67–83.

Redd, E. E., Pongstaporn, T., & Ryugo, D. K. (2000). The effects of congenital deafness on auditory nerve synapses and globular bushy cells in cats. *Hearing Research*, 147(1–2), 160–174.

Rees, S., Guldner, F. H., & Aitkin, L. (1985). Activity dependent plasticity of postsynaptic density structure in the ventral cochlear nucleus of the rat. *Brain Research*, 325(1–2), 370–374.

Rhode, W. S., & Smith, P. H. (1986). Encoding timing and intensity in the ventral cochlear nucleus of the cat. *Journal of Neurophysiology*, 56(2), 261–286.

Robertson, D. (1984). Horseradish peroxidase injection of physiologically characterized afferent and efferent neurones in the guinea pig spiral ganglion. *Hearing Research*, 15(2), 113–121.

Rose, J. E., Galambos, R., & Hughes, J. R. (1959). Microelectrode studies of the cochlear nuclei of the cat. *Bulletin of the Johns Hopkins Hospital*, 104(5), 211–251.

Rothman, J. S., Young, E. D., & Manis, P. B. (1993). Convergence of auditory nerve fibers onto bushy cells in the ventral cochlear nucleus: Implications of a computational model. *Journal of Neurophysiology*, 70(6), 2562–2583.

Rouiller, E. M., Cronin-Schreiber, R., Fekete, D. M., & Ryugo, D. K. (1986). The central projections of intracellularly labeled auditory nerve fibers in cats: An analysis of terminal morphology. *Journal of Comparative Neurology*, 249(2), 261–278.

Rubio, M. E., & Wenthold, R. J. (1997). Glutamate receptors are selectively targeted to postsynaptic sites in neurons. *Neuron*, 18(6), 939–950.

Rubio, M. E., & Juiz, J. M. (1998). Chemical anatomy of excitatory endings in the dorsal cochlear nucleus of the rat: Differential synaptic distribution of aspartate aminotransferase, glutamate, and vesicular zinc. *Journal of Comparative Neurology*, 399(3), 341–358.

Ryugo, D. K. (2008). Projections of low spontaneous rate, high threshold auditory nerve fibers to the small cell cap of the cochlear nucleus in cats. *Neuroscience*, 154(1), 114–126.

Ryugo, D. K., & Fekete, D. M. (1982). Morphology of primary axosomatic endings in the anteroventral cochlear nucleus of the cat: A study of the endbulbs of Held. *Journal of Comparative Neurology*, 210(3), 239–257.

Ryugo, D. K., & Sento, S. (1991). Synaptic connections of the auditory nerve in cats: Relationship between endbulbs of Held and spherical bushy cells. *Journal of Comparative Neurology*, 305 (1), 35–48.

Ryugo, D. K., & May, S. K. (1993). The projections of intracellularly labeled auditory nerve fibers to the dorsal cochlear nucleus of cats. *Journal of Comparative Neurology*, 329(1), 20–35.

Ryugo, D. K., & Parks, T. N. (2003). Primary innervation of the avian and mammalian cochlear nucleus. *Brain Research Bulletin*, 60(5–6), 435–456.

Ryugo, D. K., Dodds, L. W., Benson, T. E., & Kiang, N. Y. (1991). Unmyelinated axons of the auditory nerve in cats. *Journal of Comparative Neurology*, 308(2), 209–223.

Ryugo, D. K., Wright, D. D., & Pongstaporn, T. (1993). Ultrastructural analysis of synaptic endings of auditory nerve fibers in cats: Correlations with spontaneous discharge rate. In M. A. Merchán, J. M. Juiz, D. A. Godfrey & E. Mugnaini (Eds.), *The mammalian cochlear nuclei: Organization and function* (pp. 65–74). New York: Plenum Press.

Ryugo, D. K., Wu, M. M., & Pongstaporn, T. (1996). Activity-related features of synapse morphology: A study of endbulbs of Held. *Journal of Comparative Neurology*, 365(1), 141–158.

Ryugo, D. K., Pongstaporn, T., Huchton, D. M., & Niparko, J. K. (1997). Ultrastructural analysis of primary endings in deaf white cats: Morphologic alterations in endbulbs of Held. *Journal of Comparative Neurology*, 385(2), 230–244.

Ryugo, D. K., Rosenbaum, B. T., Kim, P. J., Niparko, J. K., & Saada, A. A. (1998). Single unit recordings in the auditory nerve of congenitally deaf white cats: Morphological correlates in the cochlea and cochlear nucleus. *Journal of Comparative Neurology*, 397(4), 532–548.

Ryugo, D. K., Kretzmer, E. A., & Niparko, J. K. (2005). Restoration of auditory nerve synapses in cats by cochlear implants. *Science*, 310(5753), 1490–1492.

Sachs, M. B., & Young, E. D. (1979). Encoding of steady-state vowels in the auditory nerve: Representation in terms of discharge rate. *Journal of the Acoustical Society of America*, 66(2), 470–479.

Sando, I. (1965). The anatomical interrelationships of the cochlear nerve fibers. *Acta Oto-Laryngologica*, 59, 417–436.

Schmiedt, R. A. (1989). Spontaneous rates, thresholds and tuning of auditory-nerve fibers in the gerbil: Comparisons to cat data. *Hearing Research*, 42(1), 23–35.

Sento, S., & Ryugo, D. K. (1989). Endbulbs of Held and spherical bushy cells in cats: Morphological correlates with physiological properties. *Journal of Comparative Neurology*, 280(4), 553–562.

Spirou, G. A., Brownell, W. E., & Zidanic, M. (1990). Recordings from cat trapezoid body and HRP labeling of globular bushy cell axons. *Journal of Neurophysiology*, 63(5), 1169–1190.

Spirou, G. A., May, B. J., Wright, D. D., & Ryugo, D. K. (1993). Frequency organization of the dorsal cochlear nucleus in cats. *Journal of Comparative Neurology*, 329(1), 36–52.

Spoendlin, H. (1971). Degeneration behaviour of the cochlear nerve. *Archiv für Klinische und Experimentelle Ohren-, Nasen- und Kehlkopfheilkunde*, 200(4), 275–291.

Spoendlin, H. (1973). The innervation of the cochlea receptor. In A. R. Møller (Ed.), *Mechanisms in hearing* (pp. 185–229). New York: Academic Press.

Stevens, S. S., & Davis, H. (1938). *Hearing: Its psychology and physiology*. New York: John Wiley & Sons.

Taberner, A. M., & Liberman, M. C. (2005). Response properties of single auditory nerve fibers in the mouse. *Journal of Neurophysiology*, 93(1), 557–569.

Tolbert, L. P., & Morest, D. K. (1982). The neuronal architecture of the anteroventral cochlear nucleus of the cat in the region of the cochlear nerve root: electron microscopy. *Neuroscience*, 7(12), 3053–3067.

Tolbert, L. P., Morest, D. K., & Yurgelun-Todd, D. A. (1982). The neuronal architecture of the anteroventral cochlear nucleus of the cat in the region of the cochlear nerve root: Horseradish peroxidase labelling of identified cell types. *Neuroscience*, 7(12), 3031–3052.

Tsuji, J., & Liberman, M. C. (1997). Intracellular labeling of auditory nerve fibers in guinea pig: Central and peripheral projections. *Journal of Comparative Neurology*, 381(2), 188–202.

Turecek, R., & Trussell, L. O. (2000). Control of synaptic depression by glutamate transporters. *Journal of Neuroscience*, 20(5), 2054–2063.

Uchizono, K. (1965). Characteristics of excitatory and inhibitory synapses in the central nervous system of the cat. *Nature*, 207(997), 642–643.

Vater, M., Feng, A. S., & Betz, M. (1985). An HRP-study of the frequency-place map of the horseshoe bat cochlea: Morphological correlates of the sharp tuning to a narrow frequency band. *Journal of Comparative Physiology A: Sensory, Neural, and Behavioral Physiology*, 157 (5), 671–686.

von Békésy, G. (1960). *Experiments in hearing*. New York: McGraw-Hill.

Wang, Y. X., Wenthold, R. J., Ottersen, O. P., & Petralia, R. S. (1998). Endbulb synapses in the anteroventral cochlear nucleus express a specific subset of AMPA-type glutamate receptor subunits. *Journal of Neuroscience*, 18(3), 1148–1160.

Webster, D. B. (1971). Projection of the cochlea to cochlear nuclei in Merriam's kangaroo rat. *Journal of Comparative Neurology*, 143(3), 323–340.

Weisz, C., Glowatzki, E., & Fuchs, P. (2009). The postsynaptic function of type II cochlear afferents. *Nature*, 461(7267), 1126–1129.

Weisz, C. J., Lehar, M., Hiel, H., Glowatzki, E., & Fuchs, P. A. (2012). Synaptic transfer from outer hair cells to type II afferent fibers in the rat cochlea. *Journal of Neuroscience*, 32(28), 9528–9536.

Wever, E. G., McCormick, J. G., Palin, J., & Ridgway, S. H. (1971). The cochlea of the dolphin, *Tursiops truncatus*: Hair cells and ganglion cells. *Proceedings of the National Academy of Sciences of the USA*, 68(12), 2908–2912.

Wright, D. D., Blackstone, C. D., Huganir, R. L., & Ryugo, D. K. (1996). Immunocytochemical localization of the mGluR1 alpha metabotropic glutamate receptor in the dorsal cochlear nucleus. *Journal of Comparative Neurology*, 364(4), 729–745.

Ye, Y., Machado, D. G., & Kim, D. O. (2000). Projection of the marginal shell of the anteroventral cochlear nucleus to olivocochlear neurons in the cat. *Journal of Comparative Neurology*, 420(1), 127–138.

Chapter 7
The Spiral Ganglion in an Out-of-Body Experience: A Brief History of in Vitro Studies of the Spiral Ganglion

Steven H. Green, Erin M. Bailey, Jonathan C. Kopelovich and Marlan R. Hansen

Keywords Axon · Axon guidance · Cell culture · Chemotropic factor · Cochlea · Extracellular matrix · Hair cell · Historical review · Neurite · Neurotrophic factor · Organotypic culture · Spiral ganglion neuron · Synapse · Tissue culture

7.1 Introduction

> The more closely we examine a natural object, the more beautiful, exciting and mysterious it becomes…a single living cell is much more beautiful and improbable than the solar system.
>
> – Honor Bridget Fell (lecture notes on "The cell as an individual," Bangor, March 1962)

As of this writing, we are approaching the 90th anniversary of the first successful long-term in vitro study of the cochlea by Honor Fell. Throughout most of this time, the principal use of cochlear or spiral ganglion cultures has been to facilitate the study of cochlear development: cell differentiation, structural and physiological maturation, and innervation of the sensory cells. More recently, use of spiral ganglion cultures has been extended to additional issues. One of these is neuronal survival in response to neurotrophic factors and electrical activity. The goal of such

S.H. Green (✉) · E.M. Bailey
Department of Biology, University of Iowa, 52242 Iowa City, IA, USA
e-mail: steven-green@uiowa.edu

E.M. Bailey
e-mail: erin-bailey@uiowa.edu

J.C. Kopelovich
Department of Otolaryngology, Children's Hospital Colorado and University of Colorado School of Medicine, 13123 East 16th Avenue, 80045 Aurora, CO, USA
e-mail: jokopelo@gmail.com

M.R. Hansen
Department of Otolaryngology—HNS, University of Iowa, 52242 Iowa City, IA, USA
e-mail: marlan-hansen@uiowa.edu

A. Dabdoub et al. (eds.), *The Primary Auditory Neurons of the Mammalian Cochlea*, Springer Handbook of Auditory Research 52,
DOI 10.1007/978-1-4939-3031-9_7

studies is to prevent degeneration or death of spiral ganglion neurons (SGNs) in the hearing impaired and so improve efficacy of cochlear implants. A second topic is degeneration or death of SGNs following direct trauma, particularly noise-induced excitotoxic trauma. The goal of these studies is to identify means of protecting the SGNs and their synapses on hair cells following trauma and to promote regeneration.

The success of these studies has been due to clever exploitation of several technical innovations. Culture conditions have been improved by the use of serum and specialized culture media and the use of more physiological substrate materials. Electrophysiological methods have been applied. Microscopy has advanced from conventional optical methods to the use of electron, conventional fluorescence, and confocal microscopy, greatly improving observations of fixed or live cochlear cultures. Highly specialized substrates have allowed study of SGN axon guidance by chemical or physical cues. There is a greatly expanded repertoire of small-molecule pharmacological agents, peptide growth and trophic factors targeting surface molecules and receptors, and cell membrane–permeable reagents for modulating intracellular signaling and regulation. Further expanding the range of experimental manipulations has been the introduction of molecular and genetic techniques, including gene transfer by transfection or viral transduction and culture of cells or organs from transgenic mice.

This chapter provides a historical overview of the development of cochlear and spiral ganglion culture techniques, focusing on two different types of preparations: organotypic cultures that seek to maintain the in vivo histological structure and cellular relationships and dissociated cultures in which the ganglion is enzymatically and mechanically dissociated and cultures are monolayers of dissociated cells. The chapter notes some key experiments exemplifying the application of increasingly sophisticated experimental and observational culture techniques to research goals, focusing on the following areas of inquiry: development of cochlear innervation; physiology and cell biology of SGNs; trauma to SGNs and protection; and prevention of SGN degeneration in hearing impaired individuals. The intent is that readers will obtain from this overview ideas for experimental approaches applicable to their own research questions.

7.2 Organotypic Preparations

7.2.1 Early Studies: Cultured Chick Embryo Otocysts

In explant and organotypic preparations, tissue is cultured intact without cell dissociation. In organotypic preparations, in particular, an entire organ is cultured intact, maintaining cell–cell interactions and associations among tissues. The earliest studies of the inner ear using organotypic cultures were developmental studies. These took advantage of the accessibility of cultured tissue to light microscopy to observe differentiation and morphogenesis of the live inner ear. Bright-field or phase-contrast microscopy were used (see Fig. 7.1a, b for examples). As was typical

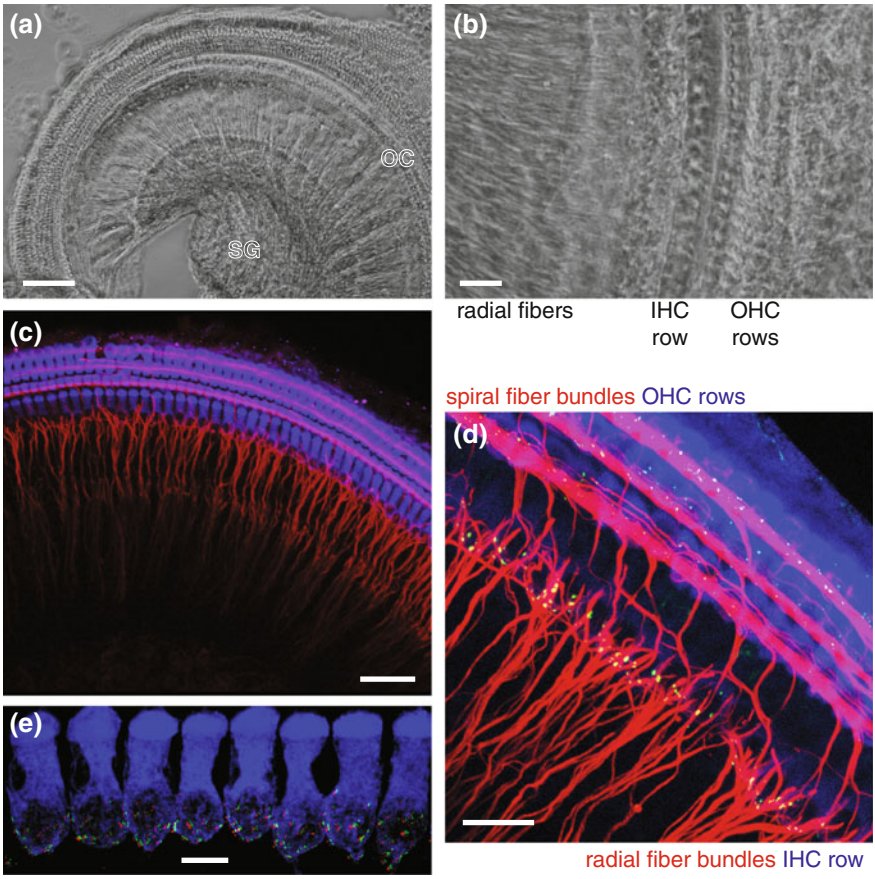

Fig. 7.1 Organotypic cochlear culture. **a**, **b** Fixed cochlear wholemounts viewed at low (**a**, scale bar = 100 µm) and high (**b**, scale bar = 20 µm) magnification. Spiral ganglion (SG) and organ of Corti (OC) are indicated in **a**. Structural elements shown in **b** are indicated by adjacent text under the panel. **c** A *z*-projection of a confocal image stack of a fixed organotypic cochlear culture at low magnification (scale bar = 50 µm) labeled with anti-HMW neurofilament (NF200, *red*) to show SGNs and their axons and with anti-myosin 7A (*blue*) to show hair cells. **d** A *z*-projection of a confocal image stack of a fixed organotypic cochlear culture at high magnification (scale bar = 20 µm) labeled, as in **c**, to show axons and hair cells and with anti-PSD95 (*green*) to show synapses. Structural elements shown in **d** are indicated by adjacent text above and below the panel. **e** A *z*-projection of a confocal image stack of a fixed organotypic cochlear culture at high magnification (scale bar = 10 µm) labeled to show hair cells (anti-myosin 6/7A mix, *blue*), presynaptic ribbons (anti-CtBP2, *red*), and postsynaptic densities (anti-PSD95, *green*)

then for many studies of organogenesis, chick embryo preparations were first used for in vitro studies of inner ear development, specifically, cultured otocysts. Honor Fell, a principal pioneer of organ culture, was also the first to succeed in long-term (up to 14-day) culture of otocysts (Fell, 1928). She described histogenesis of the sensory epithelium and differentiation of hair cells and supporting cells.

Cell and tissue cultures require incubation in medium containing all essential nutrients at physiological temperature and with physiological CO_2 concentration. For organotypic preparations there are additional considerations. The organ must attach itself to the substrate for support. The thickness of the cultured tissue impedes exchange of O_2, CO_2, nutrients, and metabolites between the culture medium and the tissue. The methods first described by Fell for successful maintenance of organ cultures were used by other investigators with little modification for several decades. To facilitate gas, nutrient, and metabolite exchange, the organ is placed on a porous substrate to which it can attach. In the earliest studies, substrates used included cellulose sponge, sterile fabric, paper, cellophane, or gelfoam. Fell's original protocol for culture of organs, including the otocyst, was to place the embryonic organ on a small clot formed of chick embryo extract and plasma at the bottom of a small glass centrifuge tube. The organ was transferred daily to a fresh medium and could be fixed and stained for microscopic observation.

Lawrence and Merchant (1953) followed up on Fell's study some 25 years later with observations of chick embryo otocyst development and differentiation in vitro. Their method was similar to that of Fell but they added a porous substrate—cellulose sponge—to which the otocyst attached to prevent the tissue from rounding up and so obtained morphogenesis more closely resembling that in vivo. They described development of all vestibular and auditory sensory epithelia. Lawrence and Merchant also reported culture of a single mammalian (rat) otic vesicle using a protocol similar to that used for the chick and observed formation of a cochlear duct and organ of Corti. However, Lawrence and Merchant did not observe full organ and cell differentiation in their chick or rat preparations and did not culture their preparations longer than 8 days.

Starting in 1956, Friedmann produced a series of publications investigating development of the chick embryo inner ear in organotypic culture. Friedmann's initial publication (Friedmann, 1956) used methods similar Fell's but the culture was on a clot in a shallow watch glass rather than in a centrifuge tube. He also included more of the surrounding mesenchyme when dissecting out the otocyst. The result was an even greater degree of differentiation of the auditory and vestibular sensory epithelia than that observed by Fell.

Up to this time, observations had focused on differentiation of the sensory structures but not innervation. Indeed, Lawrence and Merchant (1953) described efforts to remove the statoacoustic ganglion (SAG) "to have the vesicle as clean as possible." (In early embryonic development, the presumptive auditory and vestibular neurons form a continuous mass of cells, the statoacoustic ganglion, also termed the cochleovestibular ganglion [CVG] that later subdivides into the spiral ganglion and Scarpa's/vestibular ganglion.) The first ultrastructural study of inner ear development in vitro was that of Friedmann (1959) and this paper also provided the first observation of innervation in vitro, describing nonmyelinated axons extending past supporting cells into the sensory epithelium and forming contacts on hair cells. In this study Friedmann cultured the otocysts on small convex strips of voile, a sheer fabric, which supported the otocyst while allowing gas exchange.

A further technical refinement was that of Reinecke et al. (1960), who cultured chick embryo otocysts supported on cellophane strips between two glass coverslips in a Rose perfusion chamber—which allowed light microscopic observation of development of the live otocyst over periods of time up to 3–4 months after which the otocysts were fixed and stained. Reinecke et al. described differentiation of the sensory epithelium and, in cultures in which the neurons were included, growth of axons into the sensory epithelium.

Subsequent studies by Friedmann and Bird (1967), Friedmann (1968, 1969) and by Orr (1965) described in more detail innervation and synaptogenesis in organotypic cultures of chick embryo otocysts. Orr's (1965) paper was the first to focus specifically on the acoustic ganglion. In this, she used a culture system similar to that of Reinecke et al. (1960) in that the otocysts were placed directly on a coverslip in a chamber. The cultures were maintained for up to several months, observed and photographed daily by light microscopy, and ultimately fixed and stained. Orr further systematically tested a variety of culture media with respect to cell survival, neuronal differentiation, and myelination. She described neuronal differentiation and subsequent degeneration of a small number of neurons, rapid growth of axons into the sensory epithelium, and gradual myelination of a subset of the axons by Schwann cells.

Friedmann's studies pioneered the use of electron microscopy to study otocyst development in vitro. He described cell differentiation on the ultrastructural level including that of hair cells and neurons. Friedmann showed in vitro differentiation of characteristically morphologically distinct types of hair cells in auditory and vestibular sensory epithelia and "type I" and "type II" hair cells in vestibular epithelium. He showed presynaptic structures including vesicles and "bars" (ribbons) adjacent to postsynaptic terminals. With regard to neurons, he showed differentiation into morphologically distinct types resembling type I (myelinated), type II, and "intermediate" neurons adjacent to the sensory epithelia and formation of "cup-shaped" or "chalice-shaped" calyx and "bud-shaped" bouton postsynaptic terminals on, respectively type I and type II vestibular hair cells. These events closely resemble in vivo development.

Subsequent technical developments are the use of "tissue culture" dishes—dishes made of specially treated plastic to promote cell adhesion—in many cases coated with extracellular matrix proteins such as laminin, and improved formulations of culture media and non-serum supplements that have permitted some reduction in the serum concentration—although supplementation of the media with serum levels 10 % or greater has remained a common feature of organotypic cochlear cultures. This is in spite of variations among laboratories in substrates and culture media adopted for particular experimental requirements.

As methods of observation of fixed preparations have developed, fluorescence microscopy has been added to bright-field microscopy with conventional stains and to electron microscopy. Fluorescence microscopy allows selective visualization of specific molecules and cell types by immunofluorescence (see Fig. 7.1d, e for examples) or expression of appropriate fluorescent proteins. As noted previously, the earliest studies used bright-field and phase-contrast microscopy (Fig. 7.1a, b) to

observe cell movements in live preparations. More recently, differential interference contrast is used and, as described in Sect. 7.2.6, expression of fluorescent proteins in live cells.

7.2.2 *Innervation of the Mammalian Organ of Corti in Vitro*

Early efforts at long-term organotypic culture of the mammalian otocyst were unsuccessful in that significant degeneration occurred in the tissue (Lawrence & Merchant, 1953), so studies prior to and throughout the 1960s were restricted to chick embryos. A comprehensive and systematic effort by Van De Water and Ruben (1971) resulted in identification of culture conditions for mouse embryonic otocysts that maintained healthy tissue and permitted morphogenesis and cell differentiation of sensorineural elements of the inner ear, including afferent synapses on hair cells (Van de Water et al., 1973; Van De Water & Heywood, 1976). Use of mammalian cultures, including human spiral ganglion cultures (Rask-Andersen et al., 2005), allows studies more directly relevant to human health as well as exploitation of mouse genetic technology—first in studies of genetically deaf mice and, later, of transgenic mice.

These early studies highlighted requirements for proper support and substrate and for serum-supplemented medium for organotypic culture of the cochlea from avian and mammalian sources. With appropriate culture conditions, key aspects of in vivo sensorineural development, including neuronal and hair cell differentiation and synaptogenesis, proceed in vitro. Moreover, the early studies showed that conditions can be identified for microscopic observation of live tissue over time as well as for fixation and labeling of the tissue at any time. These laid the foundation for use of in vitro approaches to investigate important questions regarding innervation of the organ of Corti and the related trophic and inductive interactions among SGNs and cells of the organ of Corti.

7.2.3 *Trophic Support of Spiral Ganglion Neurons by the Organ of Corti*

A hypothesis that peripheral auditory or vestibular neurons depend on inner ear sensory epithelium for trophic support is consistent with the observation that postnatal destruction of hair cells with an aminoglycoside antibiotic results in a gradual degeneration and death of the spiral ganglion neurons in vivo (Spoendlin, 1975). Asking whether this is also the case during development and determining the mechanism, required experiments with organotypic cultures. It should be noted that at the time of these observations, neurotrophic factors other than the nerve growth factor (NGF)—which does not play a role in the cochlea (Green et al., 2012)—had not yet been characterized, although by the early 1980s there was increasing

evidence that neurotrophic factors other than NGF existed and could exert trophic or tropic influence on neurons (Barde et al., 1983).

Ard et al. (1985) tested the trophic effect of their peripheral and central targets on the survival of chick embryo cochleovestibular ganglion neurons in vitro. Explants consisting only of SAG showed relatively poor neuronal survival even in serum-supplemented and elevated potassium medium. In contrast, organotypic explants consisting of SAG with otocyst or SAG with medulla or SAG with both otocyst and medulla showed greatly increased neuronal survival. The otocyst alone provided better trophic support than did the medulla alone, but the presence of both otocyst and medulla did not increase survival significantly over otocyst alone. These experiments indicated that some neurotrophic factor(s) are available to SAG neurons from both pre- and postsynaptic sources but with additional factor(s) available only from the presynaptic sensory epithelium. Experiments in which the ganglion and otocyst were first separated from each other and then co-cultured suggested that the trophic factor is either not diffusible or, if so, operates at close range.

Experiments with mouse embryo otocysts and ganglia cultured for two weeks on hydroxyethylmethacrylate hydrogels (Zhou & Van de Water, 1987) showed results comparable to the experiments with chick embryos. In explants consisting of ganglion with attached sensory epithelium, ganglion with attached hindbrain, or ganglion with attached sensory epithelium and hindbrain, neuronal survival was evident as was axon growth into the epithelium and the hindbrain tissue. Neuronal survival was approximately equal in these three types of explants; there was no indication of better trophic support by the sensory epithelium than by the hindbrain as had been observed with chick embryo explants (Ard et al., 1985). In contrast, neuronal survival in explants consisting only of the ganglion was less than 20 % of that in ganglion with a pre- or postsynaptic target. Thus, both pre- and postsynaptic targets provide neurotrophic support to the cochleovestibular neurons.

Although these experiments could not identify the neurotrophic factors involved —a work still in progress—they did show that such factors exist and provided valuable information on their range and relative efficacy. Soon after the neurotrophic factors brain-derived neurotrohic factor (BDNF) and neurotrophin 3(NT-3) were discovered and shown to be expressed in inner ear sensory epithelium (Pirvola et al., 1992; Ylikoski et al., 1993), experiments using chick embryo SAG explants showed that BDNF and NT-3 were trophic to SAG neurons and promoted neurite outgrowth (Avila et al., 1993). Subsequent experiments, described in Sect. 7.3.3, used dissociated spiral ganglion cultures to identify neurotrophic factors—for example, NT-3, BDNF, GDNF—*sufficient* to support SGN survival (Malgrange et al., 1996; Hegarty et al., 1997). Studies showing that these factors promote SGN survival in vivo are summarized by Fritzsch et al. in Chap. 3. Experiments testing whether some of these factors are *necessary* for SGN survival, at least in development, have been performed using knockout mice in which the genes encoding BDNF or NT-3 or their receptors have been genetically deleted; these experiments are also discussed by Fritzsch et al. in Chap. 3.

Barclay et al. (2011) used cultures from P1–P7 mice maintained on polylysine-coated tissue culture plastic; explant cultures consisting of an isolated

portion of the spiral ganglion or organotypic cultures consisting of a portion of the spiral ganglion attached to the corresponding portion of the organ of Corti, with innervation remaining intact. Addition of BDNF promoted SGN survival. In the absence of added BDNF, survival of SGNs in isolated ganglia was poor; in organotypic cultures, the presence of organ of Corti appeared to result in rescue of type II, but not of type I, SGNs. However, Wang and Green (2011) did not detect SGN death over a longer culture time in P5 rat organotypic cochlear cultures similarly consisting of organ of Corti and associated ganglion. Poor SGN survival in some cultures may therefore be an artifact of the culture conditions, which can be demanding for organotypic cultures. The Wang and Green study included higher serum concentrations and culture on laminin, a more physiological substrate, which may be necessary for SGN survival in organotypic explants.

7.2.4 *Trophic/Inductive Effects of the SGNs on the OC*

Experimental manipulations of organotypic culture and co-culture systems were used to establish that there is a trophic effect of inner ear sensory epithelium on SAG neurons. Similar methods can be used to ask the reverse: Is innervation necessary for survival or differentiation of hair cells? Some early studies using chick embryo otocysts suggested that development of the sensory epithelium and differentiation of hair cells is improved by the presence in the explant of SAG tissue (Friedmann, 1968; Orr, 1968). This may be related to deficiencies in the culture conditions or to differences between avian and mammalian cultures. Van de Water (1976) compared organotypic cultures of embryonic mouse otocysts that either contained or did not contain SAG and found no difference between them in morphology of the organ of Corti, of vestibular sensory epithelia, and of the hair cells. These were cultured on tissue culture plastic with a high (20 %) serum concentration. This latter study implies that initial differentiation of inner ear sensory structures during embryonic development is independent of innervation but again implies that cell survival and differentiation in organ cultures is sensitive to culture conditions, especially substrate and serum concentration.

7.2.5 *Guidance Factors for Spiral Ganglion Neurite Growth in the Cochlea*

Organotypic cultures have been used to determine whether inner ear sensory epithelium can provide neurite guidance for neurons. Evidence that otocyst sensory epithelium can provide a chemotropic signal that attracts SAG neurites from a

distance was shown in experiments with organotypic cultures (Van De Water & Ruben 1983, 1984). In these experiments, otocysts from 11-, 12.5-, or 14-day mouse embryos, either including or lacking the ganglion, were cultured on filters in tissue culture wells adjacent to an isolated SAG. All otocysts that included a ganglion had innervation of the sensory epithelium showing that a local guidance signal was produced by the sensory epithelium. Otocysts lacking a ganglion taken from 11- and 12.5-day mouse embryos were innervated, showing that they could release a signal that attracted neurites from the separate SAG. However, otocysts from 14-day mouse embryos were unable to attract neurites from a separate SAG, implying that the chemotropic signal is available only during the time when innervation normally occurs but is not produced later. Electron microscopic observations of the vestibular sensory epithelium confirmed formation of synapses between hair cells and those neurites attracted to the otocyst (Anniko & Van de Water, 1986).

Bianchi and Cohan (1991) used chick embryo otocysts co-cultured with SAG neurons and confirmed the presence of an otocyst-derived factor that promoted neurite growth from SAG neurons. Moreover, production of the factor by the otocyst declined as development progressed from embryonic day 4 to day 13, consistent with the observation of a developmental decline in production of a chemotropic factor by mouse otocysts from embryonic day 11 to day 14 (Van de Water & Ruben, 1984). Bianchi and Cohan further showed (Bianchi & Cohan, 1993) that the factor was not one of the neurotrophic factors identified by that time —that is, not a neurotrophin or CNTF—and elicited responses only in SAG neurons and not in other peripheral neurons. More recently, this otocyst-derived chemotropic factor has been identified by Bank et al. (2012) as the inflammatory cytokine macrophage migration inhibitory factor (MIF), which promotes neurite growth from chick and from mouse SAG neurons. The MIF receptor, CD74, is present on embryonic SAG neurons and on adult mouse SGNs (Bank et al., 2012).

Another important example of the use of in vitro techniques to investigate guidance of SGN axons is investigation of the role of ephrin–Eph signaling (Cramer, 2005; Coate & Kelley, 2013). Both ephrin to Eph ("forward") signaling and Eph to ephrin ("reverse") signaling are typically repulsive to axons, contributing to axon guidance by preventing axons from growing toward inappropriate targets. Expression of Ephs and ephrins has been investigated during embryonic development in chick (Siddiqui & Cramer, 2005) and mammalian (van Heumen et al., 2000) cochleae. Although the patterns of expression differ among chick, mouse, and guinea pig (van Heumen et al., 2000), the patterns suggest Eph to ephrin "reverse" signaling as a repulsive cue for cochlear neuron axon guidance in the chick and the mouse.

This possibility was tested directly by experimentally manipulating ephrin signaling in vitro. Chick SAG neurons express ephrin-B1 and activating these receptors on cultured SAG neurons with soluble EphB–Fc fusion proteins inhibited neurite growth (Bianchi & Gray, 2002). Mouse SGNs express ephrin-B2 and ephrin-B3, both of which interact with EphA4, which is expressed in fibroblasts of

the spiral ligament and presumptive osseous spiral lamina (van Heumen et al., 2000). Brors et al. (2003) showed that EphA4 does indeed provide a repulsive cue to SGN axons, using mouse spiral ganglion explants cultured in tissue culture wells coated with stripes of different molecules: SGN neurites were repelled by EphA4-containing stripes. Coate et al. (2012) further showed, using co-cultures of SGNs with otic mesenchyme, that reducing EphA4 expression (by knockdown of the transcription factor Pou3f4) resulted in a failure of the otic mesenchyme to promote fasciculation of SGN neurites. Addition of soluble EphA4–Fc fusion proteins to the culture restored fasciculation. These experiments suggest that EphA4 in otic mesenchyme, particularly in the presumptive osseous spiral lamina, repels SGN peripheral axons, forcing them to fasciculate. For reasons not yet explained, fasciculation of these axons is necessary for normal synaptogenesis on inner hair cells (IHCs; Coate et al., 2012).

Brugeaud et al. (2014) showed that a known chemorepulsive cue, Repulsive Guidance Molecule A (RGMa), is expressed in the mouse inner ear throughout development as well as postnatally. Addition of a blocking antibody for RGMa to postnatal organ of Corti–SGN co-cultures increased the number of synapses formed between hair cells and SGN neurites and accelerated the maturation of SGN neurite morphology.

7.2.6 *Direct Observation of Spiral Ganglion Neurite Growth in the Cochlea*

As summarized in Sect. 7.2.1, direct observation of innervation of sensory epithelium in embryonic otocysts in vitro was accomplished more than half a century ago (Reinecke et al., 1960; Orr, 1965). However, the behavior of individual axons and growth cones cannot be easily observed by conventional light microscopy. The axons are bundled into fascicles in which individual axons are difficult to distinguish. Also the borders of all of the other cell types—for example, epithelial, mesenchymal, glial—in an organotypic explant obscure the thin axons in unlabeled live tissue. An elegant use of mouse genetics, combined with an innovative modification of organotypic culture, was used by Appler et al. (2013) to observe the behavior of live axons in the developing cochlea. They expressed a fluorescent protein, eGFP or tdTomato, selectively in neurons using a Cre recombinase driven by a neuron-specific promoter. Expression of the fluorescent protein only in neurons allows clear visualization of live axons in organotypic cultures by confocal microscopy without interference from other cell types. Appler et al. dissected embryonic cochleae from the transgenic mice and cultured them in serum-containing medium on filter paper in a glass-bottom (coverslip thickness) culture dish. This allowed continuous confocal imaging over many hours through a small hole in the paper over which the cochlea was placed.

An example of the use of these methods was the demonstration of aberrant axon trajectories in SGNs lacking the transcription factor Gata3. Normally, SGN axons grow from the ganglion toward the sensory epithelium with little deviation from a straight radial path. Time-lapse observation of live axons shows that for SGNs lacking Gata3 the axon trajectories clearly deviate from a radial direction and may exhibit occasional turns rather than being straight (Appler et al., 2013). The conclusion is that this transcription factor regulates expression of genes required in SGNs for sensing axon guidance cues normally used to attract SGNs to the sensory epithelium and form synapses. Further studies (Yu et al., 2013b) have shown that the transcription factor MafB acts downstream of Gata3, in particular in regulating gene expression required for normal synapse formation on IHCs. It is not yet known whether these are related to chemotropic cues explored in the studies summarized in Sect. 7.2.5, for example, macrophage MIF (Bank et al., 2012).

A further innovation is to use a "leaky" promoter (Druckenbrod & Goodrich, 2014) that results in expression of the fluorescent protein in only a small random subset of SGNs. This "sparse" labeling facilitates time-lapse observations of individual axons, even in fascicles, using culture and confocal microscopy methods like those used by Appler et al. (2013). Preliminary observations using such methods show that SGN axons initially grow rapidly through the mesenchyme toward the organ of Corti and fasciculate with the earliest emerging axons. On reaching the organ of Corti, the axons slow their growth and exhibit exploratory behavior with transient branching and contacts with inner and outer hair cells (OHCs). These dynamic changes in growth cone behavior indicate different guidance cues in different regions of the cochlea along the axon's path. Axon growth can be observed in live cultured SGNs from species other than mouse by expression of fluorescent proteins from genes introduced into the SGNs by transfection or viral transduction (Atkinson et al., 2011).

7.2.7 *Regional Specification of SGN Physiological Phenotype*

SGNs exhibit heterogeneity in several physiological and cellular characteristics, which have been reviewed (Davis & Liu, 2011; Green et al., 2012) and discussed by Davis and Crozier in Chap. 4. These include significant differences along the tonotopic (base to apex) axis in the cochlea. As summarized in these reviews, apical and basal SGNs can differ in aspects of membrane electrophysiology, expression of voltage-gated ion channels including K^+ channels and Ca^{2+} channels, expression of α-amino-3-hydroxy-5-methyl-4-isoxazolepropionic acid (AMPA)-type glutamate receptor subunit types and expression of some presynaptic proteins. To test the hypothesis that SGN regional identity along the tonotopic axis is induced by factors in the corresponding region of the organ of Corti, organotypic explants of apical or basal organ of Corti were co-cultured with explants of apical or basal spiral ganglion in immediate proximity (Flores-Otero et al., 2007). Because these physiological

properties that differ among SGNs are relevant to their function in hearing, cultures in these studies were made from neonatal, as opposed to embryonic, cochleae. The tissues were cultured in tissue culture wells in serum-containing medium.

By these means, Flores-Otero et al. demonstrated that apical organ of Corti induced an apical phenotype in SGNs—higher synaptophysin immunoreactivity—in a NT-3–dependent manner; conversely, basal organ of Corti induced a basal phenotype in SGNs—that is, higher GluA2/3 immunoreactivity—in a BDNF-dependent manner. Addition of NT-3 to cultured spiral ganglion neurons induced an apical phenotype in SGNs while addition of BDNF induced a basal phenotype with respect to membrane electrophysiological properties, expression of voltage-gated channels and AMPA-type glutamate receptors, and expression of presynaptic proteins (Adamson et al., 2002a; Zhou et al., 2005; Flores-Otero et al., 2007). This is consistent with the higher level of NT-3 expression in the apical organ of Corti relative to the basal in postnatal mice (Sugawara et al., 2007).

7.2.8 Regeneration: Studies of Postnatal Cultures

The studies summarized in Sects. 7.2.2–7.2.7 pertain to aspects of the development of cochlear innervation and have largely been confined to embryonic tissue. More recently, studies have been initiated using organotypic cultures from postnatal mice or rats to investigate trauma that affects cochlear innervation and regeneration of innervation after such trauma. Organotypic culture of postnatal cochleae poses an additional challenge relative to embryonic cochleae: more care is required in the dissection because of the tougher surrounding bone and connective tissue. This is not much of a problem in the first postnatal week as the bone has not yet ossified. Starting in the second postnatal week, dissection of a completely intact and undistorted explant in which all cells remain viable in long-term culture becomes increasingly difficult with increasing age. For this reason, current studies of postnatal organotypic cochlear explant cultures or cochlear tissue co-cultures have generally used mouse or rat pups in the first postnatal week.

Organotypic culture of postnatal cochlea was initially described by Sobkowicz et al. (1975), and the methods she developed have been reviewed in detail (Sobkowicz et al., 1993). These investigators cultured intact cochlear explants from neonatal mice consisting of the organ of Corti with a portion of attached spiral ganglion for up to 27 days, although not all SGNs survived that long and intact morphology of the explant was generally not retained for more than 2 weeks. Nevertheless, they observed a normal pattern of innervation by surviving SGNs, with both radial and spiral fiber bundles. Innervation of the apex was completed, indicating that neurite growth continued in vitro.

In the protocol used by Sobkowicz et al. (1975), the culture medium contained a high proportion of serum (initially 40 %). The sensory elements and spiral ganglia were removed intact but cut into pieces prior to plating to obtain segments that do not coil in the culture dish and that adhere well to the substrate. The explants were

cultured on glass coverslips coated with collagen (predominantly type I collagen), a substrate commonly used in cell culture. More recent studies have used similar methods with glass coverslips coated with extracellular matrix components, although laminin has proved more appropriate than type I collagen (Parker et al., 2010; Wang & Green, 2011; Tong et al., 2013) and is now generally used. In this regard, it should be noted that cochlear basal laminae are rich in laminin and collagen IV (Santi & Johnson, 2013).

Culture on a glass coverslip allows the specimen to be labeled and then observed on a microscope with an inverted stage without being moved or disturbed, thus preserving intact morphology. Sobkowicz et al. (1975) used bright-field microscopy with compatible staining, relying primarily on silver staining optimal for labeling neurons and axons. Culture on glass coverslips is also optimal for imaging by current methods of confocal microscopy. Sobkowicz et al. (1975), Rose et al. 1977) described fibers emerging from the SGN somata, projecting peripherally to the organ of Corti in radial fascicles, and becoming myelinated. These studies reported that most of the neurons were unipolar, retaining only the radially projecting processes, indicating that the centrally directed axons degenerated after the auditory nerve was severed when the cochlea was dissected and placed in culture. However, subsequent studies have shown that with proper culture conditions central axons are preserved and become myelinated with time in culture (Sobkowicz et al., 1993).

After methods for culturing postnatal cochleae were developed, studies followed on the consequences of trauma and possibility of regeneration (Rose et al., 1977; Sobkowicz & Slapnick, 1992). These described the consequences to SGN peripheral axons of mechanical injury to the explant that occurred in the culture. After displacement of the hair cells that did not result in severing the axons, the axons increased in length, presumably to relieve the tension due to the mechanical stretch, but retained the original connections. Greater displacements that caused the axons to become "disconnected"—typically breaking near the base of the hair cell — resulted in many axons growing freely, at a high rate, and in a manner apparently unrestricted by the sensory epithelium. These axons tended to extend radially past the sensory epithelium and then take apparently random paths (Rose et al., 1977). In a study using electron microscopy that focused primarily on rapid responses—within 4 h—following mechanical disruption of axons in neonatal mouse cochleae after 3 days in culture, Sobkowicz and Slapnick (1992) observed that growth cones of regenerating axons that were close to hair cells did form synapses on the hair cells. "Orphan" ribbons could be observed in the hair cells, apparently due to failure of many axons to regenerate synapses although the number of regenerated synapses was not counted in the study.

Although such an injury does not reflect typical inner ear trauma or pathology, the results are informative about the capacity of postnatal SGNs to grow neurites or even reestablish connections with hair cells. The results imply that, after trauma sufficient to sever their axons or disconnect the axons from hair cells, the damaged ends of axons of postnatal SGNs are able to acquire growth cones and elongate. However, the observation that many, if not most, axons grow past the sensory epithelium and do not track to hair cells, implies that postnatal sensory epithelium

does not provide cues sufficient to guide the axons back to the hair cells or to regenerate synapses on the hair cells. Such a conclusion is consistent with the in vitro studies of chemotropic signaling, discussed in Sect. 7.2.5, showing that the sensory epithelium provides a chemoattractant signal to SAG neurons during embryonic development when innervation is occurring but that this signal is not present in late embryonic sensory epithelium. Nevertheless, synapse regeneration is evidently possible if the growing axon does encounter a hair cell.

7.2.9 *Excitotoxic Trauma to Cochlear Synapses and Relevance to Noise Trauma*

Disconnection of SGNs from hair cells in vivo can be the result of what, unfortunately, may be a very common type of trauma: noise trauma. Pujol et al. (1985), Puel et al. (1995) showed that intracochlear perfusion with the non–*N*-methyl-D-aspartate (NMDA) glutamate receptor agonist kainic acid (KA) caused swelling and degeneration of synapses on IHCs or "synaptopathy," a type of excitotoxic trauma. Spoendlin (1971) and Pujol, Puel, and colleagues (Puel et al., 1998) noted similar swelling and loss of synapses on IHCs as a consequence of noise trauma. These observations suggested that noise damage to synapses is excitotoxic, that is, loud sound causes excessive release of the excitatory neurotransmitter glutamate from hair cells, which causes excitotoxic trauma to the synapses. In support of this hypothesis, the damage to synapses occurring after noise is prevented by kynurenic acid, a nonselective ionotropic glutamate receptor antagonist (Puel et al., 1998) while inhibition of glutamate reuptake, which increases exposure of the synapses to glutamate, exacerbates damage (Hakuba et al., 2000). Kujawa and Liberman (2006, 2009) quantified the consequences of such "moderate" noise levels and showed a reduction in the number of synapses on IHCs (OHCs do not appear to be affected.) Comparable results were found in guinea pigs (Lin et al., 2011). This could explain the observation that "moderate" noise levels, which do not destroy hair cells nor cause a permanent threshold shift, may nevertheless cause permanent hearing impairment and damage to the cochlea.

Pujol, Puel, and colleagues reported synapse regeneration in vivo after excitotoxic trauma (Puel et al., 1995) or after noise (Puel et al., 1998). This is consistent with the previous in vitro experiments (Sobkowicz & Slapnick, 1992) that suggested there was some capability of synapse regeneration after damage in vitro if the regenerating axon was in close proximity to the hair cell, as it would be after excitotoxic damage to the postsynaptic terminal. All of these observations of synapse regeneration were made by electron microscopy, making it difficult to quantify the extent of regeneration. Confocal microscopy with immunofluorescent detection of synaptic proteins allows detection of all synapses on many hair cells in a single image stack, facilitating quantitation. Using confocal microscopy, Kujawa,

Liberman, and colleagues did not detect any increase in the number of synapses on IHCs in vivo starting 3 days after noise exposure (Kujawa & Liberman, 2009).

To determine whether synapse regeneration can occur and what neurotrophic factors might promote regeneration, Wang and Green (2011) used an in vitro system that facilitates experimental analysis of excitotoxic trauma to cochlear synapses (Fig. 7.1). The methods used were similar to those originally used by Sobkowicz and colleagues to produce intact organotypic cochlear explant cultures containing a portion of the organ of Corti and the attached portion of spiral ganglion (Sobkowicz et al., 1975, 1993). Because synapses had to be counted, care was taken to ensure that the explant was intact with all cells present and viable and all synapses maintained. Neonatal rat or mouse pups were used (Wang & Green, 2013). Explants were cultured on cover glasses coated with polyornithine and laminin, in medium containing 20 % serum to improve viability. The explants were placed with the basilar membrane side down in the well, as this assists in getting them to flatten and adhere to the substrate, so preserving the morphology of the explant. Most of the medium was removed for 1–2 h, leaving only a thin film ($\sim$50 μL) on the explant, a step that has been shown to promote attachment (Parker et al., 2010). Firm attachment to the cover glass allowed labeling and confocal microscope imaging without moving the specimen, which would risk physically distorting it. Excitotoxic trauma is accomplished by exposure to the glutamate agonist KA. This recapitulates key features of excitotoxic or noise-induced synaptopathy in vivo, in particular loss of most synapses on IHCs but with those on OHCs unaffected (Pujol et al., 1985; Kujawa & Liberman, 2009). Excitotoxic trauma in vitro, like that in vivo (Puel et al., 1994), is mediated by non–NMDA-type glutamate receptors: exposure to KA in vitro results in almost complete loss of synapses, whereas inclusion of NMDA with KA has no additional effect (Wang & Green, 2011).

In this in vitro system, a limited degree of reinnervation and synapse regeneration can be detected after excitotoxic trauma, restoring approximately 12 % of synapses by 72 h post-trauma (Wang & Green, 2011). “Orphan” ribbons were found in the hair cells, presumably as a result of the persistence of ribbons in the absence of complete reinnervation, an observation made previously by Sobkowicz and Slapnick (1992). Addition of neurotrophins—NT-3 or BDNF—to the culture increases the number of synapses up to 43 % of the pre-trauma number. The endogenous NT-3 produced by the hair cells appears to be crucial for synapse regeneration on IHCs after excitotoxic trauma (Wang & Green, 2011, 2013).

In summary, use of this organotypic culture system has shown that reinnervation and synapse regeneration is possible, at least in neonatal rodents, after excitotoxic trauma has destroyed innervation of IHCs. It has also revealed dependence of reinnervation on neurotrophic factors, particularly NT-3. There is also potential for this system to be used to investigate the mechanism of excitotoxicity. Experiments using this or similar organotypic cochlear explant culture systems may be useful for prevention or recovery from noise damage.

7.2.10 Reinnervation After Replacement of Lost Hair Cells or SGNs

Prevention of excitotoxic/noise-induced synaptopathy or reinnervation after synaptopathy are situations in which in vitro studies of cochlear synapse regeneration may result in therapeutic benefits in the near future. Looking further into the future, one can envision at least two potential situations in which synapse formation on hair cells in adults will also be a necessary therapeutic goal. One is innervation of new hair cells derived from gene or stem cell therapy to replace lost hair cells (Kesser & Lalwani, 2009). The second is innervation of existing hair cells by SGNs regenerated from gene or stem cell therapy described by Nayagam and Edge in Chap. 9.

Data from the studies summarized in Sect. 7.2.8 indicate that synapse formation is possible in the postnatal rodent cochlea and can be investigated in vitro using organotypic cultures. Further support for this possibility is derived from more recent studies using co-cultured explants. Flores-Otero et al. (2007) placed micro-isolates of inner and OHCs adjacent to SGN clusters to demonstrate synaptogenesis in the presence of NT-3 and BDNF. Martinez-Monedero et al. (2006) used β-bungarotoxin to eliminate SGNs from an organotypic cochlear explant culture and then co-cultured the remaining organ of Corti with spiral ganglion neurons to determine whether these could innervate the hair cells. This experimental design is formally similar to that originally described by Van De Water and Ruben (1983, 1984), summarized in Sect. 7.2.5, that tested chemotropic attraction of SAG neurites to otocyst sensory epithelium but, in the Martinez-Monedero et al. (2006) study, instead done using cultures from postnatal mice.

Tong et al. (2013) used a similar co-culture system of postnatal organ of Corti and postnatal spiral ganglion neurons but labeled with both pre- and postsynaptic markers to unambiguously demonstrate formation of synapses. They further showed that synapse formation was significantly reduced when the organs of Corti were derived from mice lacking the vesicular glutamate transporter VGLUT3, necessary for glutamatergic neurotransmission from hair cells to SGNs. This indicates that release of glutamate from the hair cell facilitates synaptogenesis. Ruan et al. (2010) cultured SGNs with organs of Corti from neonatal mice in which spontaneous activity of IHCs prior to hearing onset was suppressed by expression of a K^+ channel, $K_{ir}2.1$. Such suppression resulted in decreased SGN survival and neurite growth, indicating a requirement for synaptic activity, consistent with Tong et al. (2013).

The studies summarized here suggest that chemotropic guidance of SGN axons to the organ of Corti is present only during innervation of the embryonic sensory epithelium. Subsequently, SGN neurites do not appear to grow preferentially toward the organ of Corti, although can evidently make synapses with hair cells on encountering them. In summary, these studies suggest that SGNs can be replaced after they are lost and that new SGNs can innervate hair cells. Although this reinnervation process is currently inefficient, these studies show that by exploiting

the relative ease of experimental manipulation in vitro and combining with the power of mouse genetics, means can be identified to improve the efficiency of reinnervation and increase the number of synapses that can be regenerated.

As described by Nayagam and Edge in Chap. 9, stem cells from a variety of sources have been shown to be able to differentiate in vitro or in vivo into neurons that have at least some of the properties of spiral ganglion neurons. To evaluate the capacity of stem cell–derived neurons to innervate hair cells, several studies have co-cultured such cells with organ of Corti explants in a manner analogous to experiments, summarized previously in this section and in Sects. 7.2.5 and 7.2.7, in which SGNs were co-cultured with organ of Corti explants (Matsumoto et al., 2005; Shi et al., 2007; Matsumoto et al., 2008; Nayagam et al., 2013). These studies did observe contacts, visualized by confocal microscopy, between hair cells and the neurites of the stem cell–derived neuron-like cells. Nevertheless, these studies have not observed typical hair cell to SGN synapses with presynaptic structures in the hair cell and postsynaptic structures in the neurite.

If lost SGNs are replaced, it is as important that the new SGNs successfully innervate the cochlear nuclei as it is that they innervate hair cells. To this end, neural stem cells have been cocultured with auditory brain stem explants (Herlenius et al., 2012). As discussed in Sect. 7.2.3, previous studies (Ard et al., 1985; Zhou & Van de Water, 1987) demonstrated trophic effects of hindbrain on statoacoustic ganglion neurons in culture. More recently, trophic effects of neural stem cells have been demonstrated by co-culture of stem cells with brain stem slices (Kaiser et al., 2014). Further work with such co-cultures may allow progress on overcoming the challenges that exist in reinnervation of the cochlear nuclei.

7.2.11 Advantages and Limitations of Organotypic Preparations

Organotypic cultures have the compelling advantage of maintaining cell–cell interactions typical of those in vivo while allowing such interactions to be observed much more closely and directly than in vivo. These include interactions of SGNs with glial cells as well as interactions with pre- and postsynaptic target tissues including hair cells, supporting cells of the sensory epithelium, mesenchymal, glial, and epithelial cells of neuronal pathways, cochlear nucleus neurons, and central glia. Nevertheless, some tissue interactions are not maintained nor are mechanical features of the inner ear. The efferent projections, including the lateral olivocochlear projection that innervates type I SGNs, are severed. Moreover, the spiral ganglion in vitro is separated from metabolic, endocrine, and other organismal factors that undoubtedly affect development and function of the cochlea. Although in some ways the simplification may be disadvantageous, it does facilitate experimental investigation of the many cell–cell interactions that are maintained in these preparations. Moreover, isolation of the cochlea from these external factors facilitates

investigating their effect on the cochlea by experimental manipulation of the culture conditions.

Organotypic preparations allow many experimental manipulations not easily performed in vivo, including compelling selected specific cell–cell interactions—achieved by appropriate co-cultures—and modifying the cellular environment by addition/deletion of appropriate factors to/from the culture medium or substrate. However, experience has indicated that some important types of observations and experimental manipulations are difficult to perform with organotypic cultures. For example, assessment of neuronal survival is made difficult by the lack of a consistent reference volume for measurement of cell density. Counting all surviving neurons in an explant does not provide the desired information because the initial number is not known, given that explants may be of different sizes when plated. Explants have been used to investigate factors affecting neurite growth but many of these factors also affect neuronal survival and counts of neurites extending from explants are affected by both neurite extension and cell number without an ability to readily determine the contribution of each variable. Another procedure that has proved technically challenging with organotypic cultures is efficient gene transfer into cells. These limitations can be overcome by the use of dissociated spiral ganglion cell cultures. This complementary method overcomes some of the technical limitations of organotypic cultures albeit with the loss of some cell–cell and cell–substrate interactions present in organotypic cultures.

7.3 Dissociated Spiral Ganglion Cultures

Dissociated spiral ganglion cultures facilitate the study of the survival, neurite regeneration, cell signaling, and electrophysiological properties of SGNs. Early work with dissociated spiral ganglion cultures was carried out using neonatal rodents and chicks (Yamaguchi & Ohmori, 1990; Lefebvre et al., 1991). Lefebvre et al. (1991) originally described the use of dissociated rat spiral ganglia cultures to study the neurotrophic requirements for SGN survival and neurite growth. Most protocols for dissociated spiral ganglion cultures follow the basic steps outlined in this chapter, including microdissection of the ganglia, enzymatic digestion, and mechanical dissociation, and plating on a substrate treated to promote adhesion, typically containing laminin. Figure 7.2 illustrates the appearance of dissociated spiral ganglia cultures with bright-field and epifluorescence microscopy. Non-neuronal cells (e.g., Schwann cells and fibroblasts) represent the majority of cells that persist in these cultures, making it necessary to distinguish cell types based on morphological criteria and expression of cell-specific markers (e.g., neurofilaments) (Hansen et al., 2001b). More than 20 years of experience in culturing SGNs since has led to a proliferation of techniques that may be applied as resources and experimental design dictate. The next sections provide an overview

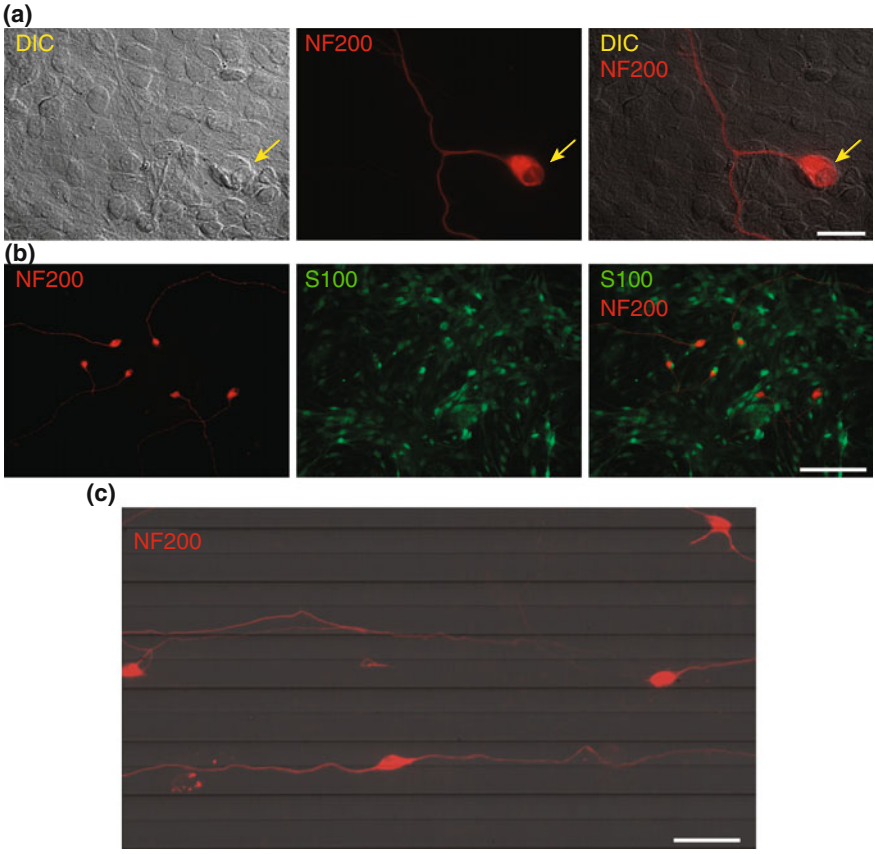

Fig. 7.2 Illustration of dissociated spiral ganglion cultures. **a** Dissociated spiral ganglion cultures immunostained with anti-neurofilament 200 (NF200, *red*) antibody and imaged with differential interference contrast (DIC) and epifluorescence microscopy. Overlay of DIC and anti-NF200 immunofluorescence images is shown in right panel. *Yellow arrow* indicates SGN cell body, which is recognized with typical large soma and prominent eccentric nucleus on DIC imaging. Scale bar = 25 µm. **b** Dissociated spiral ganglion cultures immunostained with anti-NF200 (*red*) and anti-S100 (*green*) antibodies. S100 is a Schwann cell marker. Schwann cells comprise the majority of cells in dissociated cultures. Overlay of anti-NF200 and anti-S100 images is shown in right panel. Scale bar = 100 µm. (**c**) Dissociated spiral ganglion cultures maintained on methacrylate polymer film with a micropattern consisting of parallel grooves and ridges created by photopolymerization. Cultures were immunostained with anti-NF200 (*red*) antibody. SGN neurites strongly align to the micropattern. Scale bar = 100 µm

of the general methods used to prepare dissociated spiral ganglion cultures, describe the most common types of dissociated cultures, discuss their suitability for research, and give examples of their application.

7.3.1 Types of Dissociated Spiral Ganglion Cultures

7.3.1.1 Neonatal Rodent Spiral Ganglion Cultures

Ease of dissection, incomplete ossification of the temporal bone, relatively high yield of SGNs, and similarities to other mammalian species make neonatal rat and mouse pups the most common source of dissociated spiral ganglion cultures (Lefebvre et al., 1990; Hegarty et al., 1997). Because this is before hearing onset, some physiological features of the cochlea are not yet fully mature. A mitigating factor for study of the spiral ganglion in particular is that even prior to hearing onset in neonatal rodents there is spontaneous activity and SGNs are responsive. Spontaneous neurotransmitter release from hair cells reliably elicits spikes in SGNs (Kennedy, 2012). This implies that, although hair cells and other elements of the auditory system are immature, physiology and function of SGNs may be appropriately investigated in neonatal preparations. Confirmation of this supposition depends on the ability to compare directly studies of cultures from neonates with similar studies of cultures from mature animals. This remains a critically important goal for investigators using cultured spiral ganglia.

Rats offer the advantage of larger cochleae that facilitate microdissection of the ganglia and higher yields of SGNs. In comparing the number of SGNs plated (Hegarty et al., 1997) to the number of neurons in the neonatal rat ganglion spiral ganglion (Rueda et al., 1987), plating efficiency can be estimated as approximately 25 %. Of the plated neurons, approximately 3–5 % survive in serum-free culture media devoid of other survival promoting factors after 48 h (Hegarty et al., 1997). Addition of trophic factors (e.g., serum, neurotrophins, depolarizing media, and/or cAMP analogs) significantly increases the number of SGNs that survive (Hegarty et al., 1997). Further, culture efficiency changes with age of the animal; an inverse relationship develops as the animal ages, with decreasing number of SGNs plated, but increasing survival of those that are plated (Jin et al., 2013).

Mice offer the additional experimental power of genetics. Whitlon et al. (2006) described technical details of mouse dissociated spiral ganglia cultures with approximately 30 % culture efficiency. Briefly stated, high culture efficiency in this preparation depends on serum-enriched media with inclusion of the spiral limbus during cochlear microdissection. Preservation of the spiral limbus reduces trauma and theoretically preserves developing neurites and a higher percentage of glial and supporting cells, potentially enhancing both autocrine and paracrine trophic support.

7.3.1.2 Embryonic Mouse Cultures

Cultures of neural progenitors derived from the embryonic mouse cochleovestibular ganglion mimic characteristics of mature auditory and vestibular neurons and can be used to model their interactions (Rabejac et al., 1994; Vazquez et al., 1994).

The putative benefit of embryonic material is that the tissue can be harvested with minimal mechanical trauma and provides even higher yields than cultures derived from neonatal animals.

7.3.1.3 Avian Auditory Ganglion Cultures

Embryonic and neonatal chicks have also been used as a source for auditory neuron cultures. Some of the original work identifying glutamate as the primary afferent neurotransmitter was done using stato-acoustic ganglia from embryonic chicks (Yamaguchi & Ohmori, 1990; Jimenez & Nunez, 1996). This system continues to be advantageous as a high throughput model to examine responsiveness to trophic factors including survival and neurite outgrowth (Fekete & Campero, 2007). Further, whole-cell voltage clamp recordings from dissociated chick cochlear ganglion cells have been used to identify potassium and calcium channel derived currents (Jimenez et al., 1997; Garcia-Diaz, 1999). A method for preparation of explant cultures from the chick embryo has recently been depicted on video (Fantetti & Fekete, 2011). In this preparation, polymerized collagen is used to support the cell culture while NT-3 and BDNF are used in a serum free medium to support survival and growth.

7.3.1.4 Adult Rodent and Human Spiral Ganglion Cultures

Potential differences in the behavior and electrophysiological properties between immature and mature SGNs have prompted development of methods to obtain cultures from adult rodents (Anderson et al., 2006; Jin et al., 2013). Such cultures are characterized by relatively poor yields limiting some of the experimental analyses that can be accomplished. However, SGNs derived from adult animals are more likely representative of human SGNs that are targets for stimulation by cochlear implants and regenerative strategies.

Guinea pigs and gerbils, when used as a source for spiral ganglion cultures, are primarily mature animals. In these studies the culture efficiency was low, but sufficient to characterize single-cell electrophysiological responses (Nakagawa et al., 1991; Harada et al., 1994). Techniques have been refined to culture adult guinea pig SGNs in the presence of exogenous neurotrophins (Rask-Andersen et al., 2005; Bostrom et al., 2010). Nearly identical techniques were applied to generate dissociated cultures of surgically harvested adult human SGNs from cochleae removed during transcochlear approaches to the skull base (Rask-Andersen et al., 2005). As with cultures from adult rodents, the yield of human SGNs is low but analysis of human material may be more clinically relevant.

7.3.2 Advantages and Limitations of Dissociated Spiral Ganglion Cultures

As noted in Sect. 7.2.11, dissociated cultures are preferred over explants for quantifying cell survival (Hegarty et al., 1997; Hansen et al., 2001a); analyzing neurite number, length, branching, direction and/or trajectory (Whitlon et al., 2006; Xu et al., 2012); and characterizing electrophysiological properties using single-cell patch-clamp recording techniques (Mo & Davis, 1997; Garcia-Diaz, 1999). Developmental changes can be studied by harvesting cells from animals at varying stages of development and culturing them with various cell types (Jin et al., 2013). Relative to organotypic cultures or in vivo postmortem studies, dissociated cultures provide a relatively high throughput system to quantify neuronal survival and morphology using software to analyze digital images and thus are well suited for screening of pharmacological libraries (Lie et al., 2010).

Another advantage of dissociated cultures is the greater capacity to experimentally manipulate and image the intracellular compartment. For example, dissociated cultures allow for transduction or transfection of exogenous transgenes or oligonucleotides to selectively influence specific molecular pathways. Dissociated SGNs are transduced with lentiviral vectors (e.g., feline immunodeficiency virus) with relatively high efficiency and specificity (Roehm et al., 2008). They are also amenable to transfection with expression plasmids encoding constitutively activate or dominant-negative gene isoforms, reporter constructs, and so forth, or siRNA oligonucleotides to suppress expression of specific gene products (e.g. kinases). We have used these methods to characterize signaling pathways that contribute to SGN survival and neurite growth (Bok et al., 2003; Hansen et al., 2003; Atkinson et al., 2011). Moreover, dissociated cultures facilitate observation of the intracellular environment using probes such as Ca^{2+} reporter dyes, genetically encoded fluorescent reporters for Ca^{2+}, other intracellular signals or metabolites (e.g., mitochondrial redox potential), and fluorescently tagged proteins to determine subcellular localization (Hegarty et al., 1997; Bok et al., 2003; Renton et al., 2010).

Dissociated cultures have some limitations. Unlike organotypic cultures, dissociated cultures disrupt endogenous cell–cell adhesion, trophic, and synaptic interactions. Also, plating efficiency is relatively low, usually 25–35 %, compared to explant or organotypic cultures. Dissociated spiral ganglia do not provide a pure neuronal culture as other cell types, primarily glia, are also present (Fig. 7.2b). The presence of non-neuronal cells may introduce potential confounding variables in that endogenous paracrine trophic factors or intercellular signals may still be present (Hansen et al., 2001b). The reported ratios of non-neuronal cells, mostly glial, to SGNs range from 1:1 to 20:1 (Hansen et al., 2001b; Rask-Andersen et al., 2005). The fact that macromolecules (e.g., RNA, proteins) derived from non-neuronal cells predominate in the cultures must be considered in analyses that do not distinguish the cell of origin for the macromolecule (e.g., reverse transcriptase-polymerase chain reaction or Western blot).

Most, but not all, studies employing dissociated SGN cultures make little effort to distinguish between type I and type II SGNs, which have been shown to have very different physiological properties (Reid et al., 2004). In addition, SGNs in culture may be found at different stages of differentiation and maturation. Neural stem cells have been detected in mature animals (Lopez et al., 2004; Oshima et al., 2007), and the proportion of type I and II SGNs may change with development (Barclay et al., 2011)—a process dependent on endogenous intracellular signaling.

Having described the methods, sources, advantages, and limitations of dissociated spiral ganglia cultures the following sections explore the use of such cultures to address specific experimental questions regarding spiral ganglion neurobiology.

7.3.3 Spiral Ganglion Neuron Survival and Neurite Growth

Understanding the factors that influence SGN survival during development and after damage to the cochlear epithelium represents a major thrust of inner ear regeneration strategies. The clinical success of cochlear implants has further stimulated the investigation of SGN survival and neurite regeneration. Dissociated SG cultures have been used extensively to characterize factors that promote SGN survival. In general, survival analysis is easier in dissociated cultures compared to explants as it is easier to identify and score individual neurons in dissociated cultures. For example, dissociated SG cultures were first used to demonstrate that the neurotrophins, NT-3, BDNF, and NT4/5 promote SGN survival and neurite growth (Lefebvre et al., 1991; Zheng & Gao, 1996). This observation has since been confirmed across multiple species and labs using both in vitro and in vivo preparations. In addition, transforming growth factor-β3 and -β5 promote SGN survival in vitro (Marzella et al., 1999). Neurotrophins have been reported to act synergistically with one another (Hegarty et al., 1997; Marzella et al., 1999) and with neuronal cytokines including leukemia inhibitory factor (LIF) and ciliary derived neurotrophic factor (CNTF) (Marzella et al., 1997; Whitlon et al., 2006; Jin et al., 2013) to enhance the survival and/or promote neurite growth of postnatal SGNs in vitro. Together, these results reiterate the requirement of sustained neurotrophic support for SGN survival during development and throughout adulthood.

SGN cell cultures have also been used to investigate the influence of membrane electrical activity on SGN survival and neurite growth. These studies are highly relevant to the human situation in which SGNs are subjected to electrical stimulation via a cochlear implant. In culture, SGNs are chronically depolarized by maintaining the cultures in elevated levels of extracellular K^+. SGN survival displays a dichotomous response to membrane depolarization (Hegarty et al., 1997). It is significantly enhanced by moderate depolarization but reduced by strong depolarization, presumably because of excitotoxicity. By contrast, SGN neurite growth is increasingly reduced by depolarization with the effect proportional to the level of depolarization (Roehm et al., 2008). In both cases the effect of membrane

depolarization on SGN survival and neurite growth depends on Ca^{2+} entry via voltage-sensitive Ca^{2+} channels (Hegarty et al., 1997; Roehm et al., 2008).

Studies using cultured SGNs showed that depolarization is additive with neurotrophic factors—BDNF and NT-3—in promoting survival. One implication is that different signaling pathways are used by these different survival stimuli. Indeed, studies of cultured SGNs have shown that this is the case and have identified key intracellular signals activated by neurotrophic factors or membrane depolarization to regulate SGN survival and neurite growth. These studies have taken advantage of the ability to transfect cultured SGNs with exogenous plasmids encoding mutant activated or inhibitory isoforms of key signaling proteins or siRNA oligonucleotides to suppress expression of gene products. For example, these studies demonstrated that membrane depolarization activates multiple Ca^{2+}-sensitive kinases, including protein kinase A (PKA) and Ca^{2+}/calmodulin-dependent kinase (CaMK) II and IV, to promote SGN survival and have defined intracellular compartments in which they operate (Bok et al., 2003, 2007; Hansen et al., 2003). They have also demonstrated that some signaling molecules (e.g., c-Jun N-terminal kinase) promote SGN death yet are essential for neurite growth (Renton et al., 2010; Atkinson et al., 2011) while others (e.g., Bcl-2 family members) promote SGN survival yet inhibit neurite growth (Hansen et al., 2007; Renton et al., 2010). These studies indicate that therapeutic strategies targeting survival or apoptotic signaling must contend with potential undesirable outcomes given the multiple roles played by these signaling pathways.

7.3.4 Membrane Electrophysiology and Ion Channels of SGNs

Dissociated cultures have been used as a means to define SGN membrane electrophysiological properties and channel expression, described in detail by Davis and Crozier in Chap. 4. Most studies used neonatal rodent cultures due to ease of dissection, a relatively thin myelin sheath, and cell membranes that are capable of withstanding patch clamp (Lin & Chen, 2000). A caveat is that whole-cell patch-clamp recordings of dissociated SGNs, while allowing for close scrutiny of individual neuron signaling characteristics, may differ from endogenous synaptic signaling.

Type I SGNs comprise 95 % of primary auditory neurons and have been studied in most detail (Adamson et al., 2002b; Ito & Dulon, 2002). The electrophysiological properties of type II SGNs in dissociated cultures have also been characterized, using post hoc immunolabeling with anti-peripherin antibody to identify the type II SGNs and differ from those of type I SGNs (Reid et al., 2004). Based on in vitro recordings from basal and apical SGNs, a spatial tonotopic gradient of electrophysiological properties has been identified for type I SGNs. These differences appear to be due, at least in part, to a basal-apical gradient of potassium

channel subtype expression that is influenced by exposure to specific neurotrophins (Adamson et al., 2002a, b). BDNF induces a basal SGN pattern of K^+ channel expression and basal electrophysiological properties; conversely, NT-3 induces apical phenotypes (Adamson et al., 2002a). Expression of synaptic proteins mirrors this basal-apical gradient and is also influenced by neurotrophin exposure (Flores-Otero et al., 2007). Thus, the phenotype of an SGN appears to be defined, at least in part, by its location in a basal-apical neurotrophin gradient.

Using dissociated cultures from posthearing mice, Lv et al. (2012) demonstrated that mature SGNs rely on Ca^{2+} influx through multiple types of voltage-gated Ca^{2+} channels to control resting membrane potential and encode action potentials. Lv et al. (2012) also demonstrated differences in Ca^{2+} current densities in the basal-apical axis of the adult cochlea and argue that these differences may contribute to the distinct electrophysiological features of basal and apical SGNs. It is not yet clear whether exposure to specific neurotrophins differentially regulates expression of calcium channel subunits comparable to effects on potassium channel subunits.

A recent study used dissociated SGN cultures to identify potential cellular mechanisms contributing to the SGN degeneration in DFNA2, an autosomal dominant form of progressive high-frequency sensorineural hearing loss (Lv et al., 2010). Mutation in $K_v7.4$ results in DNFA2. Inhibition of K_v7 currents promotes membrane depolarization and a sustained rise in intracellular Ca^{2+} correlated with increased SGN apoptotic death (Lv et al., 2010).

7.3.5 Interaction of SGNs with Non-Neuronal Cells

Glial co-cultures have been used to explore the influence of glial cells on SGN neurite growth. For example, Jeon et al. (2011) demonstrated that Schwann cells support neurite growth whereas astrocytes and oligodendrocytes inhibit it. Preference of SGN neurites to grow on Schwann cells has been demonstrated in other studies using dissociated SGNs (Rask-Andersen et al., 2005; Whitlon et al., 2009).

SGN survival and neurite growth can also be manipulated by inducing expression of exogenous neurotrophic factors in other cells in the culture. For example, co-culture of Schwann cells transfected with plasmids to overexpress either BDNF or NT-3 significantly enhances SGN survival in comparison to either control Schwann cells or application of recombinant neurotrophins to the culture media (Pettingill et al., 2008). Similarly, fibroblasts transfected with a fibroblast growth factor-1 expression plasmid promote and guide SGN neurite growth in culture (Dazert et al., 1998). Adenovirus mediated transfection of epithelial and mesothelial cells adjacent to the scala media with neurotophins rescues SGN cell bodies and neurites in vivo following deafening (Atkinson et al., 2012; Fukui et al., 2012), suggesting that transplantation of neurotrophin overexpressing Schwann or supporting cells into the cochlea may provide an alternative means of delivering neurotrophic factors to the deaf cochlea for therapeutic purposes (Pettingill et al., 2008).

7.3.6 SGN Neurite Guidance

Guidance of neurite growth has been extensively investigated using SGN cultures. Interest is predicated on the idea that resolution of electrical stimuli from a cochlear implant may improve with increased neurite density directed toward electrodes. Also neurite guidance will be a critical step to reestablish synaptic contact with regenerated hair cells, should inner ear regeneration prove successful. The requisite steps to implement either of these strategies are neurite initiation, directed neurite extension, and growth arrest. Of these, cultures have mostly been used to investigate neurite initiation and extension, although these events have rarely been distinguished. A variety of cell-contact, extracellular matrix, and soluble chemotactive factors have been shown to influence SGN pathfinding, including L1 (Brand et al., 2013), EphA and EphB receptors (Bianchi & Gray, 2002; Brors et al., 2003), laminin and fibronectin (Aletsee et al., 2002; Evans et al., 2007), netrin-1 (Lee & Warchol, 2008), and FGF-1 (Aletsee et al., 2003). Wittig et al. (2005) used a microfluidic chamber to demonstrate chemoattractive guidance of SGN neurites by an NT-3 gradient. In addition to biochemical cues, recent work has shown that biophysical cues guide SGN neurite growth. For example, surface topographic features created on polymer films precisely guide SGN neurite growth (Clarke et al., 2011; Tuft et al., 2013) (Fig. 7.2c). In this case, the response of SGN neurites depends both on the surface feature amplitude and frequency and the complexity of the feature (Tuft et al., 2013, 2014). Of particular relevance to cochlear implants is the observation that SGN neurites turn away from charge-balanced biphasic pulsed electrical fields whereas their response to steady or pulsed DC electrical fields depends on the substrate on which the cultures are plated (Li et al., 2010). Such observations raise the possibility that engineering appropriate physical patterns and chemical substrates onto the surfaces of cochlear implants will suffice to guide SGN neurites toward electrodes.

7.4 Relevance of These Studies to Clinical Issues and Therapy for Hearing Impairment

7.4.1 Cochlear Implants

Sensorineural hearing loss most often occurs as a consequence of loss of hair cells and affects large segments of the population (Mao et al., 2013). Loss of hair cells can result in degeneration and death of SGNs (Green et al., 2008), which takes weeks to months in animals and years to decades in humans. SGNs are the point of contact for the only established therapy to ameliorate severe to profound hearing loss: cochlear implants. Thus, degeneration or death of SGNs likely compromises the efficacy of cochlear implants. Efforts to prevent loss of SGNs or to restore the SGN population after loss are important therapeutic targets. Moreover, prevention

of degeneration of the peripheral axons is another important therapeutic target in that it could improve the fidelity of transmission of auditory information from the cochlear implant to the auditory nerve, for example, better spatial resolution and lower detection thresholds (Shibata et al., 2011). Although direct correlation of SGN survival (assessed postmortem) with measures of speech perception using a cochlear implant has yet to substantiate the hypothesis that maintenance of the SGN population or of peripheral axons improves performance with a cochlear implant (Khan et al., 2005; Fayad & Linthicum, 2006), a number of electrophysiologic and psychophysical measures correlate with neuronal survival in animal models (Kang et al., 2010). These measures may be important both in future correlations with implant performance in humans and in quantifying the success of therapies to recover neural and axonal populations (Pfingst et al., 2011). Thus, two immediately important goals of cochlear neuroscience are maintenance (or restoration) of the SGN population and maintenance (or restoration) of the peripheral axons and promotion of their growth toward cochlear implant electrodes.

With regard to maintenance of SGNs, in vitro studies of SGN survival have already led to the use of neurotrophic factors in vivo to prevent SGN death after hair cell loss in animal models. Further, in vitro demonstration of the additivity of neurotrophic factors with membrane depolarization for survival (Hegarty et al., 1997) has resulted in observations of synergism between BDNF and implant-derived electrical stimulation on SGN survival in vivo in deafened guinea pigs (Shepherd et al., 2005) and cats (Leake et al., 2013). Such studies can lead to use of cochlear implants to provide trophic support to SGNs as well as sensory information.

SGN cultures also provide a system to screen for additional molecules that alone, or in combination with electrical stimulation, prevent neurodegeneration. Small molecules that can be more readily delivered to the inner ear than growth factors, perhaps even systemically, are an especially tempting goal for testing. Some small molecules have already been shown to promote SGN survival in vivo, for example, GM1 ganglioside (Osofsky et al., 2001; Leake et al., 2007) or TrkB receptor agonists (Yu et al., 2013a). Studies summarized in Sect. 7.3.3 suggest intracellular signaling pathways that may be therapeutically relevant targets of small-molecule activators or inhibitors. However, a systematic large-scale in vitro screen is likely to be a more cost-effective and efficient means of identifying suitable molecules than in vivo testing of candidates.

A second important goal is guiding SGN peripheral axons to cochlear implant electrodes. As discussed in Sect. 7.3.6, studies using SGN cultures have identified strategies to accomplish this, including the use of diffusible chemoattractant cues to attract axon growth toward electrodes, incorporating guidance cues, such as key extracellular matrix or cell surface molecules into the substrate, or physically shaping the surface with micropatterns that direct neurite growth. Organotypic explants have been used to investigate the growth of SGN neurites within the organ of Corti during development (Appler et al., 2013; Druckenbrod & Goodrich, 2014) and in the postnatal cochlea (Wang & Green, 2011). Future studies will extend these

techniques and use them in combination to achieve the desired goal of a precise and detailed tonotopic projection from the electrode array to the cochlear nucleus.

7.4.2 Cell Regeneration

As discussed by Fritzsch et al. in Chap. 3, Davis and Crozier in Chap. 4 and Muniak et al. in Chap. 6, many crucial questions remain unanswered regarding the cell–cell and cell–substrate interactions that shape innervation of the cochlea and the cochlear nucleus during normal development. How are SGN axons guided to their peripheral and central targets? How do they make the appropriate synaptic connections to produce a tonotopic projection with appropriate and distinct synaptic morphologies? How is the proper number of synapses specified? Which external cues and which intracellular signaling pathways and regulators of gene expression are used? There are additional questions regarding specification of the physiological properties of SGNs, discussed by Davis and Crozier in Chap. 4. How can SGNs sustain firing rates of hundreds of spikes per second without fatiguing and without suffering excitotoxicity? How do SGNs acquire regionally distinct physiological properties along the tonotopic axis?

These experiments, by identifying the relevant endogenous signals, will suggest therapeutic strategies relevant to improving SGN responsiveness to cochlear implants. Similarly, they also have important implications for therapeutic strategies involving cell regeneration by gene or stem cell therapy for hearing impairment. Although cochlear implants are now and will likely remain for the foreseeable future the only means to effectively restore speech perception in sensorineural deafness, in the long term, replacement of hair cells by gene therapy and/or stem cell therapy may surpass cochlear implants in effectiveness. For such methods to be successful, the new hair cells need to be innervated. Studies of loss, due to noise, of IHC to SGN synapses in adult animals (Kujawa & Liberman, 2009; Lin et al., 2011) suggest that reinnervation is poor in spite of the fact that the original IHCs and SGNs remain and the extremity of the damaged axon is initially within 50 μm of the base of the IHC, a situation that, one might have assumed, is very favorable to synapse regeneration. Indeed, even in organotypic cultures of neonatal cochleae, discussed in Sects. 7.2.9 and 7.2.10, synapse formation between SGNs and hair cells is inefficient under similar seemingly favorable conditions.

There is compelling evidence for primary loss of SGNs in humans (Makary et al., 2011), and experiments with animal models show that such loss of SGNs, even without hair cell loss, results in a distinctive hearing impairment (Kujawa & Liberman 2006, 2009; Lin et al., 2011). Also, secondary death of SGNs may occur after loss of hair cells (Green et al., 2008; Shibata et al., 2011). Thus, replacement of SGNs by gene or stem cell therapy may be an important therapeutic tool for some hearing impairments. Progress has been made toward replacement of SGNs with stem cells (Chen et al., 2012; Rivolta, 2013). Such stem cell–derived neurons must be capable of preserving frequency and timing information in transmission of

auditory sensation from the cochlea to the brain. They must establish synapses with hair cells and with correct targets in the cochlear nuclei and possess all of the morphological and physiological properties of SGNs.

Answering these fundamental questions of ontogeny of the SGN will likely require the accessibility to observation and experimental manipulation afforded by in vitro systems. Experiments with cultured SGNs or organotypic cultures have already led to progress in answering these questions, for example, the roles of NT-3 and BDNF in specifying physiological properties of SGNs and in promoting synapse regeneration, and these models should prove valuable for further progress.

7.4.3 Protection of Cochlear Synapses

Given that there is primary loss of SGNs in humans (Makary et al., 2011) and, in animal models, this is due to noise-induced synaptopathy (Kujawa & Liberman, 2006), prevention of such trauma would obviate the need for regeneration of SGNs or their cochlear synapses. In vitro models can play a crucial role in this as a platform for testing putative neuroprotective agents in high-throughput experiments to quantify their ability to prevent excitotoxic damage to cochlear synapses. The prospect of replacing lost SGNs is exciting; equally so is the prospect of preventing their loss in the first place.

References

Adamson, C. L., Reid, M. A., & Davis, R. L. (2002a). Opposite actions of brain-derived neurotrophic factor and neurotrophin-3 on firing features and ion channel composition of murine spiral ganglion neurons. *The Journal of Neuroscience*, 22(4), 1385–1396.

Adamson, C. L., Reid, M. A., Mo, Z. L., Bowne-English, J., & Davis, R. L. (2002b). Firing features and potassium channel content of murine spiral ganglion neurons vary with cochlear location. *Journal of Comparative Neurology*, 447(4), 331–350.

Aletsee, C., Brors, D., Palacios, S., Pak, K., Mullen, L., Dazert, S., & Ryan, A. F. (2002). The effects of laminin-1 on spiral ganglion neurons are dependent on the MEK/ERK signaling pathway and are partially independent of Ras. *Hearing Research*, 164(1–2), 1–11.

Aletsee, C., Brors, D., Mlynski, R., Ryan, A. F., & Dazert, S. (2003). Branching of spiral ganglion neurites is induced by focal application of fibroblast growth factor-1. *Laryngoscope*, 113(5), 791–796.

Anderson, M., Bostrom, M., Pfaller, K., Glueckert, R., Schrott-Fischer, A., Gerdin, B., & Rask-Andersen, H. (2006). Structure and locomotion of adult in vitro regenerated spiral ganglion growth cones – a study using video microscopy and SEM. *Hearing Research*, 215(1–2), 97–107.

Anniko, M., & Van de Water, T. R. (1986). Synaptogenesis in co-cultured inner ear explants which share a single statoacoustic ganglion. *Acta Oto-Laryngologica*, 102(5–6), 415–422.

Appler, J. M., Lu, C. C., Druckenbrod, N. R., Yu, W. M., Koundakjian, E. J., & Goodrich, L. V. (2013). Gata3 is a critical regulator of cochlear wiring. *The Journal of Neuroscience*, 33(8), 3679–3691.

Ard, M. D., Morest, D. K., & Hauger, S. H. (1985). Trophic interactions between the cochleovestibular ganglion of the chick embryo and its synaptic targets in culture. *Neuroscience*, 16(1), 151–170.

Atkinson, P. J., Cho, C. H., Hansen, M. R., & Green, S. H. (2011). Activity of all JNK isoforms contributes to neurite growth in spiral ganglion neurons. *Hearing Research*, 278(1–2), 77–85.

Atkinson, P. J., Wise, A. K., Flynn, B. O., Nayagam, B. A., Hume, C. R., O'Leary, S. J., Shepherd, R. K., & Richardson, R. T. (2012). Neurotrophin gene therapy for sustained neural preservation after deafness. *PLoS One*, 7(12), e52338.

Avila, M. A., Varela-Nieto, I., Romero, G., Mato, J. M., Giraldez, F., Van De Water, T. R., & Represa, J. (1993). Brain-derived neurotrophic factor and neurotrophin-3 support the survival and neuritogenesis response of developing cochleovestibular ganglion cells. *Developmental Biology*, 159, 266–275.

Bank, L. M., Bianchi, L. M., Ebisu, F., Lerman-Sinkoff, D., Smiley, E. C., Shen, Y. C., Ramamurthy, P., Thompson, D. L., Roth, T. M., Beck, C. R., Flynn, M., Teller, R. S., Feng, L., Llewellyn, G. N., Holmes, B., Sharples, C., Coutinho-Budd, J., Linn, S. A., Chervenak, A. P., Dolan, D. F., Benson, J., Kanicki, A., Martin, C. A., Altschuler, R., Koch, A. E., Jewett, E. M., Germiller, J. A., & Barald, K. F. (2012). Macrophage migration inhibitory factor acts as a neurotrophin in the developing inner ear. *Development*, 139(24), 4666–4674.

Barclay, M., Ryan, A. F., & Housley, G. D. (2011). Type I vs type II spiral ganglion neurons exhibit differential survival and neuritogenesis during cochlear development. *Neural Development*, 6(1), 33.

Barde, Y. A., Edgar, D., & Thoenen, H. (1983). New neurotrophic factors. *Annual Review of Physiology*, 45, 601–612.

Bianchi, L. M., & Cohan, C. S. (1991). Developmental regulation of a neurite-promoting factor influencing statoacoustic neurons. *Developmental Brain Research*, 64(1–2), 167–174.

Bianchi, L. M., & Cohan, C. S. (1993). Effects of the neurotrophins and CNTF on developing statoacoustic neurons: Comparison with an otocyst-derived factor. *Developmental Biology*, 159, 353–365.

Bianchi, L. M., & Gray, N. A. (2002). EphB receptors influence growth of ephrin-B1-positive statoacoustic nerve fibers. *European Journal of Neuroscience*, 16(8), 1499–1506.

Bok, J., Zha, X. M., Cho, Y. S., & Green, S. H. (2003). An extranuclear locus of cAMP-dependent protein kinase action is necessary and sufficient for promotion of spiral ganglion neuronal survival by cAMP. *The Journal of Neuroscience*, 23, 777–787.

Bok, J., Huang, J., Wang, Q., & Green, S. H. (2007). CaMKII and CaMKIV mediate divergent prosurvival signaling pathways in response to depolarization in neurons. *Molecular and Cellular Neuroscience*, 36(1), 13–26.

Bostrom, M., Khalifa, S., Bostrom, H., Liu, W., Friberg, U., & Rask-Andersen, H. (2010). Effects of neurotrophic factors on growth and glial cell alignment of cultured adult spiral ganglion cells. *Audiology and Neurotology*, 15(3), 175–186.

Brand, Y., Sung, M., Chavez, E., Wei, E., Pak, K. K., Housley, G. D., Bodmer, D., & Ryan, A. F. (2013). Neural cell adhesion molecule L1 modulates type I but not type II inner ear spiral ganglion neurite outgrowth in an in vitro alternate choice assay. *Journal of Molecular Neuroscience*, 51(3), 663–670.

Brors, D., Bodmer, D., Pak, K., Aletsee, C., Schafers, M., Dazert, S., & Ryan, A. F. (2003). EphA4 provides repulsive signals to developing cochlear ganglion neurites mediated through ephrin-B2 and -B3. *Journal of Comparative Neurology*, 462(1), 90–100.

Brugeaud, A., Tong, M., Luo, L., & Edge, A. S. (2014). Inhibition of repulsive guidance molecule, RGMa, increases afferent synapse formation with auditory hair cells. *Developmental Neurobiology*, 74(4), 457–466.

Chen, W., Jongkamonwiwat, N., Abbas, L., Eshtan, S. J., Johnson, S. L., Kuhn, S., Milo, M., Thurlow, J. K., Andrews, P. W., Marcotti, W., Moore, H. D., & Rivolta, M. N. (2012). Restoration of auditory evoked responses by human ES-cell-derived otic progenitors. *Nature*, 490(7419), 278–282.

Clarke, J. C., Tuft, B. W., Clinger, J. D., Levine, R., Figueroa, L. S., Allan Guymon, C., & Hansen, M. R. (2011). Micropatterned methacrylate polymers direct spiral ganglion neurite and Schwann cell growth. *Hearing Research*, 278(1–2), 96–105.

Coate, T. M., & Kelley, M. W. (2013). Making connections in the inner ear: Recent insights into the development of spiral ganglion neurons and their connectivity with sensory hair cells. *Seminars in Cell and Developmental Biology*, 24(5), 460–469.

Coate, T. M., Raft, S., Zhao, X., Ryan, A. K., Crenshaw, E. B., 3rd, & Kelley, M. W. (2012). Otic mesenchyme cells regulate spiral ganglion axon fasciculation through a Pou3f4/EphA4 signaling pathway. *Neuron*, 73(1), 49–63.

Cramer, K. S. (2005). Eph proteins and the assembly of auditory circuits. *Hearing Research*, 206 (1–2), 42–51.

Davis, R. L., & Liu, Q. (2011). Complex primary afferents: What the distribution of electrophysiologically-relevant phenotypes within the spiral ganglion tells us about peripheral neural coding. *Hearing Research*, 276(1–2), 34–43.

Dazert, S., Kim, D., Luo, L., Aletsee, C., Garfunkel, S., Maciag, T., Baird, A., & Ryan, A. F. (1998). Focal delivery of fibroblast growth factor-1 by transfected cells induces spiral ganglion neurite targeting in vitro. *Journal of Cellular Physiology*, 177(1), 123–129.

Druckenbrod, N. R., & Goodrich, L. V. (2014). Timelapse imaging of live intact cochlea reveal SGNs undergo region-specific growth patterns and dynamic branching near synaptic targets during development. Paper presented at the Abstracts of Midwinter Meeting of the Association for Research in Otolaryngology, San Diego, CA.

Evans, A. R., Euteneuer, S., Chavez, E., Mullen, L. M., Hui, E. E., Bhatia, S. N., & Ryan, A. F. (2007). Laminin and fibronectin modulate inner ear spiral ganglion neurite outgrowth in an in vitro alternate choice assay. *Developmental Neurobiology*, 67(13), 1721–1730.

Fantetti, K. N., & Fekete, D. M. (2011). Dissection and culture of chick statoacoustic ganglion and spinal cord explants in collagen gels for neurite outgrowth assays. *Journal of Visualized Experiments*, doi: 10.3791/3600.

Fayad, J. N., & Linthicum, F. H., Jr. (2006). Multichannel cochlear implants: Relation of histopathology to performance. *Laryngoscope*, 116(8), 1310–1320.

Fekete, D. M., & Campero, A. M. (2007). Axon guidance in the inner ear. *The International Journal of Developmental Biology*, 51(6–7), 549–556.

Fell, H. B. (1928). The development in vitro of the isolated otocyst of the embryonic fowl. *Archiv fur experimentelle Zellforschung*, 7, 69–81.

Flores-Otero, J., Xue, H. Z., & Davis, R. L. (2007). Reciprocal regulation of presynaptic and postsynaptic proteins in bipolar spiral ganglion neurons by neurotrophins. *The Journal of Neuroscience*, 27(51), 14023–14034.

Friedmann, I. (1956). In vitro culture of the isolated otocyst of the embryonic fowl. *Annals of Otology, Rhinology, and Laryngology*, 65(1), 98–107.

Friedmann, I. (1959). Electron microscope observations on in vitro cultures of the isolated fowl embryo otocyst. *The Journal of Biophysical and Biochemical Cytology*, 5(2), 263–268.

Friedmann, I. (1968). The chick embryo otocyst in tissue culture: a model ear. *The Journal of Laryngology and Otology*, 82(3), 185–201.

Friedmann, I. (1969). The innervation of the developing fowl embryo otocyst in vivo and in vitro. *Acta Oto-Laryngologica*, 67(2), 224–238.

Friedmann, I., & Bird, E. S. (1967). Electron microscopic studies of the isolated fowl embryo otocyst in tissue culture. Rudimentary kinocilia, cup-shaped nerve endings and synaptic bars. *Journal of Ultrastructure Research*, 20(5), 356–365.

Fukui, H., Wong, H. T., Beyer, L. A., Case, B. G., Swiderski, D. L., Di Polo, A., Ryan, A. F., & Raphael, Y. (2012). BDNF gene therapy induces auditory nerve survival and fiber sprouting in deaf Pou4f3 mutant mice. *Scientific Reports*, 2, 838.

Garcia-Diaz, J. F. (1999). Development of a fast transient potassium current in chick cochlear ganglion neurons. *Hearing Research*, 135(1–2), 124–134.

Green, S. H., Altschuler, R. A., & Miller, J. M. (2008). Cell death and cochlear protection. In J. Schacht, A. N. Popper, & R. R. Fay (Eds.), *Auditory trauma, protection and repair*. New York: Springer Science + Business Media.

Green, S. H., Bailey, E., Wang, Q., & Davis, R. L. (2012). The Trk A, B, C's of neurotrophins in the cochlea. *The Anatomical Record (Hoboken)*, 295(11), 877–895.

Hakuba, N., Koga, K., Gyo, K., Usami, S. I., & Tanaka, K. (2000). Exacerbation of noise-induced hearing loss in mice lacking the glutamate transporter GLAST. *The Journal of Neuroscience*, 20(23), 8750–8753.

Hansen, M. R., Zha, X.-M., Bok, J., & Green, S. H. (2001a). Multiple distinct signal pathways, including an autocrine neurotrophic mechanism, contribute to the survival-promoting effect of depolarization on spiral ganglion neurons. *The Journal of Neuroscience*, 21(7), 2256–2267.

Hansen, M. R., Vijapurkar, U., Koland, J. G., & Green, S. H. (2001b). Reciprocal signaling between spiral ganglion neurons and Schwann cells involves neuregulin and neurotrophins. *Hearing Research*, 161(1–2), 87–98.

Hansen, M. R., Devaiah, A. K., Bok, J., Zha, X., & Green, S. H. (2003). Ca^{2+}/calmodulin-dependent protein kinases II and IV both promote survival but differ in their effects on axon growth in spiral ganglion neurons. *The Journal of Neuroscience Research*, 72 (2), 169–184.

Hansen, M. R., Roehm, P., Xu, N., & Green, S. H. (2007). Overexpression of Bcl-2 or Bcl-x_L prevents spiral ganglion neuron death and inhibits neurite growth. *Journal of Neurobiology*, 67 (3), 316-25.

Harada, N., Han, D. Y., Komeda, M., & Yamashita, T. (1994). Glutamate-induced intracellular Ca^{2+} elevation in isolated spiral ganglion cells of the guinea pig cochlea. *Acta Oto-Laryngolica*, 114(6), 609–612.

Hegarty, J. L., Kay, A. R., & Green, S. H. (1997). Trophic support of cultured spiral ganglion neurons by depolarization exceeds and is additive with that by neurotrophins or cyclic AMP, and requires elevation of $[Ca^{2+}]_i$ within a set range. *The Journal of Neuroscience*, 17(6), 1959–1970.

Herlenius, E., Thonabulsombat, C., Forsberg, D., Jaderstad, J., Jaderstad, L. M., Bjork, L., & Olivius, P. (2012). Functional stem cell integration assessed by organotypic slice cultures. *Current Protocols in Stem Cell Biology*, doi: 10.1002/9780470151808.sc02d13s23.

Ito, K., & Dulon, D. (2002). Nonselective cation conductance activated by muscarinic and purinergic receptors in rat spiral ganglion neurons. *American Journal of Physiology – Cell Physiology*, 282(5), C1121–1135.

Jeon, E. J., Xu, N., Xu, L., & Hansen, M. R. (2011). Influence of central glia on spiral ganglion neuron neurite growth. [Research Support, N.I.H., Extramural]. *Neuroscience*, 177, 321–334.

Jimenez, C., & Nunez, L. (1996). Glutamate receptors in the developing cochlear ganglion. *The International Journal of Developmental Biology*, Supplement 1, 159S–160S.

Jimenez, C., Gireldez, F., Represa, J., & Garcia-Diaz, J. F. (1997). Calcium currents in dissociated cochlear neurons from the chick embryo and their modification by neurotrophin-3. *Neuroscience*, 77(3), 673–682.

Jin, Y., Kondo, K., Ushio, M., Kaga, K., Ryan, A. F., & Yamasoba, T. (2013). Developmental changes in the responsiveness of rat spiral ganglion neurons to neurotrophic factors in dissociated culture: Differential responses for survival, neuritogenesis and neuronal morphology. *Cell Tissue Research*, 351(1), 15–27.

Kaiser, A., Kale, A., Novozhilova, E., Siratirakun, P., Aquino, J. B., Thonabulsombat, C., Ernfors, P., & Olivius, P. (2014). Brain stem slice conditioned medium contains endogenous BDNF and GDNF that affect neural crest boundary cap cells in co-culture. *Brain Research*, 1566, 12–23.

Kang, S. Y., Colesa, D. J., Swiderski, D. L., Su, G. L., Raphael, Y., & Pfingst, B. E. (2010). Effects of hearing preservation on psychophysical responses to cochlear implant stimulation. *Journal of the Association for Research in Otolaryngology*, 11(2), 245–265.

Kennedy, H. J. (2012). New developments in understanding the mechanisms and function of spontaneous electrical activity in the developing mammalian auditory system. *Journal of the Association for Research in Otolaryngology*, 32(31), 437-45.

Kesser, B. W., & Lalwani, A. K. (2009). Gene therapy and stem cell transplantation: Strategies for hearing restoration. *Advances in Oto-Rhino-laryngology*, 66, 64–86.

Khan, A. M., Handzel, O., Burgess, B. J., Damian, D., Eddington, D. K., & Nadol, J. B., Jr. (2005). Is word recognition correlated with the number of surviving spiral ganglion cells and electrode insertion depth in human subjects with cochlear implants? *Laryngoscope*, 115(4), 672–677.

Kujawa, S. G., & Liberman, M. C. (2006). Acceleration of age-related hearing loss by early noise exposure: Evidence of a misspent youth. *The Journal of Neuroscience*, 26(7), 2115–2123.

Kujawa, S. G., & Liberman, M. C. (2009). Adding insult to injury: Cochlear nerve degeneration after "temporary" noise-induced hearing loss. *The Journal of Neuroscience*, 29(45), 14077–14085.

Lawrence, M., & Merchant, D. J. (1953). Tissue culture techniques for the study of the isolated otic vesicle. *Annals of Otology, Rhinology, and Laryngology*, 62(3), 770–785.

Leake, P. A., Hradek, G. T., Vollmer, M., & Rebscher, S. J. (2007). Neurotrophic effects of GM1 ganglioside and electrical stimulation on cochlear spiral ganglion neurons in cats deafened as neonates. *Journal of Comparative Neurology*, 501(6), 837–853.

Leake, P. A., Stakhovskaya, O., Hetherington, A., Rebscher, S. J., & Bonham, B. (2013). Effects of brain-derived neurotrophic factor (BDNF) and electrical stimulation on survival and function of cochlear spiral ganglion neurons in deafened, developing cats. *Journal of the Association for Research in Otolaryngology*, 14(2), 187–211.

Lee, K. H., & Warchol, M. E. (2008). Promotion of neurite outgrowth and axon guidance in spiral ganglion cells by netrin-1. *Archives of Otolaryngology Head and Neck Surgery*, 134(2), 146–151.

Lefebvre, P. P., Leprince, P., Weber, T., Rigo, J. M., Delree, P., & Moonen, G. (1990). Neuronotrophic effect of developing otic vesicle on cochleo-vestibular neurons: Evidence for nerve growth factor involvement. *Brain Research*, 507(2), 254–260.

Lefebvre, P. P., Van de Water, T. R., Weber, T., Rogister, B., & Moonen, G. (1991). Growth factor interactions in cultures of dissociated adult acoustic ganglia: Neuronotrophic effects. *Brain Research*, 567, 306–312.

Li, S., Li, H., & Wang, Z. (2010). Orientation of spiral ganglion neurite extension in electrical fields of charge-balanced biphasic pulses and direct current in vitro. *Hearing Research*, 267(1–2), 111–118.

Lie, M., Grover, M., & Whitlon, D. S. (2010). Accelerated neurite growth from spiral ganglion neurons exposed to the Rho kinase inhibitor H-1152. *Neuroscience*, 169(2), 855–862.

Lin, H. W., Furman, A. C., Kujawa, S. G., & Liberman, M. C. (2011). Primary neural degeneration in the guinea pig cochlea after reversible noise-induced threshold shift. *Journal of the Association for Research in Otolaryngology*, 12(5), 605–616.

Lin, X., & Chen, S. (2000). Endogenously generated spontaneous spiking activities recorded from postnatal spiral ganglion neurons in vitro. *Brain Research. Developmental Brain Research*, 119(2), 297–305.

Lopez, I. A., Zhao, P. M., Yamaguchi, M., de Vellis, J., & Espinosa-Jeffrey, A. (2004). Stem/progenitor cells in the postnatal inner ear of the GFP-nestin transgenic mouse. *International Journal of Developmental Neuroscience*, 22(4), 205–213.

Lv, P., Wei, D., & Yamoah, E. N. (2010). K_v7–type channel currents in spiral ganglion neurons: involvement in sensorineural hearing loss. *The Journal of Biological Chemistry*, 285(45), 34699–34707.

Lv, P., Sihn, C. R., Wang, W., Shen, H., Kim, H. J., Rocha-Sanchez, S. M., & Yamoah, E. N. (2012). Posthearing Ca^{2+} currents and their roles in shaping the different modes of firing of spiral ganglion neurons. *The Journal of Neuroscience*, 32(46), 16314–16330.

Makary, C. A., Shin, J., Kujawa, S. G., Liberman, M. C., & Merchant, S. N. (2011). Age-related primary cochlear neuronal degeneration in human temporal bones. *Journal of the Association for Research in Otolaryngology*, 12(7), 711–717.

Malgrange, B., Lefebvre, P., Van de Water, T. R., Staecker, H., & Moonen, G. (1996). Effects of neurotrophins on early auditory neurones in cell culture. *Neuroreport*, 7(0959–4965), 913–917.

Mao, Z., Zhao, L., Pu, L., Wang, M., Zhang, Q., & He, D. Z. (2013). How well can centenarians hear? *PLoS One*, 8(6), e65565.

Martinez-Monedero, R., Corrales, C. E., Cuajungco, M. P., Heller, S., & Edge, A. S. (2006). Reinnervation of hair cells by auditory neurons after selective removal of spiral ganglion neurons. *Journal of Neurobiology*, 66(4), 319–331.

Marzella, P. L., Clark, G. M., Shepherd, R. K., Bartlett, P. F., & Kilpatrick, T. J. (1997). LIF potentiates the NT-3-mediated survival of spiral ganglia neurones *in vitro*. *Neuroreport*, 8(7), 1641–1644.

Marzella, P. L., Gillespie, L. N., Clark, G. M., Bartlett, P. F., & Kilpatrick, T. J. (1999). The neurotrophins act synergistically with LIF and members of the TGF-beta superfamily to promote the survival of spiral ganglia neurons in vitro. *Hearing Research*, 138(1–2), 73–80.

Matsumoto, M., Nakagawa, T., Higashi, T., Kim, T. S., Kojima, K., Kita, T., Sakamoto, T., & Ito, J. (2005). Innervation of stem cell-derived neurons into auditory epithelia of mice. *NeuroReport*, 16(8), 787–790.

Matsumoto, M., Nakagawa, T., Kojima, K., Sakamoto, T., Fujiyama, F., & Ito, J. (2008). Potential of embryonic stem cell-derived neurons for synapse formation with auditory hair cells. *The Journal of Neuroscience Research*, 86(14), 3075–3085.

Mo, Z. L., & Davis, R. L. (1997). Endogenous firing patterns of murine spiral ganglion neurons. *Journal of Neurophysiology*, 77(3), 1294–1305.

Nakagawa, T., Komune, S., Uemura, T., & Akaike, N. (1991). Excitatory amino acid response in isolated spiral ganglion cells of guinea pig cochlea. *Journal of Neurophysiology*, 65(3), 715–723.

Nayagam, B. A., Edge, A. S., Needham, K., Hyakumura, T., Leung, J., Nayagam, D. A., & Dottori, M. (2013). An in vitro model of developmental synaptogenesis using cocultures of human neural progenitors and cochlear explants. *Stem Cells and Development*, 22(6), 901–912.

Orr, M. F. (1965). Development of acoustic ganglia in tissue cultures of embryonic chick otocysts. *Experimental Cell Research*, 65, 68–77.

Orr, M. F. (1968). Histogenesis of sensory epithelium in reaggregates of dissociated embryonic chick otocysts. *Developmental Biology*, 17(1), 39–54.

Oshima, K., Teo, D. T., Senn, P., Starlinger, V., & Heller, S. (2007). LIF promotes neurogenesis and maintains neural precursors in cell populations derived from spiral ganglion stem cells. *BMC Developmental Biology*, 7, 112.

Osofsky, M. R., Moore, C. M., & Leake, P. A. (2001). Does exogenous GM1 ganglioside enhance the effects of electrical stimulation in ameliorating degeneration after neonatal deafness? *Hearing Research*, 159(1–2), 23–35.

Parker, M., Brugeaud, A., & Edge, A. S. (2010). Primary culture and plasmid electroporation of the murine organ of Corti. *Journal of Visualized Experiments*, doi: 10.3791/1685.

Pettingill, L. N., Minter, R. L., & Shepherd, R. K. (2008). Schwann cells genetically modified to express neurotrophins promote spiral ganglion neuron survival in vitro. *Neuroscience*, 152(3), 821–828.

Pfingst, B. E., Bowling, S. A., Colesa, D. J., Garadat, S. N., Raphael, Y., Shibata, S. B., Strahl, S. B., Su, G. L., & Zhou, N. (2011). Cochlear infrastructure for electrical hearing. *Hearing Research*, 281(1–2), 65–73.

Pirvola, U., Ylikoski, J., Palgi, J., Lehtonen, E., Arumae, U., & Saarma, M. (1992). Brain-derived neurotrophic factor and neurotrophin-3 mRNAs in the peripheral target fields of developing inner ear ganglia. *Proceedings of the National Academy of Sciences of the USA*, 89, 9915–9919.

Puel, J. L., Pujol, R., Tribillac, F., Ladrech, S., & Eybalin, M. (1994). Excitatory amino acid antagonists protect cochlear auditory neurons from excitotoxicity. *Journal of Comparative Neurology*, 341(2), 241–256.

Puel, J. L., Saffiedine, S., Gervais d'Aldin, C., Eybalin, M., & Pujol, R. (1995). Synaptic regeneration and functional recovery after excitotoxic injury in the guinea pig cochlea. *Comptes Rendus de l'Academie des Sciences III – Life Sciences*, 318(1), 67–75.

Puel, J. L., Ruel, J., Gervais d'Aldin, C., & Pujol, R. (1998). Excitotoxicity and repair of cochlear synapses after noise-trauma induced hearing loss. *NeuroReport*, 9(9), 2109–2114.

Pujol, R., Lenoir, M., Robertson, D., Eybalin, M., & Johnstone, B. M. (1985). Kainic acid selectively alters auditory dendrites connected with cochlear inner hair cells. *Hearing Research*, 18(2), 145–151.

Rabejac, D., Raymond, J., & Dechesne, C. J. (1994). Characterization of different neuron populations in mouse statoacoustic ganglion cultures. *Brain Research*, 652(2), 249–256.

Rask-Andersen, H., Bostrom, M., Gerdin, B., Kinnefors, A., Nyberg, G., Engstrand, T., Miller, J. M., & Lindholm, D. (2005). Regeneration of human auditory nerve. In vitro/in video demonstration of neural progenitor cells in adult human and guinea pig spiral ganglion. *Hearing Research*, 203(1–2), 180–191.

Reid, M. A., Flores-Otero, J., & Davis, R. L. (2004). Firing patterns of type II spiral ganglion neurons *in vitro*. *The Journal of Neuroscience*, 24(3), 733–742.

Reinecke, J., Girgis, T., Allen, G. W., & Shambaugh, G., Jr. (1960). In vitro study of the developing inner ear. *Archives of Otolaryngology Head and Neck Surgery*, 72, 599–609.

Renton, J. P., Xu, N., Clark, J. J., & Hansen, M. R. (2010). Interaction of neurotrophin signaling with Bcl-2 localized to the mitochondria and endoplasmic reticulum on spiral ganglion neuron survival and neurite growth. *The Journal of Neuroscience Research*, 88(10), 2239–2251.

Rivolta, M. N. (2013). New strategies for the restoration of hearing loss: Challenges and opportunities. *British Medical Bulletin*, 105, 69–84.

Roehm, P. C., Xu, N., Woodson, E. A., Green, S. H., & Hansen, M. R. (2008). Membrane depolarization inhibits spiral ganglion neurite growth via activation of multiple types of voltage sensitive calcium channels and calpain. *Molecular and Cellular Neuroscience*, 37(2), 376–387.

Rose, J. E., Sobkowicz, H. M., & Bereman, B. (1977). Growth in culture of the peripheral axons of the spiral neurons in response to displacement of the receptors. *Journal of Neurocytology*, 6(1), 49–70.

Ruan, Q., Chen, D., Wang, Z., Chi, F., He, J., Wang, J., & Yin, S. (2010). Effects of Kir2.1 gene transfection in cochlear hair cells and application of neurotrophic factors on survival and neurite growth of co-cultured cochlear spiral ganglion neurons. *Molecular and Cellular Neuroscience*, 43(3), 326–339.

Rueda, J., De La Sen, C., Juiz, J. M., & Merchán, J. A. (1987). Neuronal loss in the spiral ganglion of young rats. *Acta Oto-Laryngologica*, 104, 417–421.

Santi, P. A., & Johnson, S. B. (2013). Decellularized ear tissues as scaffolds for stem cell differentiation. *Journal of the Association for Research in Otolaryngology*, 14(1), 3–15.

Shepherd, R. K., Coco, A., Epp, S. B., & Crook, J. M. (2005). Chronic depolarization enhances the trophic effects of brain-derived neurotrophic factor in rescuing auditory neurons following a sensorineural hearing loss. *Journal of Comparative Neurology*, 486(2), 145–158.

Shi, F., Corrales, C. E., Liberman, M. C., & Edge, A. S. B. (2007). BMP4 induction of sensory neurons from human embryonic stem cells and reinnervation of sensory epithelium. *European Journal of Neuroscience*, 26(11), 3016–3023.

Shibata, S. B., Budenz, C. L., Bowling, S. A., Pfingst, B. E., & Raphael, Y. (2011). Nerve maintenance and regeneration in the damaged cochlea. *Hearing Research*, 281(1–2), 56–64.

Siddiqui, S. A., & Cramer, K. S. (2005). Differential expression of Eph receptors and ephrins in the cochlear ganglion and eighth cranial nerve of the chick embryo. *Journal of Comparative Neurology*, 482(4), 309–319.

Sobkowicz, H. M., & Slapnick, S. M. (1992). Neuronal sprouting and synapse formation in response to injury in the mouse organ of Corti in culture. *International Journal of Developmental Neuroscience*, 10(6), 545–566.

Sobkowicz, H. M., Bereman, B., & Rose, J. E. (1975). Organotypic development of the organ of Corti in culture. *Journal of Neurocytology*, 4(5), 543–572.

Sobkowicz, H. M., Loftus, J. M., & Slapnick, S. M. (1993). Tissue culture of the organ of Corti. *Acta Oto-Laryngologica Supplementum*, 502, 3–36.

Spoendlin, H. (1971). Primary structural changes in the organ of Corti after acoustic overstimulation. *Acta Oto-Laryngologica*, 71(2), 166–176.

Spoendlin, H. (1975). Retrograde degeneration of the cochlear nerve. *Acta Oto-Laryngologica*, 79, 266–275.

Sugawara, M., Murtie, J. C., Stankovic, K. M., Liberman, M. C., & Corfas, G. (2007). Dynamic patterns of neurotrophin 3 expression in the postnatal mouse inner ear. *Journal of Comparative Neurology*, 501(1), 30–37.

Tong, M., Brugeaud, A., & Edge, A. S. (2013). Regenerated synapses between postnatal hair cells and auditory neurons. *Journal of the Association for Research in Otolaryngology*, 14(3), 321–329.

Tuft, B. W., Li, S., Xu, L., Clarke, J. C., White, S. P., Guymon, B. A., Perez, K. X., Hansen, M. R., & Guymon, C. A. (2013). Photopolymerized microfeatures for directed spiral ganglion neurite and Schwann cell growth. *Biomaterials*, 34(1), 42–54.

Tuft, B. W., Xu, L., White, S. P., Seline, A. E., Erwood, A. M., Hansen, M. R., & Guymon, C. A. (2014). Neural pathfinding on uni- and multidirectional photopolymerized micropatterns. *ACS Applied Materials and Interfaces*, 6(14), 11265-76.

Van De Water, T. R. (1976). Effects of removal of the statoacoustic ganglion complex upon the growing otocyst. *Annals of Otology*, *Rhinology*, *and Laryngology*, 85(6 Supplement 33 Pt 2), 2–31.

Van de Water, T. R., & Ruben, R. J. (1971). Organ culture of the mammalian inner ear. *Acta Oto-Laryngologica*, 71(4), 303–312.

Van De Water, T. R., & Heywood, P. (1976). The in vitro development of innervated sensory hair cells of a mammal. *Acta Oto-Laryngologica*, 82(5–6), 337–342.

Van De Water, T. R., & Ruben, R. J. (1983). A possible embryonic mechanism for the establishment of innervation of inner ear sensory structures. *Acta Oto-Laryngologica*, 95(5–6), 470–479.

Van de Water, T. R., & Ruben, R. J. (1984). Neurotrophic interactions during in vitro development of the inner ear. *Annals of Otology*, *Rhinology*, *and Laryngology*, 93(6 Pt 1), 558–564.

Van de Water, T. R., Heywood, P., & Ruben, R. J. (1973). Development of sensory structures in organ cultures of the twelfth and thirteenth gestation day mouse embryo inner ears. *Annals of Otology*, *Rhinology*, *and Laryngology*, 82, Supplement 4:3–18.

van Heumen, W. R., Claxton, C., & Pickles, J. O. (2000). Expression of EphA4 in developing inner ears of the mouse and guinea pig. *Hearing Research*, 139(1–2), 42–50.

Vazquez, E., Van de Water, T. R., Del Valle, M., Vega, J. A., Staecker, H., Giráldez, F., & Represa, J. (1994). Pattern of trkB protein-like immunoreactivity in vivo and the in vitro effects of brain-derived neurotrophic factor (BDNF) on developing cochlear and vestibular neurons. *Anatomy and Embryology*, 189, 157–167.

Wang, Q., & Green, S. H. (2011). Functional role of neurotrophin-3 in synapse regeneration by spiral ganglion neurons on inner hair cells after excitotoxic trauma *in vitro*. *The Journal of Neuroscience*, 31(21), 7938–7949.

Wang, Q., & Green, S. H. (2013). Exogenous BDNF and NT-3 have distinct biological effects on afferent synaptogenesis on inner hair cells (IHCs) without endogenous NT-3 in vitro. Paper presented at the Abstracts of Midwinter Meeting of the Association for Research in Otolaryngology, Baltimore, MD.

Whitlon, D. S., Ketels, K. V., Coulson, M. T., Williams, T., Grover, M., Edpao, W., & Richter, C. P. (2006). Survival and morphology of auditory neurons in dissociated cultures of newborn mouse spiral ganglion. *Neuroscience*, 138(2), 653–662.

Whitlon, D. S., Tieu, D., Grover, M., Reilly, B., & Coulson, M. T. (2009). Spontaneous association of glial cells with regrowing neurites in mixed cultures of dissociated spiral ganglia. *Neuroscience*, 161(1), 227–235.

Wittig, J. H., Jr., Ryan, A. F., & Asbeck, P. M. (2005). A reusable microfluidic plate with alternate-choice architecture for assessing growth preference in tissue culture. *Journal of Neuroscience Methods*, 144(1), 79–89.

Xu, N., Engbers, J., Khaja, S., Xu, L., Clark, J. J., & Hansen, M. R. (2012). Influence of cAMP and protein kinase A on neurite length from spiral ganglion neurons. *Hearing Research*, 283 (1–2), 33–44.

Yamaguchi, K., & Ohmori, H. (1990). Voltage-gated and chemically gated ionic channels in the cultured cochlear ganglion neurone of the chick. *The Journal of Physiology*, 420, 185–206.

Ylikoski, J., Pirvola, U., Moshnyakov, M., Palgi, J., Arumäe, U., & Saarma, M. (1993). Expression patterns of neurotrophin and their receptor mRNAs in the rat inner ear. *Hearing Research*, 65, 69–78.

Yu, Q., Chang, Q., Liu, X., Wang, Y., Li, H., Gong, S., Ye, K., & Lin, X. (2013a). Protection of spiral ganglion neurons from degeneration using small-molecule TrkB receptor agonists. *The Journal of Neuroscience*, 33(32), 13042–13052.

Yu, W. M., Appler, J. M., Kim, Y. H., Nishitani, A. M., Holt, J. R., & Goodrich, L. V. (2013b). A Gata3-Mafb transcriptional network directs post-synaptic differentiation in synapses specialized for hearing. *eLife*, 2, e01341.

Zheng, J. L., & Gao, W. Q. (1996). Differential damage to auditory neurons and hair cells by ototoxins and neuroprotection by specific neurotrophins in rat cochlear organotypic cultures. *European Journal of Neuroscience*, 8(9), 1897–1905.

Zhou, X. N., & Van de Water, T. R. (1987). The effect of target tissues on survival and differentiation of mammalian statoacoustic ganglion neurons in organ culture. *Acta Oto-Laryngologica*, 104(1–2), 90–98.

Zhou, Z., Liu, Q., & Davis, R. L. (2005). Complex regulation of spiral ganglion neuron firing patterns by neurotrophin-3. *The Journal of Neuroscience*, 25(33), 7558–7566.

Chapter 8
Loss, Degeneration, and Preservation of the Spiral Ganglion Neurons and Their Processes

Hainan Lang

Keywords Age-related hearing loss · Animal models · Auditory physiology · Glia · Cell Death · Excitotoxicity · Neural degeneration · Noise-induced hearing loss · Preservation · Primary auditory nerve · Repair · Spiral ganglion · Spontaneous activities

8.1 Introduction

The auditory nerve, consisting of spiral ganglion neurons (SGNs) and their projections, is the primary carrier of auditory information from sensory hair cells of the cochlea to the central auditory system. The loss or dysfunction of SGNs can result in hearing impairment of varying degrees and forms. Loss of SGNs and their processes is frequently reported in the cochlea after hair cell death caused by exposure to noise (Kiang et al., 1976), ototoxic drugs (Bichler et al., 1983; Leake & Hradek, 1988), or genetic deficiency (White et al., 2000). Morphological evidence shows that after intracochlear perfusion with aminoglycosides, SGNs die gradually by the process of apoptosis as indicated by characteristic morphological changes including condensed cytoplasm, nonmarginal clumping of nuclear chromatin, shrinkage and fragmentation of the nucleus and cytoplasm, and the formation of the apoptotic bodies (Dodson, 1997). Pathological identification of SGN degeneration after sensory hair cell loss and the associated molecular mechanisms of neuronal death have been widely discussed (Spoendlin, 1975; Green et al., 2008; Bao & Ohlemiller, 2010). Although it is thought that aminoglycoside damage to SGNs is secondary, recent evidence suggests that there is a primary component of SGN degeneration present after gentamicin exposure (Ruan et al., 2014). This chapter focuses on findings from recent studies of primary and age-related SGN

H. Lang (✉)
Department of Pathology and Laboratory Medicine, Medical University of South Carolina, 165 Ashley Avenue, Charleston, SC 29425, USA
e-mail: langh@musc.edu

A. Dabdoub et al. (eds.), *The Primary Auditory Neurons of the Mammalian Cochlea*, Springer Handbook of Auditory Research 52,
DOI 10.1007/978-1-4939-3031-9_8

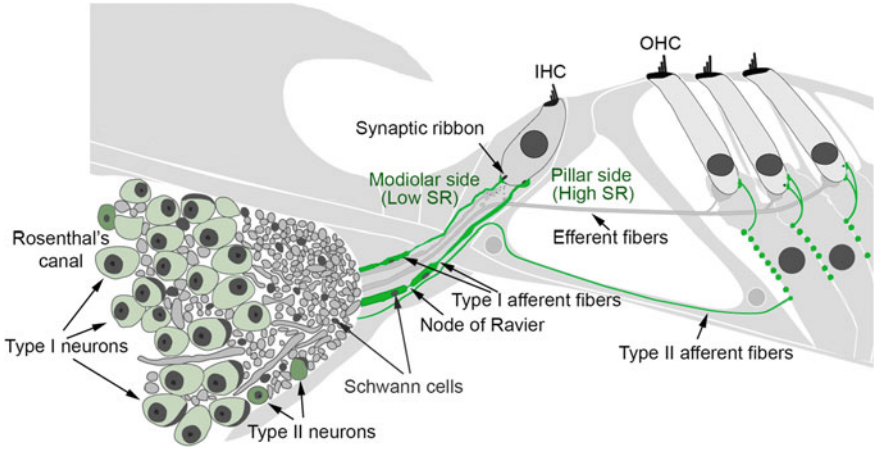

Fig. 8.1 Schematic representation of the relationships between afferent and efferent auditory nerve fibers with two types of sensory hair cells. Spiral ganglion neurons (SGNs) are clustered in Rosenthal's canal (RC) and include two groups of neuronal cells: large type I cells that make up 90–95 % of the SGN population and synapse with inner hair cells (IHCs) and small type II cells comprising 5–10 % of the neurons innervating outer hair cells (OHCs). The cell bodies of type II neurons are often seen in the periphery of RC, toward the osseous spiral lamina. Type I nerve fibers are surrounded by myelinating Schwann cells, whereas type II fibers are enclosed by nonmyelinating Schwann cells. Type I fibers lose their myelin sheath before they enter the organ of Corti through the habenular opening and can be classified into two (or three) populations based on their spontaneous discharge rate (SR). High-SR fibers are thick fibers with large terminals that contact the pillar side of IHCs. In contrast, low-SR fibers are thinner fibers with smaller terminals on the modiolar side of IHCs. Synapses on the modiolar side of IHCs have longer ribbons whereas synapses located on the pillar side of the cell have shorter ribbons. Radial innervations of efferent nerve fibers within the organ of Corti consist of (1) inner spiral fibers that run across the afferent nerve fibers under IHCs and (2) tunnel radial fibers that contact directly to OHC bodies with large nerve endings

degeneration including animal models of neuronal cell degeneration and on potential approaches for preventing auditory nerve degeneration.

The auditory nerve and its associated afferent nerve synapses form part of the structural basis for converting an acoustic signal into an electrical signal and transporting the electrical signal to the central auditory pathway (Fig. 8.1). Briefly stated, sound pressure drives the movement of the basilar membrane to generate a shearing motion of the cilia at the apex of sensory hair cells. This motion results in hair cell depolarization, triggering the exocytosis of neurotransmitter vesicles at afferent synapses located on the basolateral portion of the inner hair cells (IHCs). Neurotransmitters initiate action potentials at the ganglionic initial segments along the auditory nerve. The action potentials then propagate along the nodes of Ranvier within both peripheral and central portions of the auditory nerve carrying sound coding information to higher auditory centers (Robles & Ruggero, 2001; Fuchs et al., 2003; Hossain et al., 2005). Loss or dysfunction in any part of these structures can cause deficits in the conduction of auditory information. Note that the auditory

nerve and its associated elements discussed in this chapter include the eighth nerve extending from hair cell/synapses, dendrites under HCs, SGN cell bodies and central axons within modiolus, and the myelin sheaths provided by Schwann cells, which enclose mostly the peripheral afferent fibers and central axons of the SGNs.

There are two subpopulations of afferent neurons (types I and II) in the spiral ganglia of mammalian cochleas, each with their own morphological, immunostaining, and electrophysiological characteristics (Fig. 8.1; Davis and Crozier, Chap. 4). In most mammalian species (with the exception of humans), the cell bodies of type I SGNs are heavily myelinated. The remaining type II neuronal cells are unmyelinated and innervate the outer hair cells (OHCs) with a 1:10–20 ratio (Kiang et al., 1982; Liberman & Simmons, 1985). Both type I and type II neurons can be found within Rosenthal's canal (RC). Their central projections form the auditory nerve within the internal auditory canal. Closely associated with the peripheral and central processes of these neurons are various glial cells, including Schwann cells, satellite cells, and oligodendrocytes. The peripheral portion of the auditory nerve is surrounded by myelinating Schwann cells (for type I SGNs) and nonmyelinating Schwann cells (for type II SGNs). The central portion of the auditory nerve is also enveloped by Schwann cells in the proximal part (before the glial transition zone) and by oligodendrocytes in the distal part (after the glial transition zone). The central projections of types I and II neurons form the modiolar segment of the auditory nerve, pass through the internal auditory canal and then enter the cochlear nucleus (Nayagam et al., 2011; Muniak et al., Chap. 6).

It is well established that auditory information from the cochlea is redundantly transmitted to the brain through type I SGNs that innervate each IHC (with about 20 synapses per IHC). The functional properties of type II neurons in transmitting auditory information are still largely unknown. Voltage- and current-clamp recordings of SGNs from postnatal rodents revealed rapidly inactivating A-type–like potassium currents in type II neurons (Jagger & Housley, 2003) and slow accommodation of responses to depolarization (Reid et al., 2004). In addition, recordings at the type II synapses show that the release of synaptic vesicles by OHCs results in a small-scale depolarization (Weisz et al., 2009). These results suggest that type II neurons are less active than type I neurons during normal auditory encoding processes. The selective survival of type II neurons has been seen in several cochlear and auditory nerve injury models. For example, pathological alterations of type I SGNs but not type II SGNs were seen after ototoxic lesions of sensory hair cells (Bichler et al., 1983; Leake & Hradek, 1988), noise trauma (Spoendlin, 1975; Lim, 1976), ouabain exposures (Lang et al., 2005), and transection of the cochlear nerve (Spoendlin & Suter, 1976). Future endeavors should address whether unique functional features of type II neurons make them less susceptible to injury in pathological conditions.

Type I afferent fibers are classified into two or three subgroups based on their spontaneous discharge rate and sensitivity to sound stimulation (Fig. 8.1 and Table 8.1). Auditory nerve fibers discharge spontaneously without stimulation.

Table 8.1 Differential physiological and morphological characteristics of high-SR fibers and low- (and medium-SR) fibers

Differentiated characteristics	High-SR fibers	Low- (and medium-) SR fibers
Physiological		
Spontaneous discharge rates		
Cat	18–100 spikes/s	Low-SR: <0.5 spike/s Medium-SR: 0.5–18 spikes/s
Gerbil	18–150 spikes/s	<18 spikes/s for gerbil
Mouse	1–120 spikes/s	<1 spike/s
Response threshold	Low	High
Dynamic range	Smaller	Larger
Threshold recovery following a prior stimulation	Faster	Slower
Sensitivity to endocochlear potential	~1 dB/mV	>1 dB/mV
Morphological		
Peripheral terminal localization	Pillar pole of IHCs	Modiolar pole of IHCs
Peripheral terminal	Larger	Smaller
Ribbon	Shorter and thicker	Longer and thinner
Receptor patch	Larger	Smaller
Synapse vesicle	Less	More
Axon diameter	Larger	Smaller
Mitochondria within terminal	More	Less

The data in the table are based on previous studies in cats (Liberman & Oliver, 1984; Sewell, 1984; Kantardzhieva et al., 2013), gerbils (Schmiedt, 1989; Suryadevara et al., 2001), and mice (Taberner & Liberman, 2005)

Spontaneous rate (SR) in auditory afferent fibers was first examined by Kiang et al. (1965) and then further defined into subgroups by Liberman (1978). In the cat, auditory nerve fibers are classified into three groups: low-SR (<0.5 spikes/s), medium-SR (0.5–18 spikes/s), and high-SR (>18 spikes/s) fibers. Similar SR-based functional subdivisions of auditory nerve fibers have also been reported in other mammalian species including chinchilla (Salvi et al., 1982; Frisina et al., 1996), guinea pig (Winter et al., 1990), gerbil (Schmiedt, 1989; Ohlemiller et al., 1991), and mouse (Taberner & Liberman, 2005). Auditory afferent fibers with higher SRs have low thresholds to stimuli, whereas fibers with lower SRs have higher thresholds (see Table 8.1). In addition, morphological evidence has shown that the specialization of central projections correspond to peripheral fibers based on their SR (review by Nayagam et al., 2011; Muniak et al., Chap. 6).

8.2 Loss of Spiral Ganglion Neurons and Their Processes

Many extrinsic and intrinsic factors can cause the degeneration and dysfunction of SGNs and their processes. These factors include exposure to noise and ototoxic drugs, infection, genetic defects, aging, and absence of auditory signaling input such as loss of sensory hair cells (Liberman & Kiang, 1978; Spoendlin, 1984; Zimmerman et al., 1995). Various loci of pathology in the auditory nerve with a list of representative references are included in Table 8.2. Loss of SGNs and their processes results in auditory impairment by reduction of the auditory information (e.g., timing, neural synchrony, and phase locking) delivered to the brain and by secondary degeneration in cochlear nuclei and other components of the central auditory system.

Table 8.2 A summary on various sites of degeneration reported in SGNs and their associated elements

Anatomic site with pathological changes	General characteristics of nerve dysfunction	Representative references
1. *Synapse*		
Swelling and disruption of postsynaptic structure, reduced synapse ribbons, alterations of synapse location, orphan ribbon	Reduced activity, inexcitability, hyperexcitability (excitotoxicity), reduced activity of low-SR synapses, dys-synchronous auditory procressing, deficits in temporal coding, reduced suprathreshold amplitudes of auditory evoked potential	Liberman and Mulroy (1982), Robertson (1983), Pujol and Puel (1999)
2. *Peripheral process*		
Loss or dysfunction of afferent fibers	Inexcitability, abnormal nerve activity, reduced activity of low-SR fibers, decreased suprathreshold amplitude of auditory evoked potentials	Nadol (1979), Leake and Hradek (1988), Furman et al. (2013)
3. *Neuronal cell body*		
Reduced nuclear area neuronal apoptosis	Inexcitability, no conduction, reduced suprathreshold amplitude of auditory evoked potentials	Leake and Hradek (1988), Dodson (1997)
4. *Central axon*		
Disintegration of myelin sheath, retrograde degeneration of axon	Decreased suprathreshold amplitude, inexcitability, no conduction	Nadol (1979), Webster and Webster (1978)
5. *Myelin sheath*		
Demyelination (axon survives for short period)	Slow nerve excitability, dys-synchronous, slow conduction velocity, long latency response	Leake and Hradek (1988), Jyothi et al. (2010)

It is important to note that ears with signs of SGN degeneration do not always show a significant auditory threshold shift. Previous studies have revealed that cat cochleas with a diffuse loss of about 50 % of auditory nerves still have relatively normal thresholds as measured by behavioral tests (Schuknecht & Woellner, 1955). The amplitude of gross evoked auditory nerve responses depends on a large number of auditory nerves firing synchronously in response to sound. The loss and dysfunction of SGNs and their processes are better identified by auditory suprathreshold measurements, such as the amplitude input/output (I/O) functions of compound action potentials (CAP) (Hellstrom & Schmiedt, 1990; Kujawa & Liberman, 2009). Dysfunction of the auditory nerve can be characterized by threshold elevations, shallow slopes of I/O functions, and diminished maximum amplitudes as compared to healthy ears (see Figs. 8.4 and 8.8).

8.2.1 The Evidence of Secondary SGN Degeneration Following Hair Cell Loss

Degeneration of SGNs can occur as a secondary consequence of cochlear injury. Loss of sensory hair cells leads to a retrograde degeneration and results in a secondary SGN degeneration, a process seen in numerous animal models (see review by Spoendlin, 1984). Direct evidence is still needed to determine the primary or secondary nature of specific neuronal pathological alterations. However, there exists cumulative indirect evidence suggesting that SGN degeneration can occur after hair cell loss, including: (1) temporal patterns: loss of IHCs occurs rapidly after cochlear injury, whereas death of SGNs occurs after hair cell loss (Dupont et al., 1993; McFadden et al., 2004); (2) spatial patterns: the location of SGN loss along the cochlear spiral correlates with the location of hair cell loss (Liberman & Kiang, 1978; Bohne & Harding, 2000); and (3) manipulability of the degeneration: cochlear perfusion of the specific neurotrophic factors that are normally provided by sensory hair cell and/or supporting cells can prolong SGN survival (Ernfors et al., 1996; Altschuler et al., 1999; Stankovic et al., 2004).

Contributing factors to the degeneration of SGN after hair cell loss may include a loss of neural activity and the absence of nerve growth factors, which are critical for neuronal survival (Leake et al., 1999; Fritzsch et al., 1997; Green, 2000). In contrast to a rapid loss of hair cells in many injury models, the secondary degeneration of SGNs is often seen as a slow process with diffuse neuronal cell death. The temporal pattern of SGN death also differs across species; for example, in the rat, a loss of 90 % of the SGNs required approximately 3 months (Bichler et al., 1983). However, in the guinea pig, half of the population of SGNs was still present a year after hair cell loss (Webster & Webster, 1981). In the cat, diffuse neuronal cell loss occurred over several years (Leake & Hradek, 1988). Finally, analysis of human temporal bones suggests that SGNs can survive several decades in human ears devoid of hair cells (Nadol, 1997).

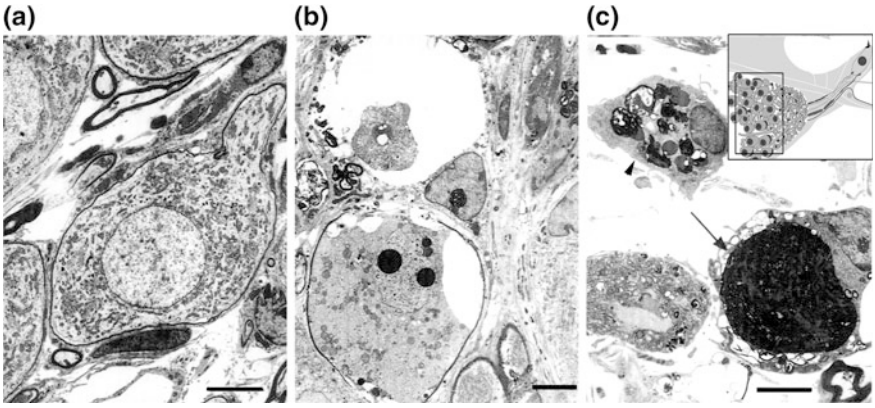

Fig. 8.2 Apoptotic cell death in type I SGNs after cochlear perfusion with aminoglycosides. **a** The ultrastructural features of type I SGNs from the basal turn of a normal guinea pig. **b** A condensed and fragmented nucleus is present in a type I SGN 10 days after aminoglycoside antibiotics were perfused into the perilymph. Separation of organelles is seen in the cytoplasm of the apoptotic neuron with a homogeneous and vesiculated appearance. **c** Another apoptotic neuron (*arrow*) is indicated by the dark chromatin masses. The *arrowhead* points to an activated macrophage identified by the irregular nucleus with clumped chromatin and myelin-associated cellular debris. Scale bars = 5 μm

Similar to other neuronal cells in the nervous system, SGN death after hair cell loss occurs through both necrosis and apoptosis (see review by Hutchins & Barger, 1998); however, apoptosis may be the key mechanism of SGN degeneration in the cochlea. Degeneration of SGNs after hair cell death may occur through two phases. Early-phase cell death occurs as necrosis and/or apoptosis in SGNs following a loss of neural activity due to sensory hair cell loss; the later phase of degeneration results in apoptosis due to pro-apoptotic signaling caused by a chronic stress condition (e.g., loss of neurotrophic support from hair cells and/or supporting cells) (reviews by Fritzsch et al., 2004; Green et al., 2008). Using intracochlear perfusion with aminoglycoside antibiotics, Dodson showed that SGN apoptosis occurred in guinea pig cochleae after hair cell loss (1997). In that study, kanamycin sulfate or gentamicin perfusion led to a rapid loss of hair cells within 3 days and 90 % SGN death within 10 days. Many of these SGNs degenerated through the process of apoptosis, as indicated by characteristic morphological changes including condensed cytoplasm, wrinkling of the nuclear membrane, nonmarginal clumping of nuclear chromatin, and shrinkage and fragmentation of the nucleus and cytoplasm into apoptotic bodies (Fig. 8.2). There is also evidence for necrotic death in SGNs present at an early survival time after kanamycin sulfate or gentamicin perfusion (Dodson, 1997).

The molecular mechanisms of SGN apoptosis have been elucidated mainly through the examination of cultured SGNs with genetic manipulation and pharmacological procedures. These in vitro studies have revealed several pro-survival signaling pathways that are involved in SGN death as a result of the absence of

neural activity or the loss of neurotrophic support (see reviews by Roehm & Hansen, 2005; Green et al., 2008). These signaling pathways include, but are not limited to (1) the cyclic AMP-dependent protein kinase and Ca^{2+}/calmodulin-dependent protein kinase II and IV systems; (2) pathways involving protein kinase C (PKC), Ca^{2+} signaling, and mitogen-activated protein kinases (MAPK)/extracellular signal-regulated kinases (ERK) activation; and (3) the c-Jun N-terminal kinase (JNK) cell death pathway (Green, 2000; Hansen et al., 2003). In addition, recent in vivo studies have demonstrated that supporting cells in the IHC region and neuregulin–erbB receptor signaling are important for survival of adult SGN (Stankovic et al., 2004; Sugawara et al., 2005, 2007).

8.2.1.1 Primary SGN Degeneration

Animal models of sensorineural hearing loss caused by exposure to noise and ototoxic agents have been established and well-characterized morphologically and functionally for several decades. In many of these models a rapid and robust loss of hair cells was seen before a significant loss of SGNs. However, in a study of aged rat ears, Keithley and Feldman (1982) reported that neuronal degeneration exceeded IHC loss, supporting the hypothesis that neuronal degeneration is not simply retrograde degeneration after loss of IHCs, but is an intrinsic degenerative process. Primary degeneration of SGNs was also seen in aged human cochlea without a robust loss of sensory hair cells (Schuknecht & Gacek, 1993; Makary et al., 2011). In addition, primary neural degeneration was reported in some cases of noise trauma (Spoendlin, 1971; Liberman & Mulroy, 1982), aminoglycoside ototoxicity (Sone et al., 1998), and in the cochleas of white cats with hereditary deafness (Pujol et al., 1977), suggesting SGN degeneration is not a unique secondary event. A series of previous studies have found that degeneration of afferent synapses and progressive loss of SGNs occur in the cochlea when the sensory hair cells are still intact and functional after exposure to an octave-band noise at moderate levels (Kujawa & Liberman, 2006, 2009; Lin et al., 2011; see Fig. 8.4). These data strongly support that SGN degeneration can be independent of the loss of sensory hair cells.

8.2.1.2 Primary SGN Degeneration as a Result of Glutamate Excitotoxicity

Glutamate is the most common excitatory neurotransmitter in the central nervous system and is believed to play an important role in cochlear mechano-neural transduction (Bird et al., 1978; Fuchs et al., 2003). The α-amino-3-hydroxy-5-methyl-4-isoxazolepropionic acid (AMPA)-type glutamate receptor has been identified in type I SGNs (Pujol et al., 1985; Liberman et al., 2011). The excessive release of glutamate results in neuronal damage through excitotoxicity. The pathophysiology of excitotoxicity includes overactivation of

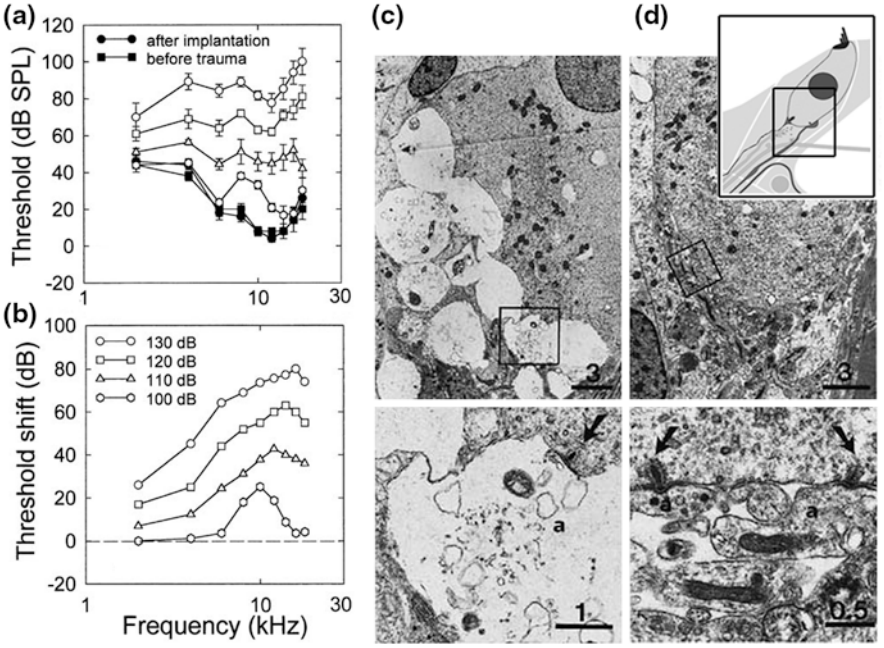

Fig. 8.3 Primary degeneration of afferent dendrites under IHCs after noise exposure in guinea pigs. **a**, **b** Compound action potential (CAP) threshold shifts are present 20 min after different levels of noise exposure (100–130 dB SPL for 15 min). Lesions in the afferent dendrites were present with noise exposures of 120 and 130 dB SPL, but not 100 and 110 dB SPL. **c** Pathological alterations of afferent dendrites are seen under IHCs. The preparation for transmission electron microscopic examination was processed 20 min after 130 dB SPL sound exposure. Massive swellings of afferent dendrites are present under an IHC. *Bottom left panel* enlargement of the area framed in (**c**). A presynaptic ribbon is seen at the basal pole of IHCs adjacent to postsynaptic membrane. **d** Significant protective effect of perilymph perfusion with kynurenate, a glutamate antagonist. No pathologic change of afferent dendrites is observed below an IHC. *Bottom right panel* higher magnification of the area framed in (**d**). An *inset* in the *upper right panel* is a schematic diagram showing the locations of images (**c**, **d**). Scale bar = 0.5 µm (Figure was modified from Puel et al., 1998)

glutamate receptors, influx of high levels of calcium ions (Ca^{2+}) to the postsynaptic cells, and neuronal cell death (Hutchins & Barger, 1998; Martin et al., 1998).

It has been hypothesized that primary SGN degeneration occurs by means of excitotoxic neural damage. Pathological characteristics of primary SGN degeneration include massive swelling of afferent nerve terminals under the basal pole of IHCs and a total disruption of the postsynaptic membrane (Fig. 8.3; Robertson, 1983; Puel et al., 1998). The pathological alterations of afferent dendrites may be caused by excessive presynaptic release of the neurotransmitter glutamate after acoustic stimulation (Eybalin, 1993; Puel et al., 1998; Hakuba et al., 2000). Local application of glutamate agonists can induce pathologic changes in afferent dendrites similar to those induced by noise trauma (Pujol et al., 1985; Zheng et al.,

1997) and the glutamate antagonist kynurenate can protect SGN dendrites from acoustic damage (Puel et al., 1998). Afferent terminals can fully or partially recover from excitotoxic damage and this recovery may play a role in the phenomenon of temporary threshold shift (TTS) (Liberman & Mulroy, 1982; Robertson, 1983; Puel et al., 1996). However, loss of presysnaptic ribbons and progressive SGN loss after TTS has also been reported in recent studies (Kujawa & Liberman, 2006, 2009; Fig. 8.4).

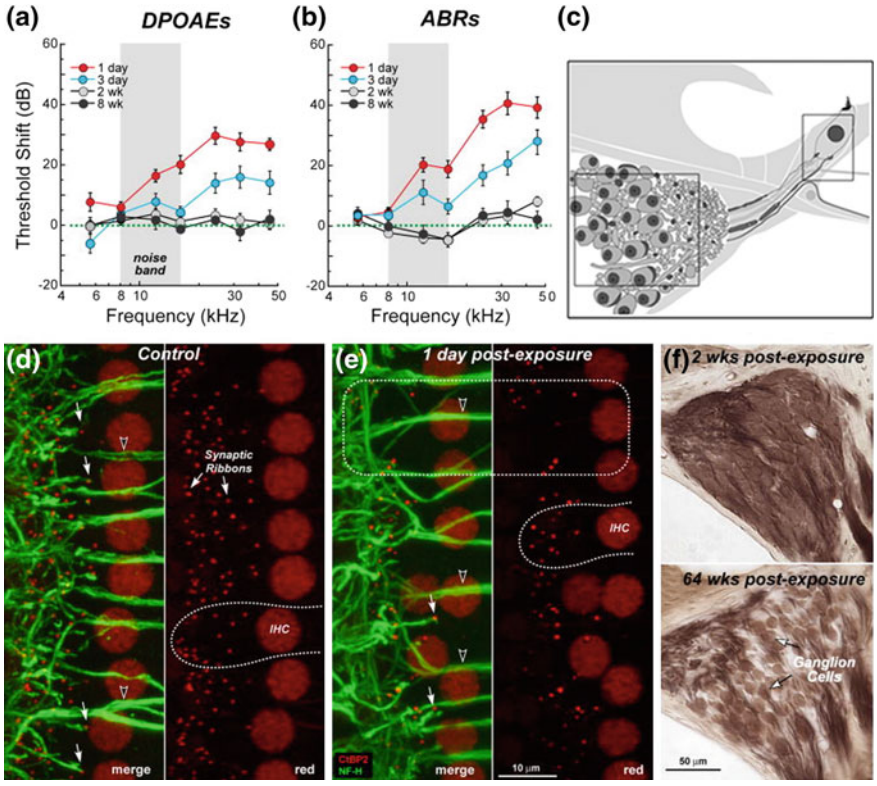

Fig. 8.4 Primary SGN degeneration following noise-induced temporal threshold shifts. **a**, **b** Temporal threshold shifts are seen in the measures of ABRs and DPOAEs in mice after exposure to an 8–16 kHz octave-band noise at 100 dB SPL for 2 h. **c** Schematic representation of the locations of the SGNs and the afferent terminals under IHCs examined in the studies. **d**, **e** A rapid and robust loss of afferent synaptic ribbons (anti-CtBP2, *red*; *arrows*) in the flat preparations of cochleae at the 32 kHz region occurred 1 day after noise exposure. Auditory nerve and afferent dendrites were stained with anti-heavy neurofilament antibody (*green*, *arrowheads*). *White dashed lines* indicate the outlines of IHCs in the control (**d**) and noise-exposed (**e**) ears. A *dashed box* in (**e**) shows the region with significant reduction of both $CtBP2^{+}$ presynaptic ribbons and $neurofilament^{+}$ postsynaptic terminals. Note that the anti- CtBP2 antibody also stains IHC nuclei and anti-neurofilament also stains efferent processes to OHCs. **f** Cross sections show a diffuse SGN loss occurring 64 weeks after noise exposure in the 32-kHz regions of the cochlea (Figure was modified from Kujawa & Liberman, 2009)

8.2.1.3 Primary SGN Degeneration After Noise Exposure

Primary degeneration of SGNs after noise exposure has been understood largely based on experiments associated with glutamate receptor antagonists. However, questions remain on several critical issues. First, high-level noise exposures (e.g., 130 dB SPL pure tone used by Puel et al., 1998) were often applied to generate at least two types of cochlear lesions: (1) loss of hair cells starting with OHCs at lower levels then including IHCs at higher levels; and (2) a massive destruction of afferent terminals below IHCs as shown in Fig. 8.3. Although pathological nerve alterations were seen as early as 20 min after sound exposure (suggesting this pathology is independent of hair cell loss), direct evidence of primary degeneration is still needed from a model with only auditory nerve injury. Also, an evaluation of whether excitotoxic lesions in the afferent nerve terminals are able to recover fully and whether auditory nerves regenerate after noise trauma is still needed. Until recently, most of the morphological observations in these studies were performed at the ultrastructural level. Longitudinal evaluations of dynamic changes in afferent synapses and afferent nerve terminals under IHCs are extremely challenging, and quantitative analysis of morphological alterations in the auditory nerve is virtually absent from these earlier studies. Finally, because lesions are mixed in these models, comprising losses of afferent synapses, SGNs, IHCs, and OHCs, it is difficult to determine which component contributes to the various noise-induced auditory functional deficits.

Recently, newly developed genetic, biochemical, electrophysiological, and high-resolution optical approaches have provided tools for the quantitative examination of the degeneration of SGNs and their associated elements (Khimich et al., 2005; Weisz et al., 2014; Rutherford and Moser, Chap. 5). Numerous biological markers for synapses and nerve terminals have been identified and characterized, including antibodies for the presynaptic ribbon (RIBEYE/transcription factor CtBP2; Khimich et al., 2005), postsynaptic glutamate receptor patches (GluR2/3; Matsubara et al., 1996), unmyelinated nerve terminals (neurofilament; Berglund & Ryugo, 1991), and afferent terminal swellings (parvalbumin; Kujawa & Liberman, 2009). A series of studies using (1) high-powered confocal imaging of sensory epithelium, (2) three-dimensional quantification of ribbon synapse numbers, and (3) histological quantification of the neuronal cells demonstrated that a moderate level of noise exposure can cause a permanent loss of afferent synapses without hair cell damage (Kujawa & Liberman, 2009; Lin et al., 2011; Furman et al., 2013). These studies showed a rapid and selective loss of afferent synaptic ribbons under IHCs after progressive degeneration of SGNs occurring in mice after exposure to an 8–16-kHz octave-band noise at 100 dB SPL for 2 h (Fig. 8.4). Shortly after noise exposure, auditory brain stem responses (ABRs) were elevated about 40 dB concurrent with a slightly smaller threshold elevation of distortion product otoacoustic emissions (DPOAEs)—a measure of OHC function. By 2 weeks after noise exposure, ABR and DPOAE thresholds were back to normal, preexposure levels. Even though cochlear threshold sensitivity fully recovered, the ABR wave I amplitudes were reduced significantly at high stimulus levels at frequencies strongly affected by the noise. Together, these groundbreaking studies provide

direct evidence that primary degeneration can occur in the inner ear in response to pathological stress conditions.

8.2.1.4 Primary SGN Degeneration and Dysfunction Associated with Gene Defects

Genetic studies of sensorineural hearing loss have progressed at a rapid pace in recent years. To date, more than 64 genes and 125 loci that link to various degrees of hearing impairment have been identified (reviews by Dror & Avraham, 2010; Angeli et al., 2012). Some of these genes play important roles in the regulation of synaptic transmission and neuronal survival and death. Deficiency of these genes likely contributes to primary SGN degeneration. Santarelli (2010) reviewed the genes associated with human auditory neuropathy, diagnostically characterized as having abnormal ABRs and completely preserved otoacoustic emissions (OAEs). Here, a brief review was given on several well-documented genes that are associated with auditory neuropathy—*SLC17A8*, *OTOF*, *PJVK*, and *DIAPH3*. In addition, animal studies of gene defects revealed two transcription factors, nuclear factor κB (NF-κB) and forkhead box O3 (FoxO3), that play important roles in maintaining the survival of SGNs and normal function of the auditory nerve and the IHC synapse (Lang et al., 2006; Gilels et al., 2013).

Vesicular glutamate transporter VGLUT3 (SLC17A8, DFNA25) and otoferlin (OTOF, DFNB9) are two key components of the afferent synapse on IHCs. VGLUT3, one of the three subtypes of vesicular glutamate transporters (VGLUT 1-3), is selectively expressed in IHCs and responsible for loading the synaptic vesicles with glutamate (Ruel et al., 2008; Seal et al., 2008). Mice lacking VGLUT3 have no auditory brainstem responses but have robust OAEs, indicating an appearance of normal OHC function. A significant reduction of IHC synapse numbers and pathological alterations of SGNs were also observed in these mice. Otoferlin is a multi-C_2 domain protein essential to the exocytosis of synaptic vesicles in IHCs and the consequent action of the Ca^{2+} sensor triggering membrane fusion at the IHC ribbon synapse (Yasunaga et al., 1999; Roux et al., 2006). Otoferlin-deficient mice ($Otof^{-/-}$) lacking exons 14 and 15, which encode most of C_2C domain, are totally deaf but have preserved OAEs. Although normal IHC ribbon synapses were observed in postnatal $Otof^{-/-}$ mice, the pathological alterations of SGNs have not been determined (Roux et al., 2006).

Pejvakin, encoded by PJVK, is a 352-residue protein belonging to the gasdermin protein family and is expressed in cochlear hair cells, supporting cells, and SGNs (Delmaghani et al., 2006). Abnormal expression of this protein is associated with nonsyndromic auditory neuropathy DFN59 and also DFNA5, which participates in the p53-regulated cellular response to DNA damage (Masuda et al., 2006). Mice lacking pejvakin ($Dfnb59t^{m1Ugds}$) show an elevation of ABR thresholds but normal OAEs at affected frequencies. Examination of the organ of Corti via scanning electron microscope revealed no structural abnormalities, but a detailed examination of auditory nerve morphology was not included. The Diaphanous homolog 3

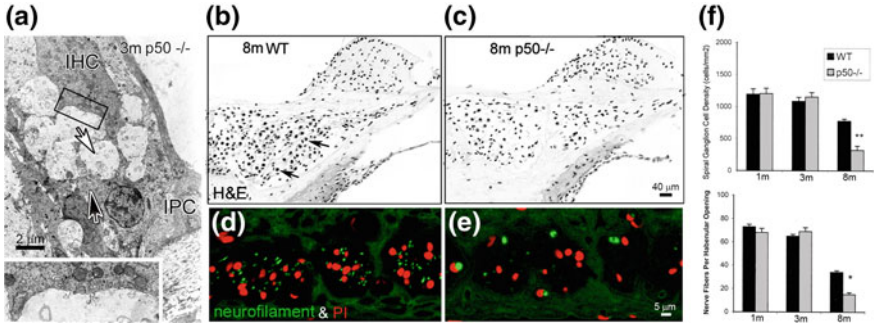

Fig. 8.5 Primary degeneration of the auditory nerve in nuclear factor-κB deficient mice. **a** Ultrastructural features of the basal half of an IHC and its subcellular synaptic region from the basal turn of a 3-month-old $p50^{-/-}$ mouse. Membranous structures presumably representing residue from degenerated cell organelles were seen in the $p50^{-/-}$ mice. Numerous small vesicles infiltrated with mitochondria and short profiles of cisternae appear in the cytoplasm in the base of the IHC. An inner pillar cell (IPC) and border cell enclosed the IHC and nerves consisting of intermingled afferent inner radial fibers (*white arrow*) and efferent spiral fibers (*black arrow*). The efferent inner spiral fibers and terminals (*white arrow*) appear normal. **b–f** Cross sections of the spiral ganglia in the basal turn of an 8-month-old wild type (WT) (B) and $p50^{-/-}$ mouse (**c**). **g** SGN counts in the basal turn in 1-, 3-, and 8-month-old WT and $p50^{-/-}$ mice. The density of SGNs in the 8-month-old $p50^{-/-}$ mice was about half that of the WT controls and the difference was significant (ANOVA, $p < 0.01$) (Figure was replotted from Lang et al., 2006)

(*DIAPH3*), which encodes the diaphanous-3 protein, was mapped to the autosomal dominant auditory neuropathy, dominant 1 (AUNA1). Analysis of lymphoblastoid cells showed an upregulation of *DIAPH3* mRNA expression suggesting a gain of function effect present in AUNA1-affected patients (Schoen et al., 2010). Expression of a constitutively active form of the diaphanous protein in *Drosophila* leads to a deficiency of auditory response from the auditory organ.

The transcription factor NF-κB has a fundamental role in regulating inflammatory responses and apoptosis in response to injury in many cell types (Barkett & Gilmore, 1999). The p50/p65 heterodimer is the predominant complex of NF κB in most mammalian cells. NF-κB is expressed and shows a low-level constitutive activity in the neurons of the central nervous system (Kaltschmidt et al., 1994). By using measures of cochlear function and histopathological evaluation, an accelerated hearing loss with correlated primary degeneration of SGNs and afferent nerve processes was seen in the SGNs of $p50^{-/-}$ mice (Lang et al., 2006). As shown in Fig. 8.5, marked excitotoxic-like alterations were seen at afferent terminals under IHCs of young adult $p50^{-/-}$ mice (1–3 month old). In contrast, no major pathological changes were seen in OHCs or the stria vascularis in the same cochleas. At 8 months of age, the density of SGNs in the basal turn of the knockouts was only about half that of wild-type mice. However, neither significant EP loss with age nor accelerated degeneration of hair cells was seen in the same cochleas, indicating that the loss of SGNs and auditory nerves is primary and independent of the degeneration of sensory hair cells.

FoxO3 is a transcription factor belonging to the forkhead O subclass, which is characterized by a distinct forkhead DNA-binding domain. It plays an important role in the regulation of stress response proteins in a variety of pathological conditions, including excitotoxic damage in brain tissue (Brunet et al., 1999; Davila et al., 2012). Adult mice lacking FoxO3 have elevated ABR thresholds but normal OHC function. Comprehensive histological examinations of cochlear tissues revealed that alterations of synapse locations and degeneration of the afferent nerve cause age-related hearing loss in these mice (Gilels et al., 2013).

8.3 Age-Related SGN Dysfunction and Degeneration

Age-related hearing impairment affects about 40 % of adults older than 65 years of age (Gates & Mills, 2005; Gordon-Salant & Frisina, 2010). By the age of 80, about half of the population suffers from varying degrees of hearing loss and/or has difficulty understanding speech under difficult listening conditions. The most widely accepted pathological categories of age-related hearing loss were established by Schuknecht and Gacek (1993). Four types of human presbycusis were initially described: (1) sensory, mainly affecting the sensory hair cells; (2) neural, typified by the loss of SGNs; (3) metabolic, characterized by atrophy of the stria vascularis; and (4) mechanical, featuring a stiffened basilar membrane and organ of Corti. After additional research on human temporal bones, Schuknecht and Gacek (1993) described neuronal loss as the most persistent and the best indicator of age-related degeneration in the cochlea. In contrast, sensory cell loss is thought to be the least important cause of hearing loss in older adults. The primary SGN degeneration has been consistently seen in a variety of inner ear disorders including Ménière's disease (Nadol & Thornton, 1987), sudden deafness (Ishii & Toriyama, 1977; Schuknecht & Donovan, 1986), Usher's syndrome (Nadol 1988), and Friedreich's ataxia (Spoendlin, 1974). Otte et al. (1978) examined 100 human temporal bones from donors in whom there was no evidence of diseases affecting the cochlea. Loss of SGNs occurred at a rate of about 2100 neurons per decade. In a more recent human temporal bone study, quantitative analysis of another 100 human temporal bones from donors, ranging in age from newborn to 100 years old, revealed a uniform progressive SGN loss at a mean rate of 100 cells per year. The human temporal bones examined in this study separated cases with and without significant cochlear hair cell loss (Makary et al., 2011; Fig. 8.6).

Degeneration and dysfunction of SGNs and their processes are also commonly seen in other types of age-related hearing loss described by Schuknecht, including hearing loss exhibiting sensory and metabolic (strial) characteristics. Damage to various cochlear components can lead to abnormal activity of the auditory nerve. Specifically, elevation of auditory nerve thresholds or changes of auditory nerve tuning curves can result from any of the following: total or partial loss of IHCs or OHCs (Kiang et al., 1976; Schmiedt & Zwislocki, 1980; Kiang et al., 1986), damage to stereocilia on IHCs or OHCs (Liberman & Kiang, 1984), and

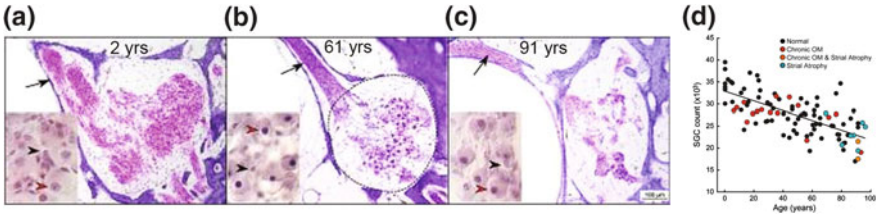

Fig. 8.6 Loss of SGNs in human cochleae. Horizontal sections of human spiral ganglions, which were obtained from donors aged 2 (**a**), 61 (**b**), and 91 (**c**) years, were stained with hematoxylin-eosin. *Black arrows* point to the peripheral portion of the auditory nerve within the osseous spiral lamina. The *dashed line* in (**b**) gives the approximate outline of Rosenthal's canal (RC). High-powered images of some cells within RC are present in the small *inset* in each panel. SGNs with a diffuse cytoplasm are indicated with *red arrowheads*. The *black arrowheads* indicate glial cell nuclei. **d** SGN counts from 100 human cochlea indicate an age-dependent loss of neuronal cells from a mean of 33,679 in the first decade to 22,444 in the tenth decade. Among the 100 ears in the studies, none had significant loss of sensory hair cells, 75 had no significant pathological changes in middle and inner ear (*black solid circles*), 7 had strial atrophy (*blue solid circles*), 16 had chronic otitis media (OM) (*red solid circles*), and two had both OM and strial atrophy (*orange solid circles*). The best-fit straight line is plotted (*solid line*) (Figure was modified from Makary et al., 2011)

degeneration or loss of the cells in the stria vascularis and spiral ligament (Kiang et al., 1986; Lang et al., 2010; Schmiedt, 2010). Comprehensive analyses with multiple functional tests, including auditory threshold and suprathreshold measurements such as CAP or ABR wave I amplitudes, DPOAEs, and endocochlear potential (EP) measurements, are necessary for discriminating SGN loss from other cochlear lesions in the aged ears.

8.3.1 Age-Related SGN Dysfunction: Selective Loss of Low-SR Fiber Activity

Primary afferent auditory nerves can be classified into two or three groups based on their SR and response threshold (Fig. 8.1 and Table 8.1). Low-SR fibers often have substantially higher thresholds and wider dynamic ranges in response to sound (Liberman & Kiang, 1978; Schalk & Sachs, 1980; Liberman, 1982) and are more resistant to masking in the presence of continuous broadband noise. Lower thresholds and smaller dynamic ranges make high-SR fibers saturate more rapidly in response to loud sounds. Consequently, low-SR fibers respond best to higher level sounds and in environments with continuous background noise (Costalupes et al., 1984; Young & Barta, 1986). Low-SR fibers at high levels preserve auditory information, especially for coding sound intensity, timing and spatial information, and amplitude modulation (Zeng et al., 1991; Frisina et al., 1996). Morphological evidence has shown that spatial segregation of central projections related to SR appears in the cochlear nucleus. Low-SR fibers give rise to larger axon arborization

and reach a wider range of regions within the cochlear nuclei than high-SR fibers (Fekete et al., 1984; Liberman, 1993; Ryugo, 2008). In addition, the central components of low-SR auditory fibers project to the areas where the neurons of the medial olivocochlear efferent system are located (Ye et al., 2000), suggesting that low-SR fibers are associated with a high threshold feedback system in the inner ear, in particular for processing loud stimuli. Moreover, human speech processing is conducted in the intensity regions (between 40 and 90 dB SPL) where the low-SR fibers become active, even while the high-SR fibers are saturated. Together, substantial evidence suggests that low-SR fibers are critical in environments that involve complicated auditory processing and speech understanding under difficult listening conditions. Thus, the age-related loss or inactivity of low-SR fibers may play a role in the decline of speech understanding in older adults (Dubno et al., 1984; Halling & Humes, 2000).

Recordings from single auditory nerve fibers can provide direct insight into the functional state of SGNs and their processes (Kiang et al., 1965). Previous studies using a well-established gerbil model of age-related hearing loss indicated reduced activity of the low-SR fiber population (Schmiedt, 1989; Schmiedt et al., 1996). These animals were raised in a sound-conditioned vivarium where the average sound level was 40 dBA. Scattered OHC loss was seen in the apical and basal turns of the aged gerbils with little or no IHC loss. The major pathological alteration in these animals was the degeneration of SGNs and cells in the cochlear lateral wall, which contributes to the generation and maintenance of the EP. Physiological characterization of single auditory-nerve fibers revealed that the percentage of low-SR fibers with characteristic frequencies (CF) greater than 6 kHz decreased from approximately 57 % in young controls to approximately 29 % in quiet-aged gerbils (Fig. 8.7), suggesting that low–SR fibers with CF greater than 6 kHz either degenerate or become inactive with increased age. To validate this result, a method for population studies of auditory nerve activity developed by Relkin et al. (1995) was also applied. This approach measures the recovery of the CAP amplitude after prior stimulation with a probe tone. CAP recovery curves include two segments: a fast segment, reflective of quick recovery of high-SR fibers, and a slow segment associated with the activities of low-SR fibers. CAP recovery curves from aged gerbils revealed a faster recovery than young controls at 8 and 16 kHz, indicating a loss of low-SR fiber activity in the aged animals.

8.3.2 Selective Loss of Low-SR Fibers as a Result of EP Reduction

In addition to the loss and/or shrinkage of the SGNs and radial fiber population seen in quiet-aged gerbils (and other aged rodents including rats and mice) compared to young controls (Keithley et al., 1989; White et al., 2000), a significant degeneration

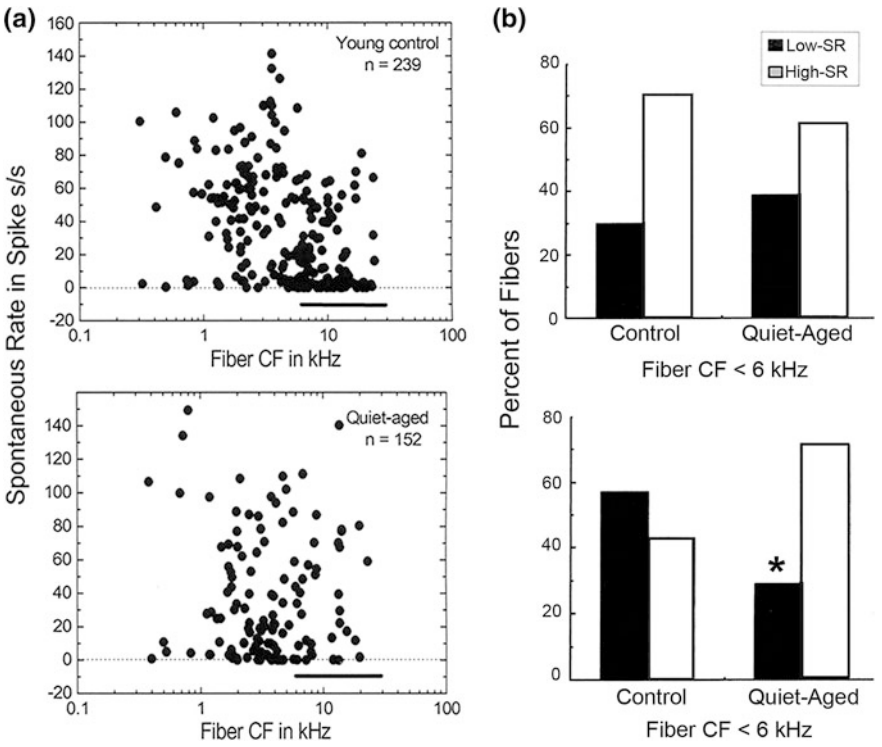

Fig. 8.7 Decline of low-SR fiber activity in quiet-aged gerbils. **a** Distribution of fiber SR plotted as a function of nerve fiber CF shows a reduction of low-SR fiber population for CFs > 6 kHz in quiet-aged gerbils as compared to young controls. **b** Percentages of low-SR fibers with CFs > 6 kHz are significantly different between quiet-aged gerbils and young controls (Figure was replotted from Schmiedt et al., 1996)

of the cochlear lateral wall is also seen in most of these older animals (Schulte & Schmiedt, 1992; Hequembourg & Liberman, 2001; Mills et al., 2006). Can a chronic EP reduction as a result of age-related degeneration of the cochlear lateral wall have a negative impact on auditory nerve activity, particularly on the activity of low-SR fibers? To test this hypothesis, the activity of single auditory nerves were recorded from a young animal model of age-related hearing loss, which was established by the chronic application of furosemide to young adult gerbils (Schmiedt et al., 2002). Application of furosemide to the round window of young animals can cause the chronic reduction of EP as seen in older animals. In this model, the only significant pathological alteration is limited to the hook region of the cochlear lateral wall including a loss of strial intermediate cells and edema in the stria vascularis, whereas the morphology of SGNs and sensory hair cells appear normal (Lang et al., 2010). Reduction of EP levels and alterations of suprathreshold neural responses in furosemide-treated animals resemble that of quiet-aged gerbils

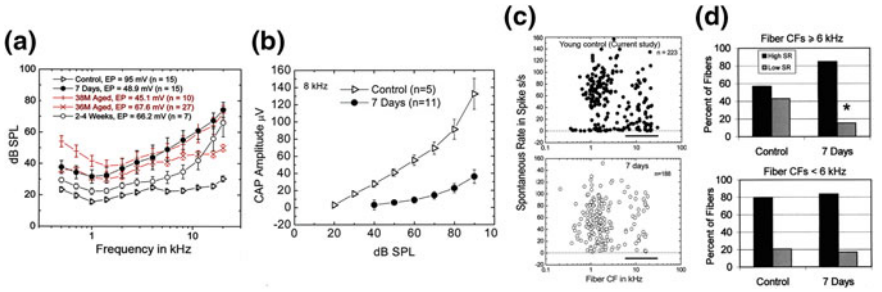

Fig. 8.8 The decline of the low-SR activity as a result EP reduction. **a** Chronic EP reduction results in CAP thresholds in the furosemide-treated ears that resemble those in quiet-aged ears. Average CAP thresholds and EPs values in gerbils treated with furosemide for 7 days are similar to the alterations of CAP thresholds and EPs values of two groups of quiet-aged gerbils (Schmiedt et al., 2002). **b** CAP amplitude input/output (I/O) functions identified the alterations of suprathreshold neural responses in the furosemide-treated ears. The flattened slope of the CAP I/O function obtained in the furosemide-treated ears indicates a decline in the evoked auditory nerve activity in those animals. **c**, **d** Single-unit recording from the auditory nerve shows alterations of SRs across CF in furosemide-treated and control animals. The percentages of low-SR fibers were significantly different in young compared to furosemide-treated animals ($p < 0.01$, chi-square test), similar to that in quiet-aged animals (Schmiedt et al., 2002). (Images were modified from Lang et al., 2010)

(Fig. 8.8a, b). Quantitative evaluation of the spontaneous activity of single auditory fibers in these animals revealed a loss of the low-SR fiber population (Fig. 8.8c, d). CAP recovery functions also indicated a decline in activity of the low-SR fibers with CFs greater than 6 kHz in the same animal model (Lang et al., 2010). These results support the hypothesis that age-related dysfunction of the auditory nerve can be a direct result of the degeneration and/or dysfunction of the cochlear lateral wall and the subsequent chronic reduction of EP levels.

8.3.3 Noise-Induced Primary SGN Degeneration in Aged Ears and Selective Loss of Low-SR Fibers After Noise Exposure

It has been generally accepted that exposing the ear to noise over a lifetime is likely to have a significant impact on the processes of normal age-related hearing loss. A longitudinal clinical study revealed that noise-induced hearing loss (NIHL) occurring at a young age accelerates the hearing loss at a frequencies adjacent to the noise bandwidth (Gates et al., 2000). However, the underlying mechanisms and interaction between NIHL and age-related hearing loss are difficult to determine in these clinical studies (Mills et al., 1998; Lee et al., 2005; Gates, 2006). Recent animal studies using mild levels of octave band noise (that result in a temporary

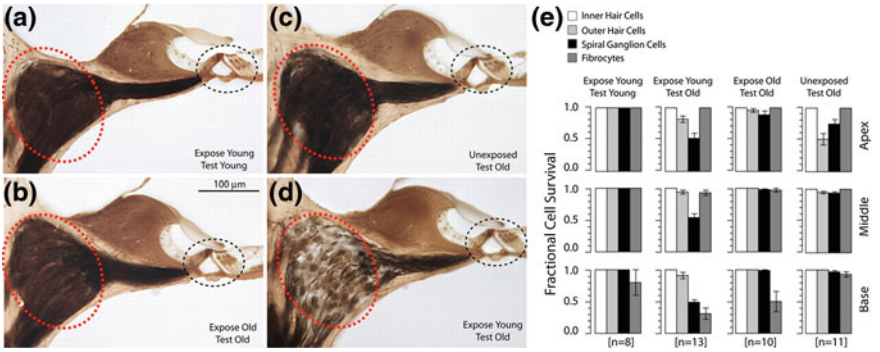

Fig. 8.9 Early noise exposure accelerates primary SGN degeneration in aged ears. Exposure of young (**a**, **d**) and old (**b**) mice with 8–16 kHz octave-band noise at 100 dB SPL for 2 h. A significant loss of SGNs with intact sensory hair cells is seen in old mice that receive noise exposure at a young age (**d**), but not in young mice that were recently exposed to noise (**a**), or in old mice that received (**b**) or did not received (**c**) noise exposure at an old age. *Large and small circles* point to SGNs and the organs of Corti, respectively. Semiquantitative analysis of IHCs, OHCs, SGNs, and spiral ligament fibrocytes shown in (**e**) are present for "Exposure Young Test Young" (exposed at 5.5 weeks and tested at 7.5 weeks), "Exposure Young Test Old" (exposed at 5 weeks and tested at 100 weeks), "Exposure Old Test Old" (exposed at 124 weeks and tested at 126 weeks), and "Unexposed Test Old" (tested at 105 weeks) animals (Figure was modified from Kujawa & Liberman, 2006)

threshold shift in mice and guinea pigs) have demonstrated that noise exposure can cause a rapid loss of nerve terminals and delayed primary SGN degeneration while leaving sensory hair cells intact. Further, early noise exposure results in a significant loss of afferent synapses, accelerated primary SGN degeneration and early onset of age-related hearing loss (Fig. 8.9; Kujawa & Liberman, 2006, 2009; Sergeyenko et al., 2013). A mild level of noise exposure also can cause a significant loss of low- and medium-SR fibers, indicated by single unit auditory nerve recordings (Furman et al., 2013). These findings provide direct evidence that age-related SGN degeneration can be a primary event following mild levels of noise exposure without a significant permanent threshold shift. Thus, noise exposure can cause loss and/or inactivation of low- and medium-SR fibers similar to that seen in aged gerbil ears (Schmiedt, 1989; Schmiedt et al., 1996).

The finding of loss and/or dysfunction of low-SR fibers in the aged cochlea with chronic EP reductions, as well as in young adult cochleas after noise exposure in animal models have broadened our understanding of the causes of the hearing deficits seen in older adults. Yet, many questions remain. For example, is the loss of low-SR fiber activity a result of degeneration of the low-SR fibers or have the characteristics of the low-SR fibers been altered? What mechanism could cause alterations in the SR of the auditory nerve with aging and noise exposure? How does the loss of afferent synapses contribute to the dysfunction of low-SR fibers?

8.4 Animal Models of Primary Spiral Ganglion Neuron Degeneration

Degeneration of SGNs accompanied by or in the absence of sensory hair cells is generally not a rapid process. The process of neuronal death is slow; in fact, it took months or years to see a significant reduction in neuron counts in injured cochleas by partially sectioning the auditory nerve through the posterior cranial fossa (Schuknecht & Woellner, 1955) or after exposure to noise or ototoxic drugs (Leake & Hradek, 1988; Kujawa & Liberman, 2006). This slow pace of neuronal degeneration makes it challenging to obtain enough protein or RNA samples associated with SGN death to investigate the underlying mechanisms of SGN degeneration using currently available cellular and molecular biological assays.

8.4.1 Primary SGN Degeneration After Ouabain Exposure

Ouabain, also known as g-strophanthin, is a cardiac glycoside that specifically binds to the plasma membrane of Na^+, K^+-ATPase and blocks its activity at higher concentrations (Hernández, 1992). Application of ouabain to the intact round window (RW) membrane of adult gerbil cochleas via acute or chronic infusion induces a rapid apoptotic death of about 90 % of the SGNs within 12–24 h. This treatment has a minimal effect on sensory hair cells and other cochlear cell functions (Schmiedt et al., 2002; Lang et al., 2005). Like that observed in adult gerbils, ouabain treatment of adult CBA/CaJ mice also causes substantially elevated neural thresholds and a loss of the majority of SGNs within a few days, whereas other cochlear cells appear intact functionally and morphologically (Fig. 8.10). Given anatomical differences of the round window niche between mouse and gerbil, the procedure used in mice has been modified by employing repeated application of a fresh solution of 1 mM ouabain to the round window at 10–15-min intervals over a 45–60-min duration (Lang et al., 2011; Yuan et al., 2014). This method has been successfully applied in several other mouse strains, revealing similar patterns of SGN degeneration.

8.4.2 Selective Loss of Type I SGNs in Ouabain-Treated Ears

In the ouabain model, apoptotic death occurs in type I SGN neurons, but not in type II SGNs (Lang et al., 2005, 2011; Fig. 8.11). Quantitative immunohistochemical analysis of ouabain-treated ears in both mice and gerbils revealed that surviving neurons (about 7 % of total SGNs) are stained positively with peripherin, a marker

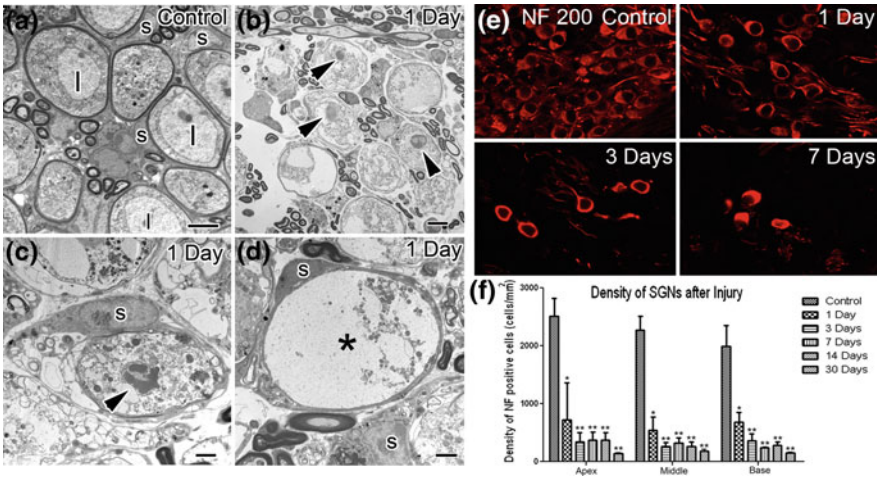

Fig. 8.10 Rapid type I SGN degeneration in ouabain-exposed mice. **a** Type I (I) SGNs are enclosed by glial cells (s) in a normal ear. **b**, **c** Apoptotic-like cell death (*arrowhead*) appears one day after ouabain exposure. **d** Surviving glial cells (s) enclose the debris of the degenerative SGN (*asterisk*). **e** SGNs were stained positively for neurofilament 200 (NF 200, a neural marker, *red*) in a young adult mouse. Many NF^+ cells are missing at 1, 3, and 7 days post-exposure. **f** Cell counts show significant losses in the mean densities of NF^+ SGNs in the apical, middle and basal portions of the cochleas from control, and 1, 3, 7, 14, and 30 days after ouabain exposure. Scale bars, 5 μm in (**a**, **b**); 2 μm in (**c**, **d**) (Figure was modified from Lang et al., 2011)

for type II neurons. The morphological and immunocytochemical features of type II neurons appeared normal even 1 month after ouabian exposure. The release of cytochrome *c*, poly (ADP-ribose) polymerase (PARP) cleavage, and activation of caspase 3 are three crucial events that initiate the processes of apoptosis (Fiskum, 2000; Ha & Snyder, 2000; Chiarugi & Moskowitz, 2002). Evidence from immunostaining shows that cytochrome c redistribution, PARP degradation, and caspase 3 activation occur in type I, but not in type II neurons (Lang et al., 2005). Calcineurin is another important signaling molecule that is involved in modulating neuronal cell survival in response to extracelluar stress (Morioka et al., 1997; Lilienbaum & Israël, 2003). The high level expression of calcineurin protein in type II but not in type I neurons may be associated with the selective survival advantage of the type II neurons (Lang et al., 2005). Ouabain-treated animals express a selective loss of type I SGNs with little effect on sensory hair cells and the cochlear lateral wall. Thus, the ouabain model is a gold standard for the study of cellular and molecular mechanisms of type I SGN degeneration. The ouabain model can also be used to (1) study how central auditory neural circuits reorganize themselves in response to the pathophysiological situation of having peripheral input from type II afferent neurons only; (2) characterize the electrophysiological and biophysical features of the type II neurons; (3) determine whether the loss of type I afferent neural activity generates central hyperacusis or tinnitus; (4) evaluate the self-repair

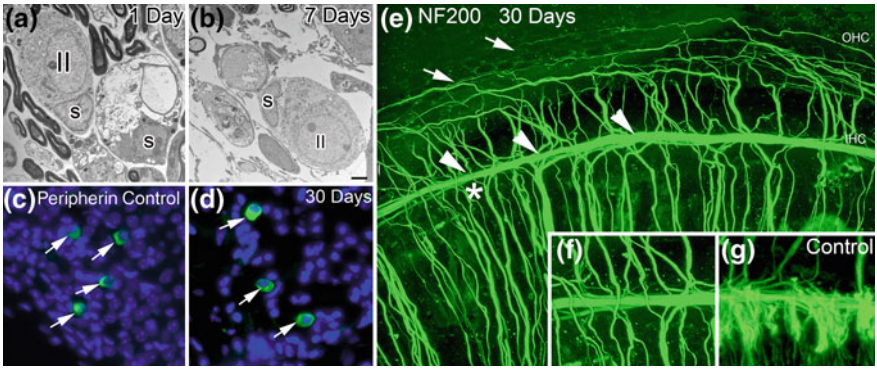

Fig. 8.11 Selective degeneration of type I SGNs in ouabain-treated mice. **a** A type II SGN with nonmyelinating glial cell (s) is present in the apical turn of a mouse 1 day after ouabain exposure. **b** Another type II SGN enclosed by a nonmyelinating glial cell (s) is present in the middle turn of a mouse 7 days post-treatment. **c**, **d** Peripherin^{+} type II SGNs (*green*, *arrows*) in the apical turns of control and 30 day post-treated ears. Nuclei were counterstained with bisbenzimide (*blue*). **e** Surface preparation from the apical turns of a mouse 30 days after treatment shows loss of NF 200^{+} afferent fibers (*arrowheads*) innervating IHCs in the apical turn of a mouse at 30 days post-treatment. **f** An *inset* shows an enlarged image in (**e**) in the area underlying IHCs (*asterisk*) compared to a similar location in a control ear (insert **g**). The absence of radial afferent fibers allows a clear view of the inner spiral bundle including both efferent and afferent fibers projecting into the outer hair cell (OHC) region. Numerous external spiral fibers are seen tracking spirally into the OHC region including long thin type II afferent fibers (*arrows*). Scale bar = 15 μm in (**a**) and (**b**) (Figure was modified from Lang et al., 2011)

potential of cells in the auditory nerve after acute injury; and (5) examine how conditions of cochlear nerve injury affect the outcome of stem cell transplantation or genetic manipulation.

8.4.3 Primary SGN Loss Induced by Central Process Lesion

A partial sectioning of the auditory nerve was first used for the treatment of Ménière's disease (Green & Douglass, 1951). In an animal study of SGN activity, Schuknecht and Woellner (1955) performed a partial section of the auditory nerve within the internal auditory meatus in cats. This surgical procedure induced a diffuse loss of SGNs to varying degrees. Primary SGN degeneration can also be induced by compression given at the internal auditory meatus in rats (Sekiya et al., 2000, 2003). In this model, retrograde degeneration of SGNs was seen after central processes of the cochlear nerve were injured using a compression-recording electrode. TUNEL (terminal deoxynucleotidyl transferase mediated dUTP nick end labeling assay)-positive apoptotic neuronal death and activation of caspase 3 were seen in the spiral ganglion within 5 days after auditory nerve compression, although the pace of SGN death was relatively slow.

8.5 Preservation of the Auditory Nerve

In the past several decades, remarkable progress was made in understanding SGN development and the critical role of neurotrophins, such as brain-derived neurotrophic factor (BDNF) and neurotrophin 3 (NT-3), in the maintenance of the auditory nerve during development and adulthood (Goodrich, Chap. 2; Fritzsch, Chap. 3; Rutherford and Moser, Chap. 5; reviews by Fritzsch et al., 2004; Ramekers et al., 2012; Green et al., 2012). Studies have also been conducted to evaluate the protective roles of neurotrophins on the auditory nerve using deafened animal models of SGN degeneration caused by exposure to ototoxic agents (reviews by Gillespie & Shepherd, 2005; Roehm & Hansen, 2005; Budenz et al., 2012). Treatment of deafened animals with exogenous neurotrophin has led to increased SGN survival rate, enlarged SGNs, regrowth of peripheral afferent processes, and auditory function recovery to various degrees. However, many questions remain to be answered before neurotrophin-associated therapeutic approaches can be safely applied to patients with sensorineural hearing loss. Do the neurotrophin-treated nerve fibers change their physiological properties? Do high- and low-SR auditory fibers respond to neurotrophins differently? What are the long-term effects of neurotrophin treatment on the survival of SGNs and related components in the central auditory system? How does the application of neurotrophin with a variety of combinations and concentrations affect the tonotopical gradient of BDNF and NT-3 expression in the surviving SGNs? How do non-neuronal cells such glial cells or endothelial cells respond to the application of neurotrophins?

Angiogenesis as well as ectopic and disorganized sprouting of auditory nerve fibers were seen in deafened cats treated with BDNF and electrical stimulation from a cochlear implant (Leake et al., 2013). Substantial angiogenesis may increase the risk of tumor formation. Disorganization of the auditory nerve outgrowth after neurotrophin treatment also may affect the functional outcome of a cochlear implant.

Proper function of SGNs require a healthy cochlear microenvironment, such as normal levels of EP, intact sensory hair cells and supporting cells, and also structural integrity of IHC/synapses and myelin sheaths provided by cochlear glial cells. Like sensory hair cells, supporting cells can be an important source of neurotrophin crucial to SGN survival (Stankovic et al., 2004; Sugawara et al., 2005). Glial cells, including Schwann and satellite cells in the auditory nerve, are thought to develop from the neural crest. Glial cells in the central nervous system are important in the regulation of tissue homeostasis, shaping synaptic connectivity and controlling adult neurogenesis after injury (Barres, 2008; Rolls et al., 2009). Previous studies indicated a protective role of Schwann cells on the maintenance of the auditory nerve. A reciprocal signaling mechanism has been found in cultured cochlear glial cells, which provide neurotrophic support to SGNs (Hansen et al., 2001). In mice without activation of the receptor tyrosine-protein kinase ErbB2, an essential protein for the development of Schwann cells, abnormal innervation of the organ of Corti is present during inner ear development (Morris et al., 2006). A loss of glial

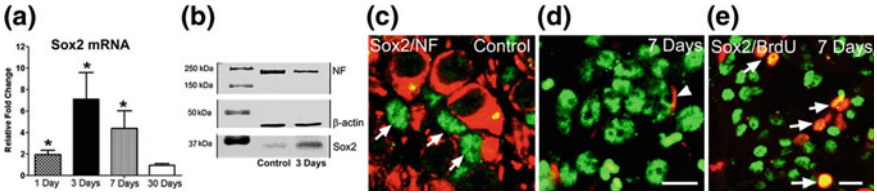

Fig. 8.12 Sox2 upregulation and cell proliferation in the injured adult auditory nerve. **a** Reverse transcriptase-polymerase chain reaction assays show fold changes for Sox2 mRNA expression in the injured auditory nerve. (n = 4–6 per group). **b** Western blot assays show increased Sox2 expression 3 days after ouabain exposure, whereas expression of NF decreased as a result of SGN loss. (**c**, **d**) Dual immunostaining for Sox2 (*green*) and NF (*red*) shows the number of $Sox2^+$ glial cells increase in the auditory nerve 7 days after ouabain exposure. The *arrowhead* indicates a surviving NF^+ SGN process. **e** Dual immunostaining for Sox2 (*green*) and BrdU (*red*) in an injured auditory nerve shows that a majority of $BrdU^+$ cells were Sox2 positive (*arrows*). Scale bars, 7 μm in (**c**, **d**); 12 μm in (**e**) (Figure was modified from Lang et al., 2011)

cells and dysfunction in fibroblast growth factor associated signaling are associated with the degeneration of SGNs and hearing loss (Wang et al., 2009).

Cochlear glial cells most likely are an important resource for the regeneration and self-repair of the adult auditory nerve. Activation of glial cells is associated with neurite growth in a mixed culture of mouse neonatal spiral ganglia (Whitlon et al., 2009). Examination of ouabain-exposed ears revealed a temporal pattern of glial cell phenotypic changes (Lang et al., 2011). Shortly after ouabain exposure, the activation of glial cells was observed in both Rosenthal's canal and osseous spiral lamina. Cell hyperplasia and hypertrophy occurred mostly in the 3 and 7 day postexposure groups. The transcription factor Sox2 is predominantly expressed in proliferating and undifferentiated neural precursors during development and adult neurogenesis in the central nervous system (Ferri et al., 2004; Pevny & Nicolis, 2010). Sox2 is also responsible for the determination of the prosensory domains and the differentiation of SGNs in the developing inner ear (Kiernan et al., 2005; Hume et al., 2007; Dabdoub et al., 2008). Sox2 upregulation and glial cell proliferation occur in the auditory nerve shortly after ouabain exposure (Fig. 8.12; Lang et al., 2011). Dual-staining of Sox2 with a neuronal marker indicates high levels of Sox2 expression in the nuclei of non-neuronal cells. In the injured auditory nerve, $Sox2^+$ cells significantly increased by 3 and 7 days post-treatment. A majority of $BrdU^+$ cells (about 70 %) in ouabain-treated auditory nerve expressed Sox2, and about 6–10 % of $Sox2^+$ cells stained positive with BrdU at 7 days post-treatment, indicating mature glial cells can change their quiescent phenotype and reenter the cell cycle in response to nerve injury. Sox2 is primarly expressed in neural stem cells (NSCs) and plays a critical role in the regulation of neural cell differentiation during development. Although a group of $Sox2^+$ glial-like cells are capable of producing neurons, glial cells, and undifferentiated neural cells in the subgranular zone of the adult hippocampus (Suh et al., 2007), some quiescent glial cells in the adult

auditory nerve also express Sox2. Further study is required to determine whether $Sox2^+$ glial cells are the resource of adult neural stem/progenitor cells (NSPs), like other glial-like NSPs identified in the central nervous system (Suh et al., 2007).

8.6 Summary, Conclusions, and a Few Unanswered Questions

The morphological integrity of the auditory nerve is required for the proper functioning of the mammalian auditory system. Functional and morphological studies conducted over the past several decades have provided insight into a wide spectrum of hearing impairments and related cellular and molecular mechanisms of degeneration of the auditory nerve. Many fundamental questions still remain. For example: how do non-neural cochlear elements contribute to the loss and dysfunction of SGNs? What are the long-term consequences of lateral wall dysfunction resulting in a lowered EP on the survival of SGNs? What is an effective strategy to preserve low-SR fibers or limit the degeneration of the SGNs after noise exposure and with aging? Is the auditory nerve capable of regeneration with the assistance of outside intervention? Do activated cochlear glial cells after auditory nerve injury have neural stem/progenitor properties?

In "Structure of the Mammalian Cochlea" in a previous SHAR volume entitled *The Cochlea*, Dr. Norma B Slepecky (1996, p. 111) wrote, "Anatomical studies on cells of the mammalian inner ear have provided us with many clues as to their different rules in the perception of sound. However, cells do not act in isolation, and hearing depends critically on interactions between cells- some structurally related, others spatially separate but functionally related." -Similarly, SGNs do not act alone; to maintain normal function, SGNs require a healthy cochlear microenvironment comprising many molecular and cellular components. Just as the importance of neural growth factors are to the survival and maintenance of SGN, interaction between SGN and adhesion molecules, extracellular matrix components, cytokines, and the physiochemical nature of the environment including ionic strength are also critical for the survival or death of SGNs with aging or in stress conditions such as noise exposure. Many types of non-neural cells in the inner ear may respond to the survival and death of SGNs. These cells include but are not limited to sensory hair cells, supporting cells, glial cells, cells in the cochlear lateral wall, or inflammatory cells engrafted from bone marrow derived cells. The complex interactions between SGNs and the cochlear microenvironment are important areas for exploration to better understand the mechanisms of SGN degeneration and dysfunction. Recent significant progress in the genetics of sensorineural hearing loss, molecular biology of the developmental auditory nerve, and biophysics of hair cell synaptogenesis, together with the application of systems biology will provide new knowledge and novel methods to answer the fundamental questions of SGN loss, degeneration, and preservation.

Acknowledgments I thank Richard Schmiedt for his encouragement and invaluable suggestions on the scope of the chapter. Many others, Judy Dubno, Jayne Ahlstrom, Emily Franko-Tobin, Kenyaria Noble, Edward Krug, Rhett Chaplin, and the editors of the SHAR series, shared their expertise and provided constructive criticism during the preparation of the text. This work supported by grants NIH grants R01 DC012058 and P50 DC00422.

References

Altschuler, R., Cho, Y., Ylikoski, J., Pirvola, U., Magal, E., & Miller, J. (1999). Rescue and regrowth of sensory nerves following deafferentation by neurotrophic factors. *Annals of the New York Academy of Sciences*, 884, 305–311.

Angeli, S., Lin, X., & Liu, X. (2012). Genetics of hearing and deafness. *Anatomical Record (Hoboken)*, 295(11), 1812–1829.

Bao, J., & Ohlemiller, K. (2010). Age-related loss of spiral ganglion neurons. *Hearing Research*, 264(1–2), 93–97.

Barkett, M., & Gilmore, T. (1999). Control of apoptosis by Rel/NF-kappaB transcription factors. *Oncogene*, 18(49), 6910–6924.

Barres, B. (2008). The mystery and magic of glia: A perspective on their roles in health and disease. *Neuron*, 60(3), 430–440.

Berglund, A., & Ryugo, D. (1991). Neurofilament antibodies and spiral ganglion neurons of the mammalian cochlea. *Journal of Comparative Neurology*, 306(3), 393–408.

Bichler, E., Spoendlin, H., & Rauchegger, H. (1983). Degeneration of cochlear neurons after amikacin intoxication in the rat. *International Archives of Otorhinolaryngology*, 237(3), 201–208.

Bird, S., Gulley, R., Wenthold, R., & Fex, J. (1978). Kainic acid injections result in degeneration of cochlear nucleus cells innervated by the auditory nerve. *Science*, 202(4372), 1087–1089.

Bohne, B., & Harding, G. (2000). Degeneration in the cochlea after noise damage: Primary versus secondary events. *American Journal of Otolaryngology*, 21(4), 505–509.

Brunet, A., Bonni, A., Zigmond, M., Lin, M., Juo, P., Hu, L., Anderson, M., Arden, K.,Blenis, J., & Greenberg M. (1999). Akt promotes cell survival by phosphorylating and inhibiting a Forkhead transcription factor. *Cell*, 96(6), 857–868.

Budenz, C., Pfingst, B., & Raphael, Y. (2012). The use of neurotrophin therapy in the inner ear to augment cochlear implantation outcomes. *Anatomical Record (Hoboken)*, 295(11), 1896–1908.

Chiarugi, A., & Moskowitz, M. (2002). Cell biology, PARP-1—a perpetrator of apoptotic cell death? *Science*, 297(5579), 200–201.

Costalupes, J., Young, E., & Gibson, D. (1984). Effects of continuous noise backgrounds on rate response of auditory nerve fibers in cat. *Journal of Neurophysiology*, 51(6), 1326–1344.

Dabdoub, A., Puligilla, C., Jones, J., Fritzsch, B., Cheah, K., Pevny, L., & Kelley, M. (2008). Sox2 signaling in prosensory domain specification and subsequent hair cell differentiation in the developing cochlea. *Proceedings of the National Academy of Sciences of the USA*, 105(47), 18396–13401.

Davila, D., Connolly, N., Bonner, H., Weisová, P., Dussmann, H., Concannon, C., Huber, H., & Prehn, J. (2012). Two-step activation of FOXO3 by AMPK generates a coherent feed-forward loop determining excitotoxic cell fate. *Cell Death & Differentiation*, 19(10), 1677–1688.

Delmaghani, S., del Castillo, F., Michel, V., Leibovici, M., Aghaie, A., Ron, U., Van Laer, L., Ben-Tal, N., Van Camp, G., Weil, D., Langa, F., Lathrop, M., Avan, P., & Petit, C. (2006). Mutations in the gene encoding pejvakin, a newly identified protein of the afferent auditory pathway, cause DFNB59 auditory neuropathy. *Nature Genetics*, 38(7), 770–778.

Dodson, H. (1997). Loss and survival of spiral ganglion neurons in the guinea pig after intracochlear perfusion with aminoglycosides. *Journal of Neurocytology*, 26(8), 541–556.

Dror. A., & Avraham, K. (2010). Hearing impairment: A panoply of genes and functions. *Neuron*, 68(2), 293–308.

Dubno, J., Dirks, D., & Morgan, D. (1984). Effects of age and mild hearing loss on speech recognition in noise. *Journal of the Acoustical Society of America*, 76(1), 87–96.

Dupont, J., Guilhaume, A., & Aran, J. (1993). Neuronal degeneration of primary cochlear and vestibular innervations after local injection of sisomicin in the guinea pig. *Hearing Research*, 68(2), 217–228.

Ernfors, P., Duan, M., EIShamy, W., & Canlon, B. (1996). Protection of auditory neurons from aminoglycoside toxicity by neurotrophin-3. *Nature Medicine*, 2(4), 463–467.

Eybalin, M. (1993). Neurotransmitters and neuromodulators of the mammalian cochlea. *Physiological Reviews*, 73(2), 309–373.

Fekete, D., Rouiller, E., Liberman, M., & Ryugo, D. (1984). The central projections of intracellularly labeled auditory nerve fibers in cats. *Journal of Comparative Neurology*, 229(3), 432–450.

Ferri, A., Cavallaro, M., Braida, D., Di Cristofano, A., Canta, A., Vezzani, A., Ottolenghi, S., Pandolfi, P., Sala, M., DeBiasi, S., & Nicolis, S. (2004). Sox2 deficiency causes neurodegeneration and impaired neurogenesis in the adult mouse brain. *Development*, 131 (15), 3805–3819.

Fiskum, G. (2000). Mitochondrial participation in ischemic and traumatic neural cell death. *Journal of Neurotrauma*, 17(10), 843–855.

Frisina, R., Karcich, K., Tracy, T., Sullivan, D., Walton, J., & Colombo, J. (1996). Preservation of amplitude modulation coding in the presence of background noise by chinchilla auditory-nerve fibers. *Journal of the Acoustical Society of America*, 99(1), 475–490.

Fritzsch, B., Farinas, I., & Reichard, L. (1997). Lack of neurotrophin 3 causes losses of both classes of spiral ganglion neurons in the cochlea in a region-specific fashion. *Journal of Neuroscience*, 17(16), 6213–6225.

Fritzsch, B., Tessarollo, L., Coppola, E., & Reichardt, L. (2004). Neurotrophins in the ear: Their roles in sensory neuron survival and fiber guidance. *Progress in Brain Research*, 146, 265–278.

Fuchs, P., Glowatzki, E., & Moser, T. (2003). The afferent synapse of cochlear hair cells. *Current Opinion in Neurobiology*, 13(4), 452–458.

Furman, A., Kujawa, S., & Liberman, M. (2013). Noise-induced cochlear neuropathy is selective for fibers with low spontaneous rates. *Journal of Neurophysiology*, 110(3), 577–586.

Gates, G. (2006). The effect of noise on cochlear aging. *Ear and Hearing*, 27(1), 91.

Gates, G., & Mills, J. (2005). Presbycusis. *Lancet*, 366, 1111–1120.

Gates, G., Schmid, P., Kujawa, S., Nam, B., & D'Agostino, R. (2000). Longitudinal threshold changes in older men with audiometric notches. *Hearing Research*, 141, 220–228.

Gilels, F., Paquette, S., Zhang, J., Rahman, I., & White, P. (2013). Mutation of foxo3 causes adult onset auditory neuropathy and alters cochlear synapse architecture in mice. *Journal of Neuroscience*, 33(47), 18409–18424.

Gillespie, L., & Shepherd, R. (2005). Clinical application of neurotrophic factors: The potential for primary auditory neuron protection. *European Journal of Neuroscience*, 22(9), 2123–2133.

Gordon-Salant, S., & Frisina, D. (2010). Introduction and overview. In S. Gordon-Salant, R. D. Frisina, A. N. Popper, & R. R. Fay (Eds.), *The aging auditory system: Perceptual characterization and neural bases of presbyacusis.* New York: Springer Science+Business Media.

Green, R. & Douglass, C. (1951). Intracranial division of the eighth nerve for Ménière's disease; A follow-up study of patients operated on by Dr. Walter E. Dandy. *Annals of Otology, Rhinology, and Laryngology*, 60(3), 610–621.

Green, S. (2000). Neurotrophic signaling by membrane electrical activity in spiral ganglion neurons. In D. J. Lim (Ed.), *Cell and molecular biology of the ear* (pp. 165–82). New York: Kluwer Academic/Plenum Press.

Green, S., Altschuler, R., & Miller, J. (2008). Cell Death and Cochlear Protection. In J. Schacht, A. N. Popper, & R. R. Fay, (Eds.), *Auditory trauma*, *protection*, *and repair* (pp. 275–319). New York: Springer Science+Business Media.

Green, S., Bailey, E., Wang, Q., & Davis R. (2012). The Trk A, B, C's of neurotrophins in the cochlea. *Anatomical Record (Hoboken)*, 295(11), 1877–1895.

Ha, H., & Snyder, S. (2000). Poly(ADP-ribose) polymerase-1 in the nervous system. *Neurobiology of Disease*, 7(4), 225–239.

Hakuba, N., Koga, K., Gyo, K., Usami, S., & Tanaka, K. (2000). Exacerbation of noise-induced hearing loss in mice lacking the glutamate transporter GLAST. *Journal of Neuroscience*, 20 (23), 8750–8753.

Halling, D., & Humes, L. (2000). Factors affecting the recognition of reverberant speech by elderly listeners. *Journal of Speech Language and Hearing Research*, 43(2), 414–431.

Hansen, M., Zha, X-M., Bok, J., & Green, S. (2001). Multiple distinct signal pathways, including an autocrine neurotrophic mechanism, contribute to the survival-promoting effect of depolarization on spiral ganglion neurons. *Journal of Neuroscience*, 21(7), 2256–2267.

Hansen, M., Bok, J., Devaish, A., Zha, X-M., & Green, S. (2003). Ca^{2+}/calmodulin-dependent protein kinases II and IV both promote survival but differ in their effects on axon growth in spiral ganglion neurons. *Journal of Neuroscience Research*, 72(2), 169–184.

Hellstrom, L., & Schmiedt, R. (1990). Compound action potential input/output functions in young and quiet-aged gerbils. *Hearing Research*, 50(1–2), 163–174.

Hequembourg, S., & Liberman, M. (2001). Spiral ligament pathology: A major aspect of age-related cochlear degeneration in C57BL/6 mice. *Journal of the Association for Research in Otolaryngology*, 2(2), 118–129.

Hernández, R. (1992). $Na^{+}/K(^{+})$-ATPase regulation by neurotransmitters. *Neurochemistry International*, 20(1), 1–10.

Hossain, W., Antic, S., Yang, Y., Rasband, M., & Morest, D. (2005). Where is the spike generator of the cochlear nerve? Voltage-gated sodium channels in the mouse cochlea. *Journal of Neuroscience*, 25(29), 6857–6868.

Hume, C., Bratt, D., & Oesterle, E. (2007). Expression of LHX3 and SOX2 during mouse inner ear development. *Gene Expression Patterns*, 7(7), 798–807.

Hutchins, J., & Barger, S. (1998). Why neurons die: Cell death in the nervous system. *Anatomical Record*, 253(3), 79–90.

Ishii, T., & Toriyama, M. (1977). Sudden deafness with severe loss of cochlear neurons. *Annals of Otology*, *Rhinology*, *and Laryngology*, 86(4 Pt 1), 541–547.

Jagger, D., & Housley, G. (2003). Membrane properties of type II spiral ganglion neurons identified in a neonatal rat cochlear slice. *Journal of Physiology*, 552(Pt2), 525–533.

Jyothi, V., Li, M., Kilpatrick, L., Smythe, N., LaRue, A., Zhou, D., Schulte, B., Schmiedt, R., & Lang, H. (2010). Unmyelinated auditory type I spiral ganglion neurons in congenic Ly5.1 mice. *Journal of Comparative Neurology*, 518(16), 3254–3271.

Kaltschmidt, C., Kaltschmidt, B., Neumann, H., Wekerle, H., & Baeuerle, P. (1994). Constitutive NF-kappa B activity in neurons. *Molecular and Cellular Biology*, 14(6), 3981–3992.

Kantardzhieva, A., Liberman, M., & Sewell, W. (2013). Quantitative analysis of ribbons, vesicles, and cisterns at the cat inner hair cell synapse: Correlations with spontaneous rate. *Journal of Comparative Neurobiology*, 521(14), 3260–3271.

Keithley, E., & Feldman, M. (1982). Hair cell counts in an age-graded series of rat cochleas. *Hearing Research*, 8, 249–262.

Keithley, E., Ryan, A., & Woolf, N. (1989) Spiral ganglion cell density in young and old gerbils. *Hearing Research*. 38, 125-33.

Khimich, D., Nouvian, R., Pujol, R., Dieck, S., Egner, A., Gundelfinger, E., & Moser, T. (2005). Hair cell synaptic ribbons are essential for synchronous auditory signalling. *Nature*, 434(7035), 889–894.

Kiang, N., Watanabe, T., Thomas, E., & Clark, L. (1965). Discharge patterns of single fibers in the cat's auditory nerve. Cambridge, MA: MIT Press.

Kiang, N., Liberman, M., & Levine, R. (1976). Auditory-nerve activity in cats exposed to ototoxic drugs and high-intensity sound. *Annals of Otology*, *Rhinology*, *and Laryngology*, 85, 752–768.

Kiang, N., Rho, J., Northrop, C., Liberman, M., & Ryugo, D. (1982). Hair-cell innervation by spiral ganglion cells in adult cats. *Science*, 217(4555), 175–177.

Kiang, N., Liberman, M., Sewell, W., & Guinan, J. (1986). Single unit clues to cochlear mechanisms. *Hearing Research*, 22, 171–182.

Kiernan, A., Pelling, A., Leung, K., Tang, A., Bell, D., Tease, C., Lovell-Badge, R., Steel, K., & Cheah, K. (2005). Sox2 is required for sensory organ development in the mammalian inner ear. *Nature*, 434(7036), 1031–1035.

Kujawa, S., & Liberman, M. (2006). Acceleration of age-related hearing loss by early noise exposure: Evidence of a misspent youth. *Journal of Neuroscience*, 26(7), 2115–2123.

Kujawa, S., & Liberman, M. (2009). Adding insult to injury: cochlear nerve degeneration after "temporary" noise-induced hearing loss. *Journal of Neuroscience*, 29(45), 14077–14085.

Lang, H., Schulte, B., & Schmiedt, R. (2005). Ouabain induces apoptotic cell death in type I spiral ganglion neurons, but not type II neurons. *Journal of the Association for Research in Otolaryngology*, 6(1), 63–74.

Lang, H., Schulte, B., Zhou, D., Smythe, N., Spicer, S., & Schmiedt, R. (2006). Nuclear factor kappaB deficiency is associated with auditory nerve degeneration and increased noise-induced hearing loss. *Journal of Neuroscience*, 26(13), 3541–3550.

Lang, H., Jyothi, V., Smythe, N., Dubno, J., Schulte, B., & Schmiedt, R. (2010). Chronic reduction of endocochlear potential reduces auditory nerve activity: Further confirmation of an animal model of metabolic presbyacusis. *Journal of the Association for Research in Otolaryngology*, 11, 419–434.

Lang, H., Li, M., Kilpatrick, L., Zhu, J., Samuvel, D., Krug, E., & Goddard, J. (2011). Sox2 up-regulation and glial cell proliferation following degeneration of spiral ganglion neurons in the adult mouse inner ear. *Journal of the Association for Research in Otolaryngology*, 12, 151–171.

Leake, P., & Hradek, G. (1988). Cochlear pathology of long term neomycin induced deafness in cats. *Hearing Research*, 33(1), 11–33.

Leake, P., Hradek, G., & Snyder, R. (1999). Chronic electrical stimulation by a cochlear implant promotes survival of spiral ganglion neurons after neonatal deafness. *Journal of Comparative Neurology*, 412, 543–562.

Leake, P., Stakhovskaya, O., Hetherington, A., Rebscher, S., & Bonham, B. (2013). Effects of brain-derived neurotrophic factor (BDNF) and electrical stimulation on survival and function of cochlear spiral ganglion neurons in deafened, developing cats. *Journal of the Association for Research in Otolaryngology*, 14(2), 187–211.

Lee, F., Matthews, L., Dubno, J., & Mills, J. (2005). Longitudinal study of pure-tone thresholds in older persons. *Ear and Hearing*, 26, 1–11.

Liberman, L., Wang, H., & Liberman, M. (2011). Opposing gradients of ribbon size and AMPA receptor expression underlie sensitivity differences among cochlear-nerve/hair-cell synapses. *Journal of Neuroscience*, 31(3), 801–808.

Liberman, M. (1978). Auditory-nerve response from cats raised in a low-noise chamber. *Journal of the Acoustical Society of America*, 63(2), 442–455.

Liberman, M. (1982). Single-neuron labeling in the cat auditory nerve. *Science*, 216, 1239–1241.

Liberman, M. (1993). Central projections of auditory nerve fibers of differing spontaneous rate, II: Posteroventral and dorsal cochlear nuclei. *Journal of Comparative Neurology*, 327(1), 17–36.

Liberman, M., & Kiang, N. (1978). Acoustic trauma in cats. Cochlear pathology and auditory-nerve activity. *Acta Oto-Laryngologica*, *Supplementum*, 358, 1–63.

Liberman, M., & Mulroy, M. (1982). Acute and chronic effects of acoustic trauma: Cochlear pathology and auditory nerve pathophysiology. In R. P. Hamernik, D. Henderson, & R. Salvi (Eds.), *New perspectives on noise-induced hearing loss* (pp. 105–151). New York: Raven Press.

Liberman, M., & Kiang, N. (1984). Single-neuron labeling and chronic cochlear pathology. IV. Stereocilia damage and alterations in rate- and phase-level functions. *Hearing Research*, 16(1), 75–90.

Liberman, M., & Oliver, M. (1984). Morphometry of intracellularly labeled neurons of the auditory nerve: Correlations with functional properties. *Journal of Comparative Neurology*, 223(2), 163–176.

Liberman, M., & Simmons, D. (1985). Applications of neuronal labeling techniques to the study of the peripheral auditory system. *Journal of the Acoustical Society of America*, 78(1 Pt 2), 312–319.

Lilienbaum, A., & Israël, A. (2003). From calcium to NF-kappa B signaling pathways in neurons. *Molecular and Cellular Biology*, 23(8), 2680–2698.

Lim, D. (1976). Ultrastructural cochlear changes following acoustic hyperstimulation and ototoxicity. *Annals of Otology, Rhinology & Laryngology*, 85(6 PT. 1), 740–751.

Lin, H., Furman, A., Kujawa, S., & Liberman, M. (2011). Primary neural degeneration in the guinea pig cochlea after reversible noise-induced threshold shift. *Journal of the Association for Research in Otolaryngology*, 12(5), 605–616.

Makary, C., Shin, J., Kujawa, S., Liberman, M., & Merchant, S. (2011). Age-related primary cochlear neuronal degeneration in human temporal bones. *Journal of the Association for Research in Otolaryngology*,12(6), 711–717.

Martin, L., Al-Abdulla, N., Brambrink, A., Kirsch, J., Sieber, F., & Portera-Cailliau, C. (1998). Neurodegeneration in excitotoxicity, global cerebral ischemia, and target deprivation: A perspective on the contributions of apoptosis and necrosis. *Brain Research Bulletin*, 46(4), 281–309.

Masuda, Y., Futamura, M., Kamino, H., Nakamura, Y., Kitamura, N., Ohnishi, S., Miyamoto, Y., Ichikawa, H., Ohta, T., Ohki, M., Kiyono, T., Egami, H., Baba, H., & Arakawa, H. . (2006). The potential role of DFNA5, a hearing impairment gene, in p53-mediated cellular response to DNA damage. *Journal of Human Genetics*, 51(8), 652–664.

Matsubara, A., Laake, J., Davanger, S., Usami, S., & Ottersen, O. (1996). Organization of AMPA receptor subunits at a glutamate synapse: A quantitative immunogold analysis of hair cell synapses in the rat organ of Corti. *Journal of Neuroscience*, 16(14), 4457–4467.

McFadden, S., Ding, D., Jiang, H., & Salvi, R. (2004). Time course of efferent fiber and spiral ganglion cell degeneration following complete hair cell loss in the chinchilla. *Brain Research*, 997(1), 40–51.

Mills, J., Dubno, J., & Boettcher, F. (1998). Interaction of noise-induced hearing loss and presbyacusis. *Scandinavian Audiology*, *Supplementum*, 48, 117–122.

Mills, J., Schmiedt, R., Schulte, B., & Dubno, J. (2006). Age-related hearing loss: A loss of voltage, not hair cells. *Seminars in Hearing*, 27, 228–236.

Morioka, M., Nagahiro, S., Fukunaga, K., Miyamoto, E., & Ushio, Y. (1997). Calcineurin in the adult rat hippocampus: different distribution in CA1 and CA3 subfields. *Neuroscience*, 78(3), 673–684.

Morris, J., Maklad, A., Hansen, L., Feng, F., Sorensen, C., Lee, K., Macklin, W., & Fritzsch, B. (2006). A disorganized innervation of the inner ear persists in the absence of ErbB2. *Brain Research*, 1091(1), 186–199.

Nadol, J., Jr. (1979). Electron microscopic findings in presbycusic degeneration of the basal turn of the human cochlea. *Otolaryngology – Head and Neck Surgery*, 87(6), 818–836.

Nadol, J., Jr. (1988). Innervation densities of inner and outer hair cells of the human organ of Corti. Evidence for auditory neural degeneration in a case of Usher's syndrome. *ORL; Journal of Oto-Rhino-Laryngology and Its Related Specialties*, 50(6), 363–370.

Nadol, J., Jr. (1997). Patterns of neural degeneration in the human cochlea and auditory nerve: Implications for cochlear implantation. *Otolaryngology-Head and Neck Surgery*, 117(3), 220–228.

Nadol, J., Jr., & Thornton, A. (1987). Ultrastructural findings in a case of Menière's disease. *Annals of Otology*, *Rhinology & Laryngology*, 96(4), 449–454.

Nayagam, B., Muniak, M., & Ryugo, D. (2011). The spiral ganglion: Connecting the peripheral and central auditory systems. *Hearing Research*, 278(1–2), 2–20.

Ohlemiller, K., Echteler, S., & Siegel, J. (1991). Factors that influence rate-versus-intensity relations in single cochlear nerve fibers of the gerbil. *Journal of the Acoustical Society of America*, 90, 274–287.

Otte, J., Schuknecht, H., & Kerr, A. (1978). Ganglion cell populations in normal and pathological human cochleae. Implications for cochlear implantation. *The Laryngoscope*, 88(8 Pt 1), 1231–1246.

Pevny, L., & Nicolis, S. (2010). Sox2 roles in neural stem cells. *The International Journal of Biochemistry & Cell Biology*, 42(3), 421–424.

Puel, J., D'Aldin, C., Safieddine, S., Eybalin, M., & Pujol, R. (1996). Excitotoxicity and plasticity of IHC-auditory nerve contributes to both temporay and permanebt threshold shift. In A. Axelsson, H. Borchgrevink, R. P. Hamernik, P. A. Hellstrom, D. Henderson, & R. J. Salvi (Eds.), *Scientific basis of noise-induced hearing loss* (pp. 36–42). New York: Thieme.

Puel, J., Ruel, J., D'Aldin, C., & Pujol, R. (1998). Excitotoxicity and repair of cochlear synapses after noise-trauma induced hearing loss. *NeuroReport*, 9, 2109–2114.

Pujol, R., & Puel, J. (1999). Excitotoxicity, synaptic repair, and functional recovery in the mammalian cochlea: A review of recent findings. *Annals of the New York Academy of Sciences*, 884, 249–254.

Pujol, R., Rebillard, M., & Rebillard, G. (1977). Primary neural disorders in the deaf white cat cochlea. *Acta Oto-Laryngologica*, 83(1–2), 59–64.

Pujol, R., Lenoir, M., Robertson, D., Eybalin, M., & Johnstone, B. (1985). Kainic acid selectively alters auditory dendrites connected with cochlear inner hair cells. *Hearing Research*, 18(2), 145–151.

Ramekers, D., Versnel, H., Grolman, W., & Klis, S. (2012). Neurotrophins and their role in the cochlea. *Hearing Research*, 288(1–2), 19–33.

Reid, M., Flores-Otero, J., & Davis, R. (2004). Firing patterns of type II spiral ganglion neurons in vitro. *Journal of Neuroscience*, 24(3), 733–742.

Relkin, E., Doucet, J., & Sterns, A. (1995). Recovery of the compound action potential following prior stimulation: Evidence for a slow component that reflects recovery of low spontaneous-rate auditory neurons. *Hearing Research*, 83(1–2), 183–189.

Robertson, D. (1983). Functional significance of dendritic swelling after loud sounds in the guinea pig cochlea. *Hearing Research*, 9(3), 263–278.

Robles, L., & Ruggero, M. (2001). Mechanics of the mammalian cochlea. *Physiological Reviews*, 81(3), 1305–1352.

Roehm, P., & Hansen, M. (2005). Strategies to preserve or regenerate spiral ganglion neurons. *Current Opinion in Otolaryngology & Head and Neck Surgery*, 13(5), 294–300.

Rolls, A., Shechter, R., & Schwartz, M. (2009). The bright side of the glial scar in CNS repair. *Nature Reviews Neuroscience*, 10(3), 235–241.

Roux, I., Safieddine, S., Nouvian, R., Grati, M., Simmler, M., Bahloul, A., Perfettini, I., Le Gall, M., Rostaing, P., Hamard, G., Triller, A., Avan, P., Moser, T., & Petit, C. (2006). Otoferlin, defective in a human deafness form, is essential for exocytosis at the auditory ribbon synapse. *Cell*, 127(2), 277–289.

Ruan, Q., Ao, H., He, J., Chen, Z., Yu, Z., Zhang, R., Wang, J., & Yin, S. (2014). Topographic and quantitative evaluation of gentamicin-induced damage to peripheral innervation of mouse cochleae. *Neurotoxicology*, 40, 86–96.

Ruel, J., Emery, S., Nouvian, R., Bersot, T., Amilhon, B., Van Rybroek, J., Rebillard, G., Lenoir, M., Eybalin, M., Delprat, B., Sivakumaran, T., Giros, B., El Mestikawy, S., Moser, T.,Smith, R., Lesperance, M., & Puel, J. (2008). Impairment of SLC17A8 encoding vesicular glutamate transporter-3, VGLUT3, underlies nonsyndromic deafness DFNA25 and inner hair cell dysfunction in null mice. *The American Journal of Human Genetics*, 83(2), 278–292.

Ryugo, D. (2008). Projections of low spontaneous rate, high threshold auditory nerve fibers to the small cell cap of the cochlear nucleus in cats. *Neuroscience*, 154(1), 114–126.

Salvi, R., Ahroon, W., Perry, J., Gunnarson, A., & Henderson, D. (1982). Comparison of psychophysical and evoked-potential tuning curves in the chinchilla. *American Journal of Otolaryngology*, 3(6), 408–416.

Santarelli, R. (2010). Information from cochlear potentials and genetic mutations helps localize the lesion site in auditory neuropathy. *Genome Medicine*, 2(12), 91.

Schalk, T., & Sachs, M. (1980). Nonlinearities in auditory-nerve fiber responses to bandlimited noise. *Journal of the Acoustical Society of America*, 67(3), 903–913.

Schmiedt, R. (1989). Spontaneous rates, thresholds and tuning of auditory-nerve fibers in the gerbil: Comparisons to cat data. *Hearing Research*, 42(1), 23–35.

Schmiedt, R. (2010). The physiology of cochlear presbyacusis. In S. Gordon-Salant, R. D. Frisina, A. N. Popper, & R. R. Fay (Eds.), *The aging auditory system: Perceptual characterization and neural bases of presbyacusis.* New York: Springer Science+Business Media.

Schmiedt, R., & Zwislocki, J. (1980). Effects of hair cell lesions on responses of cochlear nerve fibers. II. Single- and two-tone intensity functions in relation to tuning curves. *Journal of Neurophysiology*, 43(5), 1390–1405.

Schmiedt, R., Mills, J., & Boettcher, F. (1996). Age-related loss of activity of auditory-nerve fibers. *Journal of Neurophysiology*, 76(4), 2799–2803.

Schmiedt, R., Okamura, H., Lang, H., & Schulte, B. (2002). Ouabain application to the round window of the gerbil cochlea: A model of auditory neuropathy and apoptosis. *Journal of the Association for Research in Otolaryngology*, 3(3), 223–233.

Schoen, C., Emery, S., Thorne, M., Ammana, H., Sliwerska, E., Arnett, J., Hortsch, M., Hannan, F., Burmeister, M., & Lesperance, M. (2010). Increased activity of Diaphanous homolog 3 (DIAPH3)/diaphanous causes hearing defects in humans with auditory neuropathy and in *Drosophila*. *Proceedings of the National Academy of Sciences*, *of the USA*, 107(30), 13396–13401.

Schuknecht, H., & Woellner, R. (1955). An experimental and clinical study of deafness from lesions of the cochlear nerve. *The Journal of Laryngology & Otology*, 69(2), 75–97.

Schuknecht, H., & Donovan, E. (1986). The pathology of idiopathic sudden sensorineural hearing loss. *Archives of Otolaryngology*, 243(1), 1–15.

Schuknecht, H., & Gacek, M. (1993). Cochlear pathology in presbycusis. *Annals of Otology, Rhinology, and Laryngology*, 102(1 Pt 2), 1–16.

Schulte, B., & Schmiedt, R. (1992). Lateral wall Na,K-ATPase and endocochlear potentials decline with age in quiet-reared gerbils. *Hearing Research*, 61(1–2), 35–46.

Seal, R., Akil, O., Yi, E., Weber, C., Grant, L., Yoo, J., Clause, A., Kandler, K., Noebels, J., Glowatzki, E., Lustig, L., & Edwards, R. (2008). Sensorineural deafness and seizures in mice lacking vesicular glutamate transporter 3. *Neuron*, 57(2), 263–275.

Sekiya, T., Hatayama, T., Shimamura, N., & Suzuki, S. (2000). An in vivo quantifiable model of cochlear neuronal degeneration induced by central process injury. *Experimental Neurology*, 161(2), 490–502.

Sekiya, T., Yagihashi, A., Shimamura, N., Asano, K., Suzuki, S., Matsubara, A., Namba, A., & Shinkawa, H. (2003). Apoptosis of auditory neurons following central process injury. *Experimental Neurology*, 184(2), 648–658.

Sergeyenko, Y., Lall, K., Liberman, M., & Kujawa, S. (2013). Age-related cochlear synaptopathy: An early-onset contributor to auditory functional decline. *Journal of Neuroscience*, 33(34), 13686–13694.

Sewell, W. (1984). The relation between the endocochlear potential and spontaneous activity in auditory nerve fibres of the cat. *The Journal of Physiology*, 347, 685–696.

Slepecky, N. (1996). The cochlea. In P. Dallos, A. N. Popper, & R. R. Fay (Eds.). *Structure of the mammalian cochlea.* New York: Springer-Verlag.

Sone, M., Schachern, P., & Paparella, M. (1998). Loss of spiral ganglion cells as primary manifestation of aminoglycoside ototoxicity. *Hearing Research*, 115(1–2), 217–223.

Spoendlin, H. (1971). Primary structural changes in the organ of Corti after acoustic overstimulation. *Acta Oto-Laryngologica*, 71, 166–176.

Spoendlin, H. (1974). Optic cochleovestibular degenerations in hereditary ataxias. II. Temporal bone pathology in two cases of Friedreich's ataxia with vestibulo-cochlear disorders. *Brain*, 97(1), 41–48.

Spoendlin, H. (1975). Retrograde degeneration of the cochlear nerve. *Acta Oto-Laryngologica*, 79, 266–275.

Spoendlin, H. (1984). Factors inducing retrograde degeneration of the cochlear nerve. *Annals of Otology, Rhinology, and Laryngology Supplement*, 112, 76–82.

Spoendlin, H., & Suter, R. (1976). Regeneration in the VIII nerve. *Acta Oto-Laryngologica*, 81(3–4), 228–236.

Stankovic, K., Rio, C., Xia, A., Sugawara, M., Adams, J., Liberman, M., & Corfas, G. (2004). Survival of adult spiral ganglion neurons requires erbB receptor signaling in the inner ear. *Journal of Neuroscience*, 24(40), 8651–8661.

Sugawara, M., Corfas, G., & Liberman, M. (2005). Influence of supporting cells on neuronal degeneration after hair cell loss. *Journal of the Association for Research in Otolaryngology*, 6 (2), 136–147.

Sugawara, M., Murtie, J., Stankovic, K., Liberman, M., & Corfas, G. (2007). Dynamic patterns of neurotrophin 3 expression in the postnatal mouse inner ear. *Journal of Comparative Neurology*, 501(1), 30–37.

Suh, H., Consiglio, A., Ray, J., Sawai, T., D'Amour, K., & Gage, F. (2007). In vivo fate analysis reveals the multipotent and self-renewal capacities of Sox2+ neural stem cells in the adult hippocampus. *Cell Stem Cell*, 1(5), 515–528.

Suryadevara, A., Schulte, B., Schmiedt, R., & Slepecky, N. (2001). Auditory nerve fibers in young and quiet-aged gerbils: Morphometric correlations with endocochlear potential. *Hearing Research*, 161(1–2), 45–53.

Taberner, A., & Liberman, M. (2005). Response properties of single auditory nerve fibers in the mouse. *Journal of Neurophysiology*, 93(1), 557–569.

Wang, S., Furusho, M., D'Sa, C., Kuwada, S., Conti, L., Morest, D., & Bansal, R. (2009). Inactivation of fibroblast growth factor receptor signaling in myelinating glial cells results in significant loss of adult spiral ganglion neurons accompanied by age-related hearing impairment. *Journal of Neuroscience Research*, 87(15), 3428–3437.

Webster, D., & Webster, M. (1978). Cochlear nerve projections following organ of Corti destruction. *Otolaryngology*, 86(2), 342–353.

Webster, M., & Webster, D. (1981). Spiral ganglion neuron loss following organ of Corti loss: A quantitative study. *Brain Research*, 212, 17–30.

Weisz, C., Glowatzki, E., & Fuchs, P. (2009). The postsynaptic function of type II cochlear afferents. *Nature*, 461(7267), 1126–1129.

Weisz C., Glowatzki, E., Fuchs, P. (2014). Excitability of type II cochlear afferents. *Journal of Neuroscience* 34(6), 2365–2373.

White, J., Burgess, B., Hall, R., & Nadol, J. (2000). Pattern of degeneration of the spiral ganglion cell and its processes in the C57BL/6J mouse. *Hearing Research*, 141(1–2), 12–18.

Whitlon, D., Tieu, D., Grover, M., Reilly, B., & Coulson, M. (2009). Spontaneous association of glial cells with regrowing neurites in mixed cultures of dissociated spiral ganglia. *Journal of Neuroscience*, 161(1), 227–235.

Winter, I., Robertson, D., & Yates, G. (1990). Diversity of characteristic frequency rate-intensity functions in guinea pig auditory nerve fibres. *Hearing Research*, 45(3), 191–202.

Yasunaga, S., Grati, M., Cohen-Salmon, M., El-Amraoui, A., Mustapha, M., Salem, N., El-Zir, E., Loiselet, J., & Petit, C. (1999). A mutation in OTOF, encoding otoferlin, a FER-1–like protein, causes DFNB9, a nonsyndromic form of deafness. *Nature Genetics*, 21(4), 363–369.

Ye, Y., Machado, D., & Kim, D. (2000). Projection of the marginal shell of the anteroventral cochlear nucleus to olivocochlear neurons in the cat. *Journal of Comparative Neurology*, 420 (1), 127–138.

Young, E., & Barta, P. (1986). Rate responses of auditory nerve fibers to tones in noise near masked threshold. *Journal of the Acoustical Society of America*, 79(2), 426–442.

Yuan, Y., Shi, F., Yin, Y., Tong, M., Lang, H., Polley, D., Liberman, M., & Edge, A. (2014). Ouabain-induced cochlear nerve degeneration: Synaptic loss and plasticity in a mouse model of auditory neuropathy. *Journal of the Association for Research in Otolaryngology*, 15(1), 31–43.

Zeng, F., Turner, C., Relkin, E. (1991). Recovery from prior stimulation. II: Effects upon intensity discrimination. *Hearing Research*, 55(2), 223–230.

Zheng, X., Henderson, D., Hu, B., & McFadden, S. (1997). Recovery of structure and function of inner ear afferent synapses following kainic acid excitotoxicity. *Hearing Research*, 105, 65–76.

Zimmerman, C., Burgess, B., & Nadol, J. (1995). Patterns of degeneration in the human cochlear nerve. *Hearing Research*, 90(1–2), 192–201.

Chapter 9
Stem Cells for the Replacement of Auditory Neurons

Bryony A. Nayagam and Albert S.B. Edge

Keywords Cell transplantation · Differentiation · Hair cell · Inner ear • innervation · Regeneration · Spiral ganglion neuron · Synaptogenesis

9.1 Introduction

Stem cells offer the potential to replace damaged or diseased cells and tissues of the body, by providing an unlimited new source of cells. The possibility of cell replacement is dependent on the ability to guide cell fate to relevant phenotypes. The understanding of cell fate draws from molecular biology and development, and in many organs has led to information on controlled differentiation of many of the cell types in the body. For inner ear neural replacement, stem cell therapy ultimately requires the meaningful reconnection of stem cell-derived auditory neurons to their peripheral and central targets, to faithfully reproduce a functional, tonotopic circuit. Learning how a stem cell is programmed for neural differentiation, how a neuron sends out a process to find a target, how it comes to recognize the appropriate site for synaptogenesis on a target cell, and how to express the molecular machinery needed for conducting an action potential and integrating with the functional circuit are all needed for rebuilding a damaged circuit [recently reviewed by Needham et al. (2013), Shi and Edge (2013)]. In instances where the peripheral targets (the sensory hair cells) have undergone severe degeneration these new neurons could be encouraged to grow processes toward a cochlear implant. This neural prosthesis

B.A. Nayagam
Department of Audiology and Speech Pathology, University of Melbourne, Parkville, VIC 3010, Australia
e-mail: b.nayagam@unimelb.edu.au

A.S.B. Edge (✉)
Eaton-Peabody Laboratory, Massachusetts Eye and Ear Infirmary, Harvard Medical School, Boston, MA 02114, USA
e-mail: albert_edge@meei.harvard.edu

A. Dabdoub et al. (eds.), *The Primary Auditory Neurons of the Mammalian Cochlea*, Springer Handbook of Auditory Research 52,
DOI 10.1007/978-1-4939-3031-9_9

could then directly stimulate stem cell-derived auditory neurons in the absence of the hair cells, to provide sound information to the brain. The need for accurate reproduction of a tonotopic neural circuit makes inner ear stem cell therapy particularly challenging. Despite these challenges, progress is being made toward the use of stem cells for auditory neural replacement, and these studies are discussed in detail in the sections that follow.

9.2 Auditory Neurons Do Not Regenerate Spontaneously

Loss of auditory neurons has been recognized as a cause of hearing loss for many years. Although its pathogenesis has been disputed, the loss does not appear to be reversible (Kujawa & Liberman, 2006, 2009). Neural cell death can be a secondary consequence of primary loss of hair cells (Spoendlin, 1971; Liberman & Mulroy, 1982), but more recent studies suggest that neural loss can also be a primary effect of insults to the neurons themselves. Cell replacement would allow recovery of function from synaptic loss or neural cell death.

9.2.1 Synaptic Loss as a Primary Cause of Hearing Loss

Damage to the synapse between spiral ganglion neurons and hair cells has come to be seen as a primary cause of hearing loss as a result of recent work in which noise exposure caused primary afferent degeneration (Kujawa & Liberman, 2006). Loss of hearing due to damage to afferent synapses and retraction of fibers has become increasingly recognized. Hair cells were apparently normal but afferent synapses were affected after a 105 dB exposure for 2 h in this model. A profound reduction in the threshold and wave 1-amplitude of the auditory brain stem response (ABR) followed by recovery of threshold within weeks was the hallmark of the functional assessment. This loss of amplitude correlated with the loss of synapses with hair cells and also with a concomitant decrease in the number of ribbons. The low spontaneous rate, high-threshold neurons were more susceptible to degeneration than the high spontaneous rate fibers (Kujawa & Liberman, 2009).

9.2.2 Cell Death Can Result from Long-Term Synaptopathy

Slow primary loss of neurons after recovery from the initial damage overturns a long-held view that recovery from a temporary threshold shift signals a restoration of normal cochlear function after noise-induced hearing loss. Temporary threshold shifts can be a harbinger of future problems due to neural degeneration, and neural

loss without hair cell loss has been observed in human autopsy specimens (Makary et al., 2011).

A similar pattern of synaptic loss followed by degeneration of neurons was also seen with aging (Sergeyenko et al., 2013). Animals that were aged without an overt, deafness-inducing noise had slow loss of synapses with hair cells and an attendant loss of ABR wave 1-amplitude. Subsequent degeneration and death of neurons was seen, as in the noise-exposed mice.

9.2.3 Neural Loss Can Be Secondary to Hair Cell Loss

Degeneration of hair cells is another cause of hearing loss. A variety of insults cause hair cell death, and neural degeneration occurs as a secondary consequence of hair cell loss (Spoendlin, 1971; Liberman & Mulroy, 1982; Robertson, 1983). Hair cell loss has been recognized as a cause of deafness from the examination of human temporal bones. Neural counts were performed as a part of these studies and supported the idea that loss of neurons was secondary to hair cell loss.

9.2.4 Unlike Other Peripheral Nerves the Auditory Nerve Does Not Regenerate Spontaneously

Regrowth of auditory neurons after loss due to noise or toxin damage does not appear to occur (Starr et al., 2004; Kujawa & Liberman, 2009). Although there is a possibility of some regeneration of afferent synapses immediately postinjury (Lerner-Natoli et al., 1997), other mechanisms such as partial repair of damaged hair cells could account for recovery. There was no evidence of regenerated fibers or synapses in careful studies that quantified synaptic contacts after the retraction of peripheral fibers due to noise damage (Kujawa & Liberman, 2009; Lin et al., 2011), and after loss of fibers or of the neurons themselves, synaptogenesis with hair cells does not appear to be a mechanism for recovery. This lack of spontaneous regrowth of fibers or regeneration of new cells prevents recovery of function after damage (Kujawa & Liberman, 2006, 2009).

9.2.5 Some Evidence of Regrowth and Functional Synapses in Newborns

In work using spiral ganglion neurons from newborn mice there is conclusive evidence that the neurons send out fibers that make synapse with hair cells (Martinez-Monedero et al., 2006; Tong et al., 2013; Brugeaud et al., 2014). These

models involve replacement of lost neurons by addition of exogenous neurons to the organ of Corti. Only in an in vitro model of newborn rat cochlear explants has there been any evidence that peripheral fibers could spontaneously regrow to hair cells (Wang & Green, 2011).

9.3 Stem Cells to Auditory Neurons: Can We Make an Auditory Neuron?

A key question in stem cell biology is how cell fate is determined for the numerous cell types in the body. Genomic approaches have defined promoter and enhancer elements controlling gene expression that determine the fate of specific cell types (Forrest, 2014), and these data on regulation of cell specific genes direct protocols for differentiation of specific cell types. The quest to understand cell fate determination has given rise to a new tool for the study of human disease by using stem cells from human donors with specific diseases. Induced pluripotent stem cells (iPSCs) derived from humans will allow drug screening for the disease in question and will also be useful for therapies that use the cells for transplantation.

Attempts to generate functional neurosensory progenitors for cell replacement have led to cell phenotypes that closely resemble the auditory (spiral ganglion) neurons from a variety of stem cell sources in vitro, including mouse embryonic stem cells (Coleman et al., 2007a; Reyes et al., 2008; Purcell et al., 2013), mouse inner ear stem cells (Martinez-Monedero et al., 2008), human fetal (Chen et al., 2007, 2009) and embryonic (Shi et al., 2007; Chen et al., 2012; Nayagam et al., 2013) stem cells, mesenchymal stem cells (Kondo et al., 2011; Bas et al., 2013), and iPSCs (Nishimura et al., 2009; Gunewardene et al., 2014). These differentiated stem cells express a relevant cohort of neuronal genes, and several are electrically active and capable of forming new synapses on appropriate peripheral and central target tissues in vitro (summarized in Table 9.1).

9.3.1 Directed Differentiation of Stem Cells to Auditory Neurons

Directed differentiation of cells toward an auditory neural-like lineage has taken two approaches; either the application of soluble factors in the media or the genetic modification of stem cells to express relevant transcription factors or proteins essential for normal auditory neural development. Soluble factors have included retinoic acid (Coleman et al., 2007a), bone morphogenetic proteins (Shi et al., 2007; Nayagam et al., 2013), basic fibroblast growth factor, insulin-like growth factor 1 and epidermal growth factor (Chen et al., 2007, 2009), fibroblast growth factors 3 and 10 (Chen et al., 2012), conditioned medium (Coleman et al., 2007a; Kondo et al., 2011),

Table 9.1 Summary of in vitro studies deriving auditory-like neurons from human stem cells, and their reinnervation potential

Cell type/preparation	Auditory neural markers detected	Electrical activity detected ✓ or ×	New synapses detected ✓ or ×	References
Embryonic stem cells				
HESC	*Pax2*, *Brn3a*, *GATA3*, βIII tubulin, peripherin	×	✓ Synapsin +ve new synapses on hair cells	Shi et al. (2007)
HESC	*Pax2*, *Sox2*, *NeuroD1*, *Islet1*, *Brn3a*, *GATA3*, NF, peripherin, VGLUT1	×	✓ Synapsin1 +ve new synapses on hair cells and cochlear nucleus neurons	Hyakumura et al. (2012), Gunewardene et al. (2014)
HESC	*Pax2/8*, *Sox2*, *Six1*, *NeuroD1*, *Islet1*, *Brn3a*, *GATA3*, βIII tubulin, NF, NTRK2	✓	✓ New synapses detected in vivo	Chen et al. (2012)
HESC	*Pax2*, *Brn3a*, peripherin, NF	✓	✓ Synapsin1 +ve new synapses on hair cells	Nayagam et al. (2013)
HESC	*NeuroD1*, *Brn3a*, VGLUT1, NFM,	✓	Not examined	Needham et al. (2014)
Induced pluripotent stem cells				
HIPSC	*Pax2/7*, *Sox2*, *NeuroD1*, *Islet1*, *Brn3a*, *GATA3*, NF, peripherin, VGLUT1	✓	✓ Synapsin1 +ve new synapses on hair cells	Gunewardene et al. (2014)
Inner ear stem cells				
IESC	*Pax2*, *Brn3a*, *GATA3*, *Islet*, peripherin, calretinin, NTRK2/3	✓	Processes extended to hair cells	Martinez-Monedero et al. (2008)
HFASC	*Pax2*, *Sox2*, *Ngn1*, Nestin, *Brn3a/c*, GATA3, βIII tubulin	×	×	Chen et al. (2007)

(continued)

Table 9.1 (continued)

Cell type/preparation	Auditory neural markers detected	Electrical activity detected ✓ or ×	New synapses detected ✓ or ×	References
HFASC	*Pax2*, *Sox2*, *Ngn1*, Nestin, *Brn3a/c*, *GATA3*, βIII tubulin, NF	✓	×	Chen et al. (2009)
Mesenchymal stem cells				
HMSC	Nestin, Tuj-1	×	×	Bas et al. (2013)

IESC inner ear stem cells; *HESC* human embryonic stem cells; *HIPSC* human induced pluripotent stem cells; *MIPSC* mouse induced pluripotent stem cells; *MESC* mouse embryonic stem cells; *HFASC* human fetal auditory stem cells; *IPSCs* induced pluripotent stem cells; *MMSCs* mouse mesenchymal stem cells; *HMSCs* human mesenchymal stem cells; *NTRK2/3* neurotrophic tyrosine kinase receptor B/C

or small molecules such as Y27632 (Nayagam et al., 2013; Gunewardene et al., 2014). Alternatively, the forced expression of transcription factors relevant for auditory neural differentiation such as *Ngn1* (Reyes et al., 2008; Purcell et al., 2013) and *Tlx3* (Kondo et al., 2011) has generated sensory neurons from mouse embryonic and human mesenchymal stem cells, respectively. Although the aforementioned protocols can produce auditory-like neurons, it has been challenging to derive this particular cell population conclusively in the absence of a single specific marker to define the lineage. As a result, these studies have relied on groups of relevant markers to characterize the lineage, together with electrophysiological characterization of ion channels underlying their electrical activity.

More specifically, auditory-like neurons derived from embryonic stem cells have been reported to express several characteristic proteins and transcription factors to their endogenous counterparts including (but not limited to) *Ngn1*, *NeuroD1*, *Brn3a*, *GATA3*, and neurofilament. A summary of key findings in relation to this is provided in Table 9.1. Although these cells cannot be defined as auditory neurons, in many instances they show a bipolar morphology and neurosensory protein and/or transcription factor expression (Shi et al., 2007; Chen et al., 2012; Nayagam et al., 2013). Ultimately, these auditory-like sensory neurons could provide a source for functionally relevant replacement of cells in a deaf ear.

Recent experiments have shown that human and mouse embryonic stem cells after appropriate differentiation function as replacement cells in the auditory system (refer to Tables 9.1 and 9.2). The use of induced pluripotent stem cells has opened a new avenue of investigation for pluripotent stem cell research, given that these cells facilitate the derivation of patient-specific cells for transplantation. Initial experiments differentiated murine-derived iPSC lines into a neural lineage using stromal cell coculture (Nishimura et al., 2009, 2012). This culturing method has been used to produce dopaminergic neurons from the midbrain (Kawasaki et al., 2000, 2002). More recent experimentation has compared the efficiency of deriving neurosensory

Table 9.2 Summary of stem cell transplantation studies for auditory neural replacement

Cell type/preparation	Cell survival time (weeks)	Reference
Mouse stem cells		
Mouse ESCs	1–14	Corrales et al. (2006), Lang et al. (2008), Reyes et al. (2008)
Mouse IPSCs	1–4	Nishimura et al. (2009, 2012)
Mouse ASCs/MSC	1–4	Matsuoka et al. (2006), Kondo et al. (2011), Sullivan et al. (2011)
Mouse NSCs	1–9	Regala et al. (2005), Parker et al. (2007), Sekiya et al. (2007)
Rat stem cells		
Rat NSCs	2–9	Regala et al. (2005), Sekiya et al. (2007), Fu et al. (2009)
Guinea pig stem cells		
Guinea pig ASCs	4	Ogita et al. (2010)
Chinchilla stem cells		
Chinchilla ASCs	3	Naito et al. (2004)
Human stem cells		
Human ESCs	8.6–10	Shi et al. (2007), Chen et al. (2012)
Human ASCs/MSCs	2–8.5	Revoltella et al. (2008), Cho et al. (2011), Pandit et al. (2011)

ESC embryonic stem cell; *IPSC* induced pluripotent stem cell; *ASC* adult stem cell; *MSC* mesenchymal stem cell; *NSC* neural stem cell

progenitors from several human iPSC lines using noggin, epidermal growth factor, basic fibroblast growth factor, and the small molecule and Rho kinase inhibitor Y27634. Human iPSC lines were shown to express sequentially many of the key proteins and transcription factors found in the differentiating otic placode and auditory neurons in situ, including (but not limited to) *NeuroD1*, *Islet1*, *Brn3a*, *GATA3*, neurofilament, and VGLUT1 (Gunewardene et al., 2014). Although the expression of these markers was more variable in the human iPSC lines examined (in comparison to human embryonic stem cells grown under the same conditions), these data illustrated that auditory neuron-like cells could be generated from several human iPSC lines. How these progenitors survive and integrate into the deaf ear remains to be demonstrated.

Mesenchymal stem cells, have been differentiated into auditory-like sensory neurons that express a number of relevant genes including *Ngn1*, *NeuroD1*, *Brn3a*, *GATA3*, and *GluR4* (Kondo et al., 2011). Similar to iPSCs, mesenchymal stem cells are a potential source of autologous donor cells capable of avoiding issues of immune rejection. In addition to deriving cells with an appropriate phenotype, replacement neurons would also need specific physiological characteristics, and auditory-like neurons derived from mesenchymal stem cells have been shown to possess similar markers but not electrophysiological properties of auditory neurons.

9.3.2 *Are Stem Cell-Derived Auditory Neurons Electrically Active?*

In addition to their characteristic biochemistry, the primary auditory neurons of the cochlea are glutamatergic and capable of firing at high rates. The spike rate in response to acoustic stimulation is on the order of 200–400 spikes/s (Kiang et al., 1965; Javel & Viemeister, 2000); however, rates up to 1000 spikes/s are evinced by electrical stimulation (Shepherd & Javel, 1997; Javel & Viemeister, 2000). This raises important considerations for any cell type that may be used in a cell replacement therapy, including the following: Are stem cell-derived neurons electrically active? Do they possess an appropriate compliment of ion channels? Can they fire action potentials? Will they respond to the high stimulus rate provided by the cochlear implant?

A smaller number of studies have investigated the ability of stem cell-derived auditory-like neurons to generate action potentials in response to intracellular current injection (Martinez-Monedero et al., 2008; Nayagam et al., 2013; Purcell et al., 2013). These studies have illustrated that stem cell-derived auditory-like neurons possess key potassium and sodium currents necessary for neural communication. Among these are the inward sodium currents (I_{Na}) and sustained outward potassium currents (I_K). These are arguably the most basic currents necessary to instigate action potentials, and therefore communicate meaningful signals to their target(s).

Although capable of basic electrical communication, stem cell-derived auditory-like neurons do not fire action potentials with the same efficiency as adult mammalian auditory neurons (Needham et al., 2014). Their firing profile resembles that of mammalian embryonic auditory neurons in situ (Marrs & Spirou, 2012), with increased latency and broader action potentials when compared to early postnatal mammalian auditory neurons (Needham et al., 2014). Despite extended culture in vitro, these stem cell-derived auditory-like neurons did not mature into more electrically mature phenotypes, suggesting that additional factors, and potentially synapse formation, might be necessary to reach functional maturity. This idea is consistent with other reports that detail the importance of synaptogenesis between hair cells and auditory neurons (and thus spontaneous activity), in producing electrically mature auditory neurons in situ (Lippe, 1994; Marrs & Spirou, 2012). These findings set the stage for new in vitro models that incorporate both differentiation and synapse formation to determine whether more physiologically mature auditory-like neurons can be produced. An important additional feature of auditory neural physiology is the ability to respond at high rates to process sound information. This has been investigated recently with interesting findings (Needham et al., 2014).

The afferent neurons of the auditory system can follow high-frequency stimulation, as well as the electrically encoded input from a cochlear implant. Pitch discrimination deteriorates as stimulation levels approach 300 pulses per second (Shannon, 1983; Zeng, 2002; Vandali et al., 2013). Although human stem

cell-derived auditory-like neurons can reliably entrain to pulsatile stimulation rates of approximately 20 pulses per second, firing entrainment fell to 50 % at approximately 50 pulses per second. Moreover, entrainment of stem cell-derived neurons became statistically poorer than auditory neurons at stimulation rates of 67 pulses per second. A reduction in firing entrainment would likely affect the amount of information encoded in the signal. Thus, an effective auditory neural replacement strategy, irrespective of which stem cell type was ultimately chosen, would likely incorporate the transplantation of functional neurosensory progenitors that were capable of firing entrainment of 300 pulses per second.

9.3.3 Can Stem Cell-Derived Auditory Neurons Make Functional Connections on Appropriate Tissues In Vitro?

As adult spiral ganglion neurons do not appear to regrow and form synapses with hair cells, assays for afferent synaptogenesis have been developed using newborn cochlear tissues where regrowth can be studied (Flores-Otero et al., 2007; Nayagam et al., 2013; Brugeaud et al., 2014). Synaptogenesis has been studied using both stem cell-derived neurons (Matsumoto et al., 2008; Nayagam et al., 2013) and newborn spiral ganglion neurons (Flores-Otero et al., 2007; Brugeaud et al., 2014; Tong et al., 2013). In vitro synaptogenesis assays have examined whether the peripheral and central tissues of the postnatal auditory system are reinnervated by stem cell-derived auditory neurons.

Synaptogenesis has been examined after toxin-induced or mechanical denervation of the organ of Corti (Martinez-Monedero et al., 2006; Flores-Otero et al., 2007). Mouse spiral ganglion neurons grew to the denervated hair cells and formed synapses that were immunopositive for the synaptic marker, synapsin (Martinez-Monedero et al., 2006). Terminals formed by stem cell-derived neurons were similar to those formed by the spiral ganglion neurons (Fig. 9.1b; Flores-Otero et al., 2007; Martinez-Monedero et al., 2008; Nayagam et al., 2013): Human stem cell-derived auditory-like neurons extended processes toward the hair cells where they formed synapsin-positive synapses (Shi et al., 2007; Nayagam et al., 2013; Gunewardene et al., 2014); neurons derived from mouse embryonic stem cells formed synapsin- and/or synaptophysin-positive terminals with hair cells after 7 days in vitro (Matsumoto et al., 2005, 2008). The staining of presynaptic markers in the neurons suggests that the polarity of the synapse was initially reversed (Martinez-Monedero et al., 2006). Importantly, the pattern of innervation between stem cell-derived neurons and hair cells is disorganized and new synapses are en passant-like, rather than bouton-like in ultrastructure (Fig. 9.1e; Nayagam et al., 2013). Rewiring of hair cells will need to be carefully controlled to regenerate a functional system, which may be possible by the careful application of guidance molecules (refer to Sect. 9.5).

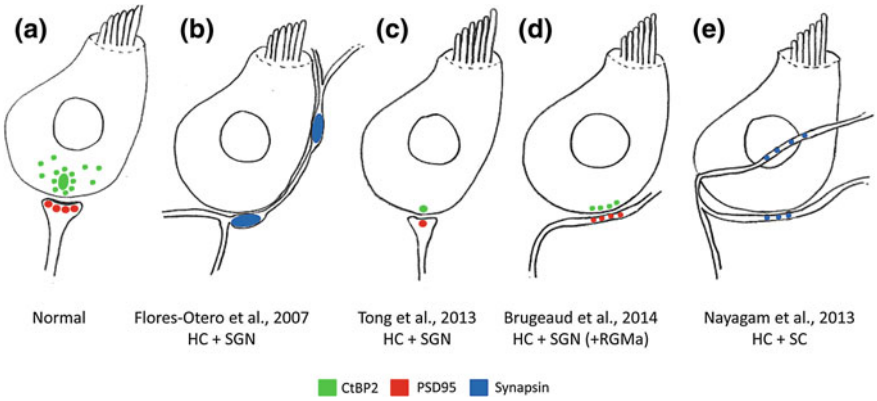

Fig. 9.1 Schematic overview of in vitro auditory synaptogenesis assays and their major findings. **a** Normal afferent innervation in the mammalian cochlea illustrating close association between hair cell (HC) CtBP2-positive (*green*) ribbon synapses and PSD95 positive (*red*) afferent terminal from type I spiral ganglion neurons (SGN). **b** Following denervation, early postnatal SGNs reinnervated HCs and their neurites made large, putative, presynaptic (synapsin-positive; *blue*) terminals on contact with the HCs. **c** Using the same experimental design as (**b**), single, correctly opposed synapses were observed between HCs (CtBP2-positive puncta, *green*) and SGNs (PSD95-positive puncta, *red*). **d** The reinnervation described in C was enhanced by the application of RGMa to the cell culture media, to give greater numbers of new, correctly opposed synaptic connections. **e** Experimentation using the same in vitro model, but replacing SGNs with stem cell (SC)-derived neurons, showed extensive reinnervation of HCs by SC-derived neurites as illustrated by synapsin-positive puncta (*blue*) at sites of HC innervation. CtBP2, C-terminal binding protein 2; HC, hair cell; SC, stem cell; SGN, spiral ganglion neuron; PSD95, postsynaptic density protein 95; RGMa, repulsive guidance molecule for retinal axons

Although these initial reports of synaptogenesis are promising, it will be important to demonstrate that these apparently presynaptic terminals ultimately mature into postsynaptic densities. Small numbers of postsynaptic densities have been reported in recent experimentation using human embryonic stem cells (Nayagam et al., 2013). These postsynaptic densities need to be correctly aligned with hair cell ribbon synapses for fast neural transmission. Early postnatal auditory neurons developed postsynaptic densities that stained for PSD95 (Fig. 9.1c, d; Tong et al., 2013; Brugeaud et al., 2014). Functionally immature stem cell-derived neurons (Nayagam et al., 2013; Needham et al., 2014) may not be capable of making mature synapses with hair cells with the same propensity as early postnatal auditory neurons, which are already specified and fully differentiated (Tong et al., 2013; Brugeaud et al., 2014). The afferent synapse may mature once connections are made to hair cells and may be assisted by the application of appropriate soluble guidance molecules, as recently reported (Brugeaud et al., 2014; see also Sect. 9.5).

In addition to peripheral innervation, a smaller number of central innervation assays have been used to examine whether stem cell-derived neurons form synapses with neurons in slices of developing mammalian cochlear nucleus (Glavaski-Joksimovic et al., 2009; Hyakumura et al., 2012). A study using murine

embryonic stem cell-derived neurons reported the presence of synaptic vesicles in stem cell processes contacting the edge of the auditory brain stem slice. More recently, auditory-like neurons derived from human embryonic stem cells were found to innervate the auditory brain stem extensively and to make synapsin1-positive glutamatergic terminals on neurons in the cochlear nucleus. Like their peripheral counterparts, central processes must form appropriate tonotopic connections with neurons located in the anatomically correct regions of the brain stem. To date, there are no published in vitro or in vivo studies describing the cochleotopic innervation of the cochlear nucleus by stem cells. Given the difficulty in tracing central stem cell-derived neural processes in vivo, assays for central innervation may prove useful in screening different stem cell types (and different stages of differentiation), in addition to various compounds and guidance molecules for their ability to improve brain stem innervation.

9.4 The Current Status of Stem Cell Transplantation for Replacement of Auditory Neurons in the Deafened Ear

Although it is promising to be able to generate appropriate and functional sensory progenitors in vitro, the ultimate challenge in stem cell therapy for hearing loss is the successful delivery and functional integration of the progenitors with residual elements in the deafened ear. Substantial loss of auditory neurons is often found in ears that are profoundly deaf. If hair cells are severely depleted, stem cell therapy could potentially be combined with a cochlear implant. Alternatively, if hair cells are intact, as in auditory neuropathy, stem cell-derived neurons might replace the link between the sensory organ and the brain stem. In either case, challenges remain because the transplantation of stem cells into the inner ear requires precise surgery to reach the appropriate anatomical compartments (the modiolus or auditory nerve). In addition, stem cell-derived neural processes must grow or be guided peripherally toward residual hair cells and centrally into the brain stem. These new neurons must also be capable of synaptogenesis in the periphery and the brain stem, if they are to recapitulate the tonotopic wiring of the cochlea and cochlear nucleus long term. When combined with a cochlear implant, stem cell-derived neurons must respond to high stimulation rates (Needham et al., 2014). As described in Sects. 9.3.1 and 9.3.3, substantial progress toward these challenges has been made in vitro. Additional advances have been described in vivo over the last decade, and key findings from these studies are described in detail in the following section.

Cochlear transplantation studies have targeted the damaged neural elements (summarised in Table 9.2), or have investigated the potential to replace the sensory hair cells (Iguchi et al., 2004; Hildebrand et al., 2005; Han et al., 2010). Despite subtle differences in the type of stem cell delivered and the transplantation technique adopted, the collective results from these studies support several conclusions: (1) exogenous stem cell types can survive in the deafened mammalian cochlea;

(2) stem cells are capable of extensive migration/dispersal after their delivery into the cochlea; (3) a proportion of stem cells express neuronal and glial proteins following their transplantation in vivo; and (4) transplantation of stem cells into the cochlea elicits a small, localised tissue response (if at all; Coleman et al., 2006; Nayagam et al., 2012). These studies have employed embryonic, adult, induced pluripotent, and mesenchymal stem cells for neural replacement in the deafened ear. Infusion of mouse embryonic stem cells into the fluid-filled cochlear scalae, while evoking no tissues response, yielded only small numbers of cells within their target location (Coleman et al., 2006). Transplantation of stem cells into the cochlear modiolus or auditory nerve (Corrales et al., 2006; Shi et al., 2007; Chen et al., 2012) led to larger numbers of neurons in an appropriate location and similarly produced a relatively minor tissue response (Backhouse et al., 2008; Nayagam et al., 2012). Importantly, studies using a mammalian neuropathy model demonstrated that the early postinjury period was an optimal time window for engraftment and survival of embryonic stem cell-derived neural cells (Lang et al., 2008).

9.4.1 Stem Cell Therapy to Treat Auditory Neuropathy

Several groups have reported that mouse (Corrales et al., 2006; Reyes et al., 2008; Yuan et al., 2012) and human (Shi et al., 2007; Chen et al., 2012) embryonic stem cells engraft and integrate into the cochlea. These in vivo studies used a deafferented model (Corrales et al., 2006) and looked at stem cell-derived neurons transplanted into the cochlea. The embryonic stem cells are pluripotent and thus have the possibility of becoming neurons phenotypically identical to auditory neurons. These studies demonstrated that (1) auditory-like neurons can be derived from embryonic stem cells and these cells differentiate into glutamatergic neurons in vitro (Reyes et al., 2008); (2) stem cell-derived neurons extend processes toward both the sensory epithelium housing the hair cells (Corrales et al., 2006; Shi et al., 2007; Chen et al., 2012) and the cochlear nucleus in the brain stem (Shi et al., 2007; Chen et al., 2012; Yuan et al., 2012); and (3) stem cell transplants result in improved function as measured by electrophysiology (auditory evoked responses) and new synapse formation (Chen et al., 2012; Yuan et al., 2012). Both of these studies used a model of auditory neuropathy previously described (Corrales et al., 2006) and reported improvements in hearing thresholds approximately 3 months after transplantation. Improvements in function were demonstrated by electrophysiology, and synaptic marker expression was used to demonstrate synapses in both the periphery, at the basal surface of the hair cells, and centrally in the brain stem (with second-order neurons in the cochlear nucleus).

Interestingly, these two studies differed in the extent to which functional recovery was observed. Whereas Chen et al., (2012) reported extensive functional recovery (albeit to varying degrees) throughout the cochlea in all stem cell transplanted animals (n = 18), Yuan and colleagues (Yuan et al., 2012) observed reinnervation of hair cells (and functional recovery) only in the basal (high frequency)

regions of the cochlea of transplanted animals. Furthermore, Chen et al., (2012) noted that there were considerably fewer stem cell-derived central projections growing to the cochlear nucleus (in comparison with numbers of transplanted somata). Taken collectively, these data suggest that further work is required to elucidate fully the mechanism(s) by which function is restored and to achieve better integration of transplanted embryonic stem cells into the host to reliably restore function. One route to improved functional integration could be electrical stimulation/depolarization using a cochlear implant as discussed in more detail in Sect. 9.4.2.

9.4.2 Treating Sensorineural Hearing Loss Using Stem Cells

A related strategy for hearing restoration is being investigated for severe-to-profound sensorineural hearing loss, where there is extensive damage to hair cells and resulting progressive degeneration of auditory neurons (Coleman et al., 2007b; Gunewardene et al., 2012). In such cases, rather than reinnervating residual hair cells, stem cell-derived neurons may be stimulated with a cochlear implant. For sensorineural hearing loss, stem cell-derived neurons would need to extend organized peripheral processes into either the osseous spiral lamina or the scala tympani to contact appropriate electrodes (Coleman et al., 2007b). Such a therapy may ultimately prove useful for a variety of etiologies of hearing loss (Coleman et al., 2007b; Gunewardene et al., 2012).

Electrical stimulation alone could improve firing properties, survival, neurite outgrowth, and synapse formation of transplanted neurons. Electrical stimulation may provide an in situ replacement for the spontaneous activity in developing auditory nerve fibers, which is essential for the survival of target neurons in the cochlear nucleus (Rubel & Fritzsch, 2002). Spontaneous firing may also assist in directing the formation of specific synaptic connections and in activating auditory neurons during embryogenesis (Lippe, 1994; Tritsch et al., 2007). Similarly, electrical stimulation has been shown to promote survival of auditory neurons in vitro (Hegarty et al., 1997; Hansen et al., 2001) and in vivo (Shepherd et al., 2005) and promotes the differentiation of stem cells into neural phenotypes in vitro (Yamada et al., 2007). These findings are further supported by a study showing that normal synaptic structure can be recovered after chronic electrical stimulation in congenitally deaf mammals (Ryugo et al., 2005). Stem cell-derived neurons send fibers into the brain stem along the neural scaffold that remains after nerve loss, and the cochlear implant may enhance cochleotopic reconnection between the new neurons and cochlear nucleus cells.

Several studies have demonstrated cell survival and neural differentiation after transplantation, but a major challenges that remains to be addressed is how to overcome the differences in tonotopic gradients present in auditory neurons [which are still being discovered (Flores-Otero et al., 2007)] and encourage the organised growth of peripheral and central stem cell-derived processes in a cochleotopic manner.

9.4.3 Stage of Stem Cell Differentiation for Integration, Targeting, and Cell Survival

The stage of differentiation of the stem cell used for implantation plays a key role in functional integration. Completely differentiated neurons, although attractive because of the inherent electrical properties of the neurons at late stages of differentiation, display less capacity to survive and integrate into the host. Although further differentiation increases the electrophysiological match to the endogenous circuit, manipulating (i.e., putting into suspension in medium and injected into the animal) highly differentiated neurons leads to death of a large number of the neurons. Partially differentiated stem cells, which have been specified but not fully differentiated, survive transplantation in higher numbers. Local cues that guide the final steps of differentiation may achieve phenotypic characteristics needed for the particular neuron at the time of transplantation. The stage of differentiation of the implanted cells also influences the growth of neurons and their processes to the brain stem. In addition the surgical approaches could be important, as a barrier to growth has been described in crossing from peripheral to central regions.

Cell division by the transplanted cells interacts with cell death in determining the outcome of a neural graft. The number of neurons to be transplanted is influenced by the extent of cell division and is higher for the progenitors at earlier stages of differentiation. Completely undifferentiated cells with high rates of cell division have a risk of tumor or teratoma formation.

9.4.4 Results Using Other Stem Cell Types

Although embryonic stem cell transplants are promising for auditory neuron replacement, iPSCs are likely to have similar functional properties (Takahashi & Yamanaka, 2006) but are immunocompatible with the host (Gunewardene et al., 2012). Recent experiments show that these cells can differentiate into both neural progenitors (Nishimura et al., 2009, 2012) and sensory auditory-like neurons (Gunewardene et al., 2014). Mouse iPSC-derived neural progenitors extended neurites toward hair cells in vitro (Nishimura et al., 2009) and survived following transplantation into the cochlea (Nishimura et al., 2009, 2012). Although no evidence of synapse formation has been reported, some of the iPSCs were glutamatergic following transplantation (Nishimura et al., 2009). In addition, human iPSCs can be directed to differentiate into sensory neurons expressing a cohort of relevant auditory neural proteins, including *Pax 2/7*, *NeuroD1*, *Brn3a*, *Islet1*, and *GATA3* (Gunewardene et al., 2014), and extend neurites toward hair cells in vitro where they make synapsin1-positive presynaptic terminals. The human cells are being tested for transplantation. Although iPSCs are currently under investigation for potential tumor formation (Nishimura et al., 2012) and long-term engraftment (Fu & Xu, 2012), they may present a viable alternative to the clinical use of embryonic stem cells.

Similarly, mesenchymal stem cells, which can be derived from the adult and used for autologous transplantation, may confer additional benefits because of their immunosuppressive properties (Ohtaki et al., 2008; Uccelli et al., 2008), their ability to secrete soluble trophic factors (Neuhuber et al., 2005; Yu et al., 2008), and their clinical use over many decades. Historically, the use of mesenchymal stem cells has been limited because of more limited differentiation capacity. However, recent in vitro studies suggest that mouse mesenchymal stem cells can be directed to differentiate into otic progenitors expressing *Pax2/8*, *GATA3*, and *Sox2*, followed by expression of sensory auditory neural transcription factors *Ngn1*, *Brn3a*, and neural protein neurofilament (Boddy et al., 2012). Interestingly, human nasal mesenchymal stem cells were reported to repopulate the spiral ganglion in an in vitro auditory neural lesion model, and extended TuJ1-positive neurites toward the sensory epithelium (Bas et al., 2013). Initial transplantation studies also report their survival in the deaf (Cho et al., 2011; Kondo et al., 2011) and normal ear (Kasagi et al., 2013). Most notably, the combined transplantation of mesenchymal stem cells with Wnt1 infusion, significantly promoted engraftment and differentiation of mesenchymal stem cells into neurons located within the spiral ganglion (Kondo et al., 2011). Collectively, these studies illustrate the potential of alternative stem cell sources for cochlear rehabilitation. The success of both induced pluripotent and mesenchymal stem cell types for auditory neural replacement ultimately rests on their long-term survival and functional integration.

If stem cells can make functional and cochleotopic connections, they may broaden the indications for cochlear implants. Importantly, research in this field has the potential to inform other emerging therapies that combine cell transplantation with electrical stimulation of tissue, including cardiac pacemakers with stem cell-derived cardiac tissue for improved heart function (Ma et al., 2011; Rajala et al., 2011; Chiu et al., 2012), or retinal prostheses combined with stem cell-derived retinal tissues to restore sight (Merabet, 2011; Singh & MacLaren, 2011).

9.5 Probing for Targets that Influence Regrowth and Synaptogenesis

The formation of synapses with hair cell and the brain stem by transplanted neurons are exciting advances. There are, however, sharp limits to the reinnervation that can be achieved, and a better understanding of growth promoting or inhibitory signals could improve regrowth to the hair cells and brain stem. What genes have emerged as potential targets for intervention and improvement on these results?

9.5.1 Guidance Systems for Development May Inhibit Regeneration

After their genesis, spiral ganglion neurons project peripherally to hair cells and centrally to cells in the cochlear nucleus. Axonal guidance molecules such as netrins, semaphorins, slits, and ephrins that exert repulsive and attractive forces on growth cones at the tips of axons and dendrites are important for the development of auditory circuitry. Axonal growth can also be guided by permissive substrates in the matrix and by soluble trophic factors. Soon after spiral ganglion neurons are born, they become bipolar and are guided to their targets through the mesenchyme and Kölliker's organ (Tritsch et al., 2007). The transiently present Kölliker's organ provides the early spontaneous activity present in the developing organ of Corti (before the onset of hearing). Thus, guidance information comes from surrounding tissues, such as Kölliker's organ, mesenchyme, and glia. Repulsive slit and ephrin ligands are expressed in nonsensory tissues of the ear and function to keep axonal growth within the spiral lamina (Bianchi & Liu, 1999; Pickles et al., 2002; Battisti & Fekete, 2008). Moreover, netrin1 promotes neurite outgrowth of cultured spiral ganglion neurons, whereas ephrinB1 inhibits outgrowth (Bianchi & Gray, 2002; Lee & Warchol, 2008). Despite the presence of many host molecules in the inner ear, specific functions remain unclear. Brain-derived neurotrophic factor and neurotrophin 3, neurotrophins expressed in the ear, may have some guidance activity, but that role is hard to dissect from the overall role in neuronal growth, survival and innervation (Fritzsch et al., 2004).

Manipulation of developmentally relevant guidance molecules is likely to be important for rewiring auditory circuitry. Inhibition of neuronal regeneration in the nervous system of adults by axonal guidance molecules that guide innervation in the embryo has been described (Pasterkamp et al., 1998; Harel & Strittmatter, 2006). The guidance molecules do not necessarily recapitulate their role in embryonic guidance but may inhibit regeneration at glial scars (Pasterkamp et al., 1998; Hata et al., 2006; Pasterkamp & Verhaagen, 2006). The neuropilin 1/semaphorin 3a and neogenin 1/RGMa receptors and ligands have been shown to prevent regeneration of axons in peripheral neurites (Kyoto et al., 2007; Tang et al., 2007; Tannemaat et al., 2007).

We have found a negative influence of some axonal guidance molecules on spiral ganglion neuron regeneration. Repulsive guidance molecule, RGMa, is expressed in the developing as well as the postnatal cochlea (Brugeaud et al., 2014). The timing of its expression after birth suggested a possible role in regenerating neurons. Inhibition of RGMa increased reinnervation of hair cells in organ of Corti explants, suggesting that expression of the molecule in the tissue of the adult after damage may inhibit spiral ganglion neuron regeneration. Thus, a better understanding and subsequent application of a defined cocktail of guidance molecules, will likely assist in the correct rewiring of auditory circuitry by stem cell-derived neurons in the adult.

Penetration of new (stem cell-derived) neurites through the Schwann-glial border remains one of the key challenges in the successful development of a stem cell therapy for auditory neural replacement. The auditory nerve is comprised of peripheral fibers that interact with peripheral glia and central fibers that interact with central glia, and a replacement neuron would confront the central glia as it exits the cochlea and enters the brain stem (Schwann-glial border). This transitional zone is known to be particularly hostile to new axon growth and thus strategies to facilitate growth through this zone are essential. Functional restoration (as measured by electrophysiology) shows that some of these connections are made, however, as it could not have occurred without the formation of new synapses in the cochlear nucleus (Chen et al., 2012; Yuan et al., 2012). Thus, the key questions remaining are how central reinnervation can be maximized and tonotopic reorganization achieved. Application of repulsive guidance molecule inhibitors to the injury site, by facilitating significantly more growth of axons through a glial scar, have been successful in the spinal cord (Hata et al., 2006; Kyoto et al., 2007). Stem cell-derived axons would also likely benefit from remyelination following the establishment of new connections. Although this remains an area of potential study in this field, it may be achieved via activation of endogenous populations of appropriate glia (Schwann cells and oligodendrocytes, provided these remain), or by the stem cells themselves. An interesting in vitro observation was the spontaneous ensheathing of stem cell-derived neural processes in glial fibrillary acidic protein (Shi et al., 2007), highlighting the potential of stem cell differentiation to provide neural and glial cell types that could enhance transplantation outcomes.

9.5.2 Activators of Afferent Synaptogenesis

Neurons placed in culture extended processes to denervated organ of Corti (Martinez-Monedero et al., 2006, 2008; Flores-Otero et al., 2007). The synaptic complexes at the ribbon of the inner hair cell, and postsynaptic densities in the spiral ganglion neuron, characteristic features of the glutamatergic synapse, have been exploited to detect and quantify new synapses. Cultured spiral ganglion neurons at contacts with denervated hair cells had PSD95-immunopositive puncta directly facing the hair cell ribbons. Application of brain-derived neurotrophic factor and neurotrophin 3, known to promote spiral ganglion neuron survival and neurite outgrowth (Pirvola et al., 1992; Ernfors et al., 1995; Fritzsch et al., 1997), significantly increased the number of new synapses in this system (Tong et al., 2013).

Glutamate released from presynaptic neurons is known to play an important role in establishing synaptic contacts (Wong & Wong, 2001; Tashiro et al., 2003; Sabo et al., 2006). In the auditory system, glutamate is loaded into synaptic vesicles of inner hair cells by VGLUT3, and mice lacking VGLUT3 are profoundly deaf due to the lack of release of glutamate into synaptic zones (Ruel et al., 2008; Seal et al., 2008). Glutamate release also played a role in the formation of synapses in these studies, and glutamate from presynaptic terminals of hair cells is important for

inducing cochlear synaptogenesis during regeneration in the in vitro system. The number of new synapses in VGLUT3 mutant mice was reduced, suggesting that glutamate release facilitated synaptogenesis (Tong et al., 2013).

9.6 Summary

The irreversible loss of auditory neurons is a recognised cause of sensorineural hearing loss, and thus new generation therapies aimed at restoring this population of cells are understandably appealing. Stem cells may provide a source of replacement neurons for the deaf cochlea, provided that they can be routinely encouraged to differentiate into appropriate phenotypes; extend new dendrites and axons in an organized manner; form synapses on appropriate target cells; and, ultimately, reestablish a functional and tonotopic circuit. Although the application of new auditory neurons derived from stem cells is challenging, remarkable progress has been made in a short time. Future advances in this field will involve the integration of advances across multiple disciplines, including neurosensory differentiation and development, neurite outgrowth and pathfinding, cochlear cell transplantation techniques, electrical stimulation, and immunocompatibility. In the future, if stem cell-derived neurons from any source can be encouraged to make functional and cochleotopic central connections using the combined approaches, there may be a broader population of deaf patients that experience improvements in hearing and/or are able to derive benefits from a cochlear implant. Importantly, advances in this field have the potential to inform related stem cell therapies for neurodegenerative disease, as the auditory system provides a unique model whereby the function of new (stem cell-derived) neurons can be measured using electrophysiology.

References

Backhouse, S., Coleman, B., & Shepherd, R. (2008). Surgical access to the mammalian cochlea for cell-based therapies. *Experimental Neurology*, 214(2), 193–200.

Bas, E., Van De Water, T. R., Lumbreras, V., Rajguru, S., Goss, G., Hare, J. M., & Goldstein, B. J. (2013). Adult human nasal mesenchymal-like stem cells restore cochlear spiral ganglion neurons after experimental lesion. *Stem Cells and Development*.

Battisti, A. C., & Fekete, D. M. (2008). Slits and robos in the developing chicken inner ear. *Developmental Dynamics*, 237(2), 476–484.

Bianchi, L. M., & Liu, H. (1999). Comparison of ephrin-A ligand and EphA receptor distribution in the developing inner ear. *The Anatomical Record*, 254(1), 127–134.

Bianchi, L. M., & Gray, N. A. (2002). EphB receptors influence growth of ephrin-B1-positive statoacoustic nerve fibers. *European Journal of Neuroscience*, 16(8), 1499–1506.

Boddy, S. L., Chen, W., Romero-Guevara, R., Kottam, L., Bellantuono, I., & Rivolta, M. N. (2012). Inner ear progenitor cells can be generated in vitro from human bone marrow mesenchymal stem cells. *Regenerative Medicine*, 7(6), 757–767.

Brugeaud, A., Tong, M., Luo, L., & Edge, A. S. (2014). Inhibition of repulsive guidance molecule, RGMa, increases afferent synapse formation with auditory hair cells. *Developmental Neurobiology*, 74(4), 457–466.

Chen, W., Cacciabue-Rivolta, D. I., Moore, H. D., & Rivolta, M. N. (2007). The human fetal cochlea can be a source for auditory progenitors/stem cells isolation. *Hearing Research*, 233 (1–2), 23–29.

Chen, W., Johnson, S. L., Marcotti, W., Andrews, P. W., Moore, H. D., & Rivolta, M. N. (2009). Human fetal auditory stem cells can be expanded in vitro and differentiate into functional auditory neurons and hair cell-like cells. *Stem Cells*, 27(5), 1196–1204.

Chen, W., Jongkamonwiwat, N., Abbas, L., Eshtan, S. J., Johnson, S. L., Kuhn, S., Milo, M., Thurlow, J. K., Andrews, P. W., Marcotti, W., Moore, H. D., & Rivolta, M. N. (2012). Restoration of auditory evoked responses by human ES-cell-derived otic progenitors. *Nature*, 490(7419), 278–282.

Chiu, L. L., Iyer, R. K., Reis, L. A., Nunes, S. S., & Radisic, M. (2012). Cardiac tissue engineering: Current state and perspectives. *Frontiers in Bioscience*, 17, 1533–1550.

Cho, Y. B., Cho, H. H., Jang, S., Jeong, H. S., & Park, J. S. (2011). Transplantation of neural differentiated human mesenchymal stem cells into the cochlea of an auditory-neuropathy guinea pig model. *Journal of Korean Medical Science*, 26(4), 492–498.

Coleman, B., Hardman, J., Coco, A., Epp, S., de Silva, M., Crook, J., & Shepherd, R. (2006). Fate of embryonic stem cells transplanted into the deafened mammalian cochlea. *Cell Transplantation*, 15(5), 369–380.

Coleman, B., Fallon, J. B., Pettingill, L. N., de Silva, M. G., & Shepherd, R. K. (2007a). Auditory hair cell explant co-cultures promote the differentiation of stem cells into bipolar neurons. *Experimental Cell Research*, 313(2), 232–243.

Coleman, B., de Silva, M. G., & Shepherd, R. K. (2007b). Concise review: The potential of stem cells for auditory neuron generation and replacement. *Stem Cells*, 25(11), 2685–2694.

Corrales, C. E., Pan, L., Li, H., Liberman, M. C., Heller, S., & Edge, A. S. (2006). Engraftment and differentiation of embryonic stem cell-derived neural progenitor cells in the cochlear nerve trunk: Growth of processes into the organ of corti. *Journal of Neurobiology*, 66(13), 1489–1500.

Ernfors, P., Van De Water, T., Loring, J., & Jaenisch, R. (1995). Complementary roles of BDNF and NT-3 in vestibular and auditory development. *Neuron*, 14(6), 1153–1164.

Flores-Otero, J., Xue, H. Z., & Davis, R. L. (2007). Reciprocal regulation of presynaptic and postsynaptic proteins in bipolar spiral ganglion neurons by neurotrophins. *The Journal of Neuroscience*, 27(51), 14023–14034.

Forrest, A. R. R. (2014). A promoter-level mammalian expression atlas. *Nature*, 507(7493), 462–470.

Fritzsch, B., Silos-Santiago, I., Bianchi, L. M., & Farinas, I. (1997). The role of neurotrophic factors in regulating the development of inner ear innervation. *Trends in Neuroscience*, 20(4), 159–164.

Fritzsch, B., Tessarollo, L., Coppola, E., & Reichardt, L. F. (2004). Neurotrophins in the ear: Their roles in sensory neuron survival and fiber guidance. *Progress in Brain Research*, 146, 265–278.

Fu, X., & Xu, Y. (2012). Challenges to the clinical application of pluripotent stem cells: Towards genomic and functional stability. *Genome Medicine*, 4(6), 55.

Fu, Y., Wang, S., Liu, Y., Wang, J., Wang, G., Chen, Q., & Gong, S. (2009). Study on neural stem cell transplantation into natural rat cochlea via round window. *American Journal of Otolaryngology*, 30(1), 8–16.

Glavaski-Joksimovic, A., Thonabulsombat, C., Wendt, M., Eriksson, M., Ma, H., & Olivius, P. (2009). Morphological differentiation of tau-green fluorescent protein embryonic stem cells into neurons after co-culture with auditory brain stem slices. *Neuroscience*.

Gunewardene, N., Dottori, M., & Nayagam, B. A. (2012). The convergence of cochlear implantation with induced pluripotent stem cell therapy. *Stem Cell Reviews and Reports*, 8(3), 741–754.

Gunewardene, N., Dottori, M., Needham, K., & Nayagam, B. A. (2014). Directing human induced pluripotent stem cells into a neurosensory lineage for auditory neuron replacement. *Bioresearch Open Access*, 3(4), 162–175.

Han, Z., Yang, J. M., Chi, F. L., Cong, N., Huang, Y. B., Gao, Z., & Li, W. (2010). Survival and fate of transplanted embryonic neural stem cells by *Atoh*1 gene transfer in guinea pigs cochlea. *NeuroReport*, 21(7), 490–496.

Hansen, M. R., Zha, X. M., Bok, J., & Green, S. H. (2001). Multiple distinct signal pathways, including an autocrine neurotrophic mechanism, contribute to the survival-promoting effect of depolarization on spiral ganglion neurons in vitro. *The Journal of Neuroscience*, 21(7), 2256–2267.

Harel, N. Y., & Strittmatter, S. M. (2006). Can regenerating axons recapitulate developmental guidance during recovery from spinal cord injury? *Nature Reviews Neuroscience*, 7(8), 603–616.

Hata, K., Fujitani, M., Yasuda, Y., Doya, H., Saito, T., Yamagishi, S., Mueller, B. K., & Yamashita, T. (2006). RGMa inhibition promotes axonal growth and recovery after spinal cord injury. *Journal of Cell Biology*, 173(1), 47–58.

Hegarty, J. L., Kay, A. R., & Green, S. H. (1997). Trophic support of cultured spiral ganglion neurons by depolarization exceeds and is additive with that by neurotrophins or cAMP and requires elevation of $[Ca^{2+}]_i$ within a set range. *The Journal of Neuroscience*, 17(6), 1959–1970.

Hildebrand, M. S., Dahl, H. H., Hardman, J., Coleman, B., Shepherd, R. K., & de Silva, M. G. (2005). Survival of partially differentiated mouse embryonic stem cells in the scala media of the guinea pig cochlea. *Journal of the Association for Research in Otolaryngology*, 6, 341–354.

Hyakumura, T., Dottori, M., Needham, K., & Nayagam, B. A. (2012). Innervation of peripheral and central auditory tissues by human embryonic stem cell-derived neurons in vitro (T-2294). Paper presented at the International Society for Stem Cell Research 10th Annual Meeting, Yokohama, Japan.

Iguchi, F., Nakagawa, T., Tateya, I., Endo, T., Kim, T. S., Dong, Y., Kita, T., Kojima, K., Naito, Y., Omori, K., & Ito, J. (2004). Surgical techniques for cell transplantation into the mouse cochlea. *Acta Oto-Laryngologica Supplementum* (551), 43–47.

Javel, E., & Viemeister, N. F. (2000). Stochastic properties of cat auditory nerve responses to electric and acoustic stimuli and application to intensity discrimination. *Journal of the Acoustical Society of America*, 107(2), 908–921.

Kasagi, H., Kuhara, T., Okada, H., Sueyoshi, N., & Kurihara, H. (2013). Mesenchymal stem cell transplantation to the mouse cochlea as a treatment for childhood sensorineural hearing loss. *International Journal of Pediatric Otorhinolaryngology*, 77(6), 936–942.

Kawasaki, H., Mizuseki, K., Nishikawa, S., Kaneko, S., Kuwana, Y., Nakanishi, S., Nishikawa, S. I., & Sasai, Y. (2000). Induction of midbrain dopaminergic neurons from ES cells by stromal cell-derived inducing activity. *Neuron*, 28(1), 31–40.

Kawasaki, H., Suemori, H., Mizuseki, K., Watanabe, K., Urano, F., Ichinose, H., Haruta, M., Takahashi, M., Yoshikawa, K., Nishikawa, S., Nakatsuji, N., & Sasai, Y. (2002). Generation of dopaminergic neurons and pigmented epithelia from primate ES cells by stromal cell-derived inducing activity. *Proceedings of the National Academy of Sciences of the U S A*, 99(3), 1580–1585.

Kiang, N. Y., Watanabe, T., Thomas, E. C., & Clark, L. F. (1965). *Discharge patterns of single fibers in the cat's auditory nerve*. Cambridge, MA.: MIT Press.

Kondo, T., Matsuoka, A. J., Shimomura, A., Koehler, K. R., Chan, R. J., Miller, J. M., Srour, E. F., & Hashino, E. (2011). Wnt signaling promotes neuronal differentiation from mesenchymal stem cells through activation of Tlx3. *Stem Cells*, 29(5), 836–846.

Kujawa, S. G., & Liberman, M. C. (2006). Acceleration of age-related hearing loss by early noise exposure: Evidence of a misspent youth. *The Journal of Neuroscience*, 26(7), 2115–2123.

Kujawa, S. G., & Liberman, M. C. (2009). Adding insult to injury: Cochlear nerve degeneration after "temporary" noise-induced hearing loss. *The Journal of Neuroscience*, 29(45), 14077–14085.

Kyoto, A., Hata, K., & Yamashita, T. (2007). Synapse formation of the cortico-spinal axons is enhanced by RGMa inhibition after spinal cord injury. *Brain Research*, 1186, 74–86.

Lang, H., Schulte, B. A., Goddard, J. C., Hedrick, M., Schulte, J. B., Wei, L., & Schmiedt, R. A. (2008). Transplantation of mouse embryonic stem cells into the cochlea of an auditory-neuropathy animal model: Effects of timing after injury. *Journal of the Association for Research in Otolaryngology*, 9(2), 225–240.

Lee, K. H., & Warchol, M. E. (2008). Promotion of neurite outgrowth and axon guidance in spiral ganglion cells by netrin-1. *Archives of Otolaryngology–Head & Neck Surgery*, 134(2), 146–151.

Lerner-Natoli, M., Ladrech, S., Renard, N., Puel, J. L., Eybalin, M., & Pujol, R. (1997). Protein kinase C may be involved in synaptic repair of auditory neuron dendrites after AMPA injury in the cochlea. *Brain Research*, 749(1), 109–119.

Liberman, M. C., & Mulroy, M. J. (1982). Acute and chronic effects of acoustic trauma: Cochlear pathology and auditory nerve pathophysiology. In R. P. Hamernik, D. Henderson, & R. Salvi (Eds.), *New perspectives on noise-induced hearing loss* (pp. 105–151). New York: Raven Press.

Lin, H. W., Furman, A. C., Kujawa, S. G., & Liberman, M. C. (2011). Primary neural degeneration in the guinea pig cochlea after reversible noise-induced threshold shift. *Journal of the Association for Research in Otolaryngology*, 12(5), 605–616.

Lippe, W. R. (1994). Rhythmic spontaneous activity in the developing avian auditory system. *The Journal of Neuroscience*, 14(3 Pt 2), 1486–1495.

Ma, J., Guo, L., Fiene, S. J., Anson, B. D., Thomson, J. A., Kamp, T. J., Kolaja, K. L., Swanson, B. J., & January, C. T. (2011). High purity human-induced pluripotent stem cell-derived cardiomyocytes: Electrophysiological properties of action potentials and ionic currents. *American Journal of Physiology–Heart and Circulatory Physiology*, 301(5), H2006–2017.

Makary, C. A., Shin, J., Kujawa, S. G., Liberman, M. C., & Merchant, S. N. (2011). Age-related primary cochlear neuronal degeneration in human temporal bones. *Journal of the Association for Research in Otolaryngology*, 12(6), 711–717.

Marrs, G. S., & Spirou, G. A. (2012). Embryonic assembly of auditory circuits: Spiral ganglion and brainstem. *Journal of Physiology*, 590(Pt 10), 2391–2408.

Martinez-Monedero, R., Corrales, C. E., Cuajungco, M. P., Heller, S., & Edge, A. S. (2006). Reinnervation of hair cells by auditory neurons after selective removal of spiral ganglion neurons. *Journal of Neurobiology*, 66(4), 319–331.

Martinez-Monedero, R., Yi, E., Oshima, K., Glowatzki, E., & Edge, A. S. (2008). Differentiation of inner ear stem cells to functional sensory neurons. *Developmental Neurobiology*, 68(5), 669–684.

Matsumoto, M., Nakagawa, T., Higashi, T., Kim, T. S., Kojima, K., Kita, T., Sakamoto, T., & Ito, J. (2005). Innervation of stem cell-derived neurons into auditory epithelia of mice. *NeuroReport*, 16(8), 787–790.

Matsumoto, M., Nakagawa, T., Kojima, K., Sakamoto, T., Fujiyama, F., & Ito, J. (2008). Potential of embryonic stem cell-derived neurons for synapse formation with auditory hair cells. *Journal of Neuroscience Research*, 86(14), 3075–3085.

Matsuoka, A. J., Kondo, T., Miyamoto, R. T., & Hashino, E. (2006). In vivo and in vitro characterization of bone marrow-derived stem cells in the cochlea. *Laryngoscope*, 116(8), 1363–1367.

Merabet, L. B. (2011). Building the bionic eye: An emerging reality and opportunity. *Progress in Brain Research*, 192, 3–15.

Naito, Y., Nakamura, T., Nakagawa, T., Iguchi, F., Endo, T., Fujino, K., Kim, T. S., Hiratsuka, Y., Tamura, T., Kanemaru, S., Shimizu, Y., & Ito, J. (2004). Transplantation of bone marrow stromal cells into the cochlea of chinchillas. *NeuroReport*, 15(1), 1–4.

Nayagam, B. A., Backhouse, S. S., Cimenkaya, C., & Shepherd, R. K. (2012). Hydrogel limits stem cell dispersal in the deaf cochlea: Implications for cochlear implants. *Journal of Neural Engineering*, 9(6), doi: 10.1088/1741–2560/9/6/065001

Nayagam, B. A., Edge, A. S., Needham, K., Hyakumura, T., Leung, J., Nayagam, D. A., & Dottori, M. (2013). An in vitro model of developmental synaptogenesis using cocultures of human neural progenitors and cochlear explants. *Stem Cells and Development*, 22(6), 901–912.

Needham, K., Minter, R. L., Shepherd, R. K., & Nayagam, B. A. (2013). Challenges for stem cells to functionally repair the damaged auditory nerve. *Expert Opinion on Biological Therapy*, 13 (1), 85–101.

Needham, K., Hyakumura, T., Gunewardene, N., Dottori, M., & Nayagam, B. A. (2014). Electrophysiological properties of neurosensory progenitors derived from human embryonic stem cells. *Stem Cell Research*, 12(1), 241–249.

Neuhuber, B., Timothy Himes, B., Shumsky, J. S., Gallo, G., & Fischer, I. (2005). Axon growth and recovery of function supported by human bone marrow stromal cells in the injured spinal cord exhibit donor variations. *Brain Research*, 1035(1), 73–85.

Nishimura, K., Nakagawa, T., Ono, K., Ogita, H., Sakamoto, T., Yamamoto, N., Okita, K., Yamanaka, S., & Ito, J. (2009). Transplantation of mouse induced pluripotent stem cells into the cochlea. *NeuroReport*, 20(14), 1250–1254.

Nishimura, K., Nakagawa, T., Sakamoto, T., & Ito, J. (2012). Fates of murine pluripotent stem cell-derived neural progenitors following transplantation into mouse cochleae. *Cell Transplantation*, 21(4), 763–771.

Ogita, H., Nakagawa, T., Sakamoto, T., Inaoka, T., & Ito, J. (2010). Transplantation of bone marrow-derived neurospheres into guinea pig cochlea. *Laryngoscope*, 120(3), 576–581.

Ohtaki, H., Ylostalo, J. H., Foraker, J. E., Robinson, A. P., Reger, R. L., Shioda, S., & Prockop, D. J. (2008). Stem/progenitor cells from bone marrow decrease neuronal death in global ischemia by modulation of inflammatory/immune responses. *Proceedings of the National Academy of Sciences of the U S A*, 105(38), 14638–14643.

Pandit, S. R., Sullivan, J. M., Egger, V., Borecki, A. A., & Oleskevich, S. (2011). Functional effects of adult human olfactory stem cells on early-onset sensorineural hearing loss. *Stem Cells*, 29(4), 670–677.

Parker, M. A., Corliss, D. A., Gray, B., Anderson, J. K., Bobbin, R. P., Snyder, E. Y., & Cotanche, D. A. (2007). Neural stem cells injected into the sound-damaged cochlea migrate throughout the cochlea and express markers of hair cells, supporting cells, and spiral ganglion cells. *Hearing Research*, 232(1–2), 29–43.

Pasterkamp, R. J., & Verhaagen, J. (2006). Semaphorins in axon regeneration: Developmental guidance molecules gone wrong? *Philosophical Transactions of the Royal Society of London B: Biological Sciences*, 361(1473), 1499–1511.

Pasterkamp, R. J., De Winter, F., Holtmaat, A. J., & Verhaagen, J. (1998). Evidence for a role of the chemorepellent semaphorin III and its receptor neuropilin-1 in the regeneration of primary olfactory axons. *The Journal of Neuroscience*, 18(23), 9962–9976.

Pickles, J. O., Claxton, C., & Van Heumen, W. R. (2002). Complementary and layered expression of Ephs and ephrins in developing mouse inner ear. *Journal of Comparative Neurology*, 449 (3), 207–216.

Pirvola, U., Ylikoski, J., Palgi, J., Lehtonen, E., Arumae, U., & Saarma, M. (1992). Brain-derived neurotrophic factor and neurotrophin 3 mRNAs in the peripheral target fields of developing inner ear ganglia. *Proceedings of the National Academy of Sciences of the U S A*, 89(20), 9915–9919.

Purcell, E. K., Yang, A., Liu, L., Velkey, J. M., Morales, M. M., & Duncan, R. K. (2013). BDNF profoundly and specifically increases KCNQ4 expression in neurons derived from embryonic stem cells. *Stem Cell Research*, 10(1), 29–35.

Rajala, K., Pekkanen-Mattila, M., & Aalto-Setala, K. (2011). Cardiac differentiation of pluripotent stem cells. *Stem Cells International*, 2011, 383709.

Regala, C., Duan, M., Zou, J., Salminen, M., & Olivius, P. (2005). Xenografted fetal dorsal root ganglion, embryonic stem cell and adult neural stem cell survival following implantation into the adult vestibulocochlear nerve. *Experimental Neurology*, 193(2), 326–333.

Revoltella, R. P., Papini, S., Rosellini, A., Michelini, M., Franceschini, V., Ciorba, A., Bertolaso, L., Magosso, S., Hatzopoulos, S., Lorito, G., Giordano, P., Simoni, E., Ognio, E., Cilli, M., Saccardi, R., Urbani, S., Jeffery, R., Poulsom, R., & Martini, A. (2008). Cochlear repair by transplantation of human cord blood CD133+ cells to nod-scid mice made deaf with kanamycin and noise. *Cell Transplantation*, 17(6), 665–678.

Reyes, J. H., O'Shea, K. S., Wys, N. L., Velkey, J. M., Prieskorn, D. M., Wesolowski, K., Miller, J. M., & Altschuler, R. A. (2008). Glutamatergic neuronal differentiation of mouse embryonic stem cells after transient expression of neurogenin 1 and treatment with BDNF and GDNF: In vitro and in vivo studies. *The Journal of Neuroscience*, 28(48), 12622–12631.

Robertson, D. (1983). Functional significance of dendritic swelling after loud sounds in the guinea pig cochlea. *Hearing Research*, 9(3), 263–278.

Rubel, E. W., & Fritzsch, B. (2002). Auditory system development: Primary auditory neurons and their targets. *Annual Reviews of Neuroscience*, 25, 51–101.

Ruel, J., Emery, S., Nouvian, R., Bersot, T., Amilhon, B., Van Rybroek, J. M., Rebillard, G., Lenoir, M., Eybalin, M., Delprat, B., Sivakumaran, T. A., Giros, B., El Mestikawy, S., Moser, T., Smith, R. J., Lesperance, M. M., & Puel, J. L. (2008). Impairment of SLC17A8 encoding vesicular glutamate transporter-3, VGLUT3, underlies nonsyndromic deafness DFNA25 and inner hair cell dysfunction in null mice. *American Journal of Human Genetics*, 83(2), 278–292.

Ryugo, D. K., Kretzmer, E. A., & Niparko, J. K. (2005). Restoration of auditory nerve synapses in cats by cochlear implants. *Science*, 310(5753), 1490–1492.

Sabo, S. L., Gomes, R. A., & McAllister, A. K. (2006). Formation of presynaptic terminals at predefined sites along axons. *The Journal of Neuroscience*, 26(42), 10813–10825.

Seal, R. P., Akil, O., Yi, E., Weber, C. M., Grant, L., Yoo, J., Clause, A., Kandler, K., Noebels, J. L., Glowatzki, E., Lustig, L. R., & Edwards, R. H. (2008). Sensorineural deafness and seizures in mice lacking vesicular glutamate transporter 3. *Neuron*, 57(2), 263–275.

Sekiya, T., Holley, M. C., Kojima, K., Matsumoto, M., Helyer, R., & Ito, J. (2007). Transplantation of conditionally immortal auditory neuroblasts to the auditory nerve. *European Journal of Neuroscience*, 25(8), 2307–2318.

Sergeyenko, Y., Lall, K., Liberman, M. C., & Kujawa, S. G. (2013). Age-related cochlear synaptopathy: An early-onset contributor to auditory functional decline. *The Journal of Neuroscience*, 33(34), 13686–13694.

Shannon, R. V. (1983). Multichannel electrical stimulation of the auditory nerve in man. II. Channel interaction. *Hearing Research*, 12(1), 1–16.

Shepherd, R. K., & Javel, E. (1997). Electrical stimulation of the auditory nerve. I. Correlation of physiological responses with cochlear status. *Hearing Research*, 108(1–2), 112–144.

Shepherd, R. K., Coco, A., Epp, S. B., & Crook, J. M. (2005). Chronic depolarization enhances the trophic effects of brain-derived neurotrophic factor in rescuing auditory neurons following a sensorineural hearing loss. *Journal of Comparative Neurology*, 486(2), 145–158.

Shi, F., & Edge, A. S. (2013). Prospects for replacement of auditory neurons by stem cells. *Hearing Research*, 297, 106–112.

Shi, F., Corrales, C. E., Liberman, M. C., & Edge, A. S. (2007). BMP4 induction of sensory neurons from human embryonic stem cells and reinnervation of sensory epithelium. *European Journal of Neuroscience*, 26(11), 3016–3023.

Singh, M. S., & MacLaren, R. E. (2011). Stem cells as a therapeutic tool for the blind: Biology and future prospects. *Proceedings of the Royal Society of London B: Biological Sciences*, 278 (1721), 3009–3016.

Spoendlin, H. (1971). Primary structural changes in the organ of Corti after acoustic overstimulation. *Acta Oto-Laryngologica*, 71(2), 166–176.

Starr, A., Isaacson, B., Michalewski, H. J., Zeng, F. G., Kong, Y. Y., Beale, P., Paulson, G. W., Keats, B. J., & Lesperance, M. M. (2004). A dominantly inherited progressive deafness affecting distal auditory nerve and hair cells. *Journal of the Association for Research in Otolaryngology*, 5(4), 411–426.

Sullivan, J. M., Cohen, M. A., Pandit, S. R., Sahota, R. S., Borecki, A. A., & Oleskevich, S. (2011). Effect of epithelial stem cell transplantation on noise-induced hearing loss in adult mice. *Neurobiology of Disease*, 41(2), 552–559.

Takahashi, K., & Yamanaka, S. (2006). Induction of pluripotent stem cells from mouse embryonic and adult fibroblast cultures by defined factors. *Cell*, 126(4), 663–676.

Tang, X. Q., Heron, P., Mashburn, C., & Smith, G. M. (2007). Targeting sensory axon regeneration in adult spinal cord. *The Journal of Neuroscience*, 27(22), 6068–6078.

Tannemaat, M. R., Korecka, J., Ehlert, E. M., Mason, M. R., van Duinen, S. G., Boer, G. J., Malessy, M. J., & Verhaagen, J. (2007). Human neuroma contains increased levels of semaphorin 3A, which surrounds nerve fibers and reduces neurite extension in vitro. *The Journal of Neuroscience*, 27(52), 14260–14264.

Tashiro, A., Dunaevsky, A., Blazeski, R., Mason, C. A., & Yuste, R. (2003). Bidirectional regulation of hippocampal mossy fiber filopodial motility by kainate receptors: A two-step model of synaptogenesis. *Neuron*, 38(5), 773–784.

Tong, M., Brugeaud, A., & Edge, A. S. (2013). Regenerated synapses between postnatal hair cells and auditory neurons. *Journal of the Association for Research in Otolaryngology*, 14(3), 321–329.

Tritsch, N. X., Yi, E., Gale, J. E., Glowatzki, E., & Bergles, D. E. (2007). The origin of spontaneous activity in the developing auditory system. *Nature*, 450(7166), 50–55.

Uccelli, A., Moretta, L., & Pistoia, V. (2008). Mesenchymal stem cells in health and disease. *Nature Reviews Immunology*, 8(9), 726–736.

Vandali, A., Sly, D., Cowan, R., & van Hoesel, R. (2013). Pitch and loudness matching of unmodulated and modulated stimuli in cochlear implantees. *Hearing Research*, 302, 32–49.

Wang, Q., & Green, S. H. (2011). Functional role of neurotrophin-3 in synapse regeneration by spiral ganglion neurons on inner hair cells after excitotoxic trauma in vitro. *The Journal of Neuroscience*, 31(21), 7938–7949.

Wong, W. T., & Wong, R. O. (2001). Changing specificity of neurotransmitter regulation of rapid dendritic remodeling during synaptogenesis. *Nature Neuroscience*, 4(4), 351–352.

Yamada, M., Tanemura, K., Okada, S., Iwanami, A., Nakamura, M., Mizuno, H., Ozawa, M., Ohyama-Goto, R., Kitamura, N., Kawano, M., Tan-Takeuchi, K., Ohtsuka, C., Miyawaki, A., Takashima, A., Ogawa, M., Toyama, Y., Okano, H., & Kondo, T. (2007). Electrical stimulation modulates fate determination of differentiating embryonic stem cells. *Stem Cells*, 25(3), 562–570.

Yu, K., Ge, J., Summers, J. B., Li, F., Liu, X., Ma, P., Kaminski, J., & Zhuang, J. (2008). TSP-1 secreted by bone marrow stromal cells contributes to retinal ganglion cell neurite outgrowth and survival. *PLoS One*, 3(6), e2470.

Yuan, Y., Mizutari, K., Cheng, Y., Lang, H., Liberman, C., Shi, F., & Edge, A. (2012). Reinnervation of hair cells and cochlear nucleus by engrafted neurons derived from stem cells. In *ARO 35th Annual Meeting, Abstract #*355.

Zeng, F. G. (2002). Temporal pitch in electric hearing. *Hearing Research*, 174(1–2), 101–106.